CORA Cork Open Research Archive
Cartlann Taighde Oscailte Chorcaí

Title	Exploiting the power of continuous flow chemistry in the synthesis and reactivity of alpha-diazosulfoxides
Authors	McCaw, Patrick G.
Publication date	2018
Original Citation	McCaw, P. G. 2018. Exploiting the power of continuous flow chemistry in the synthesis and reactivity of alpha-diazosulfoxides. PhD Thesis, University College Cork.
Type of publication	Doctoral thesis
Rights	© 2018, Patrick G. McCaw. - http://creativecommons.org/licenses/by-nc-nd/3.0/
Download date	2026-11-16 14:25:47
Item downloaded from	https://hdl.handle.net/10468/6909

UCC
University College Cork, Ireland
Coláiste na hOllscoile Corcaigh

Exploiting the power of continuous flow chemistry in the synthesis and reactivity of α-diazosulfoxides.



ucc

Coláiste na hOllscoile Corcaigh, Éire
University College Cork, Ireland

Patrick G. McCaw, B. Sc.

A Thesis Presented for the Degree of

Doctor of Philosophy

to

The National University Of Ireland, Cork

School of Chemistry,

University College Cork

Supervisors: Prof. Anita Maguire and Dr. Stuart Collins

Head of School of Chemistry: Prof. Justin Holmes

February 2018

Thesis Outline

Declaration by candidate		*iii*
Acknowledgements		*iv*
Abstract		*v*
Chapter 1 Introduction		1
Chapter 2 Results and Discussion		55
Chapter 3 Experimental		305
Appendix I		
	NCI – 60 One-Dose Mean Graphs and Table of abbreviations	*On CD*
Appendix II		
	Publications	*On CD*
Appendix III		
	X-ray crystallography data	*On CD*

DECLARATION BY CANDIDATE

I declare that this thesis contains my own work and has not been submitted for another degree, either at University College Cork, or elsewhere.

Patrick G. McCaw

Acknowledgements

First of all I'd like to express my sincere gratitude to my supervisors Prof. Anita Maguire and Dr. Stuart Collins for the extensive amount of encouragement, and support throughout the duration of my PhD. work. Additionally, I'd like to thank the technical staff at UCC for the support they have provided over the years including, Dr. Dan McCarthy, Dr. Lorraine Bateman and Dr. Denis Lynch for NMR work, Dr. Florence McCarthy and Mick O'Shea for mass spec, Dr. Simon Lawrence and Dr. Udaya Khandivalli for single crystal X-ray crystallographic data, Dr. Michael Cronin for thermogravimetric analysis and Derry Kearney for glass blowing services. Thanks also to Tina Kent and Noel Browne.

Thanks to the members of the ARM and SGC research group members, past and present, especially Debbie Curran whose work is greatly appreciated, Dr. Alan Ford, Dr. Francis Harrington, Dr. Nuala Maguire and Dr. Ben Deadman whose ideas and expertise were greatly appreciated at all times. Thanks also to Rose O'Mahony, Aaran Flynn, Laura Cooke, and Christian Mulcahy who worked with me as undergraduates on some of this project, and whose input was always appreciated.

The greatest thanks of all goes to my friends and family, the group of people that supported me on the challenging days and celebrated with me on the good days. The friendship and encouragement was invaluable, and they always kept me motivated with questions such as "any breakthroughs today?" or "how's the science going?". To Will, Marty, Donal, Niall, Eoghany Griffs and Tom, for the friendship, banter, holidays, and nights out over the years. To my friends from home; Alan, Emma, Angie, Steven, Mairéad, John, Francis and Katie for the road trips and concerts. Thanks to Brian, Kieran, and Emmet, for the random chats, cinema trips, quizzes, beer pong tournaments, for the unreal years as housemates that made Cork into a home from home, and for practically adopting me to their native Athea! A special thanks goes to Davy Sulls, Fiona, and Rachel, having you three by my side for the duration of my time in UCC, has made the experience so much easier and all the better.

And lastly to my family, my sisters, Geraldine, Michelle, and Aisling, for the unlimited support, understanding and encouragement. Thanks to Granda Joe and Nellie, and finally to my parents, Paddy and Anna, who never left me wanting in any aspect of my life and whose support over the past few months has been invaluable. This thesis is dedicated to you all, and I hope I make you proud.

_____

Patrick G. McCaw.

Abstract

The research described in this thesis is an extensive study on the synthesis and reactivity of α-diazosulfoxides utilising continuous flow processing, and contrasting the outcomes from a synthetic perspective with traditional batch reaction conditions. Using continuous flow processing leads to increased efficiency and yields of the α-diazosulfoxides. Inducing the hetero-Wolff rearrangement of α-diazosulfoxides to form α-oxo sulfines in both batch and continuous flow conditions was also explored, together with subsequent trapping in cycloaddition reactions. Both Diels-Alder cycloadditions and 1,3-dipolar cycloadditions with sulfines acting as the dipolarophiles were carried out. Overall it was established that although the diastereomeric ratios for Diels-Alder cycloadditions are comparable in batch and flow, the yields are significantly enhanced from the flow process in addition to the benefit of a metal free process. The study of 1,3-dipolar cycloadditions with nitrones and nitrile oxides led to isolation of a number of novel heterocycles, and highlighted interesting differences in reactivity patterns between the lactone and ketone derived α-oxo sulfines.

The introductory chapter is an extensive review of sulfines with a focus on both the synthesis and reactivity of sulfines and α-oxo sulfines. The methods discussed for the generation of sulfines include oxidation of thioketones, sulfenylation with sulfur dioxide, rearrangement reactions and dehydrochlorination reactions. The physical properties of the compounds are also summarised, and the final portion of the review focuses on the diverse reaction pathways which are observed with sulfines and α-oxo sulfines, including the most widely reported Diels-Alder cycloadditions. Other reaction pathways covered include, 1,3 dipolar cycloadditions, in which the sulfine can act as the dipole or dipolarophile, oxygen extrusion, sulfur extrusion, and dimerization.

The results of this research programme are discussed in the second chapter. While the synthesis of α-diazosulfoxides has been explored for many years in the research team, the synthetic potential has been limited by very poor yields, typically less than 30%. A major advance in this work demonstrated that through use of continuous flow processing, the exposure of the α-diazosulfoxide products to the basic reaction conditions could be controlled and reduced, resulting in significant yield enhancement, up to three fold, in both the ketone and lactone derived series. Building on the insight developed through optimisation in continuous flow, a modified set of batch conditions was developed which resulted in enhanced yields through reduction in product deterioration by ameliorating exposure to base. Use of continuous flow leads to isolation of the desired compounds in enhanced yields relative to standard batch conditions, with short reaction times, increased safety profile and potential to scale up.

Generation of the α-oxo sulfines from α-diazosulfoxides has been explored in continuous flow using transition metal catalysis, thermolysis and photolysis; this process is more amenable to scale up in continuous flow than in traditional batch conditions. The thermolytic conditions are the most advantageous synthetically, leading to the cycloadducts in a metal free process. Diels-Alder trapping of the α-oxo sulfines has been demonstrated under continuous flow, in general leading to similar diastereoselectivities to those seen in batch but with higher yields, improved safety and potential for scale up. Critical to the success of the α-oxo sulfine cycloaddition was use of a sufficiently concentrated diene trap; in the absence of this, alternative α-oxo sulfine reaction pathways competed with the Diels-Alder cycloaddition. Reactivity differences between the lactone and ketone series of α-diazosulfoxides was explored.

One of the highlights of this work was the demonstration of proof of concept in telescoping the diazo transfer to generate the α-diazosulfoxide, with the thermal rearrangement to the α-oxo sulfine, and

Diels-Alder cycloaddition to provide direct access to a stable thiopyran-*S*-oxide, with clear potential benefits from a safety and scale up perspective.

Investigation of 1,3-dipolar cycloadditions of α-oxo sulfines with nitrile oxides and nitrones, proved very interesting from both a synthetic and mechanistic perspective. Focusing initially on the nitrile oxides the 1,3-dipolar cycloadditions with lactone and ketone derived α-oxo sulfines exhibited opposite regiochemical outcomes leading to isolation of 1,2,5-oxathiazole-*S*-oxides, only two of which have previously been reported, and 1,4,2-oxathiazole-*S*-oxides. An interesting and unanticipated epimerisation was seen in the 1,2,5-oxathiazole-*S*-oxides. Cycloaddition of the α-oxo sulfines with nitrones leads to both approaches to form regioisomeric cycloadducts, but in this case both of the novel heterocycles undergo subsequent spontaneous reaction to aziridines and other products. Detailed analysis of the spectroscopic features of the novel heterocycles is a key element of this investigation.

Representative examples of compounds from across the research programme including 1,2,5-oxathiazole-*S*-oxides and 1,4,2-oxathiazole-*S*-oxides were sent to U.S. National Cancer Institute (NCI) for anticancer screening.

The third chapter details the full experimental procedures which were used throughout the project and includes all the spectroscopic characterisation and analytical data which were obtained for the novel compounds synthesised.

For Mam and Dad

"You have brains in your head.

You have feet in your shoes.

You can steer yourself any direction you choose."

Dr. Seuss

Chapter 1

Introduction

Contents

1.1 Introduction 3
1.1.1 Sulfine characteristics. 3
1.1.2 Sulfines in nature 4
1.2 Preparation of sulfines 6
1.2.1 Oxidation to sulfines 7
1.2.2 Dehydrochlorination and elimination reactions of sulfinyl halides 11
1.2.3 Sulfenylation of activated methylene compounds 14
1.2.4 Alkylidenation of sulfur dioxide 16
1.2.5 Rearrangement and elimination reactions from sulfoxides 17
1.2.6 *In situ* by hetero retro-Diels-Alder 21
1.3 Structural characteristics of sulfines 23
1.4 Reactions of sulfines 24
1.4.1 [4+2] Diels-Alder cycloadditions 24
1.4.2 [1+2] Cycloadditions 29
1.4.3 [3+3] Cycloadditions 29
1.4.4 1,3-Dipolar cycloadditions 30
1.4.5 Nucleophilic addition to sulfines 34
1.4.6 Thiophilic nucleophilic attack 34
1.4.7 Carbophilic nucleophilic attack 38
1.5 Miscellaneous 41
1.5.1 Rearrangements of sulfines 41
1.5.2 Thioepoxidation using sulfines as sulfur-atom transfer reagents 45
1.6 Additional relevant updates: 46
1.6.1 Oxidation to sulfines 46
1.6.2 Structural characteristics of sulfines 47
1.6.3 [4+2] Diels-Alder cycloadditions 47
1.6.4 Miscellaneous 48
1.7 Conclusion 48
Bibliography 49

1.1 Introduction

Note: this introduction is reproduced from:

"*Generation, Reactivity and Uses of Sulfines in Organic Synthesis*"

Patrick G. McCaw, Naomi M. Buckley, Stuart G. Collins and Anita R. Maguire, European Journal of Organic Chemistry, **2016**, 9, 1630 – 1650.

Naomi M. Buckley and I were the primary authors of this review. Dr. Stuart Collins and Prof. Anita Maguire provided assistance in terms of proof-reading and help with the overall construction of the manuscript.

Updates to this review article appear at the end in Section 1.6.

The name 'sulfine' was first proposed by Sheppard and Dieckmann in 1964 to indicate the structural relationship with thiocarbonyl *S*-dioxides, known as sulfenes.[1] Sulfines are the *thio* analogues of carbonyl oxides (the intermediates in the ozonolysis of alkenes) with the general structure XYC=SO. These thione *S*-oxides are short-lived and highly reactive. Many routes to these reactive intermediates are known and examples of their reactivity include Diels-Alder cycloadditions, dipolar cycloadditions, nucleophilic attack, self-reactions and rearrangements. Sulfines have also been shown to act as sulfur transfer reagents and metal complexation ligands.[2,3] This review aims to highlight the broad range of routes to sulfines and their uses in organic synthesis. The chemistry of sulfines has recently been summarised by Zwanenburg.[4-7] Recently developed routes are more robust and more widely applicable than earlier routes and so make the chemistry of sulfines more attractive from a synthetic perspective. Other sulfur functional groups such as sulfones and sulfoxides are widely studied in organic synthesis and have found uses as building blocks and as chiral auxiliaries. Sulfines, being sulfur functional groups also have the potential to be used in this manner.

1.1.1 Sulfine characteristics.

Sulfines are sulfur-centred heterocumulenes with the C=S=O moiety. They can be described as being derived from sulfur dioxide but with an oxygen atom replaced by carbon, or by nitrogen for *N*-sulfinylamines. The sulfine moiety is non-linear, which is in agreement with what is to be expected for a triatomic molecule with 18 valence electrons. Although the name sulfine corresponds to the non-classical structure (i) (Figure 1) below, sulfines are alternatively viewed in terms of charge-separated resonance structures (ii) and (iii), where (ii) can be interpreted as the

oxide of a thiocarbonyl compound. Although many authors prefer the structure (i), most theoreticians do not regard the participation of sulfur d-orbitals as high, therefore the resonance structures (ii) and (iii) might actually be considered more accurate representations.[8] This resonance hybrid constitutes a 1,3-dipole.

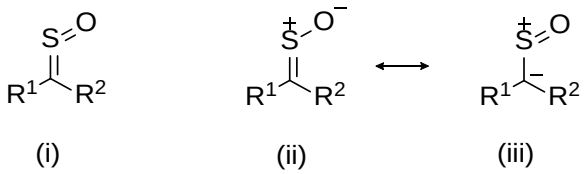


Figure 1: Three representations of sulfines.

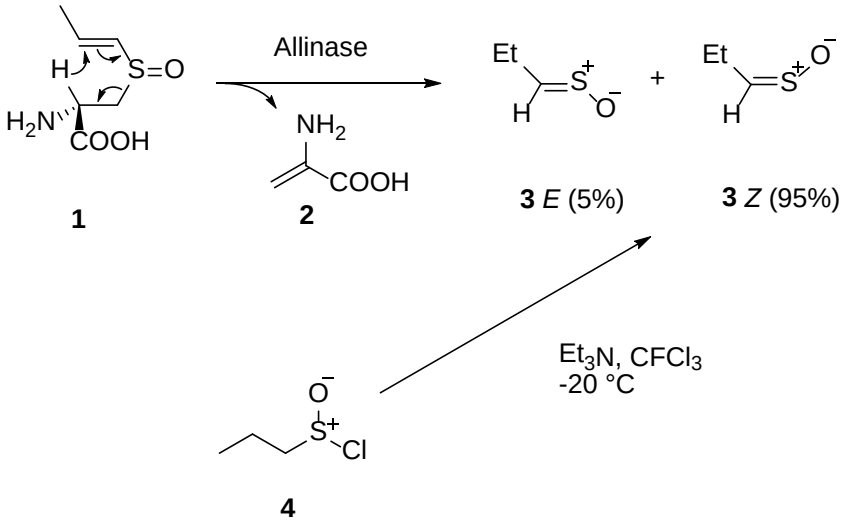
In recent years, measurements of sulfines have proven the structure to be non-linear and have shown the predominant form to be structure (**ii**) in Figure 1. The studies have established this with evidence from, the dipole moment, microwave spectroscopy, proton NMR and X-ray structure determinations.[9-12] A consequence of the non-linear structure of sulfines is that they exist as geometrical isomers, provided that the substituents at the sulfine carbon are different. Herein is where the potential to use sulfines in asymmetric synthesis can be found. The ability of sulfines to exist as *E*- and *Z*- isomers allows for the formation of isomerically distinct products on treatment with nucleophiles and 1,3-dienes. [13,14]

1.1.2 Sulfines in nature

The interesting pathways for sulfine formation and their scope for reactivity can be illustrated by examining the few known naturally occurring sulfines. In 1961, advances in the understanding of organosulfur compounds of the onion (*allium cepa*) allowed Virtanen *et al.* to demonstrate that *trans*-(+)-*S*-1-propenyl-L-cysteine *S*-oxide **1** is the precursor of the principal lachrymatory factor of onions (Scheme 1).[15] Virtanen also showed that onion allinase was the enzyme responsible for the conversion.[16] At the same time, Wilkens independently isolated and described the structure of the lachrymatory factor of onions as the sulfine (*Z*)-propanethial *S*-oxide **3** (Scheme 1).[17] These compounds, through dimerisation and self-condensation reactions have been found to lead to the unusual and interesting heterocycles shown below (Scheme 2).

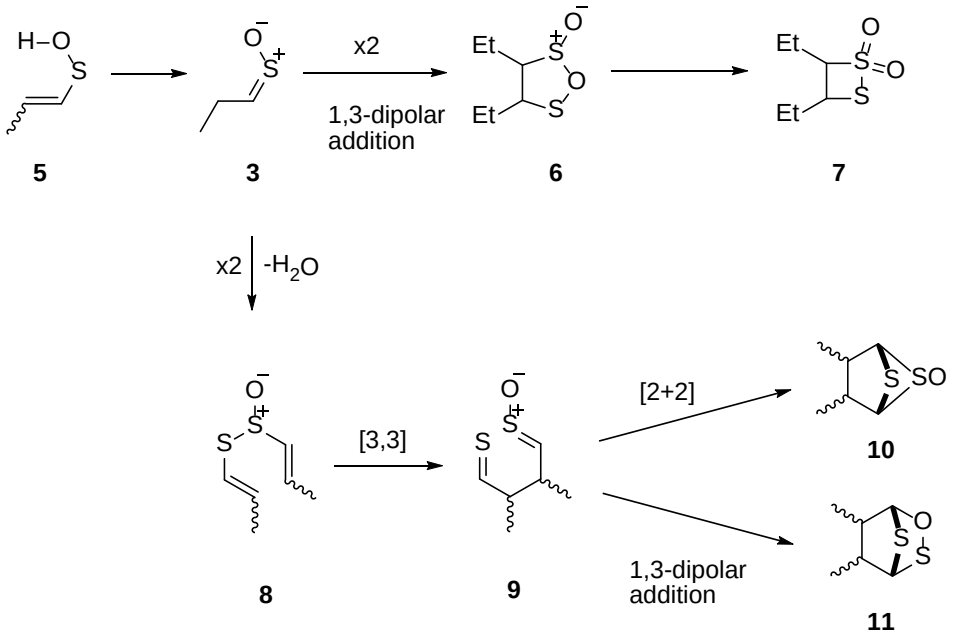
The discovery of the first naturally occurring sulfine **3** certainly stimulated the early development of sulfine chemistry throughout the 1960s and 1970s. The biological mechanism for its formation, was provided by Brodnitz and Pascale in 1971. The authors also spectroscopically confirmed Wilkins' assignment by synthesising propanethial *S*-oxide **3** from dehydrochlorinating propanesulfinyl chloride **4** (Scheme 1).[18] Finally, the *Z*-stereochemistry was confirmed by Block *at*

al.[19] Recent advances in DART-MS has also allowed the detection of naturally occurring butanethial *S*-oxide from a related plant, *allium siculum*. [20]



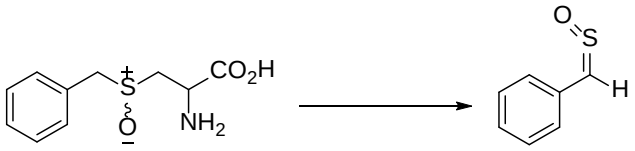
Scheme 1

The reactivity of the labile and naturally occurring compounds 1-propenesulfenic acid **5** and (*Z*)-propanethial *S*-oxide **3** attracted the attention of Block *et al.* and led to the isolation of a number of unusual and interesting heterocyclic compounds by the routes shown in Scheme 2. Notably, the proposed intermediate **9** is formed *via* a [3,3]-sigmatropic rearrangement. [21]



Scheme 2

More recently in 2003, Kubec *et al.* isolated the lachrymatory factor *Z*-thiobenzaldehyde *S*-oxide **13** from the root of *Petiveria alliacea*, a perennial shrub found widely in South and Central America.[22] The *E*-isomer was not found and the mechanism for its formation remains unclear, although the authors suggest *S*-benzylcysteine sulfoxide (petiveriin) **12** as its precursor. Interestingly, the authors also reported moderate antimicrobial activity of the sulfine, which was tested against a panel of gram positive and gram negative bacteria (Scheme 3).[22]



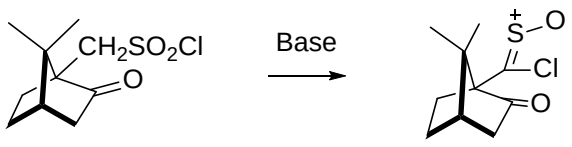
12 **13**

Scheme 3

The lability of these compounds presumably explains the relatively few examples of naturally occurring sulfines which have been isolated to date. These reports of sulfines isolated from nature are partly responsible for the increased interest in both the synthesis and reactivity of sulfines.

1.2 Preparation of sulfines

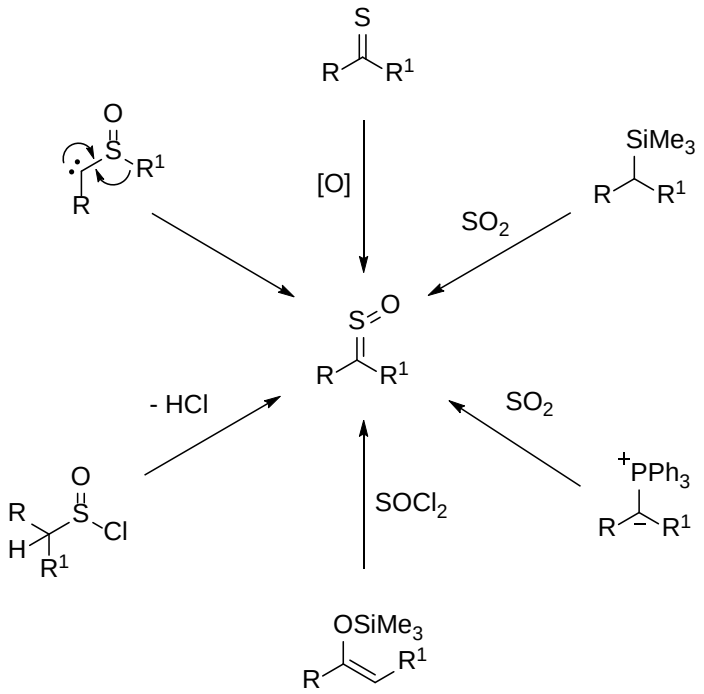
In 1923, the first synthetic route to a sulfine was published by Wedekind.[23] It was synthesised *via* the reaction of an alkyl sulfonyl chloride **14** with a tertiary amine base. Camphor-10-sulfonyl chloride **14**, in the presence of pyridine or triethylamine produced the product **15** which was tentatively assigned as a sulfine (Scheme 4). The sulfine product was confirmed years later in 1963 by King and Durst, who also confirmed the existence of sulfines as stable geometrical isomers.[9] The assignment of the *E* and *Z* geometry was made by proton NMR spectroscopy, melting points and dipole moment differences. Although the mechanism for the sulfine formation has since been elucidated[9,24] and yields have been increased by addition of *p*-toluenesulfonyl chloride,[25] this method used to generate the first sulfine is not very widely used nowadays (Scheme 4).



14 **15**

Scheme 4

Instead, multiple other methods have since been established and each of these will be discussed further (Scheme 5).

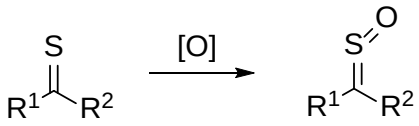


Scheme 5

1.2.1 Oxidation to sulfines

The conversion of ketones and aldehydes to thiocarbonyl compounds is a simple, one pot, one step reaction often carried out under microwave irradiation and resulting in high yields (Scheme 6).[26-28] Due to this ease of access to thiocarbonyl compounds, oxidation of these is a widely used route to sulfines.

The oxidation of thiocarbonyl compounds to sulfines has been reported using *m*-CPBA,[6] and monoperphthalic acid.[29] As well as singlet oxygen,[30] ozone has been used for sterically hindered thiocarbonyl compounds, and boron trisulfide (Stelios's reagent)[31] in limited cases.



Scheme 6

The first reported synthesis of a sulfine by oxidation of a thiocarbonyl compound was by Walter in 1960.[32] Walter showed that oxidation of thioamides with hydrogen peroxide produced thioamide-*S*-oxides, but these were previously believed to have been iminosulfenic acids. The

sulfines were isolable on the condition that there was an amide proton available for intramolecular stabilisation of the sulfine through hydrogen bonding. Initial investigations following these reported methods for the synthesis of sulfines proved unsuccessful. However, that changed when Zwanenburg reported that careful treatment of fused aromatic thioketones with monoperphthalic acid gave the corresponding sulfines in excellent yields.[29,33] Zwanenburg found that fused, aromatic thioketones gave the best results for the synthesis of sulfines. Zwanenburg treated thioketones with dimethyldioxirane to produce the corresponding *S*-oxides **16**-**21** in high yield (Figure 2).

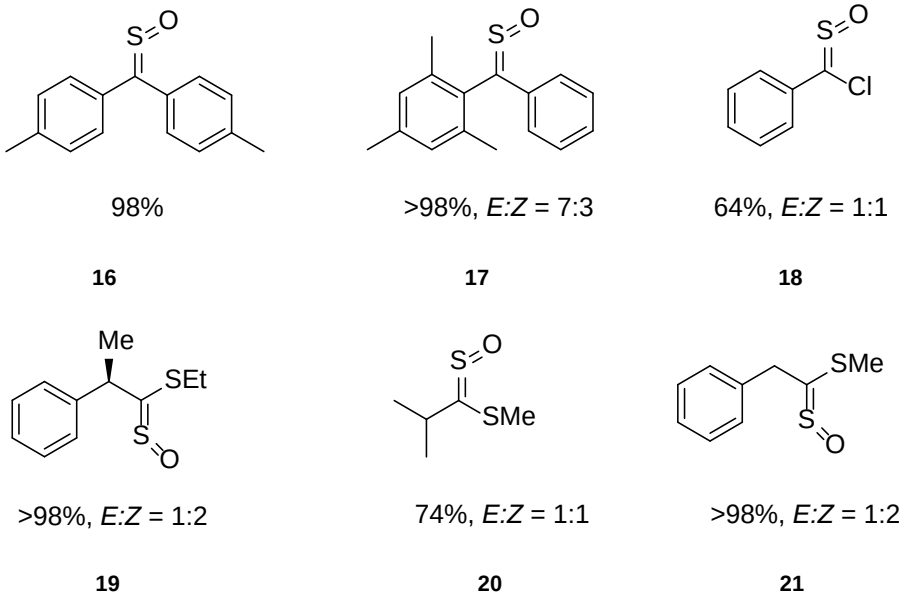
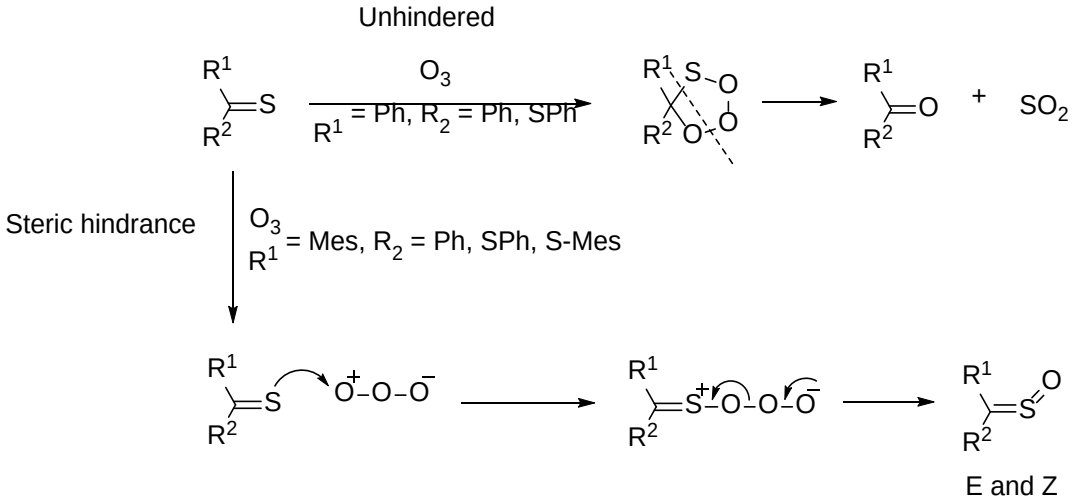


Figure 2: Zwanenburg's sulfines by oxidation.

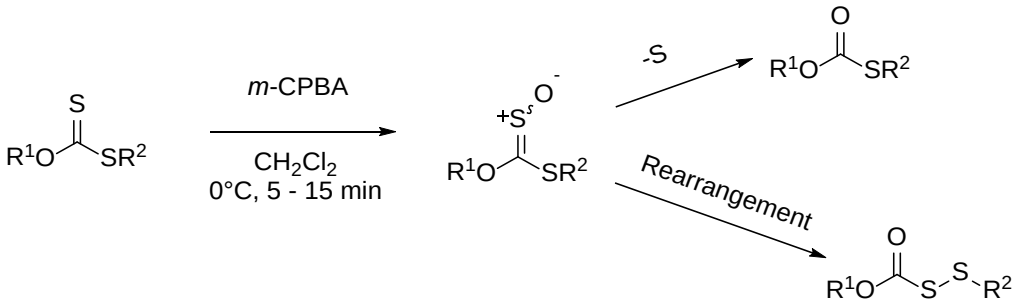
Significantly, this proved a departure from the previously held assumption that only sulfines derived from non-enethiolisable thiocarbonyls **16**-**18** and not sulfines derived from enethiolisable thiocarbonyl compounds **19**-**21** would yield sulfines on oxidation.

Zwanenburg has also reported the use of ozone as an oxidising agent for this transformation. While it has been found that sterically hindered thiocarbonyl compounds successfully produce sulfines upon treatment with ozone, unhindered thiocarbonyls give the corresponding carbonyl compounds (Scheme 7).[34] Zwanenburg rationalised these results by theorising that unhindered thiocarbonyls undergo cycloaddition with ozone, with subsequent loss of sulfur dioxide, to yield carbonyl compounds. However, the same cycloaddition would be much more difficult with a sterically hindered thiocarbonyl compound, instead resulting in nucleophilic attack of the thiocarbonyl sulfur on ozone, with elimination of molecular oxygen giving the sulfine (Scheme 7).



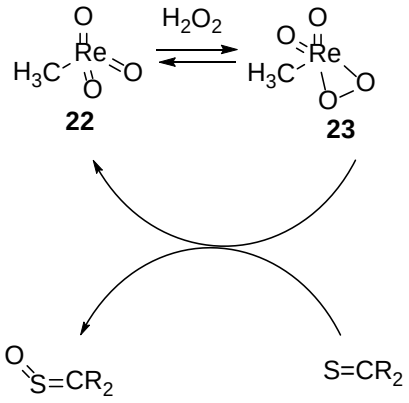
Scheme 7

The oxidation of xanthates has been described by Metzner and co-workers.[35] *m*-CPBA is used in the oxidation of the thiocarbonyl compounds to generate the exceptionally unstable sulfines, which in turn undergo a transformation. Unless the sulfine is sterically hindered it undergoes a transformation at room temperature either through the loss of elemental sulfur, or by intramolecular rearrangement. The first crystal structure of a kinetically stable sulfine was obtained using a sterically hindered xanthate oxide.



Scheme 8

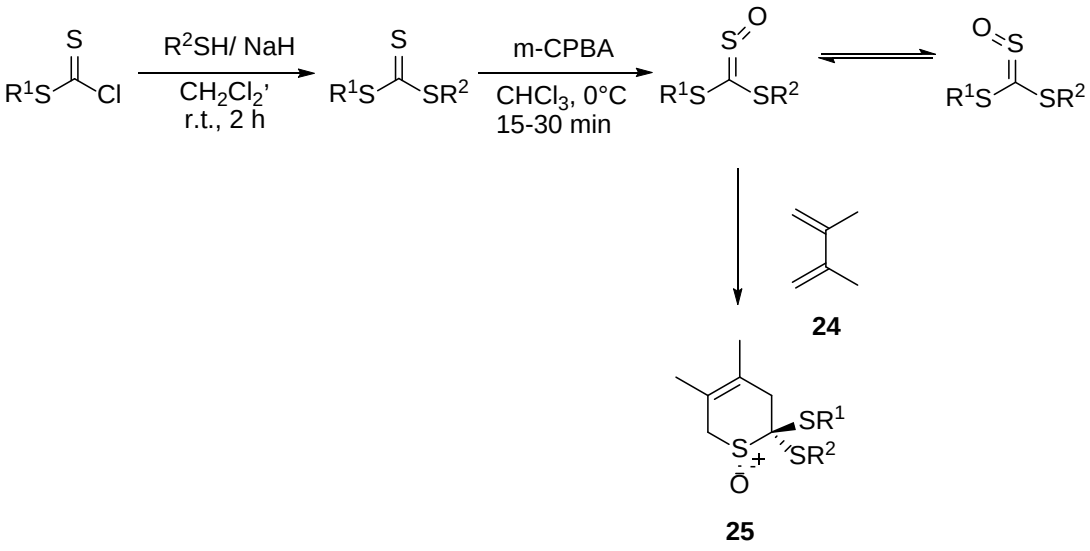
Espenson has described an interesting metal catalysed thiocarbonyl oxidation to sulfines[36] using hydrogen peroxide and catalytic methyltrioxorhenium, CH_3ReO_3 (MTO) **22**, to oxidise thiobenzophenones to their sulfines. The author describes this method as superior to the other methods because it is higher yielding and complete within five minutes, even on scale up. Conversions are high with peracids however, the yields are often lower, and with ozonation, a temperature of -70°C and a nitrogen blanket are needed.[34,37] The chemistry of this highly effective method is summarised in Scheme 9. The sulfine is formed by nucleophilic attack of the sulfur atom on the electron deficient oxygen atom of the peroxorhenium complex that is the active intermediates in the reaction.



Scheme 9

Rees *et al.* also found that on treatment of 1,2,3-dithiazoles with tetracyanoethylene oxide, the more nucleophilic thione sulfur was oxidised to the sulfine.[38] The sulfines formed were unstable and quickly revert to the thione on heating. Interestingly, only one configuration of sulfine was detected, the *Z* sulfine and it is suggested the reason for this is the electronic and steric repulsions that would arise in the *E* sulfine are unfavourable.

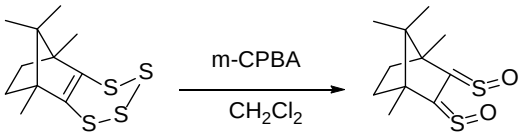
El Gokha *et al.* have shown that when trithiocarbonates are oxidised to the corresponding sulfine with *m*-CPBA, only one stable isomer is formed, the *Z* isomer (Scheme 10).[39] On cycloaddition with diene **24**, in chloroform, at 60 °C, and following analysis of the crystal structure by X-ray crystallography, it was confirmed the only product is the diastereomer **25** from the *E*-sulfine. This suggests thermal isomerisation of the sulfines during cycloaddition or else initial formation of the *cis* cycloadduct followed by diastereomerisation into the more stable *trans* cycloadduct *via* a retro-Diels-Alder reaction.[39]



Scheme 10

This research, along with others, has helped to establish that the isomeric ratio of *E*/*Z* is dependent on the unsymmetrical structure of the thiocarbonyl compound and the stability of the kinetic and thermodynamic isomers.

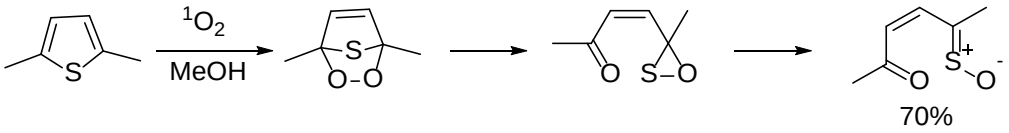
An unusual class of sulfines, α-disulfines were recently prepared by treating thiocamphor derived tetrathiin, with *m*-CPBA (Scheme 11). Spectroscopic analysis indicated the existence of the α-disulfine in the *E,Z*-form.[40] These unusual α-disulfines **27** were also prepared by Schutz *et al.* who generated them through oxidation of 1,2-dithietes **26** and confirmed the structure using X-ray crystallography.[41]



26 **27**

Scheme 11

A unique method for the synthesis of a sulfine exists using singlet oxygen as the reagent. The proposed mechanism for the photo-oxidation of the thiophene system **28** is the formation of a thiazonide intermediate **29**, which rearranges to an oxathiirane **30** which undergoes further rearrangement to form the sulfine **31** (Scheme 12). [42]



28 **29** **30** **31**

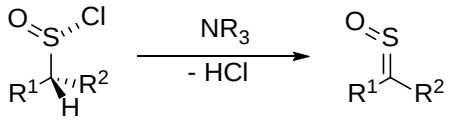
Scheme 12

The methods for the preparation of sulfines are diverse, each having its own advantages. These routes to sulfines has proven the most widely applicable and widely used in organic synthesis, having many oxidising reagents available, and having been applied to many types of compounds including α,β-unsaturated thiones,[6,29,33] trithiocarbonates,[6] dithiocarboxylic esters[43] and thioketones.[3]

1.2.2 Dehydrochlorination and elimination reactions of sulfinyl halides

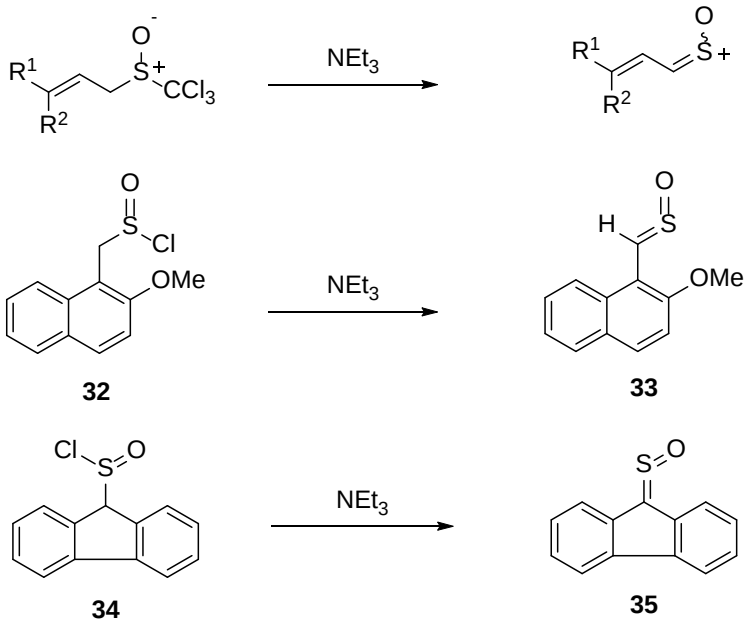
Some thiocarbonyl compounds are inherently unstable, and because of this, other routes to the target sulfine are required. Dehydrohalogenation is often used to access reactive intermediates such as 1,3-dipoles and in the same way, sulfines can be generated through base-induced

dehydrohalogenation of 1,2-sulfinyl halides. One of the first methods developed in the preparation of sulfines involved the elimination of hydrogen chloride from sulfinyl chlorides bearing an α-hydrogen atom (Scheme 13).[25] This method of accessing sulfines is usually only used for aliphatic substituted sulfines and rarely for aromatic substituted sulfines as the parent sulfinyl halide is difficult to access.



Scheme 13

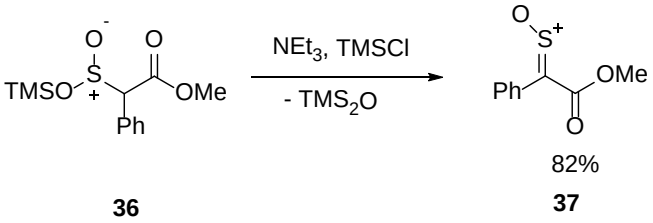
Notably, the first thioaldehyde *S*-oxide and the first thioketone *S*-oxide were prepared by this method. Zwanenburg and co-workers prepared the first thioaldehyde *S*-oxide in 1964,[25] the same year in which Dieckmann and Sheppard prepared fluorenethione *S*-oxide, employing the same dehydrohalogenation method.[1] The first stable α,β-unsaturated thioaldehyde *S*-oxide was isolated by Gottlieb *et al.* using this method,[44] albeit, with the elimination of chloroform instead of HCl, from a trichloromethyl sulfoxide. Notably, this reaction resulted in the formation of both the *E* and *Z*-isomers of the sulfine and isomerisation of the sulfines was observed in the presence of triethylamine. The authors proposed that the *E*-sulfine was the kinetic product and that the *Z*-sulfine was the thermodynamic product and that the conversion of *E* to *Z* could be explained by an addition-elimination reaction of triethylamine.



32 **33** **34** **35**

Scheme 14

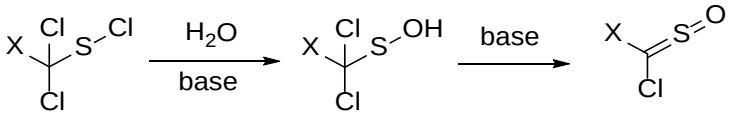
Scheme 14 illustrates that by elimination of good leaving groups such as HCl from **32** and **34**, sulfines **33** and **35** can be generated. This is also true for the elimination of trimethylsilanol from a sulfoxide **36** to form sulfine **37** (Scheme 15).[7] Although not widely applicable it is a mild method for the synthesis of sulfines which, when in the presence of an acid scavenger, can yield sulfines up to 82%.



36 **37**

Scheme 15

The same can be said for the elimination of a methanol anion from diarylmethanesulfinates.[45] On treatment with amines or a methoxide anion at room temperature, deprotonation occurs alpha to the sulfoxide with the elimination of the methoxide leaving group. Surprisingly, the elimination is faster than the substitution reaction. Other similar routes to sulfines include the elimination of phthalimide from *N*-phthaloylsulfinamide.[46] Also reported for the generation of sulfines *via* dehydrohalogenation, is the 1,3-dehydrochlorination of 1,3-chlorosulfenic acids (Scheme 16). The proposed route to the sulfines is hydrolysis of a sulfenyl chloride **38** to an intermediate sulfenic acid **39** which undergoes dehydrohalogenation in slightly basic conditions to form the sulfine product **40**.[47,48]



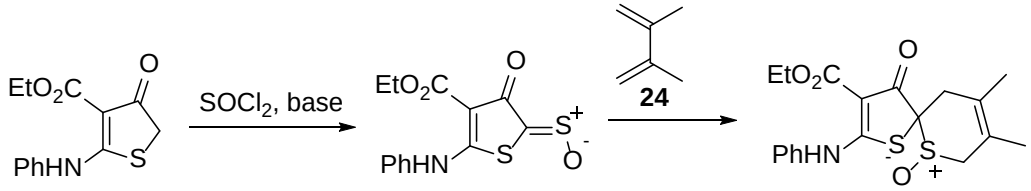
38 **39** **40**

Scheme 16

Overall, this dehydrohalogenation method has become an important and widely used route to sulfines, aided by the publication of efficient routes to the required sulfinyl chlorides.[5,7] This method has been used in the synthesis of natural products, specifically to access ethylsulfine, the lachrymatory factor in onions.[18,49]

1.2.3 Sulfenylation of activated methylene compounds

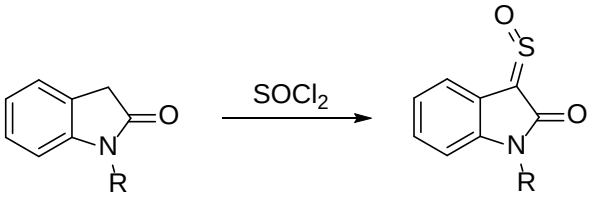
On combination of activated methylene compounds and thionyl chloride under basic conditions, an intermediate alkyl sulfinyl halide is formed and quickly undergoes dehydrohalogenation to the α-oxo sulfine. The first example of this was reported in 1981 and by trapping the sulfine **42** with diene **24** and confirming the product **43** with a crystal structure, the generation of an intermediate sulfine **42** was determined unambiguously (Scheme 17). [50]



41 **42** **43**

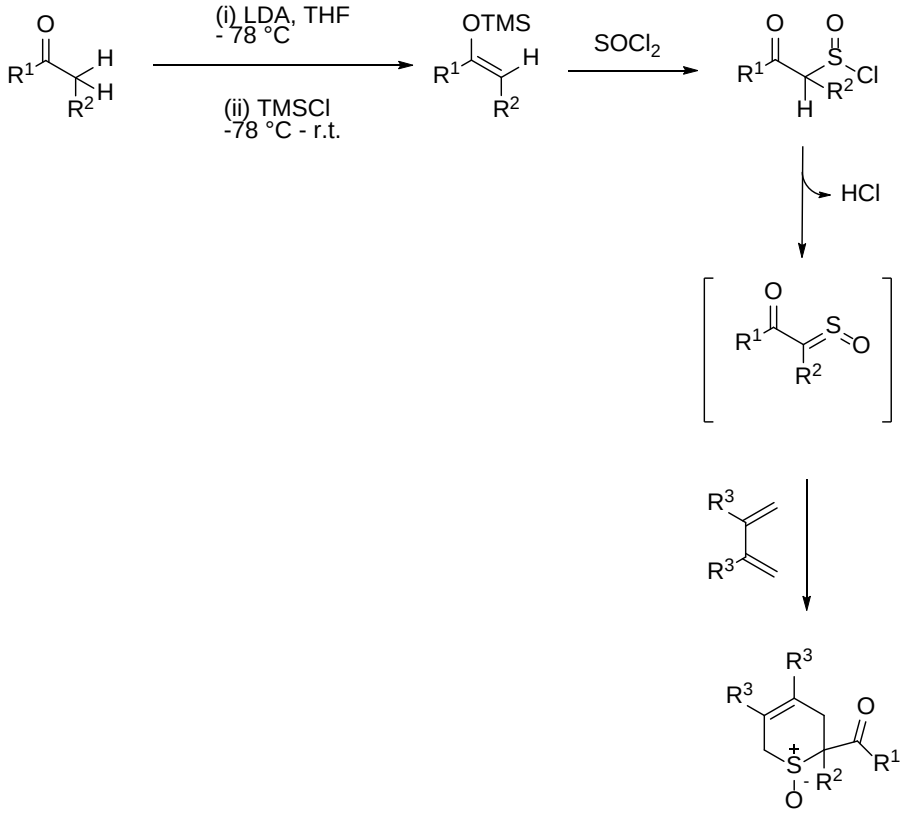
Scheme 17

This sulfenylation method towards sulfines, and trapping them to generate synthetically interesting compounds has been exploited extensively in the literature. Examples of tertiary amine bases used in this methodology include triethylamine, pyridine, and 2,6-lutidine. Interestingly, these bases can also be used in catalytic amounts.[51,52] In contrast to this, oxindoles were recently found to react readily with thionyl chloride to give the respective sulfines and in excellent yield (Scheme 18). Unusually, activation of the methylene group was not required, due to the aromaticity of the system. [53]



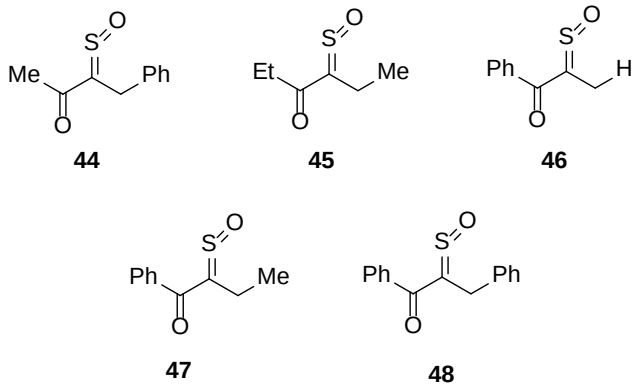
Scheme 18

The fact that some reactions require only catalytic amounts of base can be explained under the premise that the enol tautomer of the ketone is partly responsible for the sulfenylation reaction. This has been proven by utilising the enol tautomer as the silyl enol ether. This efficient route towards α-oxosulfines was developed by Zwanenburg using readily available methylene ketones. A variety of silyl enol ethers have been treated with thionyl chloride to give α-oxosulfines and their cycloadducts in good yields (Scheme 19).[54,55]



Scheme 19

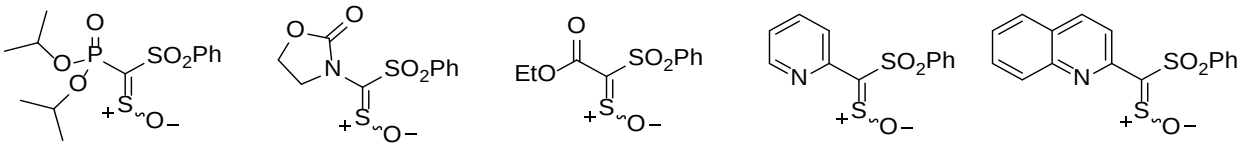
The range of labile α-oxosulfines **44**-**48** which were prepared by Zwanenburg using this method are illustrated in Figure 3.[44,45]



44 **45** **46** **47** **48**

Figure 3: α-oxo sulfines generated by Zwanenburg.

Other examples of sulfines generated in this way include substituted methyl sulfones with the substituents varying from phosphonyl **49**, carboxyoxazolidinone **50**, carboxylate **51**, 2-pyridyl **52**, or 2-quinolyl **53** groups (Figure 4). These sulfonyl sulfines are trapped with dienes and the resulting cycloadducts have been isolated in yields up to 88% and d.r. up to 100%. [56]

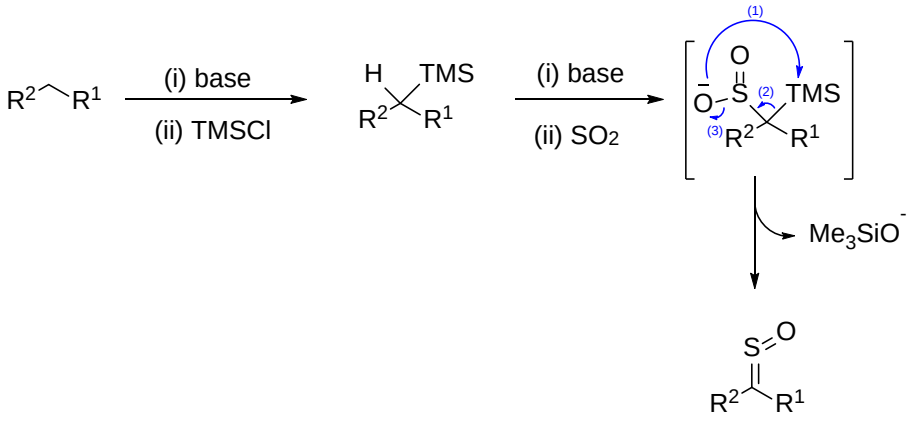


49 **50** **51** **52** **53**

Figure 4: Range of sulfonyl sulfines generated.

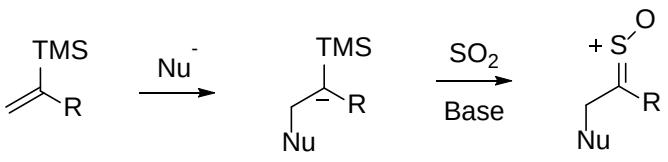
1.2.4 Alkylidenation of sulfur dioxide

Sulfines can be considered as the alkylidene derivatives of sulfur dioxide. It was first reported by Peterson that alkylidenation of α-silyl carbanions with sulfur dioxide is an attractive route towards sulfines.[57] This route proceeds by initial reaction of an α-silyl carbanion with sulfur dioxide, resulting in the formation of an α-silyl sulfinate, which undergoes the loss of trimethylsilanoate to form the sulfine. This sequence can thus be referred to as a modified Peterson olefination reaction and is widely used for the synthesis of sulfines (Scheme 20).



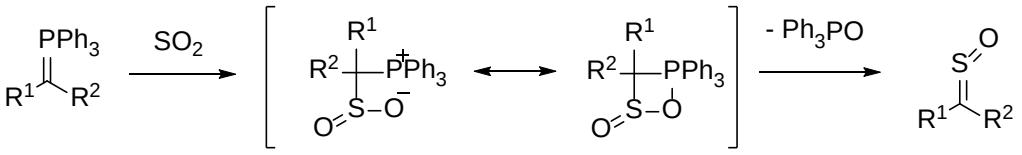
Scheme 20

The attractiveness of this route is the α-silyl carbanions are easily accessible and it is a one-pot procedure which produces sulfines in moderate to high yields. Also due to differing routes to α-silyl carbanions, preparation of more derivatives of sulfines have been possible which would not have been available by other methods. An example of this was reported by Van der Leij, where β-addition of nucleophiles on vinyl silanes leads to sulfines with a hydrogen atom alpha to the sulfur, which would not be accessible by other routes (Scheme 21).[58]



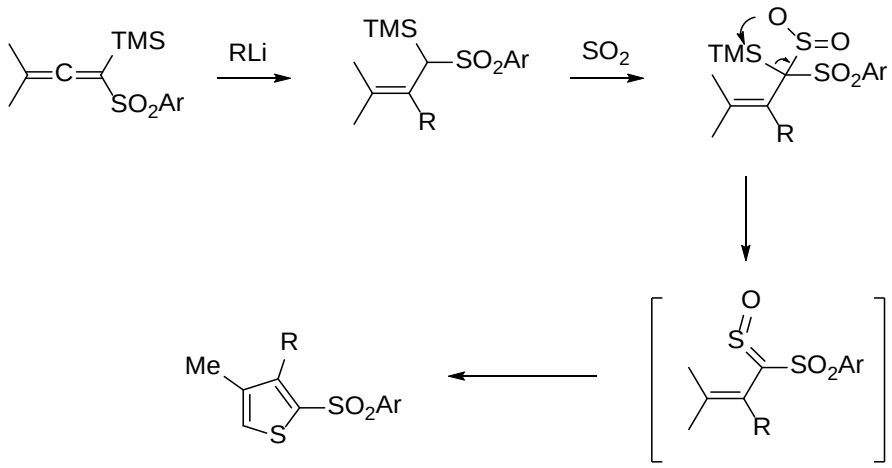
Scheme 21

Reactions of phosphonium ylides with sulfur dioxide were first investigated by Staudinger in 1922, but the isolated products were not sulfines. They were established to be a diaryl ketone and sulfur; in retrospect this can be explained by decomposition of the unstable sulfine intermediate.[59] Further work by Zwanenburg established that stable phosphonium ylides react with excess sulfur dioxide, in polar solvents, undergoing an elimination reaction to form sulfines, which when sterically hindered can be isolated. The initial combination of the ylide with the sulfur dioxide results in the formation of a sulfobetaine which collapses to form triphenylphosphine oxide and the desired sulfine.[60] Using this method, by treating (diarylmethylene)triphenylphosphoranes with sulfur dioxide, diarylsulfines have been prepared in moderate to good yields (Scheme 22).



Scheme 22

A modified Peterson olefination reaction, involving the alkylidenation of sulfur dioxide with an α-trimethylsilylated allenic sulfone, was developed by Zwanenburg and co-workers to prepare α,β-unsaturated sulfines. The sulfine species were formed as intermediates and then rapidly cycloaromatised to form thiophene. This cycloaromatisation took place at a rate even faster than Diels-Alder cycloaddition; when the reaction was carried out in the presence of 2,3-dimethyl-1,3-butadiene, there was no effect on the formation of thiophene (Scheme 23).[61]

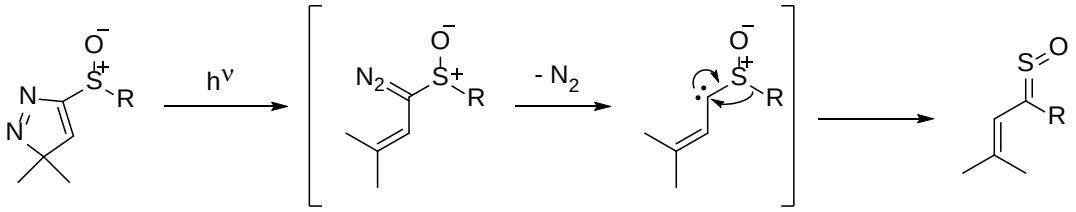


Scheme 23

1.2.5 Rearrangement and elimination reactions from sulfoxides

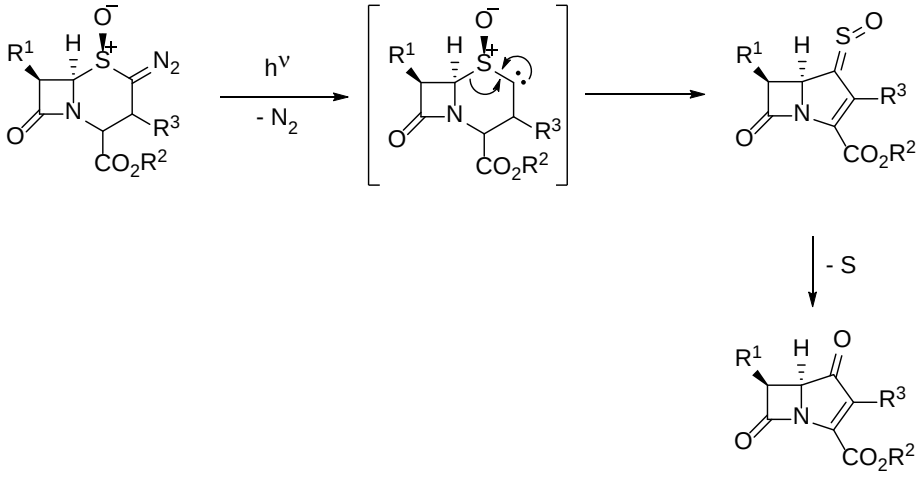
Sulfides are easily oxidised to sulfoxides by many different methods and due to this variation of routes, a route to sulfines using sulfoxides as precursors would be widely applicable in organic

synthesis. There are various reported methods for this type of transformation. The first example was in 1970, photolysis of sulfinylpyrazoles generated the sulfinylvinyl carbene intermediates, which formed the sulfines. The sulfines, however, were reported as quite unstable compounds and readily decomposed by desulfurisation to ketones (Scheme 24).[62]



Scheme 24

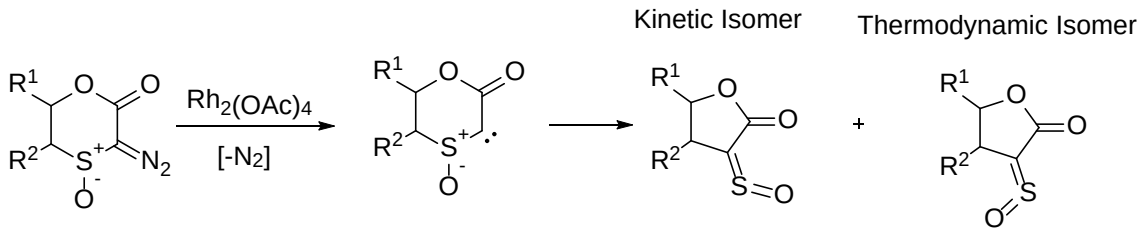
Rosati *et al.* also reported a rearrangement of sulfoxides as a route to sulfines in 1980.[63,64] Under photochemical conditions α-diazosulfoxides undergo dediazotisation to form the carbene, which undergoes a hetero-Wolff rearrangement to give the sulfine. Again, the unstable sulfine undergoes desulfurisation resulting in formation of the ketone. Rosati showcased this reaction with the conversion of a cephalosporinate to a carbapenem product (Scheme 25).[65]



Scheme 25

Recently, Maguire *et al.* have demonstrated rhodium carboxylate- or carboxamide-catalysed decomposition of cyclic α-diazosulfoxide precursors results in formation of both *E*- and *Z*-α-oxosulfines by this method of ring contraction. [66-68] The authors have also demonstrated that the *Z*-sulfine is the kinetically formed isomer, and the *E*-sulfine is the thermodynamically formed isomer. These α-oxosulfines have been detected in argon matrices and in some instances can be

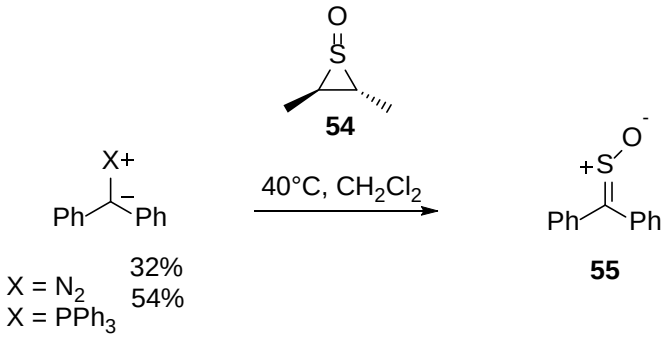
isolated and characterised directly from transition metal catalysed decompositions (Scheme 26).[66,69]



Scheme 26

This route is a useful tool in the preparation of α-oxosulfines.[70] Efficient hetero-Wolff rearrangements of α-diazosulfoxides to α-oxosulfines has been reported under microwave conditions in the absence of a transition metal catalyst. The outcome of the transformation was very similar to the outcome under thermal conditions, with no evidence of specific microwave effects.[67] Photochemical, metal-free conditions have also been used to generate sulfines from these α-diazosulfoxides.[71]

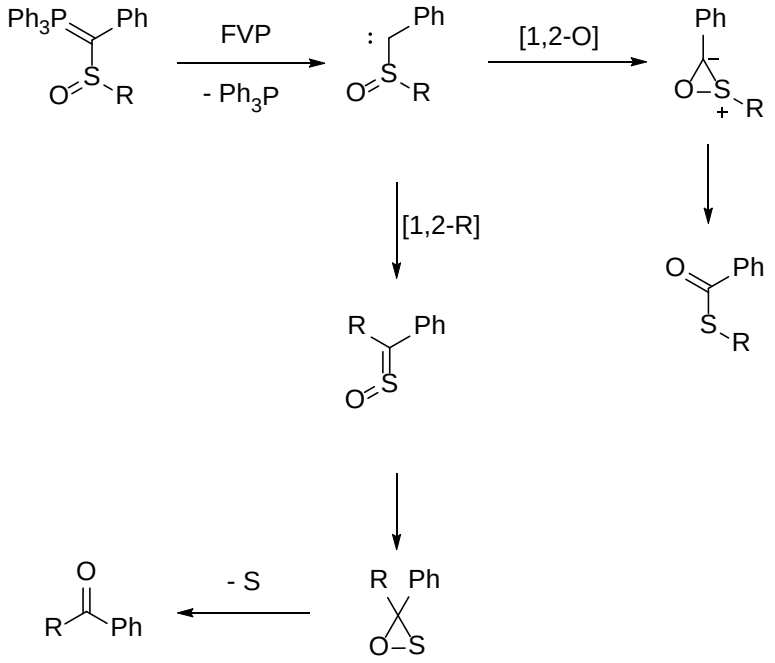
Another route to sulfines through the use of sulfoxides is the reaction of diazoalkanes, phosphonium ylides, sulfonium ylides and pyridinium ylides with sulfur monoxide.[72,73] Sulfur monoxide is generated from *trans*-2, 3-diphenylthiirane **54** oxide in refluxing dichloromethane and reacts *in situ* (Scheme 27).



Scheme 27

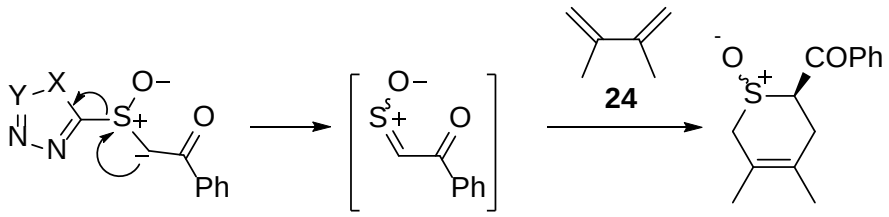
The thermolysis of sulfoxides using flash vacuum pyrolysis has also been shown as a route to sulfines. Although the parent sulfine is unstable, with an estimated lifetime of 30 minutes at room temperature, it can be isolated in an argon matrix at 18 K and studied in this way.[74] The sulfines generated by this method are often either trapped[75] or readily decompose to a thermodynamically more stable product.[76] Aitken and co-workers carried out flash vacuum pyrolysis of α-sulfinyl phosphorus ylides (500 °C, 10^{-2} Torr) and found that triphenylphosphine, as

opposed to triphenylphosphine oxide, was mainly extruded from these compounds.[77] While formation of thioesters was one of the main pathways observed, ketones were also observed. Wolff rearrangement of the sulfinyl carbenes and the subsequent formation of ketones was attributed to extrusion of sulfur from the intermediate oxathiiranes which had been formed by electrocyclisation of the sulfines (Scheme 28).



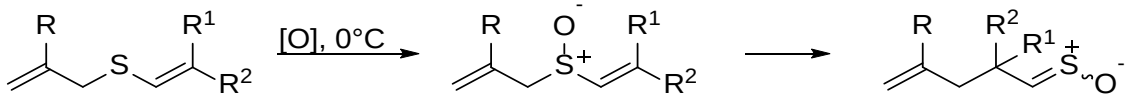
Scheme 28

The thermolysis of sulfoxides to produce sulfines has also been exploited by Morita and co-workers.[78] β-Ketosulfoxides bearing heterocycles such as thiadiazole, triazole and tetrazole were heated in the presence of base and a diene trap in dioxane. On deprotonation of the activated methylene group the nitrogen containing heteroaromatic group is eliminated and the sulfine **56** generated (Scheme 29). The cycloaddition with the diene **24** occurs rapidly and the stereochemistry of the cycloadduct **57** by the hetero Diels-Alder reaction is dependent on the ratio of E/Z of the sulfine. Although these sulfines are not isolated, this is another one step route to sulfines from activated sulfoxides.



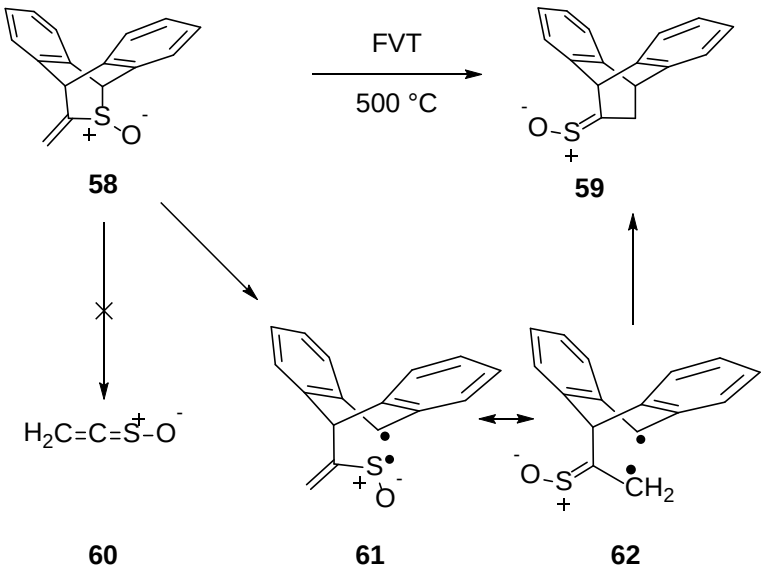
Scheme 29

A unique method, published by Block *et al.* in 1985 generates sulfines through a thio-Claisen rearrangement.[79] On oxidation of a 1-alkenyl-2-alkenyl sulfide to the corresponding sulfoxide the rate of [3,3]-sigmatropic thio-Claisen rearrangement is considerably enhanced, leading to isolable sulfine in excellent yields and, *E*/*Z* ratios of up to 2 : 98 depending on the substitution pattern of the sulfoxides (Scheme 30).



Scheme 30

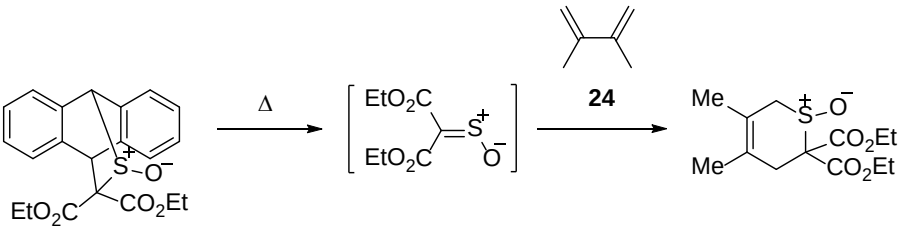
Interestingly, Vallée and co-workers discovered the rearrangement of a vinyl sulfoxide **58** to a sulfine **59** during an attempt to synthesise the thioketene-*S*-oxide **60** by retro-Diels-Alder reaction. The rearrangement did not involve a [3,3]-sigmatropic rearrangement and was proposed to proceed by homolytic cleavage of the dibenzylic C–S bond followed by recyclisation on the reverse side of the diradical **62** (Scheme 31). [80]



Scheme 31

1.2.6 *In situ* by hetero retro-Diels-Alder

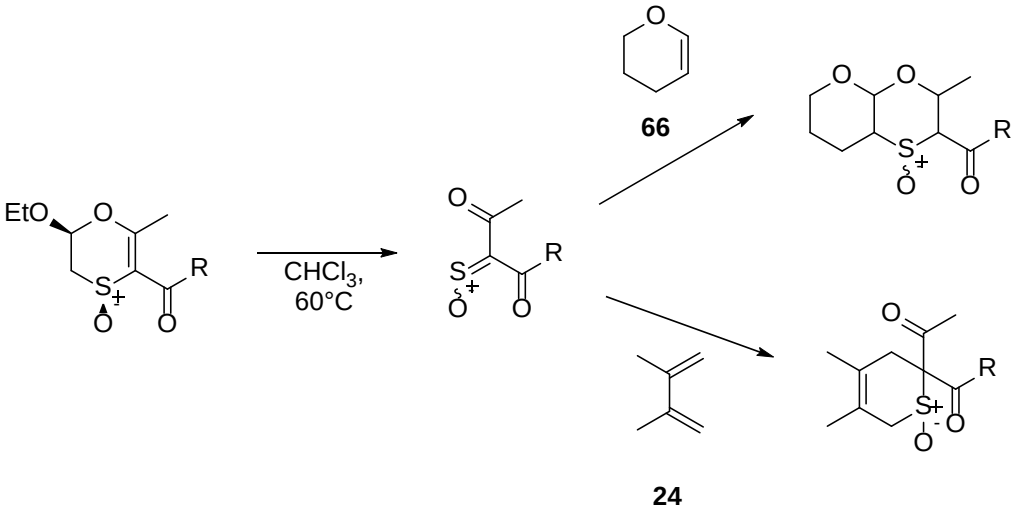
Retro-Diels-Alder reactions of appropriate precursors can afford sulfine products. Kirby and McGregor heated the anthracene cycloadduct **63** in the presence of 2,3-dimethyl-1,3-butadiene **24** (Scheme 32).[81] The isolation of the cycloadduct **65** as a product of the reaction provided evidence that the sulfine **64** had been formed as an intermediate by retro-Diels-Alder reaction of the sulfoxide.



63 **64** **65**

Scheme 32

As can be seen, the stereochemistry of the sulfine is retained in the cycloaddition to the sulfoxide products. Other dienes used to trap sulfines generated in this way include thebaine and cyclopentadiene.[81] These hetero retro-Diels-Alder reactions are also an easy route to α,α-dioxo sulfines which can be isolated through further trapping reactions (Scheme 33).[82,83]

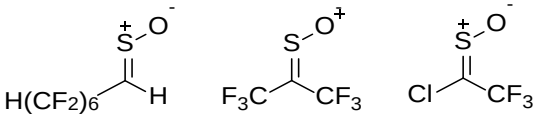


Scheme 33

Due to the fact that cycloadditions of sulfines are widely reported, it is understandable that some cycloadducts will quickly revert to the starting sulfine and another reagent. However, if the cycloadduct is generated in another way, as for example in Scheme 32, the cycloreversion could be an easy method of generating the sulfine. This is the case in the reaction of *N*-

sulfinylcarboxamides and ynamines. The 1,4,3-oxathiazine 4-oxides undergo a hetero-retro-Diels-Alder reaction under mild conditions to form the sulfine which in turn can be trapped to generate a more stable cycloadduct.[84]

Most recently, a series of fluorinated sulfines have been synthesised by Bouillon *et al.* from their corresponding anthracene cycloadducts.[85] This hetero retro-Diels-Alder route to fluorinated compounds is used as a route to sulfines, which were found to be stable for about an hour and could be characterised by NMR spectroscopy (Figure 5). The sulfines also acted as hetero-dienophiles in Diels-Alder cycloadditions to be trapped with 2,3-dimethyl-1,3-butadiene.



67 **68** **69**

Figure 5

1.3 Structural characteristics of sulfines

Ever since sulfines were first isolated and theorised in the 1920's, there has been an effort to fully characterise and understand them. As detailed above the first confirmation of a sulfine structure was published by King and Durst.[9] They also showed for the first time the existence of sulfines as two isomers, with differing dipole moments. The differences in the two isomers were initially observed by the difference in their dipole moments, and then by the differing signals in the proton NMR spectra.[11]

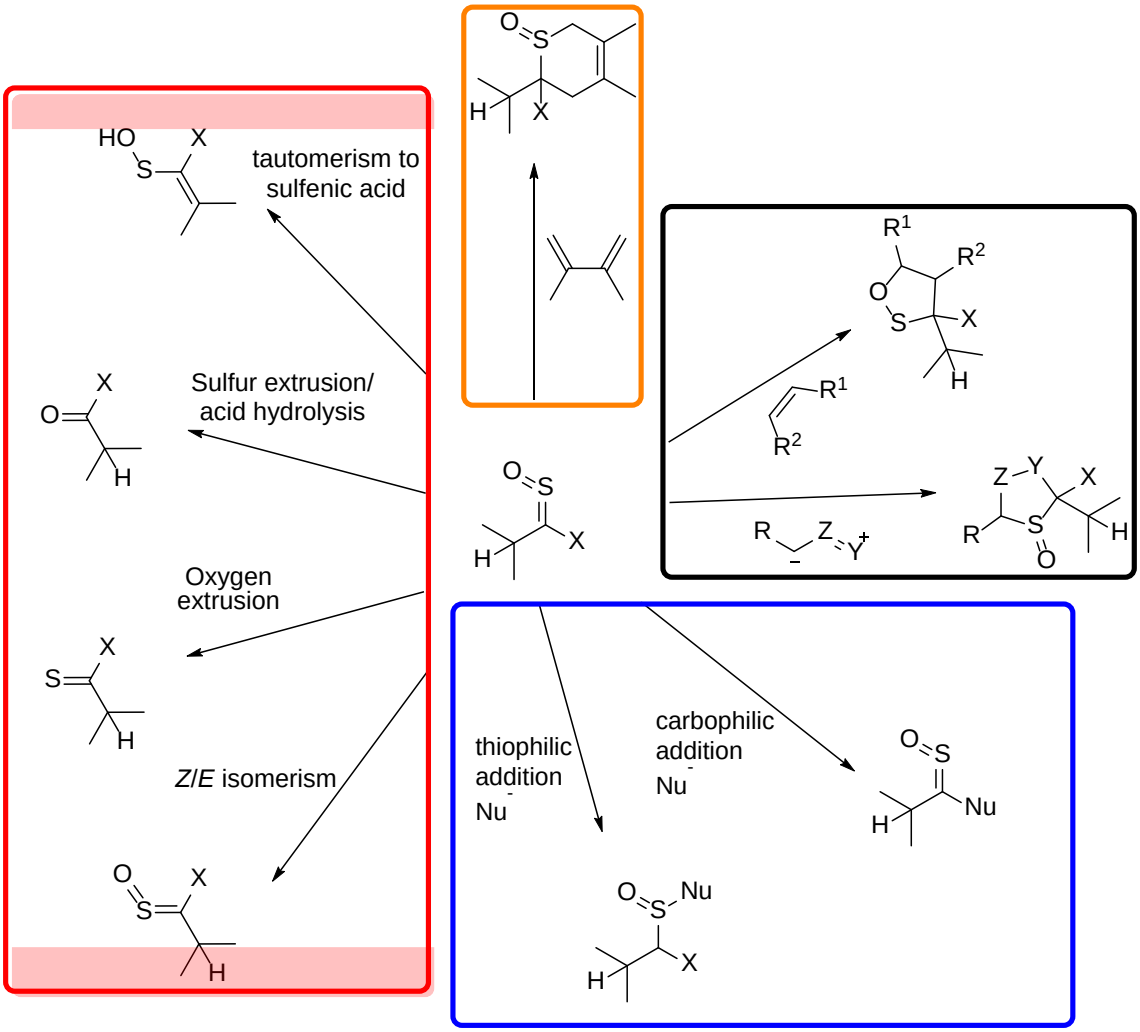
The physical characteristics of sulfines have been successfully investigated; the non-linearity of the C=S=O system has been established by X-ray crystallography (C-S, 1.62 Å; S-O, 1.46 Å; CSO angle, 114°).[86] The S=O bond length of the sulfine has been found to be closer to that of the typical S=O double bond length of 1.43 Å, rather than the sulfoxide S-O single bond length of 1.53 Å.[13,14] The IR spectra of sulfines also show characteristic absorptions in the sulfoxide region 1000-1150 cm^{-1}. The parent sulfine, CH_2=S=O shows symmetric and asymmetric stretching vibrations at 1165 and 1357 cm^{-1} respectively.[74]

Most recently, sulfines have been observed in argon matrices at 10 K.[69] The generation of these α-oxo sulfines occurs on dediazotisation of α-diazosulfoxides followed by hetero-Wolff rearrangement (Scheme 26). On irradiation at λ > 375 nm or under rhodium catalysis the thermodynamic isomer of the sulfine is predominantly seen. The asymmetric stretch of the sulfine

is recorded at 1289 cm $^{-1}$ and the symmetric stretch is recorded at 1084cm^{-1}. The *E*-sulfine was observed under irradiation at 248 nm in the argon matrix and subsequently rearranged to further products. Sulfines usually show the characteristic absorptions in this region with both symmetric and asymmetric stretches.[74,87,88] The UV absorption of sulfines has also been recorded with typical absorptions around 270 nm. [89,90]

1.4 Reactions of sulfines

With multiple routes to sulfines, and wide variation of their structures, the synthetic uses and reactivity of sulfines have been widely studied and will be reviewed in the next section. The main important reaction pathways are carbophilic and thiophilic nucleophilic addition to sulfines, and cycloaddition reactions including Diels-Alder and 1,3-dipolar cycloadditions (Scheme 34).

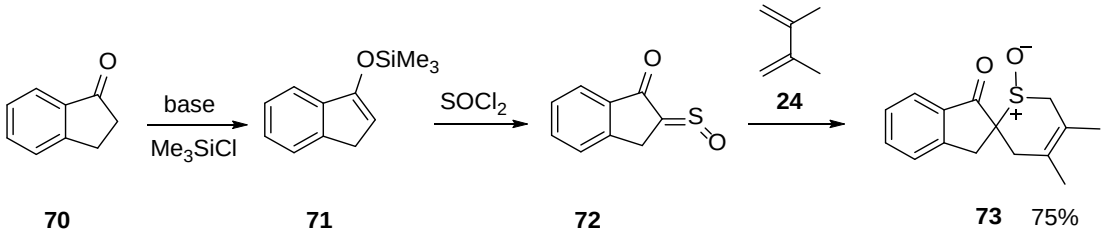


Scheme 34

1.4.1 [4+2] Diels-Alder cycloadditions

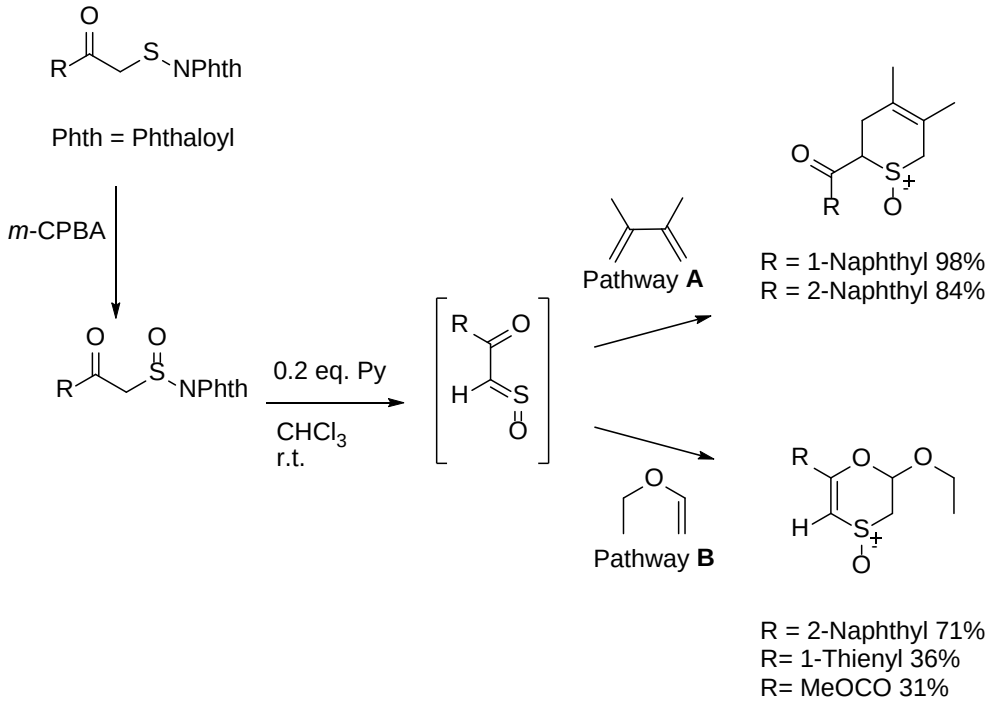
The most widely studied reaction pathway of sulfines are Diels-Alder cycloadditions, which proceed with the retention of stereochemistry. Due to the labile nature of sulfines, they are most commonly entrapped with 2,3-dimethyl-1,3-butadiene **24**[5,6,91] to verify a sulfine as an intermediate in a reaction mechanism.[92] This diene has been found to react with even moderately dienophilic sulfines. The cycloadducts derived from these reactions, dihydro-2*H*-thiopyran *S*-oxides, are of synthetic value and can be used as precursors for the synthesis of bioactive compounds.[93-96] For example, these cycloadducts have been used in Pummerer-like reactions[97] and as intermediates on the way to potential anti-HIV compounds[98] and cephalosporin derivatives.[99]

Sulfines can act as dienophiles and dipolarophiles in cycloaddition reactions with both 1,3-dienes and various 1,3-dipoles[100] leading to synthetically valuable cycloadducts and heterocycles. Sulfines with electron-withdrawing groups readily undergo Diels-Alder type cycloadditions with the stereochemical relationship of the sulfine substituents being retained in the cycloadduct.[101] The first report of a Diels-Alder cycloaddition of a sulfine was by Zwanenburg.[55] The α-oxosulfine **72** was prepared from 1-trimethylsilyloxy-1-indene **71** and treated with 1,3-dimethyl-2,3-butadiene **24** in a Diels-Alder fashion to form the dihydro-2*H*-thiopyran *S*-oxide **73** in good yield (Scheme 35). Interestingly, the formation of diastereomers was not reported.



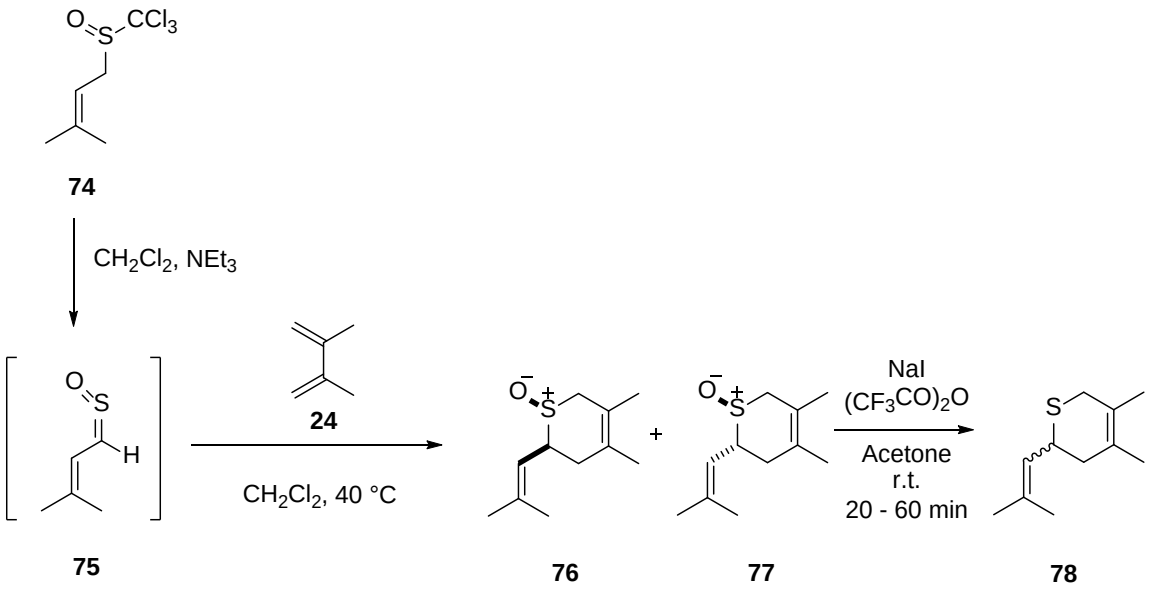
Scheme 35

Zwanenburg *et al.* have also reported the application of Lewis acid catalysts, especially $SnCl_4$, to decrease reaction times from 18 h to 1 h.[54] Research by Capozzi *et al.* has utilised the Diels-Alder cycloaddition of sulfines on multiple occasions. [46,82,83] Their work has involved generation of the sulfine *via* rearrangement of a sulfoxide which in turn is generated by *m*-CPBA oxidation of α-oxothiophthalimides. On generation of the sulfine under basic conditions the intermediate can be trapped as an electron poor dienophile (pathway **A**, Scheme 36) or alternatively as an electron poor 4π acceptor using electron rich dienophiles (pathway **B**, Scheme 36) producing predominantly *trans* dihydrothiopyran *S*-oxides (Scheme 36).



Scheme 36

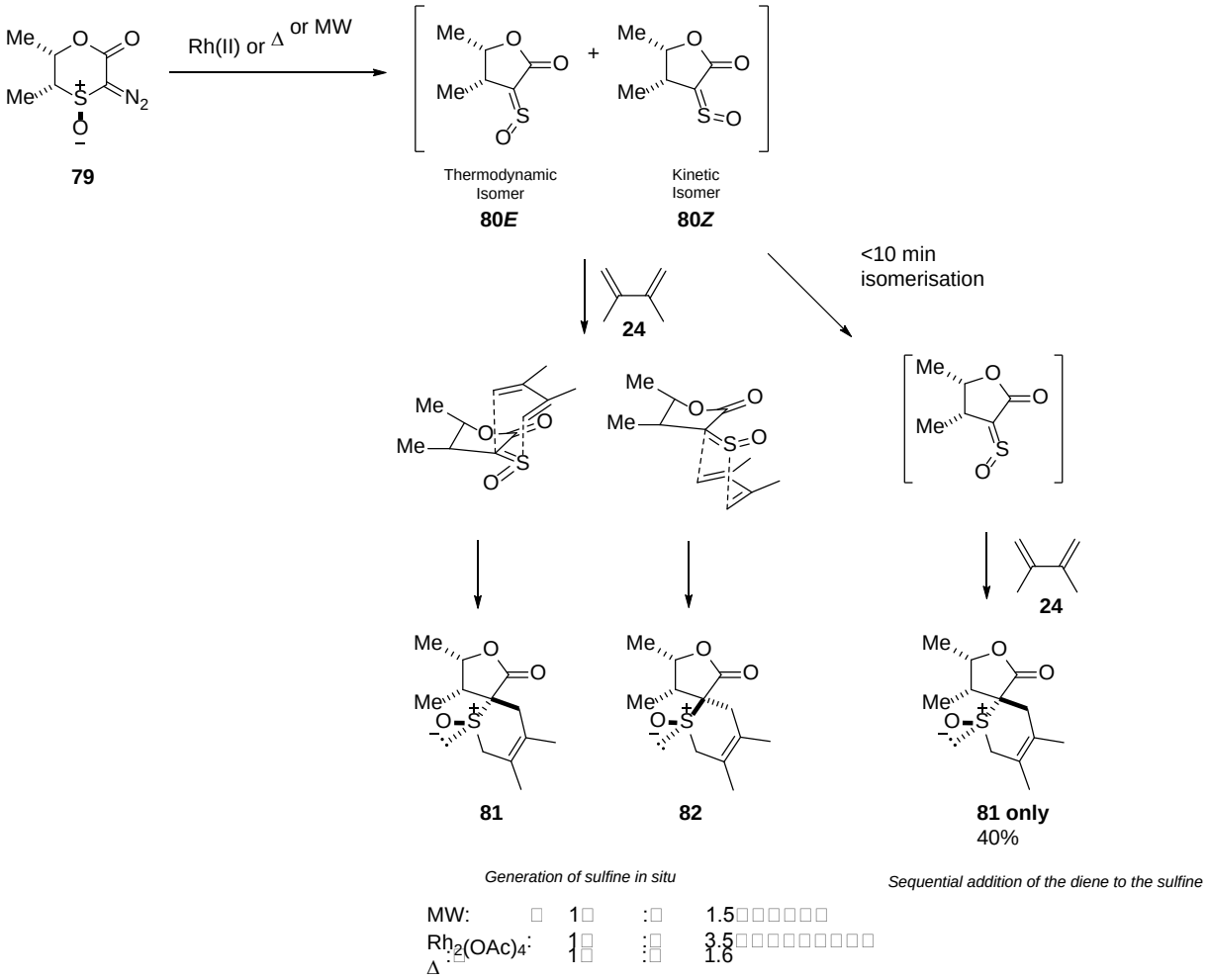
The first report of diastereomer formation in cycloadducts of sulfines was by Bonini[102] in 1993; this was followed by further work by Braverman and Gottlieb giving a mixture of two diastereomeric cycloadducts (**76**/**77**, 1:4.5) from the conjugated vinyl *Z*-sulfine **75**, which was generated *in situ* from the sulfoxide **74** (Scheme 37).[103]



Scheme 37

The cycloadduct products **76** and **77** have been successfully deoxygenated to produce 3,6-dihydro-2H-thiopyran **78**. In this way, the sulfines can be used as synthetic equivalents of thiocarbonyl compounds.[7,54]

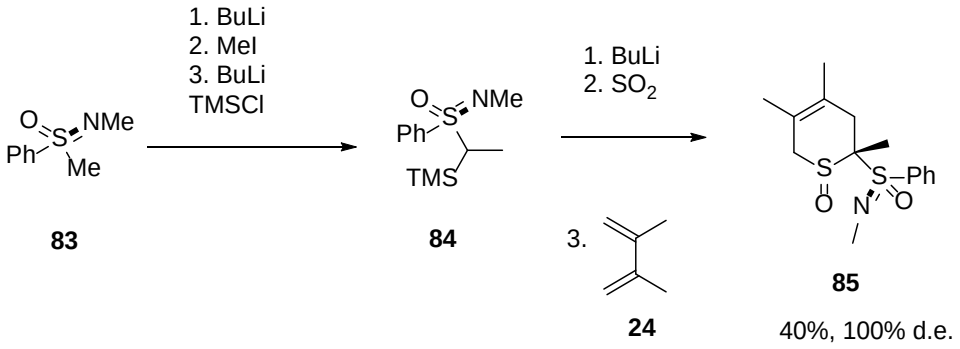
Recent research by the Maguire group has also involved the trapping of α-oxo sulfines with 2,3-dimethyl-1,3-butadiene **24**. The α-oxo sulfines **80** ***E*** and **80** ***Z*** were generated from the α-diazosulfoxide **79** (Scheme 38). On dediazotisation, the carbene undergoes a hetero-Wolff rearrangement.[104] Herein, Maguire discusses the formation of two separate diastereomers as products, **81** and **82**, arising from cycloaddition reactions with the isomers of the sulfine, *E* being the thermodynamic isomer and *Z* being the kinetic isomer (Scheme 38).[67-69,91] Depending on the method used to generate and trap the sulfine with the diene, preferential formation of one diastereomer is possible. Any one of microwave irradiation, transition metal catalysis and thermolysis can be used for this transformation.[68,69,91,105]



Scheme 38

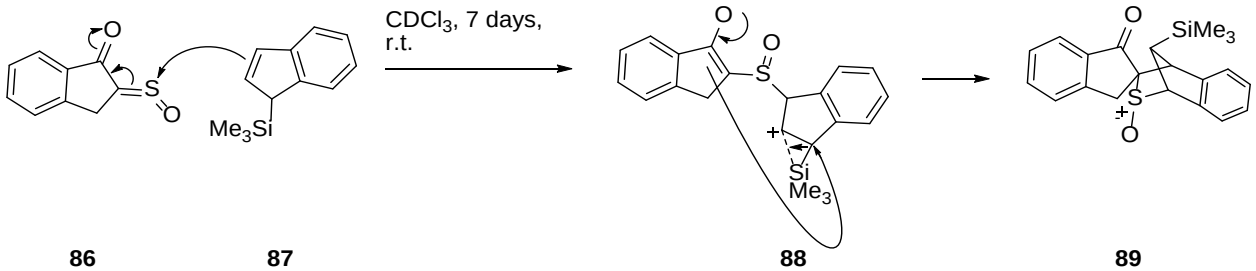
The rationale for the altered stereoselectivity depending on conditions, is that with *in situ* diene trapping, the principal cycloadduct is derived from approach of the diene from below to the kinetic, *Z*-isomer of the α-oxosulfine **80 *Z*.** In the absence of a diene trap, the (*Z*)-oxosulfine isomerises to the thermodynamically more stable *E*-oxosulfine **80 *E*** over time (<10 min). Direct evidence for this was obtained by initially forming the *E*-oxosulfine **80 *E*** as a single product, from the α-diazosulfoxide in the absence of diene. **80 *E*** was subsequently reacted with 2,3-dimethyl-1,3-butadiene **24** to generate the cycloadduct **81** derived from approach of the diene from above to the *E*-isomer, thus confirming the α-oxosulfine interconversion.[67]

To date, asymmetric Diels-Alder cycloadditions of sulfines have had very limited success except for one example. A report by Zwanenburg details an asymmetric Diels Alder cycloaddition of a sulfoximino substituted sulfine, which was generated *in situ* by reaction of an α-silylcarbanion with sulfur dioxide followed by an elimination (Scheme 39).[106] Here, the chirality of the sulfoxide is responsible for the selectivity in the cycloaddition.



Scheme 39

Zwanenburg and Rewinkel have described a regioselective cycloaddition of the sulfine **86**. On analysis of the HOMO/LUMO energy gaps between the two π systems they suggested the substituents on the sulfine are responsible for the regiochemistry observed in the Diels-Alder cycloaddition to form the cycloadduct **89** (Scheme 40).[107]

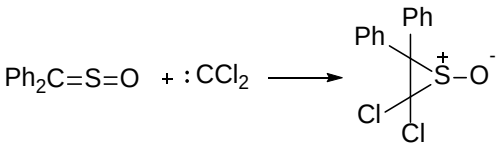


86 **87** **88** **89** Quantitative

Scheme 40

1.4.2 [1+2] Cycloadditions

The only reported example of a sulfine reacting with a carbene was in 1970 by Zwanenburg *et al.*[108] Dichlorocarbene **91** reacts with diphenyl sulfine **90** which acts as a dipolarophile to form the episulfoxide product **92** (Scheme 41).

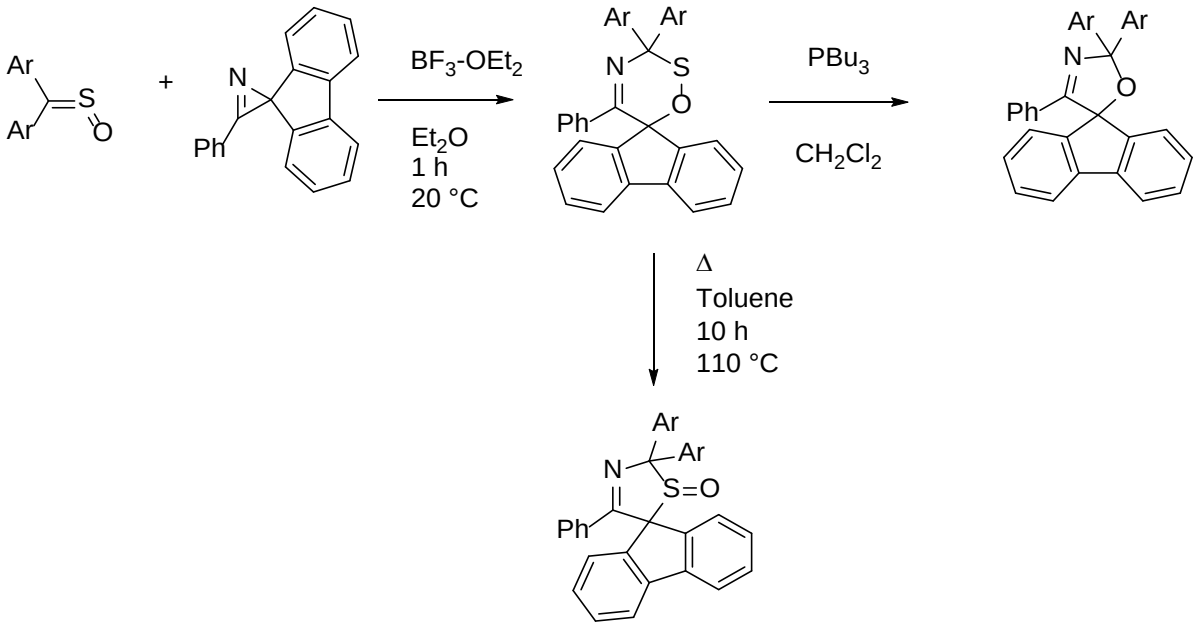


90 **91** **92** 18%

Scheme 41

1.4.3 [3+3] Cycloadditions

An interesting [3+3] cycloaddition reaction of diarylsulfines with a 2H-azirine has also been reported.[109] Under vigorous thermal conditions, the sulfine failed to react with the azirine but when the reaction was carried out in the presence of a Lewis acid, the oxathiazine was formed *via* a stepwise pathway. To date, this is the only report of a sulfine undergoing a [3+3] cycloaddition. When the intermediate cycloadduct was heated in toluene under reflux for 10 h, a sulfenate-sulfoxide rearrangement was observed and the sulfoxide was isolated (Scheme 42). Desulfurisation was also possible on these cycloadducts by treatment with tributylphosphine in dichloromethane producing the desulfurized products in quantitative yield. This further highlights the potential for the use of sulfines in organic synthesis.

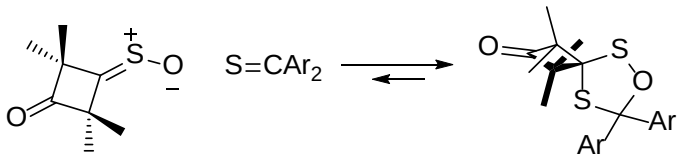


Scheme 42

1.4.4 1,3-Dipolar cycloadditions

The highly polar sulfines, can act as 1,3-dipoles or indeed as dipolarophiles demonstrating excellent synthetic versatility. Sulfines have been described as acting as dipolarophiles, towards diazoalkanes, nitrile ylides, nitrile imines, nitrile oxides and nitrones.[100] 1,3-Dipolar cycloaddition reactions proceed with a concerted mechanism leading to the retention of stereochemistry.[110,111] Due to the ability of the sulfine to isomerise between the kinetic and thermodynamic isomers, cycloaddition reactions can produce differing diastereomeric products. The stereochemistry in the cycloadduct is a result of the stereochemistry of the sulfine, suggesting a concerted cycloaddition reaction.

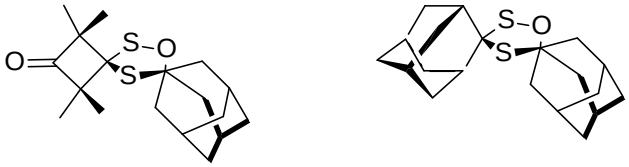
Recently, sulfines have been studied theoretically using density functional theory. Furan 2,3-dione was the dipolarophile used in the theoretical study.[112] This reactivity of the sulfines acting as dipoles has been established practically. The first example of sulfines as dipoles was reported in 1996,[100] Huisgen reported a 1, 3-dipolar cycloaddition of a sulfine **93** with a thione where the sulfine acted as a dipole and the thione as a "*superdipolarophile"* (Scheme 43). The product of the dipolar reaction of a sulfine and thione is a cyclic sulfenic ester.



93

Scheme 43

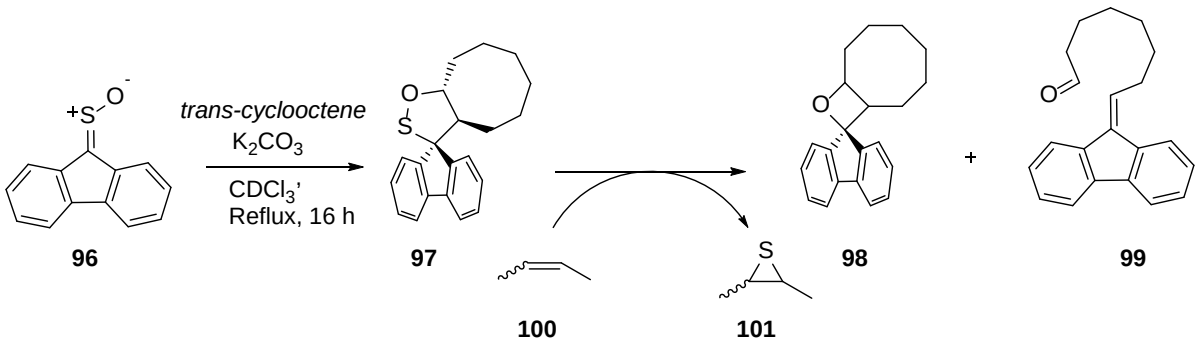
In a subsequent study rearrangement of the initial cycloadduct from reaction of an aromatic sulfine with a thione was reported.[113] Cycloadducts of sulfines with aliphatic thiones are more stable, this is shown by work carried out by Huisgen who isolated spiroadamantine derived cycloadduct **94,** and bis-spiroadamantane derived cycloadduct **95** in high yields from cycloaddition reactions (Figure 6).[114]



94 86% **95** 85%

Figure 6

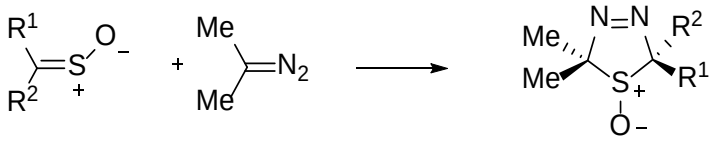
Further reports by Waldemar *et al.* describe a sulfine acting as a dipole for a carbon carbon double bond,[115] or a carbon carbon triple bond.[116] For example, the cycloaddition between fluorenethione *S*-oxide **96** and *trans*-cyclooctene is a 1,3-dipolar cycloaddition with a sulfine acting as dipole (Scheme 44). Further investigation on the thermal and photochemical reactions of sulfines, with the strained triple bond of cyclooctyne established that it undergoes a 1,3-dipolar cycloaddition and subsequently rearranges from the 1,2-oxathiole **97** to more stable products, through desulfurisation.



96 **97** **98** **99** **100** **101**

Scheme 44

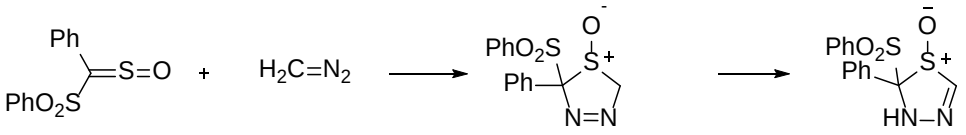
When sulfines act as dipolarophilles, thiadiazoline adducts have been formed in a regio- and stereospecific manner in the cycloaddition of a sulfine with 2-diazopropane **102** (Scheme 45).[117] Similar adducts also form with diazomethane, however the reaction is much more sluggish and the product quickly decomposes by a cycloreversion reaction.



102

Scheme 45

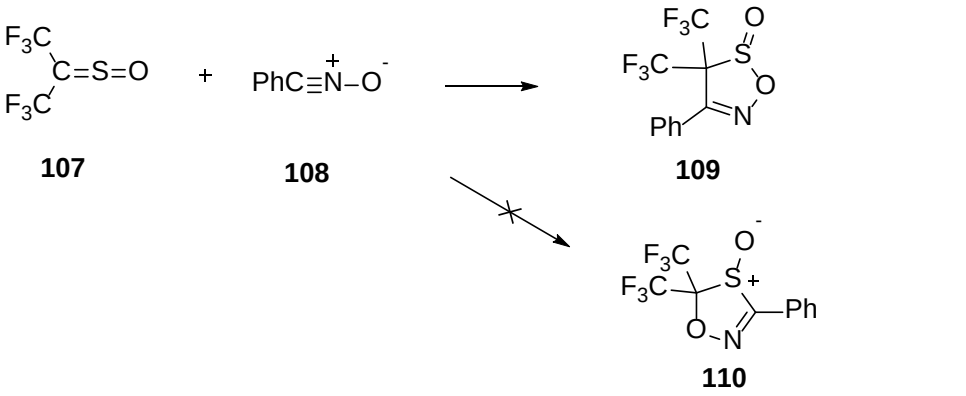
Sulfines containing sterically demanding substituents react with 2-diazopropane to give episulfoxides as a mixture of diastereomers. This reaction proceeds in a non-concerted fashion and *via* zwitterionic intermediates. Aliphatic sulfines react in the same manner producing dihydro-1,3,4-thiadiazole-*S*-oxides in high yields.[117] Other diazo dipoles also undergo cycloaddition with sulfines. Diazomethane **104** successfully undergoes [3+2] dipolar cycloadditions with sulfines. The cycloaddition with the arylsulfonyl substituted sulfine **103** produces an unstable cycloadduct **105**, which quickly rearranges or decomposes at room temperature to the thiadiazole **106** (Scheme 46).[118]



103 **104** **105** **106**

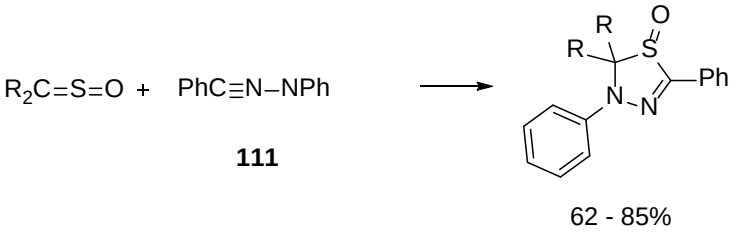
Scheme 46

Cycloaddition reactions of sulfines occur smoothly with benzonitrile oxide **108**, forming 1,4,2-oxathiazole-*S*-oxides in good yields and in a regiospecific manner.[119] The cycloadducts are heat sensitive and lose sulfur monoxide on heating, resulting in the formation of diaryl ketones and benzonitrile.[119] The only reported exception to this regiospecific addition, is the cycloaddition reaction of benzonitrile oxide **108** with the sulfine **107** in which the cycloadduct formed is the 1,2,5-oxathiazole-*S*-oxide **109** (Scheme 47). [119]

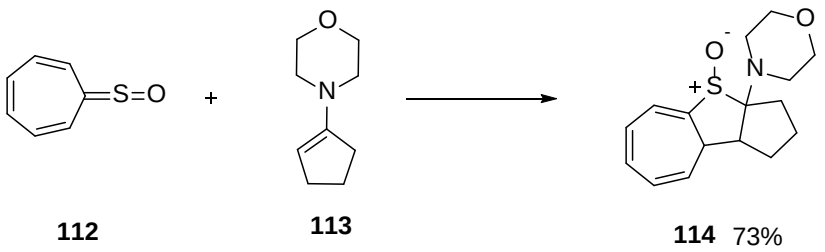


Scheme 47

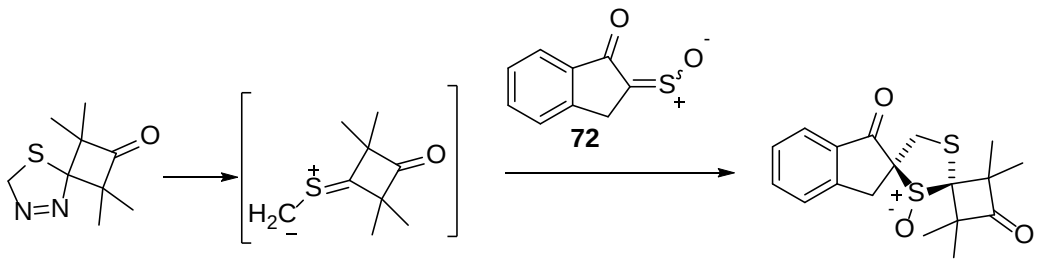
It has also been reported, diphenylnitrilimine **111** undergoes a 1,3-dipolar cycloaddition with diaryl substituted sulfines in a stereospecific manner to form 1,3,4-thiadiazoline *S*-oxides (Scheme 48).[120]In the reaction of the sulfine tropothione *S*-oxide **112** with an enamine **113**, Machiguchi and coworkers describe an unusual regiochemical outcome in the 1,3-dipolar cycloaddition with the enamine leading to the sulfoxide **114** (Scheme 49).[121] Synthesis of 1,3-dithiolane-*S*-oxides by the dipolar addition of the sulfine **72**, acting as a dipolarophile with a thiocarbonyl-*S*-ylide, generated by the elimination of nitrogen from a thiadiazole, occurs in a regiospecific manner (Scheme 50). [122,123]



Scheme 48

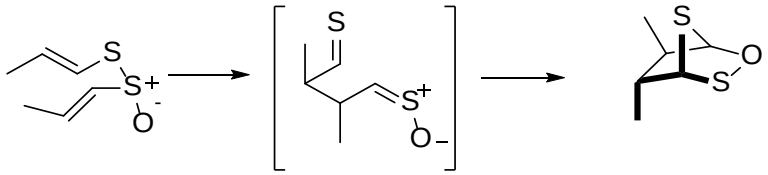


Scheme 49



Scheme 50

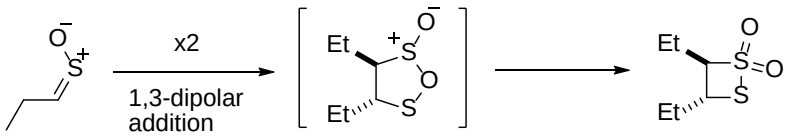
There have also been reports of intramolecular cyclisations of sulfines. Block *at al.* reported that on oxidation of a disulfide, and on analysis of the product obtained, **117**, the only explanation was a thio-Claisen rearrangement to the sulfine **116** followed by an intramolecular 1,3-dipolar cycloaddition between the sulfine and the thioaldehyde to form the product (Scheme 51).[124]



115 **116** **117**

Scheme 51

The dimerisation of sulfines to give 1,3-dithietane *S*-oxides was initially suggested by Wilkens,[17] who reported that onion lachrymatory factor **3** dimerised to give 2,4-diethyl-1,3-dithietane-1,3-dioxide. Block subsequently investigated the dimerisation in more detail and found that the product was, in fact, a 1,2-dithietane **7** which was formed by a cycloaddition of the sulfine **3**, acting both as a 1,3-dipole and dipolarophile, followed by rearrangement of the unstable cyclic sulfenyl sulfinate ester **6** (Scheme 52). [19] This highlights the properties of the sulfine to act both as dipole and dipolarophile.



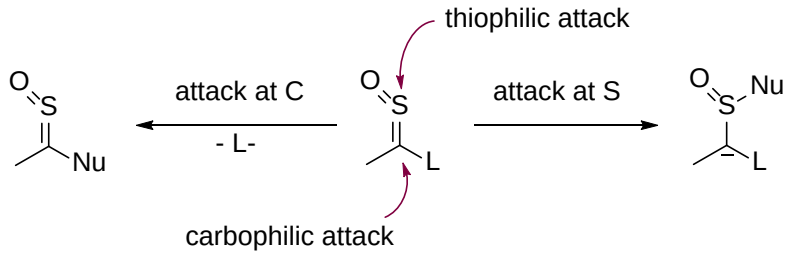
3 **6** **7**

Scheme 52

1.4.5 Nucleophilic addition to sulfines

A synthetically powerful transformation of sulfines is *via* nucleophilic addition. With potential for nucleophilic attack at both the carbon (carbophilic) and sulfur (thiophilic) sites, attack at the

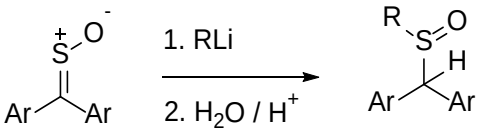
electrophilic sulfur is more common, but attack at carbon occurs when there is an appropriate leaving group attached (Scheme 53). The most common type of thiophilic reactions of sulfines are those with alkyllithium reagents, but the reaction depends both on the structure of the sulfine and the nucleophile.



Scheme 53

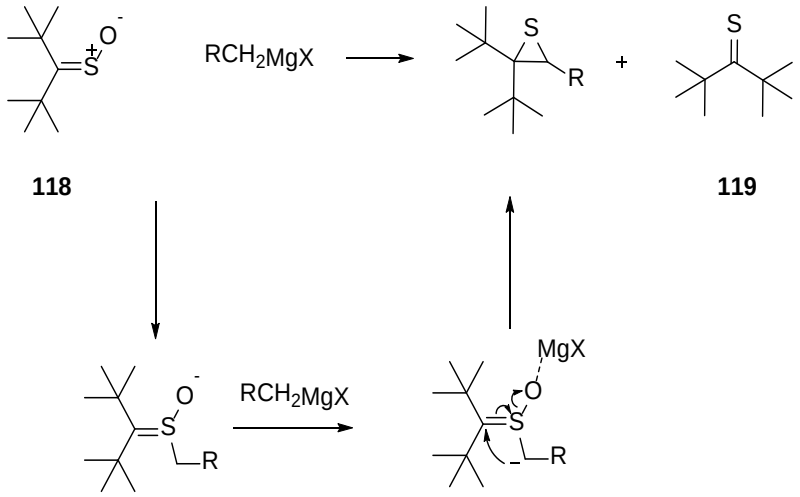
1.4.6 Thiophilic nucleophilic attack

Schlessinger and Schultz first described thiophilic addition of organolithiums to sulfines in 1970.[125] Soon after, Zwanenburg described thiophilic addition of alkyllithium compounds to aromatic alkylthio and arylthio sulfines.[126] The reaction of these diarylsulfines with alkyllithium reagents produce sulfoxides in high yields (Scheme 54).



Scheme 54

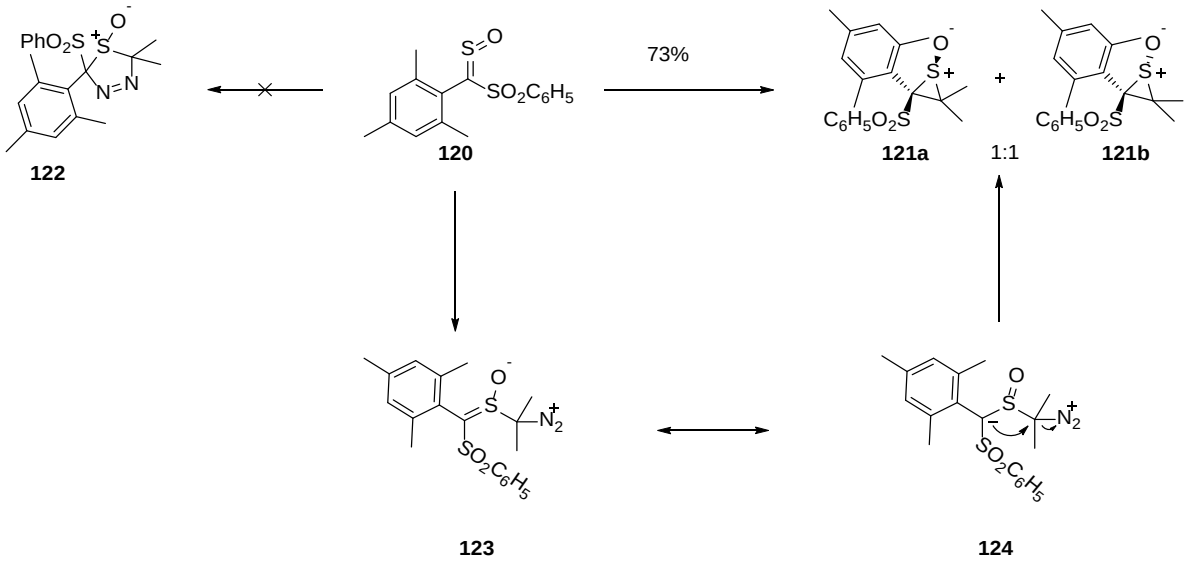
Thiophilic nucleophilic attack of alkyllithiums and Grignard reagents have been reported for the aliphatic compound di-*tert*butyl sulfine **118**. This activity is different to that of di-arylsulfines and two equivalents of the organometallic reagents are needed to give episulfides in good yields (Scheme 55).[127] This product is formed by the rearrangement and cyclisation of the intermediate carbanion generated by the nucleophilic attack.



118 **119**

Scheme 55

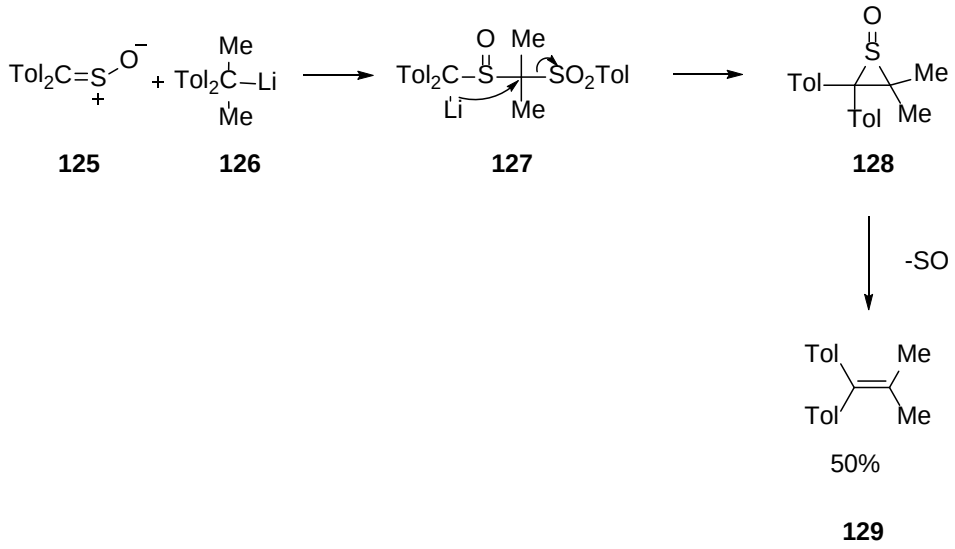
When sterically hindered sulfines react with 2-diazopropane they undergo a nucleophilic thiophilic addition and not the intended cycloaddition (Scheme 56). The rearrangement of the zwitterionic species and loss of nitrogen from the intermediate **124**, leads to a non-stereospecific cyclisation and formation of episulfoxides, in place of the expected five membered cycloadduct. [128]



122 **120** **121a** **121b** **123** **124**

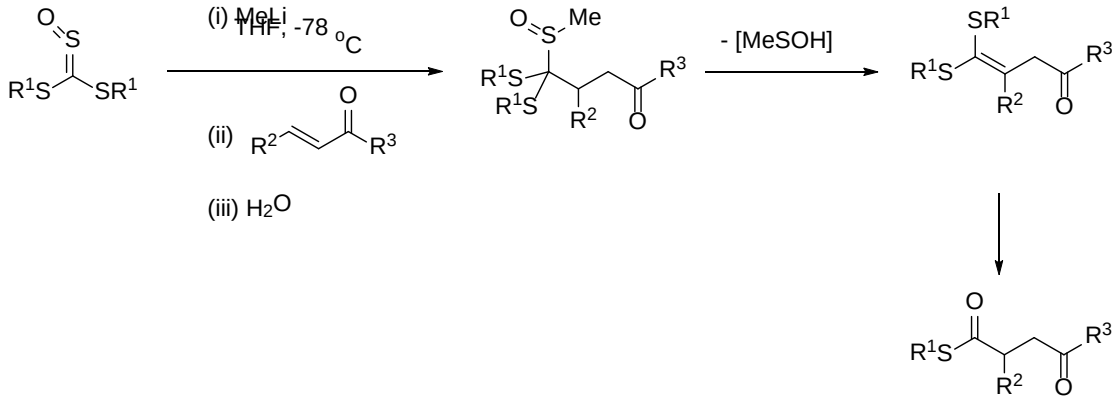
Scheme 56

Another example of cyclisation of an intermediate carbanion formed by nucleophilic thiophilic attack was reported by Zwanenburg.[129] On having an excellent leaving group α to the newly formed sulfoxide **127**, cyclisation occurs producing an episulfoxide **128** as the primary product which undergoes elimination of sulfur monoxide to form the alkene **129** in 50% yield (Scheme 57).



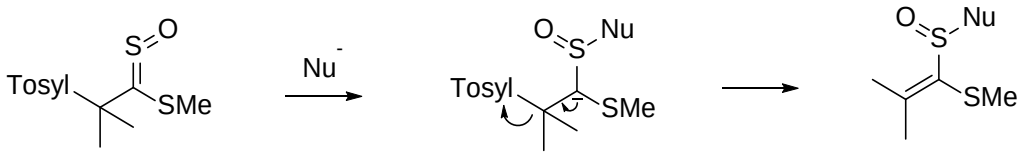
Scheme 57

Metzner also reported thiophilic addition of alkyllithium reagents to trithiocarbonate oxides where the carbanion was stabilised by the three sulfur groups.[130] On treatment of the carbanions with electrophiles, trithioorthoester oxides are formed. These trithioorthoester oxides are unstable and quickly decompose to thioesters, disulfides, thioformate with the elimination of methanesulfenic acid (Scheme 58). Low temperature conditions are vital for these reactions due to the high reactivity of sulfines towards methyl lithium. The authors also describe the 1,4 addition of the sulfine carbanion to enones, leading to intermediates which readily rearrange to β-ketene dithioacetals. The overall sequence allowed the use of an alkyl-thiocarbonyl anion synthon for Michael addition in polarity reversal reactions. The authors were interested in the umpolung aspect of this chemistry, which involved the generation of a carbanion using an addition reaction, and not a deprotonation (Scheme 58).



Scheme 58

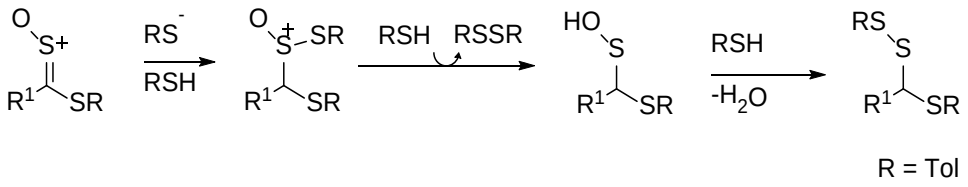
Zwanenburg has also shown that the thiophilic reaction of an α-tosyl substituted stable sulfine **130** proceeds with a concurrent elimination reaction proceeds with yields up to 92% (Scheme 59).[131] The reaction depends on the strength of the nucleophile, and lower pKa values lead to lower yields. Thiophilic attack of α-functionalised carbanion nucleophiles (α-sulfonyl, α-oxo, and α-cyano) produced ketene dithioacetal monoxide derivatives.



130

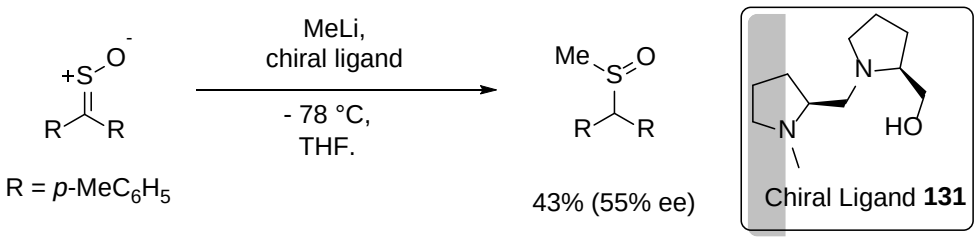
Scheme 59

By taking advantage of the reactivity of sulfines a route to disulfides has also been established. Treatment of the sulfine with a thiolate anion in basic solution leads to thiophilic nucleophilic attack. [132] The proposed mechanism suggests the thiosulfinate is formed initially but reacts further with thiol forming a sulfenic acid which then forms the disulfide through loss of a sulfonate anion (Scheme 60).



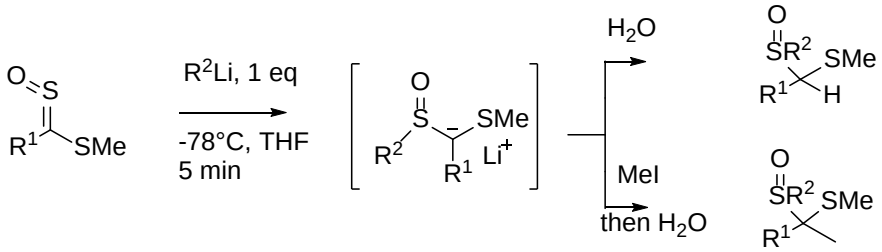
Scheme 60

Zwanenburg *et al.* have also described the asymmetric addition of methyl lithium to di-*p*-tolylsulfine in the presence of chiral ligands with yields varying from 5% to 43% (Scheme 61).[133] These additions to sulfines in an asymmetric manner have the potential to produce asymmetric sulfoxides which are of particular use as chiral auxiliaries' in organic synthesis, but to date optical yields obtained have been low, with a maximum e.e. recorded of 55%. As the maximum enantioselectivities recorded were 55% ee it does not compete with the other methods in asymmetric synthesis.[134,135]



Scheme 61

Similar to this, Metzner *at al.*[136] have described the diastereoselective formation of dithioacetal oxides from aliphatic sulfines by thiophilic attack. The sulfines were directly subjected to organolithium compounds at -78 °C in THF for five minutes, with thiophilic attack observed. Protonation of the intermediate carbanions gave dithioacetal oxide products exclusively with the diastereomeric ratio varying from 52 : 48 to 100 : 0 depending on the substitution pattern. Reaction of the carbanions with electrophiles led to predominantly unstable dithioacetal oxides and little diastereoselectivity was seen on alkylation (Scheme 62).

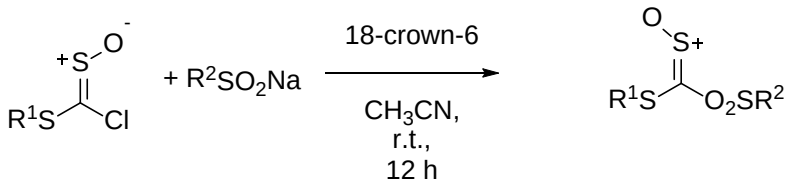


Scheme 62

These example of thiophilic nucleophilic addition to sulfines highlight the potential use of these reactive intermediates for the synthesis of multiple functional groups including disulfides, episulfides, sulfoxides and episulfoxides. Although limited success has been achieved to date in the area of asymmetric synthesis using sulfines, the presence of a thermodynamic and kinetic isomer may lead to some selectivity.

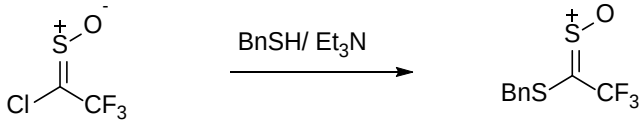
1.4.7 Carbophilic nucleophilic attack

In contrast to thiophilic nucleophilic attack, carbophilic nucleophilic attack only occurs when a suitably good leaving group is attached to the sulfine. Chlorosulfines are accessed by the oxidation of the corresponding thioketone with *m*-CPBA.[137] In the presence of a crown ether, the sulfinate anion of sodium sulfinate displaces the chloro anion with complete inversion of stereochemistry (Scheme 63). The author is unsure whether this is because of an S_N2 type reaction or if it is because the kinetic *Z* diastereomer quickly converts to the thermodynamic *E* diastereomer leading to one stereoisomer. [137]



Scheme 63

Most recently, a unique example of carbophilic nucleophilic attack of a thiolate anion on a sulfine has been reported by Bouillon.[85] An α-chloro substituted sulfine **132** undergoes an addition elimination reaction with the thiolate anion forming a thio derivative of the original sulfine, **133** (Scheme 64). Both sulfines **132** and **133** acted as dienophiles in Diels-Alder cycloadditions and the structures of the resulting cycloadducts were proved unambiguously.

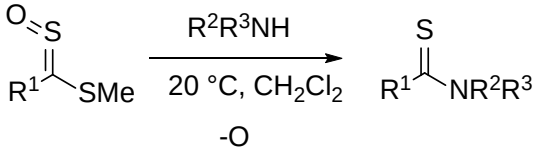


132 **133**

Scheme 64

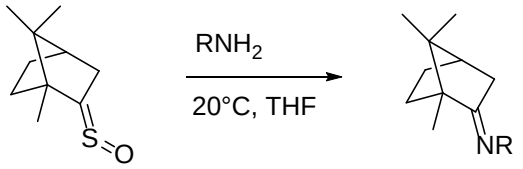
This example of carbophilic attack can be explained by the electronegativity of the attached groups. Other examples of carbophilic attack with thiolate anions, all have excellent leaving groups attached to the carbon atom. These chlorosulfines easily undergo displacement and stereochemistry is usually retained in the product.[138] A report by Baltas *et al.* also shows carbophilic nucleophilic attack of amine on intermediate sulfines.[92] In this report the product of carbophilic nucleophilic attack on a sulfine is unstable and quickly reacts further with itself.

Metzner *at al*. reported an interesting example of carbophilic nucleophilic attack on sulfines in the absence of a strong leaving group such as a chloride anion.[139] The sulfines used were prepared by oxidation of dithioesters and these compounds were stable with a half life of 1 – 4 days. The dithioester sulfines reacted with amines at room temperature to produce thioamides (Scheme 65).



Scheme 65

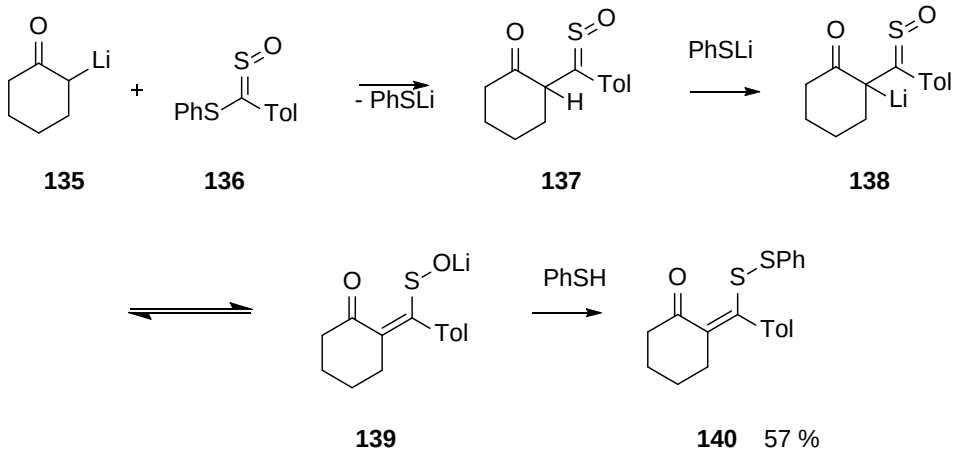
The authors also investigated the behaviour of a chiral sulfine, derived from a thioketone, with the aim of preparing new chiral sulfinamides. However, the sulfine **134**, obtained from (-)-thiocamphor, when treated with primary amines, instead gave easy access to enantiopure imines with elimination of methanesulfonic acid (Scheme 66).[139]



134

Scheme 66

Zwanenburg *et al.*[140] has also described carbophilic nucleophilic attack of α-oxo carbanions. This was the first example of carbon nucleophiles reacting with sulfines. The anions used in this study, 2-lithiocyclohexanone **135** and α-tetralone had previously been shown to not react with di-*p*-tolylsulfine in a thiophilic manner. This lack of thiophilic reactivity made them good reagents to choose for a carbophilic nucleophilic addition. The carbanion of 2-lithiocyclohexanone reacts in a carbophilic manner, however the newly formed sulfine **137** rearranges to a more stable disulfide **140** in the presence of the phenylthiolate anion giving the product in 57% yield (Scheme 67). The same rearrangement pathway occurs for the tetralone anion producing the analogous disulfide in 40% yield (Scheme 67).



135 **136** **137** **138**

139 **140** 57 %

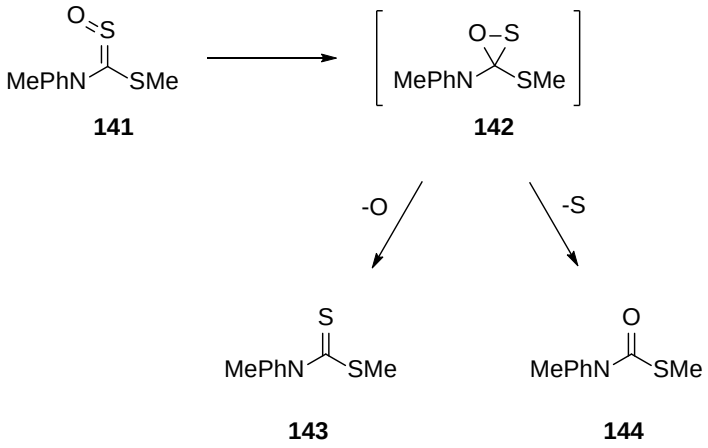
Scheme 67

1.5 Miscellaneous

1.5.1 Rearrangements of sulfines

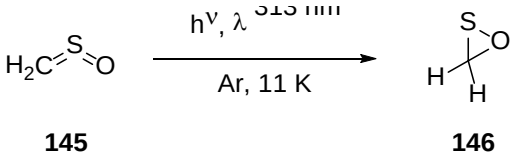
A characteristic behaviour of many sulfines is loss of elemental sulfur to give ketones under thermal and photolytic conditions.[125,141-144] This process occurs *via* an electrocyclic ring closure of the sulfine to give an oxathiirane intermediate which then extrudes sulfur forming the ketone product. Sulfines can also be reduced to thiocarbonyl compounds using phosphorus pentasulfide or thiophosphoryl bromide[145] and deoxygenation has also been observed with triphenylphosphine,[146] $Fe_2(CO)_9$ and $Mo_2(CO)_{10}$.[147]

Deoxygenation of sulfines has also been reported in the literature.[29,144] The proposed mechanism involves rearrangement to an oxathiirane intermediate **142** (Scheme 68), as reported by Metzner.[144] The thiocarbamate **14** is generated by extrusion of sulfur from the oxathiirane ring, while the dithiocarbamate **143** was formed *via* extrusion of oxygen.



Scheme 68

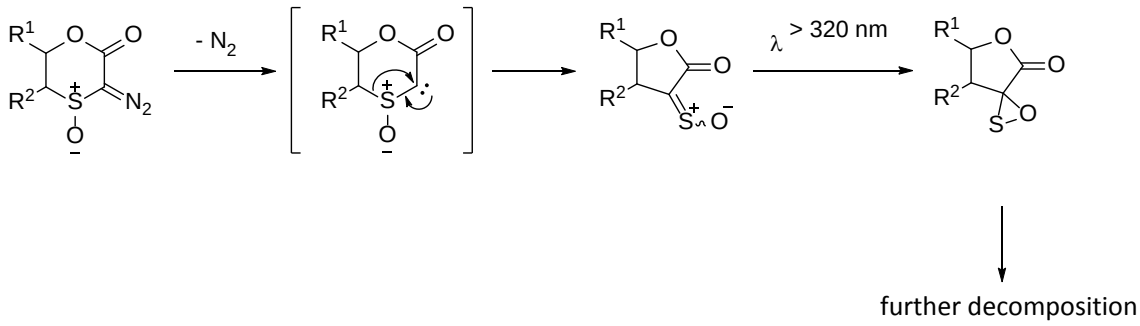
Oxathiiranes are unstable species which have been used as reactive intermediates in a variety of sulfine transformations. The electrocyclisation of sulfines to oxathiiranes has been well established by matrix isolation studies.[5,148] Oxathiiranes have proven elusive intermediates, and the photochemical generation and matrix isolation of the first experimentally observable oxathiirane **146** from thioformaldehyde *S*-oxide **145** was only recently reported by Schreiner e*t al.* (Scheme 69).[149] Related reports from this team[150] on the photochemical reactions of the sulfines and oxathiiranes in low temperature matrices provide very interesting insight into the mechanism of reactions of the highly strained oxathiiranes including desulfurisation. The generation of the parent sulfine has also been achieved *via* high vacuum flash pyrolysis with subsequent investigation of photochemical reactions. [151]



145 **146**

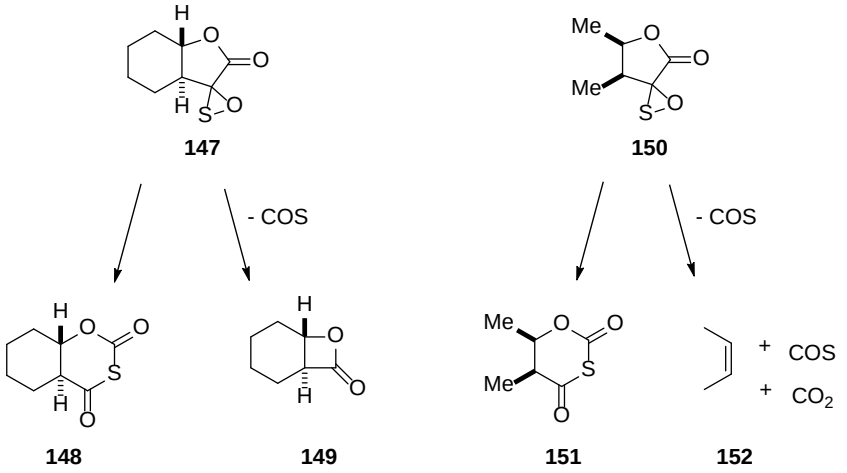
Scheme 69

Oxathiiranes are also formed as reactive intermediates in photo-catalysed rearrangement of α-diazosulfoxides in solid argon at 10 K. Characterisation by IR and UV/Vis spectroscopy by the groups of Maguire and Sander confirmed the intermediacy of the α-oxosulfine.[66,69] This photochemically induced hetero-Wolff rearrangement of the sulfinyl carbenes gave the α-oxosulfine intermediates (Scheme 70). Irradiation at λ > 320 nm resulted in decomposition of the α-oxosulfines *via* oxathiirane intermediates. A recent laser flash photolysis study by Bucher *et al.* has shown that on formation of the α-sufinyl carbene, the preferred reaction pathway is to form the sulfine, which in turn rearranges further. [152]



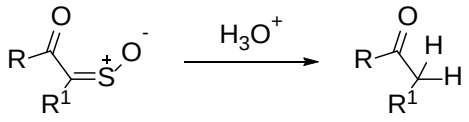
Scheme 70

The matrix-isolated species, **148 - 152** shown in Scheme 71 are formed by photochemically induced rearrangement of these oxathiiranes. The species were identified by the authors by comparison of experimental and calculated IR spectra, providing excellent insight into the nature of sulfine decomposition under cryogenic conditions. [66,69]

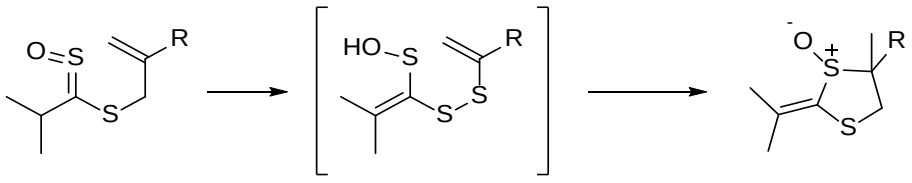


Scheme 71

α-Oxo sulfines are also known to undergo reductive hydrolysis (Scheme 72). The CSO moiety is replaced by a methylene group *via* a sulfinic acid intermediate which collapses with the loss of sulfur dioxide to form the ketone.[7] Differing to these reactivities again was the report of Zwanenburg[153] that describes tautomerisation of a sulfine to the corresponding vinylsulfenic acid followed by an intramolecular cyclisation of the sulfenic acid to the corresponding alkene (Scheme 73).

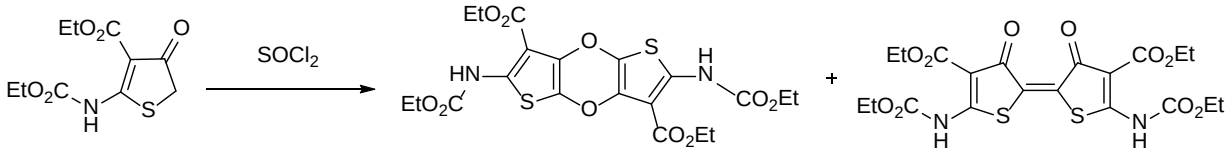


Scheme 72



Scheme 73

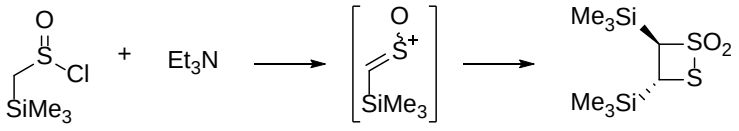
Notably, when Faull and Hull treated dihydrothiophene **153** with thionyl chloride in an attempt to generate the sulfine, they isolated two unexpected products, **154** and **155,** caused by rearrangement of the sulfine (Scheme 74).[154] The authors suspected oxidative condensation of the sulfine to give either the dioxane or the alkene dimer. Zwanenburg later confirmed that an α-oxo sulfine is indeed formed as an unstable intermediate by carrying out the reaction in the presence of 2,3-dimethyl-1,3-butadiene.[155]



153 **154** **155**

Scheme 74

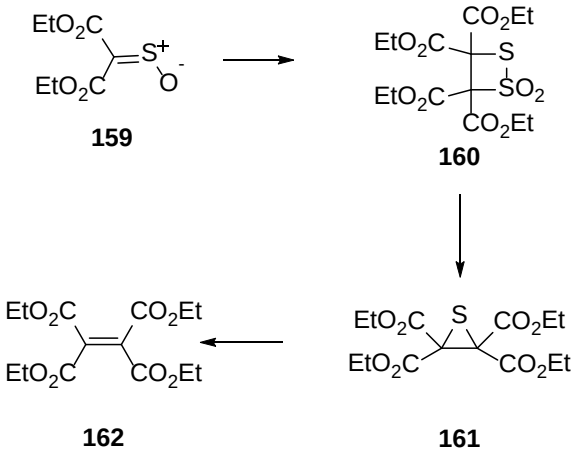
This is not the only example of dimerisation of sulfines. As seen earlier the dimerisation of propanethial-*S*-oxide is reported whereby it acts as both the dipole and dipolarophile (Scheme 52). Another paper by Block *et al.* describes the generation and dimerisation of a silicon substituted sulfine **157**, with slow dimerisation occurring over a period of four days (Scheme 75).[156]



156 **157** **158**

Scheme 75

Similar to this, Saalfrank and Rost formed the dimeric alkene **162** from the sulfine intermediate **159** (Scheme 76).[157] The mechanism they proposed was dimerisation of the sulfine and transfer of the oxygen from one sulfur to the other to give the unstable dimer which then suffered loss of SO_2 and sulfur extrusion from the episulfide to give the stable product.

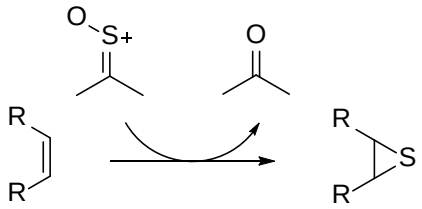


159 **160** **161** **162**

Scheme 76

1.5.2 Thioepoxidation using sulfines as sulfur-atom transfer reagents

The reactivity of sulfines has been widely studied, with regards to cycloadditions and nucleophilic additions. The unusual reactivity of the sulfur-centred heterocumulene has also found some miscellaneous uses in synthetic organic chemistry. One example of this was reported by Weinkotz in 1997.[158] Under photolytic conditions, in the absence of an alkene, bulky diaryl substituted sulfines are converted to ketones with the extrusion of elemental sulfur, this desulfurisation is a common decomposition reactions of unstable sulfines. In the presence of strained cyclic alkenes, diastereoselective sulfur transfer occurs to form thiiranes, in yields up to 94% (Scheme 77). The mechanism proposed is initial formation of the oxathiirane intermediate under photolytic conditions followed by sulfur transfer in a concerted mechanism. The suggestion is made that sulfines have the potential to be used in preparative methods of thioepoxides.

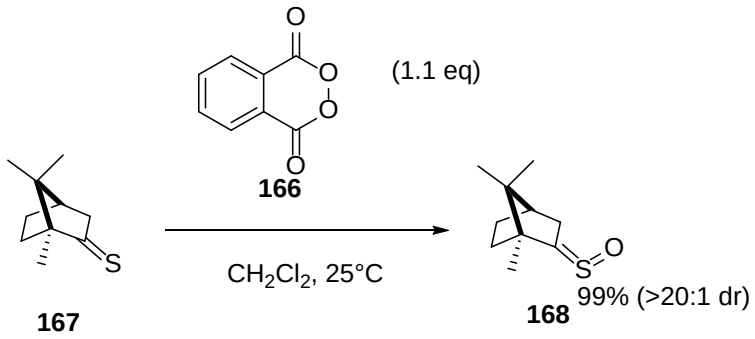


Scheme 77

1.6 Additional relevant updates:

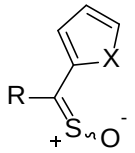
1.6.1 Oxidation to sulfines

Another oxidant has recently been reported for the generation of sulfines. Shi *et al.*[159] describe a metal free and additive free oxidation of sulfides, but also applied the methodology to thioketones producing sulfines. Mono-oxidation of the thioketones was selectively carried out with phthaloyl peroxide **166** providing the sulfine **168** in almost quantitative yields, and no evidence for the sulfene was observed (Scheme 78). The yields for oxidation to either sulfine or sulfoxide were consistently good to excellent and tolerated a wide range of functionalities. Cyclic diacyl peroxides are used for the oxygen transfer and two possible mechanisms are suggested in this report, either an ionic pathway or a radical pathway.[159]



Scheme 78

Recently, Mloston has reported the synthesis of a range of novel heteroaryl sulfines from the corresponding hetaryl thioketones.[160] Although the oxidations are carried out using *m*-CPBA as standard, the benefit of this work is providing access to, and identification of a range of novel, highly functionalised heterocyclic derived sulfines, albeit as mixtures of *E* and *Z* isomers. The pure sulfines were isolated, after chromatography on silica gel in moderate to excellent yields, between 59 and 93% (Figure 7).

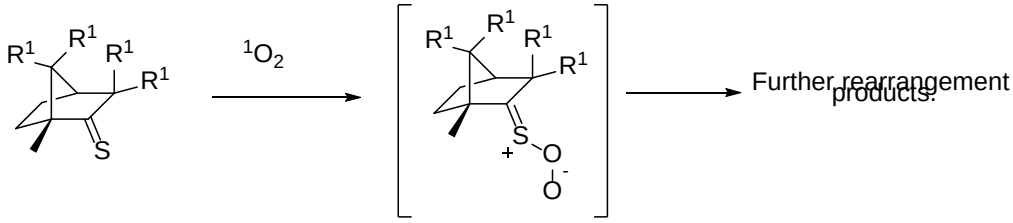


R = Ph X = S
R = Ph X = Se
R = 2-Furyl X = S
R = Selenophen-2-yl X = Se

Figure 7

1.6.2 Structural characteristics of sulfines

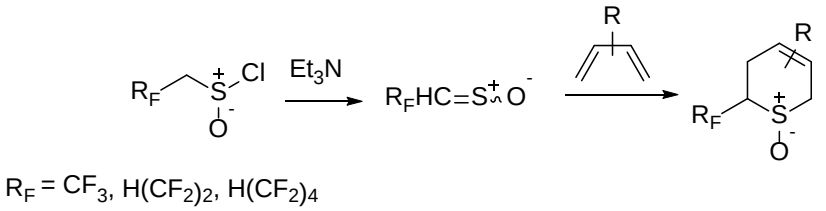
A recent study on the photochemistry of sulfines by Martinez *et al.* [161] has shown that photoexcitation of the sulfine thioformaldehyde *S*-oxide can be achieved using using wavelength 313 nm. Following photoexcitation to the first excited electronic state, it can either return to the ground state geometry or trigger the formation of the oxathiirane.[161] Returning to the ground state provides a large kinetic energy which in turn can be used to form other species; this high energy ground state is described as a "rich athermal ground state". In this example, a large diversity of 9 photoproducts are seen from one sulfine. In this manner, this report by Martinez is similar to that reported by Garcia-Fresnadillo[162] who investigated the photosensitive oxidation of trimethyl[2.2.1]-bicycloheptane thioketones (Scheme 79). The investigation by Garcia-Fresnadillo established that under conditions of low substrate concentrations the ketone is the major rearrangement product from the sulfine. This differs to under conditions of high substrate concentration where the sulfines are the major photoproducts in protic conditions. However in aprotic solvents, the ketone products are preferentially formed.



Scheme 79

1.6.3 [4+2] Diels-Alder cycloadditions

Recently, a series of polyfluoroalkanethial-*S*-oxides have been prepared by the group of Shermolovych through a dehydrochlorination reaction of 1,1-dihydropolyfluoroalkanesulfinyl chlorides.[163] The sulfines are generated under basic conditions and undergo subsequent Diels-Alder [4+2] cycloaddition reactions in good yields and good diastereoselectivity, providing access to novel polyfluorinated thiopyran-*S*-oxides (Scheme 80).



R_F = CF_3, $H(CF_2)_2$, $H(CF_2)_4$

Scheme 80

1.6.4 Miscellaneous

A recent review by Zhang *et al*[164] focuses on non-cytochrome P450-mediated bioactivation and its toxicological relevance highlighting both the formation and reactivity of sulfines *in vivo*. It is reported that thioureas can undergo oxidation to sulfines, which in turn can undergo redox cycling or can undergo a further oxidation step to form a reactive sulfenic acid. The report suggests that this is an important mechanism in the lung and liver toxicity of thioureas.[165] Additionally, further oxidation of the intermediate sulfine can lead to sulfenes, which have a comparable reactivity and possess the potential to covalently bond to lipids[166] and cellular proteins.[167] It is also reported that sulfines *in vivo* can rearrange to the reactive oxathiirane intermediate which has the potential to modify proteins or can undergo a desulfurisation process.[164]

1.7 Conclusion

This review has shown that sulfines, especially α-oxo sulfines, merit broader exploration in organic synthesis. The methods used until recently for generation of these highly reactive compounds has been superseded by more robust methods occurring under milder methods, such as the rearrangement of α-sulfinyl carbenes.[67,69] These new methods allow for the design and synthesis of a broader range of sulfines. The reactivity of these sulfines has been manipulated to generate wide libraries of compounds through either thiophilic or carbophilic nucleophilic attacks or cycloadditions such as Diels-Alder reactions and dipolar cycloadditions. Although the high reactivity associated with sulfines presents a challenge to control and exploit, there is no doubt sulfines are useful reactive intermediates with great potential.

Bibliography

(1) Sheppard, W. A.; Diekmann, J. *J. Am. Chem. Soc.* **1964**, *86*, 1891.
(2) Shimada, K.; Kodaki, K.; Aoyagi, S.; Takikawa, Y.; Kabuto, C. *Chem. Lett.* **1999**, *28*, 695.
(3) Okuma, K.; Shigetomi, T.; Nibu, Y.; Shioji, K.; Yoshida, M.; Yokomori, Y. *J. Am. Chem. Soc.* **2004**, *126*, 9508.
(4) Zwanenburg, B. *J. Sulfur Chem.* **2013**, *34*, 142.
(5) Zwanenburg, B. *Phosphorus, Sulfur Silicon Relat. Elem.* **1989**, *43*, 1.
(6) Zwanenburg, B. *Recl. Trav. Chim. Pays-Bas* **1982**, *101*, 1.
(7) Zwanenburg, B.; Damen, T. J. G.; Philipse, H. J. F.; De Laet, R. C.; Lucassen, A. C. B. *Phosphorus Sulfur Silicon Rel. Elem.* **1999**, *153*, 119.
(8) Bent., H. A. *Organic Chemistry of Sulfur*; Plenum Press: New York, 1977.
(9) King, J. F.; Durst, T. In *Tetrahedron Lett.* 1963, p 585.
(10) Block, E.; Penn, R. E.; Olsen, R. J.; Sherwin, P. F. *J. Am. Chem. Soc.* **1976**, *98*, 1264.
(11) Zwanenburg, B.; Thijs, L.; Tangerman, A. *Tetrahedron* **1971**, *27*, 1731.
(12) Tangerman, A.; Zwanenburg, B. *Tetrahedron Lett.* **1973**, *14*, 79.
(13) Lippert, E. *Angew. Chem.* **1960**, *72*, 602.
(14) Benson, S. W. *J. Chem. Educ.* **1965**, *42*, 502.
(15) Virtanen, A. I. *Angew. Chem. Int. Ed. Engl.* **1962**, *1*, 299.
(16) Virtanen, A. I. *Phytochemistry* **1965**, *4*, 207.
(17) Wilkens, W. F., Cornell University, 1961.
(18) Brodnitz, M. H.; Pascale, J. V. *J. Agric. Food. Chem.* **1971**, *19*, 269.
(19) Block, E.; Penn, R. E.; Revelle, L. K. *J. Am. Chem. Soc.* **1979**, *101*, 2200.
(20) Kubec, R.; Cody, R. B.; Dane, A. J.; Musah, R. A.; Schraml, J.; Vattekkatte, A.; Block, E. *J. Agric. Food. Chem.* **2010**, *58*, 1121.
(21) Block, E.; Bayer, T. *J. Am. Chem. Soc.* **1990**, *112*, 4584.
(22) Kubec, R.; Kim, S.; Musah, R. A. *Phytochemistry* **2003**, *63*, 37.
(23) Wedekind, E.; Schenk, D.; Stüsser, R. *Ber. Dtsch. Chem. Ges.* **1923**, *56*, 633.
(24) Opitz, G. *Angew. Chem. Int. Ed.* **1967**, *6*, 107.
(25) Strating, J.; Thijs, L.; Zwanenburg, B. *Recl. Trav. Chim. Pays-Bas* **1964**, *83*, 631.
(26) McGregor, W. M.; Sherrington, D. C. *Chem. Soc. Rev.* **1993**, *22*, 199.
(27) Varma, R. S.; Kumar, D. *Org. Lett.* **1999**, *1*, 697.
(28) Pathak, U.; Pandey, L. K.; Tank, R. *J. Org. Chem.* **2008**, *73*, 2890.
(29) Zwanenburg, B.; Thijs, L.; Strating, J. *Recl. Trav. Chim. Pays-Bas* **1967**, *86*, 577.
(30) van Tilborg, W. J. M. *Recl. Trav. Chim. Pays-Bas* **1976**, *95*, 140.
(31) Khan, A. Z.-Q.; Sandstrom, J.; Wang, S.-L. *J. Chem. Soc., Perk. Trans 2* **1991**, 913.
(32) Walter, W. *Justus Liebigs Annalen der Chemie* **1960**, *633*, 35.
(33) Strating, J.; Thijs, L.; Zwanenburg, B. *Tetrahedron Lett.* **1966**, *7*, 65.
(34) Zwanenburg, B.; Janssen, W. A. J. *Synthesis* **1973**, *1973*, 617.
(35) Marriere, E.; Chevrie, D.; Metzner, P. *J. Chem. Soc., Perk. Trans. 1* **1997**, 2019.
(36) Huang, R.; Espenson, J. H. *J. Org. Chem.* **1999**, *64*, 6935.
(37) Tabuchi, T.; Nojima, M.; Kusabayashi, S. *J. Chem. Soc., Perk. Trans. 1* **1991**, 3043.
(38) A. Koutentis, P.; W. Rees, C. *J. Chem. Soc., Perk. Trans. 1* **1998**, 2505.
(39) El Gokha, A. A.; Ali, O. M.; Zeid, I. F.; Kudoh, T.; El-Sayed, I. *Phosphorus Sulfur Silicon Rel. Elem.* **2013**, *189*, 185.
(40) Okuma, K.; Munakata, K.; Tsubota, T.; Kanto, M.; Nagahora, N.; Shioji, K.; Yokomori, Y. *Tetrahedron* **2012**, *68*, 6211.
(41) Nakayama, J.; Mizumura, A.; Yokomori, Y.; Krebs, A.; Schütz, K. *Tetrahedron Lett.* **1995**, *36*, 8583.
(42) Skold, C. N.; Schlessinger, R. H. *Tetrahedron Lett.* **1970**, *11*, 791.

(43) Zwanenburg, B.; Thijs, L.; Strating, J. *Tetrahedron Lett.* **1968**, *9*, 2871.
(44) Braverman, S.; Grinstein, D.; Gottlieb, H. E. *Tetrahedron* **1997**, *53*, 13933.
(45) Kice, J. L.; Rudzinski, J. J. *J. Am. Chem. Soc.* **1987**, *109*, 2414.
(46) Capozzi, G.; Corti, A.; Menichetti, S.; Nativi, C. *Tetrahedron Lett.* **1997**, *38*, 5041.
(47) Phillips, W. G.; Ratts, K. W. *J. Org. Chem.* **1972**, *37*, 3818.
(48) Braverman, S.; Sredni, B. *Tetrahedron* **1974**, *30*, 2379.
(49) Block, E.; Revelle, L. K.; Bazzi, A. A. *Tetrahedron Lett.* **1980**, *21*, 1277.
(50) Faull, A. W.; Hull, R. *J. Chem. Soc., Perkin Trans. 1* **1981**, 1078.
(51) Black, D.; Fallon, G.; Gatehouse, B.; Wishart, J. *Aus. J. Chem.* **1984**, *37*, 777.
(52) H.R. Barton, D.; Wozniak, J.; Z. Zard, S. *Tetrahedron* **1989**, *45*, 3741.
(53) Bergman, J.; Romero, I. *J. Heter. Chem.* **2010**, *47*, 1215.
(54) Aggarwal, V. K.; Bellus, D.; Collier, S. J.; Dabdoub, M.; Eberbach, W.; Fisera, L.; Heydt, H.; Kappe, C. O.; Kim, S.; Li, J. *Science of Synthesis: Houben-Weyl Methods of Molecular Transformations Vol. 27: Heteroatom Analogues of Aldehydes and Ketones*; Thieme, 2014.
(55) Lenz, B. G.; Regeling, H.; Van Rozendaal, H. L. M.; Zwanenburg, B. *J. Org. Chem.* **1985**, *50*, 2930.
(56) Dentel, H.; Lohier, J.-F.; Gulea, M. *ARKIVOC* **2011**, *6*, 62.
(57) Peterson, D. J. *J. Org. Chem.* **1968**, *33*, 780.
(58) van der Leij, M.; Zwanenburg, B. *Tetrahedron Lett.* **1978**, *19*, 3383.
(59) Braunholtz, W. T. K. *Journal of the Chemical Society, Transactions* **1922**, *121*, 300.
(60) Zwanenburg, B.; Venier, C. G.; Porskamp, P. A. T. W.; van der Leij, M. *Tetrahedron Lett.* **1978**, *19*, 807.
(61) Braverman, S.; van Asten, P. F. T. M.; van der Linden, J. B.; Zwanenburg, B. *Tetrahedron Lett.* **1991**, *32*, 3867.
(62) Franck-Neumann, M.; Lohmann, J. J. *Tetrahedron Lett.* **1979**, *20*, 2397.
(63) Rosati, R. L.; Kapili, L. V.; Morrissey, P.; Bordner, J.; Subramanian, E. *J. Am. Chem. Soc.* **1982**, *104*, 4262.
(64) Rosati, R. L.; Kapili, L. V.; Morrissey, P.; Retsema, J. A. *J. Med. Chem.* **1990**, *33*, 291.
(65) Ebbinghaus, C. F.; Morrissey, P.; Rosati, R. L. *J. Org. Chem.* **1979**, *44*, 4697.
(66) O'Sullivan, O. C. M.; Collins, S. G.; Maguire, A. R.; Bohm, M.; Sander, W. *Eur. J. Org. Chem.* **2006**, 2918.
(67) O'Sullivan, O.; Collins, S.; Maguire, A. *Synlett* **2008**, 659.
(68) Maguire, A. R.; Kelleher, P. G.; Lawrence, S. E. *Tetrahedron Lett.* **1998**, *39*, 3849.
(69) Sander, W.; Strehl, A.; Maguire, A. R.; Collins, S.; Kelleher, P. G. *Eur. J. Org. Chem.* **2000**, 3329.
(70) Collins, S. G.; O'Sullivan, O. C. M.; Kelleher, P. G.; Maguire, A. R. *Org. Biomol. Chem.* **2013**, *11*, 1706.
(71) O'Sullivan, O. C. M.; Collins, S. G.; Maguire, A. R.; Bucher, G. *Eur. J. Org. Chem.* **2014**, 2297.
(72) Bonini, B. F.; Maccagnani, G.; Mazzanti, G. *J. Chem. Soc., Chem. Comm.* **1976**, 431.
(73) Bonini, B. F.; Maccagnani, G.; Mazzanti, G.; Pedrini, P.; Piccinelli, P. *J. Chem. Soc., Perk. Trans. 1* **1979**, 1720.
(74) Powers, D. E.; Arrington, C. A.; Harris, W. C.; Block, E.; Kalasinsky, V. F. *J. Phys. Chem.* **1979**, *83*, 1890.
(75) Karakasa, T.; Motoki, S. *Tetrahedron Lett.* **1979**, *20*, 3961.
(76) Karakasa, T.; Ohmura, H.; Motoki, S. *Chemistry Lett.* **1980**, *9*, 825.
(77) Aitken, R. A.; Drysdale, M. J.; Ryan, B. M. *J. Chem. Soc., Chem. Comm.* **1993**, 1699.
(78) Morita, H.; Takeda, M.; Yoshimura, T.; Fujii, T.; Ono, S.; Shimasaki, C. *J. Org. Chem.* **1999**, *64*, 6730.
(79) Block, E.; Ahmad, S. *J. Am. Chem. Soc.* **1985**, *107*, 6731.

(80) Pelloux-Léon, N.; Minassian, F.; Levillain, J.; Ripoll, J.-L.; Vallée, Y. *Tetrahedron Lett.* **1998**, *39*, 4813.
(81) Kirby, G. W.; McGregor, W. M. *J. Chem. Soc., Perkin Trans. 1* **1990**, 3175.
(82) Capozzi, G.; Fratini, P.; Menichetti, S.; Nativi, C. *Tetrahedron* **1996**, *52*, 12247.
(83) Capozzi, G.; Fratini, P.; Menichetti, S.; Nativi, C. *Tetrahedron* **1996**, *52*, 12233.
(84) Pfeifer, K.-P.; Himbert, G. *Tetrahedron Lett.* **1990**, *31*, 5725.
(85) Siry, S. A.; Timoshenko, V. M.; Bouillon, J.-P. *J. Fluo. Chem.* **2012**, *137*, 6.
(86) van Lierop, J.; Avoird, A. v. d.; Zwanenburg, B. *Tetrahedron* **1977**, *33*, 539.
(87) Sander, W.; Henn, R.; Sundermeyer, W. *Spectrochimica Acta Part A: Molecular Spectroscopy* **1986**, *42*, 1281.
(88) Suzuki, E.; Watari, F. *Spec. Acta Part A: Mol. Biomol. Spec.* **1995**, *51*, 779.
(89) Zwanenburg, B.; Wagenaar, A.; Thijs, L.; Strating, J. *J. Chem. Soc., Perkin. Trans. 1* **1973**, 73.
(90) Petiau, M.; Fabian, J.; Rosmus, P. *Phys. Chem. Chem. Phys.* **1999**, *1*, 5547.
(91) O'Sullivan, O. C. M.; Collins, S. G.; Maguire, A. R.; Böhm, M.; Sander, W. *Eur. J. Org. Chem.* **2006**, 2918.
(92) Baltas, M.; Raouf-Benchekroun, K.; De Blic, A.; Cazaux, L.; Tisnès, P.; Gorrichon, L.; Hussein, K.; Barthelat, J. C. *Tetrahedron* **1996**, *52*, 14865.
(93) Bastin, R.; Albadri, H.; Gaumont, A.-C.; Gulea, M. *Org. Lett.* **2006**, *8*, 1033.
(94) Heras, M.; Gulea, M.; Masson, S.; Philouze, C. *Eur. J. Org. Chem.* **2004**, *2004*, 160.
(95) Watanabe, Y.; Sakakibara, T. *Tetrahedron* **2009**, *65*, 599.
(96) Lucassen, Andre C. B.; Zwanenburg, B. *Eur. J. Org. Chem.* **2004**, *2004*, 74.
(97) Veerapen, N.; Taylor, S. A.; Walsby, C. J.; Pinto, B. M. *J. Am. Chem. Soc.* **2006**, *128*, 227.
(98) Yoshimura, Y.; Yamazaki, Y.; Kawahata, M.; Yamaguchi, K.; Takahata, H. *Tetrahedron Lett.* **2007**, *48*, 4519.
(99) Spry, D. O. *Tetrahedron Lett.* **1972**, *13*, 3717.
(100) Huisgen, R.; Mloston, G.; Polborn, K. *J. Org. Chem.* **1996**, *61*, 6570.
(101) Zwanenburg, B.; Thijs, L.; Broens, J. B.; Strating, J. *Recl. Trav. Chim. Pays-Bas* **1972**, *91*, 443.
(102) Bonini, B. F. *Phosphorus Sulfur Silicon Rel. Elem.* **1993**, *74*, 31.
(103) Braverman, S.; Grinstein, D.; Gottlieb, H. E. *J. Chem. Soc., Perkin Trans. 1* **1998**, 103.
(104) Collins, S. G.; O'Sullivan, O. C. M.; Kelleher, P. G.; Maguire, A. R. *Org. Biomol. Chem.* **2013**, *11*, 1706.
(105) O'Sullivan, O. C. M., University College Cork, 2008.
(106) Porskamp, P. A. T. W.; van der Leij, M.; Lammerink, B. H. M.; Zwanenburg, B. *Recl. Trav. Chim. Pays-Bas* **1983**, *102*, 400.
(107) Rewinkel, J. B. M.; Zwanenburg, B.; García-Granda, S.; Beurskens, P. T.; Raaijmakers, R. *Recl. Trav. Chim. Pays-Bas* **1989**, *108*, 61.
(108) Bonini, B. F.; Maccagnani, G. *Tetrahedron Lett.* **1973**, *14*, 3585.
(109) Bonini, B. F.; Maccagnani, G.; Mazzanti, G.; Zwanenburg, B. *J. Chem. Soc., Chem. Comm.* **1985**, 237.
(110) Di Valentin, C.; Freccero, M.; Gandolfi, R.; Rastelli, A. *J. Org. Chem.* **2000**, *65*, 6112.
(111) Tanaka, J.; Kanemasa, S. *Tetrahedron* **2001**, *57*, 899.
(112) Emamian, S.; Ali-Asgari, S.; Zahedi, E. *J. Chem. Sci.* **2014**, *126*, 293.
(113) Huisgen, R.; Mloston, G.; Polborn, K.; Palacios-Gambra, F. *Liebigs Annalen* **1997**, *1997*, 187.
(114) Huisgen, R.; Mloston, G.; Polborn, K.; Sustmann, R.; Sicking, W. *Liebigs Annalen* **1997**, *1997*, 179.
(115) Adam, W.; Weinkotz, S. *J. Am. Chem. Soc.* **1998**, *120*, 4861.
(116) Adam, W.; Fröhling, B.; Weinkötz, S. *J. Org. Chem.* **1998**, *63*, 9154.

(117) Bonini, B. F.; Maccagnani, G.; Wagenaar, A.; Thijs, L.; Zwanenburg, B. *J. Chem. Soc., Perkin Trans. 1* **1972**, 2490.
(118) Elsäßer, A.; Sundermeyer, W. G. *Chem. Ber.* **1985**, *118*, 4553.
(119) Bonini, B. F.; Maccagnani, G.; Mazzanti, G.; Thijs, L.; Ambrosius, H. P. M. M.; Zwanenburg, B. *J. Chem. Soc., Perkin Trans. 1* **1977**, 1468.
(120) Bonini, B. F.; Maccagnani, G.; Mazzanti, G.; Thijs, L.; Veenstra, G. E.; Zwanenburg, B. *J. Chem. Soc., Perkin Trans. 1* **1978**, 1218.
(121) Machiguchi, T.; Hasegawa, T.; Otani, H.; Yamabe, S.; Mizuno, H. *J. Am. Chem. Soc.* **1994**, *116*, 407.
(122) Mlostoń, G.; Linden, A.; Heimgartner, H. *Helv. Chim. Acta* **1996**, *79*, 31.
(123) Mloston, G.; Heimgartner, H. *Pol. J. Chem.* **1995**, 1649.
(124) Block, E.; Thiruvazhi, M.; Toscano, P. J.; Bayer, T.; Grisoni, S.; Zhao, S.-H. *J. Am. Chem. Soc.* **1996**, *118*, 2790.
(125) Schultz, A. G.; Schlessinger, R. H. *J. Chem. Soc. D: Chem. Comm* **1970**, 748.
(126) Veenstra, G. E.; Zwanenburg, B. *Tetrahedron* **1978**, *34*, 1585.
(127) Ohno, A.; Uohama, M.; Nakamura, K.; Oka, S. *J. Org. Chem.* **1979**, *44*, 2244.
(128) Thijs, L.; Wagenaar, A.; van Rens, E. M. M.; Zwanenburg, B. *Tetrahedron Lett.* **1973**, *14*, 3589.
(129) Loontjes, J. A.; van der Leij, M.; Zwanenburg, B. *Recl. Trav. Chim. Pays-Bas* **1980**, *99*, 39.
(130) Leriverend, C.; Metzner, P.; Capperucci, A.; Degl'Innocenti, A. *Tetrahedron* **1997**, *53*, 1323.
(131) van der Leij, M.; Strijtveen, H. J. M.; Zwanenburg, B. *Recl. Trav. Chim. Pays-Bas* **1980**, *99*, 45.
(132) Veenstra, G. E.; Zwanenburg, B. *Recl. Trav. Chim. Pays-Bas* **1976**, *95*, 195.
(133) Rewinkel, J. B. M.; Porskamp, P. A. T. W.; Zwanenburg, B. *Recl. Trav. Chim. Pays-Bas* **1988**, *107*, 563.
(134) O'Mahony, G. E.; Kelly, P.; Lawrence, S. E.; Maguire, A. R. *Arkivoc* **2011**.
(135) Castedo, L.; Chen, J.; Chiu, C.; Collins, S.; Craig, D. *Science of Synthesis: Houben-Weyl Methods of Molecular Transformations Vol. 31a: Arene-X (X=Hal, O, S, Se, Te)*; Thieme, 2014.
(136) Corbin, F.; Alayrac, C.; Metzner, P. *Eur. J. Org. Chem.* **1999**, *1999*, 2859.
(137) El-Sayed, I. *Monatshefte für Chemie / Chemical Monthly* **2005**, *136*, 543.
(138) Zwanenburg, B.; Thijs, L.; Strating, J. *Recl. Trav. Chim. Pays-Bas* **1970**, *89*, 687.
(139) Cerreta, F.; Leriverend, C.; Metzner, P. *Tetrahedron Lett.* **1993**, *34*, 6741.
(140) van der Leij, M.; Zwanenburg, B. *Recl. Trav. Chim. Pays-Bas* **1980**, *99*, 49.
(141) Schultz, A. G.; Schlessinger, R. H. *J. Chem. Soc. D: Chem. Comm.* **1970**, 747.
(142) Schultz, A. G.; DeBoer, C. D.; Schlessinger, R. H. *J. Am. Chem. Soc.* **1968**, *90*, 5314.
(143) Silhanek, J.; Zbirovsky, M. *J Chem. Soc. D: Chem. Comm.* **1969**, 878.
(144) Chevrie, D.; Metzner, P. *Tetrahedron Lett.* **1998**, *39*, 8983.
(145) Kuipers, J.; Lammerink, B.; Still, I.; Zwanenburg, B. *Synthesis* **1981**, *1981*, 295.
(146) Strating, J.; Thijs, L.; Zwanenburg, B. *Rec. Trav. Chim. Pays-Bas* **1967**, *86*, 641.
(147) Alper, H. *J. Organometallic Chem.* **1975**, *84*, 347.
(148) Mlostoń, G.; Romański, J.; Reisenauer, H. P.; Schreiner, P. R. *Phosphorus, Sulfur, Silicon. Rel. El.* **2011**, *186*, 1175.
(149) Schreiner, P. R.; Reisenauer, H. P.; Romanski, J.; Mloston, G. *J. Am. Chem. Soc.* **2010**, *132*, 7240.
(150) Reisenauer, H. P.; Mloston, G.; Romanski, J.; Schreiner, P. R. *Eur. J. Org. Chem.* **2011**, *2011*, 6269.
(151) Schreiner, P. R.; Reisenauer, H. P.; Romanski, J.; Mloston, G. *Angew. Chem. Int. Ed.* **2009**, *48*, 8133.

(152) O'Sullivan, O. C. M.; Collins, S. G.; Maguire, A. R.; Buche, G. *Eur. J. Org. Chem.* **2014**, 2297.
(153) Mazzanti, G.; Ruinaard, R.; Van Vliet, L. A.; Zani, P.; Bonini, B. F.; Zwanenburg, B. *Tetrahedron Letters* **1992**, *33*, 6383.
(154) Faull, A. W.; Hull, R. *J. Chem. Soc., Perk. Trans. 1* **1981**, 1078.
(155) Lenz, B. G.; Haltlwanger, R. C.; Zwanenburg, B. *J. Chem. Soc., Chem. Comm.* **1984**, 502.
(156) Block, E.; Yencha, A. J.; Aslam, M.; Eswarakrishnan, V.; Luo, J.; Sano, A. *J. Am. Chem. Soc.* **1988**, *110*, 4748.
(157) Saalfrank, R. W.; Rost, W. *Angew. Chem. Int. Ed.* **1985**, *24*, 855.
(158) Adam, W.; Deeg, O.; Weinkötz, S. *J. Org. Chem.* **1997**, *62*, 7084.
(159) Gan, S.; Yin, J.; Yao, Y.; Liu, Y.; Chang, D.; Zhu, D.; Shi, L. *Org. Bio. Chem.* **2017**, *15*, 2647.
(160) Mlostoń, G.; Urbaniak, K.; Gębicki, K.; Grzelak, P.; Heimgartner, H. *Heteroat. Chem,* **2014**, *25*, 548.
(161) Mignolet, B.; Curchod, B. F. E.; Martínez, T. J. *Angew. Chem.* **2016**, *128*, 15217.
(162) Sánchez-Arroyo, A. J.; Pardo, Z. D.; Moreno-Jiménez, F.; Herrera, A.; Martín, N.; García-Fresnadillo, D. *J. Org. Chem.* **2015**, *80*, 10575.
(163) Ogurok, V. M.; Siry, S. A.; Rusanov, E. B.; Shermolovych, Y. G. *J. Fluorine Chem.* **2016**, *189*, 119.
(164) Gan, J.; Ma, S.; Zhang, D. *Drug Met. Rev.* **2016**, *48*, 473.
(165) Henderson, M. C.; Krueger, S. K.; Stevens, J. F.; Williams, D. E. *Chem. Res. Toxicol.* **2004**, *17*, 633.
(166) Ji, T.; Ikehata, K.; Koen, Y. M.; Esch, S. W.; Williams, T. D.; Hanzlik, R. P. *Chem. Res. Toxicol.* **2007**, *20*, 701.
(167) Ikehata, K.; Duzhak, T. G.; Galeva, N. A.; Ji, T.; Koen, Y. M.; Hanzlik, R. P. *Chem. Res. Toxicol.* **2008**, *21*, 1432.

"If you think you'll lose, you're lost,

For out of the world we find,

Success begins with a fellow's will,

It's all in the state of mind."

Walter D. Wintle

Chapter 2

Results and Discussion

Contents

2.1 Background 62
2.2 Objectives 63
2.3 Synthesis of α-diazosulfoxides 63
2.3.1 Synthesis of sulfides 64
2.3.1.1 Synthesis of lactone derived sulfides 64
2.3.1.2 Synthesis of ketone derived sulfides 65
2.3.1.3 Synthesis of monocyclic ketone-derived sulfides 69
2.3.1.4 Synthesis of lactam derived sulfides 69
2.3.2 Synthesis of sulfoxides 73
2.3.2.1 Synthesis of lactone derived sulfoxides 73
2.3.2.2 Synthesis of β-keto sulfoxides 75
2.3.2.3 Synthesis of lactam derived sulfoxides 76
2.3.2.4 Synthesis of lactam derived β-keto sulfones 77
2.3.3 Synthesis of α-diazosulfoxides 79
2.3.3.1 Synthesis of lactone derived α-diazosulfoxides 79
2.3.3.2 Synthesis of ketone derived α-diazosulfoxides under standard batch conditions 81
2.3.3.3 Synthesis of lactam derived α-diazosulfoxides 82
2.3.4 Generation of α-diazosulfoxides in a continuous flow system 83
2.3.4.1 Application of the new continuous flow diazo transfer to ketone derived β-keto sulfoxides 94
2.3.5 Attempted generation of an acyclic α-diazo-β-keto sulfoxide 95
2.3.6 Attempted telescoping of diazo transfer to sulfoxides followed by quench 97
2.3.7 Spectroscopic characteristics of the novel α-diazosulfoxide **81** 100
2.3.8 New batch conditions for the synthesis of α-diazosulfoxides 101
2.3.9 Conclusions 108
2.4 Reactivity of α-diazosulfoxides to form α-oxo sulfines 110
2.4.1 Background 110
2.4.1 Generation of α-oxo sulfines in continuous flow, in the absence of a diene trap 112
2.4.1.1 Transition metal catalysed transformations in continuous flow 115
2.4.2 Thermolysis induced transformations in continuous flow 118
2.4.3 Pre-generation of the α-oxo sulfine in batch with subsequent reactivity in continuous flow 121
2.4.4 Photolysis transformations in continuous flow 124
2.4.4.1 Background 124

2.4.4.2 Photochemical transformations 125
2.4.5 Reactivity of methyl bridgehead α-oxo sulfine **111** 126
2.4.5.1 Reactivity of **111** in continuous flow under transition metal catalysis conditions 126
2.4.5.2 Reativity of **111** in continuous flow under under thermolysis conditions 129
2.4.6 Reactivity of dimethyl α-oxo sulfine **118** in continuous flow 130
2.5 [4+2] Diels-Alder Cycloaddition Reactions 134
2.5.1 Background 134
2.5.2 Transition metal catalysed reactions - Trapping of α-oxo sulfines in a continuous flow system 136
2.5.3 Diels-Alder cycloaddition under photochemical continuous flow conditions 140
2.5.4 Thermolysis reactions carried out in continuous flow 143
2.5.4.1 Background 143
2.5.5 Diels-Alder cycloaddition reactions of lactone derived α-diazosulfoxides in continuous flow 144
2.5.5.1 Thermolytic reactions of ketone derived α-diazosulfoxides in continuous flow conditions 152
2.5.4.2 Thermogravimetric analysis (TGA) of α-diazosulfoxides 161
2.5.5.2 Spectral characteristics of the naphthalene derived cycloadducts 162
2.5.5.3 Extension to the use of cyclopentadiene as a diene trap. 164
2.5.6 Telescoping of the diazo transfer and Diels-Alder cycloaddition reactions 183
2.5.7 Further functionalisation of sulfoxide cycloadducts 189
2.5.7.1 Oxidation of the sulfoxide moiety to sulfone 189
2.5.7.2 Reduction of the sulfoxide moiety to sulfide. 192
2.5.7.3 Pummerer rearrangement type reactions 194
2.5.7.4 Attempted generation of a sulfoximine from the cycloadduct. 197
2.5.7.5 Spectral Characteristics of products formed from these oxidation, reduction, and Pummerer rearrangement transformations 198
2.6 1,3-Dipolar cycloaddition reactions 204
2.6.1 General background 204
2.6.1.1 Sulfines as dipoles 204
2.6.1.2 Sulfines as dipolarophiles; 1,3-dipolar cycloadditions of sulfines with nitrile oxides 205
2.6.1.3 Sulfines as dipolarophiles: Background of 1,3-dipolar cycloadditions of sulfines with nitrones 208
2.6.1.4 Lability of the cycloadduct products 208
2.6.2 Synthesis of nitrones 210
2.6.3 Synthesis of nitrile oxides – experimental design 211

2.7 1,3-Dipolar Cycloaddition reaction of ketone derived α-oxo sulfines with nitrile oxides 215
2.7.1 Initial investigation 215
2.7.1.1 Optimisation of reaction conditions 222
2.7.1.2 Transition metal catalysed batch reactions – isolation of kinetic isomers 224
2.7.1.3 Evidence of proposed mechanism 227
2.7.2 Continuous flow thermolysis reactions – Isolation of thermodynamic isomers 233
2.7.2.1 α-Diazosulfoxide **14** with substituted nitrile oxides 233
2.7.2.2 α-Diazosulfoxide **80** with substituted nitrile oxides 237
2.7.2.3 α-Diazosulfoxide **83** with substituted nitrile oxides 239
2.7.3 Summary of Results 241
2.7.4 Spectroscopic characteristics of cycloadducts 243
2.7.4.1 Spectroscopic characteristics of 1,2,5-oxathiazole-*S*-oxide cycloadducts 243
2.7.4.2 Spectroscopic characteristics of 1,4,2-oxathiazole-*S*-oxide cycloadducts. 249
2.7.4.3 Spectroscopic characteristics of 1,4,2-oxathiazole cycloadducts. 254
2.8 Cycloaddition reactions of lactone derived α-oxo sulfines with nitrile oxides 256
2.8.1 Initial Investigation 256
2.8.2 Attempts at dipolar cycloaddition of lactone derived α-oxo sulfines in continuous flow, and comparison to batch thermolysis 260
2.8.3 Spectroscopic characteristics of lactone derived 1,4,2-oxathiazole-*S*-oxides 264
2.9 1,3-Dipolar cycloadditions of lactone derived α-oxo sulfines with nitrones 268
2.9.1 1,3-Dipolar Cycloadditions of lactone derived α-oxo sulfines with the nitrone 2,3,4,5-tetrahydropyridine 1-oxide **212** 268
2.9.2 1,3-Dipolar Cycloadditions of lactone derived α-oxo sulfines with the nitrone (Z)-*N*-benzyl-1-phenylmethanimine oxide **211** 270
2.9.3 Spectroscopic characteristics of nitrone cycloaddition products 275
2.10 1,3-Dipolar cycloaddition of ketone derived α-oxo sulfines with nitrones 280
2.10.1 1,3-Dipolar Cycloadditions of ketone derived α-oxo sulfines with the nitrone (*Z*)-*N*-benzyl-1-phenylmethanimine oxide **211** 280
2.10.3 Spectroscopic characteristics of nitrone cycloaddition products. 283
2.11 Biological Evaluation 287
2.11.1 Introduction to NCI-60 Cancer Cell-line Screen Programme 288
2.11.2 Evaluation of NCI-60 Cancer Cell-line Screen results 289
2.11.2.1 NCI-60 method of screening 289
2.11.2.2 Biological activity of thiopyran-*S*-oxide and thiopyran-*S,S*-dioxide cycloadducts . 291
2.11.2.3 Biological activity of oxathiazole-*S*-oxide cycloadducts 293
2.11.3 Conclusion of biological evaluation 299

2.12 Concluding remarks 301
3.0 General Procedures 306
3.1 Synthesis of α-diazosulfoxides 308
3.1.1 Procedure for Generating Sodium Methoxide 308
3.1.2 Synthesis of Epoxides 308
3.1.3 Synthesis of sulfides 309
3.1.3.1 Synthesis of lactone derived Sulfides 309
3.1.3.2 Synthesis of ketone derived sulfides 313
3.1.3.3 Synthesis of monocyclic sulfides 320
3.1.3.4 Lactam derived sulfides 321
3.1.4 Synthesis of Sulfoxides 326
3.1.4.1 Lactone derived sulfoxides 326
3.1.4.2 Benzofused Ketone derived sulfoxides 330
3.1.4.3 Monocyclic ketone derived sulfoxides 332
3.1.4.4 Lactam derived sulfoxides 333
3.1.5 Synthesis of Sulfones 334
3.1.6 Synthesis of α-diazosulfoxides under standard batch conditions 335
3.1.7 Synthesis of α-diazosulfoxides in continuous flow 340
3.1.7.1 General method for diazo transfer in continuous flow using homogeneous bases 342
3.1.7.2 Diazo transfer in a continuous flow system using solid supported bases. 343
3.1.7.3 General procedure for diazo transfer using polystyrene supported 1,8-diazabicyclo undec-7-ene (PS - DBU) as base 344
3.1.7.4 General procedure for diazo transfer using solid supported bases 344
3.1.7.5 General Procedure for the Synthesis of α-Diazosulfoxides Using Amberlyst A21 (5 eq) as base. 345
3.1.8 New batch conditions for the synthesis of α-diazosulfoxides in batch reaction conditions. 351
3.2 Reactivity of α-diazosulfoxides in continuous flow. 358
3.2.1 Sacrifical quench of Dodecylbenzenesulfonyl azide in batch [29] 358
3.2.2 Application of a sacrificial sulfonyl azide quench as reported in the literature by Maguire *et al.*[29] 358
3.2.3 Telescoped sacrificial quench study in continuous flow – modified procedure from Maguire *et al.*[29] 359
3.2.4 Reactivity and transformations of α-diazosulfoxides in continuous flow. 360
3.2.5 Reactivity of cyclohexyl derived α-diazosulfoxide. 360
3.2.6 Photochemical Decomposition Reactions: 366

3.2.7 Photochemically induced transformations of α-diazosulfoxides. 366

3.2.8 Reactivity of the methyl bridgehead α-diazosulfoxide **76** in a continuous flow system.368

3.2.9 Reactivity of the *trans* - dimethyl α-oxo sulfine in continuous flow, with pre-generation of the α-oxo sulfine using transition metal catalysis. 371

3.3 Diels-Alder cycloadditions 374

3.3.1 UV-150 reaction promoted Diels-Alder cycloaddition. 379

3.3.2 Diels-Alder cycloadditions using thermolysis. 380

3.3.3 Thermolysis conditions for Diels-Alder cycloadditions of ketone derived α-oxo sulfines. 384

3.3.4 Cycloaddition reaction with cyclopentadiene as the diene and α-oxo sulfines as the dieneophiles. 388

3.3.5 Cycloaddition of lactone derived α-diazosulfoxide **38,39** with cyclopentadiene **149** in continuous flow. 392

3.4 Telescoping the diazo transfer process, with the hetero-Wolff rearrangement and subsequent Diels-Alder cycloaddition reaction. 395

3.5 Further fuctionalisation of Diels-Alder sulfoxide cycloadducts. 398

3.5.1 Oxidation to sulfone 398

3.5.2 Oxidation to β-epoxy sulfone. 401

3.5.3 Reduction to sulfides. 402

3.5.4 Pummerer rearrangements 404

3.5.5 Attempted synthesis of sulfoximine **190** 407

3.6 Synthesis of dipole precursors and dipoles. 408

3.6.1 Generation of Nitrones. 408

3.6.2 Syntheis of Oximes 409

3.6.3 Synthesis of Imidoyl chlorides 411

3.7 1,3-Dipolar cycloaddition reaction 415

3.7.1 Nitrile oxide and ketone derived α-oxo sulfine dipolar cycloaddition reactions 415

3.7.1.1 Optimisation reactions for the dipolar cycloadditons of nitrile oxide and ketone derived α-oxo sulfine. 415

3.7.1.2 Cycloaddition reactions of α-diazosulfoxide **14** with nitrile oxide dipoles under both batch and continuous flow conditions. 425

3.7.1.3 Dipolar cycloadditions of α-diazosulfoxide **80** with nitrile oxides. 434

3.7.1.4 Dipolar cycloaddition of α-diazosulfoxide **83** with nitrile oxides 439

3.7.1.5 Attempted cycloaddition reactions with *N*-hydroxyisonicotinimidoyl chloride 445

3.7.3.7 Attempted trapping of enolate intermediate 446

3.7.2 Nitrile oxide and lactone derived α-oxo sulfine dipolar cycloaddition reactions 447

3.7.3 Cycloaddition reaction of lactone derived α-oxo sulfine with nitrile oxide dipole in continuous flow. 451

3.7.4 Nitrone and lactone derived α-oxo sulfine dipolar cycloaddition reactions 454

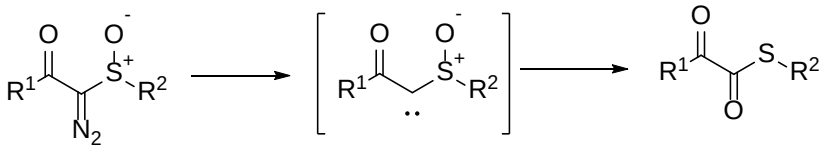
3.7.5 Nitrone and ketone derived α-oxo sulfine dipolar cycloaddition reactions 460

3.8 Bibliography 463

2.1 Background

Investigations into the synthesis and reactivity of α-diazosulfoxides has been a consistent line of research within our group with over 20 years.[1-3] Before these investigations, it was believed that α-diazosulfoxides were inherently unstable and not isolable. Work within this group has showcased both their stability and versatility in organic synthesis. Under transition metal catalysis, photolysis, thermolysis or microwave irradiation conditions, reactive α-oxo sulfines are generated.[4,5] These sulfines have great potential to be used in organic synthesis, as detailed in Chapter 1 and recent literature.[6,7]

The first two reported examples of stable α-diazosulfoxides in the literature were the cephalosporin derivatives by Rosati[8] and Campbell (Figure 1).[9,10] However, the uniqueness and importance of these isolated examples was not noted by the authors. Hodson and Holt[11] described α-diazosulfoxides as being reactive intermediates, unable to be isolated. The authors were successful in isolating thiol esters and sulfonamide by-products, which showed the α-diazosulfoxide had indeed formed, but had undergone further reaction due to its labile nature (Scheme 1).



Scheme 1

We proposed that the reason cephalosporin derived α-diazosulfoxides (Figure 1) are stable is because of the reduced conformational mobility, due to the strained bicyclic system, which depletes the chance of spontaneous diazo decomposition.

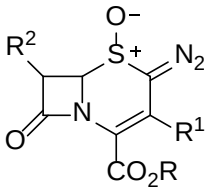
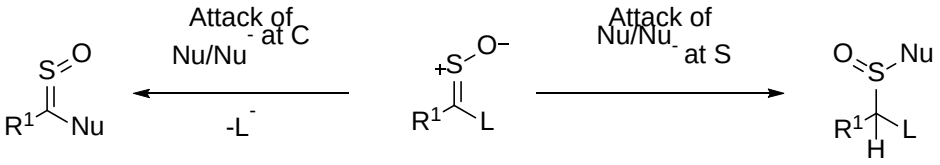


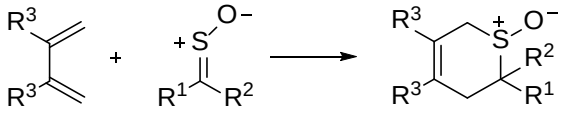
Figure 1: Cephalosporinate derived α-diazosulfoxide as described by Rosati and Campbell.

To investigate whether this was the case, a series of bicyclic lactone and lactam based sulfoxides were synthesised. These successfully underwent diazo transfer and a series of α-diazosulfoxides were isolated by Kelleher and Collins.[12-14] This work was expanded further by O'Sullivan who characterised some α-oxo sulfines and investigated conditions used for induction of the hetero-Wolff rearrangement,[4,5,15] and then Buckley who investigated nucleophilic addition (Scheme 2).

[4+2] Diels Alder cycloaddition reactions of sulfines under various reaction conditions have also been of significant interest throughout the duration of this line of research (Scheme 3).[16]



Scheme 2



Scheme 3

With this previous work in mind, the objectives for this research project were established.

2.2 Objectives

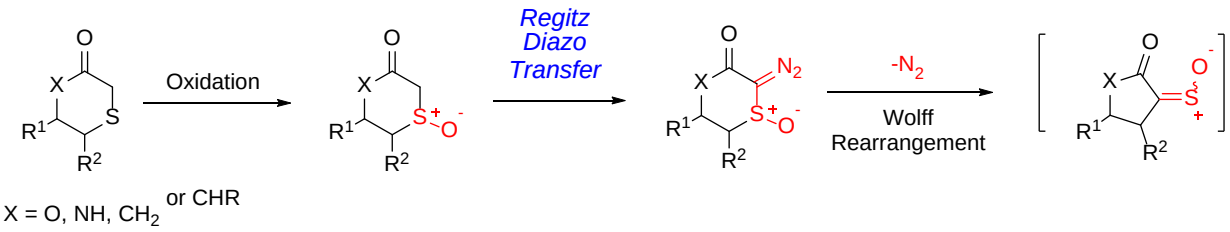
This initial aim in this work was to synthesise a series of lactone, lactam and ketone derived sulfoxides. On obtaining these compounds the focus of the work would be to:

- investigate the diazo transfer process to β-oxo sulfoxides in continuous flow, with an aim of successfully optimising the reaction conditions to provide increased yields of the desired α-diazosulfoxide.
- apply the new continuous flow diazo transfer reaction conditions to a range of substrates.
- investigate the reactivity of the α-diazosulfoxides in continuous flow.
- telescope the continuous flow diazo transfer reaction conditions with induction of the hetero-Wolff rearrangement.
- carry out an investigation in to the 1,3-dipolar cycloaddition of α-oxo sulfines with nitrone and nitrile oxide dipoles.

2.3 Synthesis of α-diazosulfoxides

Maguire and Kelleher[1] first prepared bicyclic and monocyclic lactone based α-diazosulfoxides showing that the reduced conformational mobility was responsible for their stability. Collins[13] built on this work and successfully designed and synthesised a range of lactone and lactam based α-diazosulfoxides. Buckley subsequently designed and synthesised a range of ketone derived α-diazosulfoxides. The first step in the synthesis of these labile compounds is the generation of the

sulfide precursors which can then be oxidised and undergo a Regitz diazo transfer step. The novel reactivity of these α-diazosulfoxides is their ability to undergo the hetero-Wolff rearrangement to form α-oxo sulfines in short reaction times and under mild reaction conditions (Scheme 4).

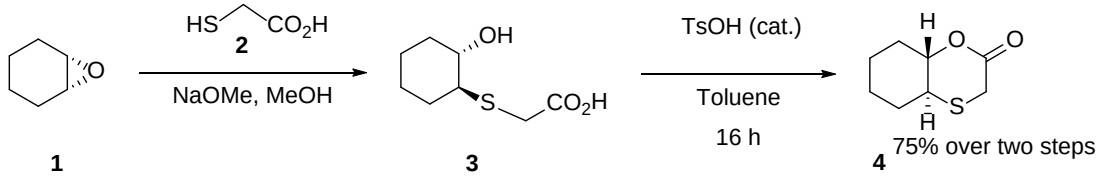


Scheme 4

2.3.1 Synthesis of sulfides

2.3.1.1 Synthesis of lactone derived sulfides

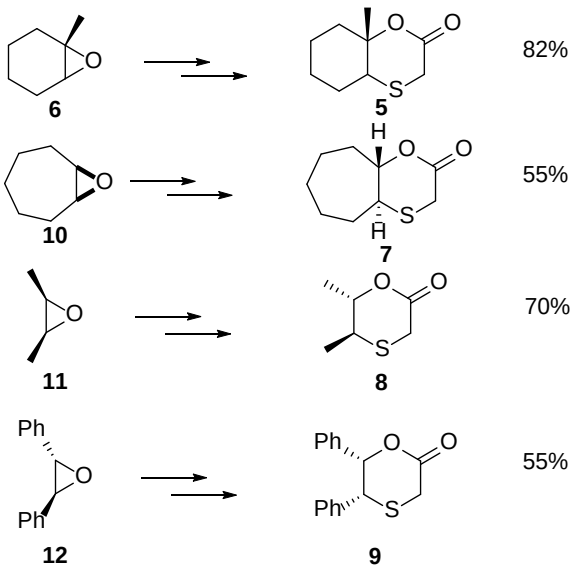
Routes to the lactone derived sulfides are reported in the literature[13] and were originally described by Koskimies.[17] For this project, the epoxide **1** is ring opened *via* a S_N2 nucleophilic attack of the thioglycolic acid **2** dianion which is prepared using freshly prepared sodium methoxide. Attack occurs only by the sulfur anion as it is more nucleophilic than the oxygen. After completion of this step, the reaction mixture is acidified with concentrated hydrochloric acid to pH 1 producing the hydroxy acid **3**. Due to the tendency of the hydroxy acid **3** to spontaneously cyclise it is not isolated, and undergoes lactonisation in Dean-Stark conditions using *p*-toluenesulfonic acid as the catalyst to generate the lactone **4** in 75% yield over the two steps. A basic workup was sufficient to remove the catalyst and provide the sulfide product (Scheme 5).



Scheme 5

This methodology was used to synthesise a range of lactone derived sulfides which are suitable for oxidation to sulfoxide level and subsequent diazo transfer to form the corresponding α-diazosulfoxides. For the methyl-bridgehead substituted sulfide **5**, the epoxide **6** is first generated through an *m*-CPBA epoxidation of the corresponding alkene and the pure epoxide **6** is isolated in a yield of 58%. The yields of sulfide **5**, **7**, **8** and **9** were moderate to good across each of the epoxide substrates **6**, **10**, **11** and **12** (Scheme 6) and the crude lactonisation products were often

pure on analysis of the ^{1}H NMR spectrum, and carried through to the next step without further purification. A hot recrystallisation from ethyl acetate was employed if purification was needed.

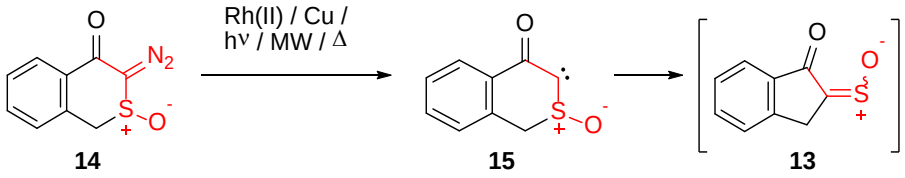


Scheme 6

Sulfides **5**, **7**-**9** have been previously characterised in the group and spectral characteristics were consistent with earlier reports. The yields and quality of the products were comparable.

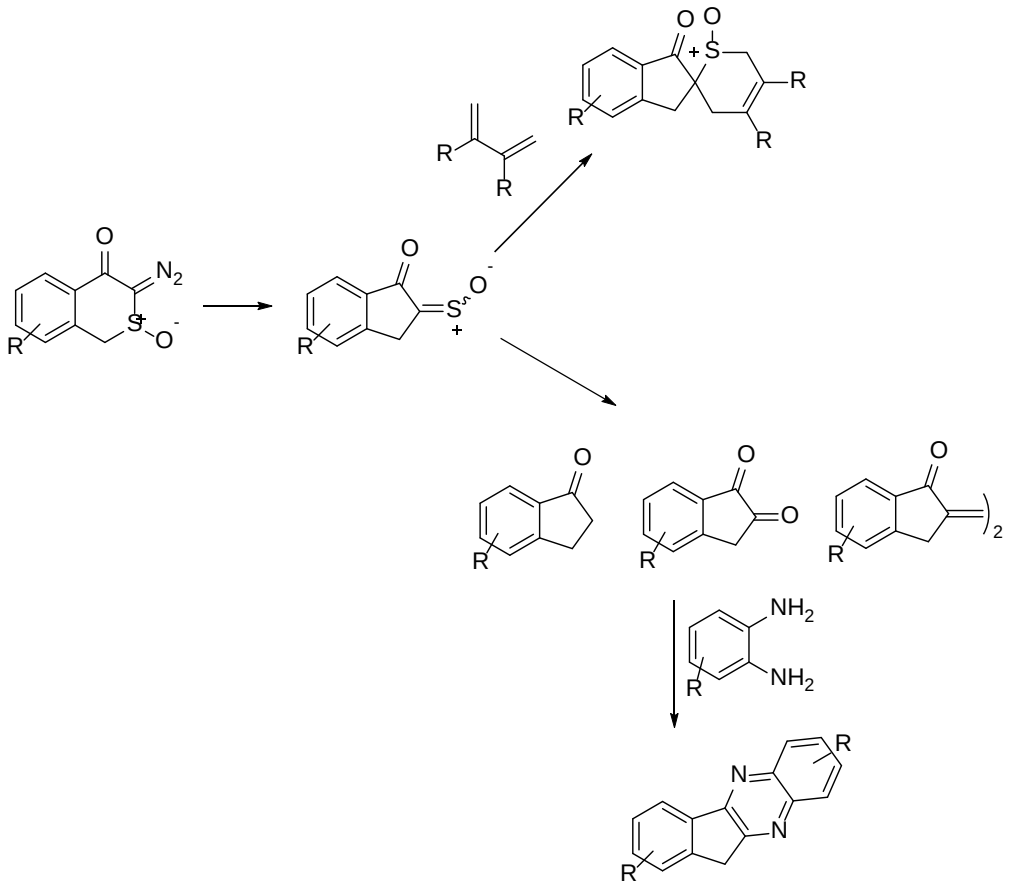
2.3.1.2 Synthesis of ketone derived sulfides

Regitz diazo transfer to β-keto sulfoxides was first carried out within our research group by Buckley, to generate novel α-diazosulfoxides.[16] Under transition metal catalysis, microwave irradiation, photolysis and thermolysis, the α-oxo-sulfine **13** is generated from the α-diazosulfoxide **14** and corresponding carbene **15** *via* the hetero-Wolff rearrangement.



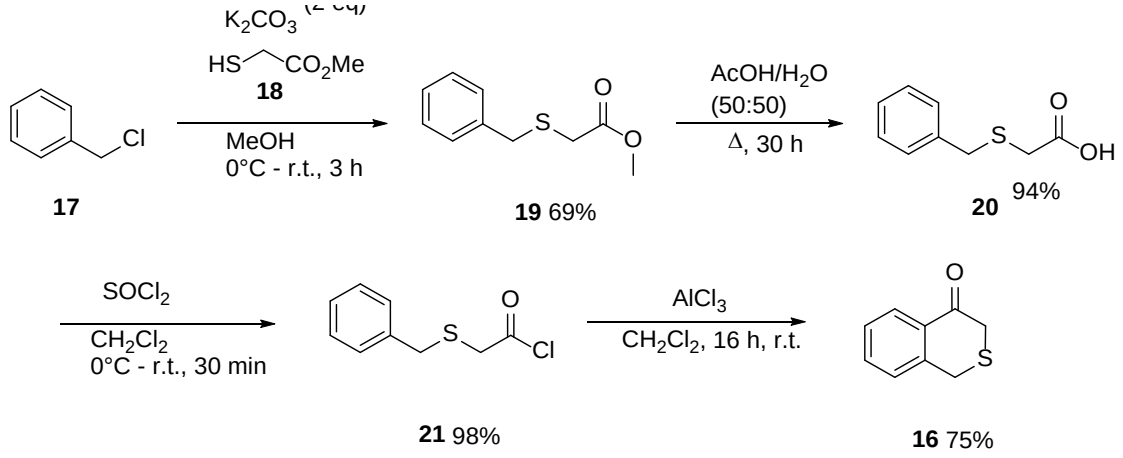
Scheme 7

The work carried out by Buckley is summarised in Scheme 8 below including Diels-Alder cycloadditions to the α-oxo sulfine along with studies of the transformation of the α-oxo sulfine in the absence of a diene trap (Scheme 8), see section 2.4 for further discussion.



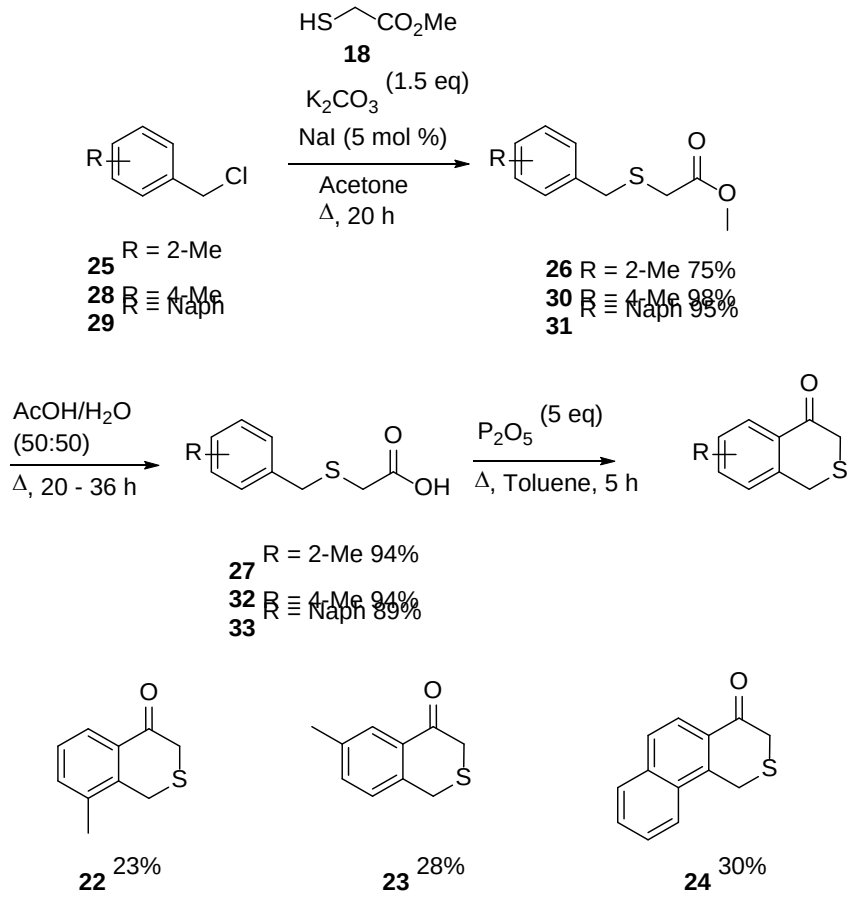
Scheme 8

The route to the ketone derived sulfide **16** was first reported by Akkurt[18] and after extensive optimisation by Buckley, an efficient synthetic route to substituted sulfides was established (Scheme 9).[16] The first step in the synthetic sequence, consists of a reaction of benzyl chloride **17** and methyl thioglycolate **18** to generate the sulfide ester **19**. Hydrolysis of the ester **19** is carried out using acetic acid/water mixture (50:50) at reflux and proceeds in an almost quantitative yield to form the desired acid **20**. The acid **20** is converted to the acid chloride **21** quantitatively using thionyl chloride and the final step is a Friedel-Crafts type cyclisation to form the ketone derived sulfide **16** (Scheme 9). The intramolecular cyclisation and dehydration was inconsistent across the acid substrates **27,32,33** (Scheme 10) with regards to the yield and some investigation in to the optimum reaction conditions were carried out during this work. A similar cyclodehydration procedure has recently been described by Aitken for the synthesis of the cyclic sulfide **16** where a combination of phosphorus pentoxide and Celite® are used to induce the transformation directly from the carboxylic acid.[19]



Scheme 9

A literature procedure described by Ramadas was applied in this work, for generation of the substituted sulfides **22, 23** and **24** (Scheme 10).[20] The final step in the synthesis of these sulfides is a direct cyclisation in a cyclodehydration step, which involved an intramolecular Friedel-Crafts reaction of the acid directly to the sulfide.[20] 2-Methylbenzyl chloride **25** was reacted with methyl thioglycolate **18** in the presence of potassium carbonate and catalytic sodium iodide to give the methyl ester **26** in a good yield. Hydrolysis of the ester **26** in refluxing acetic acid and water leads to the acid **27** in 94% yield. Using a procedure previously established by Buckley, cyclisation and dehydration *via* an intramolecular Friedel-Crafts reaction with five equivalents of phosphorous pentoxide leads to the cyclic sulfide **22** in a yield of 23 % after purification by column chromatography. The same sequence of reactions and reaction conditions are applied to the substituted benzyl chlorides **28** and **29,** resulting in the formation of the ester intermediates **30** and **31**, which are subsequently converted to the acids **32,33**. Following cyclisation the desired sulfides **23** and **24** were isolated in yields of 28% and 30% respectively after purification (Scheme 10).



Scheme 10

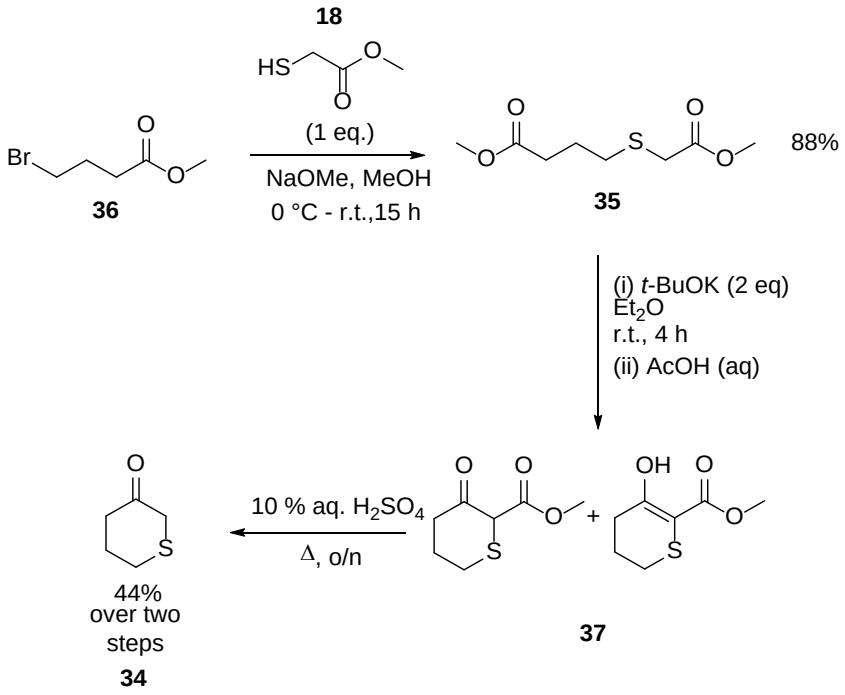
Recently, Aitken has described similar reaction conditions for this cyclodehydration step, and these were used for the synthesis of the sulfide **24** in this work.[19] The naphthalene derived acid **33** was subjected to the described reaction conditions and the reaction mixture was quenched after 3 h at reflux and the analysis of the ^{1}H NMR spectrum of the crude material showed a ratio of starting material to product as 3.5 : 2, along with the formation of impurities. Purification of this reaction mixture led to the elution of the cyclised product **24** along with a minor impurity in a yield of 8%. A third set of reaction conditions was used for the attempted cyclisation to the sulfide **24**, whereby a combination of Aitken and Buckley's methods was attempted. A mixture of Celite®, **33**, and phosphorus pentoxide (2 equivalents) was heated to reflux for 2 h. On cooling a further 3 equivalents of Celite® was added and heated to reflux again. Analysis of the crude material showed the absence of the desired sulfide **24**.

Although the yield from this cyclisation and dehydration step was moderate, the cyclised sulfides **16,22–24** were still available in multigram quantities. These sulfides were found to be relatively unstable and short lived at room temperature and were stored in the dark, in the freezer to

successfully prevent decomposition to unidentified, highly coloured, intractable material. The sulfides were typically used within 24 h of purification.

2.3.1.3 Synthesis of monocyclic ketone-derived sulfides

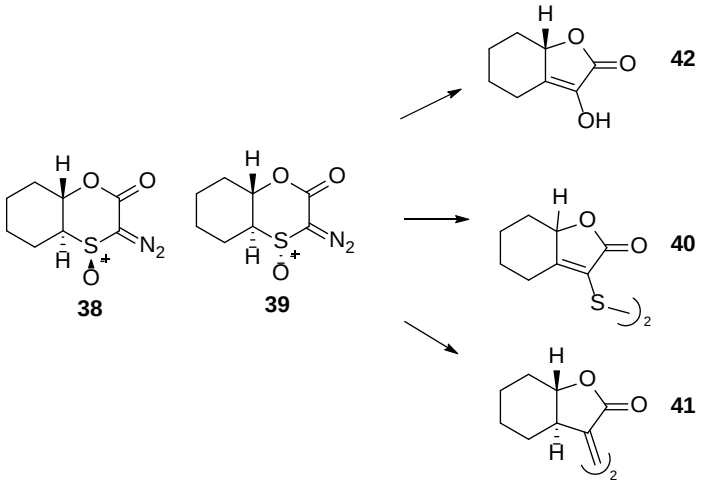
Previously, when monocyclic ketone derived sulfides were synthesised and isolated within the group, the isolated yields after purification were low.[16] The monocyclic sulfide **34** was synthesised using conditions optimized by Buckley, which were a modification of a procedure described by Kamenka.[21] Generation of the diester **35** is achieved through condensation of methyl thioglycolate **18** with the alkyl bromide **36**. Cyclisation of the diester **35** to the cyclic sulfide **34** is achieved using a Dieckmann condensation reaction. An intermediate keto-enol mixture **37** initially forms which subsequently undergoes hydrolysis and decarboxylation at high temperatures to give the desired sulfide **34** (Scheme 11) in 44% isolated yield from **35**.



Scheme 11

2.3.1.4 Synthesis of lactam derived sulfides

In this research group, investigations into the decomposition pathways of lactone derived α-diazosulfoxides, such as **38,39**, have provided invaluable insight in to the reactivity of these types of compounds and novel routes to other compounds such as the disulfide **40**, the substituted alkene dimer **41** and the enol derivative **42** (Scheme 12).



Scheme 12

With this reactivity in mind it was decided to synthesise a range of lactam derived α-diazosulfoxides and investigate their transformations to α-oxo sulfines. The synthesis, isolation and characterisation of lactam derived α-diazosulfoxides was first reported by Collins.[13] The syntheses of the lactam derived sulfides, **43** and **44** were reported by Ruano[22] in 1992 (Figure 2).

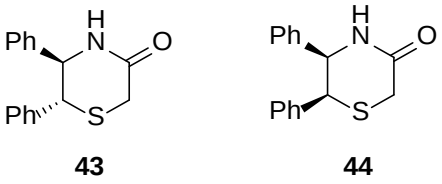
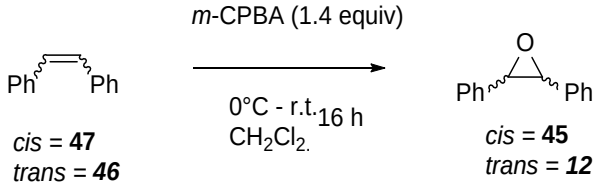


Figure 2: Di-phenyl lactam derived sulfides.

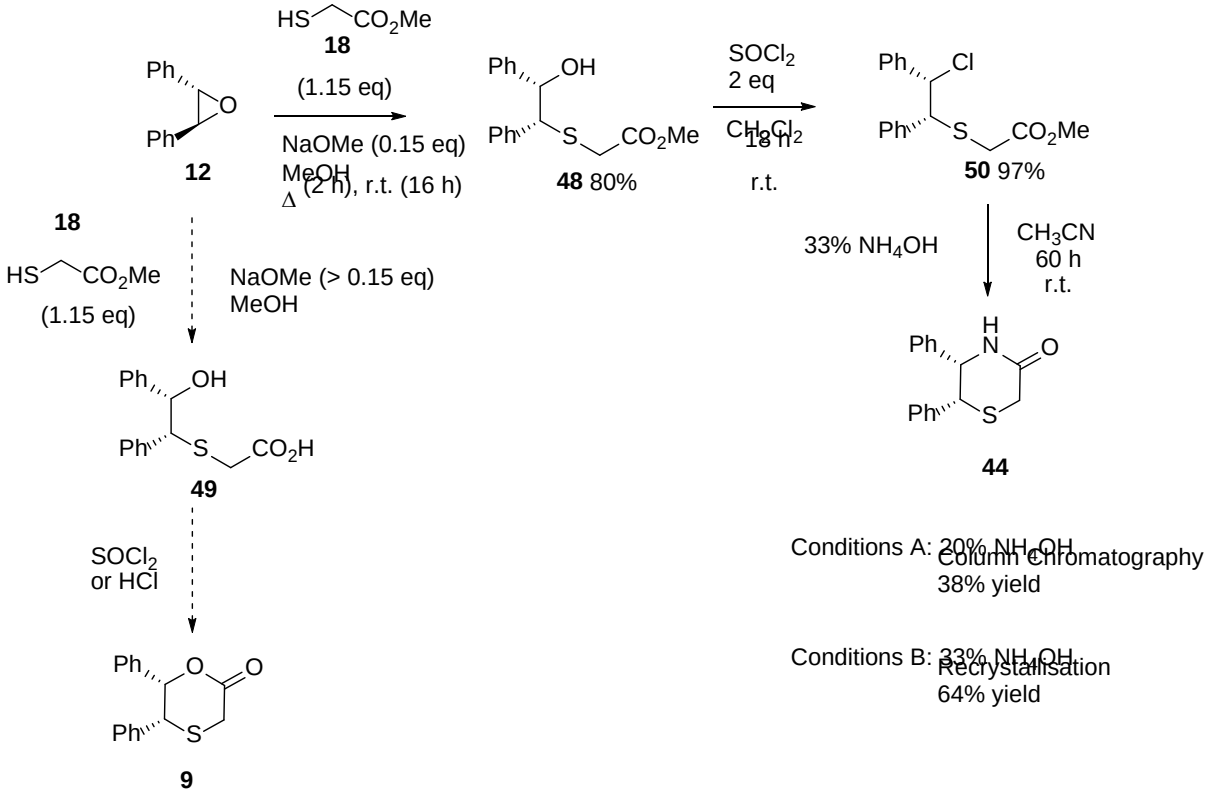
In Ruano's reported procedure the synthesis of the thiomorpholinone rings begins from their epoxide precursors; *trans* stilbene oxide **12**[14] and *cis* stilbene oxide **45**.[14] In this work, the epoxides were synthesised from *trans* stilbene **46** and *cis* stilbene **47** using *m*-CPBA at 0°C, increasing to room temperature over 16 h (Table 1).

Table 1: Yields of epoxidation reactions.



Entry	Alkene	Yield (%)
1	*cis* stilbene	93
2	*trans* stilbene	86

Methyl thioglycolate **18** was reacted with *trans*-stilbene oxide **12** and a catalytic amount of freshly prepared sodium methoxide (0.15 equiv) to give the hydroxy ester **48** in 80% yield without the need for further purification (Scheme 13). Catalytic amounts of base are needed as larger amounts result in the hydroxyacid **49**, which on treatment with thionyl chloride or hydrochloric acid would lactonise forming the undesired lactone by-product **9**. The hydroxy ester **48** was transformed to the chloro ester **50** on treatment with 2 equivalents of thionyl chloride resulting in 97% yield. The reaction of the chloroester **50** with 20% NH_4OH gave the desired lactam **44** in 38% yield after column chromatography. It was proposed that part of the reason for the low yield was difficulty in purifying the lactam **44** by column chromatography on silica gel. On repeating the procedure using 33% NH_4OH and then repeated recrystallisations with hot ethyl acetate, the desired product is isolated in an improved yield of 64%.



Scheme 13

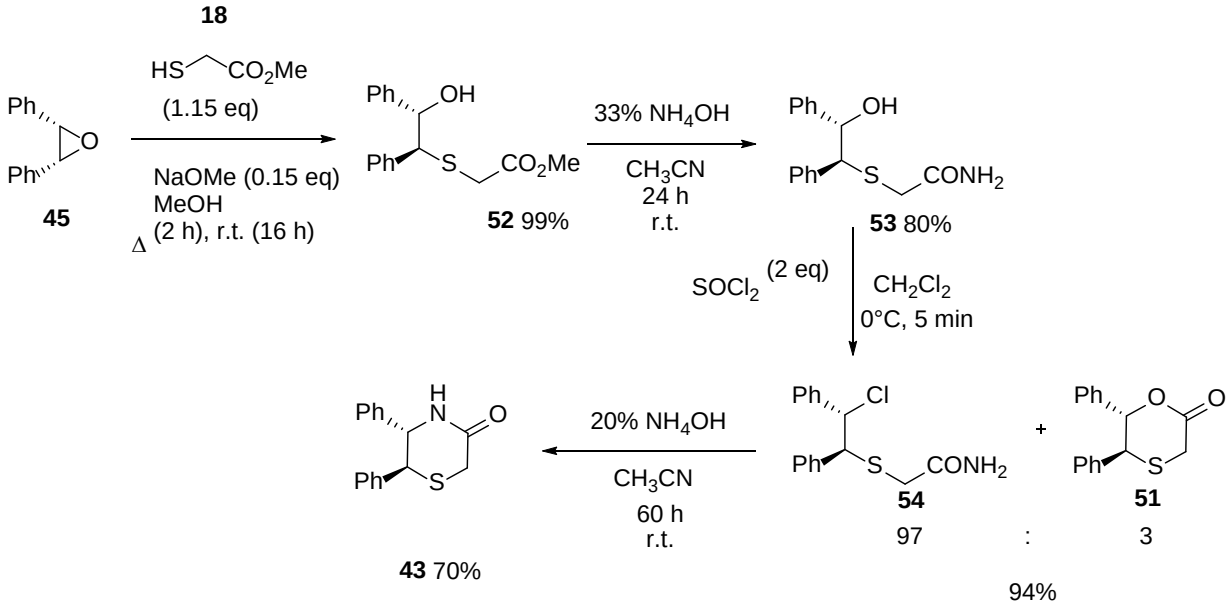
The synthesis of the *trans*-diphenyl thiomorpholinone **43** begins with *cis*-stilbene oxide **45** and methyl thioglycolate **18** (Scheme 14). Ruano reports that the trans disposition of the phenyl groups encourages the formation of the lactone **51** when reacted with thionyl chloride. To avoid this happening, it is essential to convert the ester functionality in **52** to the amide **53** before the hydroxyl group is replaced with a chloride. This transformation is carried out on treatment with

20% ammonium hydroxide for 12 h. The crude product is recrystallized from ethyl acetate providing the hydroxy amide **53** in 80% yield. Chlorination of the hydroxy amide **53** is carried out using one equivalent of thionyl chloride at room temperature. A short reaction time is needed as well as low temperature to reduce the rate of lactone **51** formation. The results with varying reaction conditions are outlined in Table 2 below**.**

Table 2: Product ratios on addition of $SOCl_2$

Temperature	Time	Ratio of chloro amide 54 : lactone 52
Room Temperature	16 h	1:1
Room Temperature	5 min	85:15
0°C	5 min	97:3

The mixture of the chloro-amide **54** and lactone **51** is used in the next step where they form the desired lactam **43** and the hydroxy amide **53** respectively. The hydroxy amide **53** is re-formed by ring opening of the lactone **51** by ammonia and the two products are easily separated by recrystallisation. The crude product is repeatedly recrystallized from ethyl acetate to isolate the pure lactam **43** in 70% yield and as a white crystalline solid. This is compared to 34% when purified by column chromatography.[14]



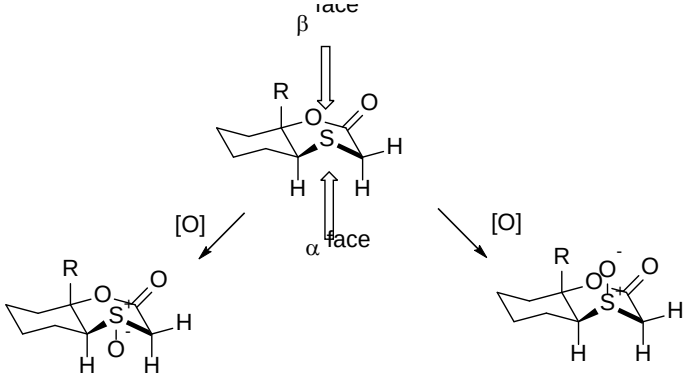
Scheme 14

Following the successful synthesis of the lactam derived sulfides **44** and **43**, in three and four steps from the *cis* and *trans* diphenyl epoxides respectively, sulfoxidation of the sulfides became the next aim of this work.

2.3.2 Synthesis of sulfoxides

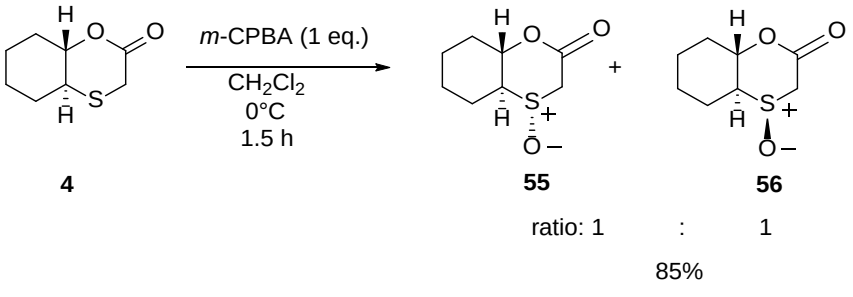
2.3.2.1 Synthesis of lactone derived sulfoxides

Oxidation of the lactone derived sulfides is carried out in dichloromethane using one equivalent of *m*-CPBA as the oxidant (Scheme 16). The sulfoxidation reactions are typically complete within 1.5 - 3 h, and the *m*-chlorobenzoic acid by-product is removed by a basic work-up. As oxidation of the sulfur forms a new chiral centre, there is the potential for the formation of 2 diastereomers, depending on whether the oxidant approached from the α or β face (Scheme 15).



Scheme 15

Typically for the oxidation of the cyclohexyl sulfide **4** the sulfoxidation shows essentially no diastereoselectivity (Scheme 16) for the formation of the pseudo[i]-equatorial **55** and pseudo-axial **56** sulfoxides in a ratio of 1:1.

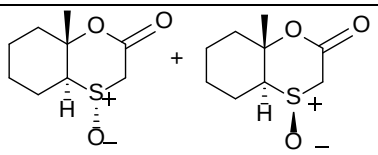
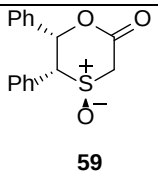
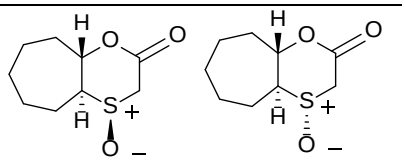


Scheme 16

[i] The term "pseudo" has consistently been used within our research group with regards to the axial or equatorial orientation of the sulfoxide oxygen.

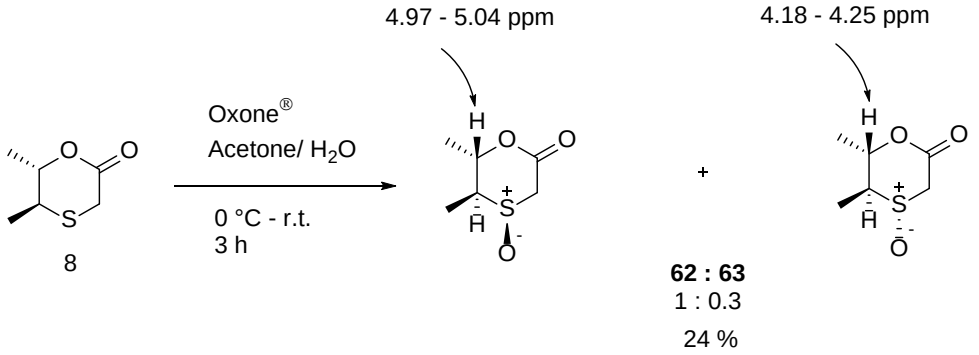
Separation of the diastereomers **55** and **56** can be achieved by repeated chromatography on silica gel, or by slow recrystallisation of the diastereomeric mixture from dichloromethane/hexane. With the range of lactone derived sulfides, oxidation is also carried out with *m*-CPBA. For the methyl bridgehead sulfide **5**, and *cis*-diphenyl derivative **9**, oxidation occurs preferentially from the β face showing high diastereoselectivity in formation of the sulfoxides **57**,**58** and **59** respectively, caused by steric hindrance to approach from the opposite face. For the cycloheptene derived sulfoxides **60** and **61**, the oxidation is carried out by sodium periodate in aqueous methanol, which were the optimal conditions for this substrate previously established within the group.[16] Purification is carried out by column chromatography on silica gel. The lower isolated yield may be due to ring opening of the lactone moiety due to adventitious methanol (Table 3).[15]

Table 3: Sulfoxidation reaction conditions and yields

Entry	**1**	**2**	**3**
Product	 **Major 57** **Minor 58**	 **59**	 **60** **61**
Conditions	*m*-CPBA/CH_2Cl_2 0°C – r.t., 1.5 h	*m*-CPBA/CH_2Cl_2 0°C – r.t., 1.5 h	$NaIO_4$/MeOH 0°C – r.t., 2.5 h
Product Ratio	9.5:1	1:0	1:1
Yield	70%	64%	28%

The *trans*-dimethyl monocyclic sulfoxides **62** and **63** were synthesised *via* oxidation of the sulfide **8** using Oxone® as the oxidising reagent in aqueous acetone which leads to the formation of two diastereomers in the ratio of 1 : 0.3 (Scheme 17). The sulfoxides **62** and **63** were fully characterised as they are both novel compounds. The stereochemistry of the major diastereomer **62**, with the pseudo-axial orientation of the sulfoxide oxygen, is assigned on the basis of the C*H*O signal in the ^{1}H NMR spectra but has not been structurally confirmed. This signal appears as a multiplet between 4.97 – 5.04 ppm, whereas the corresponding signal for the minor equatorial sulfoxide **63**

is between 4.18 – 4.25 ppm. The difference between these two signals is due to a 1,3 interaction between the sulfoxide moiety and C*H*O proton, as discussed by Collins[14] and Evans.[23] In line with the cycloheptene derivatives **60** and **61** the low yield of **62** and **63** could be due to ring opening of the lactone in the aqueous conditions and subsequent losses in water washes.



Scheme 17

2.3.2.2 Synthesis of β-keto sulfoxides

In earlier work carried out by Buckley, a range of conditions for sulfoxidation reactions were screened on each of the ketone derived sulfide precursors. The various reaction conditions used included *m*-CPBA in dichloromethane, Oxone® in aqueous acetone and sodium periodate in aqueous methanol. The optimal conditions for each derivative established by Buckley were used for the generation of the range of β-keto sulfoxides in this work. Each of the reaction conditions include addition of the oxidant at 0°C over a period 10 – 20 minutes, in an attempt to prevent over oxidation to the corresponding sulfone. The sulfoxides **64** and **65** were each synthesised using sodium periodate as the oxidant following a standard procedure while sulfides **22, 23, 24** were oxidized to the corresponding sulfoxides **66**, **67,** and **68** using Oxone® as oxidant (Figure 3).

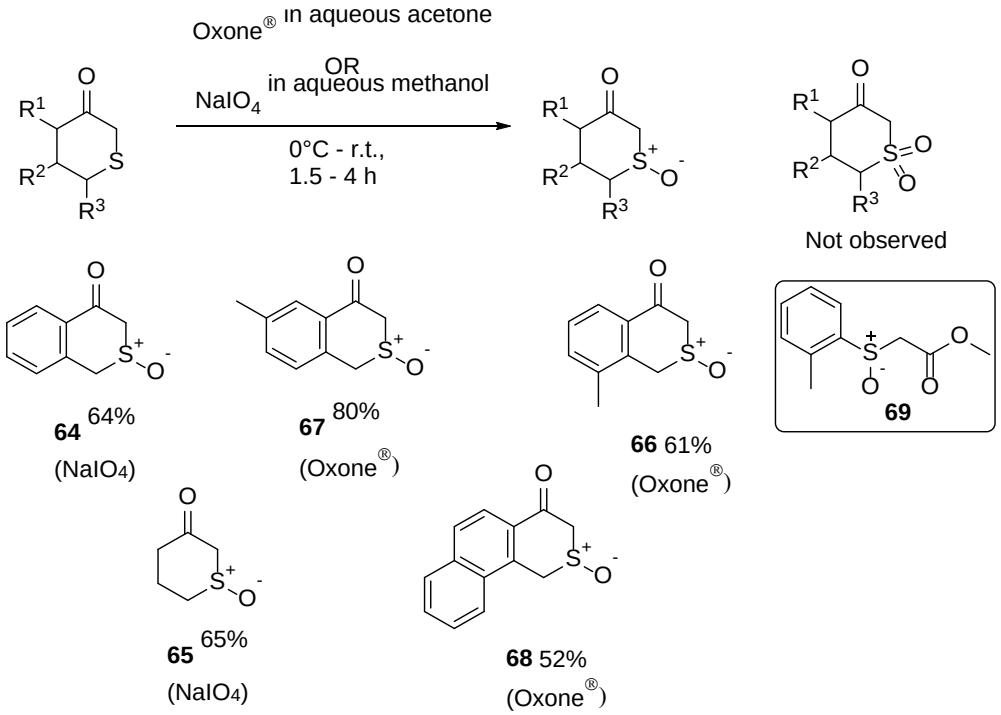
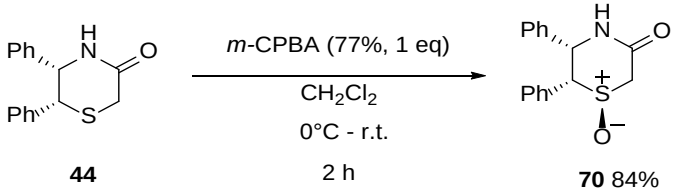


Figure 3: Results of sulfoxidation reactions.

The exceptionally polar compounds **64–68** were obtained in good yield as white crystalline solids and did not require further purification after aqueous work up. The sulfoxides **64–68** possess a similar stability profile as the sulfides and to prevent thermal or photochemical decomposition, they are kept in the freezer after preparation and used within 24 h. Notably, in one case, on sulfoxidation of an impure sample of the sulfide **22** the acyclic sulfoxide **69** was isolated in one fraction from the column (~8%) and was later used in an attempt to make an acyclic α-diazosulfoxide (Section 2.3.5).

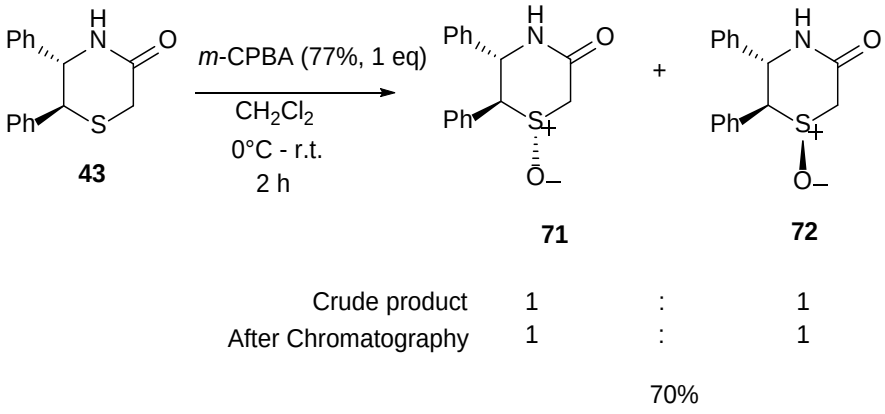
2.3.2.3 Synthesis of lactam derived sulfoxides

The oxidation of the *cis*-diphenyl lactam **44** was carried out using *m*-CPBA (77%) in dichloromethane to give the sulfoxide **70** in 84% yield after recrystallisation from ethyl acetate (Scheme 18). Only one diastereomer was present, the sulfoxide **70** with pseudo-axial orientation. This is due to oxidation from the β-face only, due to steric hindrance to approach from the α-face by the two phenyl groups.



Scheme 18

The same procedure was used for the sulfoxidation of the *trans*-diphenyl sulfide **43** leading to a 1 : 1 ratio of the diastereomeric sulfoxides **71** and **72** in the crude material.

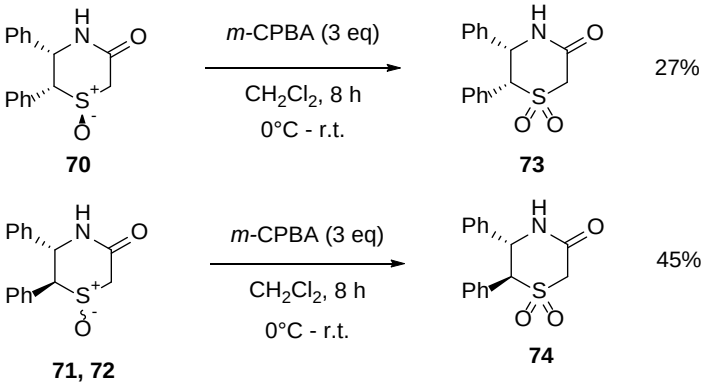


Scheme 19

The sulfoxides were purified by chromatography and and the diastereomers were isolated in the ratio 1 : 1. These results are comparable to Collins who obtained a ratio of 1 : 1 for the crude material and an isolated sample with a ratio of 2.5 : 1, equatorial : axial after recrystallisation.[14]

2.3.2.4 Synthesis of lactam derived β-keto sulfones

On one attempt to oxidise the *cis*-phenyl sulfide **44** to the sulfoxide **70,** unidentified signals at 4.06 and 4.21 ppm were seen in the ^{1}H NMR spectra (Figure 5). To determine if this extra signal was the equatorial sulfoxide or the corresponding sulfone **73**, an authentic sample of the sulfone was prepared. The synthesis and isolation of the novel sulfones **73** and **74** was carried out using 3 equivalents of *m*-CPBA in dichloromethane with an aqueous sodium bicarbonate workup on the reaction mixture providing pure sample of both sulfones (Scheme 20).



Scheme 20

The ^{1}H NMR spectrum of the sulfone **73** shows an AB quartet system (J_{AB} = 17.3 Hz) as doublets at 4.06 (finely split by W coupling) and 4.21 ppm. The C*H*S multiplet comes at 4.38 ppm and the C*H*N doublet at 5.65 ppm (J_{AB} = 4.0 Hz) (Figure 4). This is in comparison to the sulfoxide **70** which has the C*H*S signal at 4.38 ppm and the C*H*N at 5.68 ppm. An authentic sample of the *trans* diphenyl sulfone **74** was also prepared from the sulfoxides **71,72**, as a way of checking for over-oxidation of the sulfide starting material **43** (Scheme 20). The SO_2CH_2 AB quartet system (J_{AB} = 17.3 Hz) appears as doublets at 4.18 ppm and 4.26 ppm. The C*H*S is at 4.30 ppm (*J* = 10.2) and the C*H*N is at 5.23 ppm (*J* = 11.0 Hz) (Figure 4). Both sulfones **73,74** are white crystalline solids with high melting points and are novel compounds.

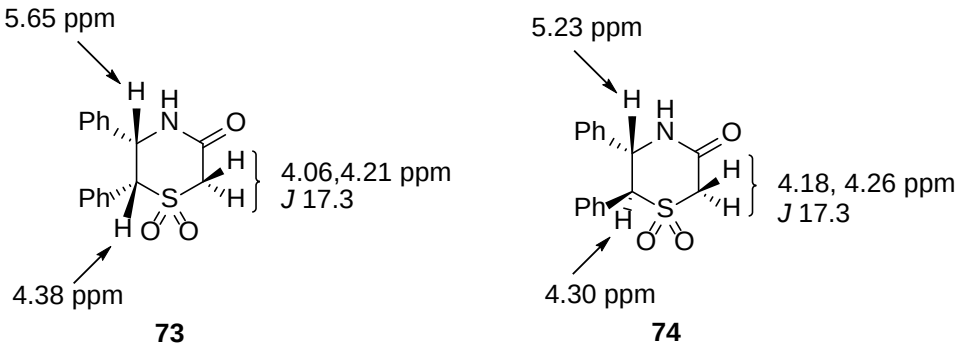


*Figure 4: ^{1}H NMR spectrum characteristic signals of sulfones **73** and **74**.*

The extra signals seen on oxidation of the sulfide **44** were confirmed as being the sulfone formed from over oxidation (Figure 5). After this result, the *m*-CPBA was assumed to be the maximum concentration of 77% to avoid further over oxidation.

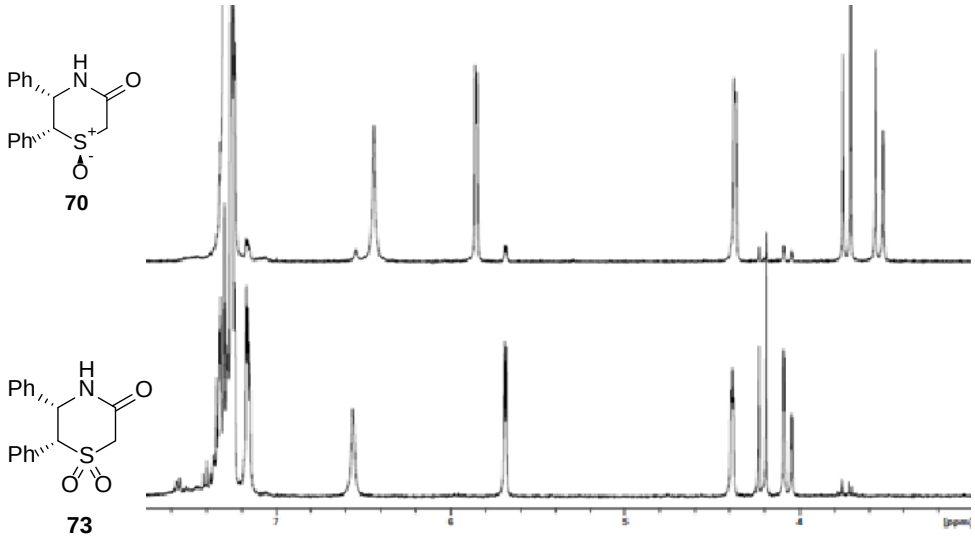


*Figure 5: ^{1}H NMR spectra of the crude sulfoxide **70** (top) from the sulfoxidation of the cis-diphenyl sulfide **45,** with an authentic sample of the sulfone **73** (bottom).*

The synthesis of the lactone, lactam[13,24] and ketone[25] derived sulfoxides (**55 - 72**), have been published by our research group.

2.3.3 Synthesis of α-diazosulfoxides

2.3.3.1 Synthesis of lactone derived α-diazosulfoxides

The standard conditions for diazo transfer to lactone derived sulfoxides have been long established within our research group, using one equivalent of triethylamine as base, acetonitrile as solvent and one equivalent of tosyl azide as diazo transfer reagent. This is the Regitz diazo transfer methodology to activated methylene groups by deprotonation.[26] The reactions are set up by cooling to 0°C, followed by the addition of the base, the reaction is stirred for 10 minutes, and subsequently followed by slow addition of a solution of a diazo transfer reagent over 10 minutes. The reaction is typically complete within 16 h with 100% consumption of the sulfoxide starting material. In this work, a series of lactone derived α-diazosulfoxides **38,39,75–79** were synthesised in this way (Figure 6), while concurrently investigating new methodologies for their synthesis in continuous flow and new conditions for the batch reaction.

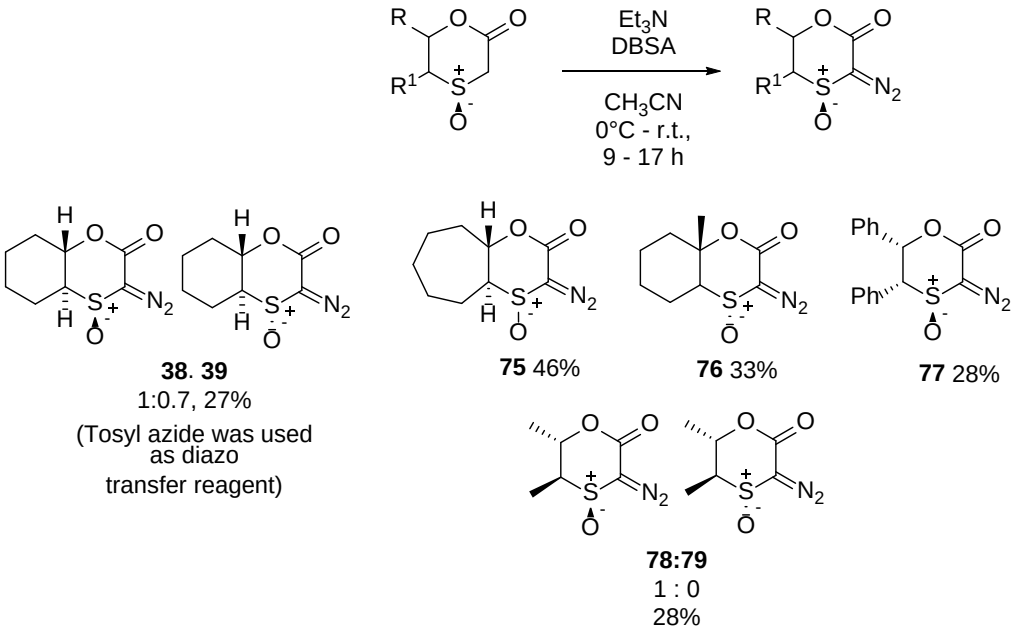


Figure 6: Isolated yields of α-diazosulfoxides from standard batch reaction conditions.

Notably, the yields for these reactions are consistently poor to moderate across a range of substrates in line with earlier work in the team. When these batch reactions are stirred for an extended period of time, the reaction mixture develops an extreme red coloration. This coloration which is caused by impurities is easily removed by column chromatography. Typically, the formation of this colour is consistent across the series and generally suggests successful diazo transfer. However, as the cause of this colouration is removed on purification, and the isolated α-diazosulfoxides are yellow crystalline solids, the colour may be due to residual by-products from decomposition. To date, no decomposition products have been isolated from a batch diazo transfer reaction. Additionally, Collins[14] highlighted the base sensitivity of this series of compounds when he carried out three different purification procedures on crude reaction mixtures which had endured the same reaction conditions. Direct purification of the crude reaction mixture by column chromatography on silica gel led to an isolated yield of the α-diazosulfoxides **38**, **39** in 40% yield. When an aqueous wash and a base wash were carried out before column chromatography on silica gel, the product was isolated in 16% yield. When a water wash only was carried out before column chromatography on silica gel the isolated yield was 24%.[14] These results by Collins indicate not only the base sensitivity of these compounds, but also the potential for hydrolysis induced losses caused by adventitious water. And as result of this observation, purification of the crude diazo transfer material is carried out by column chromatography on silica gel only.

2.3.3.2 Synthesis of ketone derived α-diazosulfoxides under standard batch conditions

Typically, α-diazoketones are more labile than α-diazoesters, therefore opening the possibility of different reactivity and more diverse synthetic applications.[27] These α-diazosulfoxide derivatives contain an α-diazoketone functionality as opposed to the α-diazolactone derivatives previously described.[13] The properties, stability and reactivity of α-diazoketones are distinctly different to those of α-diazoesters and diazo compounds derived from carboxylic acids in general. In comparison to the lactone derived α-diazosulfoxides though, this series of compounds are lacking the lactone moiety which is susceptible to hydrolysis, and base sensitive as a result.

The first syntheses of the α-diazosulfoxides **14,80–83** were reported by Buckley[16] who established the reactivity of these α-diazosulfoxides in batch reactions, under transition metal catalysis, thermolysis and photolysis conditions. The optimum conditions for the synthesis of the lactone derived α-diazosulfoxides were utilized in this work in an attempt to effect diazo transfer to the β-keto sulfoxide precursors **66, 68** and **65**. In contrast to the synthesis of the lactone derived α-diazosulfoxides, complete consumption of the sulfoxide starting material within 9 h or less is achieved, presumably as a result of the lower pKa value of approximately 11.

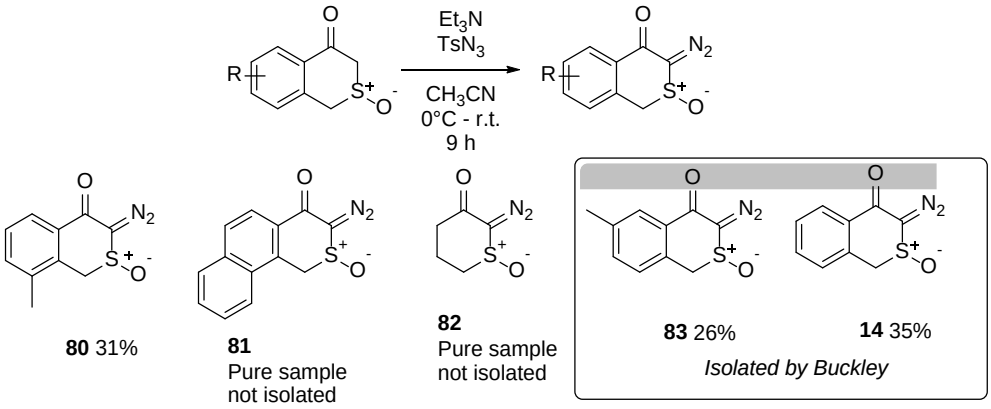


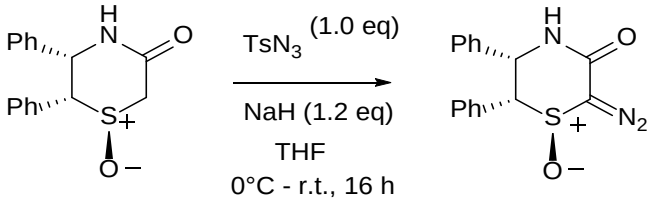
Figure 7: Isolated yields of ketone derived α-diazosulfoxides from standard batch reaction conditions.

On complete consumption of the starting material in these reactions, the ^{1}H NMR spectra of the crude material shows the disappearance of the characteristic and diastereotopic SOCH_2 signal and is accompanied by the appearance of the diazo stretch between 2111 cm^{-1} and 2120 cm^{-1} in the infrared spectrum. For the lactone and lactam derived α-diazosulfoxides the diazo stretch in the infrared spectrum is usually between 2111 cm^{-1} and 2127 cm^{-1} and in the ^{13}C NMR spectrum the $C{=}N_2$ peaks are observed between 71.3 and 79.2 ppm for both ketone and lactone derivatives. Interestingly, the naphthalene derived α-diazosulfoxide **81,** and monocyclic α-diazosulfoxide **82** were not successfully isolated as pure compounds after chromatography due to the presence of

inseparable impurities caused by product decomposition, however, the signals indicative of successful diazo transfer, such as the sulfonamide NH_2 and the diastereotopic CH_2 doublets of the corresponding α-diazosulfoxide were present in the ^{1}H NMR spectrum of the crude material.

2.3.3.3 Synthesis of lactam derived α-diazosulfoxides

The *cis*-diphenyl lactam derived α-diazosulfoxide **84** was prepared using sodium hydride as base, tosyl azide as diazo transfer reagent and THF as solvent (Scheme 21). These conditions were optimised by Collins who found triethylamine was not basic enough to deprotonate the proton alpha to the sulfoxide in the lactam **70**. [14]

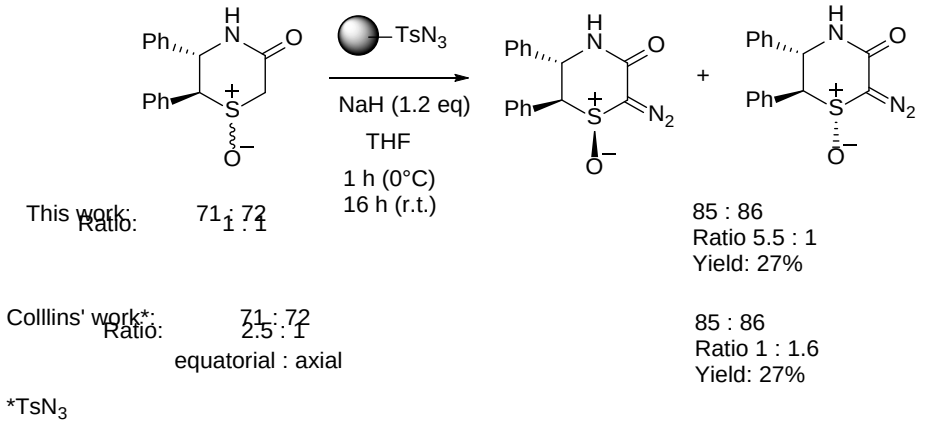


70 **84** 12%

Scheme 21

Isolation of the pure α-diazosulfoxide **84** (Scheme 21) was extremely challenging due to the similar polarity of the sulfonamide by-product. It was found that when using silica gel for column chromatography the majority of the product would not elute from the silica gel. Alumina was also used but this did not provide an efficient separation. The pure product **84** was obtained in a low yield of 12% yield after repeated column chromatography.

The *trans*-diphenyl lactam derived α-diazosulfoxides, both axial **85** and equatorial **86** were generated under the same conditions but could not be separated from the *p*-toluenesulfonamide by-product. Previous work within the group[28] had shown the effectiveness of using polymer supported benzene sulfonyl azide as the diazo transfer reagent (Scheme 22). The polymer supported reagent can be removed by filtration and eliminates the need to separate the sulfonamide by-product from the reaction product. With this in mind, the lactam derivatives **71,72** (1 : 1) were deprotonated using sodium hydride in THF, under a nitrogen atmosphere and the polymer supported sulfonyl azide was swollen separately, before the reaction, in THF (Scheme 22). The swelling of the polymers depends on the dipole moment of the solvent. THF has a similar dipole moment to dichloromethane which is usually used to swell polymer supported reagents (THF = 1.63, DCM = 1.6)[28] and so after swelling of the beads in THF for 15 minutes, they were added to the reaction mixture.

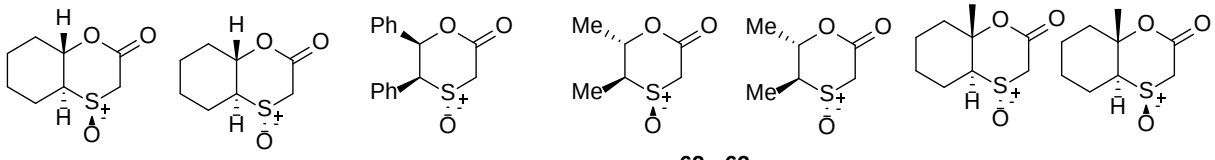


Scheme 22

After 16 h the beads were removed by Buchner filtration and rinsed with dichloromethane. After purification, the pure α-diazosulfoxide products **85** and **86** were isolated in one fraction (27%), in a ratio of 5.5 : 1 , **85 : 86**, followed by starting material (36%, 2 : 1, **71 : 72**). The low recovery is in line with Collins' work using standard tosyl azide which had a ratio of 1.6 : 1, **86** : **85**.[14] These results highlight the fact that formation or isolation of the axial diastereomer is favoured.

2.3.4 Generation of α-diazosulfoxides in a continuous flow system

The generation of α-diazocarbonyl compounds utilizing continuous flow protocols has recently been reported by our group, and others, highlighting its applicability to continuous flow.[29-31] The Regitz diazo transfer reaction to lactone derived β-oxo sulfoxides typically required 16 h at room temperature in a batch reaction and only provided moderate to good yields. A key objective of this work was to optimise the diazo transfer to form α-diazosulfoxides, in a continuous flow system. The synthesis of the sulfoxide precursors for diazo transfer is previously reported in section 2.3.2.[13] These six lactone derived substrates **55,56**,**59**,**62,63**,**57**,**58** were chosen for investigation because they would provide a good insight in to the robustness of a new methodology by variations in the steric, and conformational properties. While dr's indicated on Figure 8 refer to NMR's of samples of materials used in flow reactions, there may be alterations in the precise ratios if the diastereomer sulfoxides are not homogeneous.



55 : 56
1 : 1

59

62 : 63
1 : 0.3

57 : 58
9.5 : 1

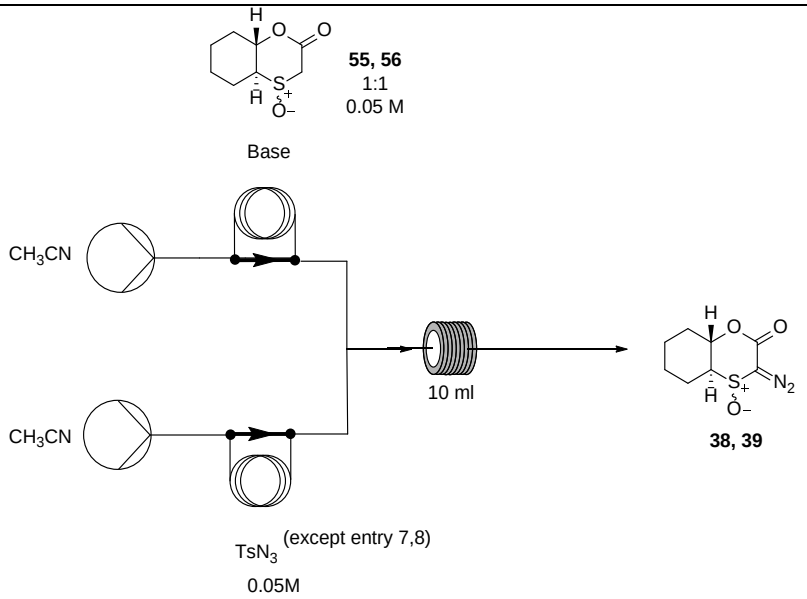
Figure 8: Sulfoxide precursors used for the diazo transfer reaction in continuous flow.

Tosyl azide is traditionally used in batch reaction conditions and was used in our initial continuous flow reactions. However, *p*-dodecylbenzenesulfonyl azide (DBSA) **87** was later used instead of tosyl azide as the diazo transfer reagent for two main reasons. Firstly the relatively low polarity of the dodecylbenzenesulfonyl amide **88** by-product makes chromatographic purification of the α-diazosulfoxides more efficient. The second reason is the additional safety aspect compared to most other diazo transfer reagents. Multiple reports exist in the literature on the safe generation and use of diazo transfer reagents,[32-37] and although tosyl azide is known to be shock sensitive and highly explosive it can be used effectively when proper precautions are taken - such as the addition of the diazo transfer to the reaction at 0°C. DBSA **87**, however, is an oil at room temperature with an approximate initiation temperature of 151°C and an impact sensitivity of 150 kg cm, compared to tosyl azide which has an initiation temperature of 120°C and an impact sensitivity of 50 kg cm.[34]

The initial study was an investigation on how a modified batch protocol (room temperature, as opposed to 0°C) would perform in a continuous flow reactor with an aim to achieve maximum conversion to the desired product (Table 4). The sulfoxides **55,56** were selected as the model substrate to begin the optimisation. As mentioned earlier, the batch procedure consists of one equivalent of tosyl azide as the diazo transfer reagent, one equivalent of triethylamine and acetonitrile as solvent. Initial results from transferring of these batch reaction conditions to continuous flow were not very promising, showing limited success (Table 4, Entries 1 – 7).

The initial optimisation investigation was carried out on the Vapourtec R-Series reactor using 2 mL injection loops, and consisted of varying the equivalents of base, residence time and temperature. The best conversion achieved in this screen of the reaction conditions was 40% consumption of the starting material (Table 4, entry 8), therefore a new approach was explored. Due to the challenge of separating the tosyl amide by-product and tosyl azide from the desired α-diazosulfoxides **38,39** the crude mixtures were not purified and the products were not isolated in these initial screening studies.

Table 4: Applying the batch reaction diazo transfer conditions to continuous flow.



Entry	Residence Time (min)	Et_3N (eq.)	Tosyl Azide	Temp (°C)	Conversion (%)[a]
1	25	1	1	22	22
2	50	3	1	25	26
3	50	1	1	25	17
4	50	1	1	40	22
5	50	1.9	2	40	38
6	25	1	1	40	26
7	50	1	1 (DBSA)[ii]	25	38
8	50	2	1 (DBSA)	40	40

[a]The conversion results were obtained from ^{1}H NMR spectroscopy analysis.

The low percentage conversion to the desired product is most likely due to the short residence time, and increasing the residence time substantially, may have provided higher conversions to the desired products. However, our aim was to achieve high conversions and high yields in short residence times, and so this approach of extending the residence time was not investigated further. The next parameter investigated was the effect of changing the base for these reactions. A series of secondary and tertiary amine bases were screened, again with limited success, except for an interesting result with DBU (Table 5, entry 5). Significant red coloration was noted at the "T"-piece, similar to what is observed after approximately 16 h with the batch reaction. Interestingly, this coloration was not observed in the other flow reactions (Table 5, entries 1 – 4). This observation was important because, as diazo transfer proceeds in the batch conditions, the colour change is from colourless to yellow, then to yellow/orange, orange, orange/red and finally

[ii] For all diazo transfer reactions using DBSA (mixture of isomers), the sulfonyl azide was sourced directly from TCI Chemicals and used without purification.

red. At this point the ^{1}H NMR spectrum of the crude material shows complete consumption of the sulfoxide starting material **55,56**. The purified α-diazosulfoxides **38,39** are yellow crystalline solids and yellow in solution, suggesting that the red coloration is associated with successful diazo transfer to the sulfoxide and formation of resulting impurities responsible for the colour. Despite the red colour, the ^{1}H NMR spectrum of the crude material from this flow reaction (Table 5, entry 5) showed starting material **55,56** and unidentified decomposition products with no α-diazosulfoxide observed. For all other previous entries in the continuous flow investigations (Table 5), no change in coloration was observed. This intense red coloration observed in the tubing suggested that among the bases used, DBU is sufficiently basic to initiate rapid diazo transfer but the sensitivity of the sulfoxide substrate to DBU as base, led to complete decomposition (Table 5, entry 5). Interestingly, Table 5 shows clearly that conversions are poor even in the presence of 2 equivalents of base and 2 equivalents of diazo transfer reagent. These results, combined with the results by Collins (Section 2.3.3.1) show that prolonged exposure to base is incompatible with a high yielding process for the synthesis of these α-diazosulfoxides.

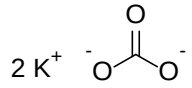
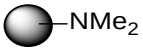
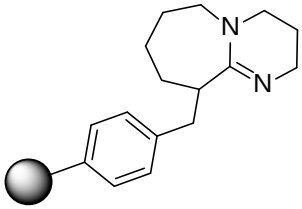
Table 5: Continuation of the Investigation into the use of homogeneous phase bases.

Entry	Base (eq.)	Diazo transfer reagent (eq.)	Residence time (minutes)	Conversion (%)[a]
1	Et_2NH (1.05)	Tosyl Azide (1.05)	25	9
2	Et_3N (2)	DBSA (1)	50	40[b]
3	Et_3N (1.9)	Tosyl Azide (2)	50	38[b]
4	DIPEA (1.05)	Tosyl Azide (1.05)	25	4
5	DBU (1.05)	Tosyl Azide (1.05)	25	-[c]

[a] Conversions were determined by ^{1}H NMR Spectroscopy.
[b] These reactions were carried out at 40°C.
[c] The percentage conversion to α-diazosulfoxide could not be determined due to the decomposition of the product to multiple unidentifiable products.

As base sensitivity of the products was a limiting factor (Section 2.3.3.1) the use of solid supported bases was attempted. This move towards polystyrene supported DBU (PS-DBU) and other solid phase bases was with the aim of formation of the product and immediate removal from the basic environment, leading to their successful isolation overcoming base mediated decomposition. These solid (K_2CO_3) or solid supported bases (Amberlyst A21, PS-DBU) are loaded in to a column reactor forming a packed bed of reagent that the substrate is flowed over. The characteristics of these bases are highlighted in Table 6.

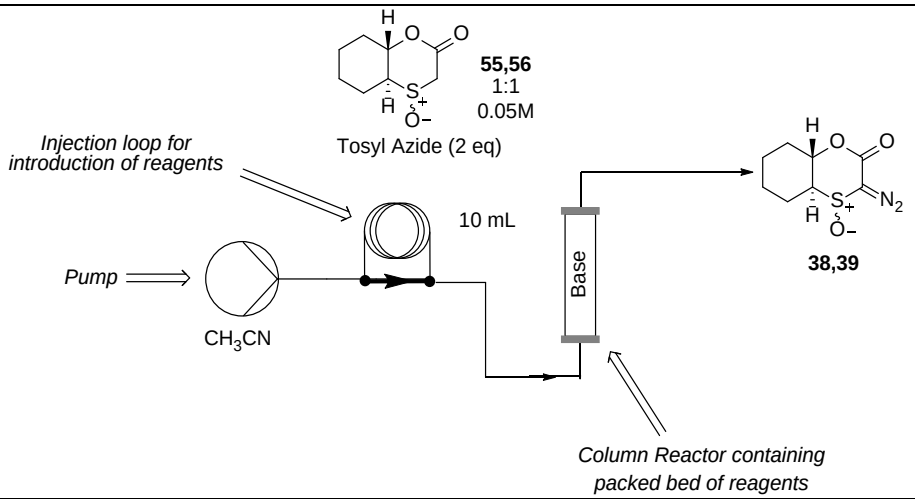
Table 6: Solid supported or insoluble bases used in the investigation.

Entry	Base	Structure	pK_a (in CH_3CN)
1	K_2CO_3		10.3
2	Amberlyst A21	Styrene divinyl benzene backbone – dimethylamine functionality at the surface 	18.4*[38]
3	PS-DBU	1% cross linked with divinyl benzene 	24.13[39]

*Using triethylamine as a model.

The combination of back pressure in the system, along with tight packing of the solid base ensures reaction of the heterogeneous reagents (Table 7). Specific control of the residence time is one of the key process control parameters in continuous flow which is easily varied by adjusting the flow rate – a control parameter which cannot be achieved in batch.

Table 7: Investigation into the use of solid phase bases.

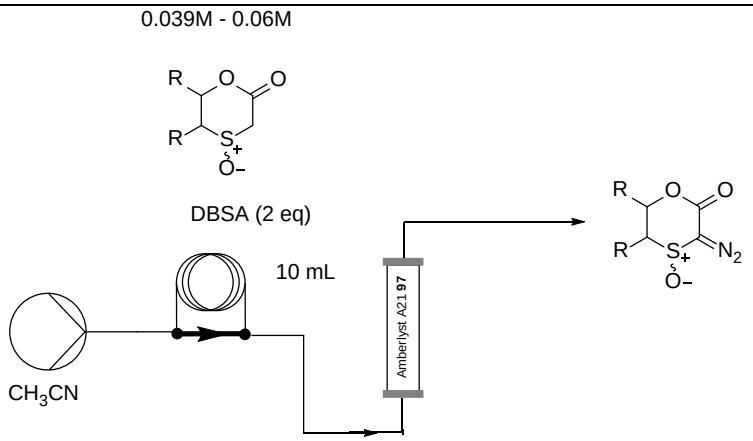


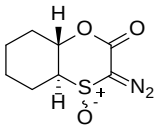
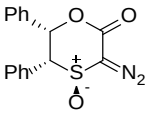
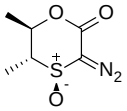
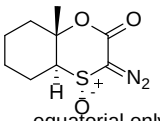
Entry	Base (equivalents)	Diazo transfer reagent (equivalents)	Residence time in reactor column (minutes)	Conversion (%)
1	PS-DBU (5)	Tosyl Azide (2)	9	100
2	K_2CO_3 (5)	Tosyl Azide (2)	15	3
3	Amberlyst A21* (20)	Tosyl Azide (2)	9	100
4	Amberlyst A21* (20)	DBSA (2)	9	100

*Amberlyst A21 is polymer supported dimethylamine (PS-NMe_2).

Using polystyrene supported DBU with tosyl azide led to 100% consumption of starting material **55,56** and critically, the intense red coloration from unidentified decomposition products, seen with the homogeneous phase DBU reaction were not observed in with the polystyrene supported DBU (Table 7, entry 1) indicating that decomposition when using DBU is avoided through immobilisation. Regeneration of the polymer supported DBU has previously been reported using a 1M solution of DBU in dichloromethane.[40] This method was successfully used in this work to regenerate the polymer supported DBU and this regenerated material was then used in turn for other successful diazo transfer reactions. These reactions gave comparable results to the commercially sourced PS-DBU, however some non bound DBU remains and subsequently leached in to the reaction mixture. Due to this challenge, the use of Amberlyst A21 was investigated, with great success (Table 8). Amberlyst A21 as a catalyst or reagent in organic synthesis and continuous flow synthesis has been previously reported and is advantageous due to its affordability and potential for regeneration.[41-43] Amberlyst A21 is reported to have excellent stability, low leaching, and resistance to thermal and mechanical shock.[44] With the excellent results we achieved using Amberlyst A21, including when DBSA was used as diazo transfer reagent (Table 7, entry 4), it was decided to focus on this solid supported base for our substrate scope, using the conditions that would afford us 100% consumption of starting material (Table 8). The conditions used were 20 equivalents of Amberlyst A21 as base, a residence time of 9 minutes and 2 equivalents of DBSA as the diazo transfer reagent. The solvent for the reaction, acetonitrile, was kept consistent to that used in the batch reaction.

Table 8: Diazo transfer in flow using Amberlyst A21 as base.



Entry	Product	Residence time (minutes)	Diastereomeric Ratio		Conversion (%)	Yield (%)[a]
			Sulfoxide	Diazosulfoxides		
1	 **38, 39 1 : 1**	9	1:1	1:1	100	49
2	 **77 -** axial only	9	Axial only	Axial only	100	30
3	 **78 -** axial only	9	1:0.3 (axial : eq)	Axial only	100[b]	47
4	 **76 -** equatorial only	9	Equatorial only	Equatorial only	100	70

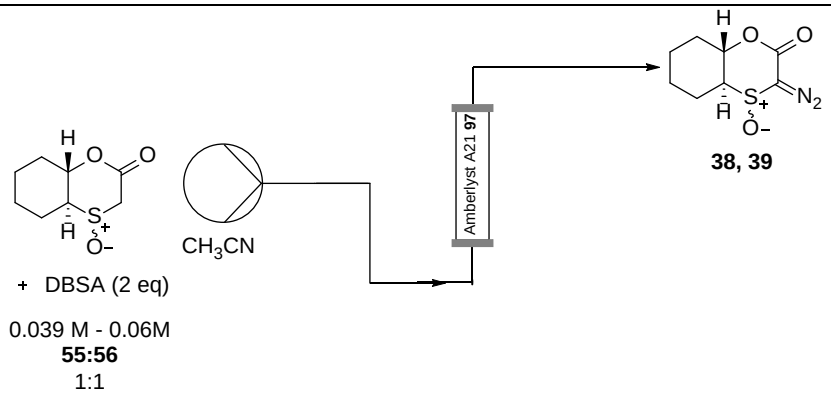
[a] After column chromatography.
[b] The sulfoxide starting material was a 1:0.3 mixture of diastereomers, axial : equatorial.

As can be seen in Table 8 yields are between 10 – 15% higher than the standard batch reaction conditions for generation of the α-diazosulfoxides **38,39,76–78** and entry 4 in particular showed the reproducible high yield of 70% for **76**. This yield of 70% for the isolation of an α-diazosulfoxide was unprecedented, and suggests that the process control which is enabled in flow, through the use of solid supported bases, leads to substantial increases in the yields for the synthesis of lactone derived α-diazosulfoxides. Interestingly, the bridgehead methyl group on **76** is anticipated to reduce the base sensitivity of this lactone relative to the others in this series, which may account

for the increased yield. Based on this exciting result, a new investigation was carried out without the use of injection loops and through the use of peristaltic pumps on the Vapourtec E-Series reactor. The low solubility of the relatively polar sulfoxide substrates made the use of peristaltic pumps a better choice than the Vapourtec R-Series reactor with HPLC pumps, for these reactions in which the consistent flow rate is important.* The solutions of sulfoxides used were between 0.039 M and 0.06 M, because of their limited solubility in acetonitrile. Table 9 illustrates the results of a yield optimisation study whereby the effect of reducing the equivalents of base, sulfonyl azide and the residence time were all investigated. It is noted that the highest yield (76%) is obtained when 5 equivalents of base are used and a residence time of nine minutes (Table 9, entry 12). A comparable yield (73%) is recorded when 20 equivalents of base are used with a short residence time (Table 9, entry 3). However, the lowest yield (46%) was recorded when there was a large excess of base and a long residence time (Table 9, entry 1). This suggests that significant decomposition occurs with prolonged exposure to basic conditions, either excess Amberlyst A21 or through a too long residence time on the Amberlyst A21. This low yield of 47% (Table 9, entry 1) is comparable to the yield from the reaction in batch, however it is much lower than the yields from the other continuous flow reactions.

*It was easier to maintain the constant flow rate with the peristaltic pump rather than with a HPLC pump.

Table 9: Yield optimisation by reduction of residence time, and equivalents of base.



Entry	Amberlyst A21	Diazo Transfer Reagent	Residence time (minutes)	Conversion	Isolated Yield
1	(20 eq)	DBSA(2)	9.5	100	47%
2	(20 eq)	DBSA (2)	9	100	49%
3	(20 eq)	DBSA (2)	4.5	100	73%
4	(20 eq)	DBSA(2)	2.25	98	73%
5	(7 eq)	DBSA (2)	4.5	96	68%
6	(7 eq)	TsN_3 (2)	6.5	100	-*
7	(7 eq)	DBSA (1.2)	6.5	73	-*
8	(7 eq)	DBSA (1.2)	9	82	-*
9	(7 eq)	DBSA (1.5)	9	85	54%
10	(5 eq)	DBSA (2)	4.5	77	68%
11	(5 eq)	DBSA (2)	9.5	95	71%
12	(5 eq)	DBSA (2)	9	86	76%

*The crude material was not purified to obtain an isolated yield.

Noteworthy, is the fact that the conditions in Table 9, entry 12, which provides us with the highest isolated yield of the product, consumption of the sulfoxide starting material **55,56** is only 86%. In all cases where 100% consumption of starting material was recorded, the isolated yields were lower. Effectively, this shows that balancing the equivalents of Amberlyst A21 and the residence time are vital parameters for a high isolated yield. Sufficient time is required to achieve diazo transfer, but if the α-diazosulfoxide products **38,39** are exposed to the basic reaction conditions for too long, decomposition begins to reduce the amount of the desired α-diazosulfoxide which can be isolated.

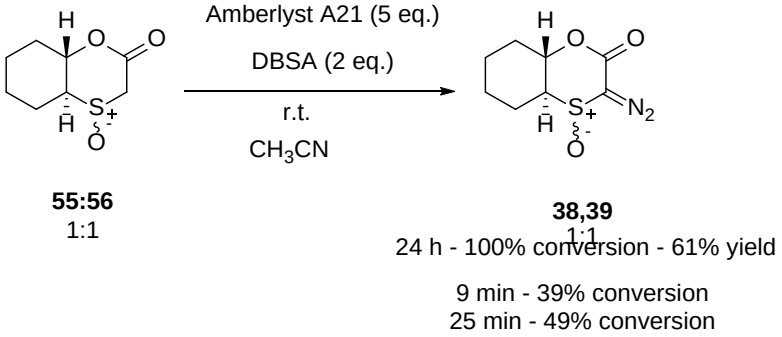
These optimised conditions (Table 9, entry 12) from the flow reaction were used for a comparison to the standard batch conditions. With 2 equivalents of DBSA **87** and 5 equivalents of Amberlyst A21, and a reaction time of 24 h, 100% conversion was achieved with an isolated yield of 61% of the α-diazosulfoxides **38,39** after column chromatography (Scheme 23). As a comparison to the flow reaction, when the reaction time in batch is reduced to 9 minutes, a conversion of 39% is

achieved, which is significantly lower. A 49% conversion was obtained after 25 min in the batch conditions, in the presence of 5 equivalents of Amberlyst A21 at room temperature (Scheme 23). Notably, while reactions were incomplete in a short period of time in batch, use of the immobilised base Amberlyst A21 led to significantly better outcomes in terms of yields and efficiency than was seen using triethylamine. Immobilisation of base also led to substantial improvement in yields (see Scheme 23, 61% *cf* circa. 40%). Notably, the ease of the protocol is enhanced by:

1. Conducting the reactions at room temperature without the need for an ice bath, and
2. The ease of sulfonamide and base removal is increased relative to tosyl azide and triethylamine.

When reactions were conducted in continuous flow, relative to batch reactions with Amberlyst A21, conversions are much higher with shorter residence times than seen in Scheme 23, presumably due to rate enhancement by better mixing and back pressure.

While batch conditions using Amberlyst A21 are an important outcome of this work, the reactions conducted in continuous flow are higher yielding because the product is completely removed from the base.

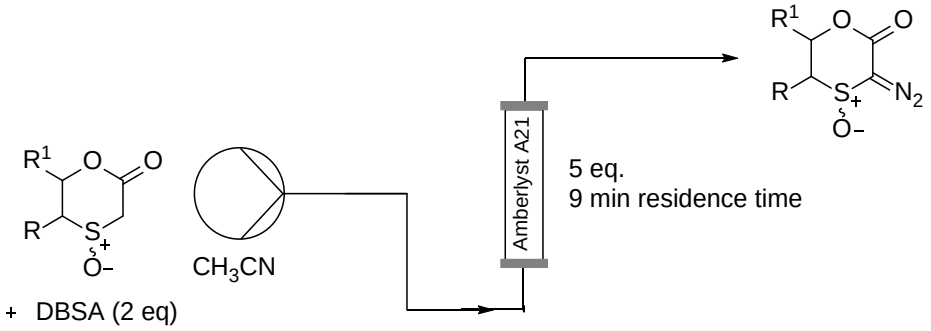


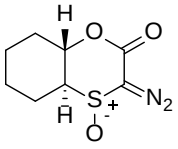
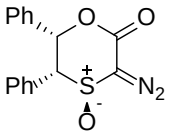
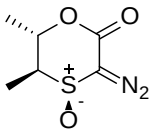
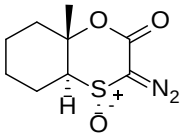
Scheme 23

Using the newly optimised conditions (Table 9, entry 12) a series of lactone derived α-diazosulfoxides were synthesised (Table 10). A significant increase in yield is achieved using the flow process and newly optimised conditions with Amberlyst A21 as base and DBSA **87** as the diazo transfer reagent across a range of substrates. To the best of our knowledge use of Amberlyst A21 for diazo transfer has not been previously reported. Although 100% conversion was achieved using the conditions outlined in Table 8, the highest yields of **38,39** were obtained using the conditions outlined in Table 9, entry 12. Interestingly for Table 10, entry 4, this sulfoxide starting material was more soluble in acetonitrile and so a test reaction was carried out the concentration of 0.09 M, instead of the usual 0.05 M. However, the yield decreased significantly to 60% under

this increased concentration, with decomposition residues remaining both on the solid supported base and on the silica gel, in a manner similar to the batch reactions.

Table 10: Isolated yields of products using the newly established flow procedure.



Entry	**1**	**2**	**3***	**4**	
Product	 **38,39**	 **77**	 **78**	 **76**	
Concentration (M)	0.05	0.04	0.06	0.05	0.09
Flow Conversion (%)	(86)	(96)	(100)	(98)	-
Flow Yield	76%	88%	86%	86%	60%
Batch Yield	34%	28%	35%	33%	33%

*Only the axial sulfoxide was used as the substrate resulting in the formation of the axial α-diazosulfoxide **78** only.

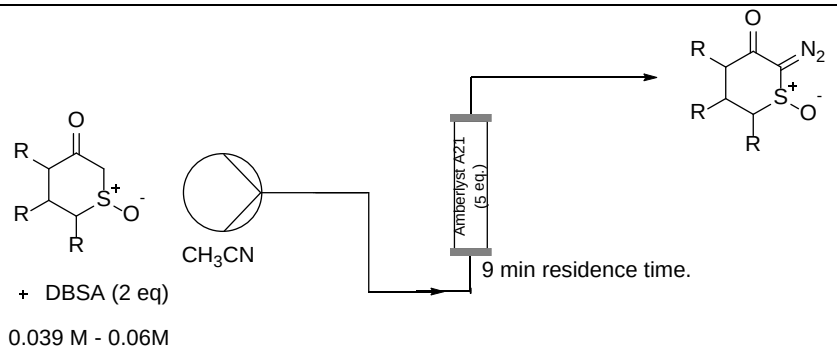
In conclusion, by using solid phase bases and in particular PS-NMe_2, in a glass reactor column, we have significantly enhanced the synthesis of α-diazosulfoxides resulting in a dramatic increase in isolated yields and reduction in reaction times. The new conditions perform consistently well across a range of lactone derived α-diazosulfoxide substrates with 2 – 3 fold increases in yield over the standard batch conditions. Both PS-NMe_2 (all series) and polystyrene supported DBU (**38,39** only) are applicable to the diazo transfer reaction. This flow method enables reproducible access to a high yielding synthesis of the α-diazosulfoxides for the first time in over 16 years of research in our team, and also shows greater potential for scale-up. This study highlights the advantages of highly controlled residence times in flow which can enable efficient synthesis of compounds that

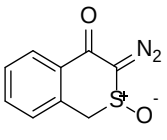
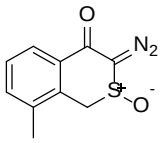
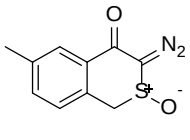
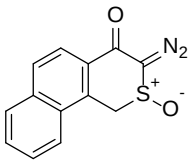
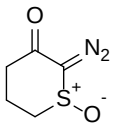
are sensitive to prolonged exposure to the reaction conditions. With this in mind this new methodology for the synthesis of lactone derived α-diazosulfoxides was also applied to the synthesis of a range of ketone derived α-diazosulfoxides.

2.3.4.1 Application of the new continuous flow diazo transfer to ketone derived β-keto sulfoxides

The standard Regitz diazo transfer methodology under batch reaction conditions was used for the generation of ketone derived α-diazosulfoxides. However, in these conditions, this led to poor to moderate yields and for some derivatives *in situ* decomposition. More specifically, in this work *in situ* decomposition was observed specifically with the naphthalene derived α-diazosulfoxide **81**; on analysis of the ^{1}H NMR spectrum of the crude material a significant amount of unknown impurities had formed. When these ketone derived β-keto sulfoxides were subjected to the continuous flow diazo transfer reaction conditions, the optimal outcome was achieved. The conditions which had been optimised for the lactone series were utilised without re-optimisation. Although discoloration of the solid supported base was observed, changing from yellow to a deep purple/black colour, analysis of the crude reaction mixtures by ^{1}H NMR spectroscopy showed excellent conversions to the desired α-diazo-β-keto sulfoxides. For the more stable α-diazosulfoxides **14,80,83** which were easily accessed from batch reactions (Table 11, entries 1 – 3), conversions were between 89 and 95% in the continuous flow reactions. For the more sensitive substrates **81,82** (Table 11, entry 4 – 5) which were challenging to synthesise and isolate from the batch reaction, their conversions were 65 and 72% respectively. However, even with these moderate conversions, the desired α-diazosulfoxides were successfully isolated and characterised in moderate yields. Notably, even when pure in the freezer both of these α-diazosulfoxides undergo transformation to a complex mixture of unknown decomposition products. The ketone derived β-keto sulfoxides are notably more labile than the lactone series, even as pure products (samples of **38**, **39** maintained their purity and quality when stored on the bench over a period of months, whereas the ketone derivative such as **82, 80** need to be kept in the freezer to maintain their quality). While the base sensitivity of the lactone derivatives is readily rationalised due to basic hydrolysis, it is less clear why the ketone derivatives are base sensitive. The properties, stability and reactivity of α-diazoketones are distinctly different to those of α-diazoesters and diazo compounds derived from carboxylic acids in general. [27] This is due to the extent of stabilisation through resonance delocalisation of the α-diazoketones compared to α-diazoesters. Typically, α-diazoketones are more labile than α-diazoesters, therefore opening the possibility of different reactivity and more diverse synthetic applications.[27]

Table 11: Synthesis of ketone derived α-diazosulfoxides in continuous flow.

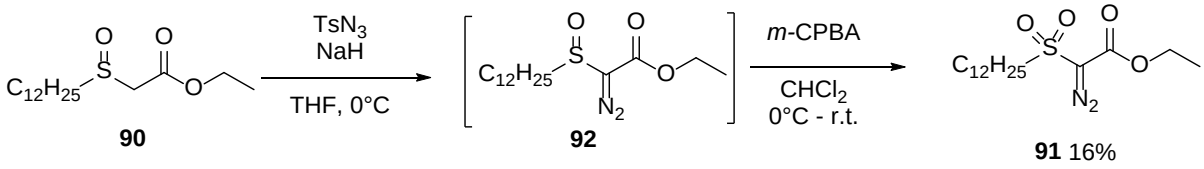


Entry	1	2	3	4	5
	 **14**	 **80**	 **83**	 **81**	 **82**
Conversion (%)[a]	95	89	95	65	72
Yield (%)[b]	80	88	60	39	19
Batch Yield (%)[b]	35[c]	33	26[c]	Not isolable	Pure sample not isolable

[a] Conversions were determined by analysis of the ^{1}H NMR spectra of the crude material.
[b] Isolated yields after purification by column chromatography on silica gel.
[c] Results reported by Buckley.

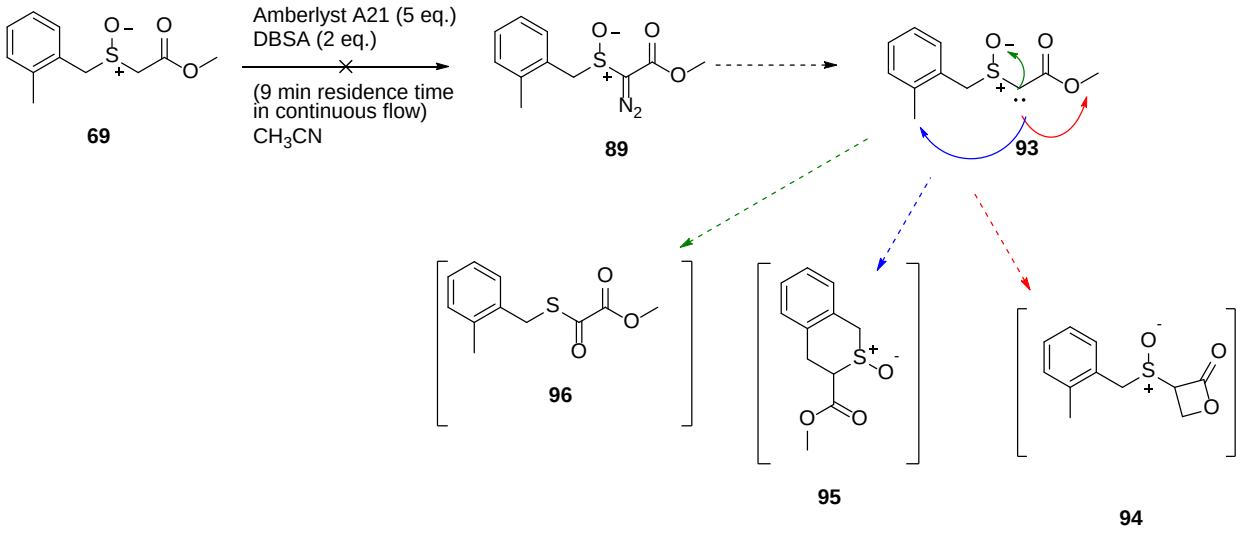
2.3.5 Attempted generation of an acyclic α-diazo-β-keto sulfoxide

The inability to isolate acyclic α-diazosulfoxides has previously been described within our group under batch reaction conditions.[14] However, with our new continuous flow reaction conditions, the synthesis of an acyclic α-diazosulfoxide **89** was attempted using this continuous flow methodology (Scheme 25). The synthesis of acyclic α-diazo-β-keto sulfoxides has been of significant interest within our research group over the years and has been investigated by both Kelleher[12] and Collins.[14] Kelleher had previously show that on addition of m-CPBA to a reaction mixture containing the β-keto sulfoxide **90** , base, and tosyl azide as the transfer reagent, the desired α-diazo-β-keto sulfone **91** was isolated. This indicated the formation of the α-diazo-β-keto sulfoxide **92** *in situ* and subsequent trapping of this compound as the sulfone derivative **91**.



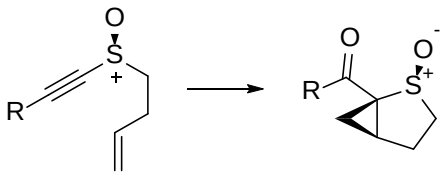
Scheme 24

Additionally, Collins had investigated the synthesis of α-sulfinyl esters, phosphonates and imidazoles to investigate whether the electron withdrawing group would prevent loss of the diazo moiety, but with no success in isolating acyclic α-diazosulfoxides. Two attempts were made for the synthesis of an acyclic α-diazosulfoxide **89** (Scheme 25) using this new methodology which provides enhanced yields of α-diazosulfoxides by preventing decomposition induced by the reaction conditions. The pure sulfoxide substrate **69** (Section 2.3.2.2) was obtained in one fraction after column chromatography, after an oxidation was carried out on an impure sample of the sulfide **22**. Polystyrene-supported DBU and Amberlyst A21 were both used as the solid supported base in two separate reactions, each reaction having a residence time of 9 minutes and 2 equivalents of DBSA **87** used as diazo transfer reagent (Scheme 25). Although successful diazo transfer from DBSA **87** occurred, as evidenced by the sulfonamide NH_2 peak on the ^1H NMR spectra of the crude material, and a colour change from colourless to yellow was observed within the reactor tubing, the desired α-diazosulfoxide **89** could not be identified after purification of the crude reaction mixture by column chromatography. The sulfoxide **69** was not isolated from the reaction mixture after purification, suggesting complete consumption in the reaction conditions. If the formation of the α-diazosulfoxide **89** occurs there are two possible further reaction pathways. The first is the instant loss of molecular nitrogen forming the carbene **93**. Two C-H insertion products, could be envisaged to form from the carbene **93** (Scheme 25). First, the formation of the lactone **94** or more favourably, the 6 membered cyclic sulfoxide **95**. Unfortunately, neither of these C-H insertion products were observed after purification of the crude reaction mixture by column chromatography on silica gel. The second, more likely, reaction pathway is similar to that described by Hodson and Holt[11] which is formation of a thiol ester **96** by oxygen abstraction from the sulfoxide.



Scheme 25

This inability to isolate an acyclic α-diazosulfoxide reflected the work by Hodson, Holt,[11] Kelleher[12] and Collins,[14] however, recently in the literature progress has been made in accessing α-sulfinyl carbenes. α-Sulfinyl metallocarbenes have been accessed by the group of Grainger[45] using oxidative gold catalysis with alkynyl sulfoxides, and in that work the subsequent reactivity was exploited to carry out intramolecular cyclopropanation reactions (Scheme 26).

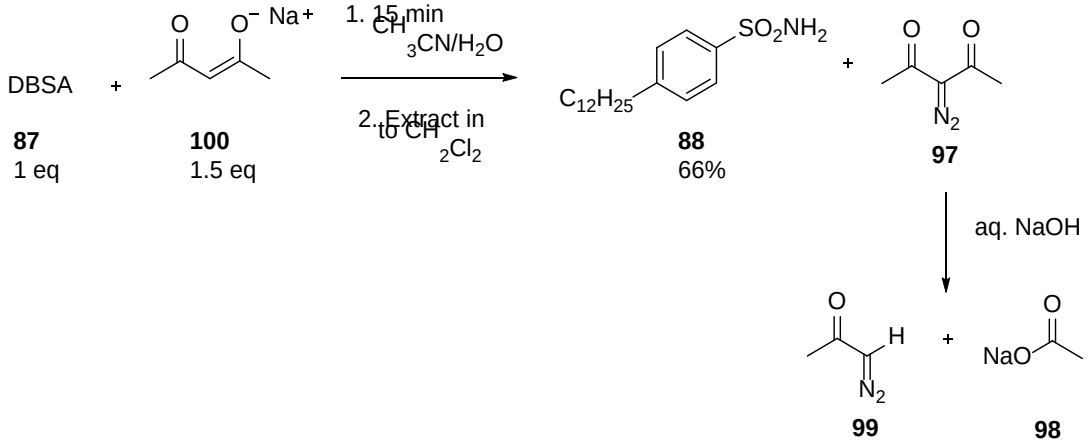


Scheme 26

2.3.6 Attempted telescoping of diazo transfer to sulfoxides followed by quench

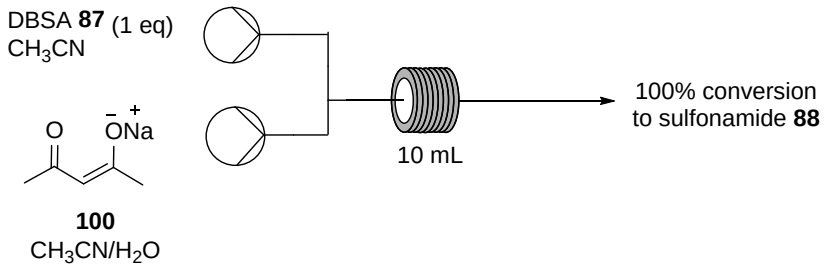
A recent report in the literature, from our research group, has shown the generation, use and subsequent quench of reactive sulfonyl azides in a continuous flow system.[29] It was envisaged that this quench method could be used in our process to safely remove the excess DBSA **87** from the system after reaction completion. In the traditional batch reaction conditions the diazo transfer reagent, tosyl azide, is 100% consumed in the reaction forming the sulfonamide by-product. This is in comparison to our new continuous flow reaction conditions whereby two equivalents of the diazo transfer reagent DBSA **87** were necessary to achieve high conversions and high yields in short residence time. Therefore any unused DBSA **87**, which is a heat and shock sensitive sulfonyl azide is a part of the crude mixture of products. With this in mind, the appropriate safety precautions were taken in all cases and crude reaction mixtures were concentrated under reduced

pressure without heating. Interestingly, on purification of the crude reaction mixtures by flash chromatography on silica gel, the excess DBSA **87** is easily separated from the dodecylbenzenesulfonyl amide by-product **88** by column chromatography on silica gel. The excess DBSA **87** elutes first, followed by the sulfonamide by-product **88** followed by the desired α-diazosulfoxide after increasing the polarity of the eluent system substantially. The sacrificial quench process reported by our group has the added safety advantage of not concentrating the unused equivalent of DBSA **87** on a rotary evaporator. We envisaged it would be possible to telescope the reaction of diazo transfer in flow using solid supported base and a subsequent sacrificial quench of the residual sulfonyl azide **87** as outlined in Scheme 27. The sacrificial quench results in formation of a labile diazoketone compound **97** which breaks down in basic aqueous solution to the benign fragment of acetate **98** and diazopropanone **99** which is subsequently quenched with sodium nitrite and dilute sulfuric acid. However, before attempting the quench in continuous flow we first had to show that the sodium acetyl acetone salt **100** would effectively quench DBSA **87** in aqueous acetonitrile. With a reaction time of 15 mins and 1.5 equivalents of the sacrificial quench solution it was established that the quench completely removes unreacted DBSA **87**. Dodecylbenzenesulfonyl amide **88** was recovered in 66% yield (Scheme 27).



Scheme 27

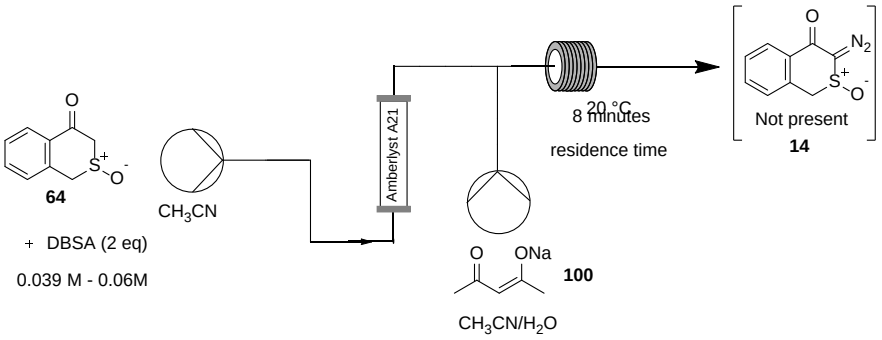
Having shown that our sacrificial quench removes unreacted DBSA **87** under batch reaction conditions, we aimed to confirm that the quench would also work in continuous flow, so that it would be applicable to our telescoped diazo transfer process and enhance the safety features of our process. Using 1.5 equivalents of the sacrificial quench solution **100** and a residence time of 15 minutes, 100% conversion of the sulfonyl azide **87** to the desired sulfonyl amide **88** was achieved with the formation of a notable yellow colour in the reactor coil (Scheme 28).



Scheme 28

For the attempted telescoping of the diazo transfer procedure and the sacrificial quench **100**, the optimum conditions for diazo transfer, as previously established, were used (9 minute residence time, 2 equivalents DBSA **87**, 5 equivalents Amberlyst A21). For the subsequent quench in line, 1.5 equivalents of the sacrificial quench solution **100** were used as reported in the literature and had been successful in our earlier quench experiments. The telescoped process (Scheme 29) was carried out with a residence time of 9 minutes for the diazo transfer reaction, and 8 minutes for the quench reaction. As expected, even with the much shorter residence time for the quench, 100% consumption of the excess DBSA **87** was achieved. However, analysis of the ^{1}H NMR spectrum of the crude material showed a complete absence of β-keto sulfoxide starting material **64** or α-diazo-β-keto sulfoxide product **14** and the presence of complex unidentified byproducts. In the reaction coil containing the quench solution intense red coloration was observed. It appears the labile α-diazosulfoxide **14** is incompatible with this sacrificial quench **100**.

It appears that the labile α-diazosulfoxide **14** is incompatible with the quench solution of sodium acetyl acetone in aqueous acetonitrile, interestingly this can not be explained solely on base lability as the pKa(BH^+) of approximately 9 in H_2O is comparable or weaker than Amberlyst A21 or DBU. The most likely rationale is that the α-diazosulfoxides are sensitive to *aqueous* base. Further investigation of this is warranted, including the lactone series. In hindsight, this quench could be attempted at lower temperatures, or with less equivalents of the quench solution to see if decomposition of the α-diazosulfoxide product is an issue. However with the establishment of a high yielding process for the synthesis of α-diazosulfoxides the focus of this work became their further reactivity.



Scheme 29

2.3.7 Spectroscopic characteristics of the novel α-diazosulfoxide **81**

Having established new reaction conditions we successfully accessed the novel naphthalene derived α-diazosulfoxide **81**. The characterisation was used to confirm the structure of the α-diazosulfoxide **81**. The characteristic $C{=}N_2$ absorption stretch in the infra-red spectrum was at 2126 cm^{-1}, all other ketone derived α-diazo-β-oxo sulfoxides are in the corresponding range of 2118 – 2129 cm^{-1}.[16] On successful diazo transfer there is complete disappearance of the $SOCH_2$ signals in the proton NMR spectrum as well as a significant change in the splitting for the AB quartet system of the methylene group alpha to the sulfoxide reflecting the altered conformation as the carbon becomes sp^2 hybridised, compared to sp^3 hybridised in the starting material (Figure 9).

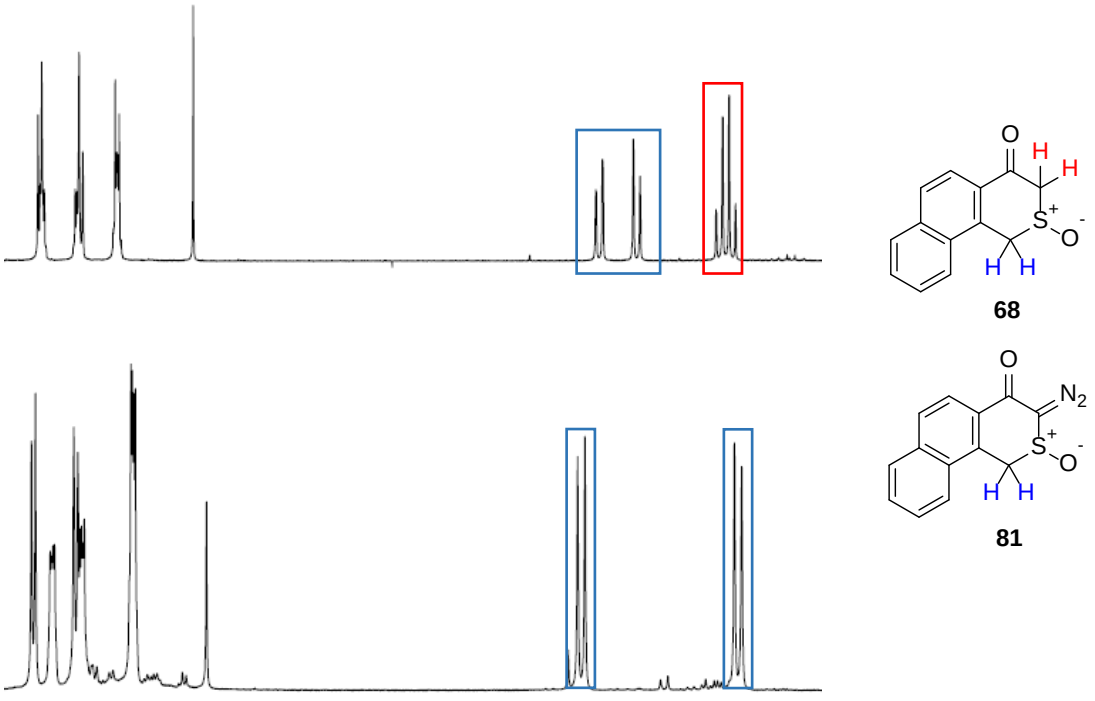


Figure 9: Comparison of the ^1H NMR spectra of the sulfoxide starting material and the α-diazosulfoxide product.

In the ^{13}C NMR spectrum there is only one CH_2 signal observed for the α-diazosulfoxide product **81**, which confirms the presence of the diazo moiety and the structure of the novel α-diazosulfoxide. The stability of this α-diazosulfoxide is further discussed in section 2.5.5.1.

2.3.8 New batch conditions for the synthesis of α-diazosulfoxides

To improve the poor yields from the diazo transfer reaction in batch conditions we investigated a combination of our optimum flow reaction conditions and the standard batch reaction conditions. Applying what we learned about the synthesis of these α-diazosulfoxides during the continuous flow optimisation, we designed new batch reaction conditions with the objective of minimising the exposure of the product to base. These new conditions were established by combining aspects of both the traditional batch reactions and the newly developed continuous flow methodology. A sulfoxide substrate is combined with 2 equivalents of the diazo transfer reagent DBSA **87**, and crucially, the base is added last, dropwise, over 20 minutes, limiting the exposure of both the substrate and product to excess base. This is in comparison to the set-up of the standard batch reaction which consists of cooling the substrate in acetonitrile to 0°C, followed by addition of the base in one portion, stirring of the reaction mixture for 10 minutes and lastly addition of a solution of the sulfonyl azide. Following completion of addition of the base, the reaction mixtures were stirred for significantly shorter times compared to traditional batch reaction conditions. While ultimately the amount of base employed is the same, the concentration of active base at any one time is reduced due to the slow dropwise addition. In all cases, the appropriate precautions were taken with reaction mixtures containing one equivalent of unreacted sulfinyl azide. The results of diazo transfer to the sulfoxide substrates under these new batch reaction conditions are outlined in Figure 10.

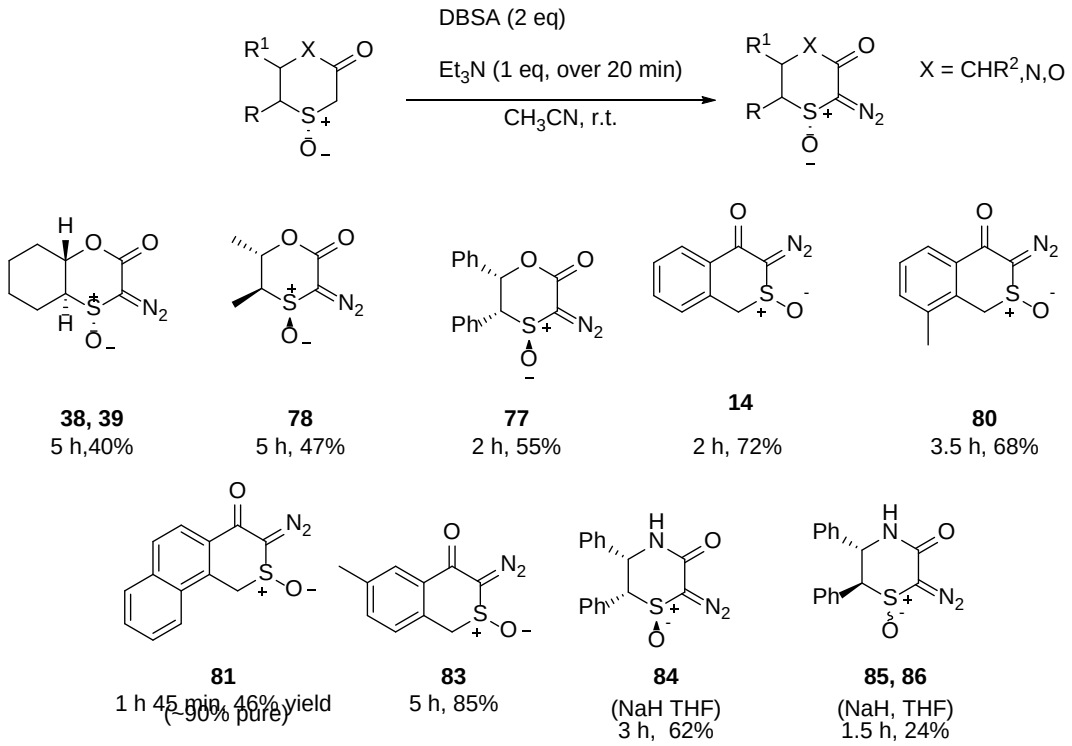


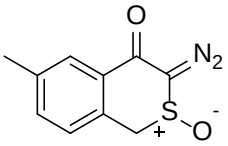
Figure 10: Isolated yields of α-diazosulfoxides from new batch reaction conditions.

The isolated yields for the ketone derived α-diazosulfoxides **14,80,81,83** and the lactam derived α-diazosulfoxides **84–86** show a significant increase in the isolated yield of product compared to the original batch conditions. Work by Collins had shown that the lactam derivatives require NaH as base for successful deprotonation, and so for these reactions, NaH in mineral oil was added portionwise to the reaction mixtures over 20 minutes. Interestingly, the lactone derived α-diazosulfoxides **38,39,77**,**78** show only a slight increase in yield, albeit with a significant reduction in reaction time. This may be due to the reactivity of the lactone moiety making it more susceptible to base mediated decomposition compared to the other derivatives. This is in contrast to the use of Amberlyst A21 in batch reaction conditions (Scheme 23) for the formation of the lactone derivative α-diazosulfoxides **38** and **39**. 100% consumption of the starting material was achieved after 24 h reaction time, giving the desired products in 61% yield. This result suggested that use of the heterogeneous base in batch reactions may lead to reduced base mediated decomposition of the lactone derived α-diazosulfoxides. Notably this may also contribute to the improved outcome in the continuous flow process.

On subjecting the sulfoxide reagents to these new batch reaction conditions (2 eq. DBSA, slow addition of 1 eq. Et_3N), each reaction was closely monitored by TLC, and more accurately by ^1H NMR spectroscopy, whereby an aliquot (<5%) was removed from the reaction mixture,

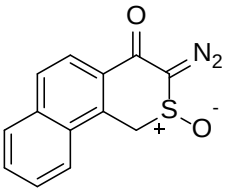
concentrated under reduced pressure without heating and analysed by ^{1}H NMR spectroscopy to determine percentage conversion (Table 12 and Graph 1).

Table 12: Monitoring percentage conversion to the desired α-diazosulfoxide using new batch reaction conditions.



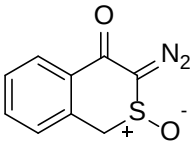
83

Time (min)	Conversion (%)
60	41
180	70
300	89



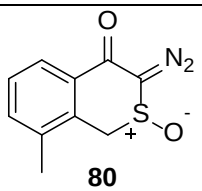
81

Time (min)	Conversion (%)
20	33
60	68
105	87



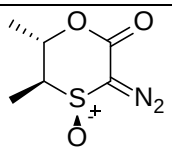
14

Time (min)	Conversion (%)
60	75
120	94



80

Time (min)	Conversion (%)
60	48
180	70
240	84



78

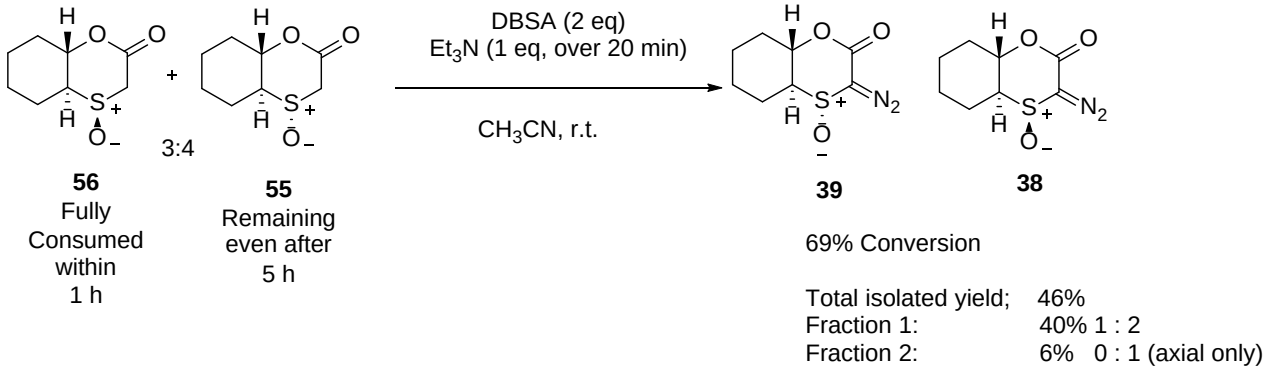
Time (min)	Conversion (%)
60	40
150	67
210	90

As seen in graph 1, the rate of the reactions in batch (2 eq. DBSA, slow addition of 1 eq. Et_3N) were significantly slower than the newly developed flow processes (5 eq. Amberlyst A21, 2 eq. DBSA, 9 min residence time) where the reaction was essentially complete after 9 minutes. This is most likely due to better mixing in continuous flow as well as the back pressure on the system which promotes reaction of the sulfoxide substrates with the heterogeneous base in the packed bed reactor.



Graph 1: Conversion versus time for diazo transfer under new batch reaction conditions.

When diazo transfer to the cyclohexyl sulfoxides **55,56** (Scheme 30) under these new conditions was monitored by ^{1}H NMR spectroscopy, all of axial sulfoxide **56** present was converted to the axial α-diazosulfoxide **38** after 1 h (Scheme 30). With continued stirring after 3 h, there was still substantial amounts of equatorial sulfoxide **55** present and this was the same result at 5 h, when the reaction was concentrated under reduced pressure. Analysis of the ^{1}H NMR spectrum showed conversion to the desired α-diazosulfoxides to be 69%.



Scheme 30

-

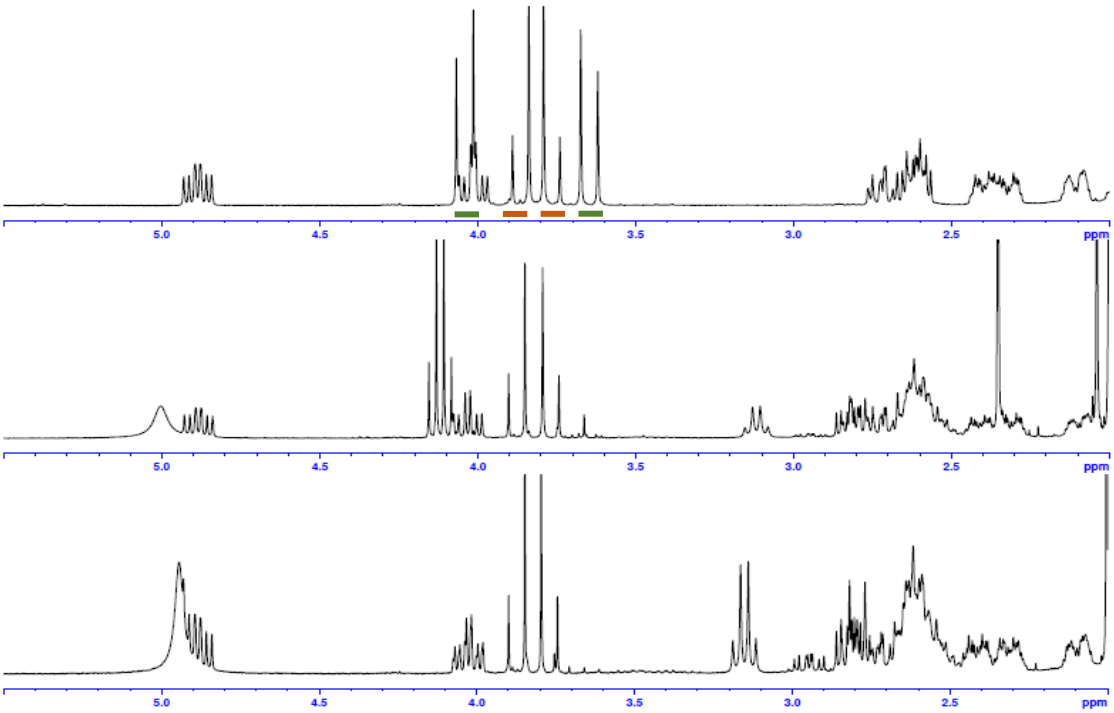


Figure 11: ^{1}H NMR spectra of the sulfoxide starting material (top), the reaction mixture after 3 h (centre) and 5 h (bottom). The disappearance of the AB_q (underlined green) of the axial sulfoxide shows it is consumed whereas the AB_q of the equatorial sulfoxide (underlined orange) remains.

Purification of the crude reaction mixture led to elution of the α-diazosulfoxide in a total yield of 46% yield. The first fraction (40%) contained a 2 : 1 mixture of the α-diazosulfoxides **38**,**39** while the second fraction (6%) contained the axial diazosulfoxide **38** only. The sulfoxide starting material was not recovered from the column. Previously within the group Kelleher[46] had noted that formation of the axial diazo sulfoxide **38** was more efficient than that of the equatorial diazosulfoxide **39** resulting in higher recoveries of **38**. Kelleher suggests that this is due to the relative stereochemistry of the sulfoxide and diazo moieties and that this relationship has a significant effect on the stability. Notably, we have seen here that this also affects the rate of reaction in the diazo transfer step. This faster formation of the axial α-diazosulfoxide is consistent across the series, with the most notable differences in rates of the diazo transfer reaction with the cyclohexyl and dimethyl substituted lactone derivatives and the *trans*-diphenyl lactam derivative.

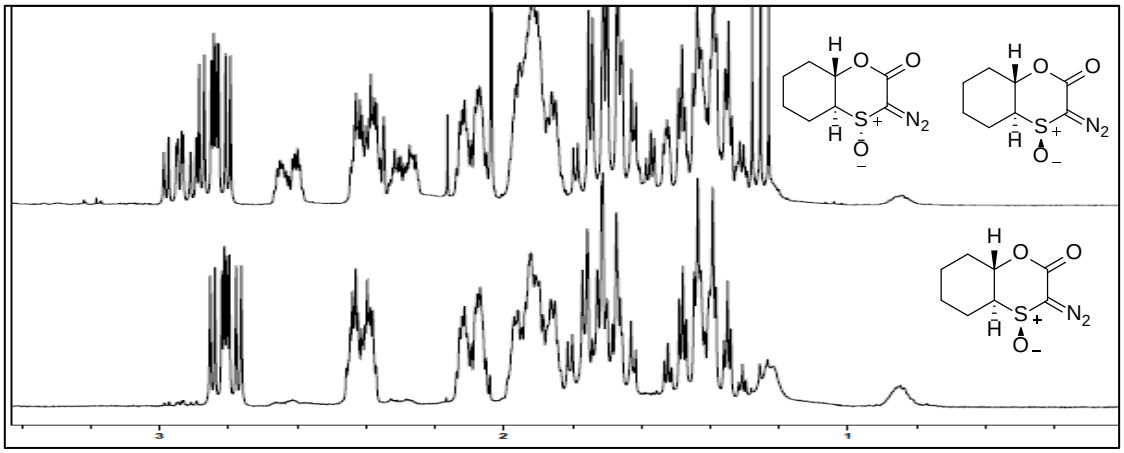
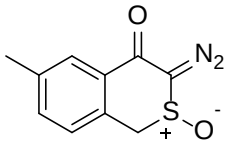


Figure 12: Comparison of the ^{1}H NMR spectra of both isolated fractions of the reaction outlined in scheme 30. The top fraction is 2 : 1, axial : equatorial and the second fraction (bottom) is axial only.

Interestingly on analysis of the diphenyl substituted derivatives, in both the lactam (NaH, THF) and lactone series (Et_3N, CH_3CN) (Figure 10), after 1.5 h they were all at 100% conversion. This was an unexpected result and in hindsight, closer monitoring of the reaction times and conversion by ^{1}H NMR spectroscopy may lead to higher isolated yields for these compounds if terminated earlier. Interestingly though, this mirrors the standard batch reaction conditions where the *cis*-diphenyl lactone derivative undergoes complete diazo transfer in 6 h. In all cases, the conversion in the reaction mixtures was monitored by ^{1}H NMR spectroscopy (Table 13, Table 12). On achieving >85% conversion, the diazo transfer reactions were concentrated under reduced pressure without heating. Purification by chromatography to provide pure α-diazosulfoxides leads to easy separation from the residual DBSA and sulfonamide byproduct.

A series of reactions were carried out to establish whether the key factor that leads to the improvement in isolated yield is the slow addition of the base, or using 2 equivalents of the diazo transfer reagent. Table 13, entry 3 shows that one equivalent of base and one equivalent of diazo transfer reagent **87**, achieved a high conversion of 84%, however a much lower yield of 54% was obtained compared to the use of 2 equivalents of DBSA **87**. Additionally, comparing Table 13 entries 3 and 4, when slow addition of the base is carried out we get high conversion of 84% and a moderate yield of 54%; but when the sulfonyl azide is added to the basic solution a much lower yield is obtained. Therefore, high conversions can be achieved using either order of addition, but for increased yields of the desired α-diazosulfoxide **83,** addition of the base last, over a period of time, is vital.

Table 13: Investigation into the parameter responsible for the increase in isolated yield.



83

Entry	Conditions*	Conversion (%)	Yield (%)
1	2 eq. of DBSA 1 eq. Et_3N[a]	89	85
2	1 eq.Et_3N 2 eq. DBSA[a]	100	84
3	1 eq. DBSA, 1 eq. Et_3N[a]	84	54
4[c]	1 eq. Et_3N 1 eq. TsN_3	100	26
5	1 eq. base	-[b]	-

[a] Added last, by slow addition, over 20 minutes.

[b] On analysis of the crude material by ^1H NMR after 5 hours, there was no change in the quality of the sulfoxide starting material.

[c] Work carried out by Buckley - A reaction time of 9 hours was used and the base was added before the sulfonyl azide.

*All reaction mixtures had a reaction time of 5 h, except for entry **4**.

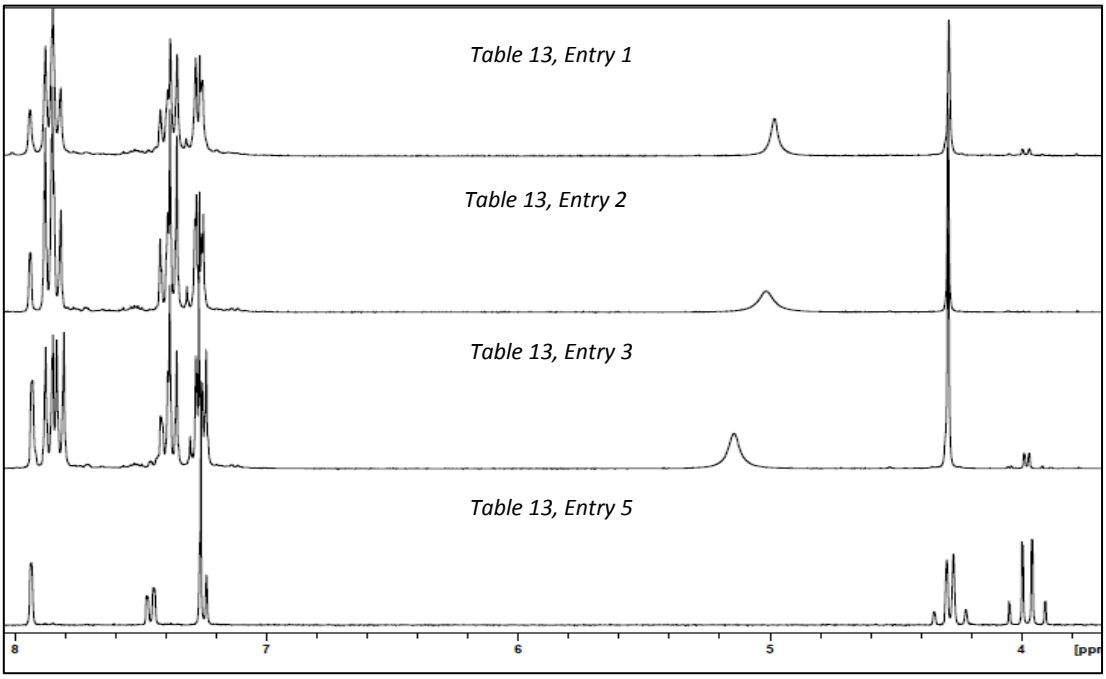


Figure 13: Stacked ^1H NMR spectra of the crude material from the reactions outlined in Table 13.

This careful control of exposure to base to achieve a higher isolated yield, is vital and can be seen by reviewing earlier results. In Table 8, entries 1-4, 2 equivalents of DBSA are used with 20 equivalents of Amberlyst A21, leading to yields which are only 10 – 15% higher than the isolated yields from the standard batch reactions. When the excess base is reduced to 5 equivalents and the residence time is carefully controlled the isolated yields undergo a 2 – 3 fold increase (Table 10, Table 11). Additionally, in Table 5, entry 3, the use of excess homogeneous base (Et_3N), with 2 equivalents of tosyl azide leads to a poor conversion of 38%, and in Table 9 modification of the extent of exposure to the base led to higher isolated yields, even when 2 equivalents of diazo transfer reagent were used in all cases.

These new conditions with shorter reaction time help achieve higher yields for the lactone derivatives. The isolable yield of the lactone derivatives may be compromised due to undergoing base mediated decomposition (either of the sulfoxide starting material **67** or the desired α-diazosulfoxide **83**) through either ring opening of the lactone moiety or hydrolysis *in situ*.

2.3.9 Conclusions

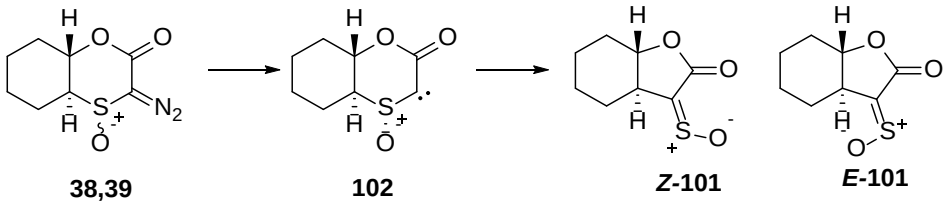
In conclusion, the first generation batch reaction conditions (1 eq. tosyl azide, 1 eq. triethylamine, 16-24 h) were used for the synthesis of a range of α-diazosulfoxides. Through optimisation of the diazo transfer process in continuous flow and utilisation of solid supported bases, in particular Amberlyst A21, we have significantly enhanced the synthesis of α-diazosulfoxides resulting in a notable increase in isolated yield. The new conditions (2 eq. DBSA **87**, 5 eq. Amberlyst A21, 9 min residence time) are consistently performing well across a range of lactone and ketone derived α-diazosulfoxide substrates with 2 – 3 fold increase in yield over the standard batch reaction. The use of Amberlyst A21 as well as polystyrene supported DBU are both applicable to the reaction, with the previously published regeneration of the PS-DBU also proving useful.[40] This method is an improvement on previous work reported from within the group and it highlights the suitability of flow for the synthesis of compounds that may be sensitive to basic conditions and also allows the synthesis in a manner which is safer, more scalable and more time efficient. Interestingly, this new method, allows access to ketone derived α-diazosulfoxides which could not be successfully isolated from batch reaction conditions. Application of these new conditions to the synthesis of lactam derived α-diazosulfoxides was not investigated in this work, as it is anticipated that the Amberlyst A21 is not a strong enough base for the deprotonation in the initial step of the Regitz diazo transfer mechanism. However solid supported organobases do exist and may be beneficial in the synthesis of lactam derived α-diazosulfoxides.[47]

Through optimisation of the continuous flow process a new batch protocol (Et_3N, CH_3CN, DBSA) was developed, utilizing dropwise addition of base to control base concentration, which proved to be successful in increasing the batch reactions yields for the synthesis of the lactone and the ketone derived α-diazosulfoxides. An increase in yield was also noted for the synthesis of the lactam derivatives (using NaH, THF, DBSA). Through optimising the diazo transfer to β-keto sulfoxides in continuous flow, design of the experimental protocol to control the base sensitivity of the desired products became apparent. Optimisation of the batch procedure, using insight from the new continuous flow reaction conditions, lead to new batch reactions conditions. Additionally, the major impact of this work, is using either the new batch conditions or the continuous flow diazo transfer conditions, it is now possible to easily access α-diazosulfoxides in synthetically useful quantities (e.g. 1.12 g of **14** was obtained from a single experiment).

2.4 Reactivity of α-diazosulfoxides to form α-oxo sulfines

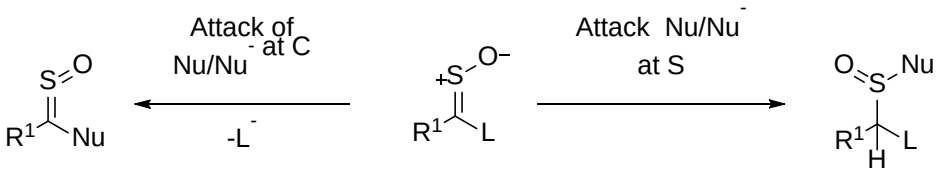
2.4.1 Background

As outlined in section 2.3, with access to a range of α-diazosulfoxides in high yields for lactone, ketone and lactam derivatives, the focus of this work now turned to their reactivity. The reactivity of both lactone and ketone derived α-diazosulfoxides has been established within the group to form α-oxo sulfines such as **101** *via* a hetero-Wolff rearrangement as the major reaction pathwway (Scheme 31). The Wolff rearrangement was first established in the early 1900's and has been widely reviewed in the literature.[48] Through loss of molecular nitrogen, induced either by transition metal catalysis, thermolysis, microwave irradiation or photolysis, a reactive carbene **102** is generated which subsequently undergoes a hetero-Wolff rearrangement to the α-oxo sulfine **101**.

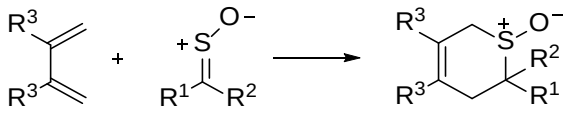


Scheme 31

Significant investigations have been carried out to understand both the reaction pathway for formation of α-oxo sulfine intermediates (**101**) and its subsequent reactivity. [4,49-51] A laser flash photolysis study has shown that on loss of molecular nitrogen, 90% of the material forms an α-oxo sulfine[49] whereas 10% forms a triplet carbene **102**. Relaxation of the triplet carbene to a singlet carbene occurs, and a ring contraction *via* the hetero-Wolff rearrangement occurs, resulting in the formation of the α-oxo sulfine **101**. The α-oxo sulfine can exist in both *E* and *Z* isomers (Scheme 31). Previous work within our group has shown that α-oxo sulfines can undergo nucleophilic attack in either a carbophilic or thiophilic manner in line with literature precedent[6,52-54] highlighting the ambiphilic nature of these reactive intermediates (Scheme 32).[16] Additionally, the lactone and ketone derived α-oxo sulfines readily undergo Diels-Alder cycloadditions with the retention of stereochemistry in the cycloadduct product (Scheme 33).[5,12-14,29,55]



Scheme 32



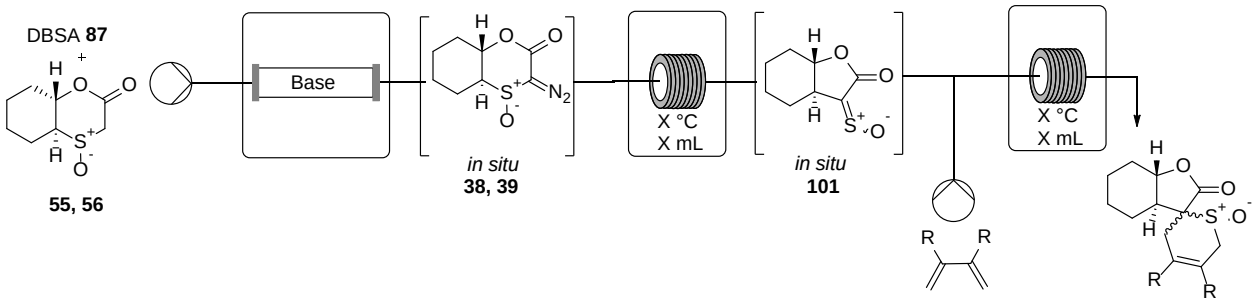
Scheme 33

With the work described in section 2.3 in mind, providing access to α-diazosulfoxides under mild reaction conditions, in a fast and efficient manner, a series of objectives were set to investigate the diverse reactivity of the α-diazosulfoxides to form the corresponding α-oxo sulfines. These objectives were to:

- Investigate the conditions available to promote the transformation of α-diazosulfoxides to α-oxo sulfines in continuous flow, and the subsequent products formed when the α-oxo sulfine is generated in the absence of a diene trap reagent.
- Investigate Diels-Alder cycloaddition reaction with α-oxo sulfines in continuous flow with an aim of increasing the isolated yield and the diastereoselectivity of the desired product.
- Establish the reactivity patterns of the thiopyran-*S*-oxides formed in the Diels-Alder cycloaddition reactions.
- Explore the reactivity of α-oxo sulfines, generated *in situ* with both nitrile oxide and nitrones in 1,3-dipolar cycloaddition reactions.

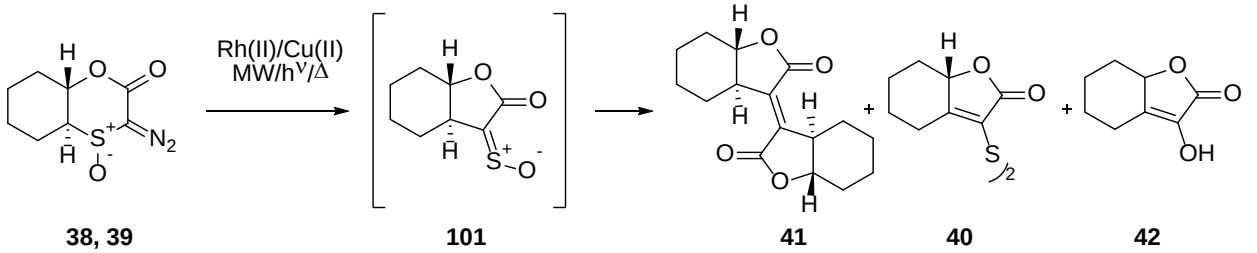
2.4.1 Generation of α-oxo sulfines in continuous flow, in the absence of a diene trap

A telescoped process from a stable β-keto sulfoxide, through to a labile α-diazosulfoxide, followed by formation of a reactive α-oxo sulfine intermediate and subsequent trapping to form a stable, isolable cycloadduct would be a useful synthetic sequence in continuous flow (Scheme 34). In this way the isolation of labile compounds is avoided and the reactivity of α-diazosulfoxides would be more readily available for synthetic utilisation.



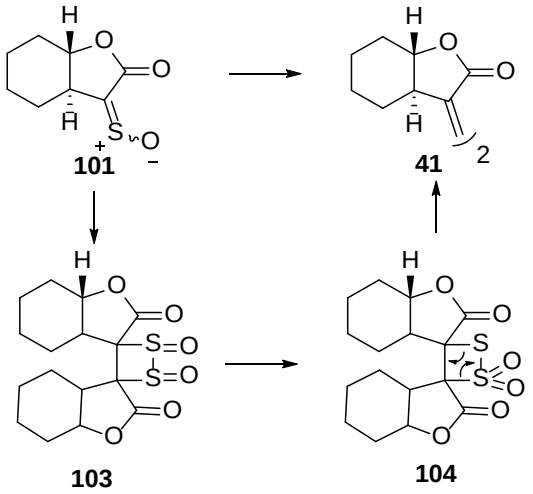
Scheme 34

To achieve this telescoped process in continuous flow, the ability to induce the hetero-Wolff rearrangement in continuous flow, was the initial goal of this work. A series of reaction conditions were investigated for their ease of loss of nitrogen. Collins has previously carried out a substantial investigation into the decomposition patterns observed of the intermediate α-oxo sulfine **101** under various batch reaction conditions including copper and rhodium transition metal catalysis, thermolysis, photolysis and microwave conditions.[14] In this work by Collins, the major products have been identified and characterised as the alkene dimer **41**, the disulfide dimer **40** and an enol **42** (Scheme 35). Additionally, the intermediate α-oxo sulfines had also been successfully isolated and characterised. [15,16]



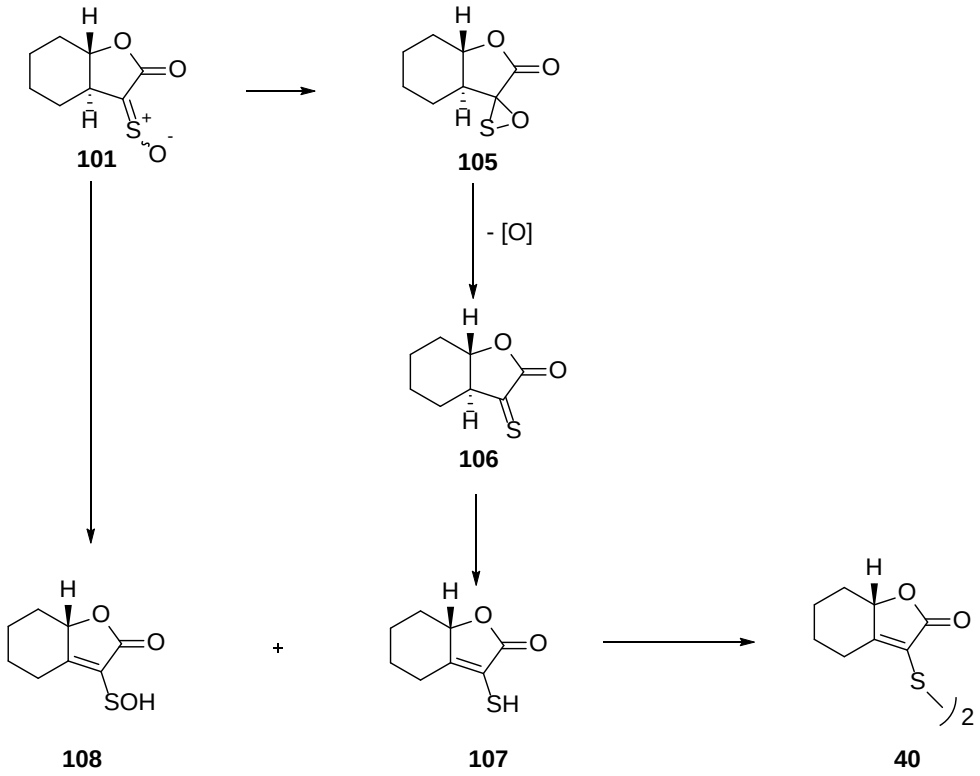
Scheme 35

The different reaction pathways for the formation of each of these products are described herein. The mechanisms of formation have previously been proposed by Collins.[14] The most likely mechanisms for the formation of the alkene dimer **41** proposed by Collins is similar to one proposed by Saalfrank and Rost for the formation of alkene dimers.[56] The tetrasubstituted alkene dimer **41** is formed by initial combination of two α-oxo sulfines **101**, giving the unstable dimer **103**, which undergoes subsequent elimination of SO_2 and sulfur from the intermediate **104** to form the product **41** (Scheme 36). The investigation by Collins had shown that the transition metal catalyst did not affect the rate of formation, or yield of the dimer. It appears that the transition metal catalyst is only involved in formation of the α-oxo sulfine **101** and not formation of the alkene dimer **41**. Additionally, the structure of the alkene dimer which was first reported by Collins[14] was later unambiguously confirmed by Buckley who obtained a crystal structure.[16]



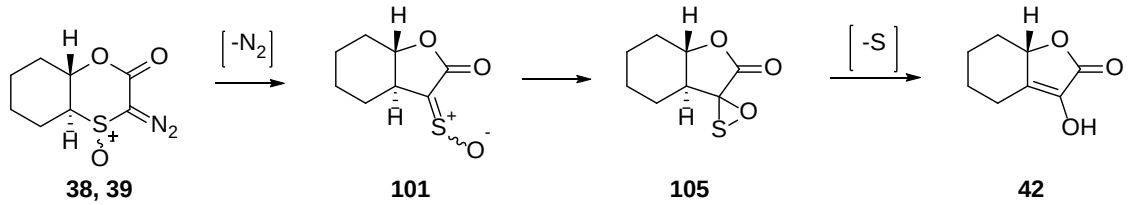
Scheme 36

For the formation of the disulfide dimer **40** (Scheme 37), Collins proposed that under copper catalysed reaction conditions the α-oxo sulfine **101** forms an intermediate oxathiirane **105**, which undergoes oxygen extrusion promoted by the copper catalyst forming a thioketone **106**. The thioketone **106** enolises to form the thioenol **107** which can dimerise with the sulfenic acid derivative **108** of the sulfine **101** to form the disulfide **40**. A similar mechanism for the formation of disulfide dimers from enolisable sulfines has been shown by Metzner. [57] Alternatively oxidative dimerization of **107** could be envisaged.



Scheme 37

The enol product **42** is formed by sulfur extrusion from the intermediate oxathiirane **105**. Interestingly, promotion of this elimination occurs primarily under photolysis conditions, but also under copper catalysed conditions (Scheme 38).



Scheme 38

The stacked spectra of each of the four main decomposition products from the α-diazosulfoxides **38,39** are outlined in Figure 14, including a ^{1}H NMR spectrum of a crude sample of the sulfine **101**. Pure ^{1}H NMR spectra of the alkene dimer **41**, the enol **42** and the disulfide dimer **40** are shown allowing for comparison and identification of the key signals.

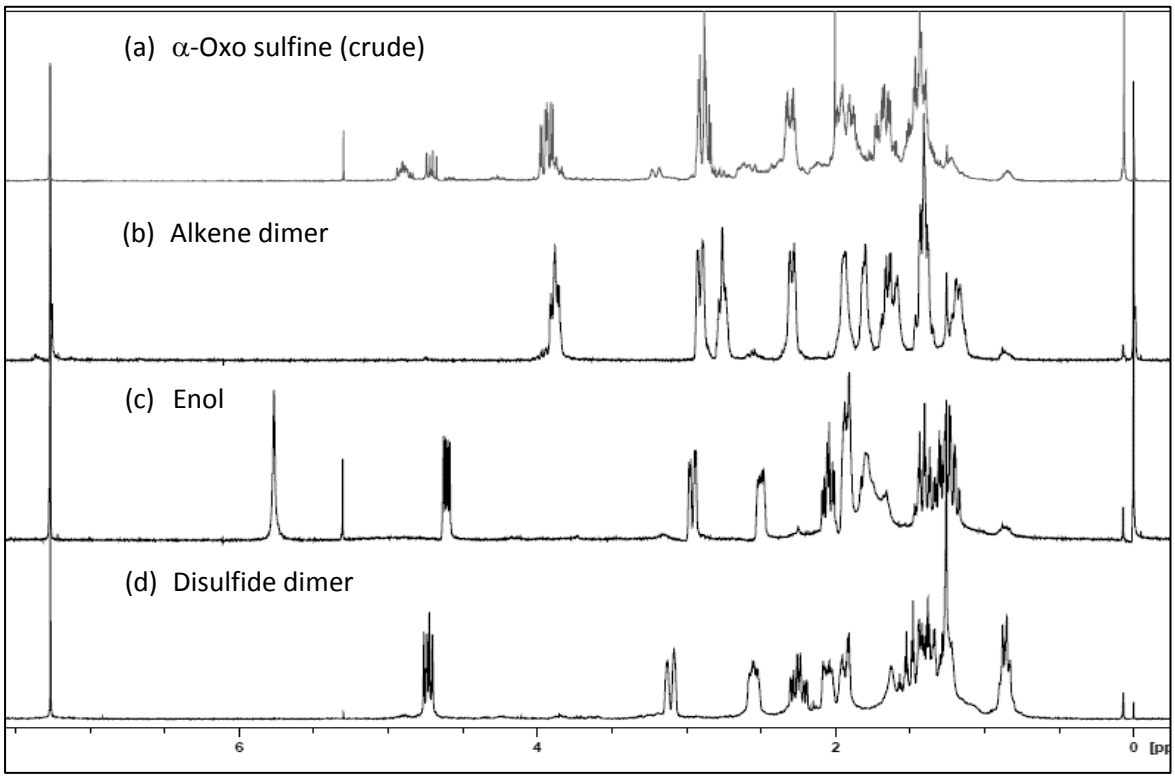
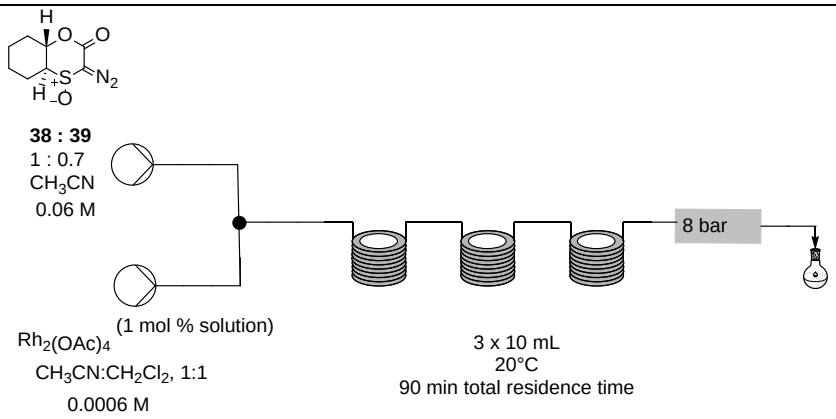


Figure 14: Stacked ^{1}H NMR spectra of (a) a crude sample of the α-oxosulfine **101***, (b) the alkene dimer* **41***, (c) the enol* **42***, and (d) the disulfide dimer* **40***.*

2.4.1.1 Transition metal catalysed transformations in continuous flow

The first set of conditions investigated for induction of the hetero-Wolff rearrangement were transition metal catalysed conditions using rhodium acetate dimer or copper trifluoromethanesulfonate. Copper trifluoromethanesulfonate was selected for its solubility. Previously in the literature[30] the use of acetonitrile and dichloromethane as solvent system has been described as completely solubilising rhodium acetate dimer, to form a purple solution, therefore making it the first choice solvent for the catalyst stream, for the continuous flow reactions.[30] Interestingly the purple colour of the solution does not persist as the reaction occurs in the continuous flow system. Acetonitrile was chosen as the solvent for the α-diazosulfoxides **38,39** solution due to the high solubility. The combination of these two solvent streams essentially equals a solvent system of 3 : 1, dichloromethane : acetonitrile for the reaction *in situ*. With a 1 mol % solution of rhodium acetate dimer and a residence time of 90 minutes, 100% consumption of the α-diazosulfoxides **38,39** were achieved (Scheme 39).



Product	Sulfine 101	Alkene dimer 41	Enol 42	Disulfide 40
Ratio	1.0	0.42	0.07	0.11

Scheme 39 [iii]

The crude reaction mixture was obtained after a Celite® filtration,[iv] followed by concentration, and on analysis by ^{1}H NMR spectroscopy, a number of components were present (Scheme 39). Interestingly, the predominant component identified in the crude material from the reaction was the α-oxo sulfine **101** with the alkene dimer **41**, trace amounts of the enol **42** and disulfide dimer **40** present in the crude material. In the analogous batch reactions carried out by Collins,[14] the major product under rhodium catalysed conditions with a reaction time of 30 minutes was also the sulfine **101**. When the reaction time was increased significantly to 16 hours the alkene dimer **41** becomes the major product, through dimerization of the intermediate α-oxo sulfine **101**. This product profile from the reaction is in line with the results from the comparable batch reaction; short reaction time batch reactions lead to the α-oxo sulfine **101** as the major product while extended reaction times lead to the dimer **41** as the major product. Noteworthy here is that a 1 mol % solution of rhodium acetate dimer, relative to the amount of the α-diazosulfoxides was efficient in inducing the transformation of all of the starting material, even in continuous flow.

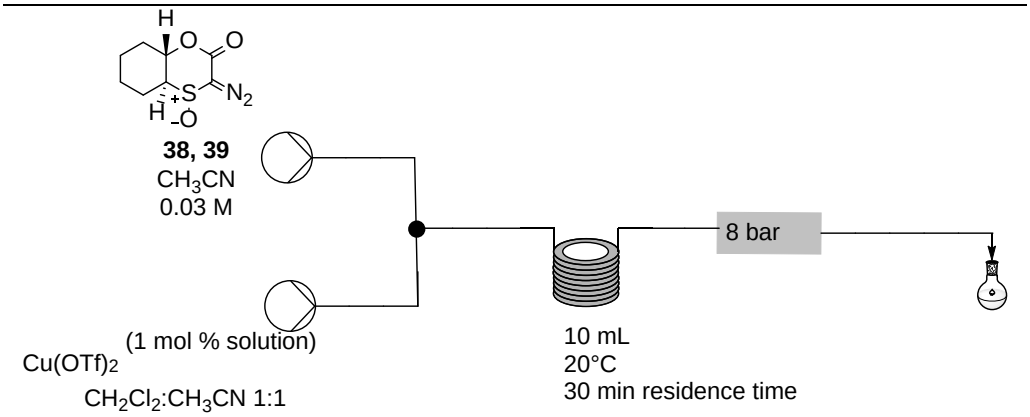
The reactivity of the α-diazosulfoxides **38,39** was also investigated using copper triflate as the transition metal catalyst *in situ.* In the batch reactions carried out by Collins[14] with a reaction time of 16 h, it was found that copper triflate promotes formation of the disulfide dimer **40** through enhancing the rate of oxygen extrusion, and enol **42** (95 : 5). The continuous flow reaction (Table 14) achieved 100% consumption of the starting material when carried out at 20°C with a 30-

[iii] For establishing the ratio of products in the crude material, the characteristic signal of each component was measured in the ^{1}H NMR spectra, resulting in the approximation of crude ratios. Characteristic peaks of each component are outlined in the experimental section.

[iv] The crude reaction mixture was filtered through a Celite® plug to remove any insoluble rhodium or transition metal catalyst.

minute residence time. On analysis of the crude material by ^{1}H NMR spectroscopy, the α-oxo sulfine was found to be the major product with the disulfide dimer **40** and enol **42** also present (Table 14). When the reaction is repeated at 65°C (Table 14) the α-oxo sulfine remains as the major product but the formation of the enol **42** is now comparable to that of the disulfide dimer **40**.

Table 14: Copper catalysed transformation of the α-diazosulfoxide in continuous flow.



Temperature	Sulfine 101	Alkene dimer 41	Enol 42	Disulfide 40
Ambient	1.82	0	0.43	1
65°C	3.5	0	0.97	1

These results are in contrast to the work of Collins where the disulfide dimer **40** was the major product from copper catalysed batch reactions [Cu(II)(OTf)$_2$] carried out under thermal conditions (dichloromethane at reflux). The difference may be due to the much shorter reaction time allowed in flow (30 minutes) compared to the batch reaction (16 hours). Also, comparable to the work by Collins, the α-oxo sulfine was the major product from room temperature copper catalysed reactions [Cu(I)Cl and Cu(0)]. Similar to these copper triflate catalyst results (Table 14), the rhodium catalysed transformation in continuous flow forms the α-oxo sulfine **101** as the major product (Scheme 39). It was noted by Collins that in rhodium acetate catalysed batch reactions, which were heated to reflux, the alkene dimer **41** was the major product isolated.[14] For the previously described batch reactions, the concentration of the α-diazosulfoxide solutions used, varied from 0.015 M to a maximum of 0.044 M for the α-diazosulfoxide starting material,[14] therefore in this continuous flow work, the concentration of solutions used are in line with previous work. Interestingly, when the copper triflate catalysed reaction was repeated with heating, a significant increase in the relative amount of enol **42** present occurs. This results agrees with work carried out by Collins who showed that when rhodium catalysed reactions are carried

out with heating, the amount of enol **42** and disulfide **40** present is greatly increased due to the increased rate of decomposition of the oxathiirane **105** and sulfine **101** intermediates.

This variation of reaction products from the continuous flow reaction compared to batch may be due to a number of factors including shorter reaction times, the pressure of the continuous flow reaction versus the batch reaction (8 Bar compared to 1 bar), the absence of oxygen in the system or the presence of acetonitrile in the solvent system (25%). Effectively, these differences in reaction conditions lead to a variation in product ratios. However the same trends in batch and flow are seen with short reaction times (sulfine **101** as the major product) and copper as the transition metal catalyst (increased the percentage of disulfide **40** and enol **42** formed in the reaction).

2.4.2 Thermolysis induced transformations in continuous flow

Thermolysis can also be used to generate α-oxo sulfines from the corresponding α-diazosulfoxides.[14,49] This effectively provides access to α-oxo sulfines under mild, metal free reaction conditions. To establish the temperature at which the α-diazosulfoxides **38,39** would undergo loss of molecular nitrogen and the subsequent rearrangement to the α-oxo sulfine **101**, a thermogravimetric analysis (TGA) was carried out. Thermogravimetric analysis is a method of determining a temperature of decomposition of a compound by monitoring the mass of the compound with respect to temperature. The sample is subjected to a controlled temperature programme in a controlled atmosphere. The heating rate was set at 5°C per minute and a maximum temperature of 250°C was set. The resulting graph of weight versus temperature (Figure 15) shows that for the lactone derived α-diazosulfoxides **38,39**, at an approximate temperature of 100°C, significant mass loss is observed. This mass loss is assigned to the loss of nitrogen. Additionally it is noted that the mass loss is gradual and steady suggesting loss of molecular nitrogen, followed by subsequent losses.

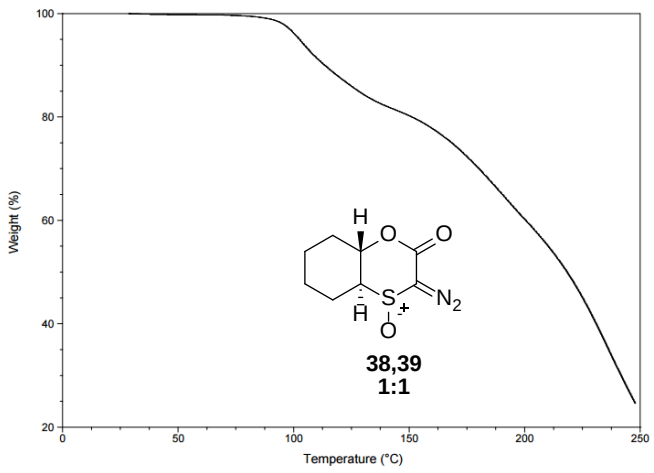
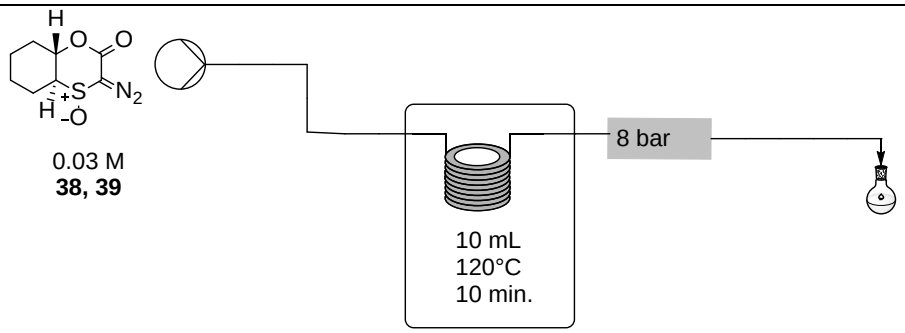


Figure 15: Thermogravimetric analysis of the α-diazosulfoxides **38**,**39**.

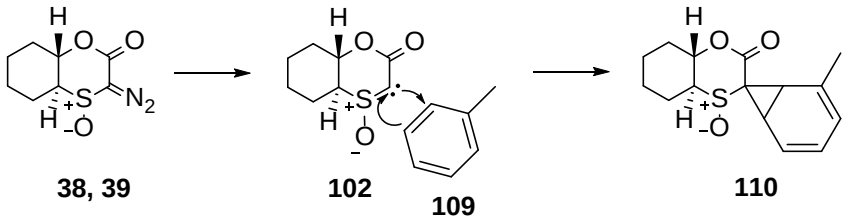
With this result from the TGA, 120°C was chosen for the continuous flow thermolysis reactions. This temperature is easily achieved in continuous flow with toluene as solvent, without causing problems with pressure regulation. With this high temperature and a residence time of 10 minutes, complete consumption of the starting material was achieved. Analysis of the crude reaction mixture by ^{1}H NMR spectroscopy showed the presence of the alkene dimer **41**, enol **42** and disulfide dimer **40** decomposition product. The disulfide dimer **40** was the major component (Scheme 40). This metal free thermolysis reaction can be compared to the microwave reaction in batch (30 mins at 135°C), carried out by O'Sullivan which resulted in the formation of complex mixture of unidentifiable products in the crude material, and after purification impure samples of the alkene dimer, the disulfide dimer and the enol were all isolated, along with other unknown decomposition products.[5] In contrast to this complex mixture from the microwave, thermolysis in the presence of rhodium acetate lead to the preferential formation of the alkene dimer **41** as the major product.[14]



Product	Sulfine 101	Alkene dimer 41	Enol 42	Disulfide 40
Ratio	0	0.31	0.13	1

Scheme 40

Interestingly the ^{1}H NMR spectrum of the crude material was quite a complex mixture, although the previously characterised products were identifiable among the components. This complexity may due to the use of toluene as solvent. O'Sullivan had previously reported similar complexities present when toluene was used as solvent and suggested it could be due to aromatic addition of the carbene **102** to the aromatic ring of toluene **109** (Scheme 41) forming an unstable intermediate **110** which undergoes further transformations to unidentifiable products.



Scheme 41

When the thermolysis reaction in continuous flow (30 min, 120°C) is repeated with dichloromethane as solvent the ^{1}H NMR spectrum of the crude material is far less complex (Figure 16). The α-oxo sulfine **101** was the major product with additional formation of the enol **42** and disulfide dimer **40**. On analysis of the reaction mixture after a further eighteen hours, at room temperature in deuterated chloroform,, the ratio of products had changed through rearrangement of the intermediate α-oxo sulfine **101**, with a slight increase in the amount of disulfide **40** and enol **42** present (Table 15 and Figure 16), highlighting the transitory nature of the α-oxo sulfine **101**.

Table 15: Thermolysis reaction using dichloromethane as solvent, and a 30 minute residence time at 120°C.

Product Ratio	Sulfine 101	Alkene dimer 41	Enol 42	Disulfide 40
After reaction	1.0	0	0.04	0.21
After 18 h	1.0	0	0.19	0.98

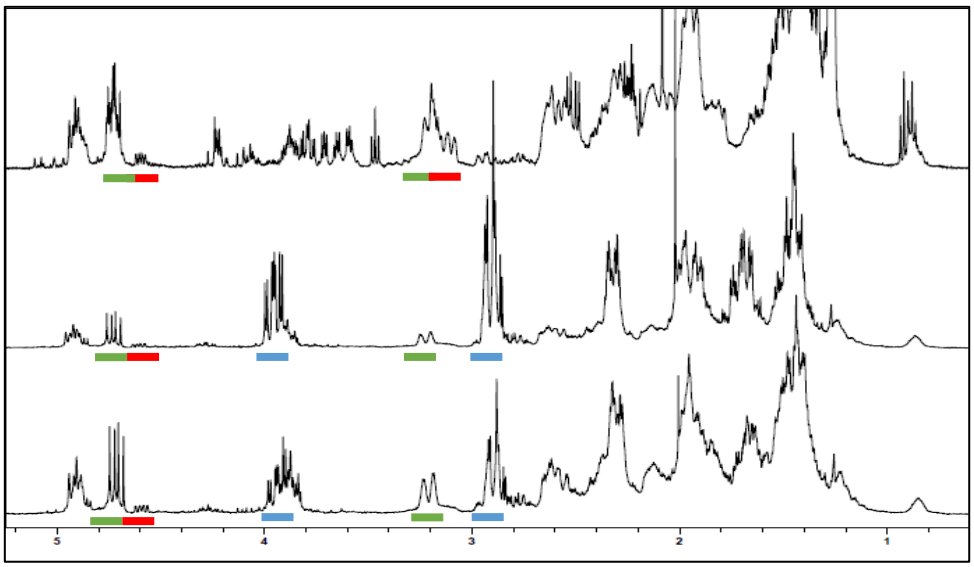


Figure 16: Comparison of the ^{1}H NMR spectra of the crude material when toluene is used as solvent (top) compared to the use of dichloromethane as solvent (centre), and when the crude material from the reaction in dichloromethane is left overnight (bottom). The sulfine **101** *signals are underlined blue, the enol* **42** *signals are underlined in red and the disulfide* **40** *signals are underlined in green.*

Additionally, we wanted to explore if concentration of the crude reaction mixture under reduced pressure, affects the ratio of rearrangement products formed in the continuous flow reactions. To investigate this possibility, before the crude reaction mixture was concentrated, a sample was analysed by infrared spectroscopy (evaporation of the crude reaction mixture on the ATR), and the major absorption peaks were recorded at 1080, 1756, 2942 cm^{-1} (Figure 17) . The collected solution was subsequently concentrated under reduced pressure and re-analysed by IR spectroscopy. No major change was recorded between the two spectra (Figure 17). The red spectrum is the analysis of the crude reaction material before concentration under reduced pressure showing the carbonyl absoprtion of the α-oxo sulfine to be the major product, and the green spectrum is after concentration under reduced pressure whereby no evidence of alteration was observed.

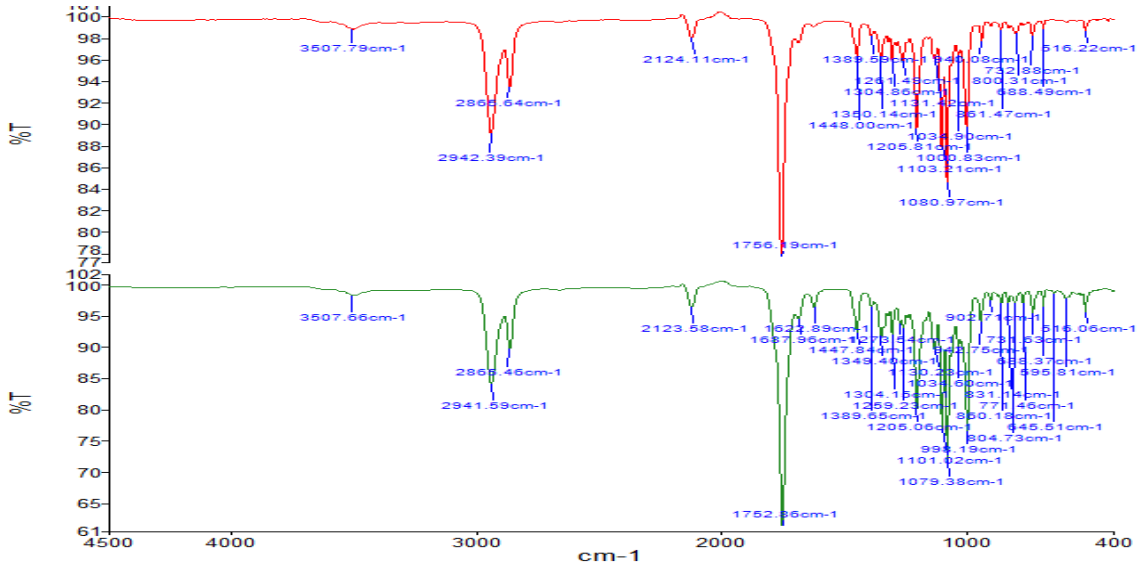


Figure 17: Comparison of the infrared absorption spectrum of the crude reaction solution before concentration (top) and after concentration under reduced pressure (bottom).

2.4.3 Pre-generation of the α-oxo sulfine in batch with subsequent reactivity in continuous flow

As part of this work, generation of the α-oxo sulfine **101** in batch reaction conditions and investigating the further reactivity in continuous flow became an objective in the context of the results in section 2.4.2. The conversion of the α-diazosulfoxides **38,39** to the α-oxo sulfine **101** was achieved under standard batch conditions using rhodium acetate dimer and was complete in 15 minutes. This transformation was monitored by IR spectroscopy with evaporation of an aliquot from the solution on the ATR crystal (Figure 18). The conversion from the α-diazosulfoxides **38,39** to the α-oxo sulfine **101** was assumed to be quantitative with all of the α-oxo sulfine **101** carried through to the reaction in flow.

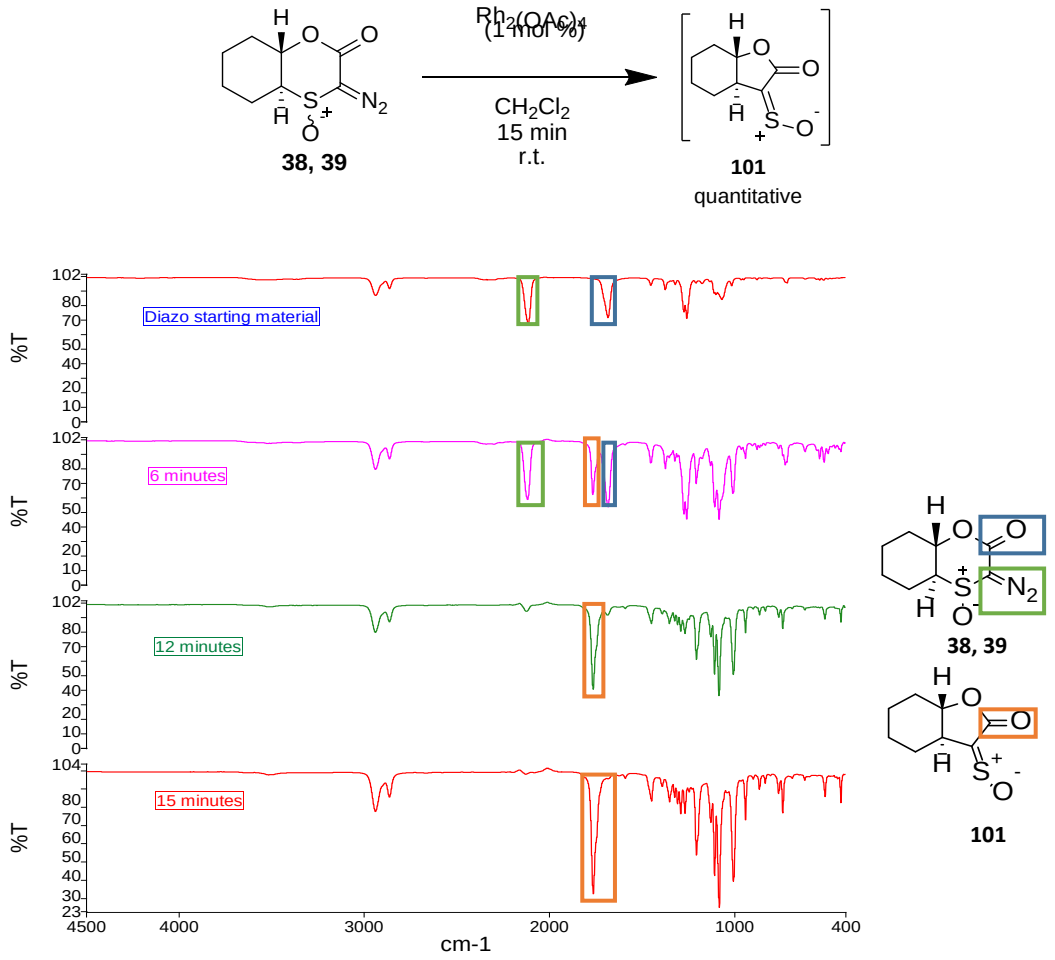
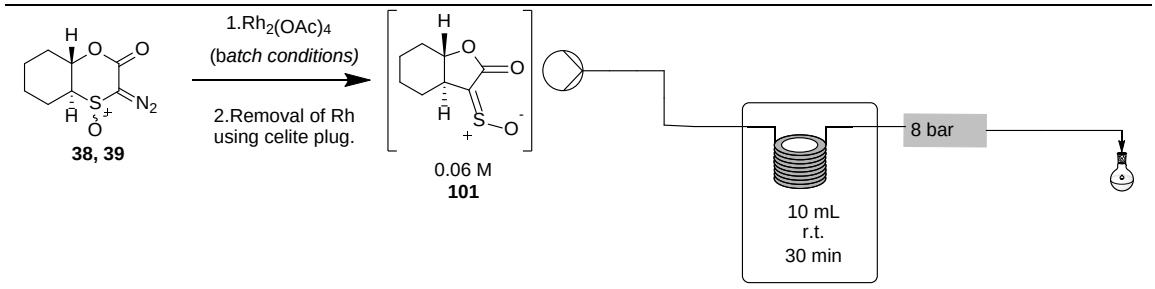


Figure 18: Monitoring of the formation of the α-oxo sulfine **101** *through disappearance of the α-diazosulfoxide carbonyl (blue) and diazo (green) stretches, followed by appearance of the α-oxo sulfine carbonyl stretch (orange).*

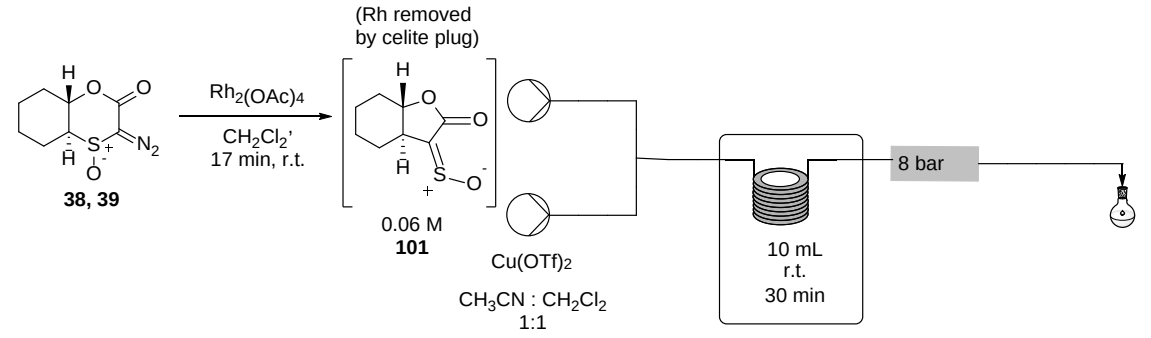
With the α-oxo sulfine **101** successfully generated in the batch reaction conditions, the batch reaction mixture was filtered through a Celite® plug to remove any insoluble transition metal catalyst. With successful generation of the α-oxo sulfine in batch reaction conditions, the reactive intermediate was pumped through the reactor coil to establish the effect of the system back pressure on the rearrangement products (Scheme 42). Analysis of the crude material by ^{1}H NMR spectroscopy showed the alkene dimer **41** to be the major product (Scheme 42) with complete consumption of the α-oxo sulfine **101**. The increased back pressure in the continuous flow system may be the parameter responsible for the increased rate of dimerization, resulting in the increased proportions of the alkene dimer product in the crude reaction mixtures.



Product	Sulfine 101	Alkene dimer 41	Enol 42	Disulfide 40
Ratio	0	4.4	1.0	1.07

Scheme 42

Similarly, generation of the α-oxo sulfine **101** was achieved in batch, with rhodium acetate dimer. After filtration through a Celite® plug, the α-oxo sulfine **101** is introduced to the continuous flow system (Scheme 43). At a T-piece the solution of α-oxo sulfine **101** is combined with a 1 mol % solution of copper triflate.



Product	Sulfine 101	Alkene dimer 41	Enol 42	Disulfide 40
Ratio	0	1.5	1.0	4.95

Scheme 43

With a residence time of 30 minutes at room temperature, analysis of this crude reaction mixture by ^{1}H NMR spectroscopy showed the disulfide **40** to be the major product, along with some alkene dimer **41** and enol **42**. The formation of the disulfide dimer **40** as the major product under copper catalysed conditions is a mirror of the results achieved in Collins' work in batch reaction conditions. Formation of the disulfide dimer as the major product is also common to the thermolysis reactions in continuous flow, when toluene is used as solvent. Purification of the reaction mixture led to elution of the disulfide dimer **40** in 35% isolated yield (Figure 19). When the α-oxo sulfine **101** was not pre-formed, the α-oxo sulfine **101** was the major product (Table 14), in this reaction where the α-oxo sulfine **101** was pre-formed and subsequently combined with the copper catalyst the disulfide **40** is the major product. This further supports that the presence of the copper catalyst enhances the rate of formation of the disulfide dimer **40**. When the α-oxo

sulfine **101** was formed *in situ* with the copper catalyst, the α-oxo sulfine **101** was the major component of the reaction mixture (Table 14). However, if the sulfine is pre-generated and subsequently combined with the copper catalyst, dimerization to form the disulfide product is the dominant reaction pathway.

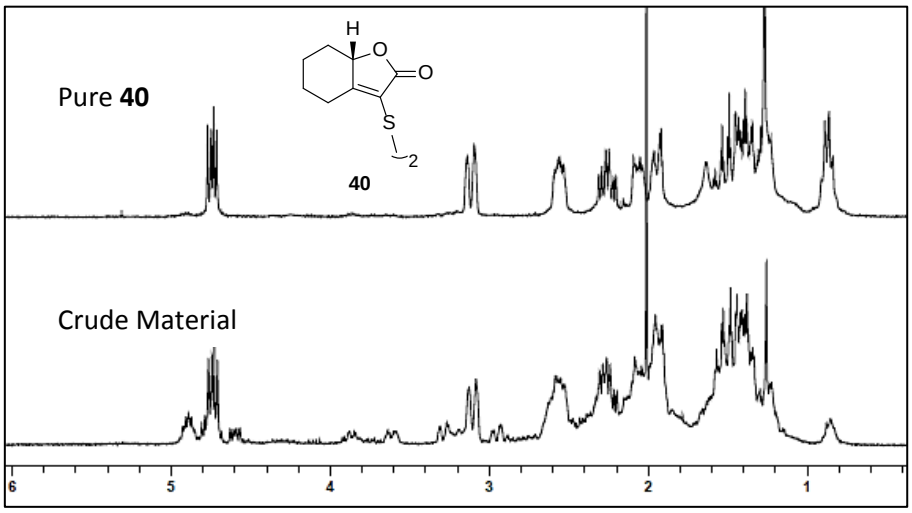


Figure 19: Comparison of the ^{1}H NMR spectrum of the crude material and the pure product.

2.4.4 Photolysis transformations in continuous flow

2.4.4.1 Background

Previously within the group Collins had demonstrated that photolysis of the α-diazosulfoxides **38,39** lead to enol product **42** almost exclusively. Collins describes that under photochemical conditions, the sulfur extrusion reaction pathway may be faster than dimerization and therefore the enol **42** is the preferentially formed product. The setup for these batch photolysis reactions included a mercury lamp being placed close to a round bottom flask and wrapped in tin foil with a reflux condenser attached. Therefore, with a more refined continuous flow photolysis setup, and having achieved successful transformation of the α-diazosulfoxides **38,39** to the α-oxo sulfine **101** in continuous flow using transition metal catalysis and thermolysis, the next part of the study was to use photolysis to promote the hetero-Wolff rearrangement. The combination of photochemistry and continuous flow chemistry is extremely useful as it allows specific control over the exposure time to the UV light, and better temperature control than in batch reaction conditions. The photochemical reactor used in this work was the UV-150 supplied by Vapourtec. The reactor coil surrounds the UV lamp whose power output and temperature can be controlled manually and whose wavelength output can be controlled by selecting an appropriate filter. It is strongly recommended by Vapourtec that a filter is always used with the UV-150 reactor as the filter will absorb a significant amount of the unwanted infra-red energy. The three filters supplied with the UV-150 photochemical reactor have different cut-off wavelengths:

Table 16: Filter Types for the UV-150 photochemical reactor.

Filter	Wavelength
Type 1 (Silver)	190 – 2000 nm
Type 2 (Gold)	250 – 390 nm
Type 3 (Red)	300 – 2000 nm

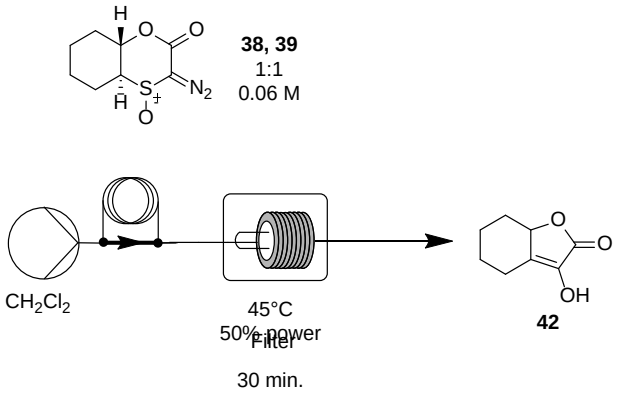
For photochemically induced transformations, it is recommended for best results to use dilute solutions as this will ensure a higher concentration of photons per reagent molecule.[58,59] Additionally, the fluoropolymer tubing has good UV transmission in the range 220 – 400 nm. Photolysis reactions which were previously carried out within the group used a mercury lamp (λ > 254 nm) with a pyrex® glass reaction vessel which has a wavelength cut off of < 300 nm.

2.4.4.2 Photochemical transformations

A series of three reactions were undertaken with variation of the filter used each time. A 0.06 M solution of the cyclohexyl α-diazosulfoxides **38,39** in dichloromethane was used (Scheme 44). The reasons for the use of this molar concentration are two fold:

1). As mentioned above the use of dilute solutions is recommended for continuous flow photolysis reactions and

2). The low solubility of the α-diazosulfoxide starting material in dichloromethane.



Scheme 44

The crude material from the reactions with filter numbers 1 and 2 were exceptionally clean with the enol **42** being the major product in greater than 90% purity (Scheme 44). Interestingly, with filter number 2 a series of unknown impurities were observed with singlets in the region between 5.77 and 6 ppm in the ^{1}H NMR spectrum. When the photochemical decomposition was carried out with filter number 3, these impurities were also present, and the enol **42** was the major

component of the reaction mixture. The ^{1}H NMR spectrum of the crude material in the case of filter 3, was much more complex compared to the results with filters number 1 and 2. This suggests that wavelengths between 190 and 300 nm are particularly suited to inducing the hetero-Wolff rearrangement in this specific substrate, as filter 3, which has uv transmission between 300 – 2000 nm resulted In a complex mixture of unidentifiable products which included the previously characterised enol **42**. It was also noted that some band broadening was observed on the ^{1}H NMR spectra of the crude mixture. This is because, as discussed earlier, as the enol **42** is formed through sulfur extrusion of the oxathiirane intermediate **105**, the elemental sulfur remains in the mixture, but this byproduct is easily removed with a Celite plug®.

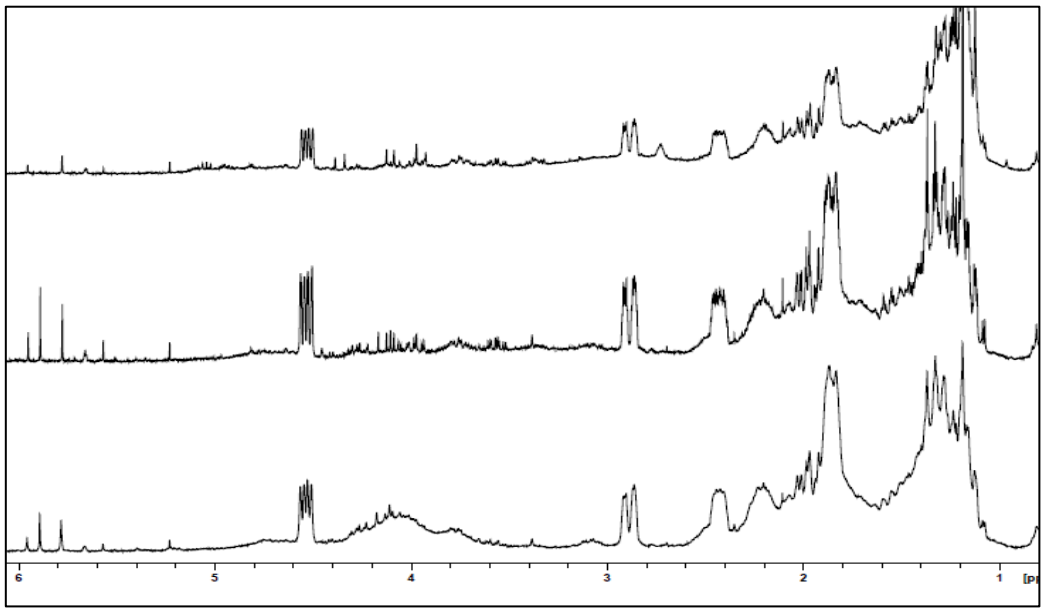


Figure 20: Stacked ^{1}H NMR spectra of the crude material from photochemically induced transformations of the α-diazosulfoxides **38,39** *using filter 1 (top), filter 2 (centre) and filter 3 (bottom).*

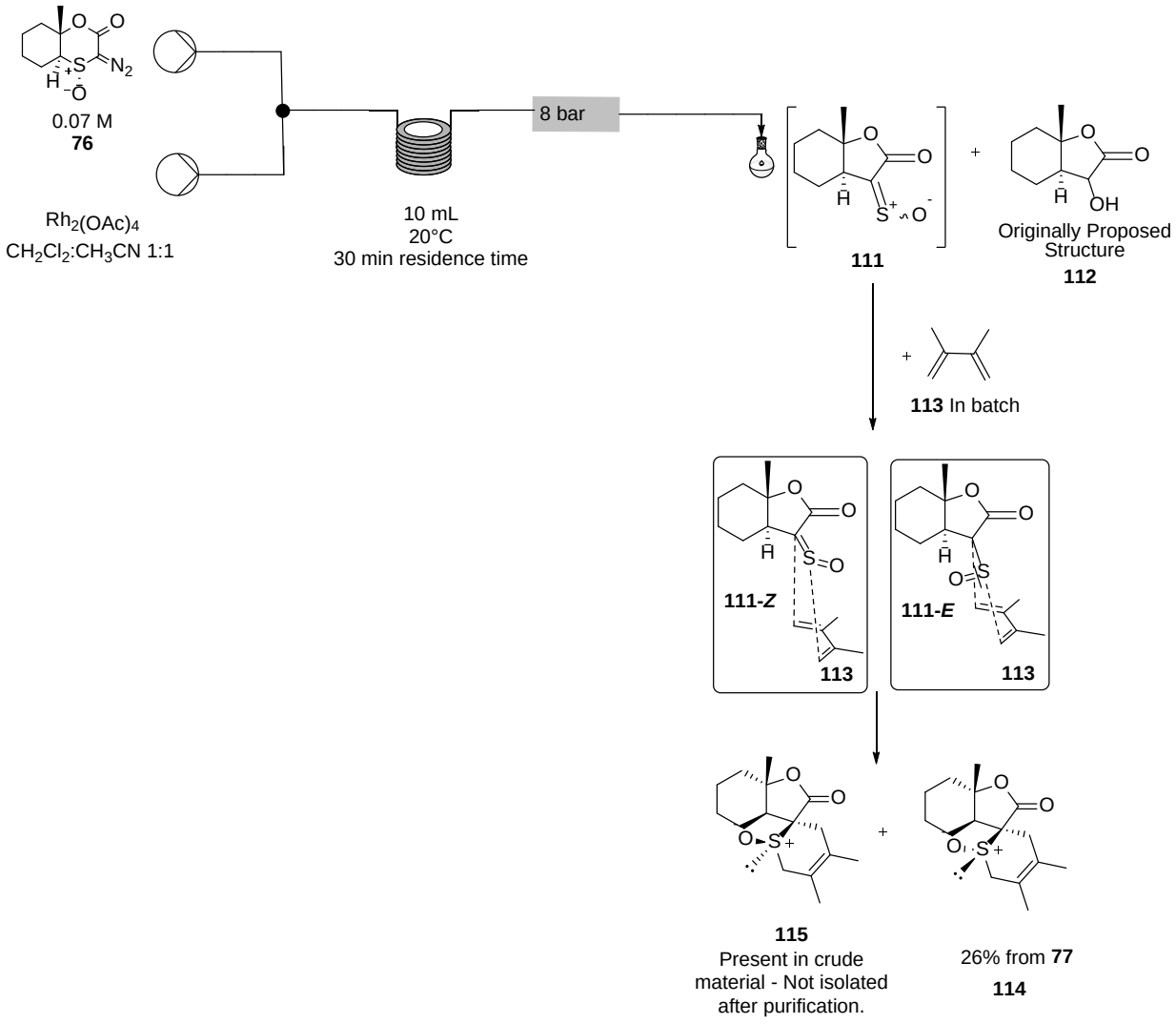
Essentially, the product profiles observed from the photolysis reactions in continuous flow are the same across each of the three filters with the enol **42** being the major product in each case. Additionally these observed results mirror the batch photolysis results reported by Collins[14] in which the enol **42** is also the major product in each case.

2.4.5 Reactivity of methyl bridgehead α-oxo sulfine 111

2.4.5.1 Reactivity of 111 in continuous flow under transition metal catalysis conditions

Having carried out a series of decomposition reaction on the α-diazosulfoxides **38,39** in continuous flow the results showed that some were in line with batch results and some were different (e.g. copper catalysed reactions in continuous flow whereby the major product was the sulfine when the major product in the batch reaction is the disulfide dimer). To continue the investigation on a second α-diazosulfoxide, the methyl bridgehead derived α-diazosulfoxide **76**

underwent a series of transformations in continuous flow which could be compared to the transformations of cyclohexyl derived α-diazosulfoxides **38,39** as detailed earlier in section 2.4.1. With a 30 minute residence time and a 1 mol % solution of rhodium acetate dimer the crude material was analysed by ^{1}H NMR spectroscopy and proved to be the intermediate α-oxo sulfine **111** but with trace amounts of an unknown product **112**. Previous work by Collins had tentatively assigned the structure of this unknown as an alcohol **112**, however, this could never be unambiguously confirmed. It was also noted by O'Sulivan that the α-oxo sulfine **111** was much more stable relative to the cyclohexyl derived α-oxo sulfine **101**, highlighted by the result that after ten hours at reflux in dichloromethane, with rhodium acetate dimer, the crude material consisted of the α-oxo sulfine **111** and the unknown **112** in a ratio of 95 : 5.[15] With the crude material from the continuous flow, rhodium catalysed transformation consisting mainly of the α-oxo sulfine **111**, it was immediately added to a solution of 2,3-dimethyl-1,3-butadiene **113** in a round bottomed flask. In this manner, the generation of the α-oxo sulfine **111** and a subsequent Diels-Alder cycloaddition was operated in a semi-continuous process (Scheme 45).

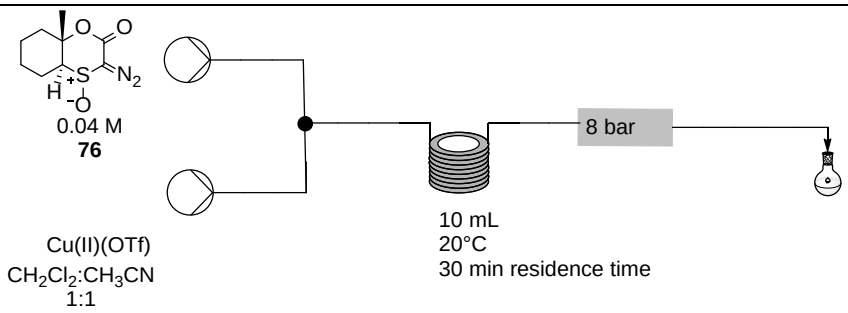


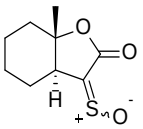
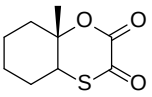
Scheme 45

Analysis of the crude reaction mixture showed the presence of a major cycloaddition product **114**, a minor cycloaddition product **115**, and the unknown **112** in a ratio of 1 : 0.2 : 0.04. Purification of the reaction mixture led to elution of the major cycloaddition product **114** in a yield of 26% (Scheme 45). The stereochemistry of the cycloadduct indicated that it was formed by addition of the diene to the *E* α-oxo sulfine **111** from below.

When the decomposition of the α-diazosulfoxide **76** was carried out in continuous flow, with copper triflate as the transition metal catalyst, the α-oxo sulfine **111** was the major product, the unknown **112** was a minor product[14] and as well as a thioester **116** previously characterised by O'Sullivan (Scheme 46).[15] Formation of the α-oxo sulfine as the major component of the reaction mixture correlated with the earlier work carried out by O'Sullivan.[15] Additionally, formation of the α-oxo sulfine as the major product reflects the results achieved with the cyclohexyl derived α-

diazosulfoxides **38,39** in continuous flow, when copper triflate is used as the transition metal catalyst also. The work carried out by O'Sullivan involved generation of the α-oxo sulfine in microwave reactions conditions which was limited by scale. This generation of α-oxo sulfine in continuous flow, represents the first scalable method for the generation of the α-oxo sulfines **101** and **111**.

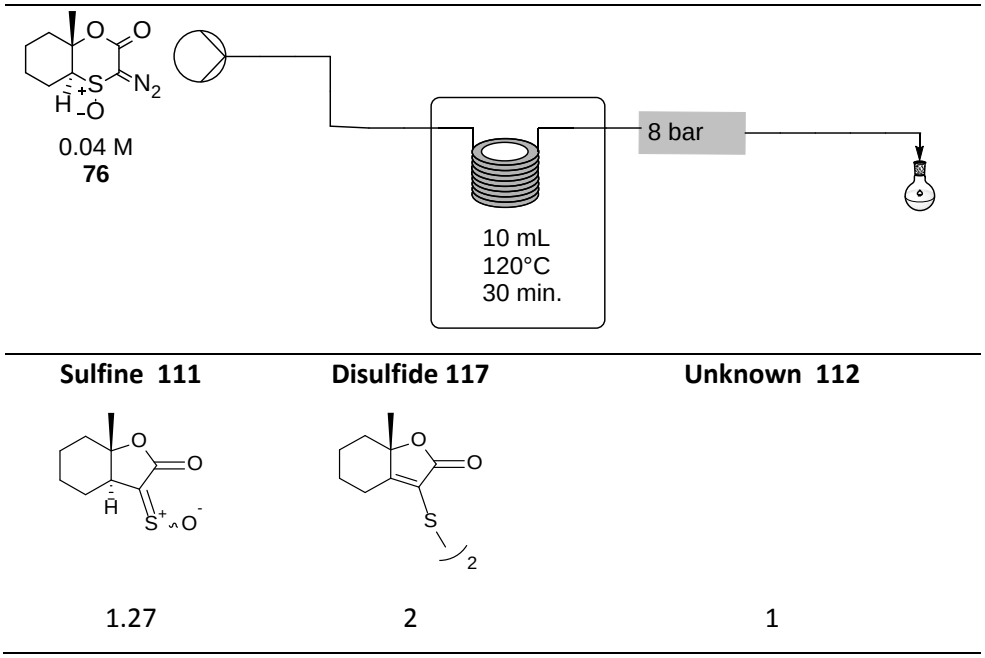


Products	Sulfine 111	Unknown 112	Thioester 116
			
Ratio	3.5	1	1.2

Scheme 46

2.4.5.2 Reativity of 111 in continuous flow under under thermolysis conditions

To compare the reactivity of the α-diazosulfoxide **76** with the cyclohexyl derived α-diazosulfoxides **38,39** under thermal conditions, the methyl bridgehead α-diazosulfoxide **76** was subjected to thermolysis conditions in continuous flow. 120°C for 30 minutes, in toluene, resulted in complete consumption of the starting material and formation of the disulfide dimer **117** as the major product with the α-oxo sulfine **111** and unknown product **112** also present (Scheme 47). Purification of the crude reaction mixture led to elution of the disulfide dimer **117** in a yield of 25%.

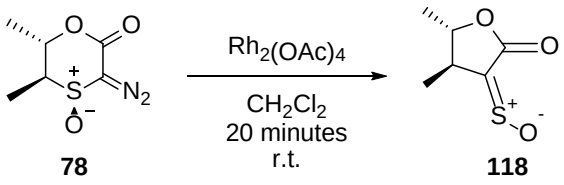


Scheme 47

The presence of the α-oxo sulfine **111** in this crude mixture, which had been subjected to high temperatures for 30 minutes, along with the α-oxo sulfine **111** being the major product under both rhodium and copper catalysed condition, highlights once again the relative stability of this methyl bridgehead derived α-oxo sulfine **111**. Previously, when decompositions of the methyl bridgehead α-diazosulfoxide **76** was carried out with $Rh(II)(pfb)_4$,[15] the sulfine **111** and the unknown decomposition product were present in the ratio of 1 : 3.75. Additionally, work by Collins[15] led to the formation of the disulfide dimer **117** as the major product under copper catalysed batch reaction conditions, and the disulfide dimer as the minor product under microwave conditions. Comparable to this result is the thermolysis reaction of the cyclohexyl derived α-diazosulfoxides **38** and **39** in toluene**,** in which the disulfide dimer **40** was the major reaction product.

2.4.6 Reactivity of dimethyl α-oxo sulfine 118 in continuous flow

For the cyclohexyl derived α-diazosulfoxides **38,39**, pre-generation of the α-oxo sulfine **101** and subsequent pumping through the continuous flow reactor produced the cleanest transformation to the disubstituted sterically-hindered alkene dimer product **41**. With an aim of synthesising another disubstituted sterically hindered alkene dimer, these conditions were applied to the *trans* dimethyl α-diazosulfoxide **78**. Generation of the proposed α-oxo sulfine **118** was achieved under batch reaction conditions, from the corresponding α-diazosulfoxide **78**, using rhodium acetate dimer as the transition metal catalyst (Scheme 48) and this transformation was monitored by infrared spectroscopy (Figure 21).



Scheme 48

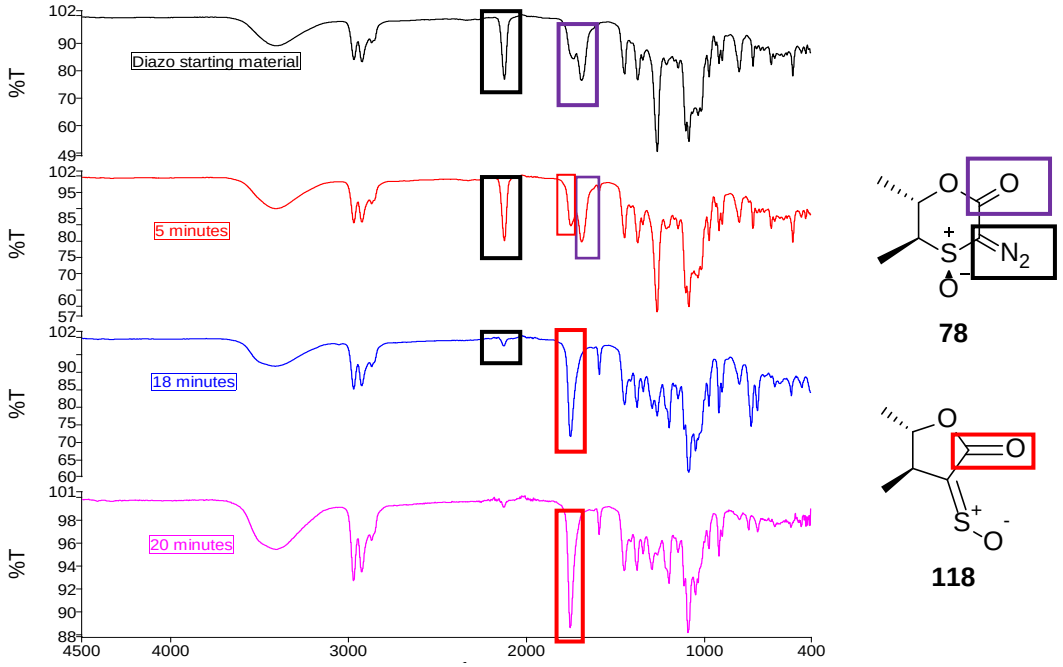
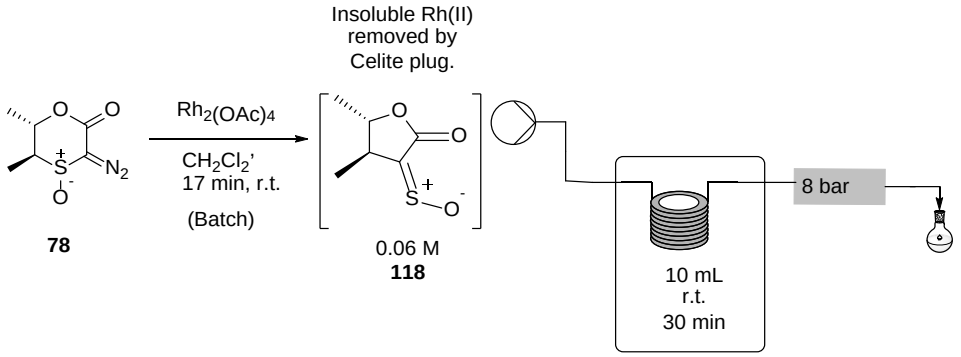


Figure 21: Formation of the desired α-oxo sulfine under batch reaction conditions is monitored by the disappearance of both the diazo stretch at 2126 cm^{-1} (black), and the carbonyl stretch of the diazosulfoxide (purple) as well as the formation of the carbonyl stretch of the α-oxo sulfine (red).

A 0.06 M solution of the proposed sulfine **118** was generated and subjected to the continuous flow conditions after removal of any insoluble rhodium acetate dimer by a Celite® plug.



Scheme 49

Analysis of the crude material showed the formation of two distinct products in a ratio of 90 : 10, and analysis of this material by infrared spectroscopy showed a spectrum identical to the material which entered the continuous flow reaction. Three possible products are the thioester **119**, the

alkene dimer **120** or a mixture of *E/Z* sulfine **118**. O'Sullivan had previously reported the formation of a comparable thioester product **121**, formed from the *cis* dimethyl α-diazosulfoxide **122** starting material.

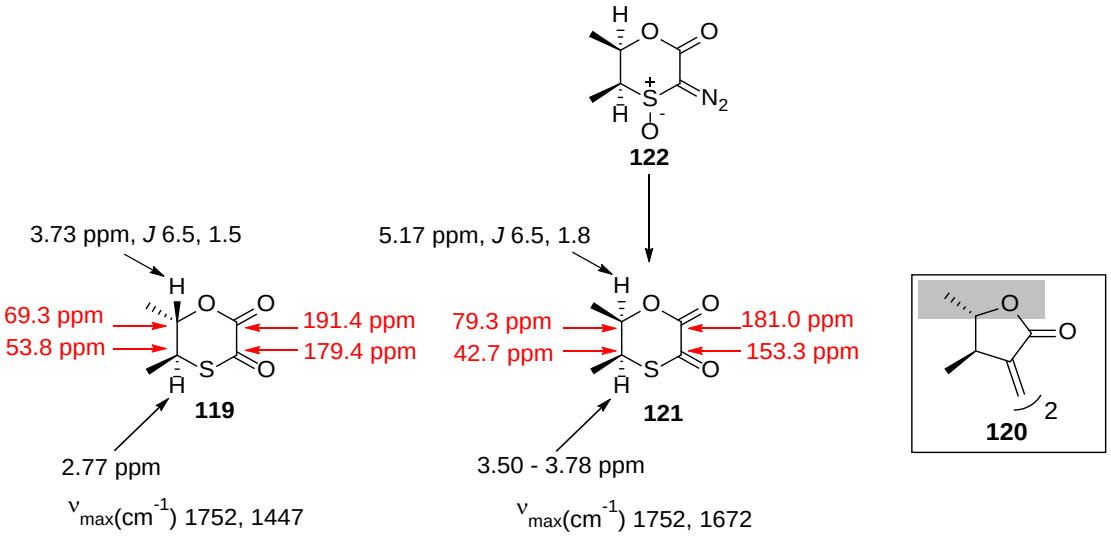


Figure 22: Tentatively assigned thioester product **119** *(left) and thioester* **121** *previously report by O'Sullivan (centre).*

The spectral characteristics of the assigned thioester **119** and the thioester **121** are summarised (Figure 22), however the structure has not been unambiguously confirmed in either case. In both cases, it was not possible to find the parent molecular ion by high resolution mass spectrometry. A literature search revealed two examples for comparison and interestingly the carbonyl signals in **123**[60] appears similar to **119** while signals for **124**[61] are consistent to **121** values.

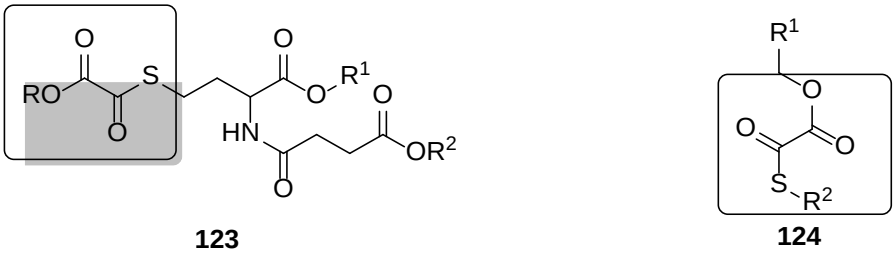


Figure 23: Compounds **123** *and* **124** *have* ^{13}*C NMR characteristics comparable to* **119** *and* **121** *respectively.*

Some evidence for the formation of the sterically hindered alkene dimer **120** which was the synthetic target of this reaction, is observed in the NMR spectra obtained.[15] In the ^{13}C NMR spectrum doubling of the CHO (69.2, 69.3 ppm) and the bridgehead CH (53.8, 54.2 ppm) signals may suggest the dimer **120**, however quarternary cabon signals for the alkene functionality of the dimer are not observed in the ^{13}C NMR spectrum. In the ^{1}H NMR spectrum the signal for one of the methyl groups appears as a doublet of doublet at 1.99 ppm whereas the other methyl signal appears as a doublet at 1.19 ppm. This extra splitting may be due to proton proton coupling across

the alkene double bond (Figure 24). This extra splitting is also seen for the CHO signal which appears as a doublet of doublets of quartets at 3.73 ppm in the ^{1}H NMR spectrum.

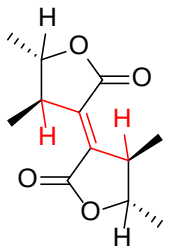


Figure 24: Alkene dimer **120**.

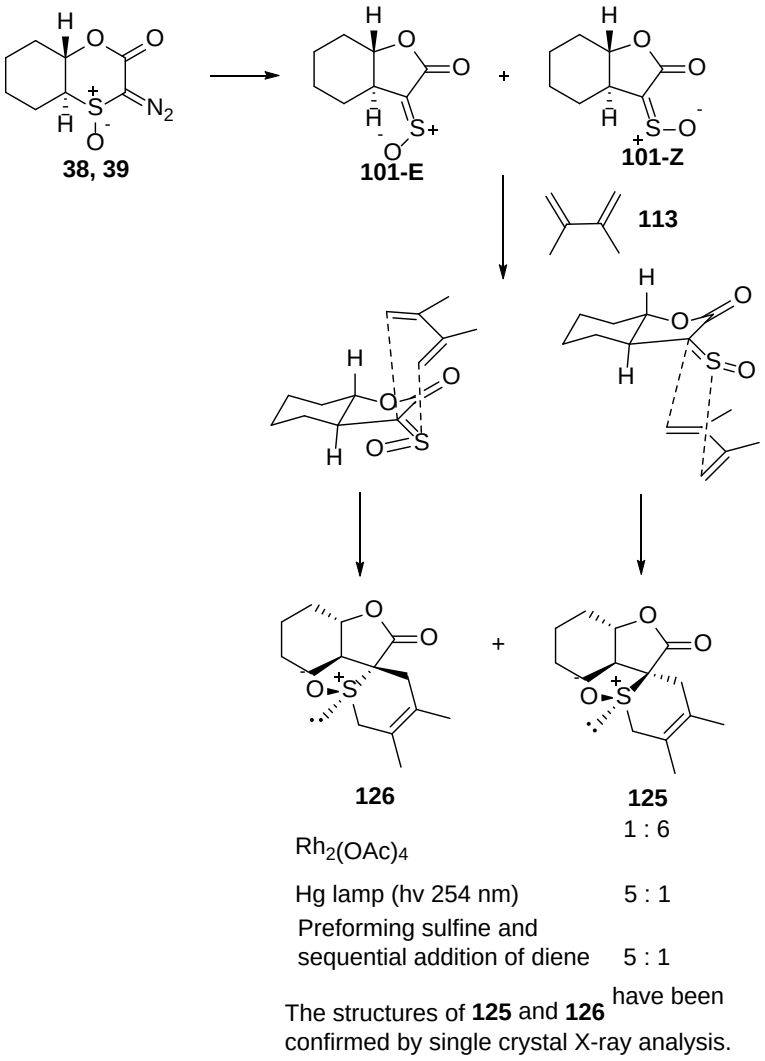
Alternatively the doubling of the key signals in the ^{13}C NMR spectrum could be due to a mixture of the *E* and *Z* sulfine being present. However, the carbonyl or thiocarbonyl signals for the sulfine are not observed and the ratio of E to Z, or further transformation into other products did not occur after 24 h. It would appears that further work will be required to unambiguously confirm the structure of the major component isolated from this reaction.

In conclusion, for this complex system where a highly reactive intermediate (α-oxo sulfine) is generated and can subsequently undergo a range of different transformations to form either the sulfine **101,** alkene dimer **41,** enol **42** or disulfide **40,** the outcome of the sulfine degradation in the absence of trapping, is remarkably consistent and predictable across a range of very different reation conditions with the same major products dominating. Clearly, alteration of the conditions leads to changes in the relative ratios but globally the outcome is consistent.

2.5 [4+2] Diels-Alder Cycloaddition Reactions

2.5.1 Background

After extensive research within our group, reactive α-diazosulfoxides are now readily accessible and in high yields under mild continuous flow and batch reaction conditions.[3,13,24,29,62] As described earlier in section 2.4, our research group has reported the transformation of α-diazosulfoxides to α-oxo sulfines *via* a hetero-Wolff rearrangement under a range of traditional batch conditions; including transition metal catalysis, thermolysis, microwave irradiation and photolysis. [4,5,62] The reactivity of these α-oxo sulfines has been recently reviewed and highlighted in the literature.[7,63] These α-oxo sulfines can undergo a wide range of transformations, and most widely reported is the Diels-Alder cycloaddition. From the reports in the literature the majority of unstable α-oxo sulfines are generated in the presence of the diene trap to promote efficient cyclisation, or to prove existence of the α-oxo sulfine as an intermediate. The Diels-Alder cycloaddition of sulfines with 1,3-dienes is widely reported as occurring with the retention of stereochemistry in the newly formed cycloadduct and work is continually ongoing to improve the novelty and range of this cycloaddition reaction.[64-67] The cycloaddition products derived from these reactions are valuable synthetic targets and have been used as intermediates or precursors on the way to biologically active molecules.[68-70] Additionally, the products from the Pummerer rearrangements and Pummerer type glycosylation reactions are under investigation for synthetic applications.[71-73] Currently, research is still ongoing in to the reactivity of α-oxo sulfines in these cycloaddition reactions and their versatility for the formation of heterocyclic compounds. Most recently, Shermolovych *et al.* [67] have reported a useful synthetic route to fluorinated sulfinyl chlorides, and subsequent generation and cycloaddition of the corresponding sulfine (Chapter 1, Scheme 81). Previous research within the Maguire group has shown generation of the α-oxo sulfine **101** from the α-diazosulfoxides **38,39** and by careful control of the reaction conditions, the isomerisation of the kinetic *Z* α-oxo sulfine **101** to the thermodynamic *E* α-oxo sulfine **101** can be limited if it is trapped in an efficient manner with a diene such as **113** (Scheme 50). Trapping of the kinetic isomer (Z*)* of the α-oxo sulfine **101** or the thermodynamic isomer (*E*) of the α-oxo sulfine **101** results in the formation of the opposite diastereomeric products, **125** and **126** respectively (Scheme 50).[5,15,16] Additionally, induction of the hetero-Wolff rearrangement and subsequent Diels-Alder cycloaddition under photochemical conditions leads to the trapping of the thermodynamic *E*-sulfine preferentially forming cycloadduct **126**.



Scheme 50

In an ongoing effort to take advantage of our efficient transformation of α-diazosulfoxides to α-oxo sulfines under mild conditions with short reaction times, as well as the remarkable diastereomeric control exhibited in these reactions, a continuous flow process for cycloaddition reactions was envisaged.[16] Excellent diastereocontrol was sought through efficient Diels-Alder trapping of α-oxo sulfines in continuous flow and an investigation in to the Diels-Alder cycloaddition of both lactone and ketone derived α-oxo sulfines in continuous flow was carried out.

Note: In subsequent reactions in this section, isolation of α-oxo sulfine **101** and the alkene dimer **41** is seen across many of the reactions indicating inefficient diene trapping of the sulfine. It is well established that the α-oxo sulfine **101** can dimerise to form **41** on storage, heating, exposure to silica gel and accordingly isolation of the dimer is in reality a measure of the proportion of sulfine left unreacted in comparison to the cycloadduct. The total amount of sulfine/dimer is a measure

of the efficiency of the cycloaddition reaction. Recovery of significant amount of the sulfine and dimer from these reactions is an indicator of the unanticipated poor efficiency of the cycloaddition under these conditions. Essentially equimolar concentrations of **38**, **39** were used unless otherwise stated.

2.5.2 Transition metal catalysed reactions - Trapping of α-oxo sulfines in a continuous flow system

To trap an α-oxo sulfine intermediate in batch reaction conditions there are two different methods:

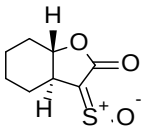
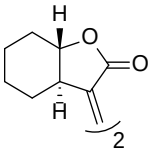
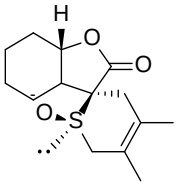
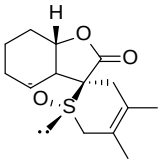
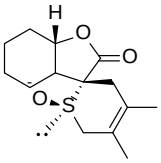
- *In situ:* Generation of the α-oxo sulfine in the presence of the diene trap or
- *Sequential:* Generation of the α-oxo sulfine followed by introduction of the diene trap.

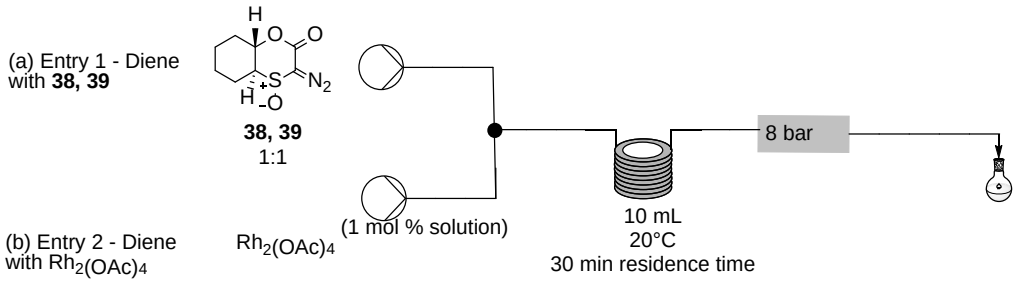
A brief investigation in to both of these trapping methods in continuous flow was carried out with an aim of developing a methodology for efficient trapping of α-oxo sulfines. A series of experiments was conducted reacting the α-diazosulfoxides **38,39** with rhodium acetate dimer at room temperature in the presence of the diene trap (20 eq.) mirroring the earlier batch reactions conducted by the group. Surprisingly the efficiency of the cycloaddition was much less under continuous flow conditions than had been seen in batch. And while some of the cycloadducts **125** and **126** were seen in many instances the α-oxo sulfine **101**, the alkene dimer **41**, the enol **42** and other sulfine byproducts were present in significant amounts. The introduction of the diene with the diazo stream (Table 17, entries 1 and 2) or $Rh_2(OAc)_4$ stream (Table 17, entry 3) led to essentially the same outcome.

In the experiment whereby the diene **113** was added after mixing of the rhodium acetate dimer and the α-diazosulfoxide starting material (Table 17, entry 3) three diastereomers of the desired cycloadduct were isolated. Earlier work by Kelleher and Collins has led to X-ray crystal structures of **125** and **126**.[12,14] Cycloadduct **125** arises from trapping of the *Z* α-oxo sulfine from below and **126** is formed by addition of the diene **113** to the thermodynamic *E*-sulfine **101** from above. O'Sullivan described a third diastereomer **127**, which is believed to be due to addition of the diene **113** from below to the *E* α-oxo sulfine but has not been confirmed crystallographically. From this experiment we isolated 6% of **125** in an early fraction and 26% of **126** and **127** (1 : 2) in a later fraction. These cycloadducts were previously described by O'Sullivan[15] However, the unreacted α-oxo sulfine **101** was again the major component of the crude reaction material. This observation was entirely unexpected as under batch conditions diene trapping has always proved very efficient. Not withstanding this observation, the outcome of the cycloaddition in terms of products

formed was similar to the outcome from the batch reaction. In addition to the three examples shown below (Table 17), further experiments were undertaken which support these results.

*Table 17: Three attempted reactions for the trapping of sulfine **101** in continuous flow.*

	101	**41**	**125**	**127**	**126**
Products					



Entry 1.

Concentration of **38,39**: 0.06 M. Diene **113** with the α-diazosulfoxides **38,39.**
(a) Diene with α-diazosulfoxides

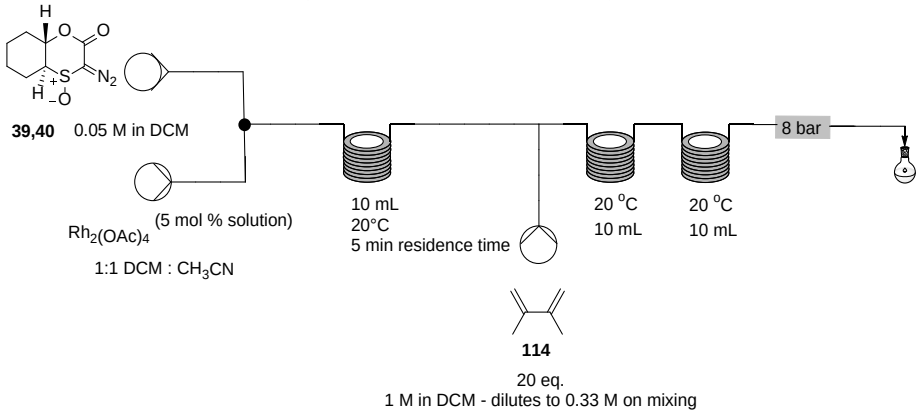
	101	**41**	**125**	**127**	**126**
Crude ratio	-	Major component	Minor reaction pathway	-	Minor reaction pathway
Isolated yield	-	56%[a]	-	-	-

Entry 2.

Concentration of **38,39**: 0.03 M. Diene **113** with the $Rh_2(OAc)_4$
(b) Diene with $Rh_2(OAc)_4$

Crude ratio[b]	Major component	-	Trace amounts in crude material	-	-

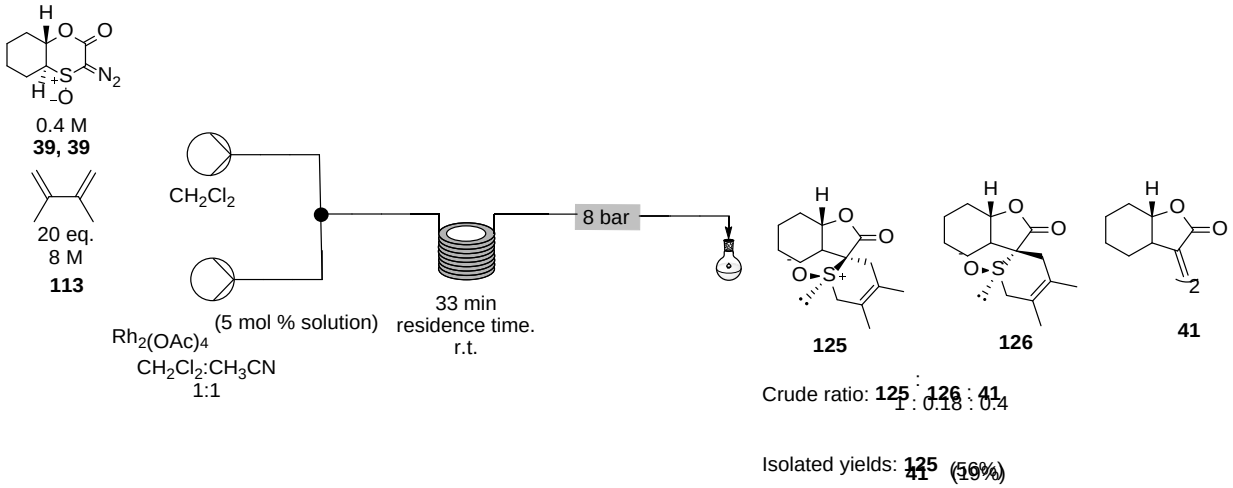
Entry 3. 5 minutes to generate sulfine, followed by introduction of diene



	101	41	125	127	126
Crude ratio	3.8	-	3.3	1	0.6
Isolated Yield	-	18%	6%	26 % (2 : 1, **127 : 126**)	

[a] Isolated yield after column chromatography on silica gel.
[b] The crude material was not purified.

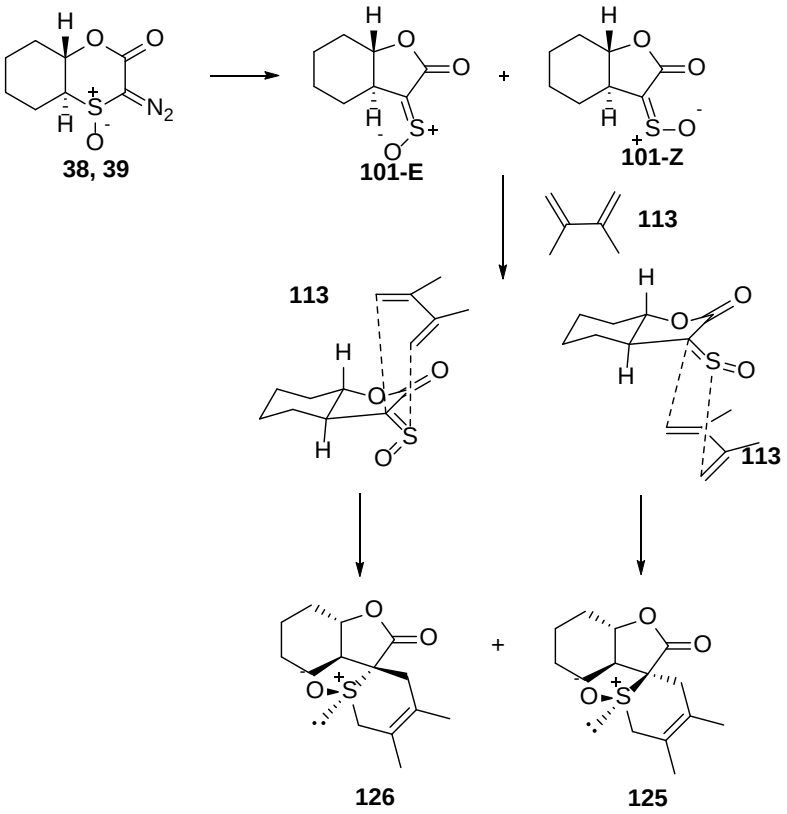
Ultimately increasing the concentration of the α-diazosulfoxides **38,39** and the diene **113** resulted in efficient cycloadduct formation as summarised in Scheme 51. Notably the batch reactions were typically conducted at 0.03 M for **38,39** and in dichloromethane only, and 0.3 M of diene **113** which led to efficient diene trapping. Conducting the same process in continuous flow with the addition of acetonitrile to the medium clearly reduced the efficiency of the diene trapping which is not easily rationalised. Medium effects (polarity, volatility of the diene, high surface area, etc.) may contribute. However, at this higher concentration in flow (0.4 M), the desired cycloadduct **125**, generated from trapping of the kinetic Z sulfine, was isolated in a yield of 56% indicating that successful cycloaddition occurs in continuous flow when high concentrations of the α-diazosulfoxides and corresponding diene are present. It is not clear if both components need to be concentrated.



Scheme 51

2.5.3 Diels-Alder cycloaddition under photochemical continuous flow conditions

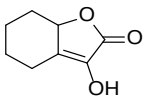
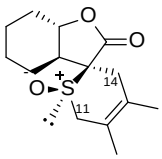
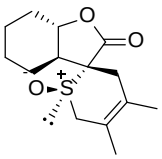
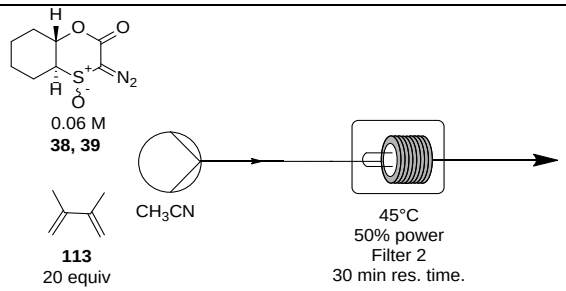
Previously within the group, Diels-Alder cycloadditions of α-oxo sulfines have been achieved using photochemical conditions to promote the hetero-Wolff rearrangement.[14] The Vapourtec UV-150 photochemical reactor was again used for inducing the hetero-Wolff rearrangement and under the described conditions (Table 18) resulted in successful Diels-Alder cycloaddition. Following chromatography of the crude reaction mixture on silica gel the major cycloadduct isolated was **126** in 14% yield. **126** is formed by addition of the diene **113** to the thermodynamic *E* α-oxo sulfine **101** (Scheme 52). The cycloadduct **125**, formed by trapping of the kinetic *Z* α-oxo sulfine **101** was also isolated in 6% yield (Table 18).



Scheme 52

Of the portion of α-oxo sulfine which did undergo cycloaddition, the results mirror the batch photochemical reactions in which trapping of the thermodynamic *E* α-oxo sulfine was favoured over the kinetic *Z* α-oxo sulfine. However, it appears that formation of the enol **42** is the major reaction pathway in these photochemical conditions at this concentration with 16% isolated yield.

Table 18: Comparison of batch and continuous flow photolysis results.

	42	**125**	**126**
Product			
Batch Results[a]			
Crude Ratio	-	1	1.5
Isolated Yield	-	19%	42%
Batch Results[b]			
Crude Ratio	-	1	5
Isolated Yield	-	6%	35%
Flow Results			
Crude ratio[c]	1	1	2
Isolated Yield[d]	16%	6%	14%

[a] Work carried out by O'Sullivan with a reaction time of 6 hours exposed to photolytic conditions and a further 48 hours stirring at room temperature. The α-diazosulfoxides **38** (axial) and **39** (equatorial) were used in a ratio of 1 : 5.6 [14]

[b] Work carried out by Collins with a reaction time of 6 hours. The α-diazosulfoxides **39** (equatorial) only was used.

[c] Crude ratio as determined by integration of the key signals in the ^{1}H NMR spectra.

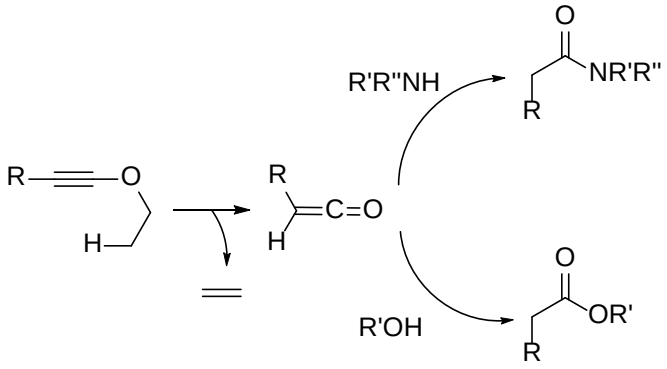
[d] Isolated yields are those of the pure material recovered after column chromatography on silica gel.

Interestingly when the α-oxo sulfine does undergo cycloaddition, the results from this photochemical continuous flow reaction, mirror the results from the batch photochemical reactions much more closely, than the continuous flow transition metal catalysed results mirror the transition metal catalysed batch results. Once again, the recovery of the enol **42** as a significant component of crude reaction mixture indicates that the cycloaddition on the flow system is significantly less efficient than in the corresponding batch process, where the enol was only seen in the absence of a diene trap. Notably the reactions were conducted at the lower concentration of 0.06 M, which as seen above in the transition metal catalysed processes led to equally inefficient trapping.

2.5.4 Thermolysis reactions carried out in continuous flow

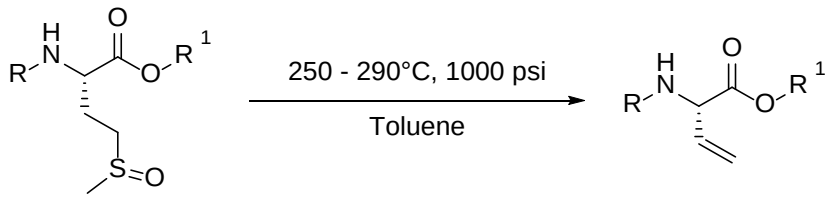
2.5.4.1 Background

Multiple advantages exist in transferring reactions which would traditionally be carried out in batch conditions and carrying them out under continuous flow reaction conditions. The benefits of this include shorter reactions times, higher selectivities of reaction products, greater control of reaction intermediates and development of greener processes.[74-76] Our aim in this work was to successfully carry out the hetero-Wolff rearrangement under continuous flow conditions by causing the loss of molecular nitrogen with thermolysis. This would induce the Hetero-Wolff rearrangement and subsequent [4+2] cycloaddition in a rapid manner. Recent reports detail the use of thermolysis in flow for the generation of ketenes, by the thermal sigmatropic rearrangement of alkoxyalkynes and then introduction of both nitrogen and oxygen nucleophiles to efficiently induce a useful chemical transformation (Scheme 53).[77,78] This is a scalable method for the generation of these reactive intermediates which subsequently undergo trapping with oxygen and nitrogen nucleophiles in short reaction times and in moderate to good yields. This process has the added advantage that no work-up is needed so it could be envisaged to be incorporated in to a multistep sequence of reactions in continuous flow.



Scheme 53

Another recent example of thermolytically induced reactions in continuous flow is the *syn* sulfoxide elimination for the generation of vinylglycine derivatives (Scheme 54). The reaction is carried out in superheated toluene at high pressure and resulted in high selectivities and high ee's (97%) of the desired product. [78]



Scheme 54

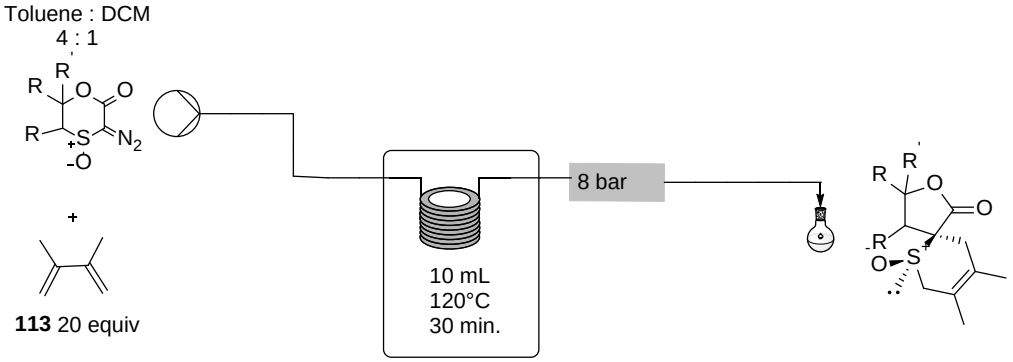
Recently, there have also been examples of Diels-Alder cycloadditions carried out in flow with excellent yields, efficiency[79] and diastereoselectivity.[80] These reactions have shown great success and increased efficiency when scaled up.[81] With precedent in the literature for the effective generation of reactive intermediates in continuous flow using thermolysis and this leading to efficient and selective reactions, our aim was to induce similar reactivity with the α-diazosulfoxides to generate the α-oxo sulfine intermediates, and subsequent [4+2] Diels-Alder cycloaddition.

2.5.5 Diels-Alder cycloaddition reactions of lactone derived α-diazosulfoxides in continuous flow

O'Sullivan had demonstrated the α-diazosulfoxides **38**,**39** could be transformed to the α-oxo sulfine **101** through thermolysis under metal free conditions and, accordingly, thermolysis of **38**,**39** was explored under continuous flow conditions with a view to generation and trapping of the α-oxo sulfine. The clear advantage of using a flow process for thermolysis is rapid and efficient heating of a portion of the reaction mixture can be achieved much more easily than under batch conditions, along with the added advantages of the increased safety profile, being scalable and metal free. The cycloadducts formed are stable in all cases, and most previously characterised examples are crystalline solids.

With thermogravimetric analysis carried out on two model substrates, both the lactones **38**,**39** (1:1) and the ketone derivative **14**, an approximate temperature necessary for generation of the intermediate α-oxo sulfine was known for both lactone and ketone derived α-diazosulfoxides.

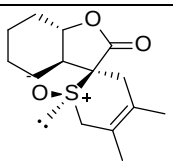
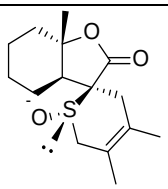
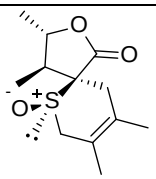
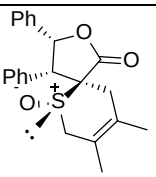
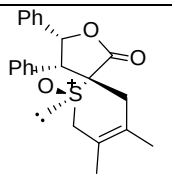
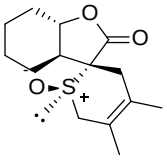
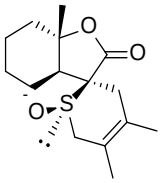
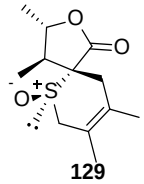
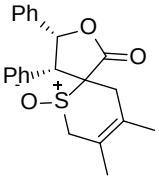
Based on the earlier results use of concentrated solutions of the α-diazosulfoxide (0.2 M) and diene (4 M) was undertaken to maximise efficiency. For each of the cycloaddition reations, the reaction mixture was pumped through a heated 10 mL reactor coil at 120°C with a residence time of 30 minutes.



Scheme 55

The solvent used for these reactions was a mixture of toluene and dichloromethane in a ratio of 4:1. Toluene was selected to achieve the high temperatures in continuous flow, but without generating excessive pressure within the system. However, due to the sparingly soluble nature of the series of lactone derived α-diazosulfoxides in toluene addition of 20% of dichloromethane to the solvent was required for sufficient solubility. It was found that with 20% dichloromethane in the solvent system there was no issue with back pressure regulation, or over pressure in the system.

Table 19: Isolated products after column chromatography on silica gel following thermolysis of the corresponding α-diazosulfoxides in continuous flow (Scheme 55 above shows the reaction setup). The results from transition metal catalysed and microwave batch reaction carried out by other members of the research group are presented for comparison.

	Entry	**1**	**2**	**3**	**4**[f]
	Major Product	 **125**	 **114**	 **128**	 **130** +  **131**
	Minor Product	 **126**	 **115**	 **129**	 MW Only **132**
		Flow [Δ in Toluene : DCM, 4: 1]			
A	**Crude** dr	84 : 16 **125 : 126**	97 : 3 **114 : 115**	72 : 28 **128 : 129**	50 : 50 **130** : **131**
	Pure Yield and dr	74%[a] (**125** only)	62%[a] (**114** only)	30% (**128** only) 30% (8 : 1, **128 : 129**)	60%[b] (1 : 1, **130** : **131**)
		Batch [MW in DCM]			
B	**Crude** dr[c] **Yield**[c]	85 : 15 **125 : 126** -	94 : 6 **114 : 115** -[e]	- -	4 : 58 : 38 **132** : **130** : **131** 72%[b]
		Batch [Rh(II)(OAc)$_4$ in DCM]			
C	**Crude**	84 : 16	83 : 17	78 : 22	55 : 45

	dr[d]	**125 : 126**	**114 : 115**	**128 : 129**	**130** : **131**
	Yield[d]	40% (**125** only)	48% (**114** only)	41% (**128** only)	51% (1.9 : 1, **130** : **131**)

[a]Isolated yield of major diastereomer

[b]Isolated yield of all diastereomers

[c] Microwave reactions were previously carried out without a transition metal catalyst present, by other members of the research group. [14,15] The reactions was heated to 135°C in a sealed 10 mL vessel.

[d] Work carried out previously within the group using Rh(II) as transition metal catalyst, the presence of the diene *in situ* and dichloromethane as solvent. [14,15]

[e] The crude reaction mixture was not purified.

[f] The diazosulfoxide starting material had a molarity of 0.1 M compared to 0.2 M for all other substrates.

On subjecting the α-diazosulfoxides **38,39** to the reaction conditions (Table 19, Entry 1A) and subsequent analysis by ^{1}H NMR spectroscopy, the absence of the alkene dimer **41**, disulfide dimer **40** and enol **42** was noted as well as 100% consumption of the α-diazosulfoxide starting material and a very clean transformation to the cycloaddition product **125** (Figure 25). A dr of 84 : 16 was recorded which is essentially the same as the microwave reaction with a dr of 85 : 15. The cycloadduct **125**, which is formed by successful trapping of the kinetic *Z* α-oxo sulfine was the major product and was isolated in 74% yield after chromatography, compared to 36% yield reported by O'Sullivan from the comparable microwave reaction.[15] This reaction was the first successful generation and trapping of the α-oxo sulfine **101** in a continuous flow manner with high selectivity and efficiency in trapping of the kinetic isomer of the α-oxo sulfine. Although the trapped form of the thermodynamic sulfine was not visible in the ^{1}H NMR spectra of the crude material, trace amounts of the cycloadduct **126** were isolated in the most polar fraction after the purification process. Notably, the stereochemical outcome both in terms of the α-oxo sulfine trapped and the facial selectivity of the cycloaddition are essentially the same for thermolysis in flow, microwave irradiation or exposure to $Rh_2(OAc)_4$. Significantly, isolation of 74% of **125** is undoubtedly the most efficient formation of this cycloadduct over two decades and renders this process synthetically useful for the first time.

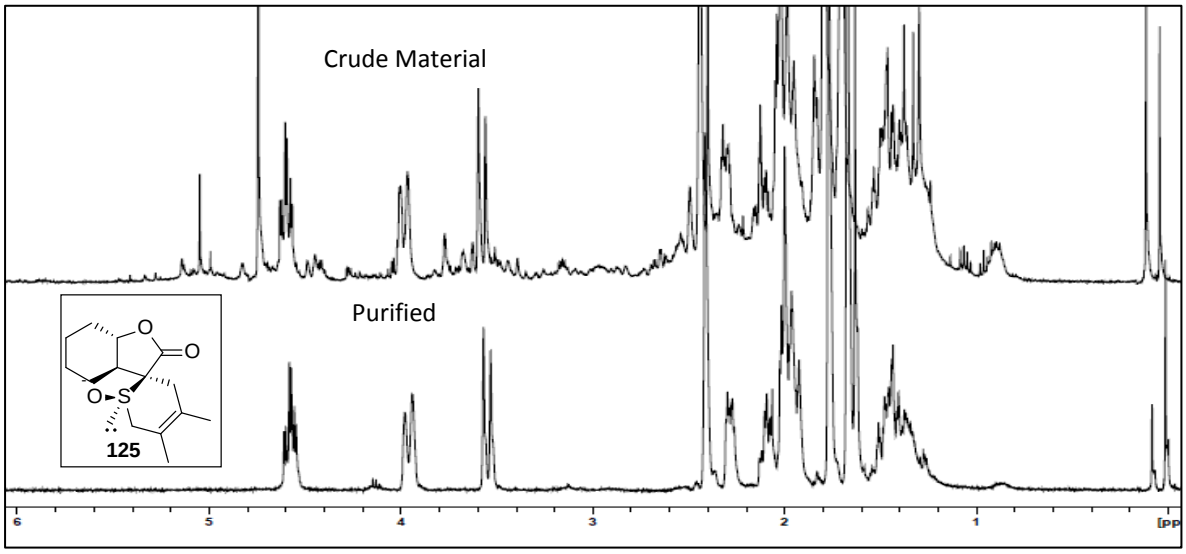
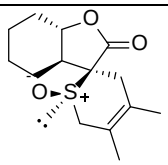
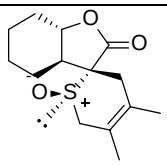
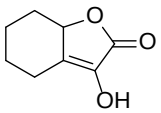
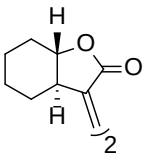


Figure 25: Comparison of the ^{1}H NMR spectrum of the crude material (top) and the purified cycloadduct (bottom).

This continuous flow thermolysis result can also be compared to the rhodium acetate catalysed reaction in continuous flow and the photolysis reaction in continuous flow. The highest yielding process is the thermolysis; however it has the added advantage of not generating the alkene dimer **41** or enol **42**, which are present in the photolysis and transition metal catalysed reactions.

*Table 20: Comparison of Diels-Alder cycloaddition results for the α-diazosulfoxides **38**, **39** under a range of continuous flow conditions.*

Entry	 **125**  **126**  **42**  **41**
	Crude ratio[a] / Isolated yields[b]
1. [Δ] Toluene : DCM 4:1 120°C, 30 min, 0.2 M	**125** : **126** (84 : 16) / **125** (74%)
2. [hv] CH_3CN : DCM, (4:1) 45°C, 30 min, 0.06 M	**125** : **126** : **42** (25 : 50 : 25) / **125** (6%) **126** (14%) **42** (16%)
3. [$Rh_2(OAc)_4$] CH_3CN : DCM, (4:1) r.t., 30 min, 0.4 M	**125 : 126 : 41** (63 : 12 : 25) / **125** (56%) **41** (19%)

[a] The crude ratio of products is determined by analysis of the key signals in the ^{1}H NMR spectrum of the crude material.

[b] The isolated yield is the amount of pure product isolated after column chromatography on silica gel.

For Table 19, entry 2A, the ^{1}H NMR spectrum of the crude reaction material showed a diastereomeric ratio of 97:3. When the reaction is carried out in batch conditions with $Rh_2(OAc)_4$, (Table 19, Entry 2C) the dr is 83 : 17. Following purification the desired cycloadduct **114** was isolated as one diastereomer in a yield of 62%, with an additional fraction isolated containing the disulfide **117** (Figure 26).

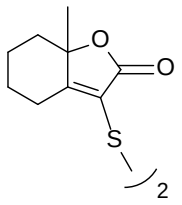
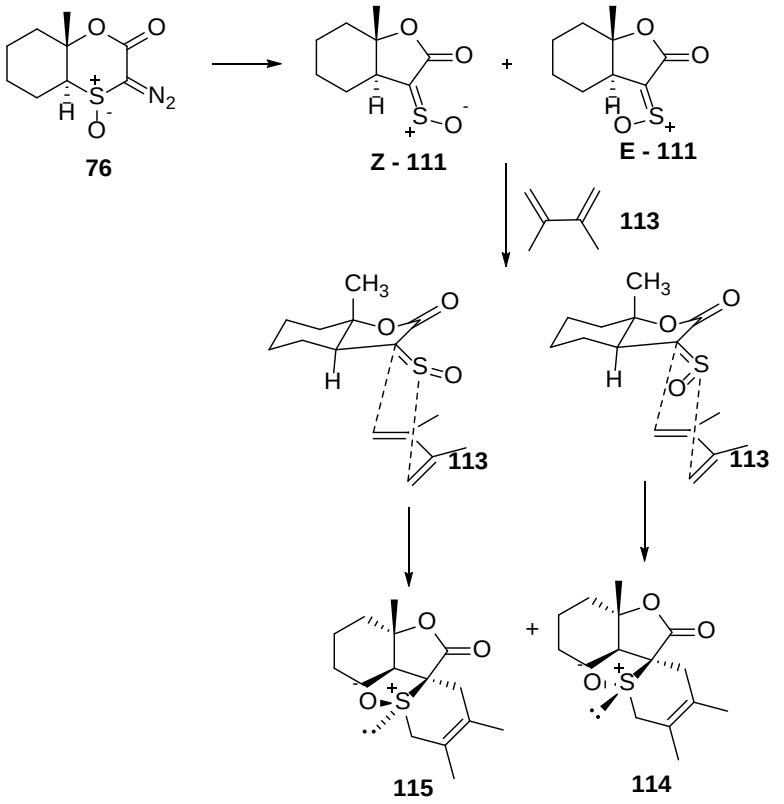


*Figure 26: Disulfide **117***

Cycloadduct **114** is formed by addition of the diene from below to the *E* α-oxo sulfine, whereas the minor diastereomer **115** is formed by addition of the diene from below to the *Z* α-oxo sulfine (Scheme 56).

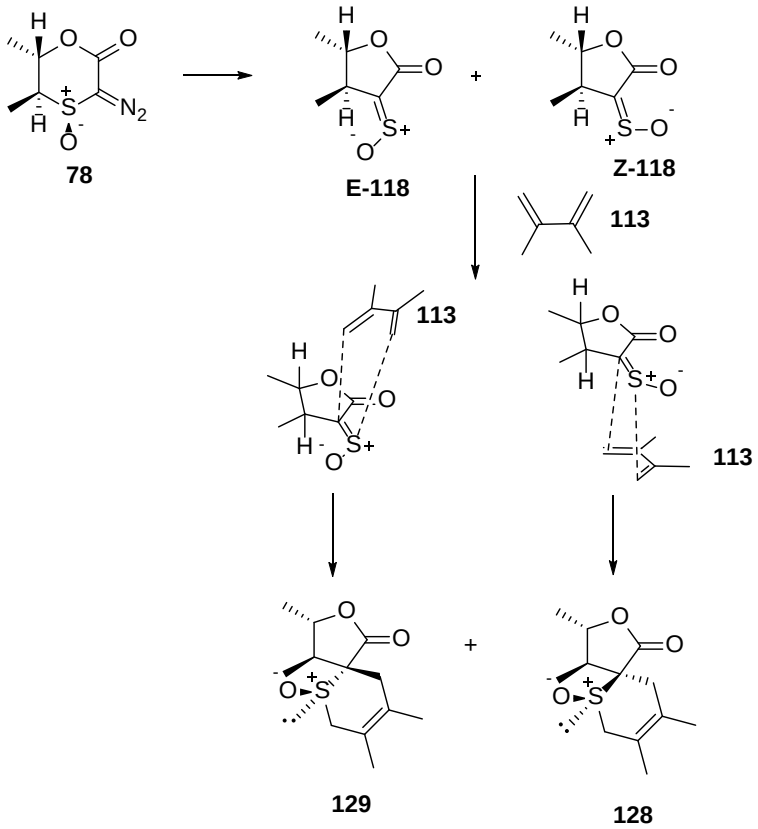


Scheme 56

When comparable trapping reactions are carried out using microwave irradiation (Table 19, Entry 2B) with the diene *in situ,* **114** is the major product when dichloromethane is used as solvent (94 : 6 dr) or with toluene as solvent (92 : 8 dr). [v]

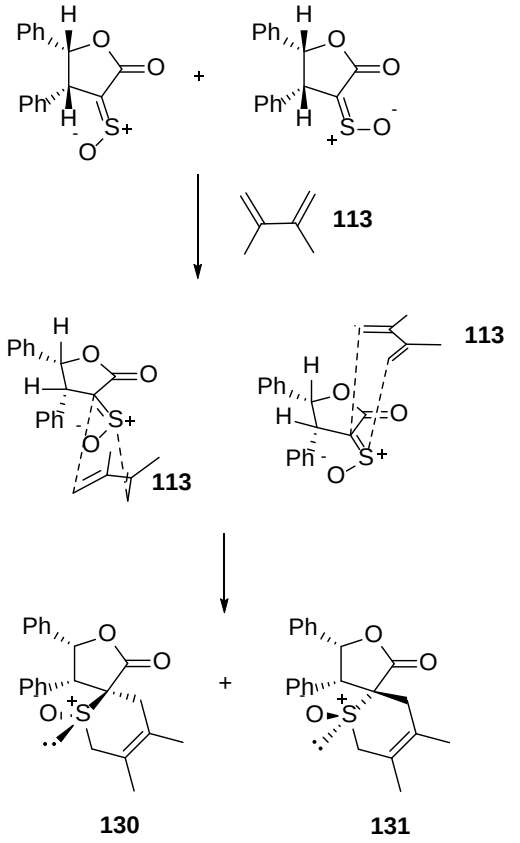
For Table 19, entry 3, when the same reaction conditions were applied to the axial *trans*-dimethyl α-diazosulfoxide **78**, with a concentration of 0.2 M, successful formation of the cycloadducts **128,129** was achieved. Interestingly, the ^{1}H NMR spectrum of the crude material showed a dr of 72 : 28 (Table 19, Entry 3A). The lower dr is due to the increased flexibility of the monocyclic ring system along with reduced steric hindrance, and so addition from both faces, to the intermediate α-oxo sulfine, occurs. The major cycloadduct **128,** formed by addition of the diene **114** to the kinetic *Z*-sulfine **118** is cleanly isolated after purification by column chromatography in 30% yield (Table 19, Entry 3A). A second fraction, containing an additional 30% of the cycloaddition material, consisted of the two diastereomers **128** and **129** in a ratio of 8:1. The stereochemistry of **128** has been assigned by Collins, by comparison of its spectroscopic data to to the spectroscopic data of **125** which was confirmed crystallographically. The data obtained here for **128** is in good agreement to that data previously obtained for **128**, although the structure has not been structurally confirmed in either case. The stereochemistry of **129** is tentatively assigned based on characteristic signals in the ^{1}H NMR spectrum of the crude material.

[v] The stereochemistry of **114** has been unambiguousy confirmed in the thesis of O'Sullivan. This single crystal data was unavailable at the time of publication of a corresponding journal article [O'Sullivan, O.; Collins, S.; Maguire, A. Synlett 2008, (5), 659-662] resulting in contrasting stereochemical reports of **114**.



Scheme 57

For Table 19, entry 4, the final lactone derived α-diazosulfoxide subjected to the new methodology was the *cis*-diphenyl α-diazosulfoxide **77** which was previously described by Kelleher[1,2] and O'Sullivan.[15] This α-diazosulfoxide **77** had previously been investigated under microwave irradiation and transition metal catalysis reaction conditions. When investigated under thermal conditions in continuous flow, the crude material consisted of 2 diastereomers (Scheme 58), **130** and **131** in a dr of 50:50 respectively (Table 19). The stereochemistry of the cycloadducts **130** and **131** is based on the work done by O'Sullivan who tentatively assigned stereochemistry to the four isolable cycloadducts.[15] This dr is even lower than the dimethyl cycloadducts and may be due to the flexibility of the monocyclic ring system allowing addition from above and below to the intermediate sulfine. After purification both diastereomers **130** and **131** were isolated as a mixture in 60% yield.



Scheme 58

What is noteworthy about carrying out these reaction in continuous flow is that the dr results obtained are comparable to that when carried out with transition metal catalysis or microwave irradiation in batch reaction conditions. The batch results (Table 19) are those previously reported by Collins and 0'Sullivan.[14,15] Overall, the best result for thermolysis induced Diels-Alder cycloaddition of a lactone derived α-oxo sulfine is achieved with the methyl bridgehead derived α-diazosulfoxide **76** with an increase in selectivity (Table 19, entry 2). The result achieved with the cyclohexyl diazosulfoxides **38,39** mirrors the analogous batch reaction for the *in situ* trapping of the α-oxo sulfine **101** (Table 19, entry 1). For both the diphenyl and the dimethyl derivatives (Table 19, entries 3 and 4) the dr's obtained in continuous flow are similar or lower than those in the comparable batch reaction. However, this methodology has multiple distinct advantages over the batch reactions. Through generation of the sulfine under thermal conditions, the use of expensive transition metal catalysis is avoided and the isolated yields of the desired cycloadducts are consistently higher, most notable for the cyclohexyl derived cycloadduct **125** with an isolated yield of 40% in batch compared to 74% from the continuous flow reaction. These metal free reactions

were found to be highly diastereoselective reactions which were efficient at high temperatures and easily scalable. Short reaction times and the added safety benefit are all advantages of the thermolytic methodology for the cycloaddition the α-oxo sulfines in continuous flow. The potential to couple the thermolysis with the diazo transfer in continuous flow is clear, enabling the use of this methodology without ever handling or isolating the diazo intermediate (see section 2.5.6).

2.5.5.1 Thermolytic reactions of ketone derived α-diazosulfoxides in continuous flow conditions

With success in achieving metal free, diastereoselective [4+2] cycloadditions of the lactone derived α-oxo sulfines we aimed to extend this selectivity and reactivity to the ketone derived α-diazosulfoxides. With the TGA analysis obtained (section 2.5.3.2) promotion of the hetero-Wolff rearrangement at lower temperatures (approx. 100°C) was anticipated, and accordingly acetonitrile was employed in place of toluene without back pressure issues. To achieve high concentrations for efficient cycloaddition, use of 4 : 1, acetonitrile : dichloromethane was employed as the diazosulfoxide substrates are more soluble in dichloromethane. The reaction conditions were subsequenty applied to each of the α-diazosulfoxide substrates **14**, **80**, **81** and **83** (Figure 27) and results are summarised in Table 21.

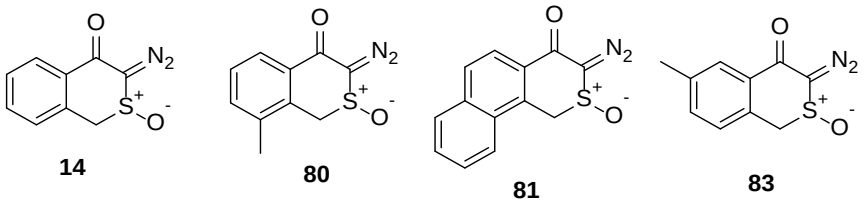
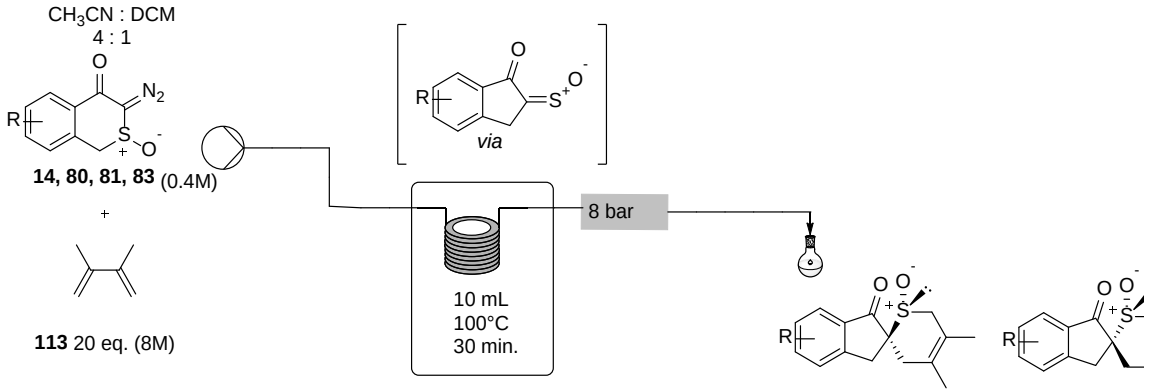
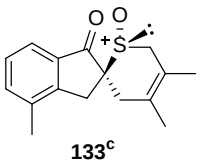
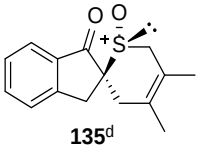
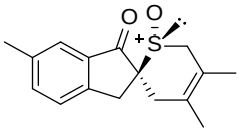
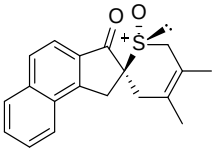
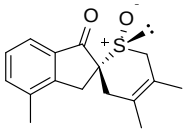
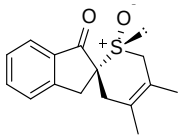
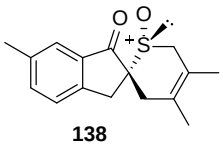
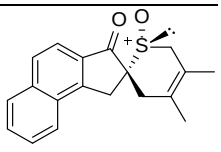


Figure 27: Range of ketone derived α-diazosulfoxides used.

Table 21:Comparison of cycloadditions under continuous flow thermolysis, microwave, and batch transition metal catalysis.

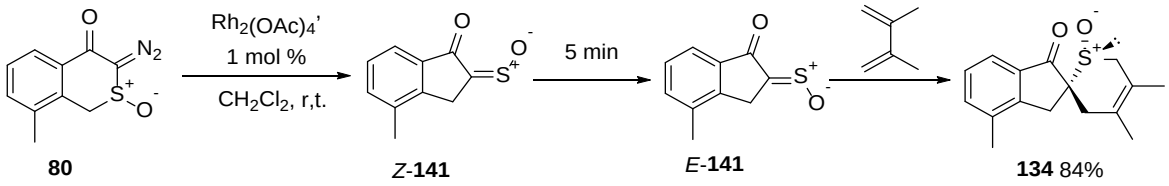


	Entry	1	2[d]	3	4
	Major Product	 **133**[c]	 **135**[d]	 **137**	 **139**
	Minor Product	 **134**	 **136**[d]	 **138**	 **140**
A	Flow dr[e]	95 : 5	95 : 5	99 : 1	73 : 27
	Δ in CH_3CN : DCM 4 : 1	**133** : **134**	**135 : 136**	**137** : **138**	**139** : **140**
	Isolated Yield[f] (%)	**133** only (64%)	**135** only (63%)	**137** only (78%)	**139** (34%) **140** (20%)
B	Microwave dr[a]	**133** only	96 : 4	90 : 10	-
	135°C for 2-3 min at 300W in DCM (No Rhodium present)		**135 : 136**	**137** : **138**	
	Isolated Yield[f] (%)	-	-	-	-
C	Batch dr[e]	96 : 4[a]	85 : 15[a]	71 : 29[a]	-

	$Rh_2(OAc_4)$ in DCM	81 : 19	-	-	
		133 : **134**	**135 : 136**	**137** : **138**	
	Yield (%)[b,f]	29%[a]	35%[a]	**137** only[a]	-
		(**133** only)	(**135** only)	(impure)	

[a]Results reported by Buckley.[16]
[b]Generation of the α-oxo sulfine was achieved using $Rh_2(OAc)_4$ *in situ* with the diene trap, in dichloromethane.
[c] The relative stereochemistry of **133** was unambiguously confirmed with a single crystal X-ray structure as part of this research.
[d] The relative stereochemistry of **135** and **136** were unambiguously confirmed with a single crystal X-ray structure as part of the research carried out by Buckley. [16]
[e] The dr values are determined by integration of the characteristic signals in the ^{1}H NMR spectra of the crude material.
[f] The yields describe the isolated yields of the products obtained after column chromatography on silica gel.

When the trapping of the α-diazosulfoxide **80** is carried out in batch reaction conditions in this work [($Rh_2(OAc)_4$, diene *in situ*, dichloromethane as solvent] the crude ratio, for the major and minor diastereomers, **133** and **134** was 81 : 19 respectively. Previously, and in comparison to this, Buckley had reported the crude ratio for this reaction as being 96 : 4 from the rhodium catalysed batch reaction (Table 21, Entry 1C). Additionally in the work by Buckley, only **133** was formed in the microwave (diene *in situ*) reaction (Table 21, Entry 1B). Buckley established that if the α-oxo sulfine was generated in the absence of a diene trap using $Rh_2(OAc)_4$ and subsequently trapped, the diastereomer **134** could be formed as the major product. This is due to isomerisation of the kinetic α-oxo sulfine *Z*-**141** to the thermodynamic isomer *E*-**141** (Scheme 59).



80 *Z*-**141** *E*-**141** **134** 84%

Scheme 59

On analysis of the dr for Diels-Alder cycloaddition of the α-oxo sulfine **141**, generated from **80** under thermolytic conditions (Table 21, Entry 1A) the ratio was found to be 95 : 5 of **133** and **134**. This highlights the efficiency and diastereoselectivity of the continuous flow procedure. Additionally due to the minor quantitites present, the minor diastereomer **134** was not recovered from the reaction mixture. Notably, Buckley had recovered this diastereomer from the reaction where the sulfine was allowed to equilibrate prior to cycloaddition, accordingly there is no evidence that **134** is unstable for example through syn elimination of the sulfoxide. The ratio of the crude products from this continuous flow protocol was consistent in scales varying from 50

mg up to 300 mg for both of the α-diazosulfoxides **80** and **14**. Similar to the other continuous flow reactions, the dr of the cycloaddition of the α-oxo sulfine generated from **80** is in line with the batch reaction, however the isolated yield after flash chromatography is much higher, 64% in this work, compared to 29% for the analogous batch reactions. A single crystal of the major cycloadduct **133**, formed by trapping of the kinetic Z sulfine **141** with diene **113**, was grown from dichloromethane and hexane (from a sample not containing **134**) and the structure and relative stereochemistry was unambiguously confirmed by single crystal X-ray diffraction (Figure 28).

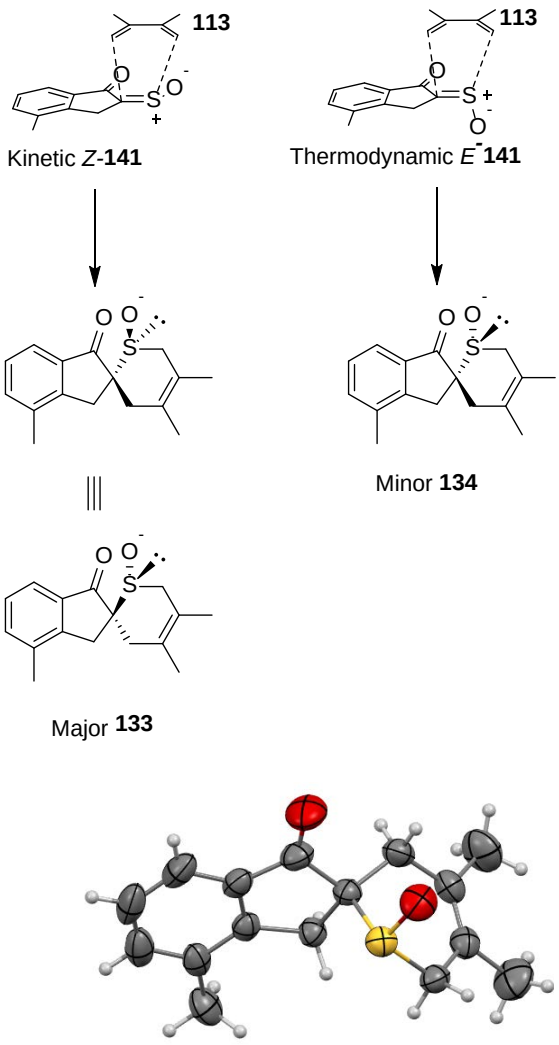
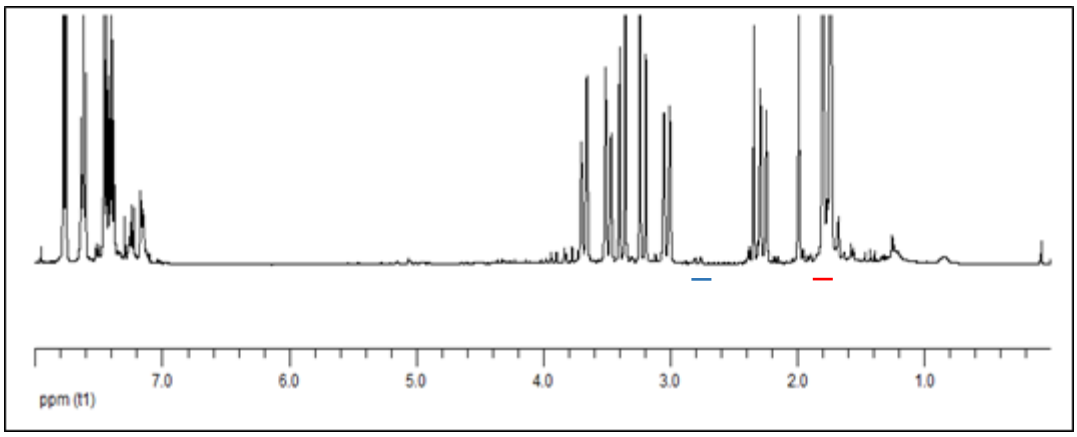


Figure 28: The crystal structure of the cycloadduct **133** *unambiguously confirmed the relative stereochemistry.*

When the same reaction conditions are applied to α-diazosulfoxide **14** (Table 21, entry 2) conversion occurs efficiently and cleanly using the thermolytic conditions, as shown by the ^{1}H NMR spectrum of the crude material (Figure 29). The crude dr of 95 : 5 for the products **135** and **136** was an improvement over the analogous transition metal catalysed batch reaction for trapping of the kinetic sulfine which was 85 : 15, and in line with the microwave reaction which

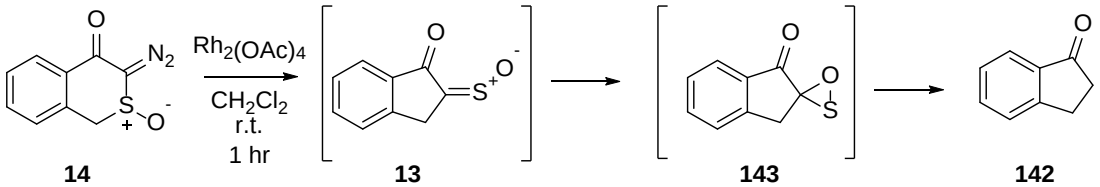
was 96 : 4 as reported by Buckley.[16] Buckley has reported the isolated yield from the transition metal catalysed batch reaction as being 35%.[16] After purification of the continuous flow thermolysis reaction mixture, the pure diastereomer **135** was isolated in 63% yield. Although the ^{1}H NMR spectrum of the crude material (Figure 29) only shows minor impurities, the loss of mass



may be due to loss of the polar cycloadduct **135** on silica gel as well as careful combination of the isolated fractions. However the ^{1}H NMR spectra highlight the remarkably clean transformation obtained from the labile precursors under these conditions.

Figure 29: The ^{1}H NMR spectrum of the crude material from the continuous flow thermolysis cycloaddition. The major peaks (underlined red) correspond to the cycloadduct **135** *while the minor cycloadduct* **136** *is also present in <5% (underlined blue). See Table 21, entry 2A.*

Interestingly, on undertaking purification of the crude material and on analysis of the first fraction isolated from the column, the ^{1}H NMR spectra showed evidence of trace amounts of the indanone **142**, presumably caused by rearrangement from the α-oxo sulfine **13** to the intermediate oxathiirane **143** and subsequent sulfur elimination (Scheme 60). However these signals are not apparent in the ^{1}H NMR spectrum of the crude material. In previous work, this indanone is only observed in the absence of a diene trap, suggesting that the efficiency of the trapping in continuous flow is less compared to batch, a result which is also seen in earlier work in this project (see section 2.5).

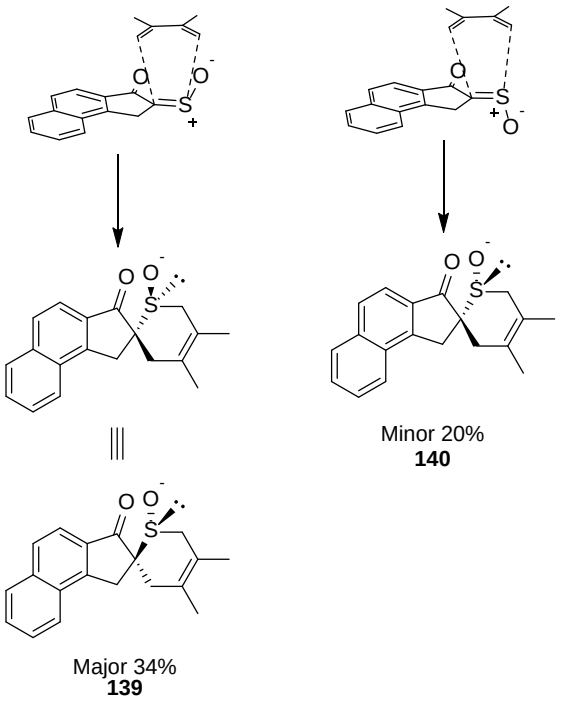


14 **13** **143** **142**

Scheme 60

On application of the cycloaddition in flow protocol to the α-diazosulfoxide **83** (Table 21, Entry 3A) successful Diels-Alder cycloaddition with a high dr is achieved again. Less than 1% of a minor diastereomer **138** is observed in the ^{1}H NMR spectrum of the crude material alongside the major cycloadduct **137**. This is in comparison to the result from the transition metal catalysed batch reaction which was 71 : 29, and the microwave reaction which formed **137** and **138** in a ratio of 90 : 10, as reported by Buckley (Table 21, Entry 3B and 3C).[16] Again, purification of a reaction using 200 mg of the starting material **83**, led to isolation of the pure diastereomer **137** in a high yield of 78%. This is the first time a pure sample of **137** has been isolated and characterised.

As discussed in section 2.3.4, the use of continuous flow chemistry to make labile α-diazosulfoxides in greater yields enabled access for the first time to the naphthalene derived α-diazosulfoxide **81,** therefore the continuous flow cycloaddition protocol was next applied to this α-diazosulfoxide **81** (Scheme 61). On analysis of the crude reaction mixture by ^{1}H NMR spectroscopy, a complex mixture of products was obtained (Figure 30). Amongst the complex mixture were two diastereomeric cycloadducts, **139** and **140** present in a ratio of 73 : 27. The major diastereomer **139** formed in the thermolysis reaction is believed to come from addition of the diene **113** to the kinetic Z-sulfine and the minor diastereomer **140** is believed to form by addition to the thermodynamic *E* sulfine. After undertaking purification of the crude reaction mixture by column chromatography on silica gel, the major and minor cycloadducts were isolated and characterised in yields of 34% for the major product **139** and 20% for the minor product **140** (each containing up to 10% of the other diastereomer).



Scheme 61

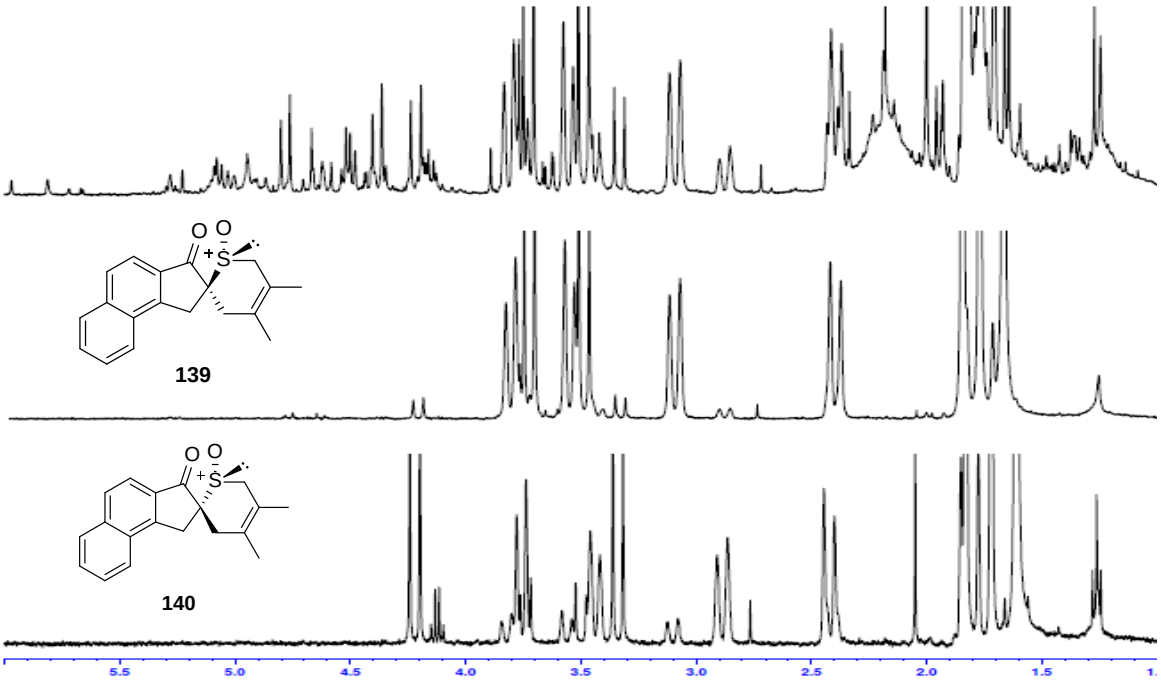


Figure 30: ^{1}H NMR spectrum of the crude material (top) showing the formation of two cycloadducts in a ratio of **139** *:* **140***, 73 : 27, and multiple unknown decomposition products. The ^{1}H NMR spectra (centre) shows the major diasteromer* **139** *on the ^{1}H NMR spectra (bottom) shows the minor diastereomer* **140** *(contains some ethyl acetate). Both spectra contain up to 10% of the opposite diastereomer.*

At this point it is difficult to rationalise the low dr in this system. The complex ^{1}H NMR spectrum of the crude material contains signals for unidentified decomposition products and this is consistent with the labile nature of the α-diazosulfoxide **81** which Buckley had been unable to access from batch reactions. It is possible that some of the α-diazosulfoxide **81** had rearranged to the corresponding α-oxo sulfine on storage prior to reaction, which would explain the enhanced trapping of the *E* α-oxo sulfine. It was noted, that on storage of the labile α-diazosulfoxide **81** in the freezer over a period of 2 months, loss of the diazo moiety (shown by disappearance of the diazo stretch in the infrared spectrum at 2126 cm^{-1}) and formation of an unidentified decomposition product occurred as the major component present. The physical appearance of the sample was not significantly altered. This aged sample showed a singlet at 4.54 ppm in the ^{1}H NMR spectrum and two key signals in the ^{13}C NMR spectrum at 183.8 and 188.4 ppm. Two possible structures were considered, either the indanedione **144** or the sulfine **145**. Previously Buckley had synthesised and characterised a range of sulfines (using rhodium acetate catalysis with a short reaction time) and indanediones, such as **146**, (using rhodium acetate catalysis with a long reaction time) (Figure 31) and by comparison of the spectroscopic characteristics the material was assigned as the sulfine **145**. It appears the thermal rearrangement of α-diazosulfoxide **81** occurs even on storage in the freezer, this explains why Buckley had not managed to isolate this compound.

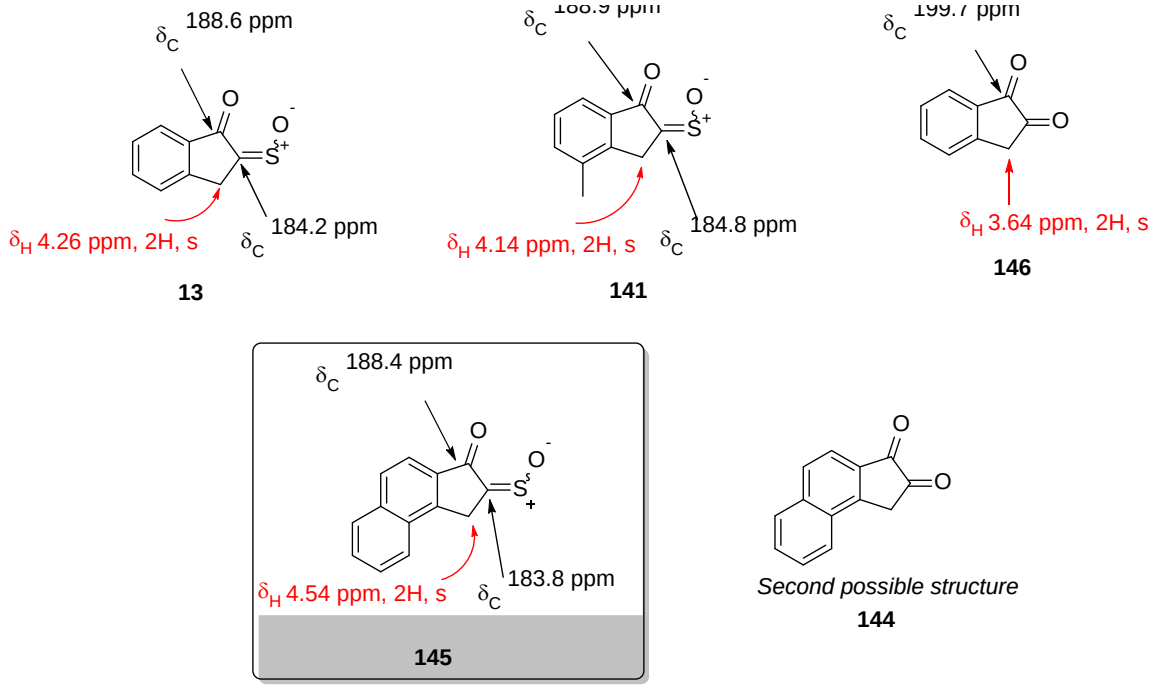
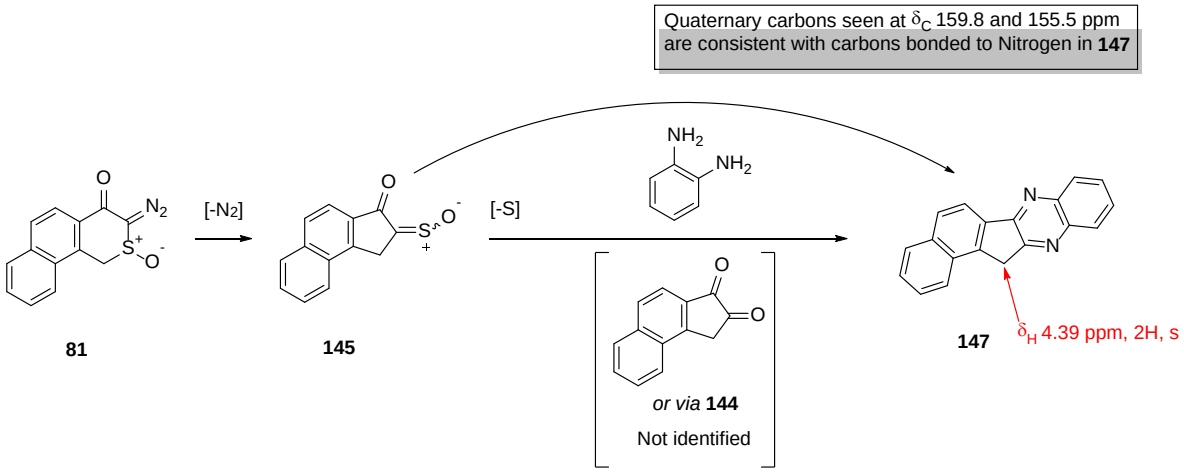


*Figure 31:Comparison of spectroscopic characteristics of **145** to sulfines and Indanediones characterised by Buckley.*[19]

Initially it was thought that the α-diazosulfoxide **81** had decomposed to the indanedione **144** on storage, to confirm this the aged sample was reacted with *ortho*-phenylenediamine, and interestingly the quinoxazoline condensation product **147** was tentatively identified as the major component of the crude mixture. This reaction was carried out on a small scale and therefore purification of the material was not carried out. The signals corresponding to the tentatively assigned product **147** were a singlet at 4.39 ppm in the ^{1}H NMR spectrum and the characteristic signals for the C=N were present at 155.5 and 159.8 ppm in the ^{13}C NMR spectrum. These characteristic signals are in line with literature precedent for quinoxazolines.[16,82] It appears that the sulfine **145** can react with *ortho*-phenylenediamine in a similar manner to a 1,2-diketone.



Scheme 62

Subsequently, an authentic fresh sample of the α-diazosulfoxide **81** was reacted with $Rh_2(OAc)_4$, for five minutes in dichloromethane at room temperature. Analysis of this reaction mixture showed a compound which possessed the same spectral characteristics as observed for the aged sample. Mass spectrometry indicated the presence of the molecular ion of the α-oxo sulfine **145**. On chromatographic purification a sample was recovered with characteristic 2H signals at 2.82 and 3.41 ppm, tentatively assigned as the indanone **148** (Figure 32). Previously, Buckley demonstrated conversion of α-oxo sulfines to indanones on chromatographic purification. This result suggests the unknown compound characterised earlier was indeed the sulfine **145** and not the indanedione **144** as conversion of the dione **144** to the indanone **148** on silica gel is not easily rationalised. Additionally, o*rtho*-phenylenediamine reacted with the sulfine in a condensation reaction, in a similar manner to what would have been expected with the indanedione **144**.

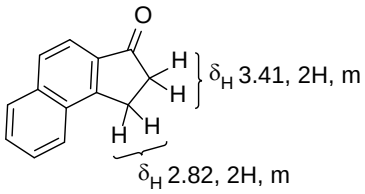


*Figure 32: Indanone **148***

2.5.4.2 Thermogravimetric analysis (TGA) of α-diazosulfoxides

Research from within our group has shown that dediazotisation of α-diazosulfoxides leads to a hetero-Wolff rearrangement, and it can be induced through various methods including thermolysis.[4,5,50,62] A thermogravimetric analysis (TGA) was carried out on a lactone derived α-diazosulfoxide (Figure 33, see section 2.4.2) so in an extension of that work a TGA on the ketone derived α-diazosulfoxide **14** was also carried out (Figure 34).

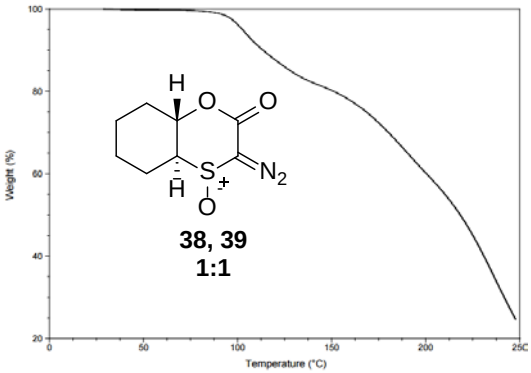


*Figure 33: TGA of α-diazosulfoxides **38,39.***

As expected, the labile ketone derived α-diazosulfoxide **14** shows a sudden and extreme loss of mass at approximately 110°C, much more distinct than in the lactone derivative, highlighting the increased sensitivity of the ketone derivatives to thermal conditions relative to the lactone, making them an excellent candidate for thermolytic conditions for induction of the hetero-Wolff rearrangement. This results agrees with literature precedent that the Wolff rearrangement is more efficient process for α-diazo ketone excited states than for the α-diazo esters, due to enhanced stability of the carbene derived from α-diazo esters, which is caused by ester resonance.[83,84]

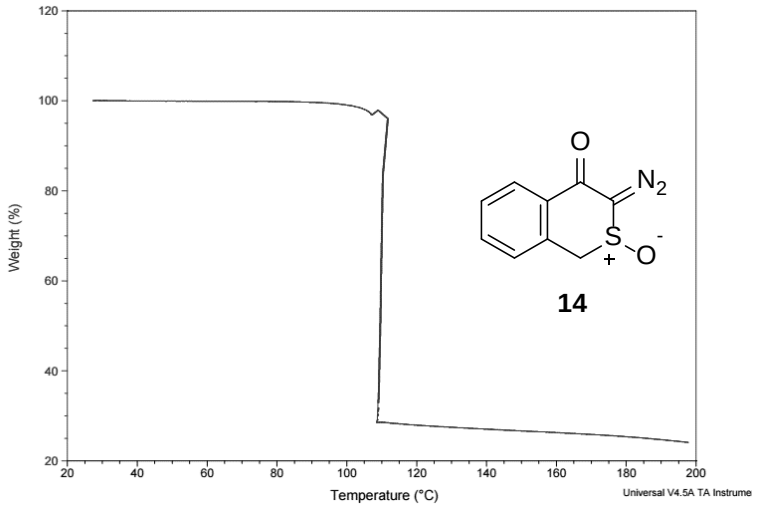
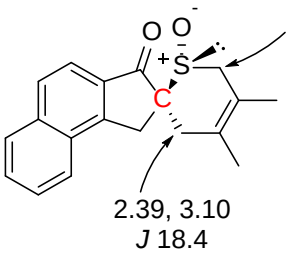
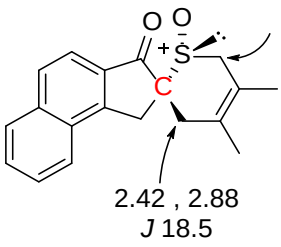


*Figure 34: Thermogravimetric analysis of the ketone derived α-diazosulfoxide **14** showing mass loss versus temperature.*

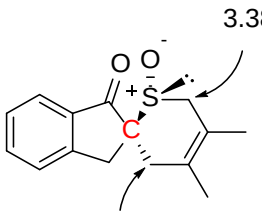
2.5.5.2 Spectral characteristics of the naphthalene derived cycloadducts

With access to the novel naphthalene derived α-diazosulfoxide **81**, and having successfully carried out the Diels-Alder cycloaddition reaction in continuous flow under thermal conditions, two diastereomeric products, **139,140** were isolated and characterised. The distinguishing signals which are characteristic in this set of compounds are the newly formed sp^3 hybridised spiro centres and the diastereotopic protons alpha to the sulfoxide. By comparison with other cycloadducts described by Buckley we have concluded that the major diastereomer **139** formed in the thermolysis reaction comes from addition of the diene **113** to the kinetic *Z*-sulfine **145** (Scheme 61 and Table 22). The spiro centre is affected by the electronic and steric effects of the relative stereochemistry at the sulfoxide and this is illustrated in the ^{13}C NMR spectrum (Figure 35).

Table 22: Comparison of the characeristic ^1H NMR signals and the ^{13}C NMR signals of the novel cycloadducts **139** *and* **140** *with the known cycloadducts* **135** *and* **136.***

Trapping of kinetic *Z* α-oxo sulfine 145 with diene 113	**Trapping of thermodynamic *E* α-oxo sulfine 145 with diene 113**
3.49-3.6, 3.8 *J* 18.0  2.39, 3.10 *J* 18.4	3.33, 3.43 *J* 16.4  2.42 , 2.88 *J* 18.5
Major **139** – more polar	Minor **140** – less polar

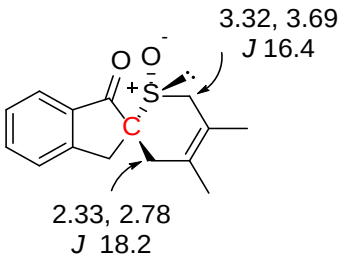
^{13}C NMR signal of $C_{Q\text{-spiro}}$ - 63.5 ppm



135* - more polar

^{13}C NMR signal of $C_{Q\text{-spiro}}$ - 63.7 ppm

^{13}C NMR signal of $C_{Q\text{-spiro}}$ - 68.4 ppm



136* - less polar

^{13}C NMR signal of $C_{Q\text{-spiro}}$ - 68.5 ppm

*The structure and stereochemistry of **135** and **136** were unambiguously confirmed in work by Buckley.[16]

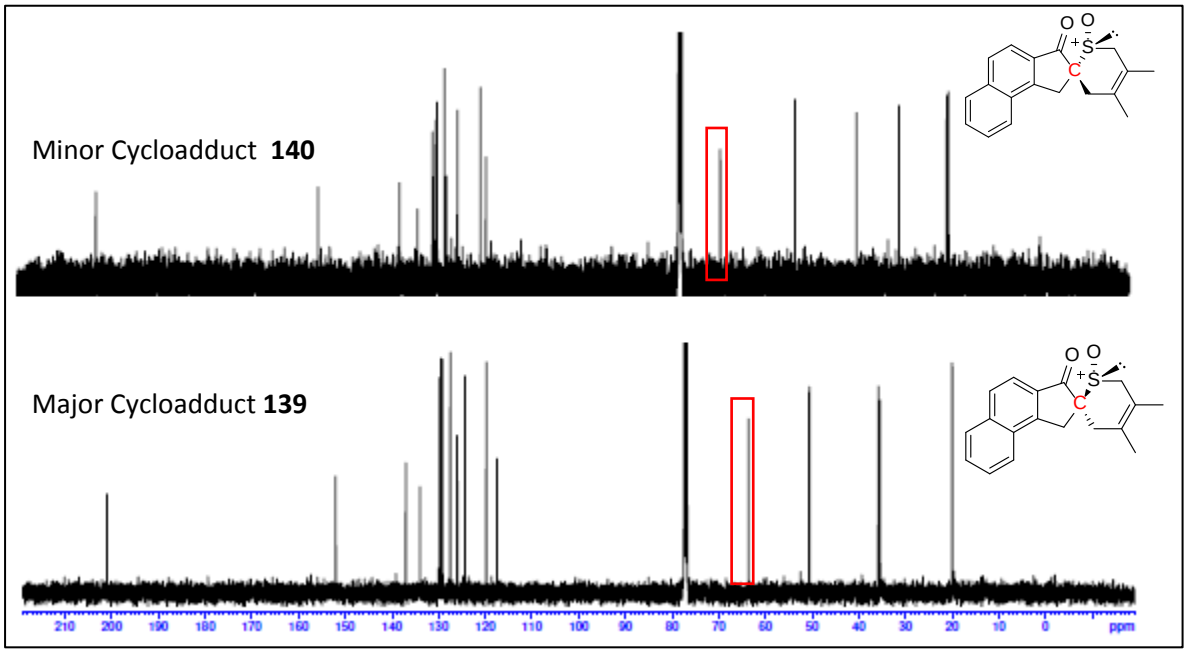


Figure 35: Comparison of the ^{13}C NMR spectrum of two diastereomeric cycloadducts.

The pattern of the signals in the ^{13}C NMR spectra shown in Figure 35, are consistent with the signals previously described for the diastereomers **135** and **136**, both of which have had their stereochemistry confirmed by single crystal X-ray diffraction. The similarities are highlighted in Table 23.

*Table 23: Similarities between the ^{13}C NMR spectra of the cycloadducts **135** and **136** which were confirmed by single crystal analysis and the novel naphthalene derived cycloadducts **139** and **140,** leading to assignment of stereochemistry. $CDCl_3$ was the solvent in all cases.*

	Compound 139	**Compound 135**
^{13}C NMR signals (ppm)	19.9	19.8
	20.0	19.9
	35.3	35.2

	35.7	37.2
	50.5	50.5
	63.5	63.7
	Compound 140	**Compound 136**
^{13}C NMR signals (ppm)	19.5	19.5
	19.9	19.8
	30.1	31.3
	39.2	39.1
	52.4	52.3
	68.4	68.5

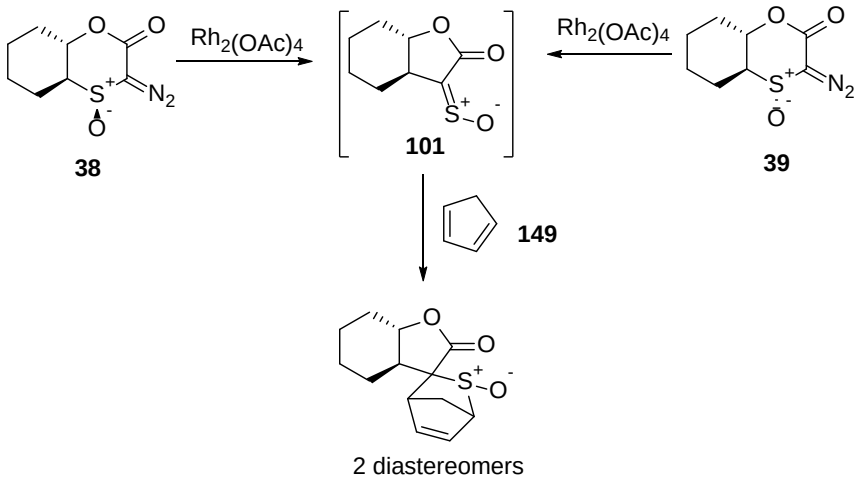
Overall, application of the new cycloaddition methodology to these ketone derivatives shows enhanced efficiency and higher dr in the new continuous flow thermolysis conditions as opposed to the standard transition metal catalysed batch reactions. It now provides access to the sulfoxide cycloadducts **133,135,137,139** in synthetically useful amounts with simple purification through recrystallisation, or flash chromatography if necessary. Of these, **137**, **139** and **140** were isolated and fully characterised for the first time. While the diastereoselectivities obtained is more or less in line with the microwave batch reactions, the increased yields and ability to scale and isolate the products as pure compounds is far easier from the continuous flow process.

In summary, use of this methodology for the Diels-Alder cycloadditions of lactone and ketone derived α-oxo sulfines in continuous flow has resulted in excellent diasteroselectivity and yield when compared to the transition metal catalysed batch reactions. The diastereoselectivity of the reactions is comparable (or better) across the series but consistently higher yields of both lactone and ketone derived cycloadducts are obtained. In some cases, this methodology has the added advantage of purification by recrystallisation or reslurry of the desired cycloadducts rather than column chromatography. As well as this, the ease of scale up, high yields, efficiency, reproducibility, metal free conditions and safety are all advantages of the continuous flow procedure. Indeed, this high yielding step allows access to the thiopyran-*S*-oxides **133**, **135** ,**137** and **139** in synthetically useful yields for the first time, promoting our interest in further derivatisation of these compounds (section 2.5.7).

2.5.5.3 Extension to the use of cyclopentadiene as a diene trap.

Having demonstrated effective cycloaddition with 2,3-dimethyl-1,3-butadiene, extension to the use of cyclopentadiene was next explored. Previously, Kelleher had undertaken a brief

investigation of the cycloaddition of α-oxo sulfine **101** with cyclopentadiene (Scheme 63). When the axial α-diazosulfoxide **38** was used as starting material two diastereomers were formed in a ratio of 2 : 1. When the equatorial diazosulfoxide **39** was used as starting material, the diastereomeric products were formed in a ratio of 3 : 2. In both cases, only one diastereomer was isolated and characterised; in 35% yield from **38** and 14% yield from **39**. The stereochemistry of the cycloadducts was not defined.

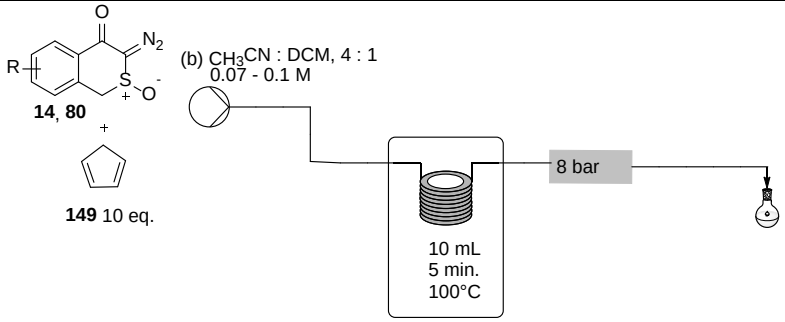


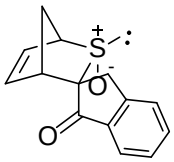
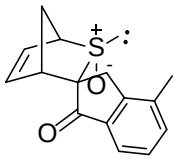
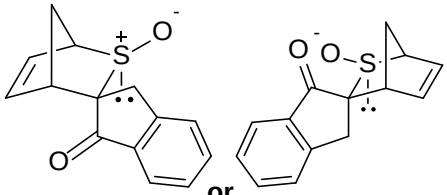
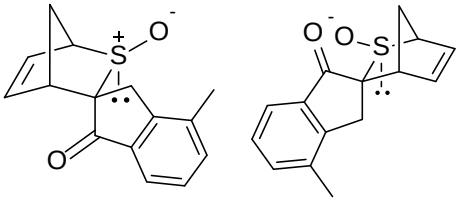
Scheme 63

The initial reactions of the ketone derived α-diazosulfoxide **14** with cyclopentadiene **149** (Table 24, entry 1) were carried out using the same conditions as had been used previously for the cycloadditions with 2,3-dimethyl-1,3-butadiene **113**. The cyclopentadiene **149** was freshly prepared by cracking dicyclopentadiene **150** at high temperature[85] and each of the Diels-Alder cycloaddition reactions were carried out within 48 h. However, it was found that sustained heating of cyclopentadiene **149** in the continuous flow setup under back pressure (8 bar, 120°C for 30 minutes) resulted in a complex mixture. The two products, diastereomer A **151** and diastereomer B **152/153** were minor components of the reacton mixture**.** Although purification was challenging, an impure fraction of diastereomer B **152/ 153** was isolated in 18% yield. At this point, it is believed that **151** and **153** are the most likely structures of the major and minor cycloadducts but this has not been confirmed.

In an attempt to reduce the complexity of the crude material the residence time of the cycloaddition reaction in flow was reduced to 5 minutes, much shorter than the previously used 30 minutes. Notably, when a 30 minute residence time was used with 2,3-dimethyl-1,3-butadiene no problems were encountered.

Table 24: Continuous flow thermolysis cycloaddition reactions with cyclopentadiene.



Entry	**1**[a]	**2**[a,vi]
Diastereomer A	 **151**	 **154**
Diastereomer B	 **152** or **153**	 **155** or **156**
Conversion[b]	100%	100%
Product dr (flow)	51 : 49 **151 : 152/153**	65 : 35 **154** : **155/156**
Isolated Yield[c] (%)	**152/153** (35%)	**154** (14%) **155/156** (25%)

[a] The reaction was carried out at 100°C.

[b] The percentage conversion and dr of the crude material were determined by analysis of the characteristic signals of each component in the ^{1}H NMR spectrum.

[c] The isolated yield refers to the amount of product isolated after column chromatography on silica gel.

[vi] Note: At this point, it is believed that the two cycloadducts are **151** and **153,** and **154** and **156.** However, distinguishing between **152** and **153,** and **155** and **156** cannot be undertaken definitively. Accordingly, in this thesis **152/153** or **155/156** is used to designate the compound Diastereomer B in each instance.

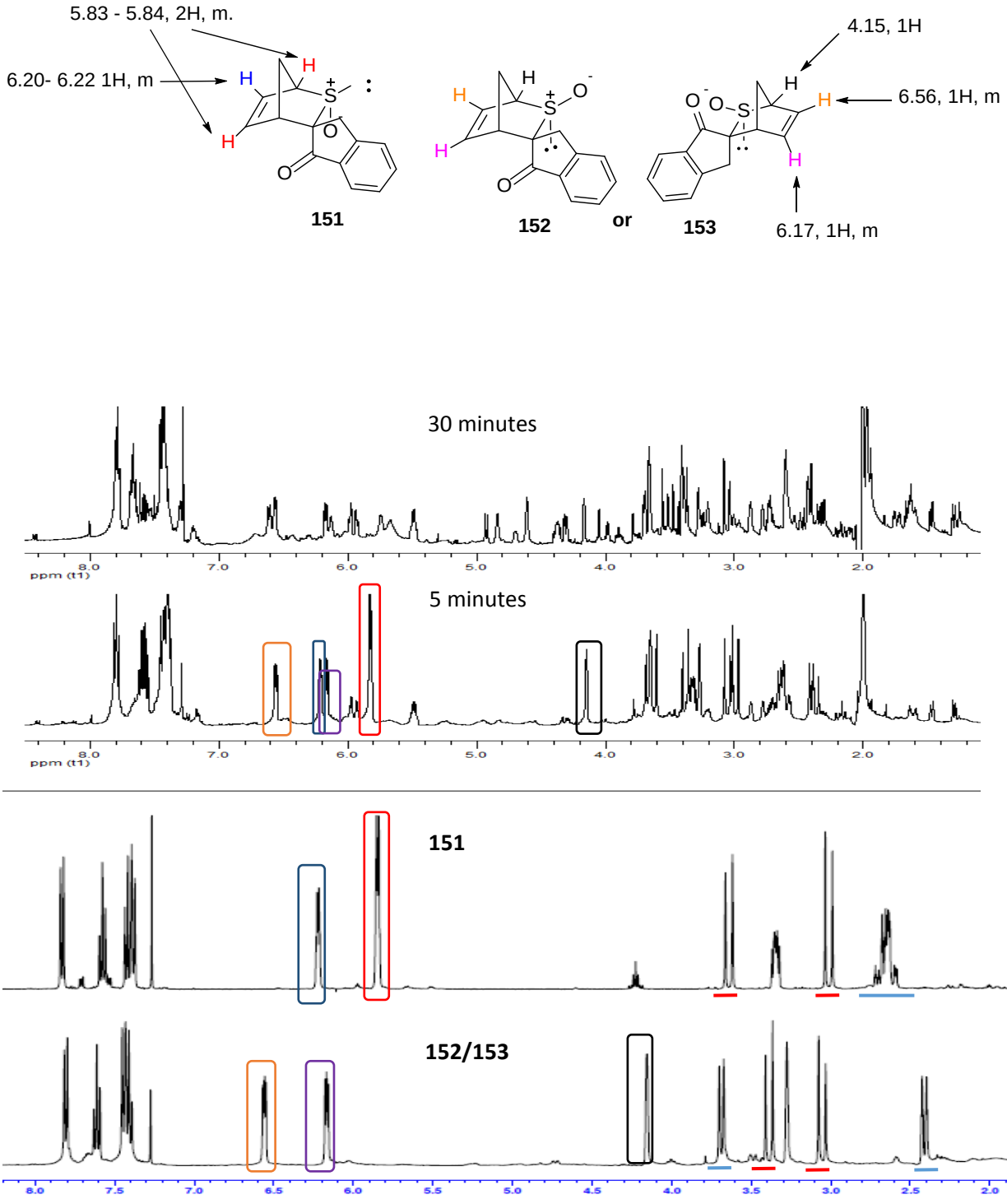


Figure 36: Comparison of the ^{1}H NMR spectrum of a 30 minute residence time versus a 5 minute residence time. Key signals corresponding to **151** *and* **152/153** *are highlighted in both the crude and pure spectra shown. In the pure spectra of* **151** *and* **152/153,** *the $ArCH_2$ AB quartet system is underlined red and the cyclopentadiene CH_2 signals are underlined blue.*

On comparison of the spectrum observed for a 30 minute residence time and a 5 minute residence time it appears the diastereomer **151** is not apparent in the crude reaction mixture from a 30

minute residence time. This may be due to **151** not surviving the longer reaction conditons or alternatively, reacting further in a second Diels-Alder cycloaddition pathway. A similar outcome was subsequently observed when the 30 minute residence time reaction conditions were applied to the α-diazosulfoxide **81** resulting in a complex mixture of crude products. Notably, from the 5 minute residence time reaction, diastereomer A **151** and diasteromer B **152/ 153** can be isolated and characterised separately each exhibiting interesting spectroscopic characteristics (Figure 36). For **151,** the bridgehead proton alpha to the sulfoxide appears at 5.83 – 5.84 ppm in the ^{1}H NMR spectrum, and the corresponding carbon at 98.3 ppm in the ^{13}C NMR. The signal for the spiro carbon is apparent at 70.4 ppm. In contrast to this, these signals for **152/ 153** appear at 4.15 ppm in the ^{1}H NMR spectrum and 70.6 ppm in the ^{13}C NMR spectrum, and the spiro signal is observed at 75.7 ppm. The substantial difference between the diastereomers A and B is presumably caused by the relative stereochemistry of the sulfoxide and ketone moieties. The shorter 5 minute residence time led to cleaner cycloaddition reactions (Table 24).

The formation of two diastereomers can be interpreted in two ways – the first being formation from cyclopentadiene addition to the *Z*-sulfine giving **151** and the *E* sulfine giving **152,** assuming maximum orbital overlap in the transition states resulting in the endo ketone. Alternatively, the two diastereomers could both be formed from the *Z* sulfine only, the endo-endo product **151** and the exo-exo product **153**. Distinguishing between **152** and **153** by spectral details is not evident, although **153** is more likely on the basis of the diastereomer ratio observed and the higher reactivity of cyclopentadiene relative to the 2,3-dimethyl-1,3-butadiene.

Utilising these conditions the cycloadditions with cyclopentadiene were carried out using both ketone and lactone derived α-diazosulfoxides **14, 80**, **77** and **38**, **39** to enable further exploration.

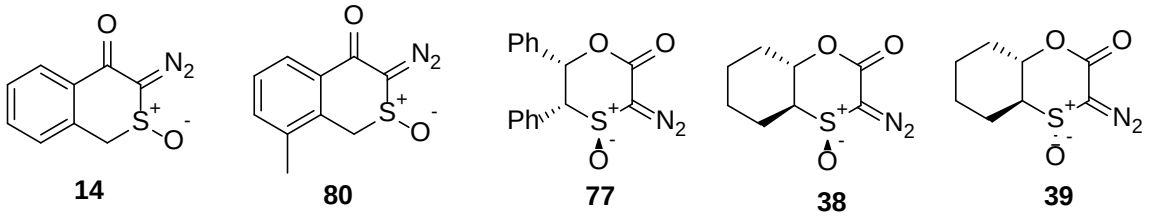


Figure 37: Lactone and ketone derived α-diazosulfoxides utilised in these reaction conditions.

For Table 24, entry 1, the 5 minute residence time leads to successful generation of two diastereomeric products, **151** and **152/153**, with the isolation of **151** in a moderate yield of 35% after column chromatography on silica gel. As described earlier a 30 minute residence time (Figure 36) results in formation of a complex mixture.

For Table 24, entry 2, on investigation of the cycloaddition reaction of cyclopentadiene **149** with the α-diazosulfoxide **80**, with a long residence time of 30 minutes, the same pattern of a complex crude mixture is seen. With a reduced residence time of 5 minutes and a temperature of 100°C, complete consumption of the α-diazosulfoxide **80** is achieved with clean conversion to the desired diastereomers A **154** and B **155** or **156**. Purification of the reaction material led to isolation and characterisation of both diastereomers, **154** and **155/156**, in separate fractions with a combined yield of 39% [**154** (14%) and **155/156** (25%)]. The patterns observed in the ^{1}H and ^{13}C NMR spectra for **154** and **155/156**, are very similar to those seen for **151** and **152/153** shown earlier (Figure 36) with characteristic shifts and coupling for the allylic and bridgehead protons.

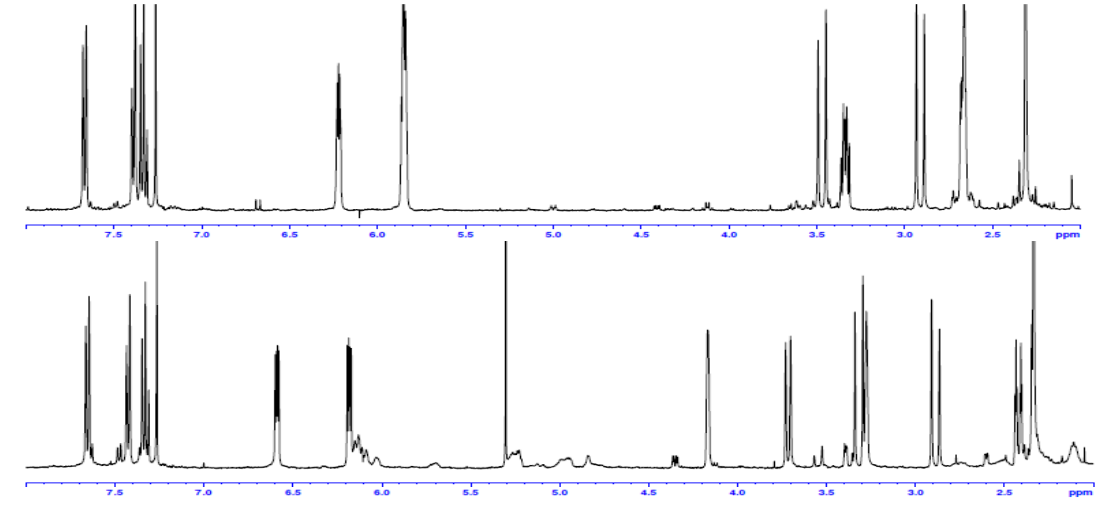
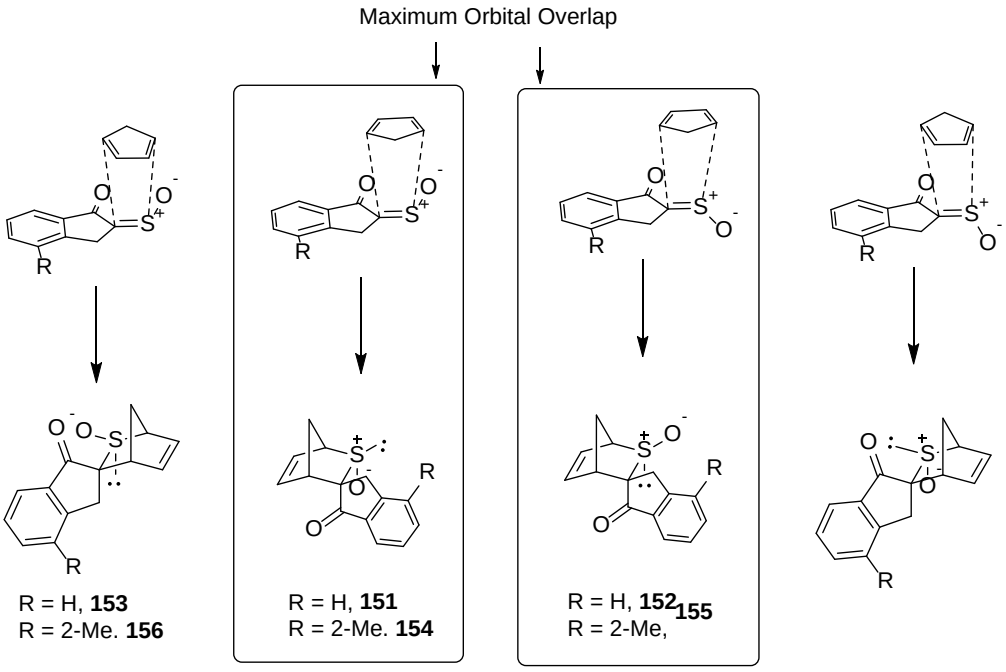


Figure 38: Stacked ^{1}H NMR spectra of **154** *(top) and* **155/156** *(bottom) showing comparable characteristic peaks to* **151** *and* **152/153** *in Figure 35.*

For Table 24, entry 2, the major product **154** formed from trapping of the kinetic *Z* α-oxo sulfine, had the spiro carbon signal at 70.2 ppm and the minor diastereomer **155/156** (from trapping of the thermodynamic *E* α-oxo sulfine or minimum orbital overlap of the *Z* sulfine) from the crude material had the spiro carbon signal of 75.4 ppm. The major cycloaddition products, **151** and **154**, have stereochemistry tentatively assigned based on these data, and the assumption that they arise from trapping of the kinetic Z isomer of the sulfine. The diastereomer B (**152/153** and

155/**156**) is derived from either the alternative approach (minimum orbital overlap) to the *Z* sulfine, or approach to the *E*-sulfine (Scheme 64).

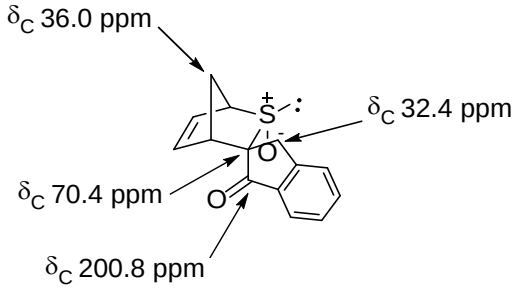
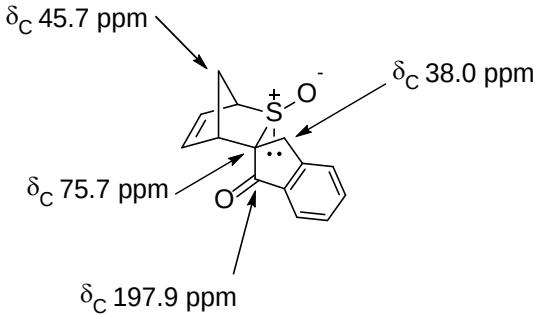
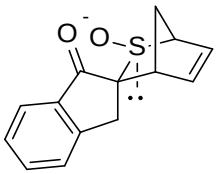
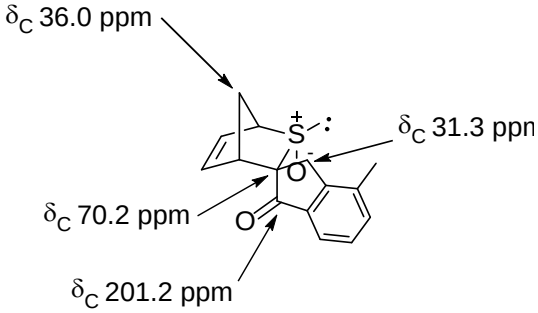
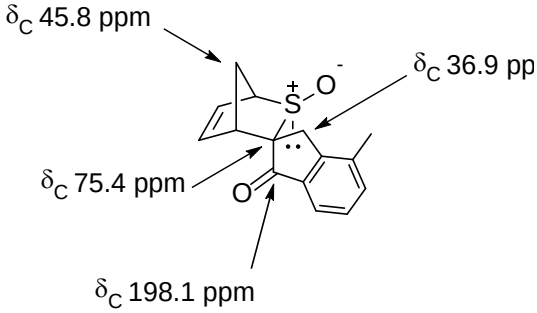
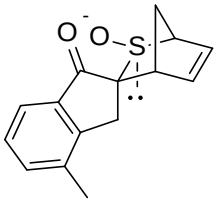
In these cycloaddition reactions there is the potential to form four diastereomeric products, however in all cases, only two are seen. Diasteromer A **151** and Diastereomer B **152** can be envisaged to form from addition to the *Z* and *E* sulfines respectively, with maximum orbital overlap in the transition state to provide the endo ketone, or alternatively both **151** and **153** are formed by trapping of the *Z* sulfine (both maximum and minimum orbital overlap) to give the endo-endo or exo-exo diastereomers.



Scheme 64

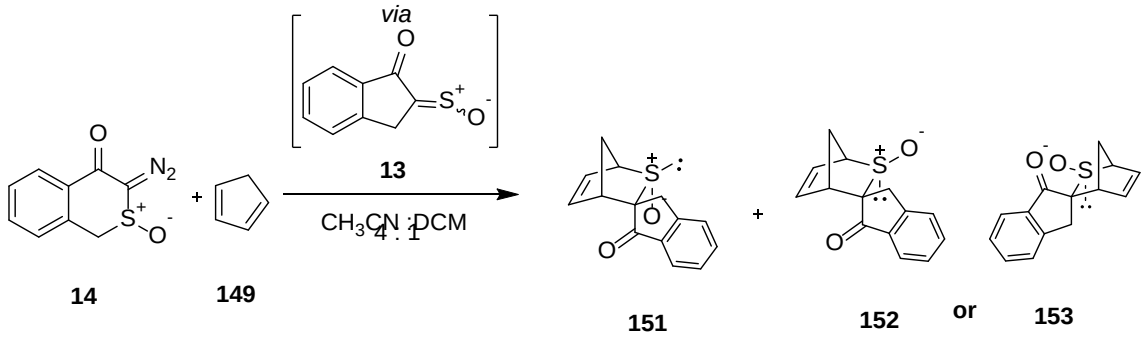
At this time, the exact stereochemistry of the cycloadducts has not been structurally confirmed, but by comparing the experimental data of the cycloadducts **151** and **154**, and **152/153** and **155**/**156** it is clear that these are structurally related. The splitting patterns and chemical shift (δ_H and δ_C) for the aryl CH_2 and the bridgehead CH_2 were very characteristic with **151** and **154** essentially identical, and likewise **152/153** and **155**/**156** were very similar. The relative polarity is also the same with diastereomer A (**151, 154**) being less polar and diastereomer B (**152/153, 155**/**156**) being more polar.

Table 25: Comparison of the ^{13}C NMR spectral data of the cycloadducts **151** *and* **154** *and****151/152*** *and* ***154/155****.*

Entry	*Diastereomer A*	*Diastereomer B*
1.	 **151**	 **152** **or**  **153**
	Diastereomer A	***Diastereomer B***
2.	 **154**	 **155** **or**  **156**

With this success in achieving the synthesis of the these novel cycloadducts in continuous flow using a 5 minute residence time, batch reactions was explored for comparison (Table 26) utilising the same solvent system across the series.

*Table 26: Cycloaddition reactions of α-diazosulfoxide **14** with cyclopentadiene **149**.*



Entry		Crude Ratio of Products	Isolated Products
1.	Continuous flow thermolysis (Δ) 30 min.	Complex Mixture	**152/153** (18% - impure)
2.	Continuous flow thermolysis (Δ) 5 min.	**151** : **152/153** 51 : 49	**152/153**(35%)
3.	Batch thermolysis (Δ) 30 min.	**151** : **152/153** 66 : 34	**151** (63%)
4.	Batch [$Rh_2(OAc)_4$, 1 mol %]. 60 min, r.t.	**151** : **152/153** 60 : 40	**152/153** (22%)

For Table 26, Entry 3, the α-diazosulfoxide **14** and cyclopentadiene **149** were reacted in acetonitrile : dichloromethane (4 : 1) for 30 minutes under batch reflux conditions with the oil bath set to 100°C. This time, on analysis of the crude reaction mixture, the ^{1}H NMR spectrum of the crude material showed a 66 : 34 ratio of major to minor diastereomers. (Although up until now, microwave batch reactions have been compared against thermolysis reactions in continuous flow, the increased pressure in the microwave would most likely cause dimerization of the cyclopentadiene, therefore the flow thermolysis reaction was compared to a batch thermolysis reaction at atmospheric pressure.) After purification of the batch thermolysis reaction (Table 26, entry 3), diastereomer A **151** is isolated in 63% yield. Interestingly, only minor amounts of the dicyclopentadiene dimer **150** were observed. This is likely due to cyclopentadiene **149** being

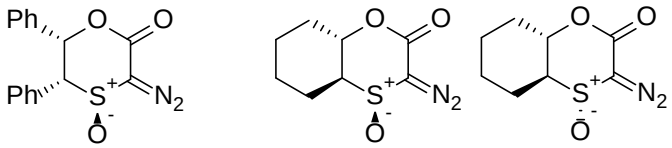
heated to reflux. In continuous flow the reaction mixture is at increased pressure and temperature promoting dimerization, however in the analogous batch reaction the diene **149** can continually evaporate and re-condense without dimerisation. Previously within the group, batch thermolysis reactions have been rarely used. O'Sullivan noted that reflux conditions in chlorobenzene were required to induce the hetero-Wolff rearrangement of lactone derived α-diazosulfoxides[15] and Buckley noted that reflux conditions with dichloromethane as solvent were not sufficient to generate the sulfine from ketone derived α-diazosulfoxides.[16]

To compare to the batch and continuous flow thermolysis reactions, a batch reaction was carried out whereby generation of the intermediate α-oxo sulfine was achieved using rhodium acetate at room temperature in the presence of a cyclopentadiene trap (Table 26, entry 4).

The two diastereomers, A **151** and B **152/153** were formed in a ratio of 60 : 40, with a significant amount of impurities which were not apparent in the thermolysis reactions. Purification of the reaction mixture led to successful isolation of the diastereomer B, **152/153** only, in a yield of 22%. Notably, the dr of the batch thermolysis reaction was the most selective whereas the continuous flow reaction and the transition metal catalysed batch reaction were less selective. However, when compared to the dr's obtained with 2,3-dimethyl-1,3-butadiene, the selectivity is much lower e.g. a crude dr of 95:5 is obtained with the thermolysis of **14** and 2,3-dimethyl-1,3-butadiene, whereas it is 51 : 49 for **14** and cyclopentadiene (Table 26, entry 2). When the reactions are carried out using rhodium acetate the crude dr's are 85 : 15 and 60 : 40 respectively (Table 26, entry 4). The most likely interpretations of these observations is that the cyclopentadiene **149** trapping of the sulfine intermediate is faster than the trapping with butadiene due to the s-*cis* conformation and therefore isomerisation to the *E* isomer does not occur prior to trapping, The highly reactive cyclopentadiene can trap from either approach to give the endo-endo **151** or exo-exo **153**. With the butadiene the diastereomers are formed in a different way due to trapping of the *E* sulfine in addition to the *Z* sulfine.

Overall, this methodology for the generation and cycloaddition of α-oxo sulfines in continuous flow was successfully applied to ketone derived α-diazosulfoxides **14** and **80** with cyclopentadiene **149**. Although it required optimisation, through modification of the residence time, successful cycloaddition was achieved to isolate novel cyclopentadiene cycloadducts with preferential *in situ* trapping of the kinetic *Z* α-oxo sulfine. However, this methodology led to novel, cycloadducts in a scalable, safe, metal-free and efficient methodology. Building on the preliminary investigation

carried out by Kelleher (Scheme 63) extension of this methodology to the *cis* diphenyl derived α-diazosulfoxide **77** and the cyclohexyl derived α-diazosulfoxides **38,39** was next explored.



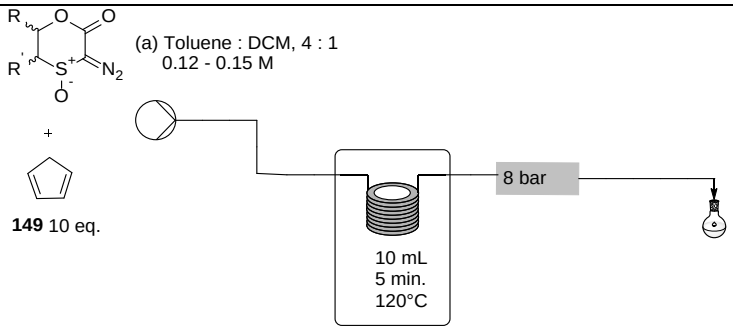
1 : 0.7

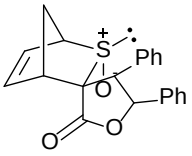
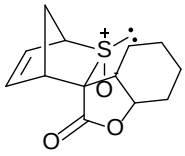
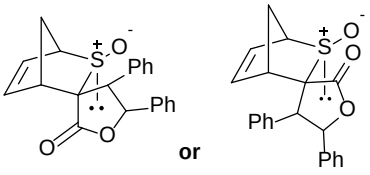
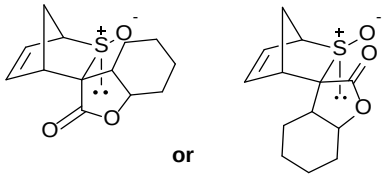
Axial : Equatorial

77 **38 : 39**

Figure 39: Lactone derived α-diazosulfoxides used in the cycloaddition reactions with cyclopentadiene.

Table 27: Cycloadditions of lactone derived α-diazosulfoxides with cyclopentadiene.

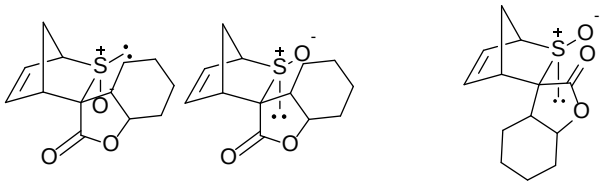


Entry	**1**	**2**
Diastereomer A	 **157**	 **158**
Diastereomer B	 **159/160**	 **161/162**
Conversion	20%	63%
Product dr (flow)	50 : 50 **A : B** **157** : **159/160**	45 : 55 **A : B** **158** : **161/162**
Isolated Yield (%)	**159/160** (11%)	**158** (19%) **161/162** (24%)

Initially, the residence time used for the lactones was the same used for both ketone derived α-diazosulfoxides **80** and **14**, however due to solubility issues and the higher temperature required (120°C compared to 100°C) to achieve the hetero-Wolff rearrangement of these derivatives, the solvent mixture used was a 4 : 1 combination of toluene and dichloromethane, the same as used previously with 2,3-dimethyl-1,3-butadiene (section 2.5.4). The initial results, as shown above (Table 27) show reduced consumption of the α-diazosulfoxide starting materials (20% for **77** and 63% for **38,39**) and lower diastereoselectivity. Notably, in the case of **38,39**, the equatorial α-diazosulfoxide **39** reacted selectively, with the presence of unreacted axial α-diazosulfoxide **38** only, observed in the ^{1}H NMR spectrum of the crude material. This increased stability of axial α-diazosulfoxides has previously been observed by both Collins and Kelleher.[12,14]

In attempting to increase the percentage conversion of the cyclohexyl α-diazosulfoxides **38,39** the residence time was increased from 5 minutes to 10 minutes. Although the conversion increased to 100%, the diastereoselectivity became 50:50. In another experiment (Table 28, Entry 3), the temperature was increased allowing a shorter residence time to also achieve 100% conversion.

Table 28: Variation of conditions used for the Diels-Alder cycloaddition for lactone derivatives.



158 **161** or **162**

Entry	**1**	**2**[a]	**3**[a]
Residence time	5	10	5
Temperature	120	120	130
Equivalents of diene 149	20	20	20
Conversion	63%	100%	100%
dr	55:45	50:50	50:50
	161/162 : 158	**161/162 : 158**	**161/162: 158**
Yield	**161/162** (24%)	-	-
	158 (19%)		

[a]Entries 2 and 3 were not purified, due to the low diastereoselectivity and excessive amounts of dicyclopentadiene dimer formed in the reaction.

Additionally, dimerisation of the cyclopentadiene **149** at the elevated temperatures became a major issue with the dicyclopentadiene dimer **150** being the major component of the crude reaction mixture. Therefore to optimise the outcome of the cycloaddition reactions with

cyclopentadiene **149** consumption of the α-diazosulfoxide starting material and dimerization of cyclopentadiene **149** must be carefully balanced.

Although the cycloaddition reactions of the α-diazosulfoxide **77** and the α-diazosulfoxides **38,39** have the potential to form eight diastereomeric cycloadducts in both cases (four from the *Z* sulfine and four from the *E* sulfine), only two diastereomers are present in the ^{1}H NMR spectrum of the crude material in both cases. For the *cis*-diphenyl diazosulfoxide **77** the dr is 50 : 50 for **159**/**160** and **157**. For the cyclohexyl derived α-diazosulfoxides **38,39** the ratio of the two cycloadducts formed is 55 : 45 (Table 27) for the **161**/**162** and **158**. These dr's are much lower when compared to the cycloadditions of lactone derived α-oxo sulfines with the 1,3-dimethyl-2,3-butadiene **113**, however they are in line with the dr results achieved for the cycloadditions of the ketone derived α-oxo sulfines with cyclopentadiene **149**, once again indicating addition to the the *Z* sulfine.

In addition, the spectral features of the lactone cycloadducts are very similar to the ketone derivatives. Therefore, it is most likely that two cycloadducts are formed from the *Z* sulfine giving both the exo-exo and endo-endo cycloadducts. At this point the relative stereochemistry at the fused bridgeheads is unknown. An alternative explanation is that one of the cycloadducts is from the *E* sulfine to form the exo-endo cycloadduct **161** and in the absence of crystallographic data, distinguishing between **161** and exo-exo **162** is not possible, although **162** is more likely (Figure 40).

Kelleher[12] had previously carried out cycloaddition reactions of the α-diazosulfoxides **38,39** with cyclopentadiene **149** and had isolated one diastereomer as the product. Comparison of the spectral data confirms it was indeed **158**, however assignment of stereochemistry to the only isolated product, **158**, was not possible at that time. In this work, the inability to grow single crystals of these cycloadducts also hindered the assignment of stereochemistry.

When the α-oxo sulfine **101** is trapped with butadiene **113**, the major products are formed from addition to the kinetic *Z* sulfine from above and the thermodynamic *E* sulfine from below, confirmed by crystallography. At this stage the relative stereochemistry of the fusion in the lactone is not defined although it is clear that only one is formed in each case.

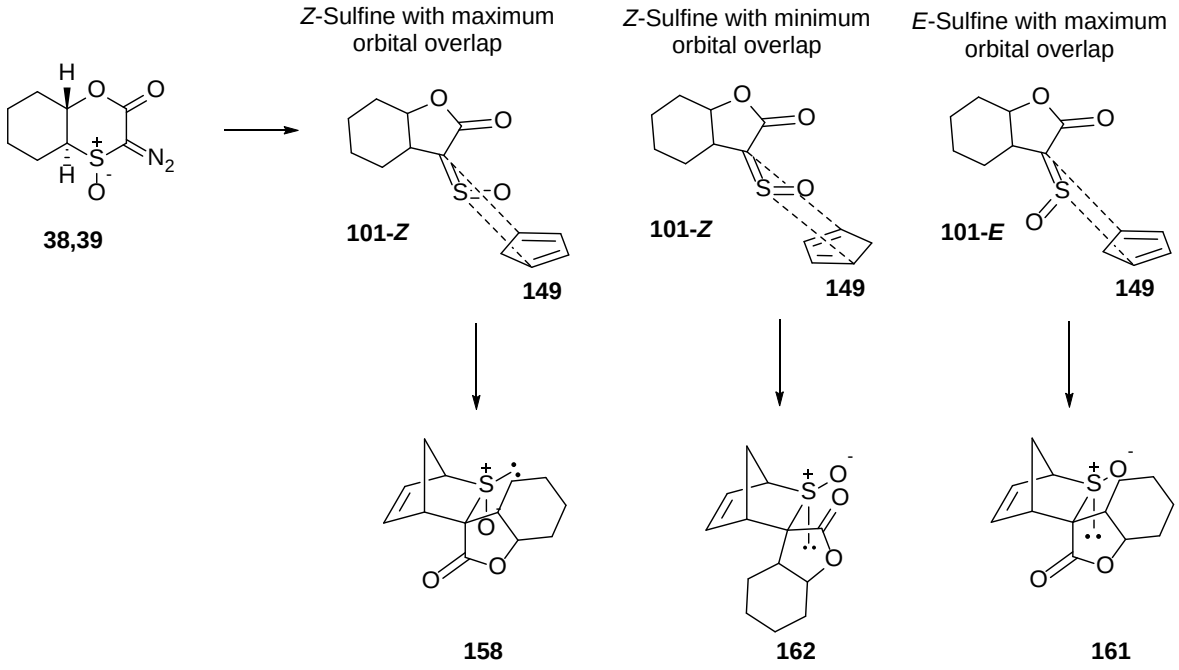


Figure 40: Possible modes of addition of cyclopentadiene **149** *with the α-oxo sulfine* ***101*** *when maximum orbital overlap occurs.*

The product **158** is the less polar of the two diastereomers. Significantly, in the ketone series, the *endo* sulfoxides **154** and **151** were also less polar than the *exo* sulfoxides **155**/**156** and **152**/**153**. Furthermore, the carbon signal for the methylene unit in the bridge is very distinctive in the cycloadducts; thus in **154** and **151** it appears at δ_C 36.0 ppm while in **152**/**153** and **155**/**156** the same carbon appears at δ_C 45.7 and 45.8 ppm respectively. Clearly the relative orientation of the sulfoxide oxygen substantially deshields this carbon when the oxygen is *exo.* Similarly in the cycloadducts **161**/**162** and **158**, this carbon appears at δ_C 45.5 ppm in **161**/**162** and δ_C 33.5 ppm in **158**. It is believed that **162** and **158** are formed both from the *Z* sulfine.

Interestingly, the chemical shift of the CH next to the carbonyl is not sensitive to alteration of stereochemistry of the carbonyl (exo/endo). Alternatively, it is possible that all stereoisomers are endo carbonyl (formed from maximum orbital overlap).

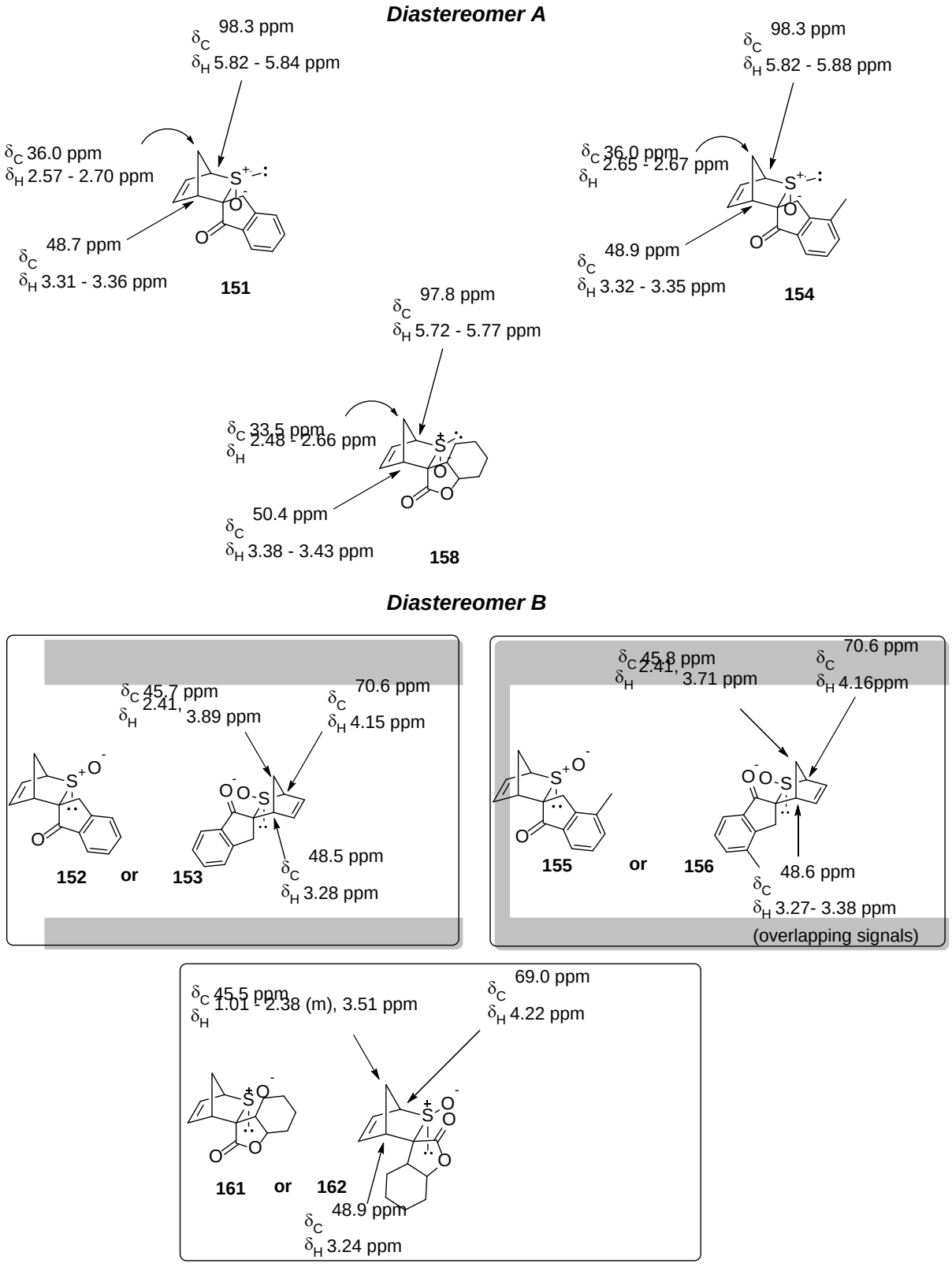


Figure 41: The endo cycloadducts **151, 154** *and* **158** *and the exo cycloadducts* **152/153, 155/156***, and* **161/162***.*

The butadiene cycloaddition has clearly shown that addition to the *Z* sulfine occurs from the alpha face of the bicyclic lactone and addition to the *E* occurs from the beta face. While it reasonable to assume similar facial discrimination with the cyclopentadiene the decreased diastereoselectivity is difficult to rationalise and therefore at this point further investigation is required to definitively determine the relative stereochemistry in the cycloadducts.

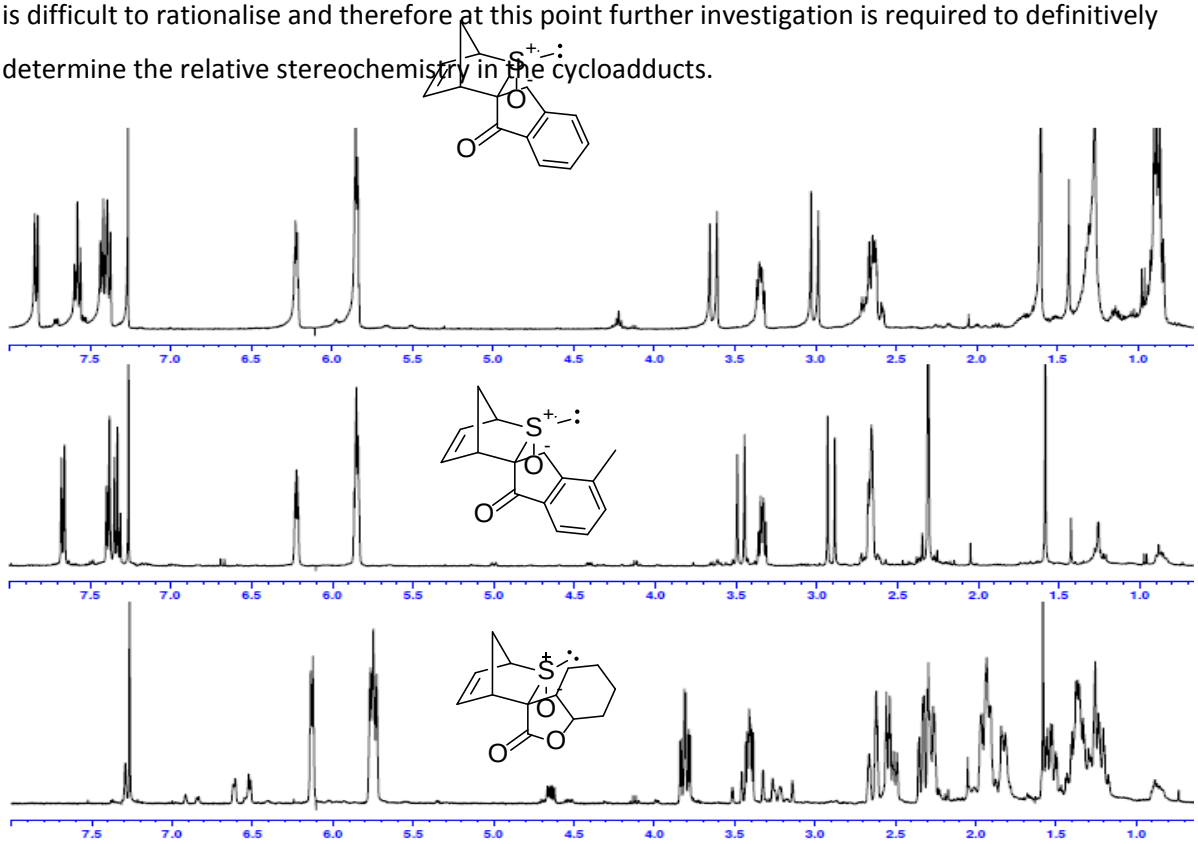


Figure 42: Stacked ^{1}H NMR spectra of diastereomers A: **151** *(top),* **154** *(centre) and* **158** *(bottom).*

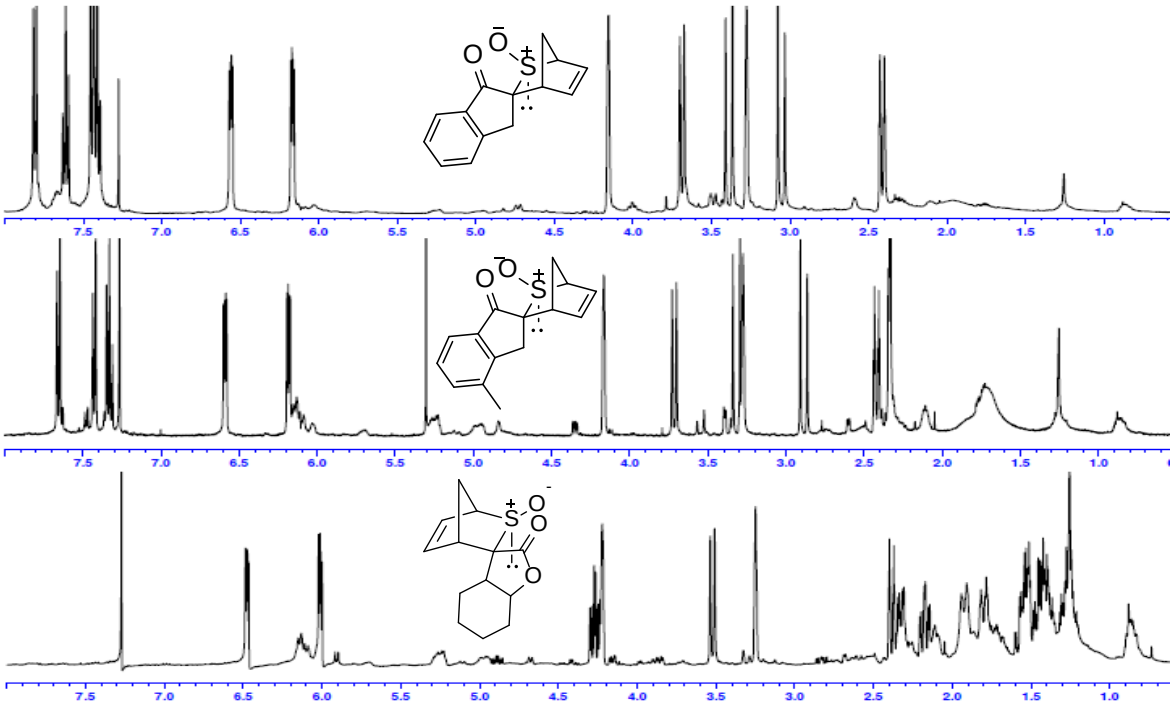


Figure 43: Stacked ^{1}H NMR spectra of diastereomers B: of **152/153** *(top),* **155/156** *(centre), and* **161/162** *(bottom).*

The orientation of the sulfoxide moiety has a significant effect of the NMR shift of both the CH signal alpha to the sulfoxide, and the cyclopentadiene CH_2 bridgehead when the oxygen is near these in space leading to significant deshielding, an effect of sulfoxides known in the literature.[17] The significant deshielding from the sulfinyl oxygen affecting the NMR characteristics is identical to the ketone derived product **154**. Further evidence for the presumed stereochemistry are the spectroscopic characteristics of **158**, **154**, and **151** are similar and **161/162** and **155/156** and **152/153** are similar with regards to the pattern in the ^{1}H and ^{13}C NMR spectra (Figure 41, 42 and 43).

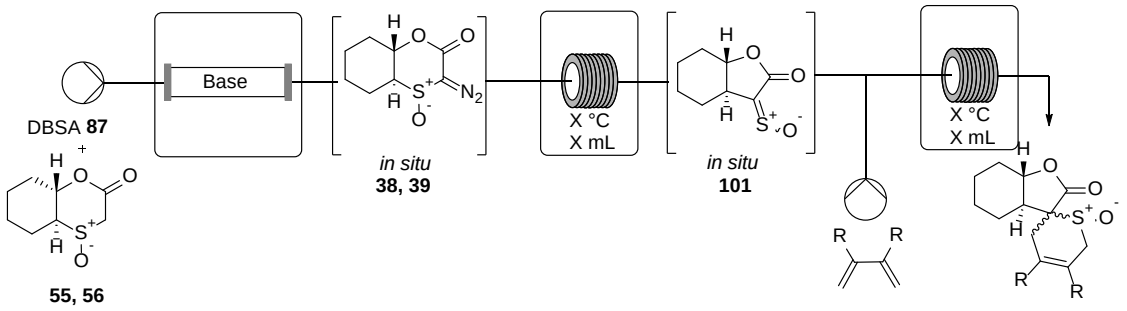
Through modification of the reaction conditions (shorter residence time for ketone derivatives) a series of novel cyclopentadiene cycloadducts were isolated and characterised for the first time. Interestingly diastereoselectivites were different using cyclopentadiene or 2,3-dimethyl-1,3-butadiene as the trap. At this stage it appears that with 2,3-dimethyl-1,3-butadiene traping of both *E* and *Z* sulfines is seen, while with the more reactive cyclopentadiene trapping with the *Z* sulfine occurs faster than isomerisation to the *E* sulfine, in this case, resulting in the formation of both exo and endo diastereomers. Further work is required to definitively establish the relative stereochemistry of the cycloadducts.

Having established conditions for the synthesis of the α-diazosulfoxides in continuous flow (section 2.3.4) and having established conditions for the successful thermal Diels-Alder

cycloadditions (section 2.5.5) telescoping these two chemical transformations in continuous flow was carried out.

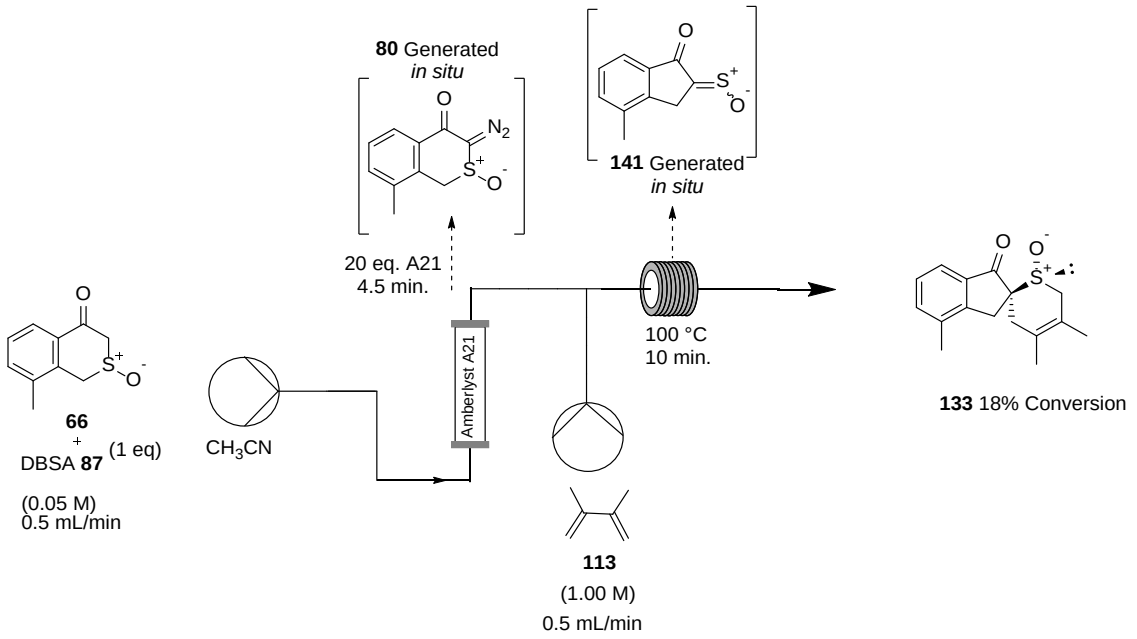
2.5.6 Telescoping of the diazo transfer and Diels-Alder cycloaddition reactions

Having achieved success in the optimisation of the diazo transfer protocol to α-diazosulfoxides in continuous flow (section 2.3.4), and success in achieving cycloaddition of α-oxo sulfines in continuous flow (section 2.5), demonstrating proof of concept that the processes could be telescoped was a priority (Scheme 65).



Scheme 65

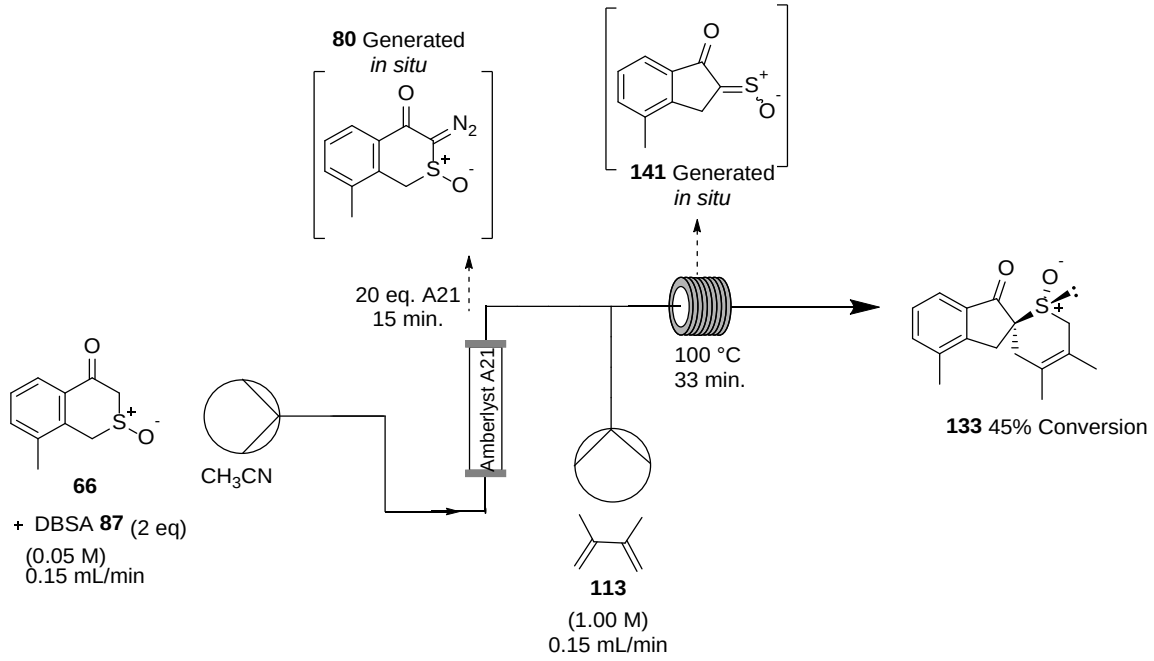
The objective was to telescope the generation of the labile α-diazosulfoxide with the hetero-Wolff rearrangement to form the reactive α-oxo sulfine, and subsequent Diels-Alder cycloaddition to form a stable, isolable, crystalline cycloadduct. The first attempt at this consisted of a 4.5 minutes residence time of the ketone derived sulfoxide **66**, on 20 equivalents of Amberlyst A21 with 1 equivalent of DBSA **87** (Scheme 66). One equivalent of the sulfonyl azide **87** was used so that on achieving complete conversion to the α-diazosulfoxide **80**, excess sulfonyl azide **87** would not be heated (Scheme 66).



Scheme 66

The output from the column reactor was combined with the 1,3-dimethyl-2,3-butadiene **113** input at a T-piece and heated to 100°C for 10 minutes in the reactor coil, to induce the hetero-Wolff rearrangement, resulting in formation of the intermediate α-oxo sulfine **141** and subsequent Diels-Alder cycloaddition (Scheme 66). On analysis of the crude reaction mixture, 18% of the desired cycloadduct product **133** was formed along with 82% residual starting material **66** (Figure 44). This low consumption of starting material **66** may be due to using only one equivalent of DBSA **87**. Our earlier investigation had shown on reduction of the equivalents of the DBSA **87** below 2 equivalents, there is a significant decrease in the percentage conversion to the desired α-diazosulfoxide **80**. Heating the reaction mixture which, in retrospect, contained residual DBSA **87** did not pose any problem in practice, within the continuous flow system; although, as it has an initiation temperature of 151°C,[33,34] 51°C higher then the temperature in the reactor coil this explains this observation.

To achieve higher percentage conversion to our desired α-diazosulfoxide **80** inline two equivalents of the diazo transfer reagent DBSA **87** were used, with the sulfoxide starting material **66**. A 15 minute residence time over 20 equivalents of Amberlyst A21 was followed by combination with the butadiene **113** stream leading to sulfine formation under thermolytic conditions followed by cycloaddition (Scheme 67).



Scheme 67

Analysis of the crude material by ^{1}H NMR spectroscopy showed 45% of the desired cycloadduct **133**, which is formed from trapping of the kinetically favoured *Z* α-oxo sulfine *in situ,* alongside 55% of the residual starting material **66** (Figure 44).

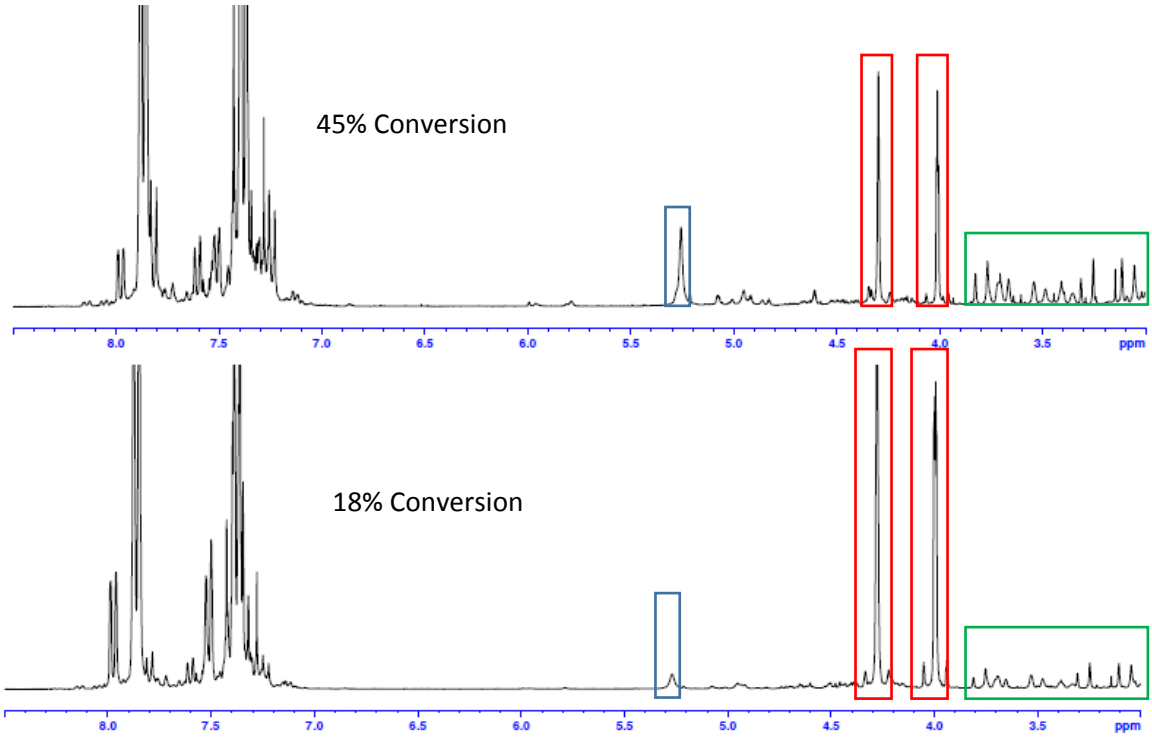
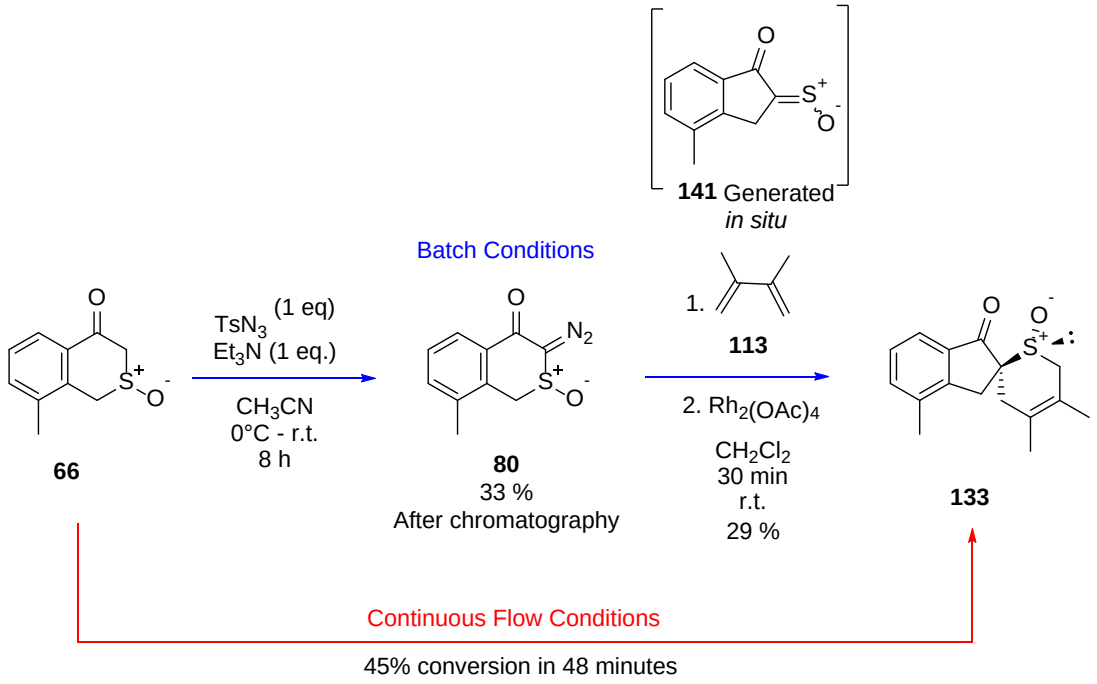


Figure 44: Comparison of 1H NMR spectra of the crude material from the telecoped reactions in scheme 67 (top) and scheme 66 (bottom). Characteristics signals of the dodecylbenzenesulfonyl amide are in blue, signals of the sulfoxide starting material **66** are in red and the cycloadduct product **133** is highlighed in green.

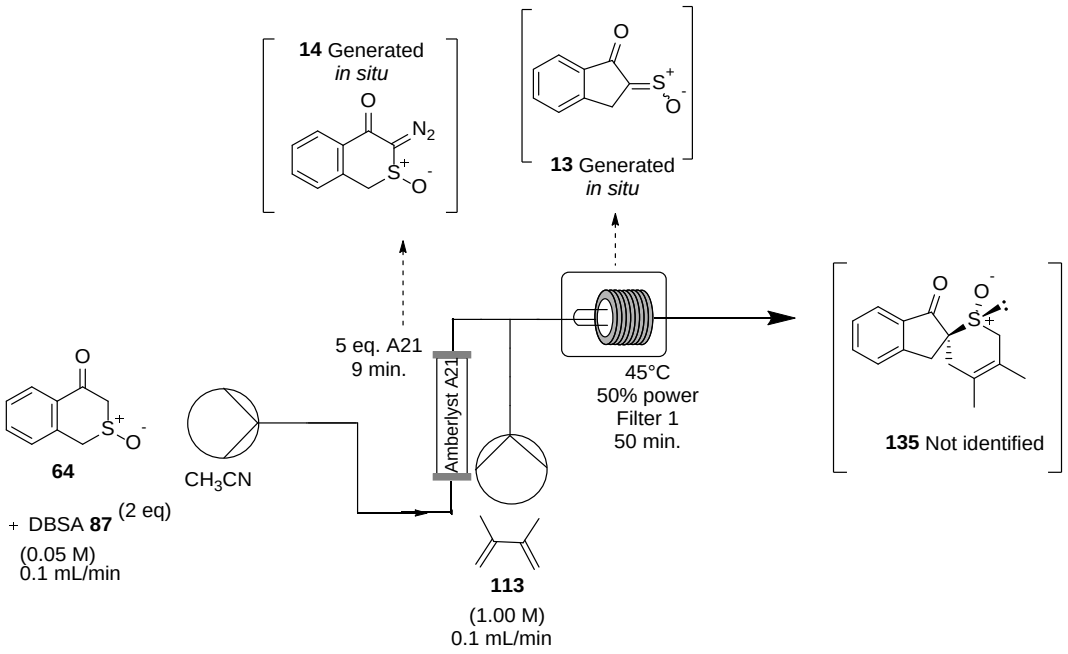
This was a significant result as it highlights the potential to go from the stable sulfoxide **66** through to a labile α-diazosulfoxide **80**, through to reactive α-oxo sulfine **141** and finally to a stable cycloadduct product **133** without isolation at any point. Although this telescoped reaction sequence will require further optimisation, it establishes proof of concept and is a scalable process. This process can be compared to the previously used batch processes which would require a 8 to 16 hour reaction time for diazo transfer resulting in a yield between 25% and 35% after column chromatography on silica gel, then is subsequently followed by the Diels-Alder cycloaddition (reaction time 3 min in microwave, 30 min in batch) with moderate yields (29% in batch and quantitative in microwave).



Scheme 68

This comparison highlights the benefits of the scalable telescoped process which generated the desired cycloadduct **133** within 14.5 minutes (18% conversion) or 48 minutes (45% conversion). Having shown proof of concept for telescoping the reaction sequence under thermolytic conditions, telescoping the reactions under photochemical conditions was also investigated. These photochemical conditions would be more desirable than thermal conditions, as heating the excess of the diazo transfer reagent DBSA **87** is avoided.[vii] Using the optimum conditions for diazo transfer in continuous flow (5 equivalents Amberlyst A21, 9 minute residence time, 2 equivalents DBSA **87**) and filter number 1 in the UV-150 reactor, these conditions were trialled with sulfoxide **64** (Scheme 69). As described earlier (Table 16) filter number 1 removes infrared light but has good transmission in the region of 190 – 2000 nm.

[vii] Sulfonyl azides are safely used under photolysis conditions for nitrone transfer.



Scheme 69

Analysis of the crude reaction mixture by ^{1}H NMR spectroscopy did not show the presence of the sulfoxide starting material **64**, α-diazosulfoxide **14**, desired cycloadduct **135**, or any rearrangement products formed from the intermediate α-oxo sulfine **13** which had been previously isolated and characterised by Buckley.[16] The complex mixture of unidentifiable products believed to be due to over exposure to the UV light reaction conditions (residence time of 50 minutes) which caused significant decomposition to form a complex mixture of unidentifiable components, and may be associated with the excess DBSA going in to the photoreactor.

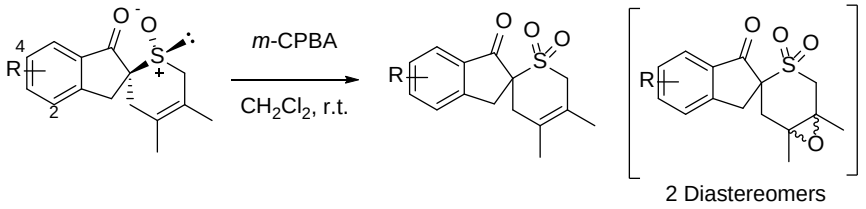
2.5.7 Further functionalisation of sulfoxide cycloadducts

As the yields of α-diazosulfoxides have been substantially enhanced during this work which enabled access to synthetically useful amounts of the sulfoxide cycloadducts in high diastereocontrol and good to excellent yields, a systematic investigation of the reactivity of these cycloadducts was possible for the first time. Previously, isolated experiments were conducted at small scale by Kelleher on a lactone derived sulfoxide cycloadduct.[12] The functionality present in the cycloadducts, namely the sulfoxide and the tetrasubstituted alkene provide opportunity for synthetically useful transformations without altering the carbon skeleton of the cycloadduct, hence a series of oxidation, reduction and rearrangement reactions were carried out to explore the broad range of synthetic transformations available. Interestingly, earlier work from our team has demonstrated activity in anticancer screens for structurally related cycloadducts to those synthesised in this work.[16]

2.5.7.1 Oxidation of the sulfoxide moiety to sulfone

Oxidation of the sulfoxide **133** with *m*-CPBA was first explored at room temperature over four hours. The major product was the sulfone **163** and interestingly, two β-epoxy sulfones over oxidation side products, **164** and **165**, were also observed in the crude material in a ratio of 3 : 1. No evidence for the β-epoxy sulfoxide is observed. This high degree of chemoselectivity for the oxidation provided the desired sulfone **163** in 75% isolated yield after column chromatography. The epoxidation products were not isolated from the reaction mixture after purification. With success in generation and isolation of the novel sulfone **163** in a good yield, these reaction conditions were also applied to the sulfoxide cycloadducts **135** and **137** (Table 29).

Table 29: Results of sulfonylation oxidation reactions.



R = 2-Me **133**
R = H **135**
R = 4-Me **137**

R = 2-Me **163**
R = H **166**
R = 4-Me **169**

R = 2-Me **164, 165**
R = H **167, 168**
R = 4-Me **170, 171**

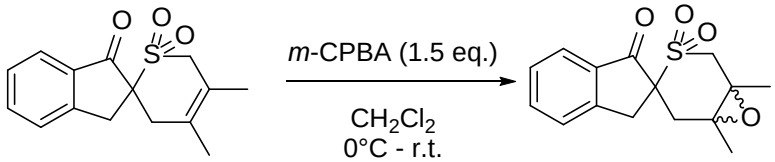
Entry	Reaction Time	Crude Ratio	Isolated products
1			
R = 2-Me	3 h	**163** : **164** : **165**	**163** (75%)
		84 : 12 : 4	
2			
R = H	3 h	**166** : **167** : **168**	**166** (72%)
		84 : 10 : 6	
3			
R = 4-Me	16 h	**169** : **170** : **171**	**169** (48%)
		52 : 37 :12	**170** : **171**, 1 : 0.7 (10%)

The crude ratio of products observed after subjecting sulfoxide **135** to the oxidation reaction conditions (Table 29, Entry 2) was consistent with that recorded for oxidation of sulfoxide **133** (Table 29, Entry 1). The sulfone was the major component (84% of the crude material) while the major β-epoxy sulfone **167** and the minor β-epoxy sulfone **168** were present in a ratio of ~ 2 : 1. Notably, the characteristic signal for the methyl groups of the β-epoxy sulfones are sharp singlets, compared to broader singlets for the allylic methyl groups present in sulfone **166** (Figure 45) and the sulfoxide analogue **135**.

On subjecting sulfoxide **137** to the reaction conditions (Table 29, Entry 3), complete consumption of the starting material was not achieved after 5 h and so the reaction was stirred for 16 h in total. Following ^{1}H NMR analysis of the crude reaction mixture, sulfone **169** and β-epoxy sulfones **170** and **171** were present in a ratio of 52 : 37 : 12 . Following purification, sulfone **169** was isolated in a moderate yield of 48% and another fraction consisted of a 1 : 0.7 mixture of β-epoxy sulfone diastereomers **170** and **171**. Interestingly, this highlights the reactivity of the sulfoxide moiety towards sulfonylation and preferential oxidation to sulfone **169** in the first instance, followed by

subsequent oxidation of the sulfone to the β-epoxy sulfone. The difficulty in isolating the minor amounts of the β-epoxy sulfones **170** and **171** should also be noted. Although signals corresponding to the β-epoxy sulfones **164**, **167**, **170** and **171** were present in the ^{1}H NMR spectra of the crude material at a level of approximately 10%, the corresponding β-epoxy sulfones **164** and **167** were not isolated, and for **170** and **171**, present at about 50% of the crude material, an isolated yield of 10% was achieved suggesting this series of compounds is sensitive to the purification conditions, and possibly labile on silica gel. When the epoxidation of the sulfone to the β-epoxy sulfone occurs the diastereomers are formed in a similar ratio in all cases, 3 : 1 for Table 29, entries 1 and 3, and 2 : 1 for Table 29, entry 2. The relative stereochemistry of the major and minor epoxide diastereomers is consistent across the series, with the same NMR signals for the CH_3 groups of the major and minor diastereomer appearing in the same pattern in all three entries.

To confirm the preferred order of reactivity, an authentic sample of sulfone **166** was isolated and subjected to 1.5 equivalents of *m*-CPBA over a period of 16 h, after which time complete consumption of the sulfone starting material was achieved. In the ^{1}H NMR spectrum of the crude material, two diastereomeric epoxides, **167** and **168** were present in a ratio of 5:1 (Scheme 70).



166

Crude: 5 : 1,
167 : 168,
major : minor

Fractions Isolated : **167** only (32%)
167 : 168, 1 : 1, (32%)
168 only (5%)
Combined yield : 69%

Scheme 70

Following purification, the less polar, major epoxide **167**, and the more polar, minor epoxide **168** were isolated in a combined yield of 69% after chromatography (Figure 45).

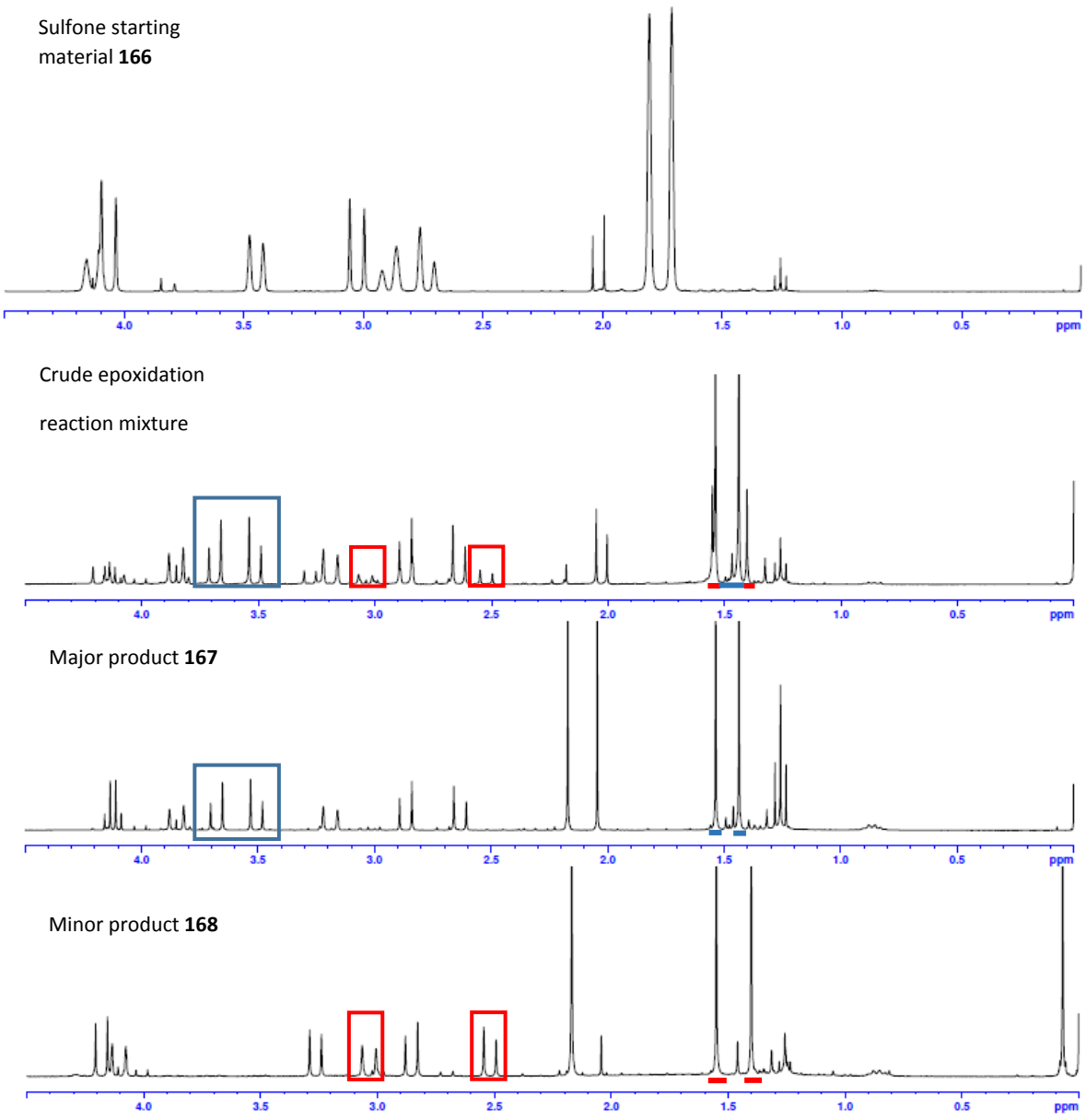
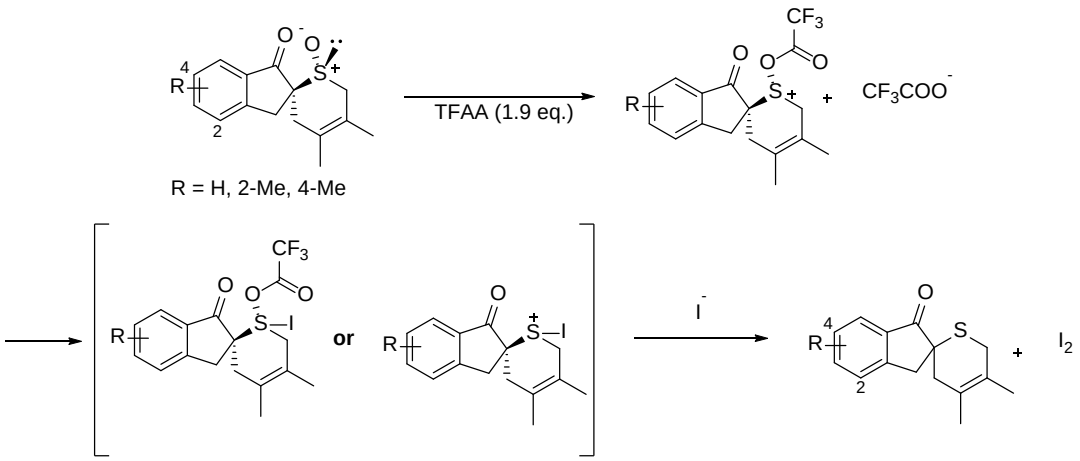


*Figure 45: Comparison of the ^{1}H NMR spectra of the crude material from oxidation of sulfone **166** with 1.5 equivalents of m-CPBA , the major β-epoxy sulfone isomer **167** and the minor β-epoxy sulfone isomer **168**.*

2.5.7.2 Reduction of the sulfoxide moiety to sulfide.

An important synthetic transformation of sulfoxides is reduction to the corresponding sulfide.[86] This transformation can be achieved under a variety of conditions, employing transition metal complexes, electrophilic reagents or Lewis acids.[86-90] The conditions used in this work, to achieve this transformation are those first described by Drabowicz *et al.,* utilizing trifluoroacetic anhydride and sodium iodide in acetone.[91] The report details how the use of mild reaction conditions and readily available reagents achieves successful reduction in short reaction times. The reduction proceeds through an intermediate acyloxysulfonium salt, which will react with the iodide anion to

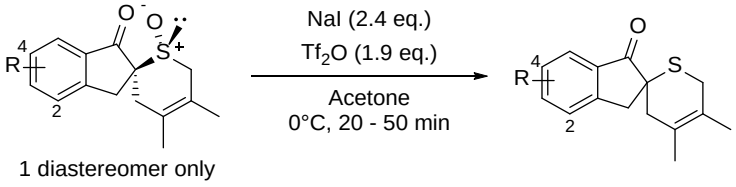
form either a sulfonium salt or a sulfurane intermediate (Scheme 71); decomposition promoted by another iodide anion results in the desired reduction products, resulting in the formation of by-products which are removed during the aqueous workup. The desired sulfide is recovered from the organic layer in high yield.



Scheme 71

When these reaction conditions (2.4 eq. NaI, 1.9 eq. trifluoroacetic anhydride in acetone) were applied to our substrate **133** (Table 30, Entry 1), the reaction was complete after 20 minutes at 0°C, with aqueous work up providing the pure sulfide **172** in a high yield of 84%, without the need for further purification. The aqueous workup includes a sodium thiosulfate wash for removal of any residual iodine formed during the reduction reaction.

Table 30: Results of sulfide reduction reactions.



R = 2-Me **133**
R = H **135**
R = 4-Me **137**

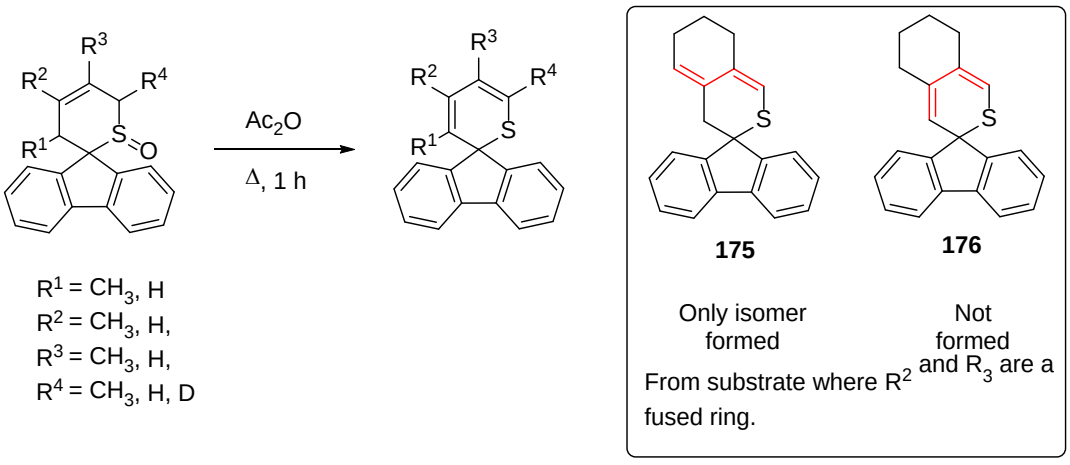
R = 2-Me **172**
R = H **173**
R = 4-Me **174**

Entry	Time	Isolated Products
1 **R = 2-Me**	20 min	**172** (84%)
2 **R = H**	20 min	**173** (81%)
3 **R = 4-Me**	50 min	**174** (75%)

The same reaction conditions were applied to the two sulfoxide substrates **135** and **137**, with the desired sulfides **173** and **174** isolated in yields of 81% and 75% respectively (Table 30), as exceptionally clean crude poducts. Sulfoxide **135** required a reaction time of 20 minutes whereas the methyl substituted sulfoxide **137** required a reaction time of 50 minutes for successful reduction. This longer reaction time was also noted with the sulfonylation reaction of sulfoxide **137**, suggesting a retarding effect on the reactivity of the sulfoxide when the methyl group is present in this position. Interestingly, by reduction of the sulfoxide cycloadducts to the corresponding sulfides, the α-oxo sulfine, which was generated *in situ,* and acted as a dienophile in the Diels-Alder cycloaddition, has been used as a synthetic equivalent for an α-oxo thiones - a class of compounds which are often challenging to access; either generated *in situ*[92] or *via* flash vacuum pyrolysis.[93]

2.5.7.3 Pummerer rearrangement type reactions

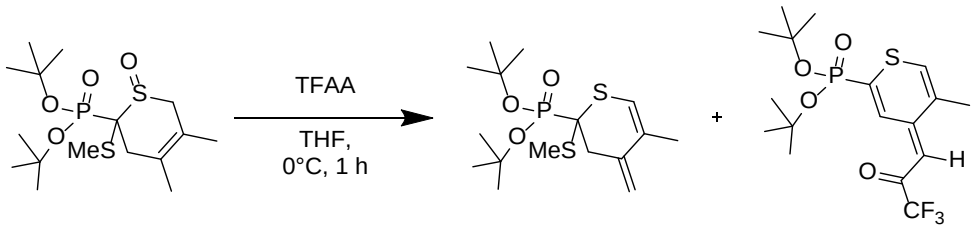
The Pummerer rearrangement and its effectiveness at promoting novel transformations has been reviewed by Procter *et al.* in 2010.[73] This review highlights the applicability of six membered cyclic sulfoxides as substrates for the Pummerer rearrangement, with an aim of generating bioactive molecules such as thioglycosides[94,95] and thionucleosides.[72] In the literature, Weichsel *et al.*[96] describe the synthesis of thiopyrans from dihydrothiopyran-*S*-oxides by vinylogous Pummerer reactions (using acetic anhydride) with the formation of endocyclic alkenes in most case, except for one specific case in which an "exocyclic" alkene **175** was formed with no evidence for the "endocyclic" isomer **176**.



R^1 = CH_3, H
R^2 = CH_3, H,
R^3 = CH_3, H,
R^4 = CH_3, H, D

Scheme 72

Additional to this, thiopyran-*S*-oxide type compounds such as **177** have been subjected to Pummerer rearrangement conditions (using trifluoroacetic anhydride), resulting in the formation of the exocyclic alkene **178** and the trifluoroacetyl derivative **179** (Scheme 73). [71]

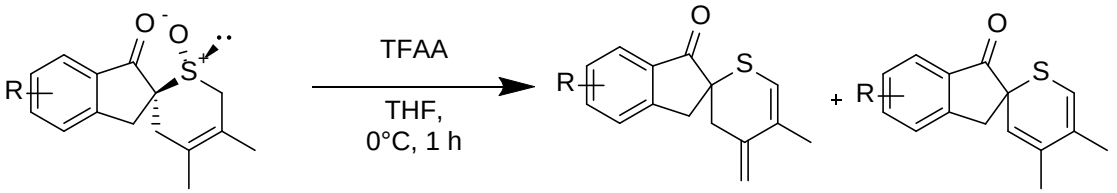


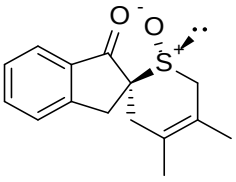
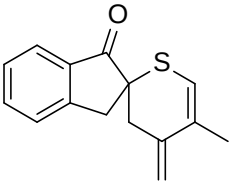
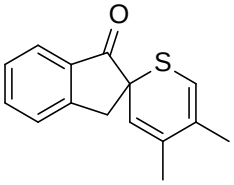
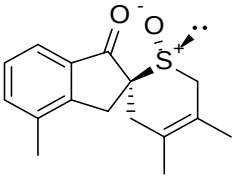
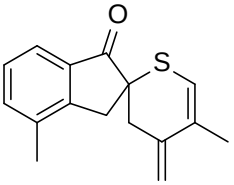
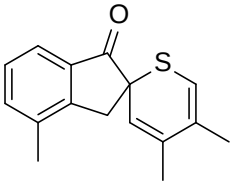
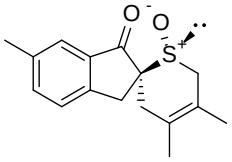
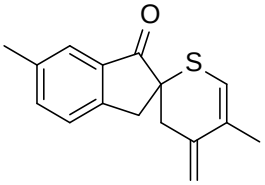
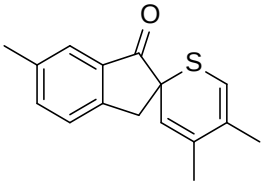
177 **178** **179**

Scheme 73

Gulea[71] describes reaction conditions for this Pummerer rearrangement affording a 1 : 1 mixture of isomeric products upon analysis of the reaction material. These conditions consist of exposure of the sulfoxide substrate to excess trifluoroacetic anhydride in tetrahydrofuran at 0°C. An investigation of use of these reaction conditions with sulfoxide **135** was undertaken leading to two isomeric products **180** and **181** in a 1 : 1 ratio after 1 hour, with 10% starting material **135** still present by ^{1}H NMR analysis. After purification, the two desired isomers were isolated and characterised — both the endocyclic alkene **181** and exocyclic alkene **180**. No evidence was observed for the formation of a trifluoroacetyl derivative, similar to **179** in Scheme 73, as described in the literature.

Table 31: Crude ratios and yields of Pummerer rearrangement reactions.

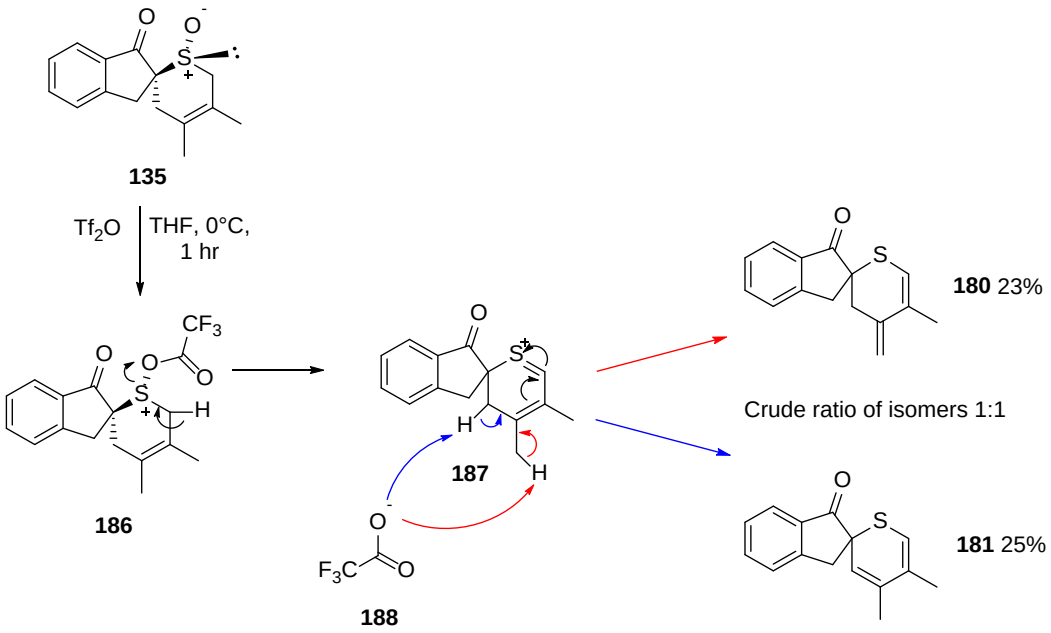


Entry	Starting Material	Exocyclic Isomer	Endocyclic Isomers
1			
	135	**180**	**181**
		Crude ratio 1 : 1[b]	
Yield[a]		23 %	25%
2			
	133	**182**	**183**
		Crude ratio 1 : 1	
Yield[a]		27%	20%
3			
	137	**184**	**185**
		Crude ratio 1 : 1	
Yield[a]		32%	21%

[a] After purification by column chromatography on silica gel.
[b] 10% of the starting material **135** was present in the ^{1}H NMR spectrum of the crude material.

When the Pummerer rearrangement reaction conditions were applied to the sulfoxides **133** and **137** the analogous diene products **182** - **185** were similarly observed, again in an equimolar ratio in each case. Complete separation of the dienes was challenging however **181** and **185** were isolated cleanly. The other dienes, **180**, **182**, **183** and **184** were isolated with <10% of the other isomer present in each case.

A mechanism for the formation of the described products is proposed (Scheme 74)[71]; one possibility is elimination from the intermediate **186** to form a thionium cation **187**, followed by deprotonation by a trifluoroacetate anion **188** to lead to either the endocyclic or exocyclic product (Scheme 74). Interestingly, the rates of formation of the two isomers appear to be the same. No evidence was seen for the interconversion of the isomers although this was not systematically examined.

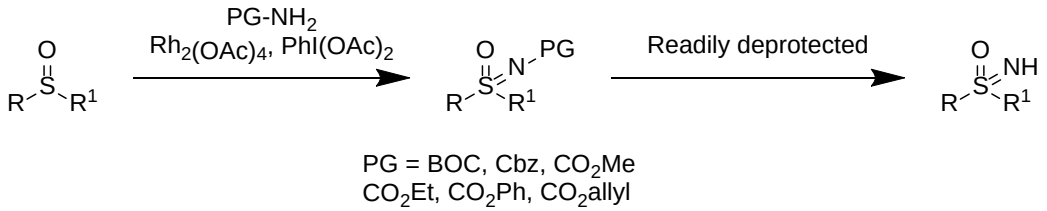


Scheme 74

As the substrates for these reactions are now readily available, this sequence may become of interest as it provides a method for cleanly accessing these novel, highly functionalised thiopyran derivatives.

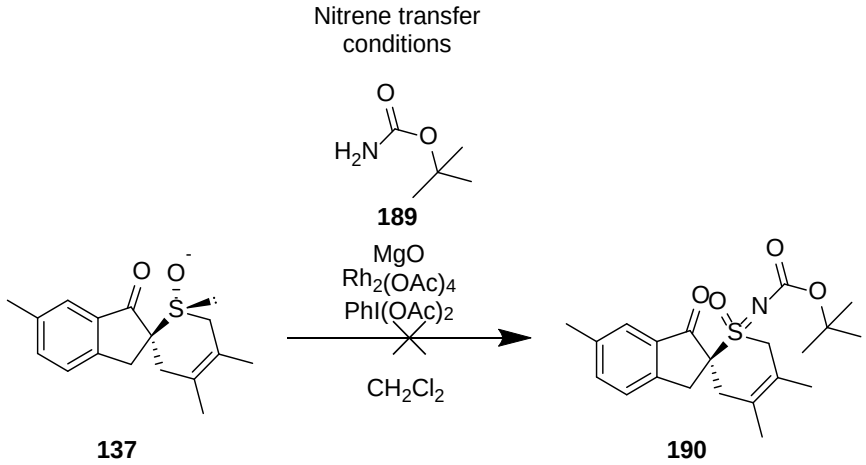
2.5.7.4 Attempted generation of a sulfoximine from the cycloadduct.

Sulfoximines have been shown to be an important motif present in some biologically active molecules[97,98] and as such generation of these compounds in an enantiomerically controlled manner could be extremely beneficial. A literature procedure using transition metal catalysis for nitrene transfer to a range of sulfoxides, including alkyl, aryl, vinyl, allylic, cyclic and acyclic derivatives under mild reaction conditions was attempted during this work for generation of BOC protected sulfoximines (Scheme 75).[99]



Scheme 75

The conditions in this report, described as extremely efficient,[99] were applied to the substrate **137** and led only to isolation of the recovered sulfoxide starting material **137** (Scheme 76) and BOC carbamate **189** after chromatography of the crude reaction material. Possible reasons for the unsuccessful synthesis of the sulfoximine **190** may be due to steric hindrance around the sulfoxide moiety of **137**.



Scheme 76

2.5.7.5 Spectral Characteristics of products formed from these oxidation, reduction, and Pummerer rearrangement transformations

Comparison of the spectroscopic features of the sulfides, sulfoxides and sulfones is very interesting with a clear impact of the level of sulfur oxidation on both the ^{1}H and ^{13}C NMR spectra (Figure 46). In the ^{1}H NMR spectra of the pure compounds, each of the methylene groups appears as a characteristic AB quartet system, due to geminal coupling, of the diastereotopic hydrogens. Interestingly, in general the ABq of C(10)H_2 was very sharp in the ^{1}H NMR spectra, while the ABq of the two allylic CH_2's were broadened somewhat due to unresolved ^{4}J coupling; this was one of the features that helped in establishing the ^{1}H NMR assignments. In the spectra of the sulfide dervatives, the ArCH_2 signal appears as a compact ABq system, however, for the sulfoxide and sulfone derivatves the analogous signal is a distinct ABq with a greater separation between the

doublets (Figure 46). Clearly, the presence of oxygens on the sulfur has a significant impact on the environment of one of the diastereotopic protons of the $ArCH_2$ moiety.

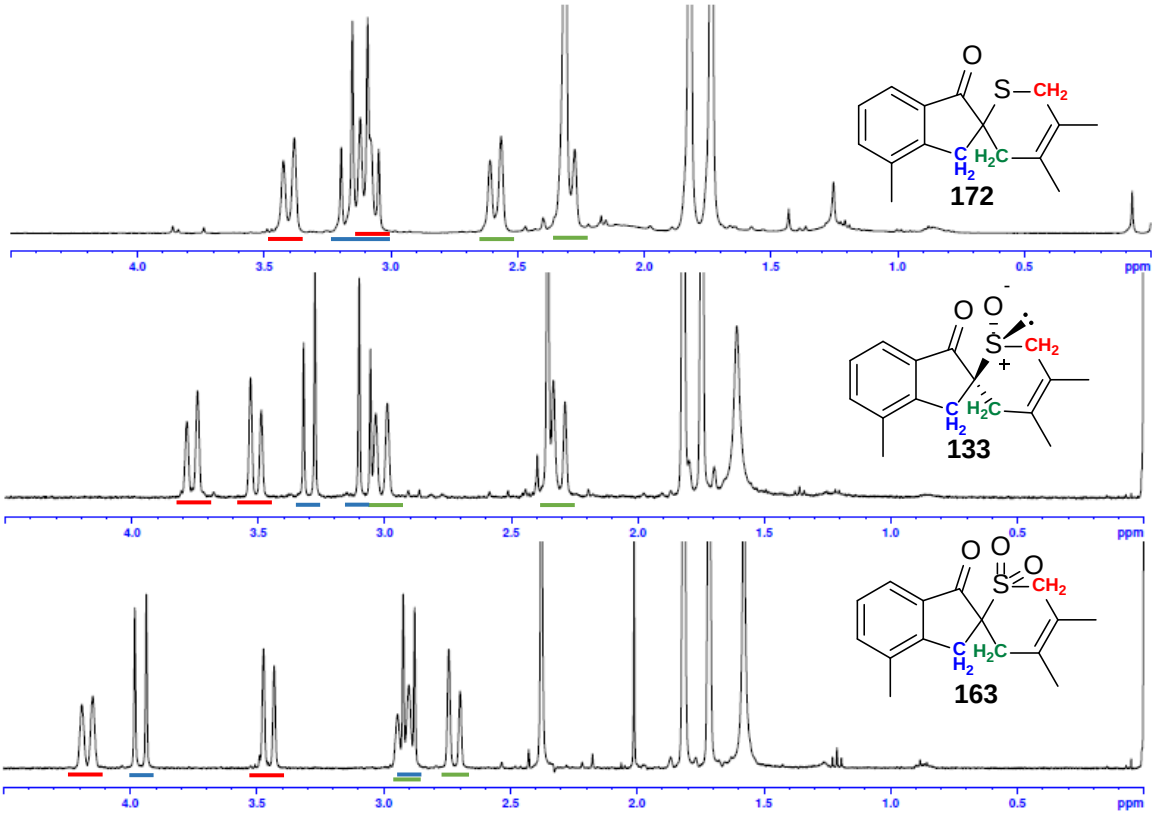


Figure 46: ^1H NMR spectra of the sulfoxide **133***, the sulfone* **163***, and the sulfide* **172***. The $ArCH_2$ signal is underlined blue, the SCH_2 signal is underlined red and the $CqCH_2$ signal is underlined green.*

In the infrared spectra of the three sulfones **163**, **166** and **169**, the carbonyl absorption was consistently observed between 1706 and 1712 cm^{-1}, while the characteristic absorption of the sulfone was consistently between 1117 and 1119 cm^{-1} for each derivative. For the sulfoxides, the characteristic carbonyl absorption appears between 1704 and 1708 cm^{-1} with the S-O bands at 1048 – 1051 cm^{-1}, and for the sulfide derivatives, the characteristic absorptions are between 1705 and 1708 cm^{-1} and 1270 – 1281 cm^{-1}. Overall, each of the sulfones **163**, **166** and **169** and the sulfoxides were high melting point crystalline solids while the sulfides were generally oils. The characteristic signals of the sulfones (Figure 47), sulfoxides (Figure 48) and sulfides (Figure 49) are summarised below

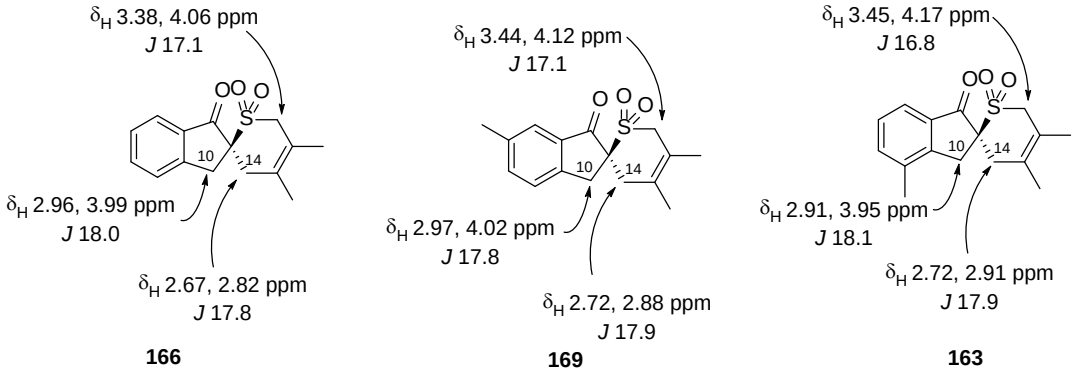


Figure 47: Characteristic ^{1}H NMR signals of the β*-keto sulfones* **166***,* **169** *and* **163***.*

.

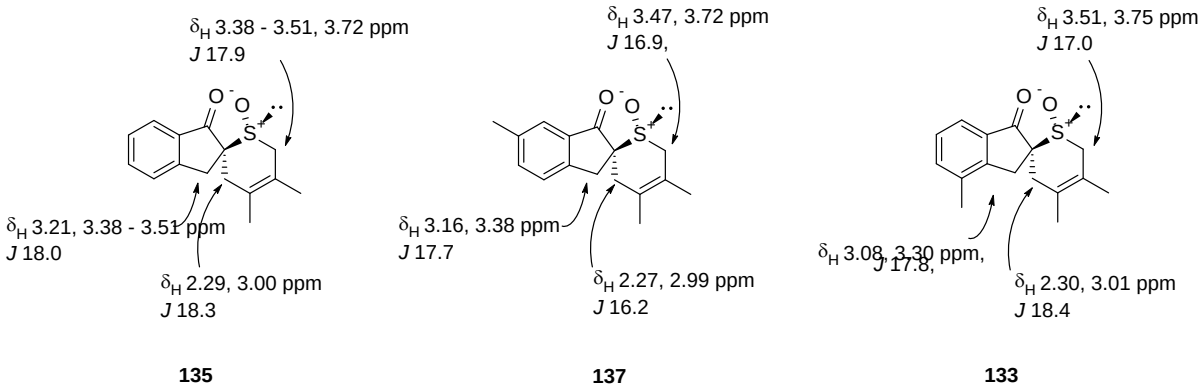


Figure 48: Characteristic ^{1}H NMR signals of the β*-keto sulfoxides* **135***,* **137** *and* **133***.*

,

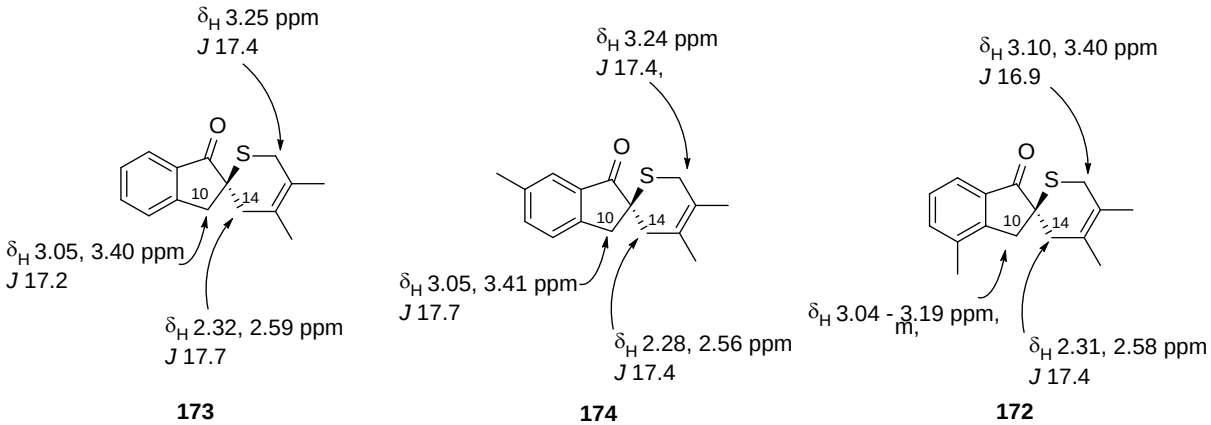


Figure 49: Characteristic ^{1}H NMR signals of the sufides ***173, 174,*** *and* ***172****.*

***Note:** The $ArCH_2$ signals are much sharper than the other CH_2 signals which have long range coupling to the CH_3 groups.

The shift of the spiro centre in the ^{13}C NMR spectra is also consistent across the three sulfones. Shifts of 67.8 ppm for **166**, 67.7 ppm for **163** and 68.2 ppm for **169** show the similarity of electronic environments experienced by each of the spiro centres. This is compared to a range of between 63.5 – 64.0 ppm observed for the corresponding sulfoxides and 49.8 – 50.3 ppm for the sulfide derivatives (Figure 50). Similaraly, the CH_2 next to the sulfur is impacted by the extent of oxidation at sulfur.

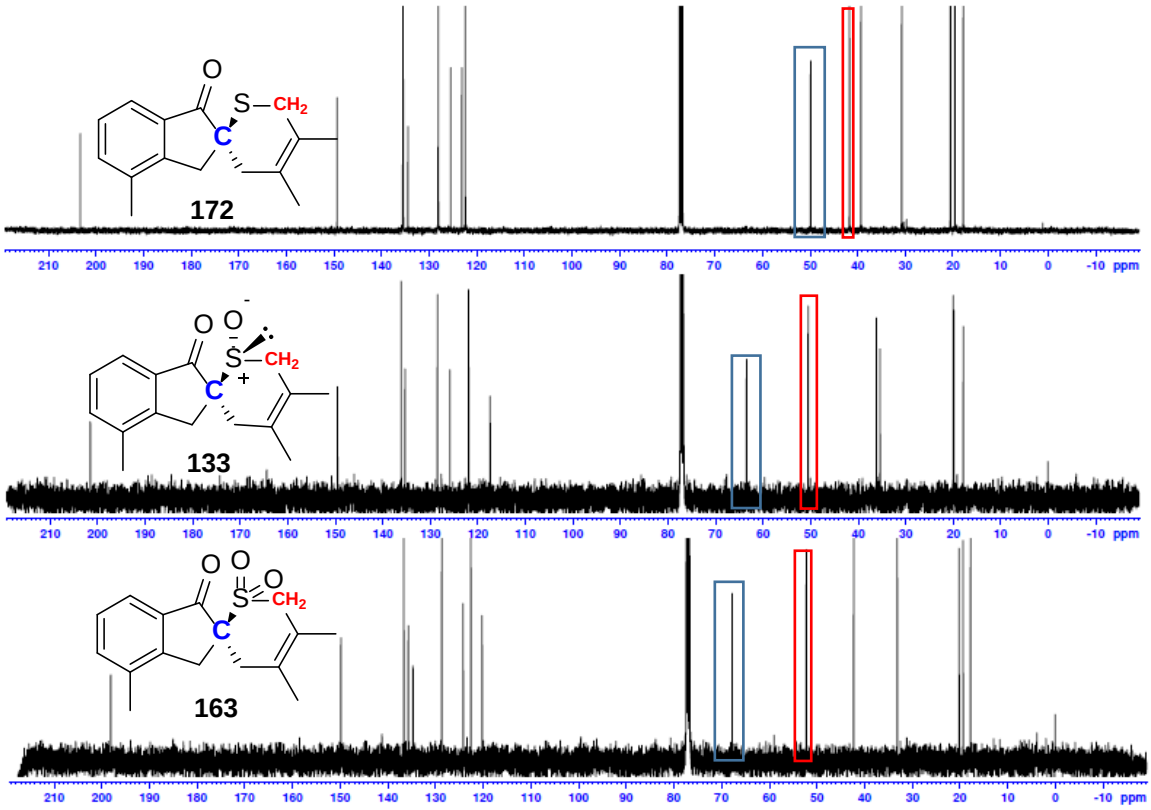


Figure 50: Comparison of the ^{13}C NMR spectra of the sulfide product **172**, *the sulfoxide starting material* **133**, *and the sulfone* **163**, *with the most notable change at the spiro centre highlighted in blue.*

The spectral characteristics of the endocyclic products **181**, **183**, **185** and exocyclic products **180**, **182**, **184** from the Pummerer reaction are also interesting. Characteristic peaks for the endocyclic alkene **181** include two vinylic singlets corresponding to the alkene protons, whereas characteristic peaks of the exocyclic alkene **180** include three singlets for the three vinylic protons (Figure 51). The CH signal alpha to the sulfur, which is observed at 6.0 – 6.1 ppm, is similar for each isomer. Both products are easily identifiable in the ^{1}H NMR spectrum of the crude reaction material (Figure 51).

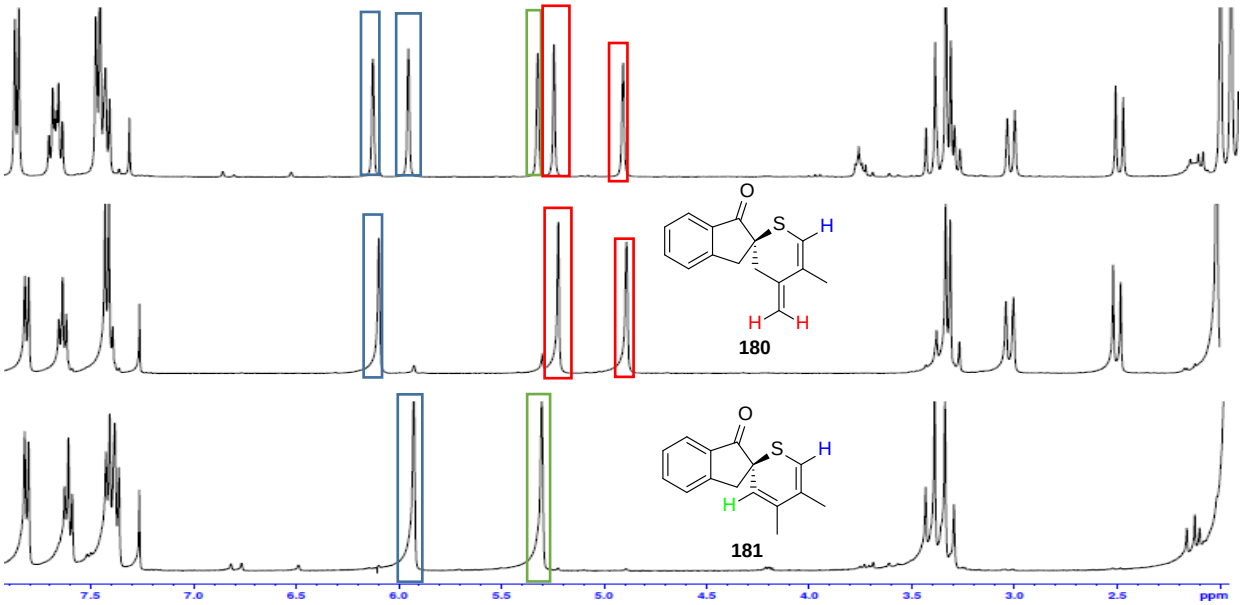


Figure 51: Comparison of crude ^{1}H NMR spectrum (top) with external alkene product (centre) and internal alkene product (bottom).

The isomeric dienes are readily identified by differences in the ^{13}C NMR spectra reflecting the endocyclic and exocyclic nature of the dienes (Figure 52). The pattern of reactivity was consistent across each of the three substrates and similar characteristic NMR signals were observed for the recovered products. HSQC and HMBC spectra were vital in establishing the assignments due to the large number of sp^2 hybridised carbons. A summary of the identifying features and characteristic signals of each isomer is described in Figure 53.

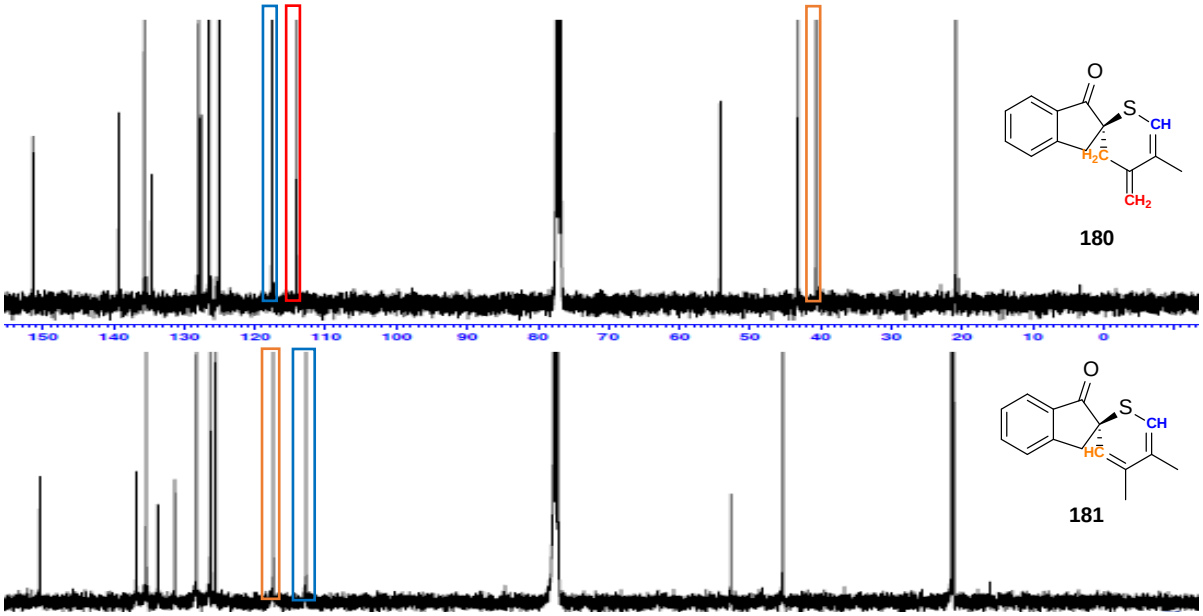


Figure 52: Comparison of the exocyclic **180** *(top) and endocyclic* **181** *(bottom) isomers of the Pummerer rearrangement products.*

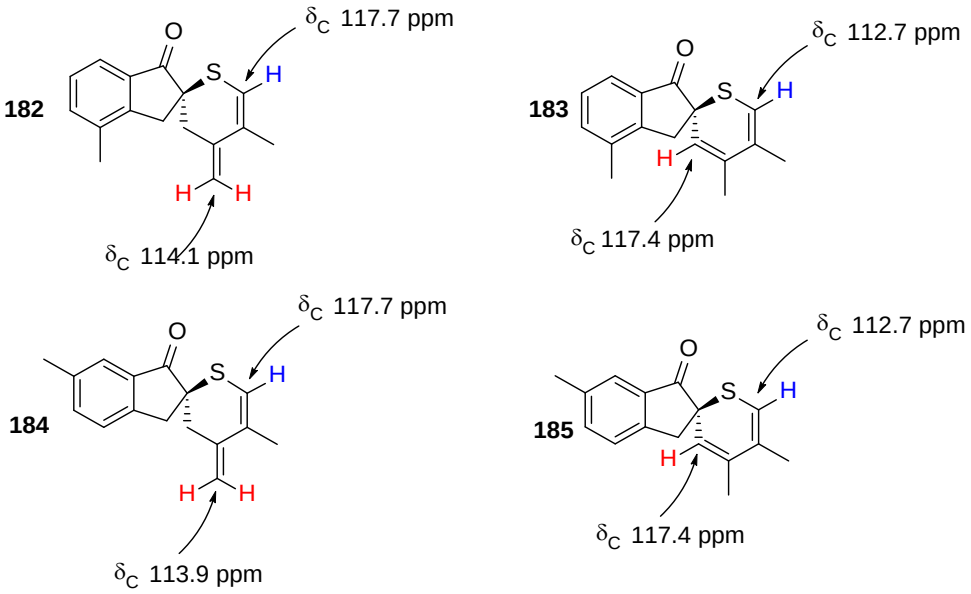
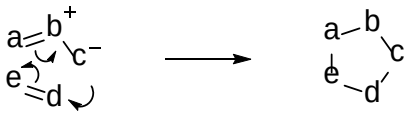


Figure 53: Comparison of ^{13}C NMR shifts for the Pummerer rearrangement products.

2.6 1,3-Dipolar cycloaddition reactions

2.6.1 General background

The most widely accepted mechanism for 1,3-dipolar cycloadditions is currently that of an asynchronous concerted process resulting in the formation of a five membered heterocycle. The α-oxo sulfine is the dipolarophile and the nitrile oxide or nitrone is used as the corresponding dipole. 1,3-Dipoles (a=b$^+$-c$^-$ or a$^+$-b-c$^-$) (Scheme 77) have been defined by Huisgen[100] such that *a* possesses an electron sextet *i.e.* an incomplete valence shell, and that *c* possess an unshared electron pair. Combination of a charged 1,3-dipole with a dipolarophile (such as any double or triple bond) results in the extinction of the formal charges and formation of a neutral species. Based on this mechanistic approach, the 1,3-dipolar cycloaddition reaction can be represented as proceeding through a transition state in which the 4π-electron component of the 1,3-dipole interacts with the 2π-electron component of the dipolarophile in a one-step reaction. The activation energy profile of this reaction would contain one activation peak, and therefore this is similar to Diels-Alder cycloadditions, and Claisen and Cope rearrangements. [101,102] The cycloaddition reaction is reported to proceed *via* a concerted mechanism, and as mentioned earlier, stereochemistry is retained in the product.

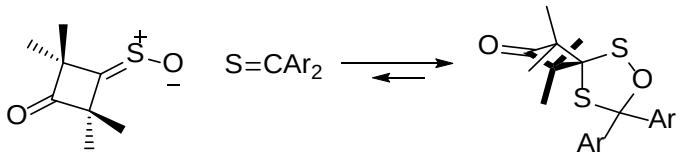


Scheme 77

Of these 6π-electron reactions for sulfines and α-oxo sulfines the Diels-Alder cycloaddition is the most widely reported. [7,63] Work within the group has shown the Diels-Alder cycloaddition reaction of ketone derived α-oxo sulfines to be highly diastereoselective,[14-16] with on-going research into the novelty, range and further functionalisation of these cycloadducts.[64-67]

2.6.1.1 Sulfines as dipoles

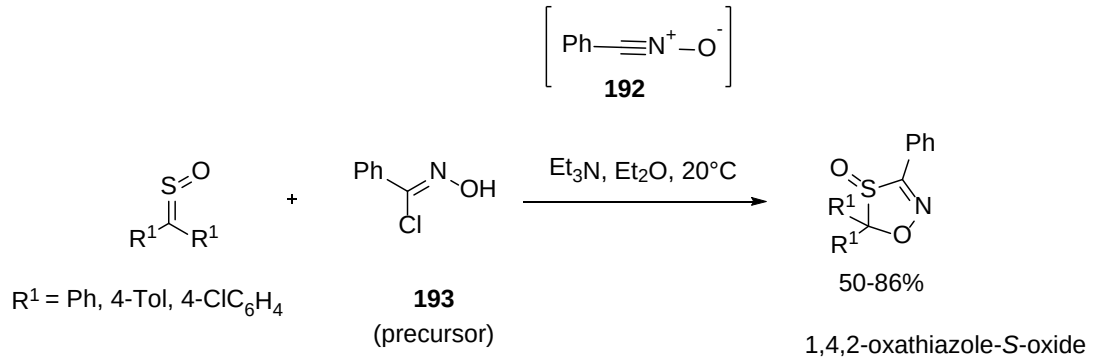
As discussed in Chapter 1 Section 1.4.4., sulfines most commonly act as dipolarophiles but have been used as dipoles when used with a "superdipolarophile" thione.[103] The first report of sulfines acting as dipoles instead of as dipolarophiles in a 1,3 dipolar cycloaddition was in 1996, by Huisgen where an aliphatic sulfine acted as a dipole with three distinct thioketones (Scheme 78).[103] The corresponding cycloadducts were isolated in moderate yields, with the rationale for this being the ease of cycloreversion of the cycloadducts.



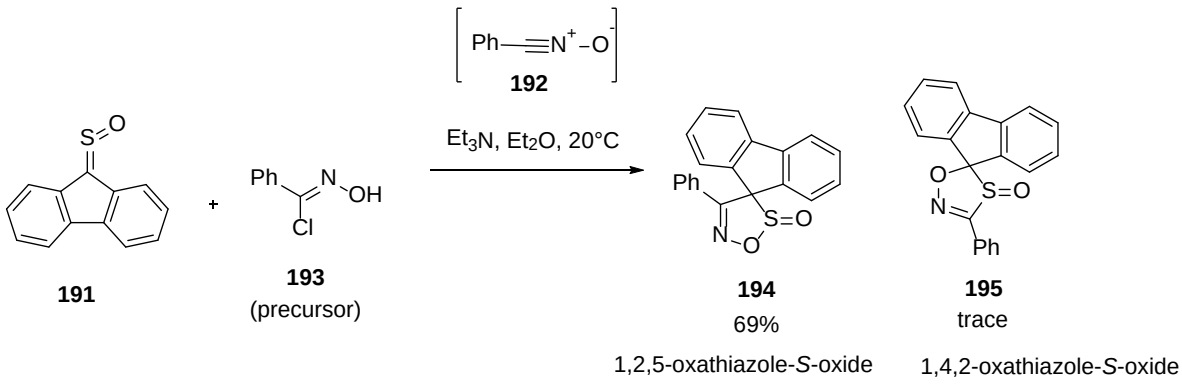
Scheme 78

2.6.1.2 Sulfines as dipolarophiles; 1,3-dipolar cycloadditions of sulfines with nitrile oxides

In the majority of 1,3-dipolar cycloaddition reaction of sulfines and nitrile oxides, the 1,4,2-oxathiazole-*S*-oxide is the major regiosiomer, and the 1,2,5-oxathiazole-*S*-oxide is a minor regioisomer.[104] 1,3-Dipolar cycloadditions of diaryl substituted sulfines progress in a regio and stereospecific manner (Scheme 79)[105] with the exception of 9*H*-fluorene-9-thione-*S*-oxide **191** which reacts with benzonitrile oxide **192**, generated *in situ* from the imidoyl chloride **193**, giving the regioisomeric 1,2,5 oxathiazole-*S*-oxide **194** as opposed to a 1,4,2 oxathiazole-*S*-oxide **195** (Scheme 80).

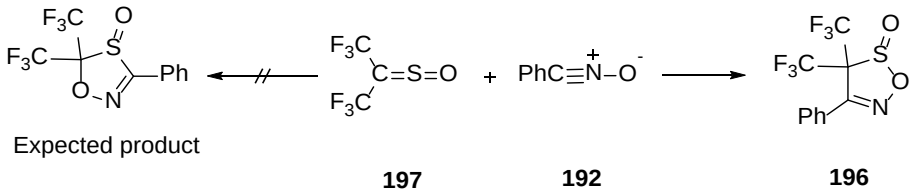


Scheme 79



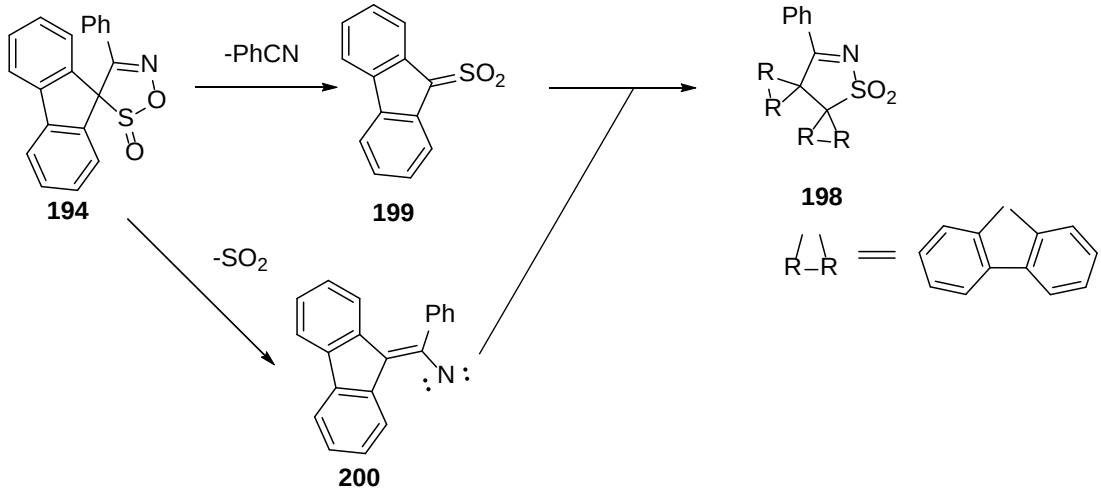
Scheme 80

There are only two example of 1,2,5-oxathiazole-*S*-oxides in the literature, and in both cases they are described as an unexpected product formed from the 1,3-dipolar cycloaddition reaction of α-oxo sulfines.[104,106,107] The two reported 1,2,5-oxathiazole-*S*-oxides in the literature are **194** (Scheme 80), and **196** (Scheme 81) formed from the α-oxo sulfine **197**.



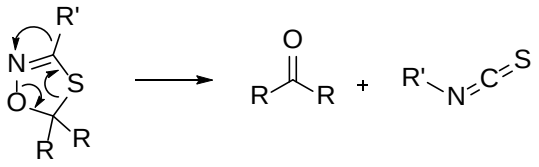
Scheme 81

Zwanenburg has investigated the thermal fragmentation of the 1,2,5-oxathiazole-*S*-oxide **194** which was isolated as an unexpected regioisomer from the cycloaddition of flourenethione-S-oxide **191** and benzonitrile oxide **192** to give the thiazole **198** through reaction of an intermediate sulfene **199** and intermediate nitrene **200** (Scheme 82).[104,106] The structure of the thiazole **198** was confirmed by single crystal analysis.



Scheme 82

Reports of cycloadditions of sulfines exist in the literature, describing successful cycloadditions and immediate rearrangement to more stable species.[104,108-110] In fact, this rearrangement to more stable species is highlighted by the fact that 1,4,2-oxathiazoles have been used as precursors of isothiocyanates with the rearrangement occurring under mild thermal conditions (Scheme 83).[111,112]



Scheme 83

There are no current examples in the literature of methodology to access 1,2,5-oxathiazoles or the corresponding 1,2,5-oxathiazole-*S*-oxides; this, combined with the absence of a reported series of these compounds, highlights their rarity.

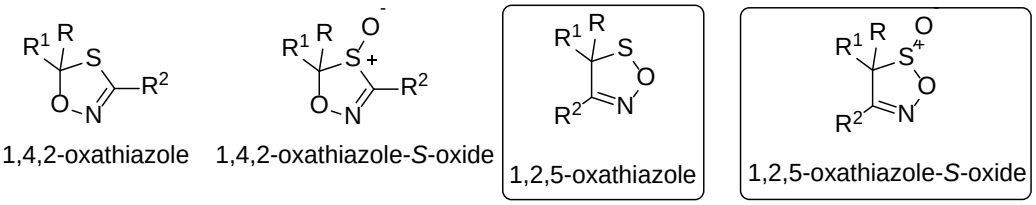
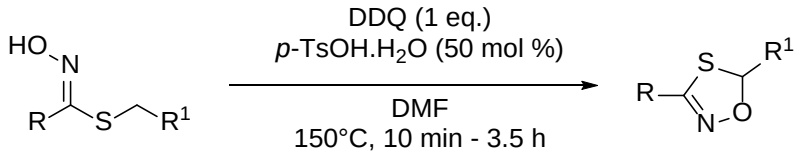
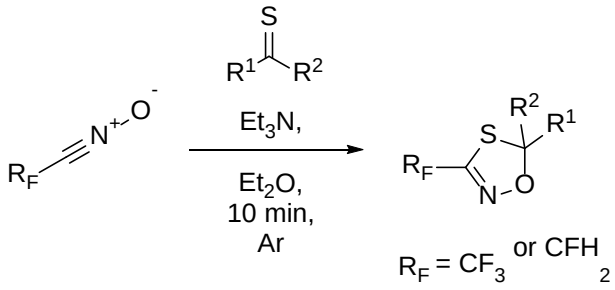


Figure 54: A range of oxathiazole heterocycles.

Showcasing the interest in these types of compounds is a recent effort by Pierce which focused on the synthesis of the related compounds, 1,4,2-oxathiazoles, through oxidative cyclisation of thiohydroximic acids[113] (Scheme 84) as well as an effort by Mloston who generated fluorinated 1,4,2-oxathiazoles (Scheme 85) through regioselective cycloaddition reactions of fluorinated nitrile oxide with thioketones.[114]



Scheme 84



Scheme 85

Routes to these types of cycloadducts are typically from dipolar cycloaddition of thioketones or thioaldehydes which are often unstable or challenging to access. In the reported examples of dipolar cycloadditions, dehydrohalogenation in basic environments or strong oxidising agents are

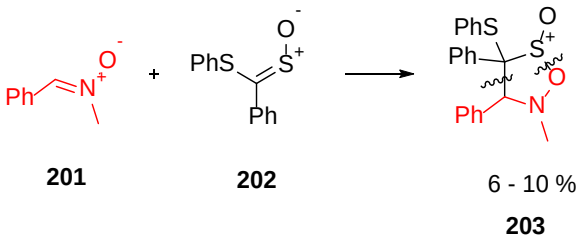
used for generation of the sulfines which subsequently undergo cycloadditions – conditions which would be incompatible with our substrates (see section 2.6.3).

2.6.1.3 Sulfines as dipolarophiles: Background of 1,3-dipolar cycloadditions of sulfines with nitrones

The cycloadducts formed from a successful 1,3-dipolar cycloaddition of sulfines and a nitrone are extremely rare, illustrated by the lack of corresponding products in the literature (Figure 55 - one report of heterocycle type A, [115] none of type B). In the report by Zwanenburg of a successful cycloaddition of *C*-phenyl-*N*-methyl nitrone **201** with a sulfine **202**,[115] the desired 1,2,5-oxathiazolidine-*S*-oxide **203** was isolated in just 6 – 10 % yield along with "other products" which were unidentified (Scheme 86).



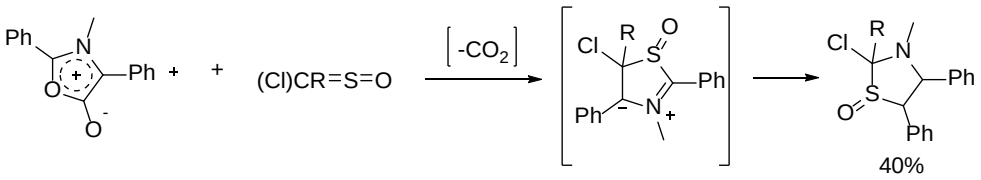
Figure 55



Scheme 86

2.6.1.4 Lability of the cycloadduct products

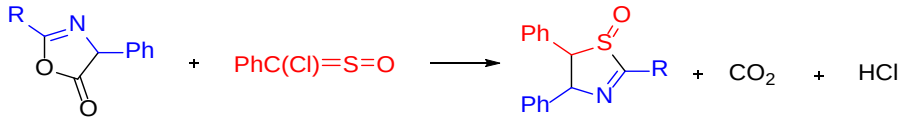
In the literature reports of cycloadditions of sulfines in 1,3-dipolar cycloaddition reactions, formation of unstable cycloadducts which undergo losses of volatile gases in subsequent rearrangements is often described. One such example in the literature describes the reaction of an oxazolium-*S*-olate **204** with the sulfine **205**, the cycloadduct initially formed expels carbon dioxide generating a new dipolar species **206**, which rearranges to the product **207** isolated in 40% yield (Scheme 87). [115]



204 **205** **206** **207**

Scheme 87

Similar to this is the 1,3-dipolar cycloaddition of an azlactone **208** with chlorophenylsulfine **209** forming an intermediate cycloadduct which loses carbon dioxide and hydrogen chloride to form the isolated product **210** (Scheme 88).[116]



208 **209** **210**

Scheme 88

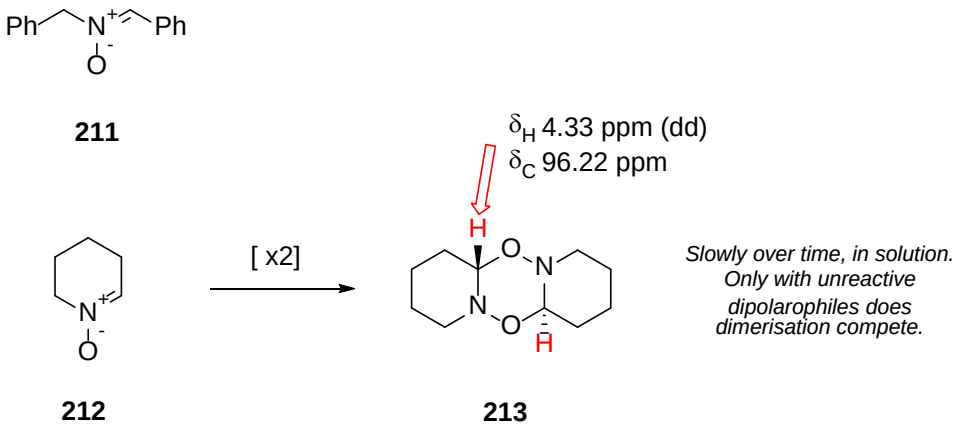
With the broad synthetic versatility of sulfines and α-oxo sulfines, the potential for the formation of regioisomers and diastereomers from dipolar cycloaddition reactions leading to product mixtures is an issue. However, building on the success of the study of [4+2] Diels-Alder cycloadditions in this work and previously undertaken within our research group,[16] and with limited research on 1,3-dipolar cycloadditions of sulfines in the literature, exploration of these dipolar cycloadditions was a significant objective of this research. The regioselectivity, diastereoselectivity, and nature of the isolated products were of significant interest. In this section of the work we aimed to explore the reactivity of α-oxo sulfines derived from both ketones and lactones with both nitrones and nitrile oxides.

The initial challenge was to find the conditions which would enable generation of both the α-oxo sulfines and 1,3-dipole, both of which are highly reactive species. From our earlier work we know that the α-oxo sulfine can be accessed thermally, photochemically or using rhodium catalysis. Establishing which approach was most compatible with the nitrile oxide and nitrones was the first step.

While the nitrone **211**[117] is a stable, isolable species, nitrone **212** must be freshly prepared for use to avoid dimerization to form the tricyclic dioxadiazinane **213** (Scheme 89).[118] In contrast nitrile oxides are generally generated *in situ* by base mediated elimination from imidoyl chlorides. Clearly, this would not be compatible with labile α-diazosulfoxides and/or α-oxo sulfines.

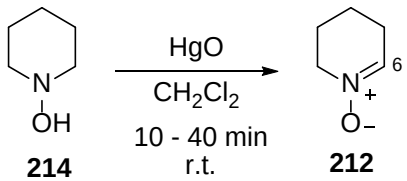
2.6.2 Synthesis of nitrones

To explore the novel reactivity patterns of α-oxo sulfines generated *in situ* from α-diazosulfoxides, with nitrone dipoles in 1,3-dipolar cycloaddition reactions, the symmetrical nitrones **212**[119,120] and **211**[117] were synthesised in this work as they avoid the potential for the formation of regioisomers. To the best of our knowledge, no reports exist on the cycloaddition of **211** or **212** with sulfines.



Scheme 89

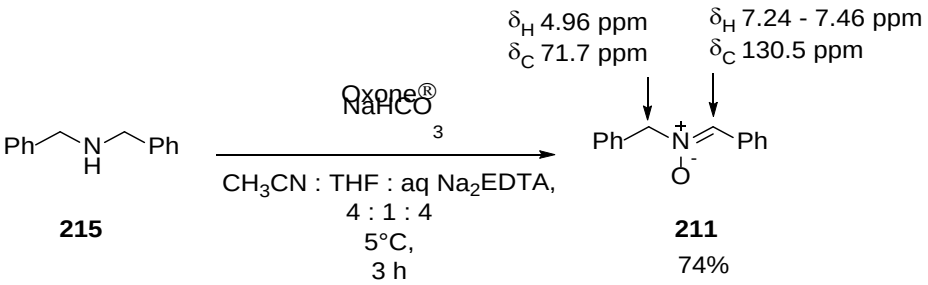
Generation of the nitrone **212** is carried out by oxidation of 1-hydroxypiperidine **214** with yellow mercuric oxide (Scheme 90).[119] The hydroxylamine reacts with the mercuric oxide forming a nitroxyl radical. This undergoes a disproportionation reaction with an excess of the oxidant giving the desired nitrone **212** as the final product. The reaction changes from the bright yellow of the mercuric oxide to a dark green/black as the reaction proceeds. This nitrone **212** was freshly prepared each time it was used, and generation of the nitrone was carefully monitored by TLC analysis to ensure complete consumption of **214**, as reaction times varied from 10 to 40 minutes, depending on scale. ^{1}H NMR spectroscopy confirmed the formation of the nitrone **212** with the characteristic [C(6)H] signal at 7.19 ppm. Dimerisation is indicated by δ_H for C*H*NO at 4.33 ppm as a 2H doublet of doublets. [121]



Scheme 90

The acyclic dibenzyl nitrone **211**, was generated through the oxidation of dibenzylamine **215** using Oxone® as the sole oxidant in a biphasic basic medium. [117] This procedure from Font *et al.* is an

efficient and metal-free route to nitrones from secondary amines.[117] The reaction mixture was kept at or below 5°C at all times as the author describes this temperature control is necessary to avoid decomposition of the Oxone®. The oxidation reaction was monitored by TLC and was complete within three hours. The work up provided the nitrone **211** in a yield of 74% and sufficient purity to be carried through to the cycloaddition with the α-oxo sulfine. The stable nitrone **211** can be stored in the freezer for months at a time, without loss of quality or dimerisation.



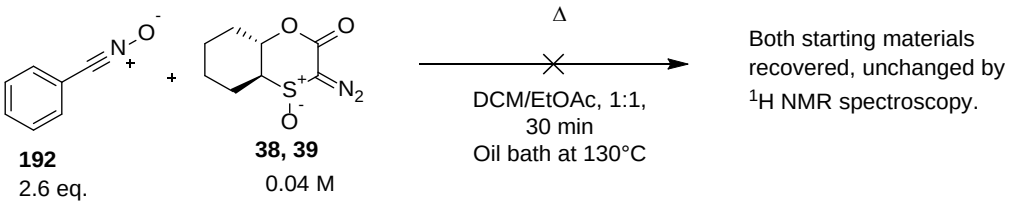
Scheme 91

2.6.3 Synthesis of nitrile oxides – experimental design

In the relevant literature, nitrile oxide dipoles are most often generated *in situ* from the parent imidoyl chloride using a non nucleophilc base such as triethylamine. In this work, it was important to avoid *in situ* base mediated dehydrohalogenation to generate the nitrile oxide due to the lability of the α-oxo sulfines and/or their α-diazosulfoxide precursors. Previously within our group, in another research project, we have described the pre-generation of nitrile oxide dipoles, with the aim of preventing nucleophilic attack of the oxyanion *in situ*.[122] In this instance, we chose to once again pre-form the nitrile oxide dipole to prevent exposure of the α-diazosulfoxide and α-oxo sulfine to conditions for generation of the nitrile oxide.[24] In this method described initially by Chopra and subsequently by Kissane,[123] the dipole is generated separately, and then added to the dipolarophile. In this work the dipole is added to the α-diazosulfoxide starting material which is then converted without delay to the α-oxo sulfine dipolarophile *in situ,* either by thermolysis, rhodium acetate dimer as a transition metal catalyst or microwave irradiation.

This protocol was designed to enable trapping of the kinetic *Z* α-oxo sulfine based on our earlier investigations as the preliminary investigation into the feasibility of heterocycle generation through this route. In this work, pre-generation of the thermodynamic *E* α-oxo sulfine with subsequent cycloaddition has not been investigated to date and is warranted in further studies. Evidently it was not clear at the outset whether the presence of the nitrile oxide would impact on the interconversion of the α-diazosulfoxide to the α-oxo sulfine, for example, through poisoning

of the rhodium catalyst, or direct reaction of the α-diazosulfoxide with the dipole through an alternative pathway. In later work, which involved heating a reaction mixture of the α-diazosulfoxides **38,39** with the nitrile oxide **192** [in dichloromethane : ethyl acetate, (1 : 1)], to a temperature (130°C) that was insufficient to induce the hetero-Wolff rearrangement, the two starting materials were evident on analysis of the crude material without substantial degradation (Scheme 92). This established that a competing reaction does not occur between the α-diazosulfoxide starting material and nitrile oxide dipole without generation of the reactive α-oxo sulfine species.



Scheme 92

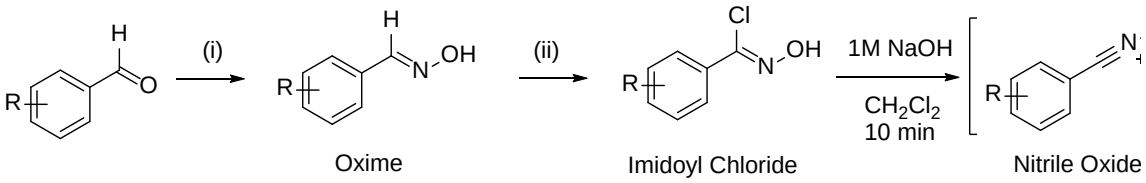
The selected nitrile oxides were generated from the corresponding imidoyl chlorides which were synthesised through chlorination of the corresponding oximes **216–221** following established literature procedures (Table 32).[124,125] A range of oximes were synthesised from the corresponding aldehydes.[126,127] Benzaldoxime **216** was commercially available, however, to access the other substituted oximes **217–221**, condensation reactions were carried out with hydroxylamine hydrochloride and the respective aldehydes, **222–227**, in the presence of excess sodium hydroxide. The nitrile oxides were selected to enable investigation of the impact of electronic effects on the aryl substituents, on the outcome of the cycloaddition reactions.

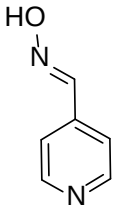
Using this procedure, the oximes **216–221** were isolated in good to excellent yields across a range of derivatives bearing electron withdrawing and electron donating substituents, and the isonicotinaldehyde derivative **221**. The exception to this is the 2,5-difluoro derivative **219**; this substrate required a reaction time of 16 h, which is in comparison to the 1 – 2 h for the other substrates and was isolated in a much lower yield of 47%. In most cases, the oximes are isolated as the pure compounds without purification. However, the isonicotinaldehyde oxime **221** was 90% pure, and was subsequently carried through to the chlorination reaction without purification. Additionally, while the *p*-nitro oxime **217** required purification by recrystallisation to remove minor impurities, it was isolated as a pure compound in 84% yield.

A range of aromatic substituted imidoyl chlorides, **193,228–232** was prepared from the corresponding oximes **216–221** (Table 32). For the electron deficient oximes **217**, **218**, **219** and

221, if the chlorination was slow to start, the reaction was heated to 40°C. With monitoring by TLC, if the reaction was deemed to not have initiated, or no visible colour change is observed, HCl vapour drawn from the headspace of a concentrated HCl bottle, with a glass syringe, was bubbled through the reaction mixture.[125] These reaction conditions led to the isolation and characterisation of a range of substituted aromatic imidoyl chlorides **193,228–232** which needed no further purification except for the 2,5-difluoro derivative **230** which was recrystallized from dichloromethane and hexane. The isonicotinaldehyde imidoyl chloride **232** and *p*-fluoro derivative **229** were lower yielding in comparison to the other substrates. This range of imidoyl chlorides can be readily converted to the corresponding nitrile oxide dipole.

Table 32: Conditions and yields for the sequence of reactions to generate the range of nitrile oxide dipoles.



R	Oxime (%)[a]	Imidoyl Chloride (%)
H	- **216**[b]	54% **193**[ref. 119,128]
4-NO_2	84% **217**[c]	79% **228**[ref. 124]
4-F	98% **218**	36% **229**[ref. 129]
2,5-difluoro	47% **219**	93% **230**[ref. 127]
4-*t*-Butyl	89% **220**	73% **231**[ref. 127]
	70% **221**	40% **232**[ref. 130]

(i) $NH_2OH.HCl$, NaOH, H_2O/Ethanol 1:1, 1 - 2 h in most cases, except for the 2,5-difluoro derivative for which 16 h were needed.

(ii) NCS, DMF, rt, 1 - 5 hr. If the chlorination reactions were slow to start for the electron deficient oximes (as evidenced by the absence of a colour change) the reaction was heated to 40°C. If the reaction still did not start HCl vapour from the headspace of a bottle of conc. HCl was bubbled through the reaction mixture from a glass syringe.

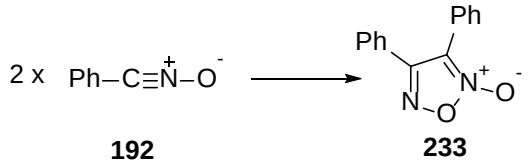
[a] Oximes were used without purification except for **217** which was recrystallized from ethanol : water, 3: 1.[124] Yields are reported for crude products.

[b] Benzaldoxime was commercially available from Sigma-Aldrich.

[c] **217** was synthesised using sodium acetate (2.5 eq) as base, and heated to reflux in ethanol for 24 h.

While a few isolated examples of the generation of nitrile oxide dipoles in the absence of base have been recently described,[131] in this work our previous strategy for pre-generation of the dipole

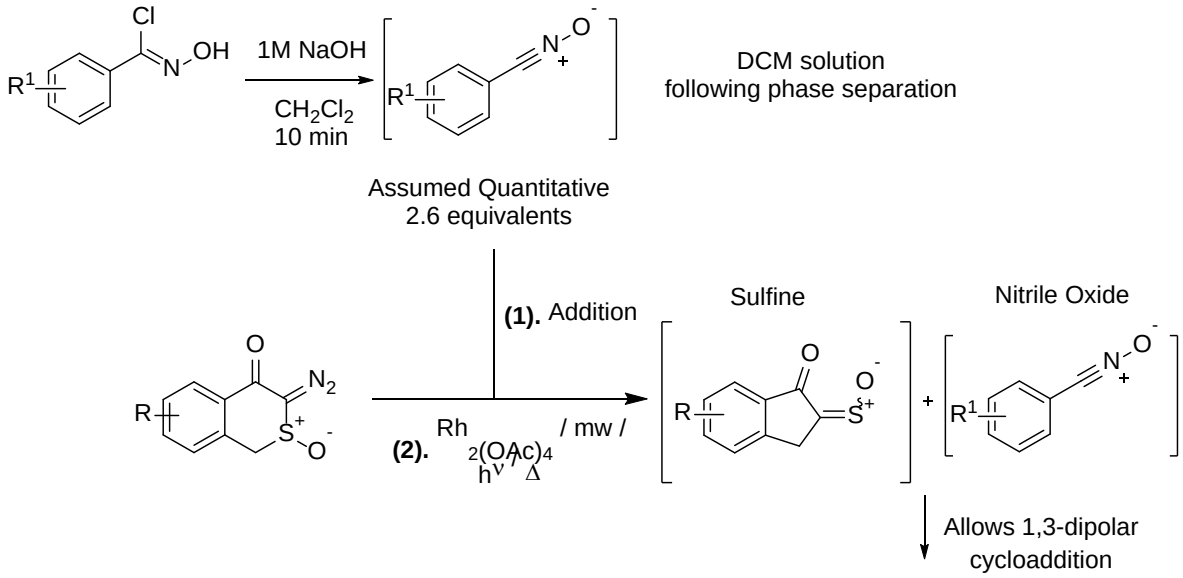
proved successful. The imidoyl chloride is added to a biphasic mixture of dichloromethane and NaOH [1 : 1, (1M NaOH)] at room temperature. Successful dehydrohalogenation is achieved in approx. 10 minutes at which point, following phase separation, the nitrile oxide in dichloromethane can be added to the α-diazosulfoxide without isolation. The transformation to the α-oxo sulfine by thermolysis, photolysis, microwave irradiation or rhodium catalysis is undertaken immediately following dipole addition. Dimerization of the nitrile oxide dipoles, such as **192**[128] to the corresponding furoxans, such as **233**, [132128] (Scheme 93) did not prove to be a problem in practice, although in a number of experiments, the furoxan derivatives were observed by ^{1}H NMR of the crude products. No attempts were made to characterise the nitrile oxides or monitor their stability – addition to the reaction mixture was carried out directly after generation.



192 **233**

Scheme 93

While nitrile oxide dipoles are commonly generated *in situ* by base mediated dehydrohalogenation, these conditions would not be compatible with base sensitive α-diazosulfoxides and their transformation to α-oxo sulfines. Our experimental design of generation of the nitrile oxide followed by immediate addition, and subsequent generation of the α-oxo sulfine (either through rhodium catalysis, phtolysis, thermolysis or microwave irradiation) enables the ability to access to two reactive species at the same time, resulting in a 1,3-dipolar cycloaddition (Scheme 94).



Scheme 94

2.7 1,3-Dipolar Cycloaddition reaction of ketone derived α-oxo sulfines with nitrile oxides

2.7.1 Initial investigation

On 1,3-dipolar cycloaddition of the ketone derived α-oxo sulfine and nitrile oxide, two possible regioisomers can be envisaged, a 1,2,5-oxathiazole-*S*-oxide or a 1,4,2-oxathiazole-*S*-oxide. Both of these regioisomers have the potential to form two diastereomers. Literature precedent would suggest that formation of the 1,4,2-oxathiazole-*S*-oxide is more likely. In this work, evidence for the formation of all four isomers by ^{1}H NMR spectroscopy was observed. It was also found that under transition metal catalysed reaction conditions, another product formed in some cases, a 1,4,2-oxathiazole (Figure 56).

The main product in all cases is the 1,2,5-oxathiazole-*S*-oxide, and the two diastereomers formed will be referred to as the kinetic diastereomer and the thermodynamic diastereomer.[viii] For the

[viii] Note: The use of the terms kinetic and thermodynamic in this instance is distinct from earlier use of kinetic and thermodynamic referring to the α-oxo sulfine. In all experiments in this work the α-oxo sulfine was generated and trapped *in situ* so it is reasonable to assume that the *Z* sulfine is the reacting species in this section.
The use of kinetic and thermodynamic for the 1,2,5-oxathiazole-*S*-oxides is due to the observation that one diastereomer (kinetic) is formed initially in the cycloaddition and over time this interconverts to the other, more stable diastereomer (thermodynamic).
Regioisomers A and B of the 1,4,2-oxathiazoles are so called as they are formed by the opposite regiochemistry of cycloaddition to that which forms the 1,2,5-oxathiazoles.
In the literature, 1,2,5-oxathiazole-*S*-oxides have been historically labelled as 1,5,2-oxathiazole-*S*-oxides. See reference 104.

minor regioisomeric products, the 1,4,2-oxathiazole-*S*-oxides, these two diastereomers will be referred to as Regioisomer A and Regiosiomer B. The reduction product of these regioisomers, is referred to as product C, and is a 1,4,2-oxathiazole (See section 2.7.4 for spectroscopic characteristics).

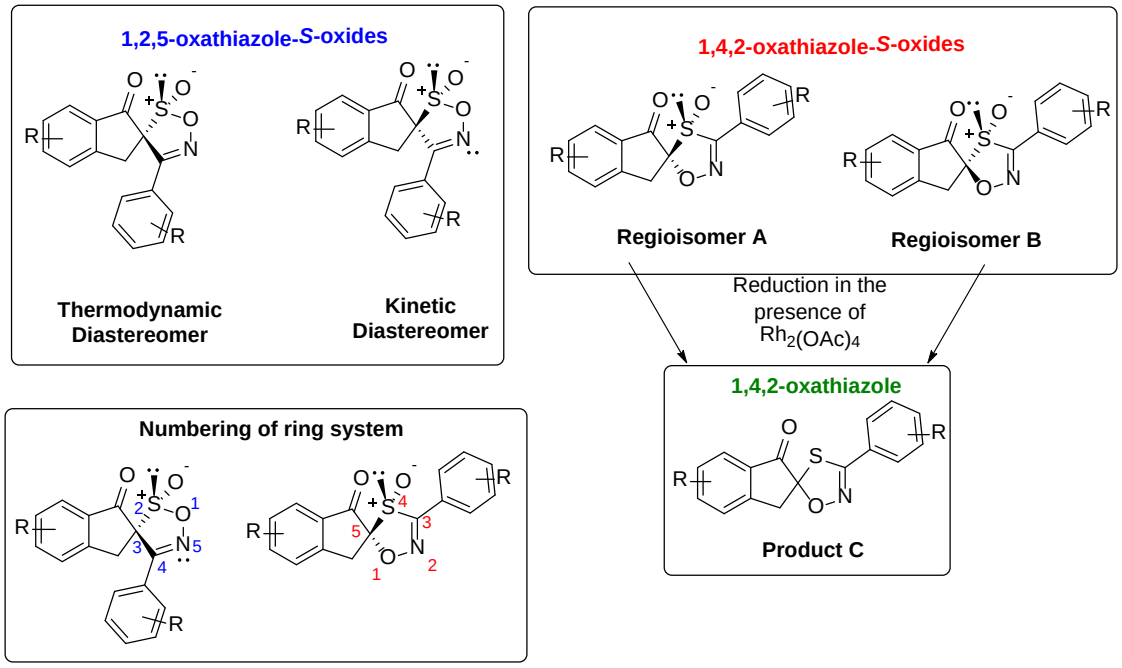
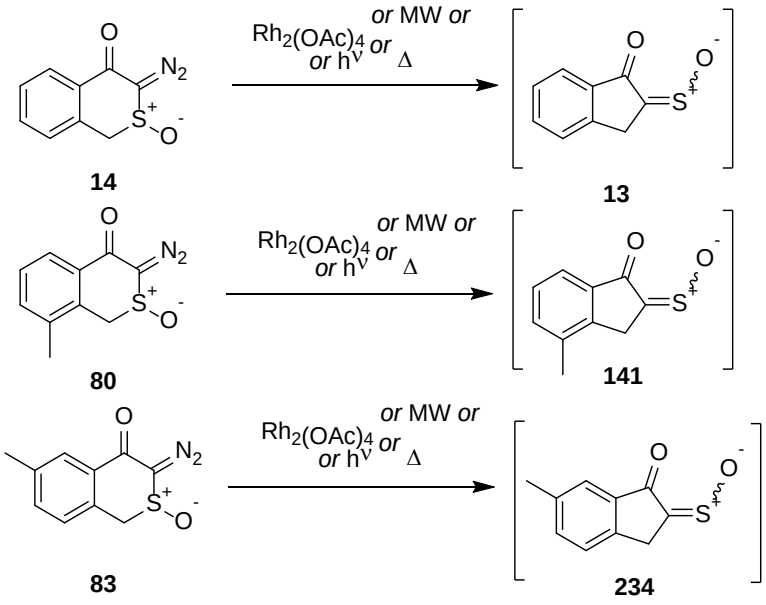


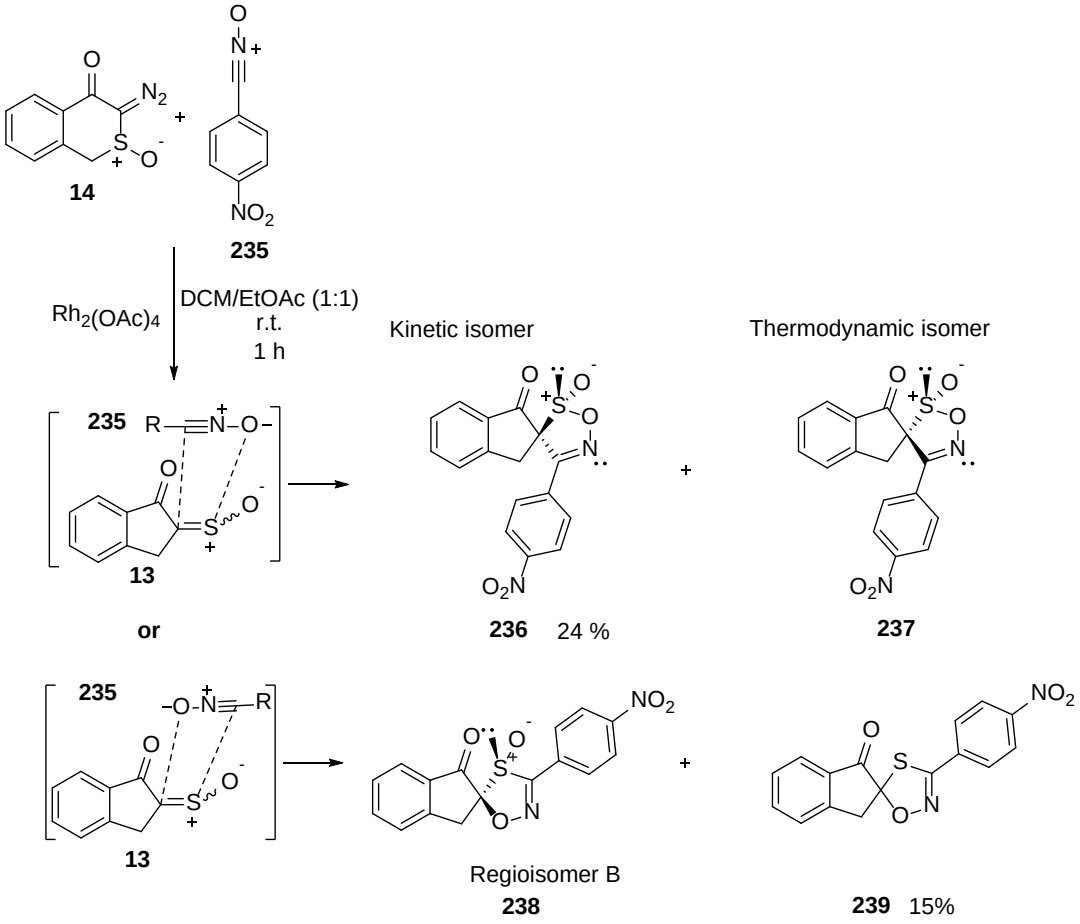
Figure 56: Range of possible products from the 1,3-dipolar cycloaddition of α-oxo sulfines with nitrile oxides.

The first challenge in this work was to induce the hetero-Wolff rearrangement of the α-diazosulfoxide **14** to form the α-oxo sulfine **13** *in situ* and investigate whether this reactive species would undergo cycloaddition with a nitrile oxide. The α-diazosulfoxides **14, 80**, and **83** were synthesised according to the work described earlier (section 2.3) and after undergoing the hetero-Wolff rearrangement, result in the corresponding α-oxo sulfines **13**, **141**, and **234** (Scheme 95)[24,13,25].



Scheme 95

The reaction of the α-oxo sulfine **13** with *p*-nitrobenzonitrile oxide **235** as an *in situ* trap was first explored, in batch reaction conditions, with induction of the hetero-Wolff rearrangement achieved through the use of rhodium acetate dimer (Scheme 96). On analysis of an aliquot withdrawn from the reaction mixture by ^{1}H NMR spectroscopy, after 1 hour, complete consumption of both the α-diazosulfoxide **14** and intermediate α-oxo sulfine **13** had occurred. The crude reaction mixture, on concentration, consisted a mixture of diastereomers and regioisomers. These components were later identified as the kinetic 1,2,5-oxathiazole-*S*-oxide **236**, the thermodynamic 1,2,5-oxathiazole-*S*-oxide **237**, a 1,4,2-oxathiazole-*S*-oxide Regioisomer B **238** and a 1,4,2-oxathiazole **239** in the ratio of 40 : 29 : 22 : 9. No evidence was observed for the Regioisomer A **240**.



Scheme 96

Purification of the crude reaction mixture led to the isolation of two pure cycloadducts; the kinetic diastereomer **236** and the 1,4,2-oxathiazole **239**, both of which had been observed in the ^{1}H NMR spectrum of the crude material. The thermodynamic isomer **237** was not isolated as a pure compound. With successful isolation of the major cycloadduct **236**, unambiguous definition of the stereochemistry and regiochemistry was required. The structure of **239** was assigned by comparison to spectroscopic data of 1,4,2-oxathiazoles reported in the literature, and was confirmed by a crystal structure of an analogous compound in the series, **241**, obtained during this work (Figure 57), which will be discussed further in section 2.7.4. [113,114]

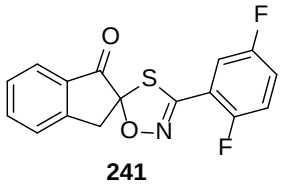
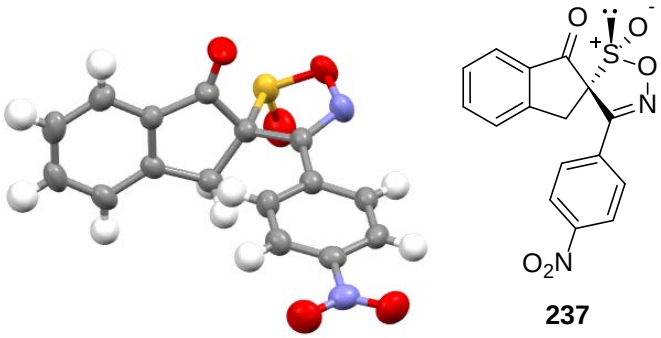


*Figure 57: 1,4,2-oxathiazole **241***

An isolated fraction which was clearly one diastereomerically pure component by ^{1}H NMR spectroscopy was recrystallised from dichloromethane/toluene and the regiochemistry and relative stereochemistry of a single crystal from this sample was unambiguously defined as the 1,2,5-oxathiazole-*S*-oxide **237**, illustrated in Figure 58. The regiochemistry of this 1,2,5-oxathiazole-*S*-oxide was unexpected, as it is the less reported regioisomer compared to the 1,4,2-oxathiazole-*S*-oxides. Furthermore in the lactone derived α-oxo sulfine studies (which will be discussed later) the 1,4,2-oxathiazole-*S*-oxide was isolated, characterised and confirmed by single crystal analysis from the cycloaddition reaction of the lactone derived α-oxo sulfine with benzonitrile oxide **192** (see section 2.8).

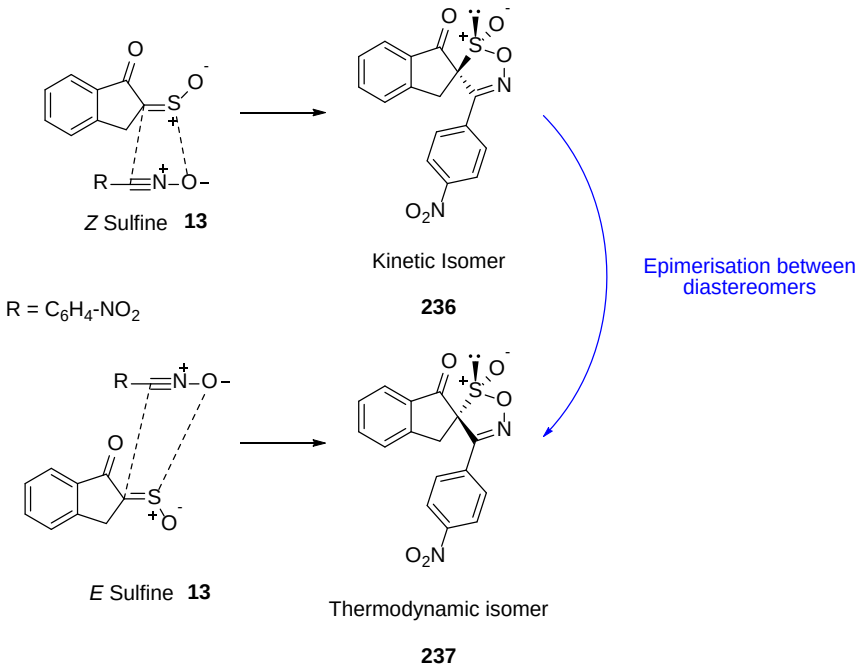


237

Figure 58: Unambiguous confirmation of the relative stereochemistry of the 1,2,5-oxathiazole-S-oxide **237**.

Following crystal structure determination the single crystal used was recovered from the crystallographic pin and analysed by ^{1}H NMR spectroscopy (600 MHz) to unambiguously confirm the relative stereochemistry. Surprisingly, it was clear that the compound present was no longer the compound originally isolated, **236**, but had rearranged completely to compound **237** during the crystallisation process. Following this unanticipated observation, the conversion of the initially isolated kinetic diastereomer to the more stable thermodynamic diastereomer was seen across this series of compounds. Having confirmed the stereochemistry of **237**, the stereochemistry of **236** can be assigned as there are just two possible diastereomers. Formation of the major kinetic diastereomer **236** can be envisaged from cycloaddition of the nitrile oxide to the *Z* sulfine as illustrated in Scheme 97. Notably, the formation of the cycloadduct **237** can be envisaged by two pathways; either cycloaddition to the *E* α-oxo sulfine or by interconversion from the kinetic isomer **236**, as evidenced by crystallographic and spectroscopic studies. As the thermodynamic isomer **237** is seen as a product in the ^{1}H NMR spectrum of the crude material it is not possible at this stage to rule out some cycloaddition as a pathway to **237**, however it is very clear that **236** does interconvert to **237**. From our earlier studies with diene traps, trapping of the *Z* α-oxo sulfine was anticipated, although we can not be definitive that the nitrile oxide trapping is as fast as the diene trapping and therefore some *Z* α-oxo sulfine to *E* α-oxo sulfine conversion may be happening.

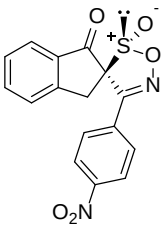
Notably, as sulfine trapping with a nitrile oxide was slower than with a diene in this work, some *Z* to *E* sulfine interconversion can be envisaged prior to trapping. Additionally, while cycloreversion to the sulfine **13** is a possible mechanistic pathway in this instance, the absence of the characteristic decomposition products e.g. diketone, does not support this pathway.



Scheme 97

Figure 59 highlights the differences in ^{1}H NMR spectrum between the kinetic isomer **236** which was originally isolated [Figure 39, (i)] and the thermodynamic isomer **237** to which it converted [Figure 39, (iii)]. Analysis of the remaining solid sample that the crystal was chosen from, showed approximately a 1 : 1 ratio of the diastereomers **236** and **237** [Figure 39, (ii)], even though this had originally been recrystallized from a sample which was excusively **236** by ^{1}H NMR spectroscopy.

Previously, low yields of cycloadducts from dipolar additions of sulfines had been rationalised by the ability to easily undergo cycloreversion reaction,[7,63,103,108,133,134] however, this ability to switch from a kinetic diastereomer to a more stable thermodynamic diastereomer was an unexpected and unforeseen property of these heterocyclic compounds.



236

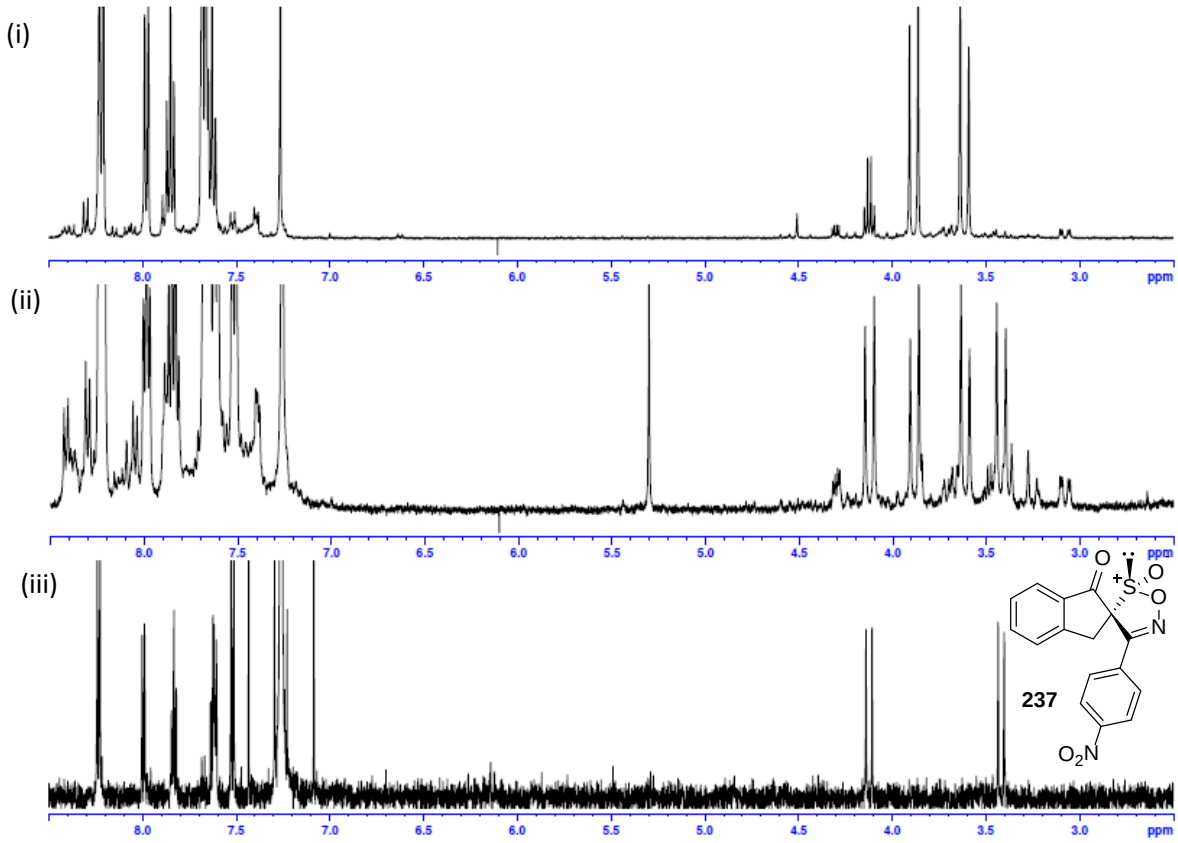


Figure 59: Conversion of the 1,2,5-oxathiazole-S-oxide **236** *isolated after purification (top – 400 MHz, contains ethyl acetate), to the 1,2,5-oxathiazole-S-oxide* **237** *identified after obtaining a crystal structure (bottom – 600 MHz). A 1 : 1 mixture of the remaining material highlights the ability to interconvert (centre – 400 MHz, contains DCM).*

To confirm the two diastereomers of the cycloadducts interconvert, a rhodium acetate catalysed batch reaction was carried out for 30 minutes (in acetonitrile : DCM, 1 : 1) at room temperature, generating the kinetic isomer **236** and thermodynamic isomer **237** in a relative ratio of 1 : 1.2 respectively in addition to other products.[ix] The remaining reaction material was subsequently heated to reflux for a further 7 h converting much of **236** into **237**, in a relative ratio to 1 : 3.3. In this instance the thermodynamic 1,2,5-oxathiazole-*S*-oxide cycloadduct **237** was isolated as a pure compound in a yield of 25% after column chromatography on silica gel, however, the major product isolated was the oxadiazole **242** in 42% yield (Figure 60), formed by the cycloaddition of the nitrile oxide dipole and acetonitrile. In subsequent reactions acetonitrile was not used as solvent, to avoid this side reaction.

[ix] Its interesting to note the relative ratios of **236** and **237** differed somewhat from the ratio in the reaction in Scheme 96 which may be due to interconversion prior to analysis or may be a solvent effect (acetonitrile compared to ethyl acetate).

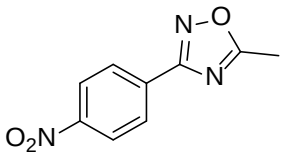


Figure 60: Oxadiazole **242**

A tentatively proposed mechanism for the interconversion is shown below (section 2.7.1.3). Notably, the kinetically formed product **236**, epimerises to the thermodynamic isomer **237** at elevated temperature, during crystallisation (Figure 59) or while in solution.

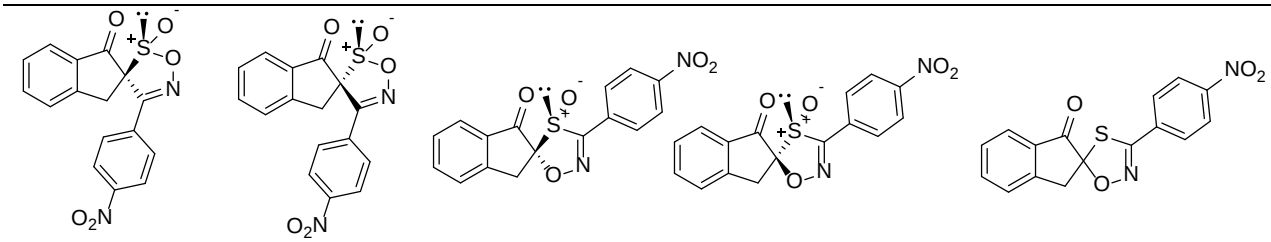
2.7.1.1 Optimisation of reaction conditions

With the crystal structure of **237** in hand, a series of reaction conditions was investigated to establish the optimum conditions for the preferential formation of either the kinetic isomer **236** or the thermodynamic isomer **237** (Scheme 96) in a synthetically viable process. As summarised in Table 33, the rhodium catalysed sulfine generation in either ethyl acetate/dichloromethane (1:1) or acetonitrile/dichloromethane (1:1) leads to mixtures of up to five cycloadducts and in general the kinetic isomer **236** is the major component, followed by the thermodynamic isomer **237** and then the regioisomeric 1,4,2-oxathiazole-*S*-oxides (Table 33 , entries 1-3). In acetonitrile, cycloaddition to form **242** is the dominant process. The best conditions for formation of the kinetic isomer **236** is rhodium catalysed batch reactions at 0°C. Using microwave irradiation to induce the hetero-Wolff rearrangement had previously been proven and widely studied within the group.[5,15] Generation of the sulfine *via* microwave heating (Table 33, entry 4) showed promise with the thermodynamic isomer **237** being the dominant cycloadduct in the crude product mixture. The recovered yield of **237** was low from this reaction and therefore this process is not a synthetically viable route. Thermal interconversion of **236** into **237** can be envisaged under these conditions, however, as the scale is limited in microwave reactions, continuous flow conditions were investigated (Table 33 , entries 5, 7, 8 - 10). The use of thermolysis in continuous flow proved successful in leading to moderate yields of the thermodynamic isomer confirming thermolysis in flow as a more controlled process. Literature precedent exists for this transformation as thermolysis reactions in continuous flow have recently been used for the generation of various reactive intermediates including ketenes and nitrenes.[77,78,135] Transition metal catalysis and thermolysis were both trialled in continuous flow, with a much cleaner transformation occurring in the absence of the rhodium acetate dimer catalyst.

A related report in the literature in the area of continuous flow dipolar cycloadditions, suggests that a column reactor loaded with a neutral alumina bed can be used for the removal of excess

nitrile oxide and furoxan dimers.[136] When two equivalents of the dipole were used, the crude material was recrystallised from ether and hexane to give the thermodynamic isomer **237** in 52% yield. When four equivalents were used (Table 33, entry 5), not all of the residual dipole and furoxan dimer was removed. Additionally, it was established that only a slight excess of 2 equivalents of the dipole were necessary for a clean transformation to occur.

Table 33: Investigation of the impact of reaction conditions on the 1,3-dipolar cycloaddition



Kinetic Diastereomer **(K)** | Thermodynamic Diastereomer **(T)** | Regioisomer A **(A)** | Regioisomer B **(B)** | 1,4,2-oxathiazole **(C)**

236	**237**	**240**	**238**	**239**

Entry	**Method** (Solvent)	**Generation of α-oxo sulfine**	**Reaction Time** (min)	**Dipole Eq.**	**Ratio K** : **T** : **A** : **B** : **C** **236** : **237** : **240** : **238** : **239** *(yield)*
1	Batch (EtOAc/DCM)	$Rh_2(OAc)_4$	60	2.3	**40 : 29 : 0 : 22 : 9** 24% : 0 : 0 : 0 : 15%
2	Batch (CH_3CN/DCM)	$Rh_2(OAc)_4$	30 (r.t.) 390 (100°C)	4	**1 : 1.2 : 0 : 0 : 0 : 5.3(242)**[g] **1 : 3.3 : 0 : 0 : 0 : 11.3(242)**[g] 0 : 25% : 0 : 0 : 0 : 42%[g]
3	Batch (EtOAc/DCM)	$Rh_2(OAc)_4$	90	4	**4 : 3 : 0 : trace : *0*** *0 : 17% : 0 : 0 : 0*
4	Microwave (DCM)	MW	10	2.5	**9 : 81 : 0 : 9 : 0** 0 : 18% : 0 : 0 : 0
5	Flow[b] (DCM)	Thermolysis[a]	10	4	**25 : 50 : 0 : 0 : 0**[f]
6	Batch[d] (Et_2O)	$Rh_2(OAc)_4$	180	1	*Complex Mixture*[e]
7	Flow[b,c] (EtOAc/DCM)	Thermolysis[a]	10	2	**10 : 56 : 0 : 14 : 0**[f] 0 : 52% : 0 : 0 : 0
8	Flow[b,c]	Thermolysis[a]	30	2	***10 : 83 : 0 : 7 : 0***[e]

	(EtOAc/DCM)				
9	Flow[b,c] (EtOAc/DCM)	Thermolysis[a]	10	4	***17 : 72 : 0 : 11 :0***[e]
10	Flow[b,c] (EtOAc/DCM)	$Rh_2(OAc)_4$	60	2	***52 : 38 : 0 : 10 : 0***[e]
11	Batch (r.t.) (EtOAc/DCM)	$Rh_2(OAc)_4$	30	2	***57 : 43 : 0 : 18 : 0***[e]
12	Batch (0°C) (EtOAc/DCM)	$Rh_2(OAc)_4$	30	2	***58 : 29 : 0 : 3 : 10***[e]

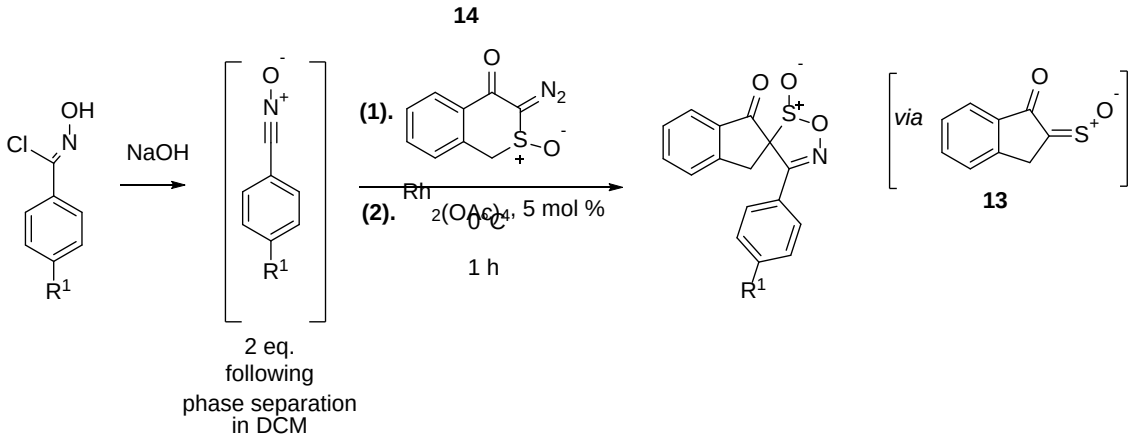
[a]Thermolysis reactions were carried out at 100°C in continuous flow.
[b]All continuous flow reaction were carried out with an 8 bar back pressure regulator fitted to the system.
[c]A packed bed of alumina was used in a 10 mm id omnifit® glass column.
[d] Following literature procedure for one of the other times a 1,2,5-oxathiazole-*S*-oxide was isolated.[137] Carried out at -20°C.
[e]The crude reaction mixture was not purified
[f] Another unknown impurity was present and made up the remainder of the material.
[g] The major product was the oxadiazole **242** from the cycloaddition of the nitrile oxide dipole and the solvent, acetonitrile.

As seen in entry 7, the thermodynamic isomer **237** is formed as the major product when the cycloaddition is conducted for 10 minutes thermolysis at 100°C in flow leading to isolation of the compound **237** in 52% yield. In addition, the kinetic isomer **236** can be formed as a major product (Table 33, entries 1,11,12), although these reaction conditions resulted in the additional formation of the thermodynamic isomer **237** and the 1,4,2-oxathiazole **239** (Table 33, entries 1 and 12). Entry 12 (rhodium acetate at 0°C) shows preferential formation of the kinetic isomer **236** over the thermodynamic isomer **237** in a ratio of 2 : 1. Thus, two different sets of reaction conditions for the preferential formation of two different diastereomeric products had been established, and subsequent application of these conditions to a range of substrates was carried out. Essentially, a viable and predictable synthetic process leading to the thermodynamic isomer *via* a metal-free thermolysis in flow was established.

2.7.1.2 Transition metal catalysed batch reactions – isolation of kinetic isomers

With reaction conditions also established for the preferential formation and isolation of the kinetic isomer **236** in pure form, we aimed to generate and isolate a series of related kinetic isomers using a series of nitrile oxide dipoles, **192,235,243–245** to confirm that the unanticipated conversion to the more stable thermodynamic isomer is consistent across the series. The kinetic isomers were generated in batch reaction conditions, at 0°C with 2 equivalents of the dipole in each case. Each of the nitrile oxide dipoles **192,235,243–245** were pre-generated as a solution in dichloromethane

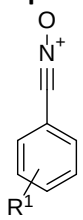
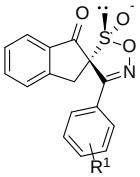
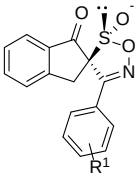
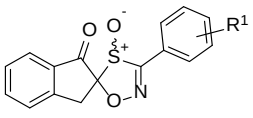
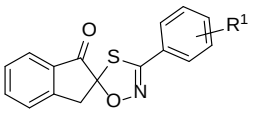
and added to the corresponding α-diazosulfoxide (Scheme 98). This was followed directly by addition of rhodium acetate dimer to promote the hetero-Wolff rearrangement to form the reactive α-oxo sulfine **13** *in situ* which is efficiently trapped with each of the nitrile oxides **192,235,243–245**.



Scheme 98

These reaction conditions were applied to the α-diazosulfoxide **14** combined with a series of five nitrile oxides **192,235,243–245** (Table 34).

Table 34: Summary of crude ratios and isolated yields of 1,3-dipolar cycloaddition reactions under rhodium catalysed batch reaction conditions.

Entry	Dipole	Thermodynamic Product	Kinetic Product	Regioisomer A/B	1,4,2-Oxathiazole
					
1[a]	Ratio (**192**) R^1 = H	8 **246**	47 6% - **247**	34 (B only) 6% **248** B[b] -	11 **249** 9%
2	Ratio (**243**) R^1 = 4-F	14 **250**	68 28% - **251**	7 (A only) 11% - **252** A	0 -
3	Ratio (**244**) R^1 = 4-*t*Bu	0 **253**	80 16% - **254**	20 (B only) **255** B	0 -
4	Ratio (**235**)	29 **237**	40 24% - **236**	22 (B only) **238** B	9 15% - **239**

	R^1 = 4-NO_2				
5	Ratio (**245**) R^1 = 2,5-difluoro	23 **256**	23 **257**	0 -	54 8% - **241**[c]

*All yields are of pure compounds isolated after column chromatography on silica gel.
[a] Minor amounts of the ketone **142** and diketone **146** (Figure 61) were also present in the ^{1}H NMR spectrum of the crude material.
[b]The Regioisomer B **248** was characterised as part of a mixture of 2 components.
[c] Repeated careful chromatography to obtain a pure product resulted in this low yield.

For Table 34, entries 1-4 the targeted kinetic isomers were successfully isolated in each case, albeit in poor yields. Although the thermodynamic isomers were present in trace amounts in the ^{1}H NMR spectrum of the crude material, the thermodynamic isomer was not isolated after purification, likely due to the minor amounts present. Significantly, while the selectivity for the kinetic isomer **236** over **237** was relatively modest, across the series of nitrile oxides, formation of the kinetic cycloadducts **247**, **251** and **254** has a much higher selectivity. This may be due to slower interconversion of the cycloadducts and/or more efficient trapping of the *Z* sulfine with the nitrile oxides. Scanning the data in Table 34 suggests there may be a relationship between the formation of the 1,4,2-oxathiazole-*S*-oxides when the ratio of the thermodynamic 1,2,5-oxathiazole-*S*-oxide isomers is lower relative to the kinetic 1,2,5-oxathiazole-*S*-oxide Isomers. There is some evidence that formation of Regioisomer B by cycloaddition to the *E* sulfine competes effectively with the 1,2,5-oxathiazole-*S*-oxide cycloaddition pathway to the same sulfine to form the thermodynamic Isomer, especially in Table 34, entries 1 and 3, but a definitive conclusion on this would require further investigation. Interestingly, the 1,4,2-oxathiazole-*S*-oxide Regioisomers A or B were present in four out of the five reactions in Table 34, whereas was present in three of the five reactions. In the case of Table 34, entry 5, only 1,4,2-oxathiazole **241** was isolated after repeated chromatography, in 8% yield. This 1,4,2-oxathiazole **241** is a reduction product and the absence of the sulfinyl oxygen may be due to oxygen transfer within the reaction conditions catalysed by the presence of rhodium or the intermediate carbene,[138] or due to intermolecular transfer of sulfinyl oxygens. The extent of formation of the 1,4,2-oxathiazole **241** in Table 34, entry 5 is much greater than in any of the other experiments, and this could potentially indicate that the proximity of the 2-fluoro substituent and the sulfoxide oxygen in space facilitates the oxygen transfer in the presence of the rhodium acetate catalyst. It should be noted that this is a once off experiment and further investigation would be required to clarify this effect.

In Table 34, entry 1 the crude material showed in addition to the products outlined above, the presence of the ketone **142** and diketone **146** as minor products, formed by rearrangement of the intermediate α-oxo sulfine **13** (Figure 61). In Table 34, entry 2, the diketone **146** was also present as a minor component in a ratio of 1 : 0.15 with the desired product. The formation of these products is as a result of transformations of the intermediate α-oxo sulfine **13** as it undergoes either sulfur extrusion, or loss of SO *via* and intermediate oxathiirane **143** (Scheme 76), these reaction pathways and products have been previously confirmed and characterised by Buckley. [16]

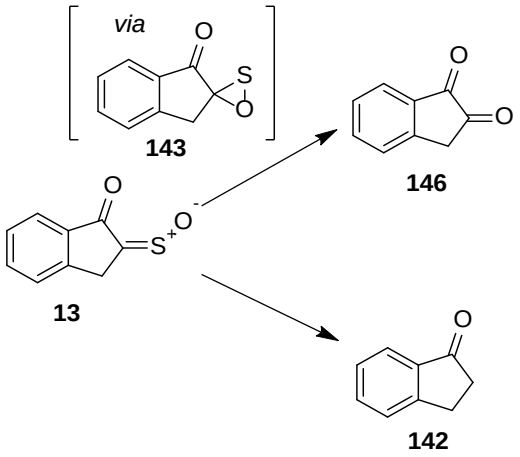
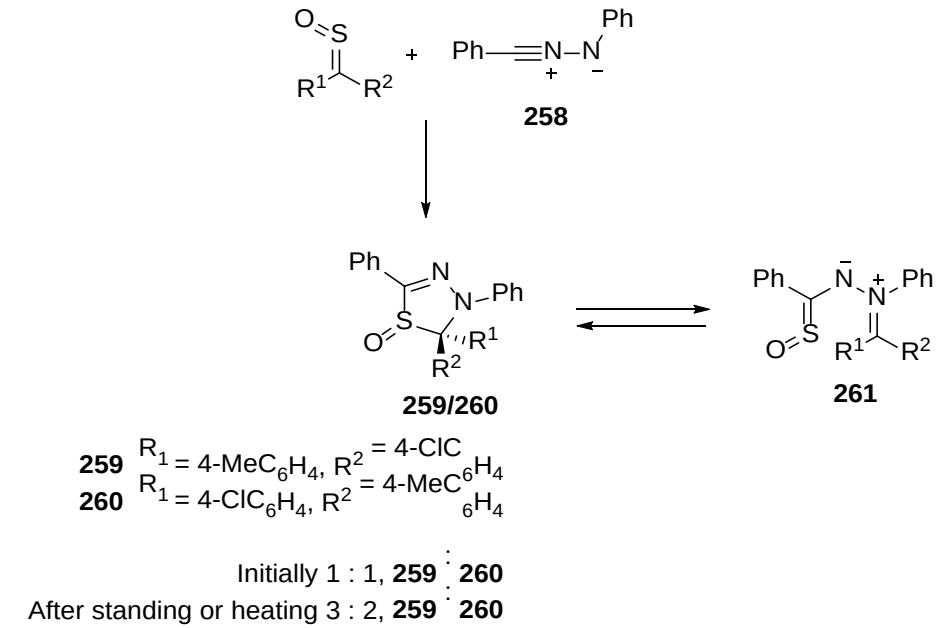


*Figure 61: Conversion of the α-oxo sulfine **13** to the ketone **142** or diketone **146** via the oxathiirane intermediate **143** .*

This set of reactions confirm that preferential formation of the kinetic isomer of 1,2,5-oxathiazole-*S*-oxides can be achieved using rhodium acetate dimer (5 mol %) at 0°C, and subsequently isolated and characterised as a pure compound in most cases (**247**, **251**, **254** and **236**). On storage of these isomers, spontaneous interconversion to the thermodynamic isomers is observed over time, as is highlighted in section 2.7.1.3.

2.7.1.3 Evidence of proposed mechanism

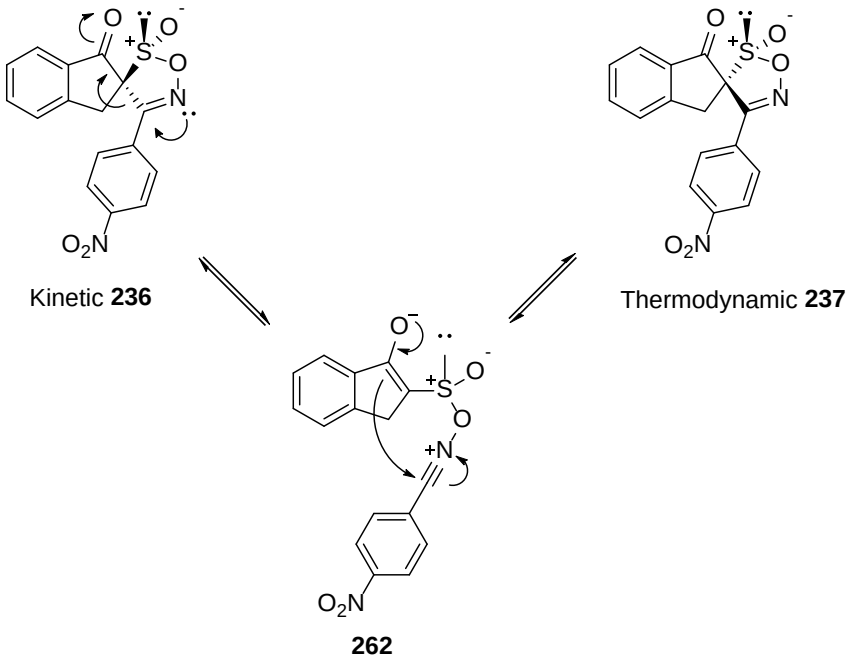
In the literature, Zwanenburg *et al*.[133] have described the 1,3-dipolar cycloaddition of sulfines with diphenylnitrilimine **258**. This led to a 1 : 1 mixture of two 1,3,4-thiadiazoline-*S*-oxides diastereomers **259** and **260** as the initial products. However, comparable to the 1,2,5-oxathiazole-*S*-oxide products in this work, the diastereomeric 1,3,4-thiadiazoline-*S*-oxide products lose their stereochemical integrity over time due to interconversion through a ring opened intermediate **261**, resulting in a ratio of 3 : 2 of the diastereomers (Scheme 99).



Scheme 99

The kinetic cycloadduct **260**, undergoes a ring opening-ring closing cycle with the loss of steric integrity, forming **259**, *via* **261**. The authors describe how the loss of stereochemical integrity is not by isomerisation of the sulfine starting material, but by product equilibration afterwards. The authors noted that equilibration happens on standing or heating, and also that inversion of the sulfoxide functionality was highly unlikely seeing as the configurational stability of sulfoxides is usually rather high. [133]

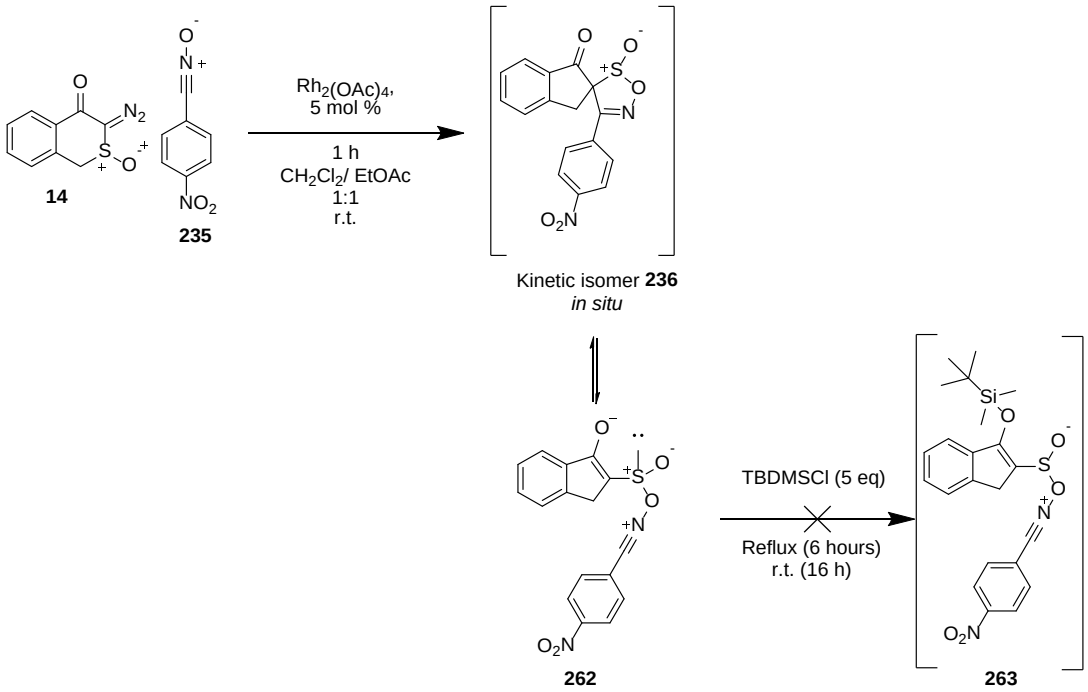
In this work, the observation of the epimerisation of the kinetic isomer **236** to the thermodynamic isomer **237** which occurs during crystallisation is comparable to Zwanenburg's observation. The kinetic isomer **236** was isolated originally and characterised as one single component, however on slow solution recrystallisation (four weeks), selecting a single crystal, and obtaining a crystal structure, analysis of the crystal following crystallography by ^{1}H NMR spectroscopy (600 MHz) showed the crystal to be the thermodynamic isomer **237**, and the residual sample from the recrystallisation was a 1 : 1 mixture of **236** and **237** by ^{1}H NMR analysis. The proposed mechanism for our derivatives is different to the mechanism proposed by Zwanenburg for his 1,3,4-thiadiazoline-*S*-oxides. Presumably, epimerisation of our 1,2,5-oxathiazole-*S*-oxides occurs *via* ring opening of the kinetic 1,2,5-oxathiazole-*S*-oxide **236** forming an enolate intermediate **262**, which on ring closure can result in inversion of stereochemistry at the spiro carbon and formation of the thermodynamic isomer **237** (Scheme 100). The conjugation with the indanone provides an electron sink enabling the fragmentation of the kinetic 1,2,5-oxthiazole-*S*-oxide Isomer.



Scheme 100

From the crystal structure of the thermodynamic isomer **237** (Figure 58), it is noted that the two electron rich oxygens are pointing away from each other. In the kinetic isomer **236**, where the relative stereochemistry is the opposite at the spiro centre, the two electron rich oxygen atoms are close in space, leading to a driving force for the rearrangement from the kinetic isomer **236** to the thermodynamic isomer **237.**

It is proposed that electron donation from the nitrogen lone pair results in the formation of an enolate intermediate **262** which subsequently ring closes, neutralising the zwitterion and forming the thermodynamic cycloadduct. Attempts to confirm this reaction mechanism included using transition metal catalysed batch reaction conditions for generation of the kinetic cycloadduct **236**, then adding TBDMSCl or MeI with the objective of trapping the enolate intermediate and thereby confirming its role in the stereochemical interconversion. In this event there was no evidence for trapping of the enolate **262**, and no evidence for any enol ether derivative such as **263** was observed (Scheme 101), and neither the thermodynamic isomer **237** nor kinetic isomer **236** was recovered from the reaction.



Scheme 101

A second possible explanation of the interconversion of the kinetic isomer **236** and the thermodynamic isomer **237** is that the cycloadduct **236** undergoes a cycloreversion reaction to re-form the *Z* α-oxo sulfine **13** which we know can isomerise to the *E* α-oxo sulfine **13**, and the *E* α-oxo sulfine **13** can subsequently undergo a cycloaddition to form the thermodynamic isomer **237**. It is believed that the first pathway is more likely as the formation of byproducts (ketone **142** and diketone **146**) of sulfine degradation would be expected if the interconversion is exclusively *via* cycloreversion. This interconversion was also studied across the cycloadducts **251** and **254**, monitoring samples of the kinetic isomers which had been stored in solution and/or as solids. Clear evidence for the interconversion was seen for all of the series with appearance of the characteristic ^{1}H NMR signals for the corresponding thermodynamic isomers from totally pure samples of the kinetic isomers as shown in Figures 61, 62 and 63. It is also noteworthy that the extent of interconversion from the kinetic isomer to the thermodynamic isomer is relatively significant for the *p*-nitro derivative **236** (Figure 62) and the *p*-fluoro derivative **251** (Figure 63). The extent of interconversion is much less with the 4-*t*Bu-substituted cycloadduct **254** (Figure 64), which showed only minor amounts (<10%) of epimerisation after 6 months, but the position of equilibrium has not been established with these derivatives. Figure 62 shows the conversion over time of the cycloadduct **236** to form **237** with 10% of the thermodynamic isomer after 2 days, increasing to a 1 : 1 mixture after 4 weeks.

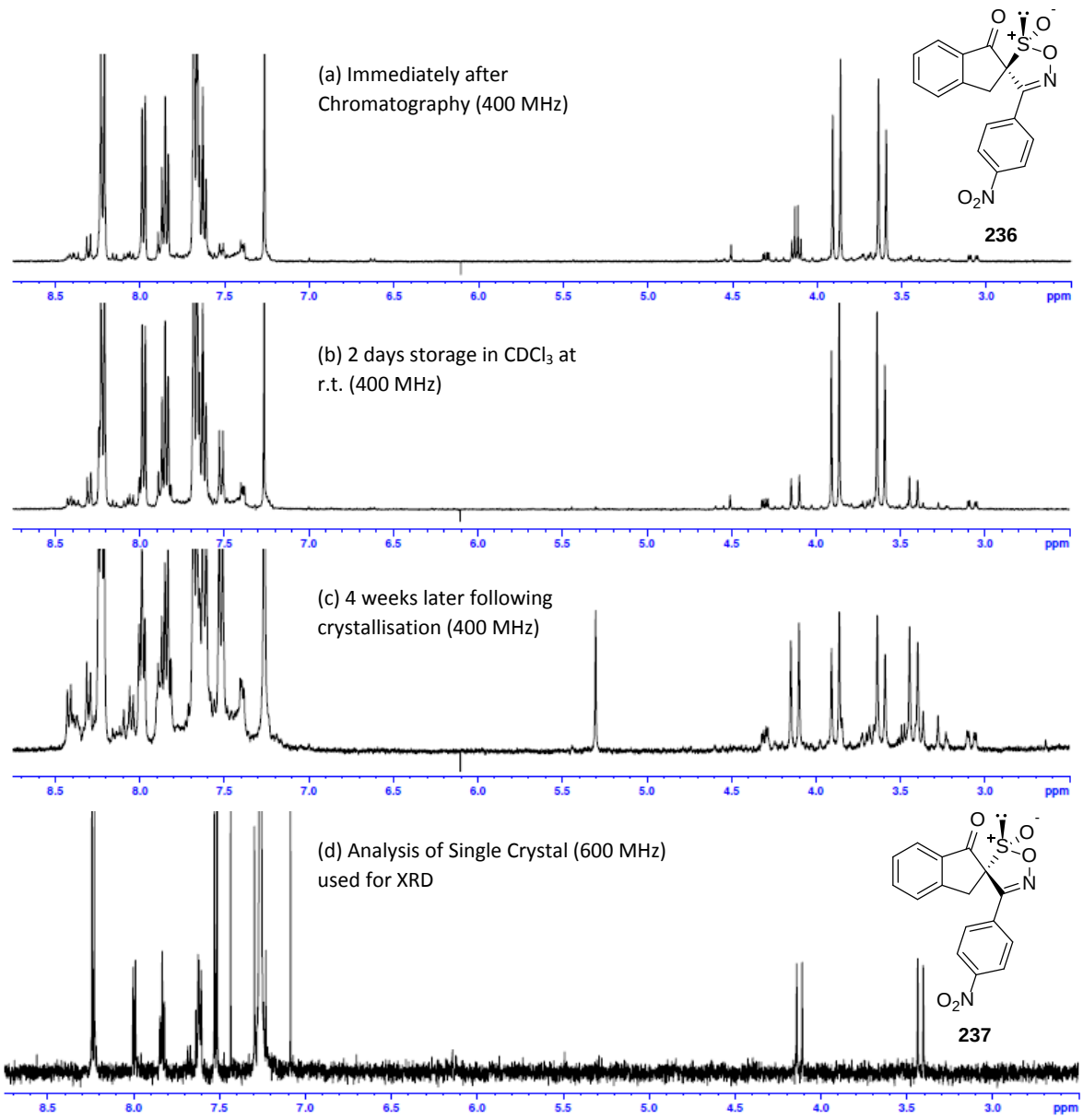


*Figure 62: Continual monitoring of the interconversion of the kinetic oxathiazole-S-oxide isomer **236** (top) to the thermodynamic isomer **237** (bottom).*

The same pattern is seen with the *p*-fluoro substituted cycloadduct **251**. Immediately after purification by column chromatography on silica gel the kinetic diastereomer **251** was isolated as one compound only. After 6 h, the material was a 93 : 7 mixture of the kinetic and thermodynamic cycloadducts, **251** and **250**, respectively. After 3 days the material had become a 83 : 17 mixture of the kinetic and thermodynamic isomers and after 5 months, 90% of the initially isolated kinetic diastereomer **251** had converted to the thermodynamic diastereomer **250** (Figure 63).

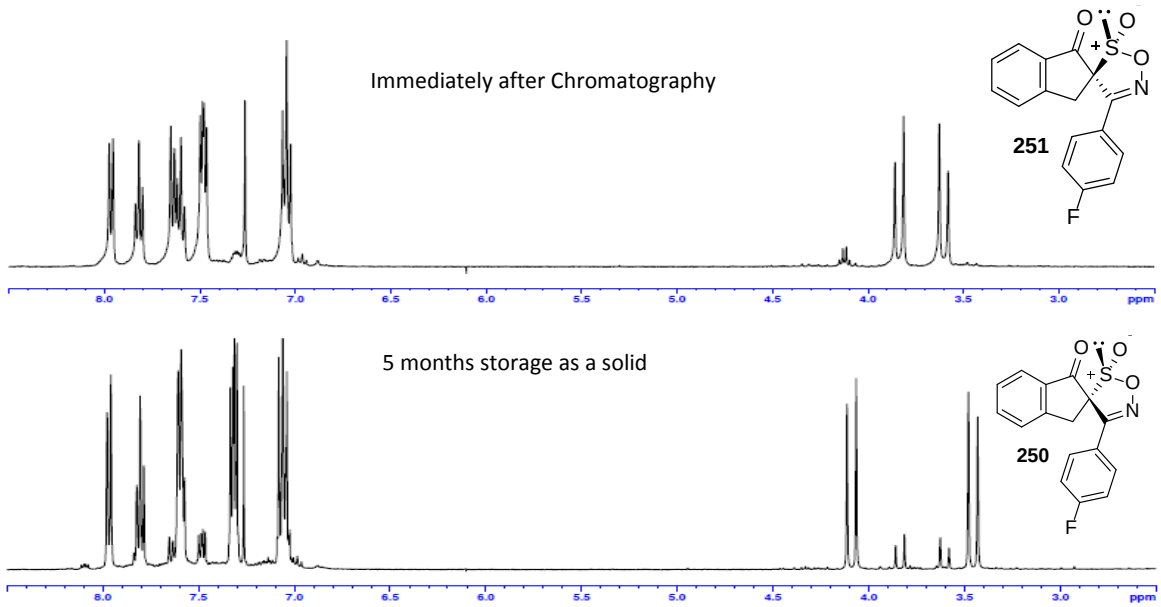


Figure 63: Comparison of the two ^{1}H NMR spectra highlights the conversion of the p-fluoro cycloadducts **251** *to* **250** *following a time lapse of 5 months on storage as a solid.*

The extent of interconversion is less on storage with the *t*-butyl substituted kinetic diastereomer **254** (Figure 64). Consistent with that seen with the other kinetic isomers, the kinetic diastereomer **254** was isolated as one isomer after chromatography (Table 34, Entry 3) (Figure 64). However, in contrast to the *p*-fluoro derivative **251** and the *p*-nitro derivative **236**, the interconversion between this kinetic isomer **254** to the thermodynamic isomer **253** is extremely limited when stored as a solid, with only 10% of the thermodynamic isomer **253** present after 6 months.

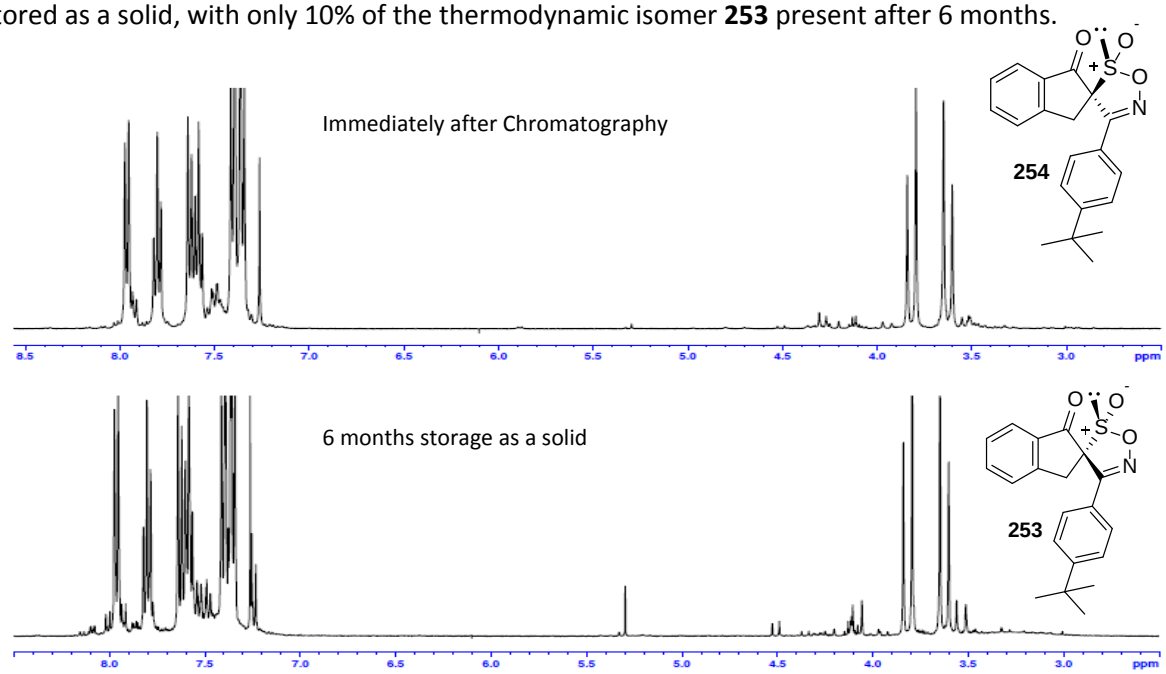


Figure 64: Stacked spectra of the kinetic 1,2,5-oxathiazole-S-oxide **254** *after purification by column chromatography on silica gel (top) with re-analysis of the material after 6 months (bottom), highlighting the slow rate of interconversion to the thermodynamic 1,2,5-oxathiazole-S-oxide* **253**.

This limited of interconversion of the *t*-butyl substituted cycloadduct **254** may indicate that in the solid state epimerisatioin is hindered by the sterically demanding *t*-butyl group.

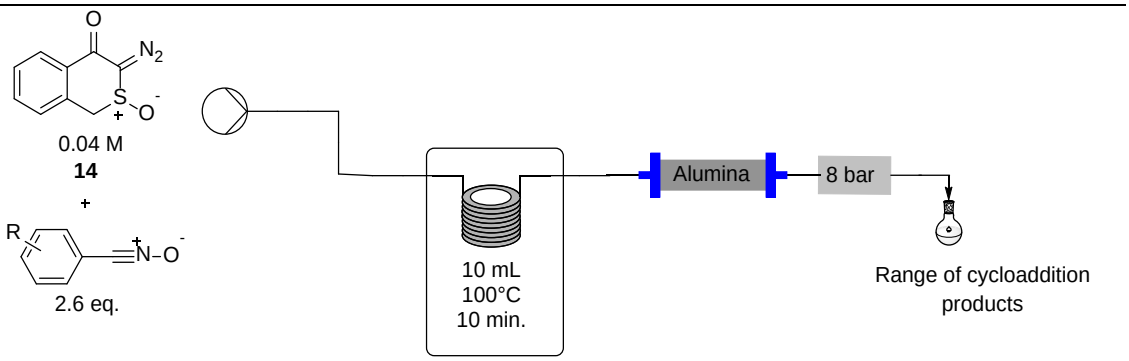
2.7.2 Continuous flow thermolysis reactions – Isolation of thermodynamic isomers

2.7.2.1 α-Diazosulfoxide **14** with substituted nitrile oxides

From the investigations to date it appears that the formation of the thermodynamic isomer as the major product from metal free, thermolysis in continuous flow, is due to efficient conversion of the initial kinetic product under these conditions. However some cycloaddition to the *E* α-oxo sulfine under these conditions may also be occurring, as Z *to E* sulfine interconversion would be expected under these conditions.

The reaction conditions identified for the preferential formation of the thermodynamic isomer **237** in good yields (Table 33, entry 8) were used with a range of nitrile oxides **192,235,243–245** to enable investigation of the influence of substituents. The electronic and steric effects were to be investigated through variation of the substituent on the nitrile oxide aryl ring. In each case the thermodynamic 1,2,5-oxathiazole-*S*-oxide is the principal product formed and was isolated in each case as a pure component following chromatography using this synthetically viable process. As summarised in Table 35, smaller amounts of the other cycloadducts were seen in the crude product mixtures including the kinetic 1,2,5-oxathiazole-*S*-oxide, the 1,4,2-oxathiazole-*S*-oxide Regioisomers A and B, and in some instances samples of these were isolated. Notably 1,4,2-oxathiazole was not formed under these conditions in any instance, indicating that the sulfoxide reduction only occurs in the presence of the rhodium catalyst. Spectral details which were employed in assigning the stereochemistry and regiochemistry of the isolated cycloadducts are outlined in section 2.7.4.

*Table 35: Results of the thermolysis in continuous flow cycloaddition reactions with the α-oxo sulfine generated from the unsubstituted α-diazosulfoxide **14**.*



Entry	Dipole	Thermodynamic Product	Kinetic Product	Regioisomer A/B	1,4,2-Oxathiazole
1	Ratio[a]:	63	12	7 – A, 15 - B	0[a]
	R^1 = H	**246** 32 %	**247**	**264** A **248** B	-
2	Ratio R^1 = 4-*t*Bu	78 **253** 30%	12 **254**	10 **265** A 5%	0 -
3	Ratio R^1 = 4-F	63 **250** 35%	18 **251** 12%	12 **252** A 4%	0[a] -
4[d]	Ratio R^1 = 4-NO_2	56 **237** 52%	10 **236**	14 **238** B	0[b] -
5	Ratio R^1 = 2,5-diF	62 **256** 11%	0 **257**	9 **266** B	0[c] -

[a] The diketone **146** was present as the remainder of the material.
[b] An unknown impurity made up the remainder of the material.
[c] The ketone **142** and diketone **146** were present as the remainder of the material in a ratio of 2 : 1.
[d] This is the same entry reported in Table 33, Entry 7.

In continuous flow, use of reaction conditions of 100°C for 10 minutes was extremely efficient at inducing the hetero-Wolff rearrangement, as well as promoting the transformation of the kinetic diastereomers to the thermodynamic diastereomers, with no starting material present on analysis of the ^{1}H NMR spectrum of the crude material in any case.

When the reaction conditions were applied to the unsubstituted nitrile oxide **192**, and the unsubstituted α-diazosulfoxide **14** the desired 1,2,5-oxathiazole-*S*-oxide **246** was isolated as one isomer in 32% yield following chromatography. Notably and unusually, both Regioisomer A and Regioisomer B of the 1,4,2-oxathiazole-*S*-oxide were present in the ^{1}H NMR of the crude material. Although the ^{1}H NMR spectrum of the crude material showed trace amounts of the diketone product **146**, formed by rearrangement of the intermediate sulfine **13**, this product was not isolated from the column after chromatography. The thermodynamic isomer **246** was isolated as a crystalline solid and a single crystal was slowly grown from dichloromethane and hexane using the vapour diffusion method leading to an unambiguous assignment of the regio- and stereochemistry of **246** (see section 2.7.4). Given the observations seen in section 2.7.1, the single crystal of the thermodynamic isomers were recovered from the XRD and analysed by ^{1}H NMR; there was no evidence of any alteration of the thermodynamic isomer, or equilibration with the kinetic isomer, in any case.

When the reaction was carried out using the *t*-butyl substituted nitrile oxide **244** (Table 35, Entry 2) the ^{1}H NMR spectrum of the crude material similarly showed an efficient transformation to the desired thermodynamic isomer **253**, as well as the presence of the Regioisomer A **265** and the kinetic isomer **254** in a ratio of 78 : 10 : 12. After purification by column chromatography on silica gel, the desired 1,2,5-oxathiazole-*S*-oxide **253** was isolated in 30% yield. In a much more polar fraction, the Regioisomer A **265** was isolated in a low yield of 5%.

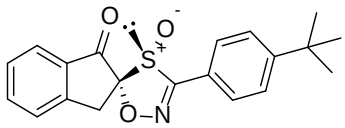


Figure 65: The Regiosiomer A **265***.*

Using the *p*-fluoro nitrile oxide **243** (Table 35, Entry 3), analysis of the crude material by ^{1}H NMR spectroscopy shows a mixture of the thermodynamic isomer **250**, the kinetic isomer **251**, the Regiosiomer A **252** and the diketone rearrangement product **146** in a ratio of 63 : 18 : 12 : 7. After purification, the desired thermodynamic 1,2,5-oxathiazole-S-oxide **250** was isolated in a yield of 35%. The minor kinetic diastereomer of the 1,2,5-oxathiazole-*S*-oxide **251** was isolated also in 12% yield, suggesting this kinetic isomer **251** did not undergo complete interconversion to the thermodynamic isomer **250** in the continuous flow thermolysis conditions (10 minutes at 100°C).

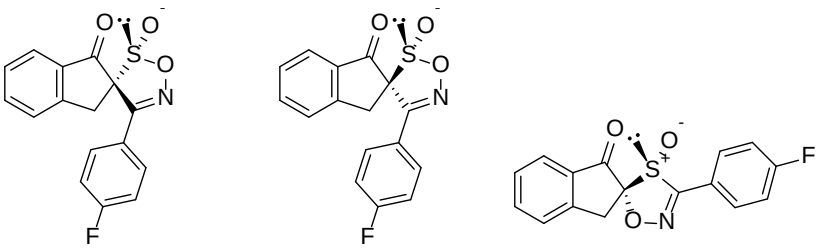
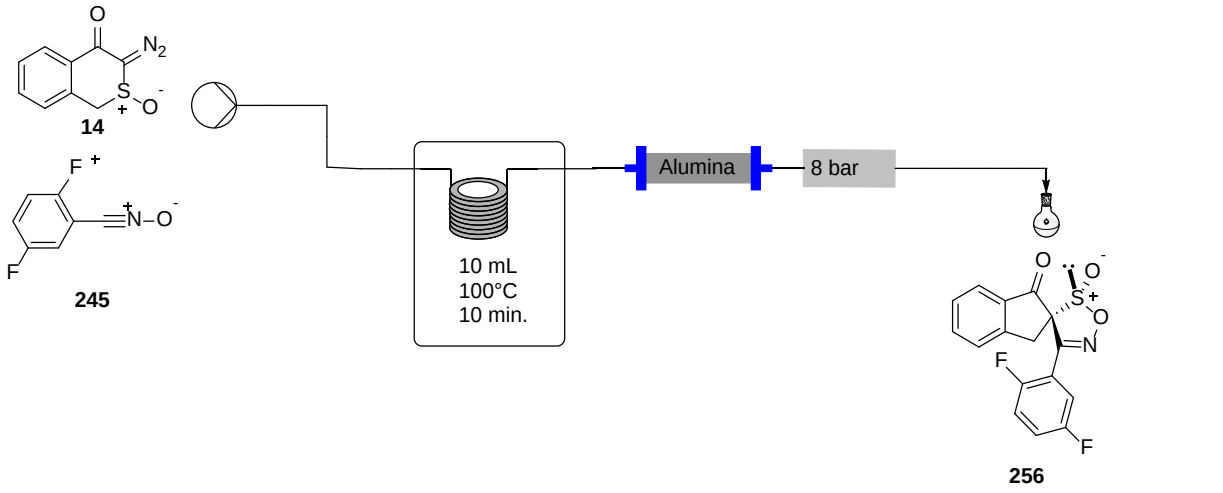


Figure 66: Cycloadducts isolated from Table 35, Entry 3 after purification by column chromatography.

Following this, a third fraction was also isolated from the column. This was assigned as the 1,4,2-oxathiazole-*S*-oxide Regiosiomer A **252**. This was a minor component of the reaction mixture and is assigned on comparison of the spectroscopic data to previously characterised 1,4,2-oxathiazoles in the literature and by comparison to our 1,4,2-oxathiazole-*S*-oxide **267** confirmed by single crystal X-ray diffraction (see section 2.8).[113,139]

The 2,5-difluoro nitrile oxide **245** (Table 35, Entry 5) and the unsubstituted α-diazosulfoxide **14** were subjected to the standard continuous flow thermolysis conditions achieving 100% consumption of the starting material and intermediate α-oxo sulfine **13** as expected. Analysis of the crude reaction mixture by ^{1}H NMR spectroscopy showed the formation of the thermodynamic isomer **256**, the ketone **142**, diketone **146** and the Regioisomer B **266** in a ratio of 62 : 20 : 11 : 9. After repeated purification, the 1,2,5-oxathiazole-*S*-oxide thermodynamic isomer **256** was isolated as a pure compound in 11% yield.



11% *After repeated chromatography*

Scheme 102

It is interesting to note from Table 33, Entry 5 and Table 35, Entry 5 that it appears the conversion of the kinetic isomer **257** with the 2,5-difluoro aryl substituent, to the thermodynamic isomer **256** occurs more easily than in the other derivatives as the extent of the kinetic isomers seen in the crude products is much less than the other derivatives in both tables. It appears that the *o*-fluoro enhances the rate of the interconversion from the kinetic to thermodynamic isomers, probably due to interaction between the fluoro and the sulfinyl oxygen. In addition, in this instance, the chromatographic purification of individual components was more challenging than for any of the other derivatives in Table 35 and only after repeated chromatography were small amounts of pure components isolated.

2.7.2.2 α-Diazosulfoxide 80 with substituted nitrile oxides

With successful cycloadditions achieved with the unsubstituted α-diazosulfoxide **14** in both batch (see section 2.7.1) and continuous flow reaction conditions (see section 2.7.2.1), an understanding of the formation of the kinetic and thermodynamic 1,2,5-oxathiazole-*S*-oxide products as well as the 1,4,2-oxathiazole-*S*-oxide regioisomers had been established. The series of stable, isolable thermodynamic 1,2,5-oxathiazole-*S*-oxide isomers was extended through combination of a range of substituted nitrile oxides **192,235,243–245** with the substituted α-diazosulfoxide **80**. Once again, the major component present in the crude reaction mixtures in each case in the thermodynamic isomer of the 1,2,5-oxathiazole-*S*-oxide cycloadduct, with smaller amounts of the kinetic isomer and the two 1,4,2-oxathiazole-*S*-oxide Regioisomers A and B. In each instance the thermodynamic 1,2,5-oxathiazole-*S*-oxide was isolated as a pure component and once again the 1,4,2-oxathiazole product was not detected in the absence of the rhodium catalyst.

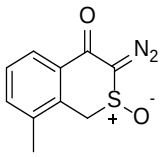
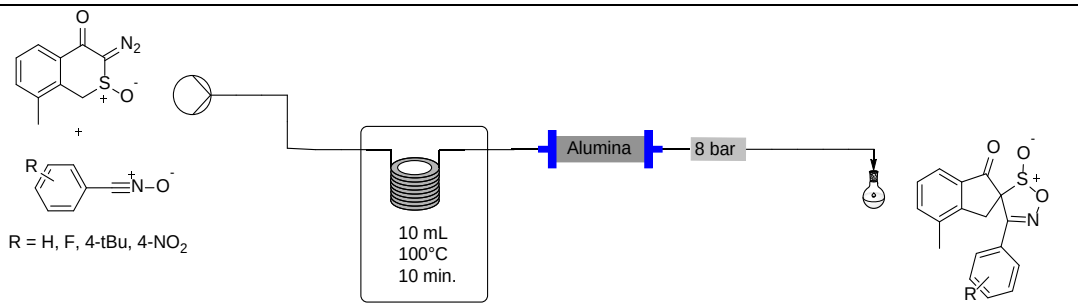


Figure 67: α-Diazosulfoxide **80**

In all cases, as with the earlier reactions, the dipole was freshly generated each time. The dipole, as a solution in dichloromethane, is added to the α-diazosulfoxide **80** and subjected to thermolysis under continuous flow. The results of each reaction are outlined below (Table 36). Under these thermolysis conditions efficient transformation of the α-diazosulfoxide to the α-oxo sulfine is achieved. Trapping of the *Z* α-oxo sulfine to form the kinetic 1,2,5-oxathiazole-*S*-oxide and the *E* α-oxo sulfine to form the thermodynamic 1,2,5-oxathiazole-*S*-oxide cycloadduct can be envisaged, with subsequent transformation of the kinetic isomer to the thermodynamic isomer effected at 100°C. With each of the α-diazosulfoxides, **14**, **80** and **83**, further investigation would be required

to clarify how much of the thermodynamic 1,2,5-oxathiazole-*S*-oxide is formed directly from cycloaddition to the *E* α-oxo sulfine, and how much from the interconversion of the kinetic isomer.

Table 36: Results of cycloaddition reactions of the α-oxo sulfine **141** *derived from α-diazosulfoxide* **80**.



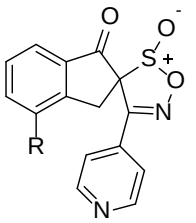
Entry	Dipole	Thermodynamic Product	Kinetic Product	Regioisomer A/B	1,4,2-Oxathiazole
1	Ratio R^1 = H	78 30% - **268**	18 **269**	8 **270** B	0 -
2	Ratio R^1 = 4-F	77 45% - **271**	11 **272**	12 12% - **273** A	0 -
3	Ratio R^1 = 4-tBu	78 26% - **274**	15 **275**	7 **276** A	0 -
4	Ratio R^1 = 4-NO_2	85 20% - **277**	11 **278**	4 **279** B	0 -

*All reactions were carried out in continuous flow using the optimum conditions of a 10 minutes residence time at 100°C with 2.6 equivalents of the pre-generated dipole, followed by an inline alumina column.
*Yields of pure compounds isolated after column chromatography on silica gel are given in the table.

In each case the desired thermodynamically stable 1,2,5-oxathiazole-*S*-oxide cycloadduct was isolated in a yield between 20 and 45% (**268**, **271**, **274**, and **277**). It is noted that in one case only, Table 36, entry 2, where the *p*-fluorobenzonitrile oxide dipole **243** is used, the 1,4,2-oxathiazole-*S*-oxide regiosiomer **273** is isolated in a significant yield of 12%. Each of the isolated cycloadducts was a crystalline solid. For the cycloadduct **271** a single crystal was grown from dichloromethane and hexane using vapour diffusion method with dichloromethane as solvent and hexane as antisolvent. The structure and stereochemistry were unambiguously defined and will be discussed further in section 2.7.4. Interestingly an investigation into extension of the residence times may

be warranted to establish if that would increase the ratio of the thermodynamic 1,2,5-oxathiazole-*S*-oxide cycloadduct relative to the kinetic 1,2,5-oxathiazole-*S*-oxide cycloadduct.

Reactions of the α-oxo sulfines derived from both the α-diazosulfoxide **14** and the α-diazosulfoxide **80** with the isonicotinaldehyde derived nitrile oxide **280**, generated from the imidoyl chloride **232**, were unsuccessful. Analysis of the crude reaction mixture, in both cases, by ^{1}H NMR spectroscopy showed a complex mixture, with no evidence of the cycloaddition products **281** or **282** (Figure 68). The preparation of the nitrile oxide **280** under these conditions has not been confirmed.



R = H **281**
R = CH_3 **282**
not isolated

Figure 68: Cycloadducts **281** *and* **282***.*

2.7.2.3 α-Diazosulfoxide 83 with substituted nitrile oxides

The reaction conditions were also applied to the synthesis of a series of 1,2,5-oxathiazole-*S*-oxides using the α-diazosulfoxide **83** (Figure 69).

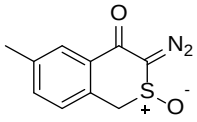
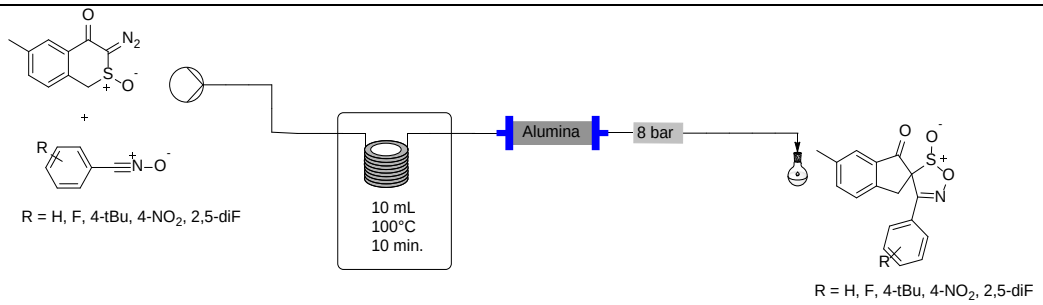


Figure 69: α-Diazosulfoxide **83**

Consistent with the α-diazosulfoxide **14** and **80** the major component in the crude material of these reactions (Table 37) is the thermodynamic isomer of the 1,2,5-oxathiazole-S-oxide.

Table 37: Results of the 1,3-dipolar cycloaddition reaction of the α-oxo sulfine derived from α-diazosulfoxide **83**.



Entry***	Dipole	Thermodynamic Product	Kinetic Product	Regioisomer A/B	1,4,2-Oxathiazole
1	Ratio R^1 = H	64 34% - **283**	16 **284**	11 25%[c] - **285** A	0[a]
2	Ratio R^1 = 4-F	73 36% - **286**	14 5% - **287**	13 10% - **288** A	0 -
3	Ratio R^1 = 4-tBu	80 15% - **289**	20 **290**	0 -	0 -
4	Ratio R^1 = 4-NO_2	77 45% - **291**	17 11% - **292**	6 **293** A	0 -
5	Ratio R^1 = 2,5-DiF	53 16% - **294**	11 **295**	0[b] -	0 -

[a]The remainder of the material consisted of an unknown with a singlet at 3.77 ppm in the ^{1}H NMR spectrum.
[b]The remainder of the material consisted of the α-oxo sulfine with the indicative signal being a singlet at 4.21 ppm in the ^{1}H NMR spectrum.
[c] Clearly the discrepancy between the recovered yield and the proportion in the crude reaction mixture reflects the accuracy of measurements in a complex mixture.
*All reactions were carried out in continuous flow using the optimum conditions of a 10 minutes residence time at 100°C with 2.6 equivalents of the pre-generated dipole, followed by an inline alumina column.
**Yields of pure compounds isolated after column chromatography on silica gel are given.

In the case of Table 37, entry 1 a minor component present is the Regiosiomer A **285**. Notably, the formation of this regioisomer was not identified when the α-diazosulfoxide **80** was used. For Table 37, entry 2 as well as successful isolation of the desired 1,2,5-oxathiazole-*S*-oxide **286**, the kinetic isomer of the 1,2,5-oxathiazole-*S*-oxides **287** and the Regioisomer A **288** are both isolated. Incomplete conversion of the kinetic isomer **272** to the thermodynamic isomer **271** is achieved in the residence time allowed. Interestingly, when the 4-F dipole **243** is used, the regioisomeric

byproduct is isolated from all continuous flow thermolysis reactions. For Table 37, entry 3, the desired 1,2,5-oxathiazole-*S*-oxide is isolated in a low yield of 15%. This is in contrast to 30% when combined with the α-diazosulfoxide **14** and 26% when reacted with the α-oxo sulfine derived from α-diazosulfoxide **80**. This lower yield is due to difficulty in purification of the reaction mixture on silica gel and corresponds to a pure isolated fraction only. For Table 37, entry 4, along with successful isolation of the thermodynamic isomer, the kinetic isomer **292** was also isolated. Across the series of five reactions, after purification of the crude reaction material the desired thermodynamic cycloadducts **283**, **286**, **289**, **291**, and **294** are isolated in poor to moderate yields principally due to the challenge in isolating pure components from complex mixtures. Interestingly, the *t*-butyl substituted derivative **289** and the 2,5-difluoro substituted cycloadducts **294** were both isolated in low yields and as oils after purification. Each of the other thermodynamic 1,2,5-oxathiazole-*S*-oxides isolated was a crystalline solid. Characterisation data of **294** was obtained from a fraction which was 90% pure; as seen with the earlier difluoro derivative **256**, purification was challenging. The Regiosiomers A **285** and **288** were isolated for entries 1 and 2 only.

2.7.3 Summary of Results

In conclusion, this part of the work has successfully established two sets of reaction conditions for the preferential formation of either the kinetic isomer or the thermodynamic isomer of a 1,2,5-oxathiazole-*S*-oxide cycloadducts by trapping of α-oxo sulfines with nitrile oxides. These cycloadducts are exceptionally rare in the literature with only two reported examples. Most reports of nitrile oxide cycloadditions are to isolated sulfines and yield the 1,4,2-oxathiazole-*S*-oxide regioisomer; we are not aware of a nitrile oxide cycloaddition to an α-oxo sulfine.[104] It is well established that the conjugation in an α-oxo sulfine alters the electronic properties and accordingly the reactivity of the sulfine moiety. In Zwanenburg's analysis of the regioselectivity of cycloaddition of α-oxo sulfines with Danishefsky's diene, he highlights the impact of the conjugation to the ketone on the orbital coefficients, thus in an isolated sulfine the largest atomic coefficient in the LUMO is on the carbon while in the oxo-sulfine the polarisation is reversed with the largest coefficient now at sulfur.[140] This is supported by the observation that the 1,2,5-oxathiazole-*S*-oxide is formed in the nitrile oxide cycloaddition of the highly conjugated sulfine **191** and also to the trifluoromethyl derivative **197** (see Section 2.6.1). Thus, the formation of the 1,2,5-oxathiazoles as the major product, while not precedented, can be rationalised on the basis of the electronic properties of the α-oxo sulfines.

Cycloaddition with nitrile oxides and electron deficient dipolarophiles are normally considered to proceed via LUMO dipole and HOMO dipolarophile.

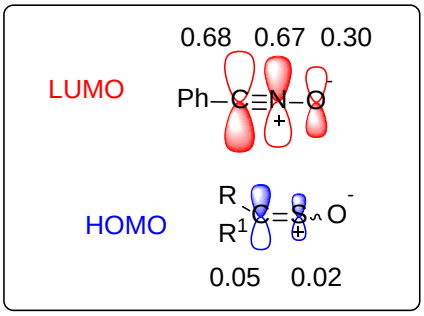
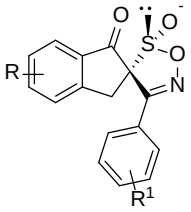
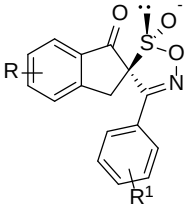
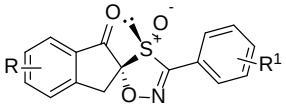


Figure 70: Frontier molecular orbital coefficients for the LUMO of benzonitrile oxide[141] and the HOMO of an α-oxo sulfine[140].

Interestingly, the 1,2,5-oxathiazole-*S*-oxides exhibited an unanticipated ability to interconvert on standing or on heating, between a kinetic isomer and a thermodynamic isomer. This interconversion was studied crystallographically and spectroscopically with significant differences apparent in the ^{1}H and ^{13}C NMR spectra of both isomers. Additionally a proposed driving force and a mechanism for the interconversion are suggested, while monitoring of the interconversion over time for a number of samples was carried out.

We have generated a series of 14 thermodynamic diastereomers and 4 kinetic diastereomers (Table 38) with regiochemistry and stereochemistry confirmed in four cases by single crystal X-ray diffraction. Additional to this novelty, are the 1,4,2-oxathiazole-*S*-oxide regioisomers formed as minor by-products in these reactions. Careful chromatography lead to the isolation, identification and characterisation of a series of 1,4,2-oxathiazole-*S*-oxides, both Regioisomer A and Regioisomer B which are diastereomers. Although a few reports of these types of compounds exist in the literature they are described as thermally unstable and quickly undergo cycloreversion reactions.[104] Additionally, three examples of a 1,4,2-oxathiazole were isolated from rhodium acetate catalysed batch reactions in moderate yields as minor byproducts, the structure and regiochemistry of one (**241**) of which was confirmed by crystallography (see Section 2.7.4.3, figure 76).

Table 38: Summary of isolated cycloadducts from continuous flow 1,3-dipolar cycloaddition reactions under thermolysis conditions.

		Thermodynamic Product 	**Kinetic Product** 	**Regioisomer** 
R= H	R^1=4-NO_2	52% - **237**	-	-
	R^1=2,5-difluoro	11% - **256**	-	-
	R^1=4-*t*Bu	30% - **253**	-	5% - **265** A
	R^1=4-F	35% - **250**	12% - **251**	4% - **252** A
	R^1=H	32% - **246**	-	-
R= 2-Me	R^1= 4-F	45% - **271**	-	12% - **273** A
	R^1= 4-*t*Bu	26% - **274**	-	-
	R^1= 4- NO_2	20% - **277**	-	-
	R^1= H	30% - **268**	-	-
R= 4-Me	R^1=H	34% - **283**	-	25% - **285** A
	R^1= 4-F	36% - **286**	5% - **287**	10% - **288** A
	R^1= 4-NO_2	45% - **291**	11% - **292**	-
	R^1= 4-*t*Bu	15% - **289**	-	-
	R^1=2,5-difluoro	16% - **294**	-	-

2.7.4 Spectroscopic characteristics of cycloadducts

2.7.4.1 Spectroscopic characteristics of 1,2,5-oxathiazole-*S*-oxide cycloadducts

With transition metal catalysed batch reaction conditions established for the preferential generation of kinetic 1,2,5-oxathiazole-*S*-oxide isomers and continuous flow thermolysis conditions to generate the thermodynamic 1,2,5-oxathiazole-*S*-oxide isomers, a series of both diastereomers were generated, isolated and characterised as pure compounds. Single crystal X-ray diffraction and subsequent analysis of the single crystals has confirmed the structure of the thermodynamic series both in terms of regiochemistry and stereochemistry. Characteristic ^{1}H NMR and ^{13}C NMR signals have also been identified for each of the series.

The signal in the ^{13}C NMR spectrum corresponding to the spiro carbon is indicative of both the stereochemistry and regiochemistry of the cycloadduct present. In addition the $ArCH_2$ signal is very sensitive in both diastereomers and can be used to indicate the relative stereochemistry.

The key spectroscopic characteristics of the thermodynamic isomers of the 1,2,5-oxathiazole-*S*-oxides are consistent across the series, presumably suggesting that the stereochemistry at the spiro centre and the sulfoxide is common to the series of compounds. The majority of these compounds are high melting point crystalline solids and the variation at the spiro centre is extremely small at a minimum of 96.5 ppm and a maximum of 97.8 ppm in the ^{13}C NMR spectrum (Figure 71) (compared to 92.5 ppm to 93.4 ppm for the kinetic 1,2,5-oxathiazole-*S*-oxide isomers). The AB_q signals for the diastereotopic CH_2 signal, in the ^1H NMR spectrum, are consistently observed between 3.25 and 3.54 ppm for the first doublet, and the second doublet is observed between 3.98 and 4.08 ppm, for all examples. The coupling constants for these signals vary from 18.8 Hz to 19.4 Hz. The characteristic signal of the cycloadducts derived from the unsubstituted indanone moiety (**237**, **246**, **253**, **250** and **256**, highlighted in red), from the 2-Me indanone moiety (**277**, **274**, **268** and **271**, highlighted in blue) and the 4-Me indanone moiety (**291**, **289**, **283**, **286** and **294**, highlighted in green) are highlighted below (Figure 71).

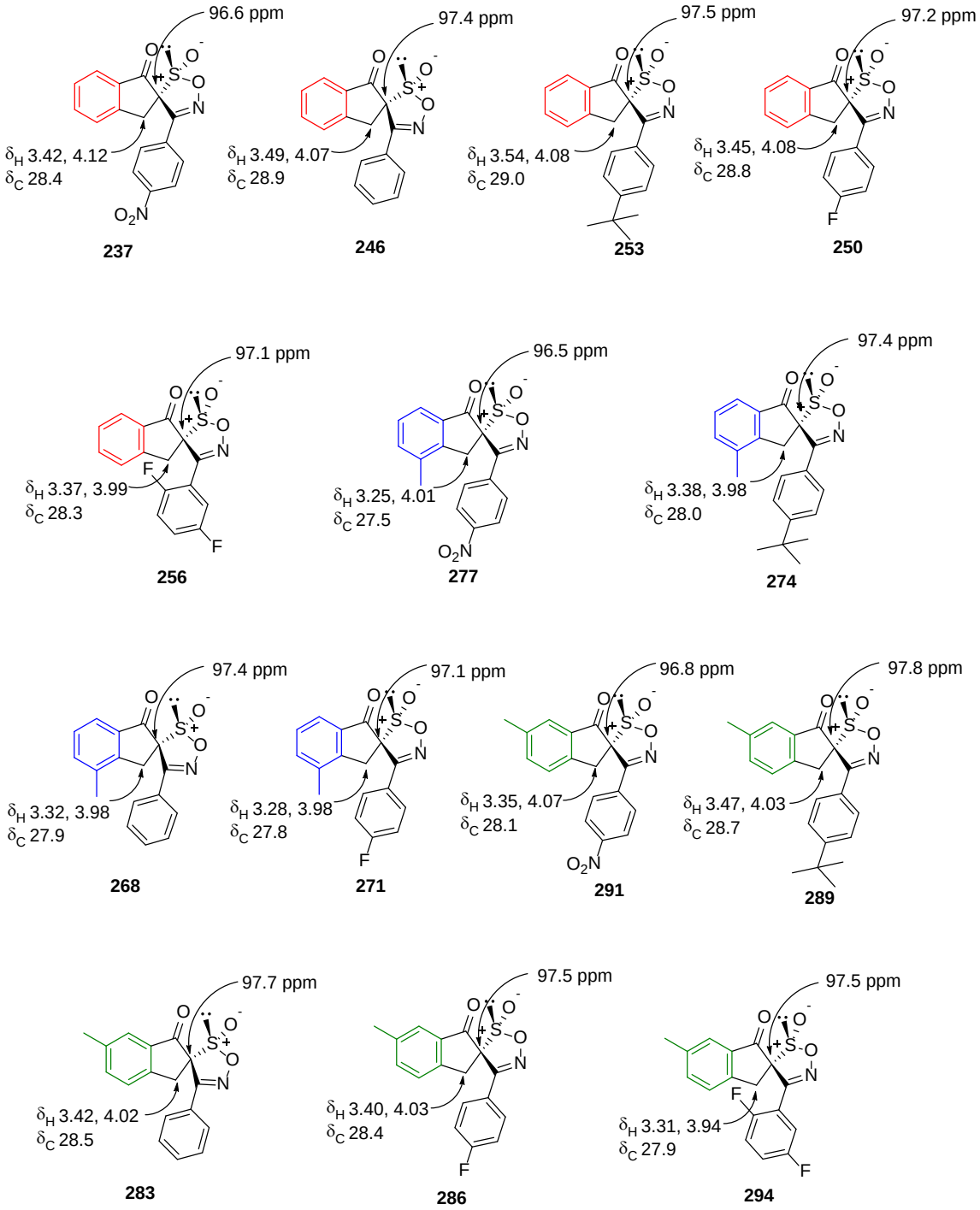


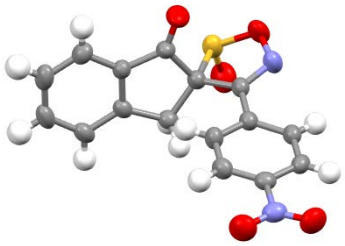
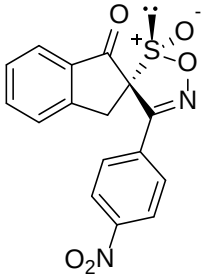
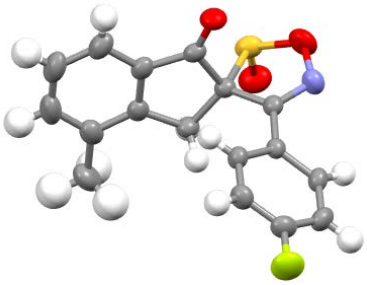
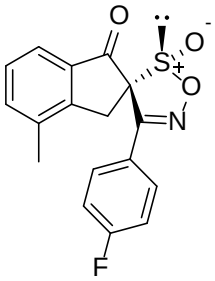
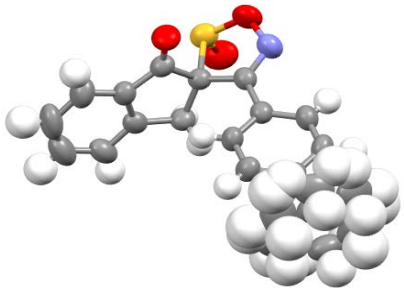
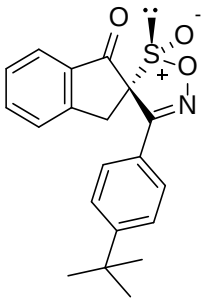
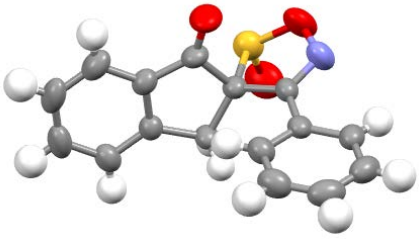
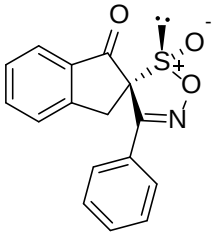
Figure 71: Characteristic ^{13}C NMR signal of the thermodynamic 1,2,5-oxathiazole-S-oxide isomers.

It appears that there is a minor difference absorption of the sulfinyl moiety in the infrared spectrum of the kinetic and thermodynamic 1,2,5-oxathiazole-*S*-oxides. For the thermodynamic isomers the signal is located between a minimum of 1149 cm^{-1} and a maximum of 1162 cm^{-1}, whereas for the kinetic isomers the absorption is consistently between 1160 and 1168 cm^{-1}. Notably, the absorption is clearly distinct from the standard sulfoxide band (1030 – 1080 cm^{-1}),

and more closely related to a sulfone band (1120 – 1160 cm^{-1}), due to the additional oxygen on sulfur.

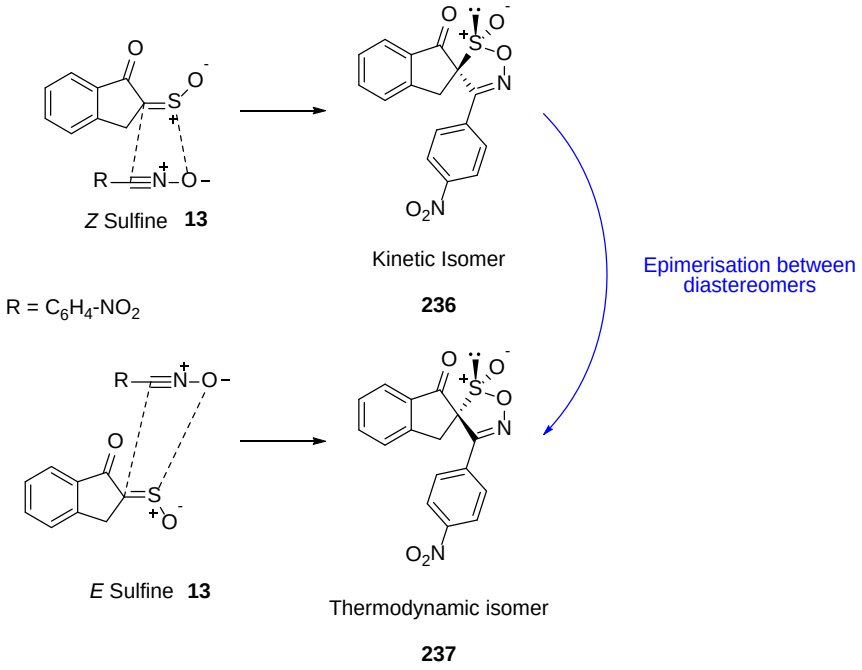
The carbonyl stretch of these thermodynamic 1,2,5-oxathiazole-*S*-oxides can not be used to distinguish whether the product is the kinetic or thermodynamic isomer. The stretches recorded for the series of kinetic isomers have a narrow range between 1711 to 1716 cm^{-1} for the carbonyl. For the thermodynamic isomers, the carbonyl stretch in the infrared spectrum varies between 1707 cm^{-1} to 1721 cm^{-1}. A number of single crystals of the thermodynamic isomers of the 1,2,5-oxathiazole-*S*-oxides were grown by the slow vapour diffusion method using dichloromethane as solvent and hexane as antisolvent. Slow evaporation resulted in the successful formation of single crystal and these underwent single crystal X-ray analysis. These structures of **237**, **271**, **253** and **246** are illustrated in Table 39.

Table 39: Confirmation of regiochemistry and stereochemistry for a range of thermodynamic 1,2,5-oxathiazole-S-oxides. Structures are displayed using the Mercury 2.7 package.

Crystal Structure	1,2,5-Oxathiazole-*S*-oxide
	 **237**
	 **271**
	 **253**
	 **246**

Noteworthy, is the fact that in each of these structures confirmed by single crystal analysis the carbonyl oxygen is located at a maximum distance away from the sulfoxide oxygen, due to electronic repulsion between the two electron rich atoms. This may be a thermodynamic driver for the interconversion from the kinetic diastereomer to the thermodynamic. The relative

stereochemistry in **237**, **271**, **253** and **246** is consistent with trapping of the thermodynamic *E* sulfine, although it appears that these isomers can also arise from initial cycloaddition to the *Z* sulfine followed by epimerisation (see section 2.7.1.3).

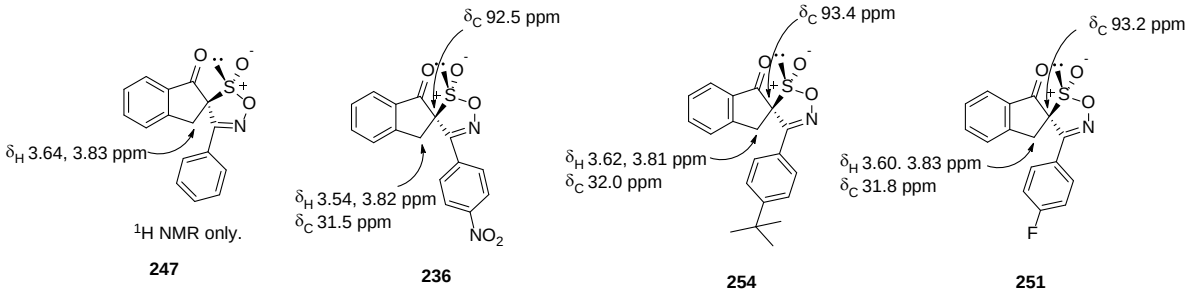


Scheme 103

In the kinetic 1,2,5-oxathiazole-*S*-oxide diastereomers, the spiro carbon is consistently observed between the narrow range of δ_C 92.5 and 93.4 ppm (Figure 72). For the diastereotopic protons alpha to the chiral spiro centre, an AB_q system is observed in the ^1H NMR spectrum. The first doublet signal is consistently observed between 3.53 and 3.64 pm for all examples, and the second is observed between δ_H 3.77 and 3.88 ppm for all examples. The coupling constants for these signals vary from 18.0 Hz to 18.5 Hz. Critically, these signals are distinct from the corresponding signals for the thermodynamic diastereomers.

The kinetic isomer **247** was isolated from a rhodium catalysed batch reaction, however when the ^{13}C NMR was obtained after eight months, the sample had converted to the thermodynamic isomer **246**. The other cycloadducts **236**, **254** and **251** were successfully isolated and characterised as the kinetic diastereomer only, from rhodium catalysed reactions (see section 2.7.1.3). One comparable cycloadduct **292**, was isolated from a continuous flow thermolysis reaction (Figure 72).

Kinetic isomers isolated from batch reactions



Kinetic isomers isolated from continuous flow thermolysis reactions

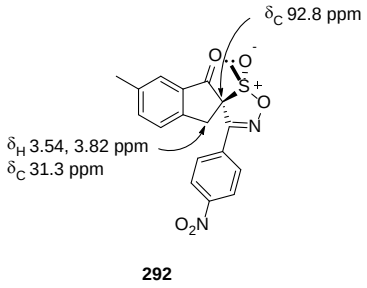


Figure 72: Characteristic signals of the kinetic 1,2,5-oxathiazole-S-oxide isomers.

In reaction conditions where both the kinetic and thermodynamic 1,2,5-oxathiazole-*S*-oxide diastereomers are present, the order of relative polarities are consistent across the series. Also, across the series the least polar compound is the 1,4,2-oxathiazole, followed by the thermodynamic 1,2,5-oxathiazole-*S*-oxide, then the kinetic 1,2,5-oxathiazole-*S*-oxide, and subsequently the 1,4,2-oxathiazole-*S*-oxide Regioisomers A and B. As Regioisomer A and Regioisomer B were not both isolated from one single reaction, their respective polarities are not known.

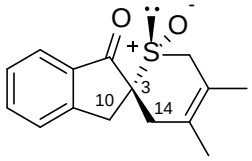
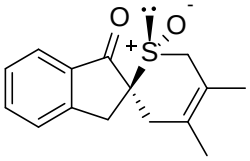
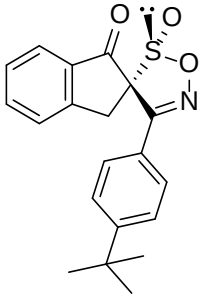
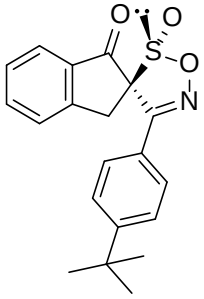
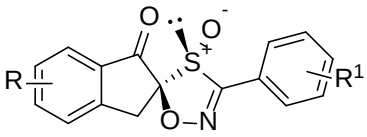
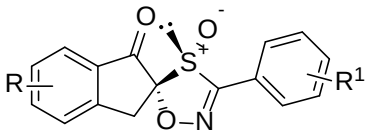
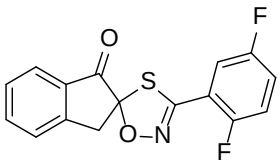
2.7.4.2 Spectroscopic characteristics of 1,4,2-oxathiazole-*S*-oxide cycloadducts.

The formation of the 1,4,2-oxathiazole-*S*-oxide Regioisomers A and B, is a minor reaction pathway under all reaction conditions. Characteristic of the 1,4,2-oxathiazole-*S*-oxide regioisomer is the carbonyl absorption at higher wavenumbers, consistently between 1721 cm^{-1} at a minimum and 1726 cm^{-1} at a maximum. Additionally, on analysis of the spectroscopic characteristics of the regioisomers, the shift of the spiro centre is characteristic of the 1,4,2-oxathiazole-*S*-oxide regiosiomer, specifically, this signal is deshielded to *ca*. 108 ppm in Regioisomer A and *ca*. 110 ppm for Regioisomer B. In the corresponding sulfide, Regioisomer C, the spiro centre appears *ca*. 102 ppm. The key evidence in the switch in regiochemistry is the deshielding of the spiro carbon due to the electronegative oxygen relative to the 1,2,5-oxathiazole-*S*-oxide. Furthermore,

depending on the diastereomer present, the CH_2 signals are very characteristic and distinctive. Analysis of this change, and comparison to similar cycloadducts allows the tentative assignment of relative stereochemistry in the regioisomers (Table 40).

The relative stereochemistry of **136**, **135** and **253** are known by single crystal X-ray diffraction. Characteristic signals for the aromatic CH_2 are shielded in the ^{13}C NMR spectrum for diastereomer 1 **136** and **253**, while with diastereomer 2, the corresponding ^{1}H NMR signals are more separated. This pattern aligns more closely with the pattern seen for Regioisomer B i.e. δ_C CH_2 appears at 28 ppm compared to 33 ppm in Regioisomer A. While X-ray crystallography would be required to definitively confirm the relative stereochemistry, Regioisomer B is tentatively assigned, as outlined in Table 40.

Table 40: Comparison of spectral characteristics for determination of stereochemistry of the 1,4,2-oxathiazole-S-oxides.

Entry		
	Diastereomer 1	Diastereomer 2
1		
	136 [a]: δ_C CH_2: 31.3, δ_C C_{spiro}: 68.5	**135** [a]**:** δ_C CH_2: 37.2, δ_C C_{spiro}: 63.7
2		
	Thermodynamic **253** [b]: δ_C CH_2: 29.0, δ_C C_{spiro}: 97.5 δ_H 3.54, 4.08	Kinetic **254**: δ_C CH_2: 32.0, δ_C C_{spiro}: 93.4 δ_H 3.62, 3.81
3		
	Regioisomer B **255** R=H, R^1 = 4-^{t}Bu δ_H 3.44, 4.19 Comparable compounds shows the following pattern: **248** R=H, R^1 = H δ_H 3.66, 4.20 δ_C CH_2: 28.6, δ_C C_{spiro}: 110.8 **270** R= 2-Me, R^1 = H δ_H 3.72, 4.28 **279** R= 2-Me, R^1 = 4-NO_2 δ_H 3.51, 4.31 **266** R=H, R^1 = 2,5-difluoro δ_H 3.26, 4.21	Regioisomer A **265** R=H, R^1 = 4-^{t}Bu δ_C CH_2: 33.6, δ_C C_{spiro}: 107.9 δ_H 3.31, 3.47 **252** R=H, R^1 = 4-F δ_C CH_2: 33.6, δ_C C_{spiro}: 108.4 δ_H 3.33, 3.51 **273** R= 2-Me, R^1 = 4-F δ_C CH_2: 32.4, δ_C C_{spiro}: 108.2 δ_H 3.15, 3.41 **288** R=4-Me, R^1 = 4-F δ_C CH_2: 33.3, δ_C C_{spiro}: 108.7 δ_H 3.26, 3.45 **285** R=4-Me, R^1 = H δ_C CH_2: 33.3, δ_C C_{spiro}: 108.5 δ_H 3.26, 3.45
4	 **241** 1,4,2-Oxathiazole **241** : δ_C CH_2: 42.5, δ_C C_{spiro}: 101.1	

	δ_H 3.78, 3.91
	239 R=H, R^1 = 4-NO_2
	δ_C CH_2: 42.3, δ_C C_{spiro}: 102.2
	δ_H 3.82, 3.95
	249 R=H, R^1 = H
	δ_C CH_2: 42.7, δ_C C_{spiro}: 101.1
	δ_H 3.79, 3.92

[a]Confirmed by single crystal X-ray diffraction by Buckley.
[b]Confirmed by single crystal X-ray diffraction in this work.

Regioisomers A and B exhibit a shift of the spiro centre in the ^{13}C NMR region between 107.9 to 108.7 ppm for Regioisomer A (Figure 73, **265**, **252**, **273**, **288**, **285**) and *ca*. 110 - 111 ppm for Regioisomer B (Figure 74, **248**, **266**, **255**, **270**, **279**). The majority of these regioisomers are isolated as pure compunds from the continuous flow thermolysis reactions. Unambiguous confirmation of the stereochemistry has not been possible to date as these Regioisomers A and B are not readily crystallised.

The infrared data is also consistent across the series of Regioisomers A, with strong absorptions for both the sulfoxide moiety (Figure 73, blue) and the carbonyl signal (Figure 73, red). Additional to this is the strong absorption for the C-O bond which appears consistently between the range of 1238 – 1280 cm^{-1} for each of the derivatives. The presence of the strong sulfoxide absorption in the infrared spectra combined with the presence of the molecular ion of each derivative in high resolution mass spectrometry strongly supports the assigned structures. Notably, the infrared absorption for the sulfoxide stretch in these derivatives appears in the expected region of 1030 – 1080 cm^{-1}, which is in contrast to the 1,2,5-oxathiazole-*S*-oxide derivatives which appear between 1149 and 1168 cm^{-1}.

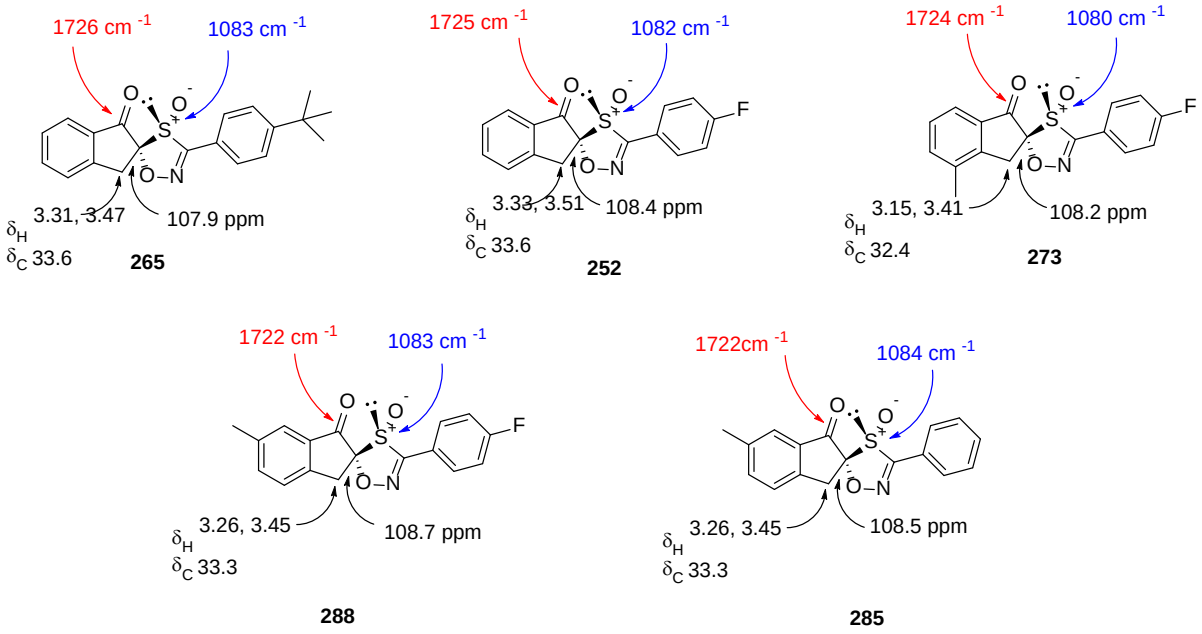


Figure 73: Characteristic signals in the ^{13}C NMR spectra and infrared spectra of the Regiosiomer A 1,4,2-oxathiazole-S-oxides.

These are in contrast to the 1,4,2-oxathiazole-*S*-oxides Regioisomers B, where only one example **248**, was isolated and characterised. In other instances, the corresponding signals to the regioisomer B were present in the ^{1}H NMR of the crude material. The one isolated sample, and the analogous compounds – are highlighted below. The fully characterised Regioisomer B **248**, is from a rhodium catalysed batch reaction, whereas **255**, **266**, **270** and **279** were all isolated from continuous flow thermolysis reactions.

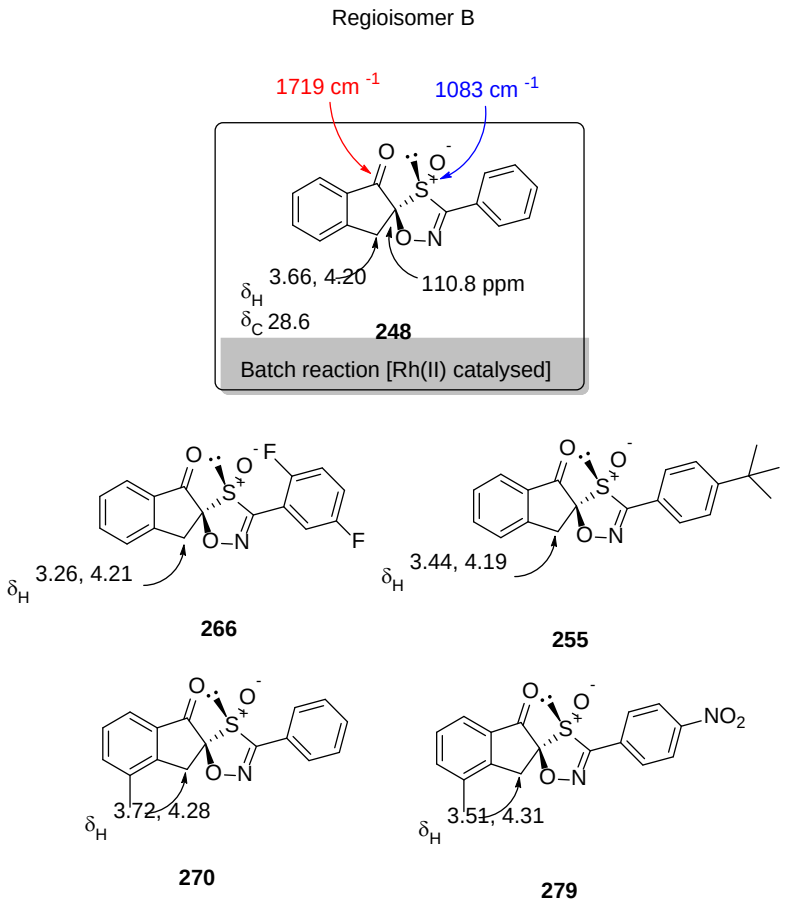


Figure 74: Characteristic signals in the ^{13}C NMR spectra and infrared spectra of the second diasteromer of the Regiosiomer B 1,4,2-oxathiazole-S-oxides.

Securing crystallographic data to definitively confirm structural and stereochemical assignments would be useful.

2.7.4.3 Spectroscopic characteristics of 1,4,2-oxathiazole cycloadducts.

Three derivatives of the 1,4,2-oxathiazoles (**239**, **249**, **241**) were isolated, and only from the rhodium catalysed batch reactions. The shift of the spiro centre is consistently observed between a narrow range of 101.1 – 102.2 ppm in the ^{13}C NMR spectrum for the three compounds (Figure 75). In the ^{1}H NMR spectrum, the aromatic-CH_2 AB_q of these sulfide derivatives, displays much less separation compared to the 1,2,5- and 1,4,2-oxathiazole-*S*-oxide derivatives. This is due to the absence of deshielding on one proton, due to the absence of the sulfinyl oxygen.

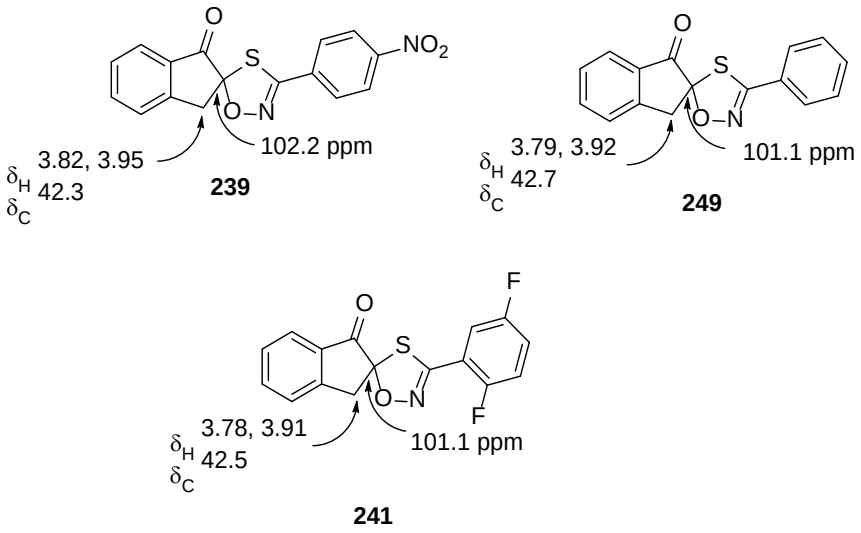


Figure 75: Characteristic signal in the ^{13}C NMR spectra of the 1,4,2-oxathiazole-S-oxide regioisomer.

The regiochemistry and sulfide oxidation level was confirmed on growing a single crystal of the regioisomer **241**.

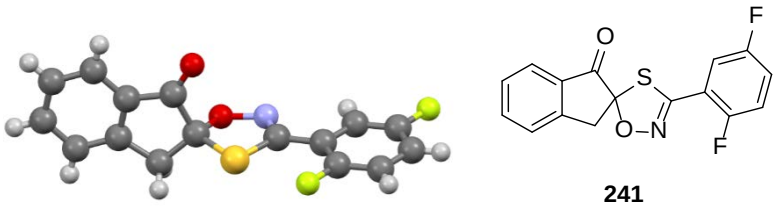


Figure 76: Single crystal analysis of **241** *confirmed the stereochemistry and regiochemistry of the sulfide, as well as the absence of the sulfinyl oxygen.*

Comparison of the 1,4,2-oxathiazoles (only one stereoisomer possible) to the Regioisomers A and B which are 1,4,2-oxathiazole-*S*-oxide derivatives is interesting; the sulfoxides are primarily isolated from the continuous flow thermolysis reactions. Notably, the 1,4,2-oxathiazole derivatives (at the sulfide level of oxidation) are the least polar cycloadducts formed in these reactions and consistently elute from the column first on purification.

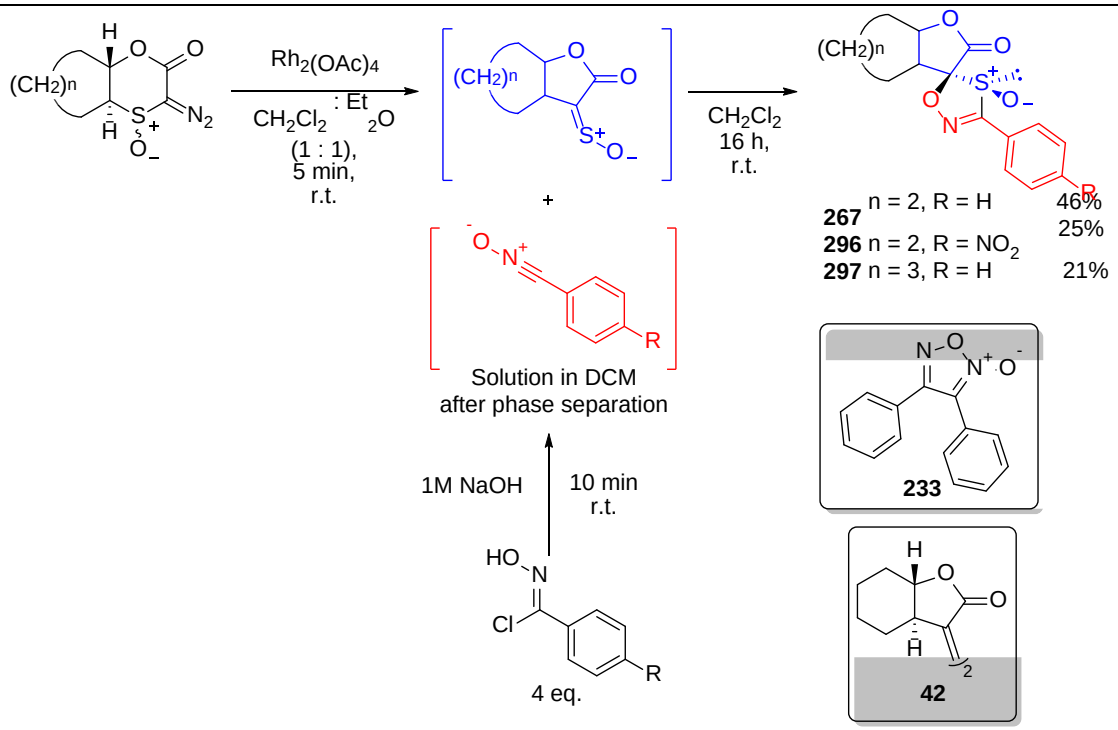
2.8 Cycloaddition reactions of lactone derived α-oxo sulfines with nitrile oxides

2.8.1 Initial Investigation

The cycloaddition of a series of lactone derived α-oxo sulfines with nitrile oxide dipoles was also explored. The objective of this exploration was to achieve generation and reaction of the reactive lactone derived α-oxo sulfines with nitrile oxides *in situ,* using either transition metal catalysis, or thermolysis and to establish the impact of the alteration from a ketone to a lactone on the sulfine reactivity. Notably, the regiochemistry of nitrile oxide cycloaddition with lactone derived α-oxo sulfines leads to 1,4,2-oxathiazole-*S*-oxides, which is in contrast to the outcome observed with the ketone derived α-oxo sulfines.

To enable the cycloaddition to occur, the nitrile oxide dipole **192** was pre-formed from the imidoyl chloride **193**, following the procedure developed by Kissane, as described above.[123] The nitrile oxide is subsequently added as a solution in dichloromethane to the corresponding cyclohexyl α -diazosulfoxide **38,39** (1 : 1), or the cycloheptyl α-diazosulfoxide **75**. This addition is followed directly by the addition of rhodium acetate dimer (1 mol %) to induce the hetero-Wolff rearrangement leading to generation of the α-oxo sulfine **101** *in situ* which provides the dipolarophile for the 1,3-dipolar cycloaddition reaction. The reaction solvent used was a mixture of dichloromethane and ether (1 : 1) and the reaction mixture is stirred at room temperature (Table 41).

Table 41: Results of dipolar cycloaddition of lactone derived α-oxo sulfines and nitrile oxides.



	n =	R =	Isolated Products	Compounds not isolated, but present in crude material
1	2 (**38** : **39**, 1 : 1)	H (dipole **192**)	**267 : A**, 10 : 1 (46%)	**233**, **41**
2	2 (**38** : **39**, 1 : 1)	NO_2 (dipole **235**)	**296** (25%)	**41**
3	3 (**75**, axial only)	H (dipole **192**)	**297** (21%) **298** (7%)	**299**[a], **300**[a], **41**

[a] Presumably these are two more minor cycloaddition products.

In Table 41, entry 1, three hours after addition of the freshly prepared nitrile oxide dipole **192**, a precipitate started to form, and after sixteen hours this precipitate was isolated by filtration. Analysis of the white precipitate led to the identification of the 1,4,2-oxathiazole-*S*-oxide cycloaddition product **267** as a single component, in a yield of 46%, with a characteristic CHO signal at 4.35 ppm in the ^{1}H NMR spectrum.[x] There was evidence for a minor cycloadduct **A**, present as <9% of the material, with a characteristic CHO signal present at 4.46 ppm, however the

[x] On repeating this reaction, the yields recovered were variable, presumably due to the efficiency of precipitation.

regio- and stereochemistry is not known but the compounds is believed to be either **301**, **302**, or **303** (Figure 77).[xi]

Analysis of the concentrated mother liquor was also undertaken to provide insight into the other components in the reaction mixture. Due to the use of excess dipole, significant amounts of the furoxan dimer **233** were formed. Both **233** and **41** were identified by characteristic signals in ^{1}H NMR spectrum of the crude material. Additionally, dimerization of the α-oxo sulfine **101** *in situ* resulted in the formation of substantial amounts of the alkene dimer **41**. The presence of the furoxan dimer **233** and alkene dimer **41** made chromatographic purification of the mother liquor challenging and as a result no other components were isolated from the reaction mixture as pure compounds. The presence of both dimers formed from the dipole and dipolarophile highlight that dimerisation competes with dipolar cycloaddition.

This 1,3-dipolar cycloaddition has the possibility of forming two regioisomers and four diastereomers per regioisomer. A single crystal of **267** was recrystallised from the precipitated material using methanol, and allowed confirmation of the regiochemistry and the relative stereochemistry. From the crystal structure it is clear that the cycloadduct is formed from addition of the nitrile oxide to the upper face of the kinetic *Z* α-oxo sulfine, as illustrated in Figure 77. As the sulfine is generated and trapped *in situ*, formation of this cycloadduct is entirely in line with our results with dienes where the *Z* α-oxo sulfine is the kinetic sulfine. This is in comparison to the Diels Alder cycloaddition with 2,3-dimethyl-1,3-butadiene in which trapping occurs from the α-face.

It seems that the regioselectivity of the dipolar cycloadditions of lactone derived α-oxo sulfines and ketone derived α-oxo sulfine is the opposite, suggesting that introduction of the lactone oxygen has a significant effect on the frontier molecular orbital coefficients of the sulfine. This is not unexpected as cycloaddition of electron rich dipolarophiles are dipole LUMO controlled whereas electron deficient dipolarophiles are both dipole HOMO and dipole LUMO controlled.

As reported in the literature and mentioned earlier, in an isolated sulfine the largest atomic coefficient in the LUMO is on the carbon while in the oxo-sulfine the polarisation is reversed with the largest coefficient now at sulfur.[140] It seems introduction of the lactone oxygen reverses the

[xi] The stereochemistry of the possible cycloadducts to be formed (**267**, **301**, **302**, and **303**) are highlighted below in Figure 77. However, aside from **267**, it is not known which signal in the ^{1}H NMR spectrum corresponds to which cycloadduct, and therefore the cycloadduct with unknown stereochemistry will be referred to as cycloadduct **A**.

polarisation of the sulfine LUMO again, leading to preferential formation of the 1,4,2-oxathiazole-*S*-oxide derivatives.

The other 1,4,2-oxathiazole-*S*-oxide diastereomers possible are **301**, **302** and **303** and one of these may correspond to the signal at 4.46 ppm assigned to cycloadduct **A**. Notably, in the isolated precipitate and in the concentrated mother liquor there was no evidence for the formation of the opposite regioisomeric products, the 1,2,5-oxathiazole-*S*-oxide. This is in contrast to the cycloadditions of the ketone derived α-oxo sulfines in which the 1,2,5-oxathiazole-*S*-oxide is the major product in all cases.

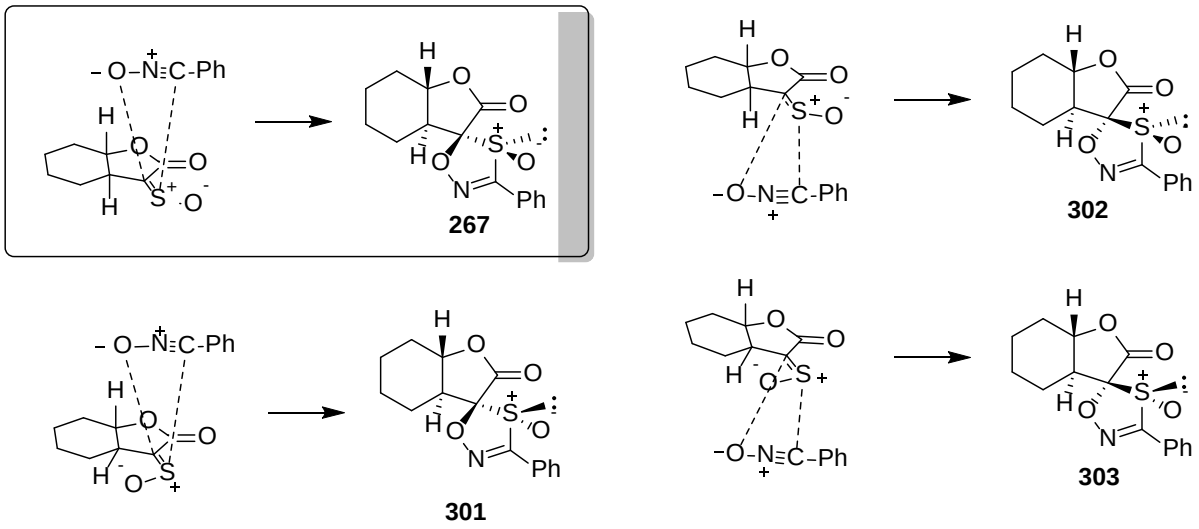
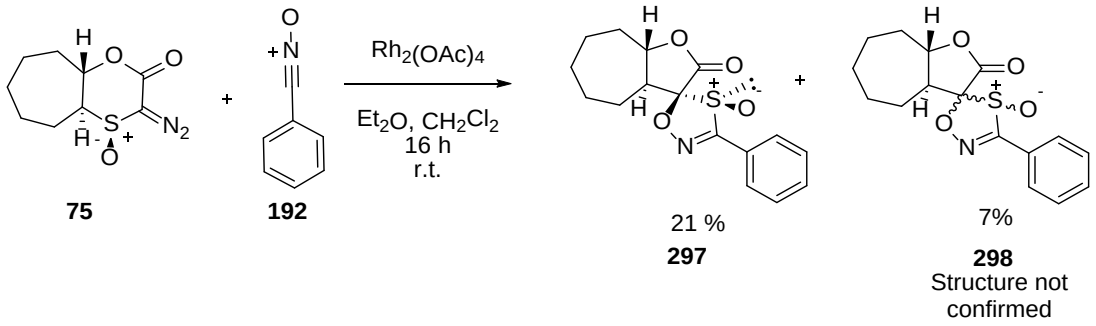


Figure 77: Four possible approaches for the formation of the diasteromers are possible. Approach of the nitrile oxide from above to the E α-oxo-sulfine leads to the cycloadduct **267** *confirmed by single crystal X-ray diffraction.*

These cycloaddition reaction conditions were subsequently applied to the *p*-nitro substituted benzonitrile oxide **235** with the α-diazosulfoxides **38,39** (Table 42, entry 2). Once again, the desired 1,4,2-oxathiazole-*S*-oxide **296** was isolated as one diastereomer in a yield of 25% after precipitation from the reaction mixture. Consistent with the previous reaction, dimerisation of the α-oxo sulfine **101** leading to formation of the alkene dimer **41** was a major reaction pathway. No other identifiable cycloadducts were recovered from the reaction mixture.

The cycloheptyl α-diazosulfoxide **75** (Table 41, entry 3) also underwent transformation to the corresponding α-oxo sulfine and subsequent cycloaddition utilising these conditions. After stirring for 16 h in the presence of the dipole and rhodium acetate dimer, a precipitate was isolated from the reaction as one diastereomer only (**297**) in 21% yield. This result was similar to the earlier cycloaddition reactions, where once again the product precipitated from the reaction mixture as a single diastereomer. Analysis of the remaining mother liquor by ^{1}H NMR spectroscopy indicated

the presence of four components, **297**, **298**, **299**, and **300** in a ratio of 0.26 : 0.12 : 1 : 0.32. The components **298**, **299**, and **300** are most likely to be cycloadducts however the corresponding regio- and stereochemistry is unknown. Following concentration of the mother liquor and chromatographic purification on silica gel a minor product, **298**, was isolated in 7% yield and characterised by ^{1}H and ^{13}C NMR. While it may be a cycloadduct the assignment is not confirmed as some spectroscopic details are not easily rationalised for the cycloadduct structure.



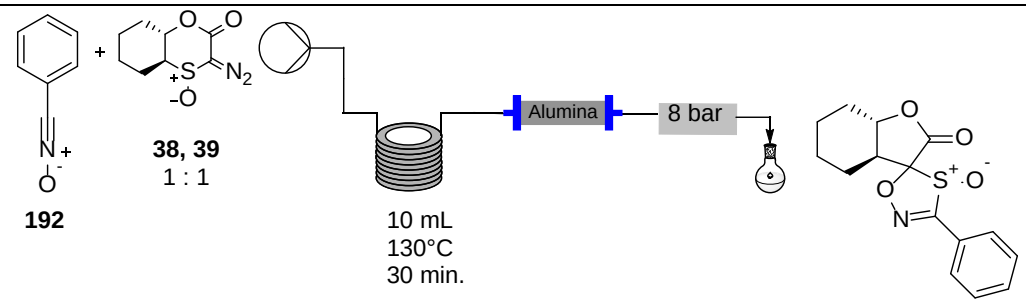
Scheme 104

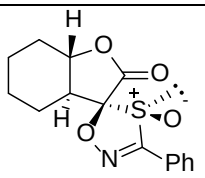
While the relative stereochemistry of the *p*-nitro derivative **296** and the cycloheptyl derivative **297** have not been characterised, it is reasonable to assume that they have the same relative stereochemistry as the structurally confirmed **267,** on the basis that both form a precipitate in the reaction solvent and all three possess similar spectral characteristics, particularly the δ_C of the quaternary spiro carbon with signals between 101.6 and 103.5 ppm. The assignment of the minor product **298** is very tentative at this stage.

2.8.2 Attempts at dipolar cycloaddition of lactone derived α-oxo sulfines in continuous flow, and comparison to batch thermolysis

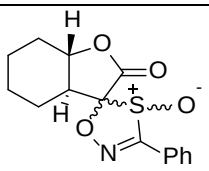
With the success seen with cycloaddition of the ketone derived α-oxo sulfines in continuous flow thermolysis conditions, and in an effort to promote more efficient cycloaddition of the lactone derived α-oxo sulfines to form the 1,4,2-oxathiazole-*S*-oxide **267** with higher yields and in greater diastereoselectivity, the 1,3-dipolar cycloaddition of lactone derived α-oxo sulfines in continuous flow was attempted. A set of three different reaction conditions were utilised to investigate the efficiency of the cycloaddition in continuous flow and these are illustrated in Table 42.

*Table 42: Results from 1,3-dipolar cycloadditions of the lactone derived α-oxo sulfine **101** in continuous flow.*

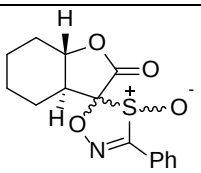




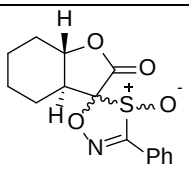
267
(4.35 ppm)[a]



A
(4.46 ppm)[a]



B
(4.11 ppm)[a]



C
(3.77 ppm)[a]

	Conditions:	**Optimum for:**	**Product Ratio** (yield)[c]
1	2.6 eq. dipole Alumina column inline CH_2Cl_2/ Ethyl Acetate 10 min residence time 100°C	*1,3-Dipolar cycloaddition* of ketone derived α-oxo sulfines in continuous flow	Unchanged starting material (80%) Unidentifiable decomp. Products (20%)
2	2.6 eq dipole Alumina column inline CH_2Cl_2/ Ethyl Acetate 30 min residence time 120°C	*1,3-Dipolar cycloaddition of lactone derived α-oxo sulfines in continuous flow*	**267 : A: B : C : 304**[b] 1.18 : 0.88 : 0.31 : 1.0 : 0 (25%) Trace : 1 : 0.6 : trace : 0 (12%)
3	2.6 eq. dipole[d] Toluene 30 min residence time 120°C	*1,3-Dipolar* cycloaddition *of lactone derived α-oxo sulfines in continuous flow*	**267 : A : B : C : 304**[b] 0 : 0.9 : 0.3 : 0 : 1 (22%) 0 : 0.9 : 0 : 0 : 1 (8%)

[a] The characteristic signal in the ^{1}H NMR spectrum for each compound is outlined.

[b] The characteristic signal in the ^{1}H NMR spectrum is a CHO signal at 4.34 ppm.

[c] Crude product ratios were not obtained from the ^{1}H NMR spectra due to the complexity of the spectra and overlapping on multiple key signals.

[d] 20 equivalents of the diene are used in the Diels-Alder cycloaddition that use these reaction parameters.

Using the conditions which were optimum for dipolar cycloaddition of ketone derived α-oxo sulfines (Table 42, Entry 1), a ten minute residence time, at 100°C, resulted in recovery of starting material (80%) along with unknown unidentifiable decomposition products (20%). The results reaffirms that the lactone derived α-diazosulfoxides are more thermally stable compared to the

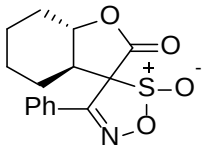
ketone derivatives and need to be heated to a higher temperature to induce the hetero-Wolff rearrangement. In each of the following continuous flow reactions, complete consumption of the α-diazosulfoxide starting material was achieved due to to higher temperature and longer residence time.

Following on from this, the optimum solvent from the 1,3 dipolar cycloaddition conditions of the ketone derived α-oxosulfines were used (DCM/Ethyl Acetate, 1 : 1) along with the optimum parameters of residence time and temperature from the Diels-Alder cycloadditions of the lactone derived α-oxo sulfines (120°C, 30 min), (Table 42, Entry 2). The higher temperature of 120°C and longer residence time of 30 minutes was needed to ensure complete conversion to the α-oxo sulfine, whereas the small excess of dipole and alumina column inline are necessary to ease purification and enable clean isolation of the desired cycloadducts. These reaction conditions (Table 42, Entry 2) resulted in formation of a complex mixture of products containing four cycloadducts. The stereochemistry of the possible cycloadducts to be formed (**267**, **301**, **302**, and **303**) are highlighted above in Figure 77. However, aside from **267** it is not known which signal corresponds to which cycloadduct and therefore the three cycloadducts with unknown stereochemistry will be referred to as cycloadducts **A**, **B** and **C**. **A**, **B** and **C** are most likely **301**, **302**, and **303** although it is not known which is which.

After purification by column chromatography on silica gel the first fraction isolated contained these four components **267** : **A** : **B** : **C** in a ratio of 1.18 : 0.88 : 0.31 : 1.0 and in 25% yield. A second fraction was also isolated in a yield of 12%, which contained the four diastereomers but consisted primarily of the cycloadducts **A** and **B**, in a ratio of 1 : 0.6 with trace amounts of both **267** and **C**. There was no evidence observed for the formation of the alkene dimer **41** which is in contrast to the batch reactions in which it was a major component of the crude material.

Additionally, thermolysis in continuous flow was carried out using toluene as the solvent (as is the case for the Diels-Alder cycloaddition reactions of these lactone derived α-diazosulfoxides) with 2.6 equivalents of the dipole **192**, which was again, pre-generated. The formation of four diastereomers was apparent in the ^{1}H NMR spectrum of the crude material. Following chromatographic purification, partial fractionating of the diastereomers occurred, however, as seen earlier, it was not possible to isolate the products as pure compounds. The first fraction (22%) contained a mixture of the 1,4,2-oxathiazole-*S*-oxides **A** and **B** and a previously uncharacterised cycloadduct **304** in a ratio of 0.9 : 0.3 : 1.0. A second fraction isolated from the column contained a mixture of **A** and **304** in a ratio of 0.9 : 1.0 and in 8% yield. The unidentified product **304** has a characteristic signal at 4.34 ppm in the ^{1}H NMR spectrum and 45.0 and 84.8 ppm in the ^{13}C NMR

spectrum. These may correspond to the other regioisomer, a 1,2,5-oxathiazole-S-oxide, however its rare occurance made full characterisation unachievable in this work. Notably this signal corresponding to an previously unseen cycloadduct was not apparent from the other reactions and this may be due to a solvent effect (toluene compared to Ethyl Acetate/DCM).



304

Figure 78

When the corresponding thermolysis reaction was carried out in batch reaction conditions (30 min, oil bath at 130°C, 2.6 eq. dipole), the crude material was a clean, unreacted combination of the α-diazosulfoxides **38,39** and the pre-generated dipole **192**. The inability to reach the suitable temperature in the solvent system of dichloromethane and ethyl acetate leads to boiling and condensing of the solvent, rather than achieving the super-heated temperatures achievable in continuous flow, this results in the hetero-Wolff rearrangement not taking place and recovery of the unchanged starting materials.

2.8.3 Spectroscopic characteristics of lactone derived 1,4,2-oxathiazole-*S*-oxides

A single crystal of the oxathiazle-*S*-oxide **267** was successfully grown from methanol, and the crystal structure has unambiguously confirmed the regiochemistry and relative stereochemistry of the cycloadduct **267** illustrated in Figure 79.

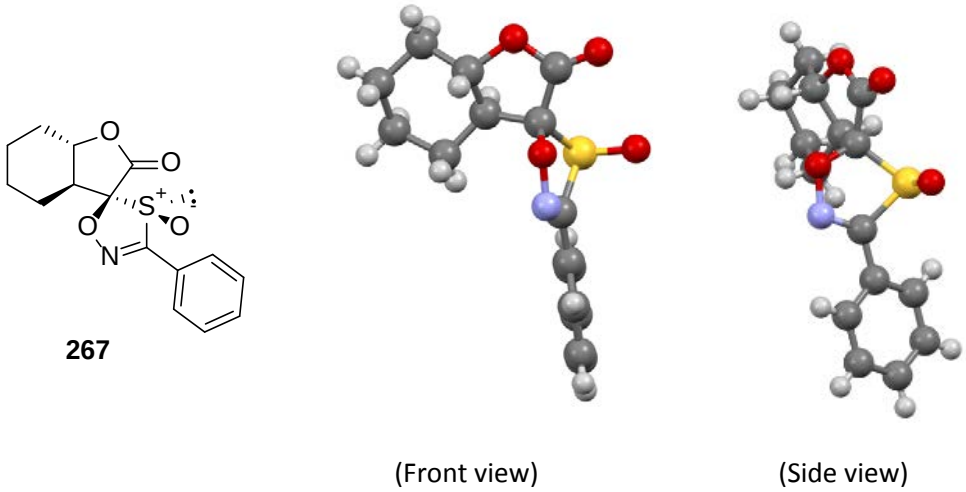


Figure 79: Structure of **267** *unambiguously confirmed by single crystal X-ray diffraction.*

Based on this, the regiochemistry and stereochemistry of other derivatives, **296** and **297**, have been assigned by comparison of their spectroscopic data. Characteristic signals are the spiro centres which are consistently observed between δ_C 101.6 and 103.5 ppm and the CHO proton which is consistenly observed between δ_H 4.27 – 4.50 ppm for the three cycloadducts. The second product **298**, isolated from the reaction of the cycloheptyl α-diazosulfoxide **75** has unknown structure and stereochemistry.

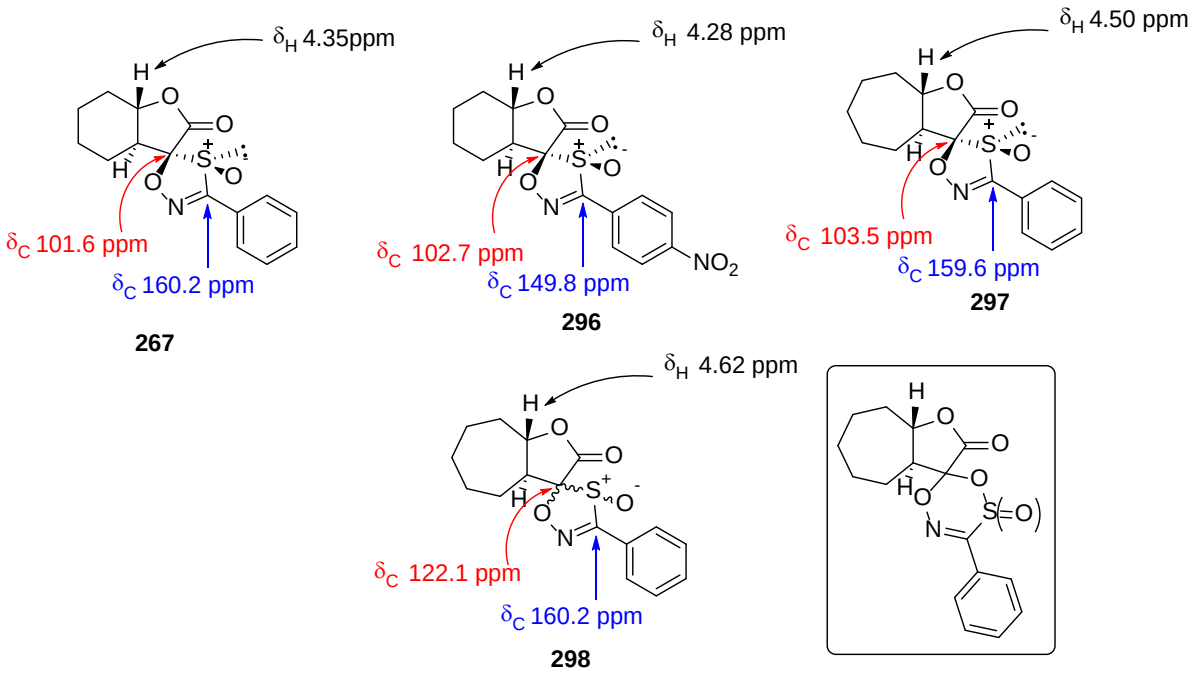


Figure 80: Characteristic signals from the ^{1}H and ^{13}C NMR spectra of the lactone derived 1,4,2-oxathiazole-S-oxides.

Interestingly, the two products **297** and **298** were isolated separately. **297** was successfully isolated by precipitation from the reaction mixture while chromatographic purification led to the isolation of **298** from the mother liquor. Illustrated below in Figure 81, **297** is in the top ^{13}C spectra and below is **298** showing the significant differences between the two products, most notable being the spiro centre, outline in blue. The alteration in the δ_C for the carbonyl, one of the methylenes and the spiro centre are difficult to rationalise for **298,** and it may be a different product other than a diastereomeric cycloadduct. During discussion at the *viva* an alternative structure for **298** was proposed as illustrated above.

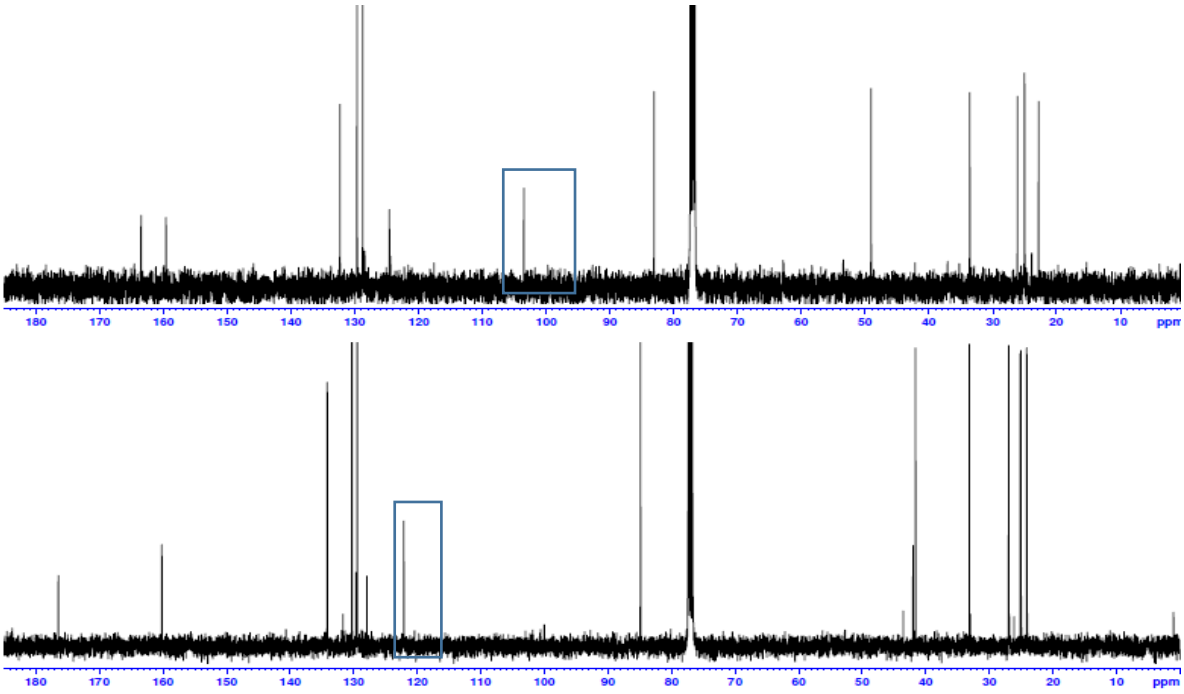


*Figure 81: Comparison of the ^{13}C NMR spectra of the 1,4,2-oxathiazole-S-*oxides **297** *(top) and minor product* **298** *(bottom)*. The signal for the spiro centre, which does not appear in a DEPT 135, is outlined in blue.

The characteristic spectroscopic signals of the product **267** are comparable to the 1,4,2-oxathiazole-*S*-oxides **265** and **248** isolated from the reactions of the ketone derived α-oxo sulfines with the nitrile oxide dipoles. The spiro carbon of **267** is recorded at 101.6 ppm, compared to 107.9 for **265** and 110.8 in **248** (Figure 82). The characteristic signals of **267** are outlined below inlcuding the distinctive C=N bond which appears at 160.2 ppm and was observed between a minimum of 156.0 and a maximum of 159.4 ppm for the majority of nitrile oxide cycloadducts discussed earlier (Figure 82). Notably the infrared absorption of the sulfoxide functionality is also comparable across the ketone and lactone derived 1,4,2-oxathiazole-*S*-oxides with a minor difference of 7 cm^{-1} between the derivatives. Once again, the S-O stretch is very characteristic of the regiochemistry of the cycloadducts with the sulfoxide in the 1,4,2-oxathiazole-*S*-oxide isomers appearing at approximately 1080 cm^{-1} while in the "sulfinate-like" 1,2,5-oxathiazole-*S*-oxides isomers, the S-O stretch appears at approximately 1160 cm^{-1}. Additional evidence for the 1,4,2-oxathiazole-*S*-oxide regiochemistry is the contrast seen when compared to the spiro centre of the series of 1,2,5-oxathiazole-*S*-oxide derivatives seen previously (section 2.7.4), both kinetic isomers such as **254** and thermodynamic isomers such as **246**. The deshielding as a result of sulfur and oxygen connectivity to the spiro centre is much more apparent in the 1,4,2-oxathiazole-*S*-oxide derivatives.

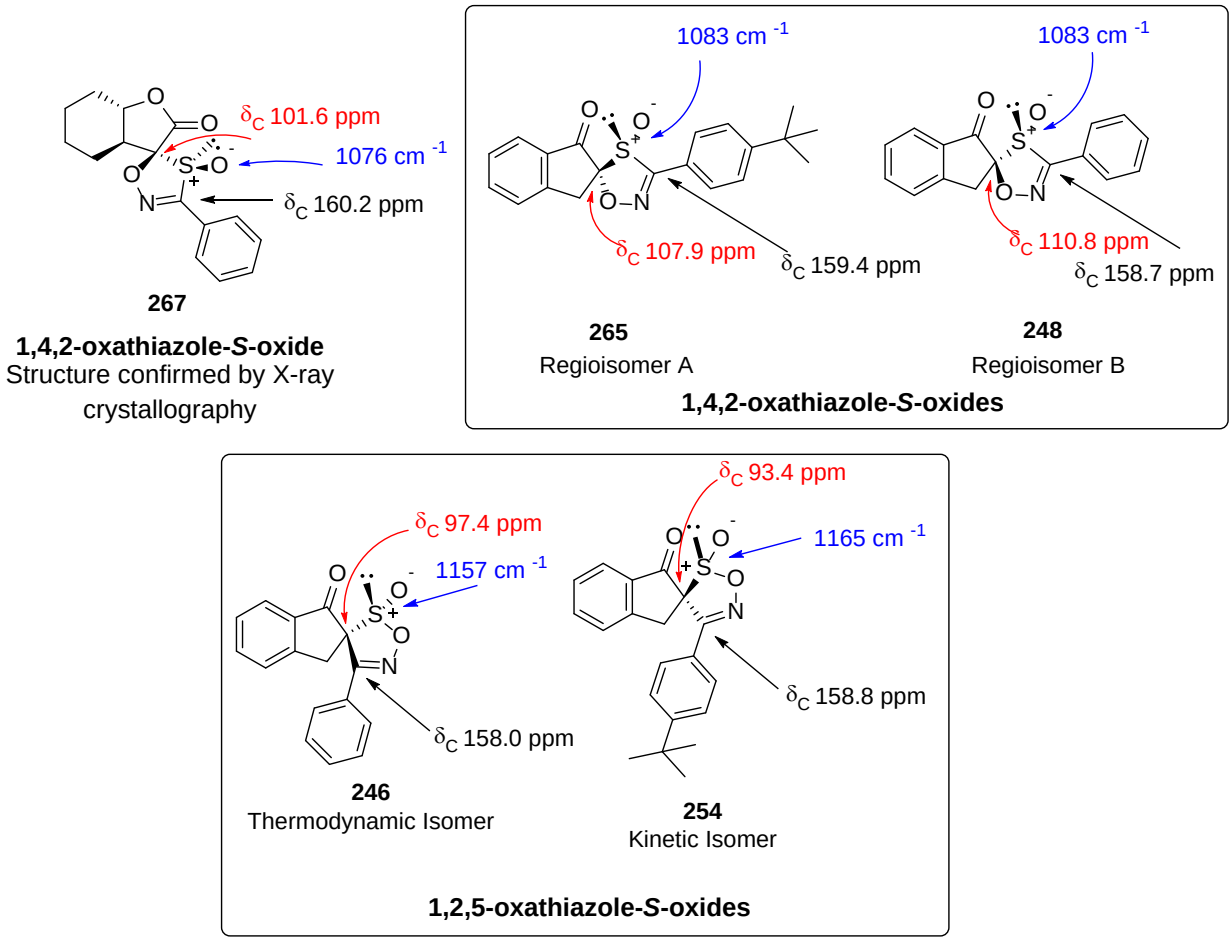
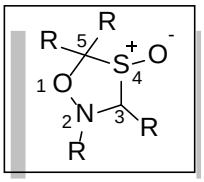


Figure 82: The structure of **267** *has been confirmed by X-ray crystallography. Assignment of the regiochemistry and stereochemistry of the 1,4,2-oxathiazole-S-oxide cycloadduct,* **265** *and* **248** *is by comparison with* **267.** *The contrasting characteristic signals of the 1,2,5-oxathiazole-S-oxide* **246** *and* **254** *are outlined also.*

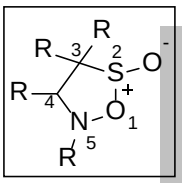
2.9 1,3-Dipolar cycloadditions of lactone derived α-oxo sulfines with nitrones

There are limited reports on the reactions of sulfines with nitrone dipoles (see Section 2.6.1.3) and as outlined above, to the best of our knowledge, no reports exist on the cycloaddition of nitrones **211** or **212** with sulfines. Having carried out an investigation in to the reaction of lactone derived α-oxo sulfines with nitrile oxides, extension of this work to the reactions with nitrones was carried out. Notably, the dipolar cycloaddition of nitrone is in the same classification as nitrile oxides, Type II.[141,142] This means that both dipole LUMO controlled cycloaddition, and dipole HOMO controlled cycloadditions can occur.

In this work, 1,3-dipolar cycloadditions of a range of lactone derived α-oxo sulfines, generated from a range of lactone derived α-diazosulfoxides, with nitrones, resulted in the isolation of a number of heterocyclic compounds. In all cases, the two regioisomeric cycloadducts which were anticipated (Figure 83) were not isolated. Instead, it is reasonable to assume, that the cycloaddition occurs and the intermediate products undergo subsequent rearrangements. It appears that both regioisomers form in the cycloaddition and each regioisomer subsequently undergoes a different rearrangement process to a stable, isolable product.



1,4,2-oxathiazolidine 4-oxide



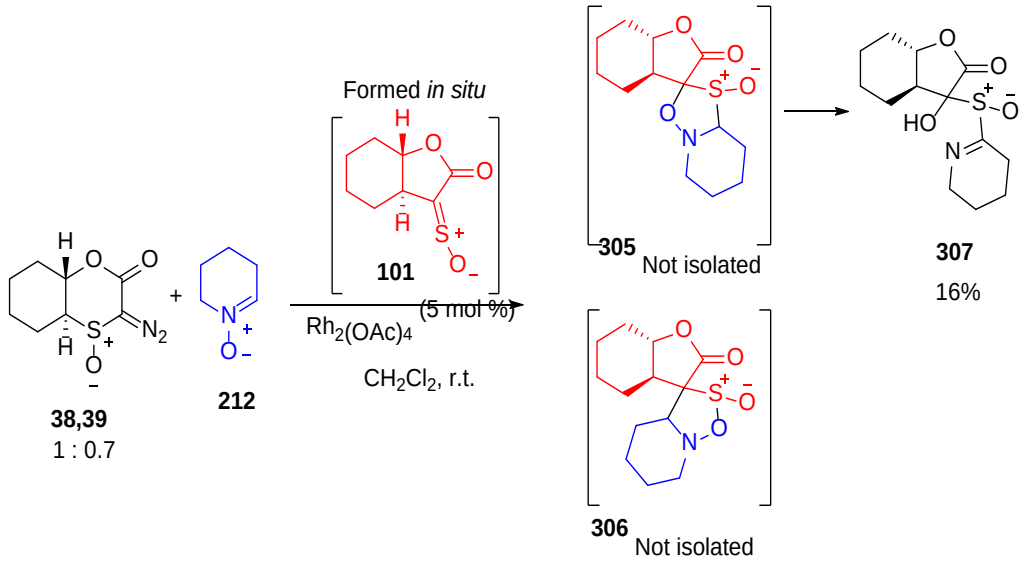
1,2,5-oxathiazolidine 2-oxide

Figure 83: Regioisomeric cycloadducts initially formed.

2.9.1 1,3-Dipolar Cycloadditions of lactone derived α-oxo sulfines with the nitrone 2,3,4,5-tetrahydropyridine 1-oxide 212

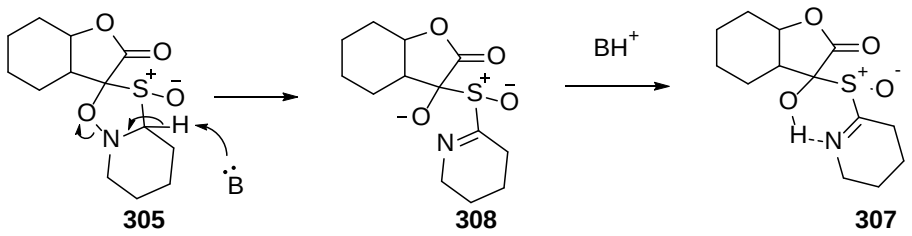
The nitrone **212** is freshly prepared for each reaction using yellow mercuric oxide and in our initial cycloaddition investigation, the α-oxo sulfine dipolarophile **101**, was generated *in situ* from the α-diazosulfoxides **38,39** (1 : 0.7) by the addition of rhodium acetate dimer, in the presence of the nitrone **212** (Scheme 105). Following addition of the rhodium acetate dimer, and on the basis of TLC analysis showing no notable changes, the reaction mixture was stirred for four days at room temperature. Two possible regioisomers could be formed, **305** and **306** from this reaction.

Following chromatographic purification of the crude reaction mixture, the intact cycloadducts **305** and **306** were not isolated.



Scheme 105

The major product in the ^{1}H NMR of the crude material was the alkene dimer **41** indicating the nitrone cycloaddition reaction was not very efficient. The only isolated product from this reaction following chromatography, has been identified on the basis of ^{1}H NMR, ^{13}C NMR, IR and HRMS analyses, as the rearrangement product **307**, a β-hydroxy imine, formed by rearrangement of the oxathiazolidine **305** and isolated in 16% yield. The spectral features did not match either **305** or **306** and the best fit to the recorded spectroscopic data is the ring opened product **307**, although confirmation by crystallography is warranted. The low isolated yield is due to dimerization of the α-oxo sulfine **101** *in situ* highlighted by a substantial amount of the alkene dimer **41** present in the ^{1}H NMR spectrum of the crude material. Interestingly, previous work within our group by Kissane, on a different research project, reported that on formation of cycloaddition products with this nitrone **212**, subsequent rearrangements to more stable products occurred also.[123] The proposed mechanism for the formation of the product **307** is a deprotonation of the bridgehead proton of the oxathiazolidine **305**, resulting in breaking of the nitrogen-oxygen bond. The alkoxide **308** is reprotonated forming the isolated product **307** (Scheme 106). Spectral characteristics of **307** are outlined in section 2.9.3.



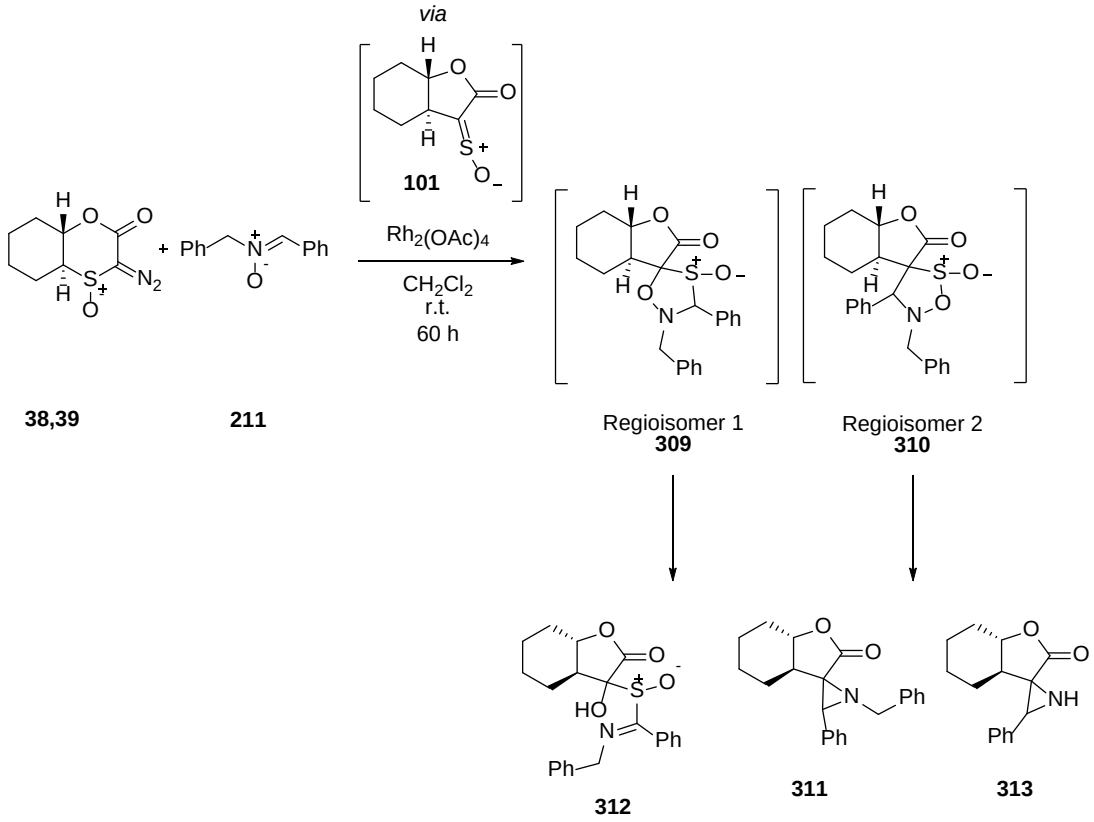
Scheme 106

It is likely that the intact cycloadducts were not isolated due to inherent instablity either due to the electronic properties of the intermediate heterocycle or due to unfavourable conformational constraint. The absence of any literature reports of stable 1,4,2-oxathiazolidine *S*-oxides, and just one report of a 1,2,5-oxathiazolidine *S*-oxide[115] is consistent with this observation. With the intermediate cycloadduct **305** not isolable, and the only identifiable product being the β-hydroxy imine rearrangement product **307**, it was investigated if changing the nitrone **212**, to the acyclic analogue **211**, to reduce the conformational strain in the product, would allow isolation of an intact cycloadduct.

2.9.2 1,3-Dipolar Cycloadditions of lactone derived α-oxo sulfines with the nitrone (Z)-*N*-benzyl-1-phenylmethanimine oxide 211

Initially a series of three reactions were carried out to establish whether the intact cycloadducts could be isolated. These reactions varied equivalents of nitrone and additive present (Table 43) and led to series of isolable compounds. This 1,3-dipolar cycloaddition reaction has the potential to form two regioisomeric cycloadducts, **309** and **310** and it is believed these undergo spontaneous rearrangement to give the isolated products. The 1,3-dipolar cycloaddition of the α-oxo sulfine generated from the α-diazosulfoxides **38,39** with the acyclic nitrone **211** (11 equivalents) was carried out at room temperature with 5 mol % of rhodium acetate dimer (Table 43, Entry 1). The α-diazosulfoxides **38,39** are dissolved in the minimum amount of dichloromethane and the nitrone **211** in dichloromethane was added in one portion, followed by the transition metal catalyst.

Table 43: Summary of cycloaddition results with the acyclic nitrone **211**.



Entry	Nitrone (eq)	Rh (mol %)	Reaction conditions	Time (h)	Outcome
1	11	5	*In situ* generation of sulfine.	60	Co-elution of **311** with byproducts
2	1	1	Formation of sulfine, sequential addition of 30 mol % $MgCl_2$, then nitrone **211**.	60	Complex Mixture of unidentifiable products
3	0.95	5	*In situ* formation of sulfine with 0.95 equiv. nitrone.	60	aziridine product **311** (5%) cycloadduct ring-opened **312** (7%) debenzylated aziridine **313** (10%)

Analysis of a ^{1}H NMR spectrum of an aliquot of the reaction mixture (Table 43, Entry 1), after 24 h, showed the presence of peaks assigned to a significant product **311** (Figure 84). These signals were apparent for the bridgehead protons at 3.60 ppm (CHO), and at 2.42 ppm (CH). Attempts to precipitate out the product or excess nitrone were made by adding ice cold ether and ice cold hexane to separate portions of the reaction, but both were unsuccessful. The reaction mixture

was concentrated after a further 36 h and purification by column chromatography led to co-elution of an aziridine rearrangement product **311**, with other unidentifiable products.

Literature precedent had shown that the addition of $MgCl_2$ to dipolar cycloadditions of nitrones could increase both the rate of reaction and yield of product through activation of the dipolarophile.[143] In a test reaction (Table 43, Entry 2), the α-oxo sulfine **101** was pre-generated using rhodium acetate dimer and filtered through a celite plug to remove insoluble rhodium catalyst. 30 mol % Magnesium chloride was added to the α-oxo sulfine **101** followed after a few minutes by one equivalent of the nitrone **211**. Analysis of the crude material after 60 h showed no evidence for the products **309**, **310**, **311**, **312** or **313** in a complex mixture of unidentifiable components. This complex mixture is likely due to the presence of the $MgCl_2$ which may be causing competing reactions or decompositions to occur.

In the initial reaction with excess nitrone **211** (Table 43, Entry 1), substantial amounts of impurities were formed - to avoid this issue, a cycloaddition with just 0.95 equivalents of the pure nitrone **211** were used (Table 43, Entry 3). After addition of the nitrone **211** to the α-diazosulfoxides **38,39** in dichloromethane, followed by rhodium acetate dimer, the reaction mixture was stirred for 60 h. The ^{1}H NMR spectrum of the crude material was much cleaner in contrast to to other reaction conditions and showed the presence of multiple components. Following chromatographic purification the isolated fractions were later assigned as the following: the least polar fraction which eluted first was the aziridine **311** (5%), followed by the β-hydroxy imine **312** (7%), a rearrangement product of the cycloadduct **309**, and lastly the debenzylated-aziridine **313** (10%) (Figure 84).

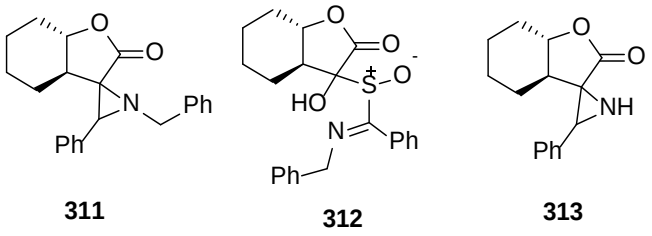
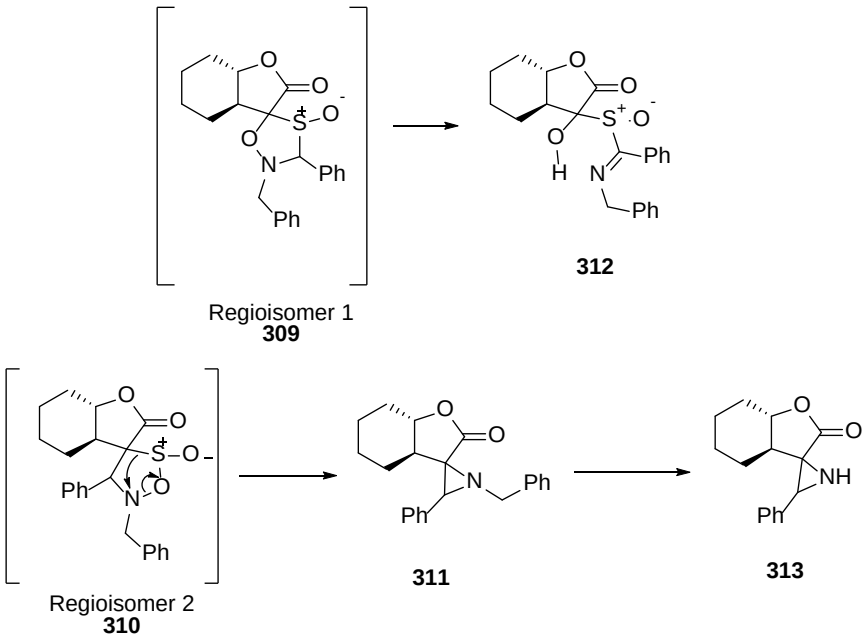


*Figure 84: Three tentatively assigned products from the cycloaddition reaction of α-diazosulfoxide **38, 39** and the nitrone.*

Formation of the β-hydroxy imine **312** can be rationalised by the rearrangement of Regioisomer 1 **309** (Scheme 107), in an identical manner to that seen for the product **307** (Scheme 106). Formation of the aziridine **311** can be rationalised *via* initial formation of the Regioisomer 2 **310** (Scheme 107), followed by subsequent extrusion of sulfur dioxide and ring contraction. It appears

that on successful cycloaddition of the dibenzyl nitrone with the lactone derived α-oxo sulfine, resulting in the formation of an aziridine **311**, a further debenzylation step can occur. This debenzylation of the aziridine **311** results in the formation of **313**.

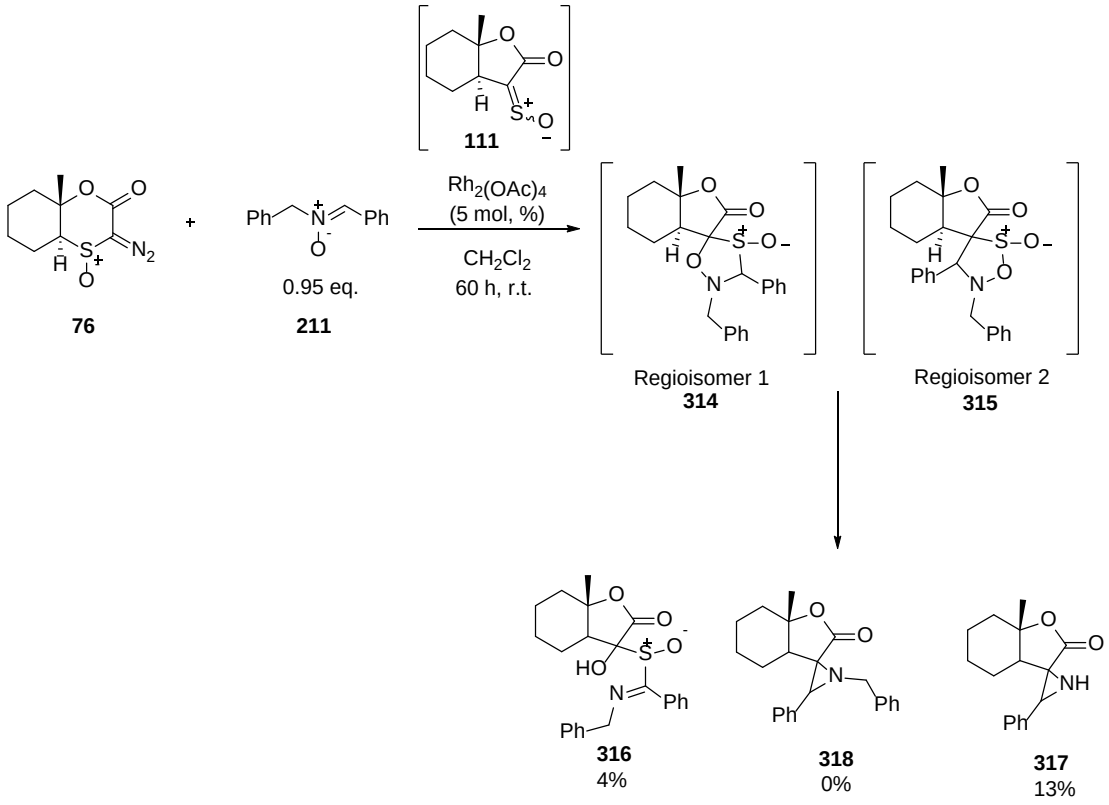


Scheme 107

In retrospect, the length of time these reactions were left may have contributed to the complexity as it is known that the α-diazosulfoxide is transformed rapidly to the labile α-oxo sulfine, which is anticipated to be transformed to the known sulfine decomposition products over this period of time. The investigation of the reactivity of α-diazosulfoxides with the acyclic nitrone **211** was extended to include the methyl bridgehead α-diazosulfoxide **76**, and the axial *trans*-dimethyl α-diazosulfoxide **78**, utilising *in situ* generation and trapping with just 0.95 equivalents of the nitrone.

The reaction of the methyl bridgehead α-diazosulfoxide **76** with the nitrone **211** was carried out at room temperature for 60 h to establish whether we could isolate an intact cycloadduct regioisomer, either **314** or **315** formed from the [3+2] cycloaddition (Scheme 108), or if aziridine products would be isolated. Earlier results from the continuous flow decomposition reactions had shown that this α-oxo sulfine **111** is particularly stable after generation, with dimerisation and other decomposition transformations occurring at a slow rate. The same methodology as the previous reactions was used i.e. addition of 0.95 equivalents of the nitrone dipole **211** to the α-

diazosulfoxide **76** followed by rhodium acetate dimer as the transition metal catalyst to induce the hetero-Wolff rearrangement.

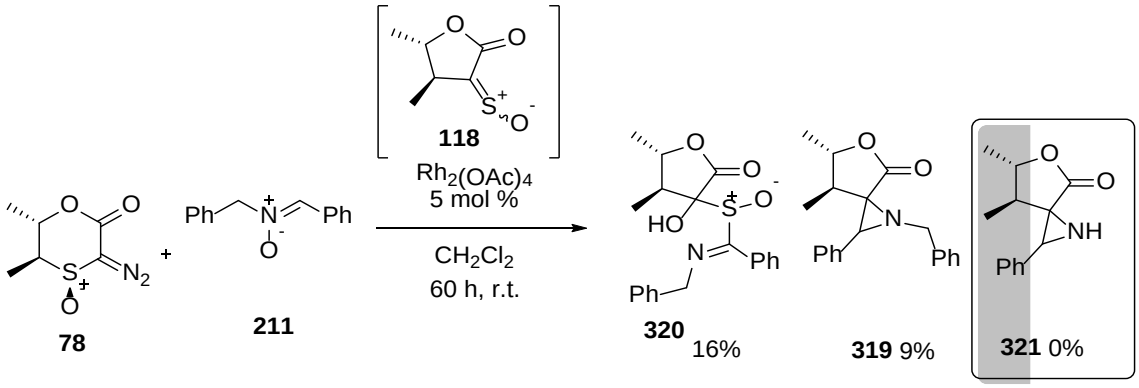


Scheme 108

On analysis of the crude reaction material a complex mixture was observed. After purification, one product isolated from the reaction was the β-hydroxy imine **316**, the same class of product previously isolated from the reaction of α-diazosulfoxides **38,39**. Also isolated was the debenzylated aziridine **317** (Scheme 108). Once again, the intact cycloadducts **314** and **315** were not isolated, supporting the earlier conclusion of the inherent instability of the intermediate heterocycles. The isolation of both the β-hydroxy imine **316** and the debenzylated aziridine product **317** are indicative of the formation of both regioisomers *in situ* with spontaneous decomposition to more thermodynamically stable products. Notably, the *N*-benzyl aziridine **318** was not isolated from the reaction mixture. Elemental anaylsis and high resolution mass spectrometry confirmed the molecular formula of the heterocycle **317** which is a vital result in confirming that in fact these aziridine heterocycles are formed from the cycloaddition of α-oxo sulfines and nitrones.

When the reaction conditions were applied to the monocyclic α-diazosulfoxide **78** analysis of the crude reaction material again showed a complex mixture, however, on purification a series of

products were successfully isolated and characterised. The aziridine product **319** was isolated in 9% yield, and the β-hydroxy imine rearrangement product **320** was also isolated, albeit in a higher yield of 16% (Scheme 109).



Scheme 109

Interestingly, the debenzylated cycloaddition product **321** was not isolated from the reaction mixture, however, characteristic signals were present in the ^{1}H NMR spectrum of the crude material, with a signal tentatively assigned as the CHO present at 3.88 ppm, and the aziridine CH present as a doublet at 4.04 ppm as a minor product in a complex mixture.

Most notable across the series of nitrone cycloadditions is that the β-hydroxy imine class of products such as **316** are consistently formed across the reactions of lactone derived α-oxo sulfines with the nitrones **211** and **212**. However, the aziridnes and debenzylated aziridines were not consistently isolated after chromatographic purification across the substrates. This may be as a result of challenges in isolating minor components from complex mixtures or maybe due to the different reactivity profiles between the α-oxo sulfines. However, formation of the two series of products shows the nitrone cycloaddition occurs with both regiochemical outcomes, in contrast to the nitrile oxides, which is the result expected for Type II 1,3-dipolar cycloadditions. Notably, the isolated products were isolated as a single diastereomer in each case, however as the crude spectra were complex mixtures it is not definitive if another diastereomer was formed.

2.9.3 Spectroscopic characteristics of nitrone cycloaddition products

In all cases the intact regioisomeric cycloadducts were not isolated, however a series of three types of product were isolated that were consistent to each of the four reactions. The first products which were consistent across the series from the cycloaddition reaction of lactone derived α-oxo sulfines with nitrone dipoles are the β-hydroxy imine class of products.

The structure **307**, which was the first derivative isolated, was assigned based on the ^{1}H and ^{13}C NMR data observed. Interestingly, **307** shows a broad 1H singlet at 8.62 ppm in the ^{1}H NMR spectrum, which exchanges rapidly in D_2O. On this basis, and evidence from a HSQC experiment, we have tentatively assigned the signal as an OH, as this proton is on a heteroatom. A paper by Matysiak[144] has shown protons in a similar system **322** (a sulfide compared to the sulfoxide in **307**), were observed at 14.26 ppm in DMSO. He also states the conformation of the molecule **322** is stabilised by an intramolecular hydrogen bond with a distance of 1.77 Å between the OH and N lone pair. Is it possible that a similar interaction in our rearrangement product **307** is occurring, resulting in the deshielding of the OH signal to 8.62 ppm.

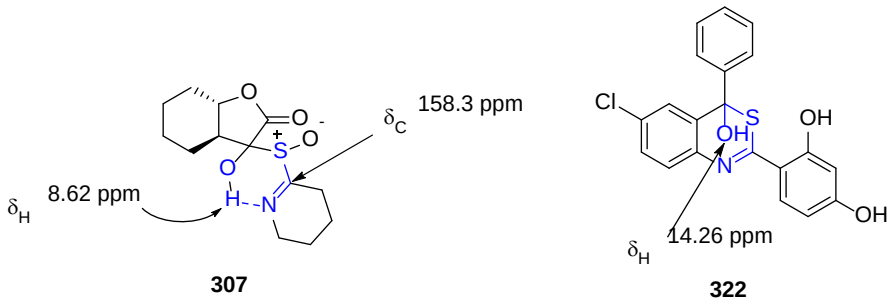


Figure 85: NMR signals of the rearrangement product **307***, and the heterocycle* **322***, reported by Matysiak.*[144]

The spectral characteristics of the series of isolated β-hydroxy imines; **307**, **312**, **316** and **320** are outlined below, with the most distinguishing features highlighted (Figure 87). Notably, the OH signal in each of these rearrangement products (**312**, **316**, **320**) appears between 8.38 and 8.79 ppm as a broad triplet. This triplet is believed to be due to through space coupling of the OH to the benzylic CH_2 through the nitrogen hydrogen bond acceptor, equally, the N-CH_2 signal of **312**, **316** and **320** appears as a doublet in the ^{1}H NMR spectrum.

On conducting a D_2O shake with the product **312**, the benzyl CH_2 signal at 4.08 ppm, originally a doublet becomes a singlet, with the loss of "OH" signal also observed. The original doublet for this signal is likely due to ^{3}J scalar coupling through hydrogen bonding (Figure 86) to the OH signal. Across the hydrogen bond the nucleus-electron-nucleus magnetisation transfer mechanisms are still effective. These electron mediated couplings, are through non-bonded interactions and referred to as through space (TS) internuclear spin-spin couplings, with multiple reviews in the literature.[145-147] The conversion of this doublet to a singlet is due to disruption of the intramolecular hydrogen bonding interaction when D_2O is present (Figure 86).

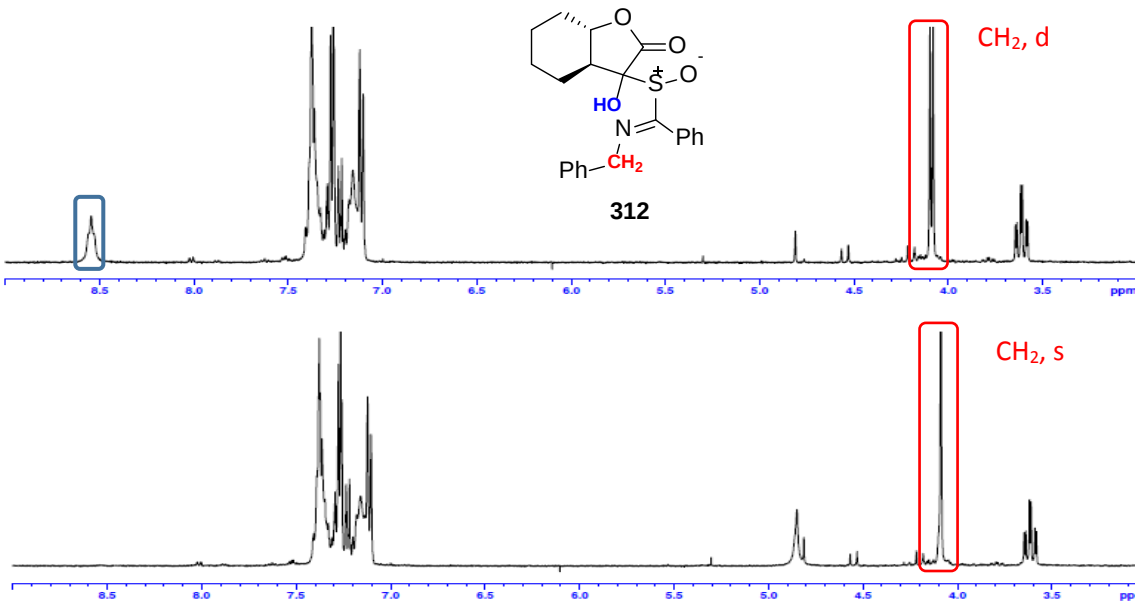


Figure 86: Stack of original ^{1}H NMR of compound **312** *(top) and after D_2O shake (bottom) in $CDCl_3$ (400 MHz).*

As summarised in Figure 87, the ^{13}C signals for the spiro carbon (*circa.* 88 – 95 ppm) and the imine carbon (*circa* 158 – 160 ppm) were very characteristic across the series and indeed were very similar to the signals seen for the 1,4,2-oxathiazole-*S*-oxide **267** which had been characterised crystallographically.

The carbonyl absorption varies in the infrared spectrum from 1674 cm^{-1} up to 1688 cm^{-1} for the 4 comparable compounds, **307, 312**, **316** and **320**, this is contrast to **267** which has its carbonyl IR absorption band at 1764 cm^{-1}. Additionally, the absorption corresponding to the sulfoxide moiety varies between 1055 and 1076 cm^{-1} for **307, 312**, **316** and **320** but is observed at 1076 cm^{-1} for **267.**

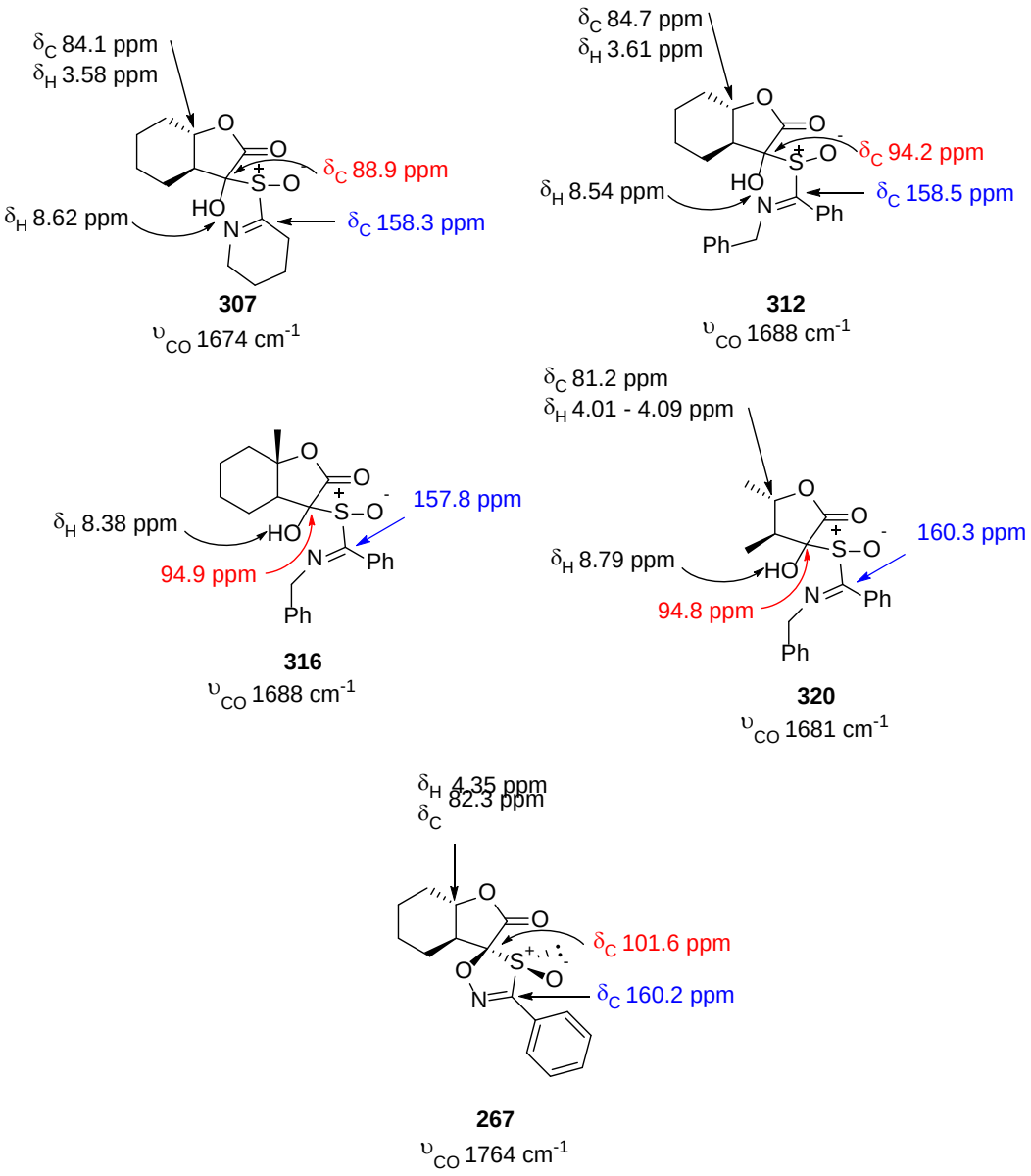


Figure 87: Spectral characteristics of rearrangement products, consistent to all nitrone cycloaddition reactions, and comparison of the spiro centres (red) and imine signal (blue) to the 1,4,2-oxathiazole-S-oxide **267** .

The second type of products isolated are the aziridines, **311** and **319**, both with similar spectral characteristics. Key to their assignment is finding the molecular ion of both aziridines in both nominal and high resolution mass spectrometry and the absence of the molecular ion of the intact cycloadduct products in both the nominal and high resolution mass spectra, and in particular the absence of sulfur. For the aziridines **319** and **311** it is to spiro centre is consistently located around 50.1 ppm, while for **313** and **317**, the spiro signal is not apparent in the ^{13}C NMR spectrum. These signals for **319** and **311** are comparable to the literature values for spiro centres on aziridine heterocycles. [148,149]

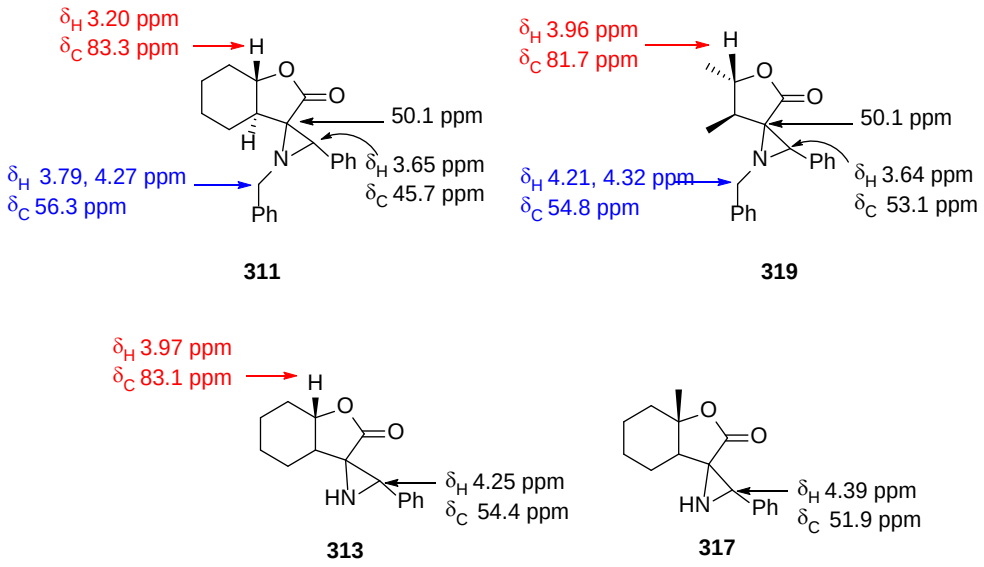


Figure 88: Characteristic ^{1}H NMR signals of the aziridine products **311**, **319, 313** *and* **317**.

Elemental analysis on the debenzylated aziridine **317** confirmed the empirical formula is correct and reaffirmed the absence of the sulfoxide moiety. Notably, a debenzylated aziridine was not isolated from the reaction of the dimethyl derived α-diazosulfoxide **78**, however the corresponding benzylated aziridine **319** was isolated.

The debenzylated aziridine **313** is the most polar fraction isolated after chromatographic purification of the reaction mixture and is isolated in 10% yield. Interestingly, in the ^{1}H NMR spectrum of the product, the bridgehead CH signal at 2.58 ppm shows evidence of ^{4}J coupling to the NH in addition to ^{3}J coupling to the CHO and CH_2 of the cyclohexyl ring (Figure 89).

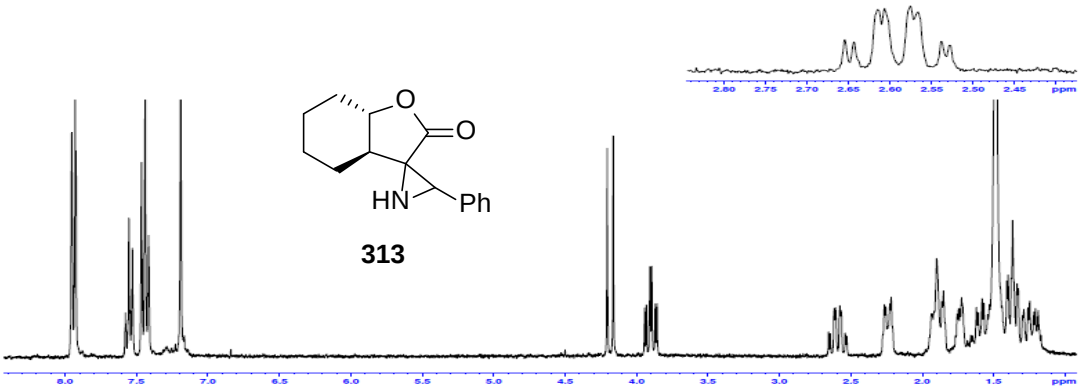


Figure 89: ^{1}H NMR spectrum of the debenzylated aziridine **313**

2.10 1,3-Dipolar cycloaddition of ketone derived α-oxo sulfines with nitrones

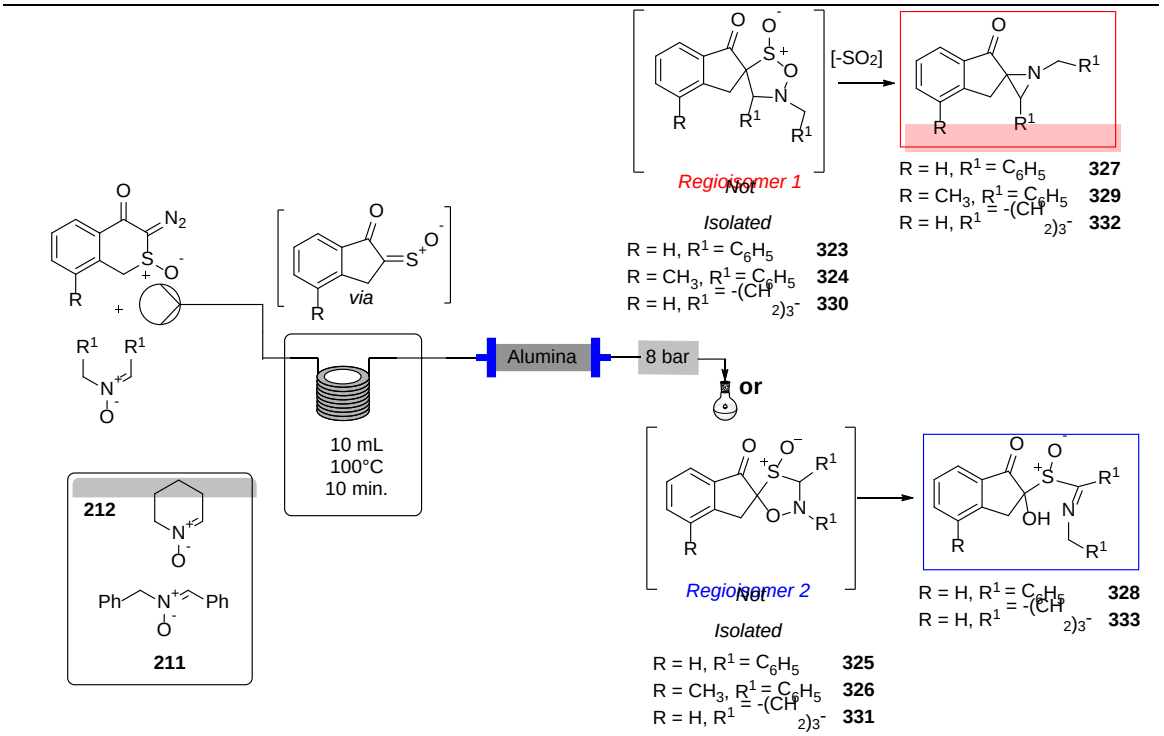
Having studied cycloadditions to the lactone derived α-oxo sulfines with nitrones and nitrile oxides, and in particular the cycloadditions of the ketone derived α-oxo sulfines with nitrile oxides in continuous flow, the next phase in the investigation was to explore the cycloadditions of the ketone derived α-oxo sulfines with nitrones. In particular, it was important to establish if use of metal free conditions by conducting the sulfine synthesis by thermolysis in continuous flow would lead to improved outcomes for the nitrone cycloadditions. Both the acyclic nitrone **211**[117] and the cyclic nitrone **212**[117] (see section 2.6.2) were used in this study. As seen earlier with the lactone derivatives, the cycloadducts formed were not detected or isolated; instead a number of products were recovered and characterised including aziridine derivative and compounds assigned as β-hydroxy imines. At this point it appears that the aziridines are formed by extrusion of sulfur dioxide from the 1,2,5-oxathiazole-*S*-oxides, while the β-hydroxy imines appear to be derived from the regioisomeric 1,4,2-oxathiazole-*S*-oxides although their structure is not fully confirmed at this stage. Thus, it appears that the ketone derived α-oxo sulfines and the nitrones undergo cycloaddition to form both possible regioisomers.

2.10.1 1,3-Dipolar Cycloadditions of ketone derived α-oxo sulfines with the nitrone (*Z*)-*N*-benzyl-1-phenylmethanimine oxide 211

The optimum conditions for the 1,3-dipolar cycloaddition of nitrile oxides in continuous flow were applied to these nitrone dipoles with ketone derived α-oxo sulfines i.e. 100°C for 10 minutes, with a packed bed reactor containing alumina (Table 44). In all cases, neither of the intact Regioisomers 1 (**323**, **324**) or Regioisomers 2 (**325**, **326**) were isolated and in each instance, complete consumption of the α-diazosulfoxide starting material was achieved. In contrast to the dipolar additions with the nitrile oxides which consistently produced clean transformation to the desired products, the reactions afforded the crude material as a complex mixture of products. When compared to the cycloaddition reaction of ketone derived α-oxo sulfine with the nitrile oxide, Regioisomer 1 would be comparable to the 1,2,5-oxathiazole-*S*-oxides, whereas Regioisomer 2 is comparable to the 1,4,2-oxathiazole-*S*-oxide products. It is noted that under these conditions with nitrile oxides, in continuous flow the 1,2,5-oxathiazole-*S*-oxides are the major products in all cases. Notably, in the nitrone cycloadditions summarised in Table 44, the aziridines formed from Regioisomer 1 are the major products recovered. This suggests that the regioselectivity is

consistent for the 1,3-dipolar cycloaddition of ketone derived α-oxo sulfines with both nitrone and nitrile oxide dipoles.

Table 44: 1,3-Dipolar cycloaddition of ketone derived α-oxo sulfines with nitrone **211**.



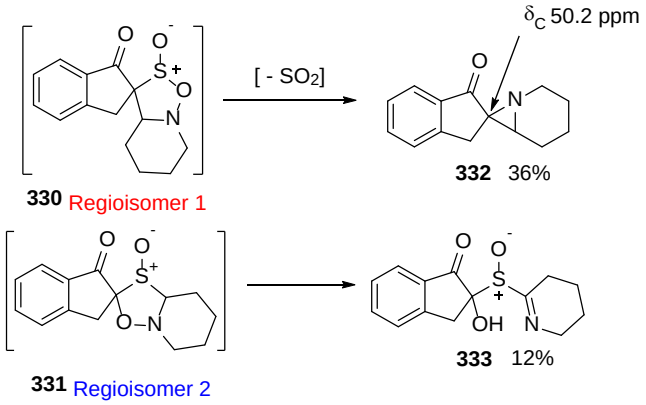
Entry	R = (α-diazosulfoxide)	Nitrone	Regio 1	Regio 2	Isolated **Products** (yield)
1	H (**14**)	**211**	**323**	**325**	**327** (18%), **328** (8%)
2	CH_3 (**80**)	**211**	**324**	**326**	**329** (32%)
3	H (**14**)	**212**	**330**	**331**	**332** (36%), **333** (12%)

Reacting α-diazosulfoxide **14** and nitrone **211** in these conditions (Table 44, entry 1) results in a complex crude mixture, and after chromatographic purification, isolation of the aziridine **327** as one diastereomer in 18% yield is achieved. The aziridine **327** is presumably formed from sulfur dioxide extrusion from Regioisomer 1 **323**. The diastereomeric control originates from the initial 1,3-dipolar cycloaddition. Although the isolation of the aziridine **327** is achieved, the efficiency is low, partly due to challenging purification. Successful isolation of the β-hydroxy imine product **328** in 8% yield means that Regioisomer 2 **325** is also formed in the cycloaddition. The spectroscopic characteristics of the isolated products are discussed below (section 2.10.3).

Utilising the α-diazosulfoxide **80** in these conditions (Table 44, entry 2) results in the isolation of the aziridine rearrangement product **329** only after chromatography. It is believed that regioselective dipolar cycloaddition results in the formation of the intermediate Regioisomer 1 **324** *in situ*, sulfur dioxide is subsequently and spontaneously extruded from the intermediate heterocycle, resulting in formation of the isolated aziridine product **329**. The structure was established based on the characteristic ^{1}H and ^{13}C NMR signals, and comparison to literature values for aziridines[149-151] as well as comparison to the aziridines characterised in the earlier Section 2.9.

Although the spectroscopic assignments of both compounds could be similar (Regioisomer 1 **324**, and the aziridine **329**), the assignment was made predominantly on the absence of the molecular ion of the intact cycloadduct **324** via high resolution mass spectrometry as well as the characteristic signal of the spiro carbon in the ^{13}C NMR spectrum at 54.6 ppm. As seen earlier, spiro carbons attached to both a sulfoxide moiety and oxygen moiety appear in the area of 100 ppm due to increased deshielding. To date, a crystal structure of the product **329** has not been obtained to unambiguously define the stereochemistry and regiochemistry as it is an oil, however 2D NMR studies have been used to investigate the structure (see Section 2.10.3).

To establish whether the same pattern reactivity is seen with the cyclic nitrone **212**, the unsubstituted α-oxo sulfine **13**, derived from α-diazosulfoxide **14,** was reacted with the nitrone **212** (Table 44, Entry 3). As with the earlier reactions, potential for the formation of two regioisomers is possible, **330** and **331** (Scheme 110).



Scheme 110

The less polar product identified from the reaction was the β-hydroxy imine **333**, formed by initial formation of the cycloadduct Regioisomer 2 **331** and subsequent rearrangement to the product **333** (Scheme 110), in a manner similar to that seen before. The more polar product isolated and identified was the aziridine rearrangement product **332**, formed through sulfur dioxide extrusion

from Regioisomer 1 **330**. This class of products are also consistent with the dibenzyl nitrone series of reactions. The characteristic spiro carbon signal of **332** is observed at 50.2 ppm in the ^{13}C NMR spectrum.

In summary, the reactions of the nitrone dipoles **212** and **211** with the ketone derived α-oxo sulfines consistently provided the isolation and identification of rearrangement products, without isolation of the intact intermediate cycloadducts on any occasion. In comparison to the cycloadducts formed from the reactions with nitrile oxide dipoles, the intact cycloadducts from 1,3-dipolar cycloadditions of nitrones are extremely labile, and rearrange to more stable species. As the same rearrangements are seen with the lactone derivatives in batch reaction conditions with rhodium acetate dimer, as are seen with the ketone derivatives in continuous flow, the high temperature and high pressure conditions in continuous flow are presumably not a factor in driving the rearrangement of the initially formed cycloadducts.

2.10.3 Spectroscopic characteristics of nitrone cycloaddition products.

From the successful 1,3-dipolar cycloaddition reaction of ketone derived α-oxo sulfines with nitrone dipoles, a series of compounds with comparable spectroscopic characteristics were identified, assigned as the aziridines **327**, **329**, and **332**. In the ^{1}H NMR spectra characteristic signals of the aziridines are the 2 AB quartet systems for both sets of diastereotopic protons, the aziridine CH signal, and the spiro centre in the ^{13}C NMR spectrum. The spiro carbon signals show up at 54.5, 54.6, and 50.2 ppm respectively for **327**, **329**, and **332** (Figure 90). A literature report by Luisi *et al.*[148] described the synthesis of a series of enantioenriched aziridines, including some with similar substitution patterns to our derivatives. In almost all case the characteristic spiro centre and CH signal for phenyl substituted derivatives were located in the region 52 – 60 ppm.[148] Characteristic signals in the ^{1}H and ^{13}C NMR for the indanone CH_2, the benzylic CH_2, and the aziridine CH are very consistent across the series and illustrated in Figure 90.

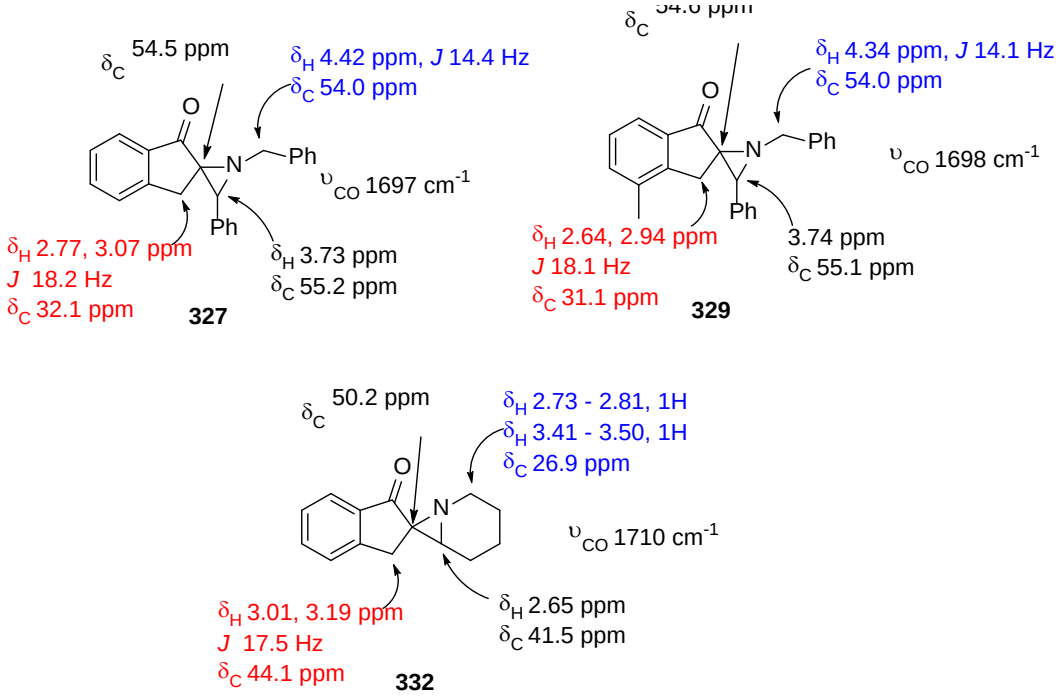


Figure 90: Characteristic ^{1}H NMR signals of the aziridines **327**, **329** *and* **332**.

Additionally, elemental analysis of the aziridine **317** earlier, confirms the formation of aziridine rearrangement products by the expulsion of sulfur dioxide from the intermediate cycloadducts. DEPTQ analysis was also used to establish the hybridisation of the three signals which were consistently located close together in the ^{13}C NMR and this is illustrated below in Figure 91.

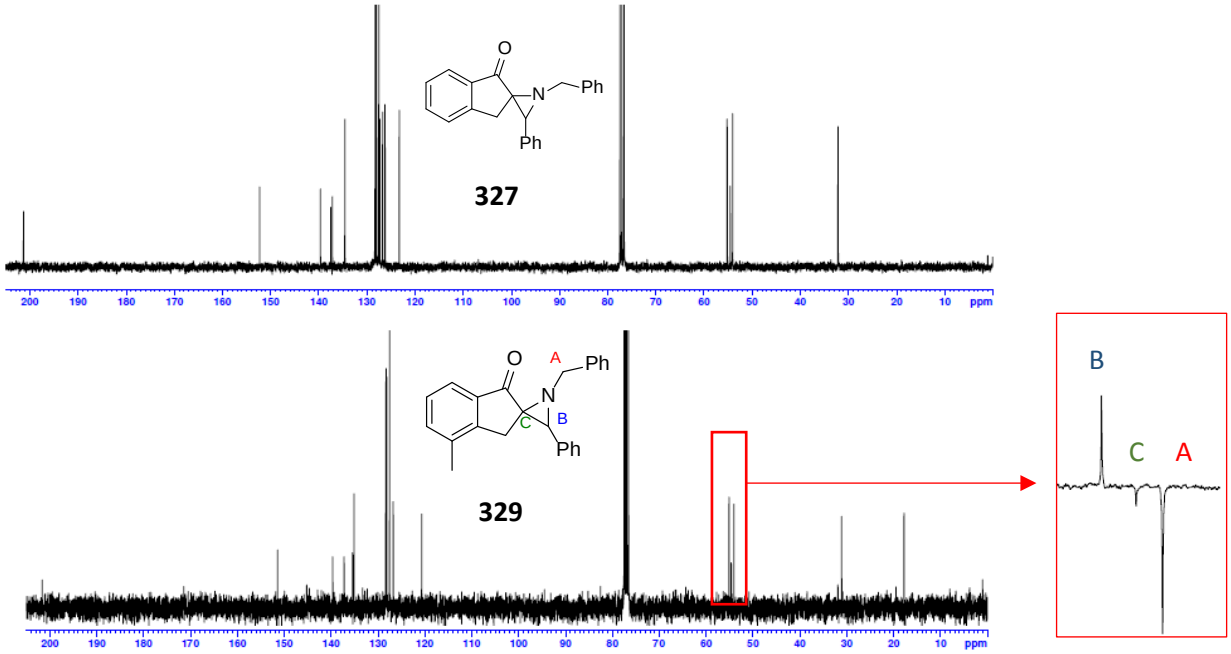
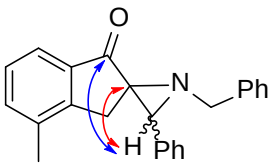


Figure 91: Through a DEPTQ NMR experiment, assignments are made to the three signals located close together; the benzyl CH_2 at 54.0 ppm (A), followed by the spiro centre at 54.5 ppm (C), followed by the CH signal at 55.1 ppm (B).

A HMBC experiment on **329** shows an interaction between the CH singlet at 3.74 ppm with the quaternary spiro carbon at 54.6 ppm (Figure 92). Additionally, there is an interaction between the CH singlet and the carbonyl at 201 ppm indicative of a 3 bond coupling. No interaction between the benzyl CH_2 signal at 4.34 ppm with the quaternary carbon was observed. The structure was assigned as the aziridine **329** based on the combined spectroscopic evidence.



329

Figure 92: A HMBC NMR experiment showed interaction between the CHPh singlet and the carbonyl at 201 ppm indicative of a 3 bond coupling as well as an interaction between the CH singlet at 3.74 ppm with the quaternary spiro carbon at 54.6 ppm.

As seen earlier with the lactone derived cycloadducts, a series of β-hydroxy imines were also isolated from the reactions of ketone derived α-oxo sulfines. These include **333** and **328** which are crystalline solids. The defining feature is the presence of the quaternary centre in the ^{13}C NMR spectrum which is recorded at 105.3 ppm and 102.6 ppm for **328** and **333** respectively. This is in comparison to the lactone derived β-hydroxy imine **312** whose spiro centre is recorded at 88.9 ppm (Figure 93).

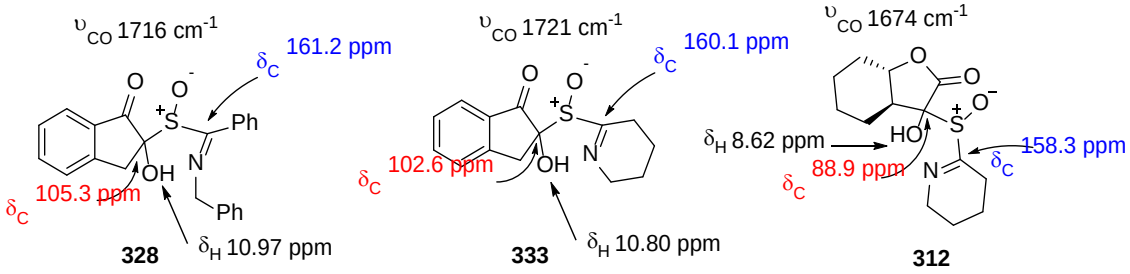


Figure 93: Structures of the β-hydroxy imines, formed from in situ rearrangements.

The characteristic data of the β-hydroxy imines **328** and **333** include a broad 1H singlet at 10.97 and 10.80 ppm respectively in the ^1H NMR spectra. Key signals in the ^{13}C NMR spectrum are the quaternary and imine signals. Noticeably, when the quaternary carbon is attached to the electron rich oxygen as in the β-hydroxy imines, significant deshielding of the signal occurs relative to the aziridine derivatives. As seen earlier with the lactone derived β-hydroxy imines, the *N*-benzylic CH_2 signal in the ^1H NMR spectrum appears as a doublet, due to ^3J coupling with the hydroxy proton, through space.[145-147] When acetone-d_6 was used as the solvent for analysis of **328** (instead of $CDCl_3$) this doublet becomes a singlet. This same effect was seen for **312** in D_2O (Figure 86, Section 2.9.3). This observation is explained by disruption of the intramolecular hydrogen

bonding, which allows through space planar coupling. When acetone-d_6 is used, the hydrogen bonding becomes intermolecular with the solvent, eliminating the ability of through space coupling and the benzylic CH_2 appears as a singlet.

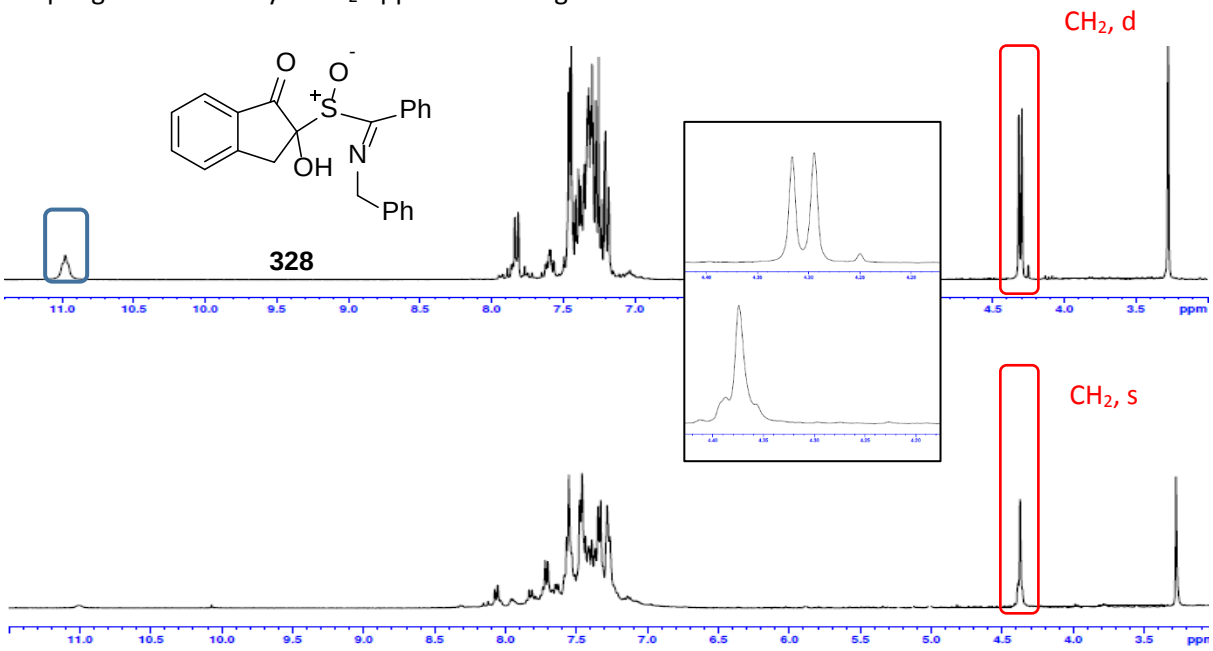


Figure 94: Comparison of ^1H NMR spectrum of **328** *in $CDCl_3$ (top, 400 MHz) and in d_6-acetone (bottom, 300 MHz). Most notable is the disappearance of the OH broad triplet, and conversion of the benzylic CH_2 from a doublet to a singlet.*

Overall, the nitrone cycloadditions to sulfines derived from α-diazosulfoxides lead to two series of products which can be rationalised as forming from each of the two regioisomeric cycloadducts. Yields are low due to the complexity of the crude reaction mixtures and the reactions are noticeably less efficient than the nitrile oxide cycloadditions. One series of the products isolated are aziridines derived from sulfur dioxide extrusion from the 1,2,5-oxathiazolidine *S*-oxide, while the other series has been assigned as the β-hydroxy imines, formed through fragmentation of the other regioisomeric cycloadduct. It's interesting to note each product was isolated as a single diastereomer, and while it is impossible to exclude the presence of other diastereomers in the complex mixture, this suggests diastereoselectivity in the cycloadditions. In contrast to the nitrile oxides, both regioisomers of cycloadducts appear to form in the reactions of both the lactone and ketone series with nitrones. While the assignments of the β-hydroxy imines is not definitive, this is our best interpretation of the data at this point.

2.11 Biological Evaluation

With the novel heterocyclic functionality installed in a large range of novel compounds throughout this project, a selection of these derivatives was submitted for screening of their biological activity in a range of anticancer screens (Figure 95) to the National Cancer Centre in Maryland, USA. These included four sulfoxide cycloadducts generated through Diels-Alder cycloadditions (**128**, **125**, **154**, **139**) one sulfone derivative (**163**), a lactone derived 1,4,2-oxathiazle-*S*-oxide (**296**) and six ketone derived 1,2,5-oxathiazole-*S*-oxides (**246**, **253**, **250**, **271**, **274**, **268**). Every compound that was submitted to be tested was accepted and subsequently screened for one dose testing. This series of compounds was successfully investigated for initial one-dose (10 µM) tumour cell line activity, and the resulting pattern of growth inhibition of these agents on the NCI-60 human tumour cell line panel is outlined herein.

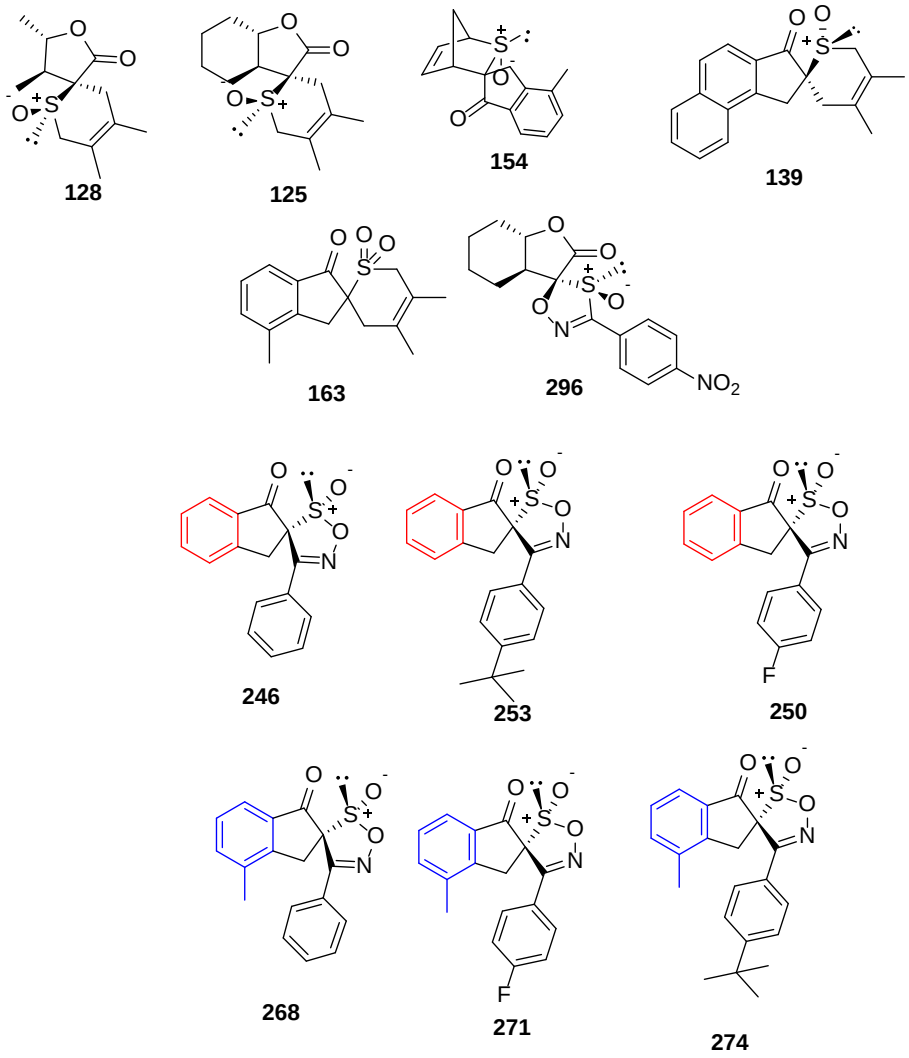


Figure 95: Range of heterocycles which were tested for their anticancer activity.

2.11.1 Introduction to NCI-60 Cancer Cell-line Screen Programme

The National Cancer Institute (NCI) screens compounds which may exhibit interesting biological activity against cancer cell lines as part of their Developmental Therapeutics Programme (DTP). Sixty human tumour cell lines are tested *in vitro* against the compounds to check for anticancer activity. The screening methodology and centre of research was established in the late 1980's with an emphasis on drug discovery. It is a strategic high-throughput screening tool which has proved beneficial over the years for providing access to novel highly effective anticancer medications and treatments. Some of the best known success stories are reported below (Table 45) including Paclitaxel (Taxol®) **334** which is one of the most widely prescribed anticancer drugs on the market and Bortezomib (Velcade®) **335** which went from one-dose testing with the NCI to full FDA approval in 8 years.

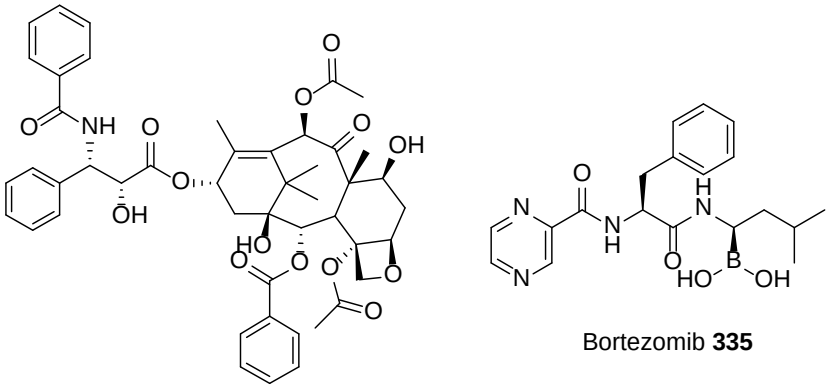


Figure 96: Structures of the anticancer agents Paclitaxel and Bortezomib.

The NCI has established a significant database of over 100,000 compounds and their corresponding cytotoxicity data in an effort to find the next generation of anticancer drugs.

Table 45: Anticancer agents developed with DTP involvement.

Year	Drug	Year	Drug
2015	Dinutuximab	**1979**	Daunorubicin
2012	Omacetaxine	**1978**	Cisplatin
2010	Eribulin	**1977**	BCNU
2010	Sipuleucel-T	**1976**	CCNU
2009	Romidepsin	**1975**	Dacarbazine
2004	Erbitux®	**1974**	Adriamycin
2003	Velcade®	**1974**	Mitomycin C
1996	Gliadel®	**1967**	Hydroxyurea
1996	Topotecan	**1966**	Pipobroman
1995	All-*t*-retinoic acid	**1966**	Thioguanine
1992	Chorodeoxyadenosine	**1964**	Actinomycin D
1992	Taxol®	**1963**	Vincristine
1992	Teniposide	**1962**	Fluorouracil
1991	Fludarabine Phosphate Pentostatin	**1961**	Vinblastine
1990	Hexamethylmelamine	**1959**	Cyclophosphamide
1990	Levamisole	**1959**	Thiotepa
1989	Carboplatin	**1957**	Chlorambucil
1988	Ifosfamide		
1987	Mitoxantrone		
1983	Etoposide		
1982	Streptozotocin		

The DTP programme has been responsible or involved in the discovery or development of more than 70% of the anticancer drugs currently available for treatment.[152,153] Recently, the NCI has began establishing investigations into new combination strategies to overcome drug resistance in patients with advanced cancer. Over 5,000 pairs of currently FDA-approved cancer drugs have been screened, and this new screening method has demonstrated value in identifying promising combinations.[154]

2.11.2 Evaluation of NCI-60 Cancer Cell-line Screen results

2.11.2.1 NCI-60 method of screening

To investigate the biological activity of the desired compounds for cytotoxic or noncytotoxic effects, a number of key steps are necessary before addition to the various cancer cell lines. The first step is the preparation of a stock solution in DMSO, followed by dilution in a medium containing 5% fetal bovine serum and 2 mM L-Glutamine. This solution is exposed to each previously cultured cell line for 24 h. After incubation for 48 h the required steps of media removal,

cell fixation and staining (with sulforhodamine B), prior to a 1% acetic acid wash and finally followed by air drying. Analysis by colorimetric growth inhibition-dependent absorbance at 515 nm is measured and calibrated against the DMSO control.[155,156] On obtaining the results of the *in vitro* screening, the results are presented by the NCI as a "mean graph" for interpretation, as illustrated in Figure 97.

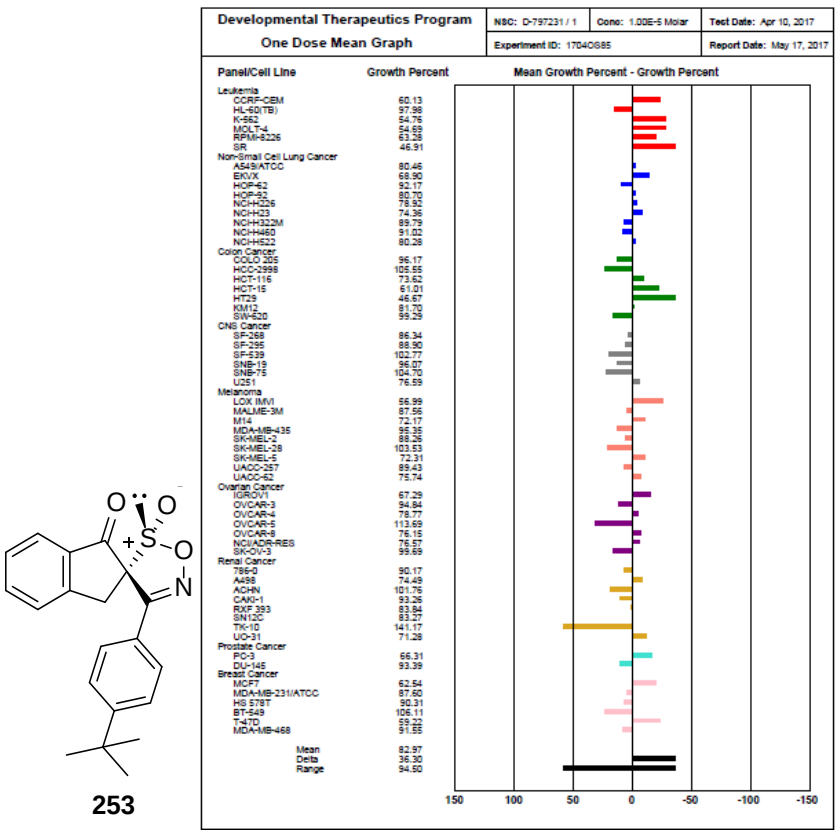


Figure 97: "Mean growth" graph of compound **253**.

The mean growth across the cancer cell line is the centre of the line graph (0). As an indicator, the bar charts which extend to the right of the mean indicate selective positive growth inhibition, while those to the left of the mean are indicative of a chemoprotective or non-cytotoxic effect on the specific cell line. Typically, if a mean growth of <60% is achieved, and the Data Review Committee at the NCI is interested in further screening of a compound, it is selected for 5 dose screening. This compares the growth inhibition, across the 60 cancer cell lines, at 5 different concentration levels. Following this screening, determination of three key response parameters can be achieved; GI_{50}, TGI and LC_{50}. If success in this screening is achieved, lead compounds can be progressed to *in vivo* hollow-fibre testing in mouse models.

2.11.2.2 Biological activity of thiopyran-*S*-oxide and thiopyran-*S,S*-dioxide cycloadducts

The furanone moiety has been incorporated into a wide variety of therapeutically interesting drug candidates such as Basidalin **336**. There are butenolide natural products which show antitumour activity (Figure 98);[157] the dihydrofuranone Bacillariolide II is **337** known to possess significant inhibitory activity against phospholipase A_2. [158]

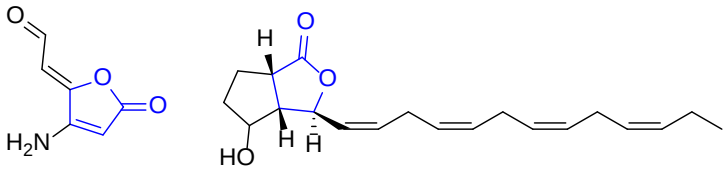


Figure 98: Biologically active furanone derivatives.

The indanone moiety has been studied for various biological activity against diseases such as cancer and Alzheimer's. Indanocine **338** (Figure 99) and its analogues were explored to combat drug-resistant malignancies.[159] Another indanone analogue Donepezil hydrochloride **339** has been approved by US-FDA for the treatment of mild to moderate Alzheimer's disease (Figure 99).

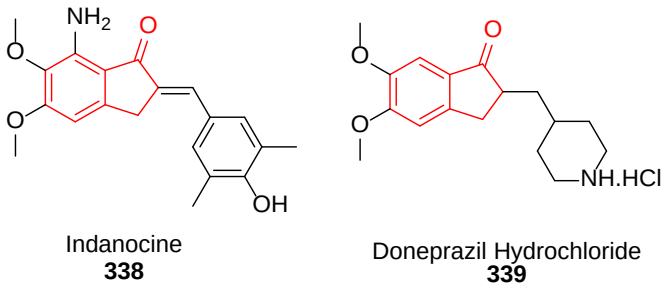


Figure 99:Indanone derived biologically active heterocycles **338** *and* **339** .

Doneprazil hydrochloride **339** acts as an AChE (Acetylcholinesterase) inhibitor.[160] Gallic acid-based indanone derivatives showed very good anticancer activity in MTT (Malignant triton tumor) assay against various human cancer cell lines. [161] The most potent indanone (IC50 = 2.2 uM), is against a hormone-dependent breast cancer cell line (MCF-7), showed no toxicity to human erythrocytes even at higher concentrations (100 ug/ml, 258 uM).[161]

The first two compounds in the series of thiopyran-*S*-oxides sent for biological testing are generated through Diels-Alder cycloaddition of the lactone derived α-oxo sulfines resulting in furanone derived cycloadducts **128** and **125** (Figure 100). Previously the cycloadduct [14] **125** had been requested by the NCI for testing, but was only screened on two cancer cell lines at this time. This compound, **125**, was re-submitted during this work for testing against the sixty cancer cell

lines now established at the NCI along with **128**, and the thiopyran-*S*-oxide cycloadducts **154**, **139** and **163** which are indanone derived (Figure 100). With interesting biological activity established in indanones and our efficient route to the synthesis of diastereomerically pure indanone containing compounds, in good yields, analysis and understanding of their cytotoxicity was of interest.

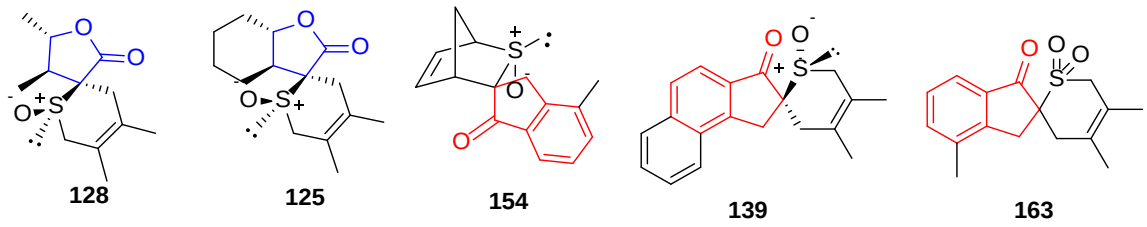
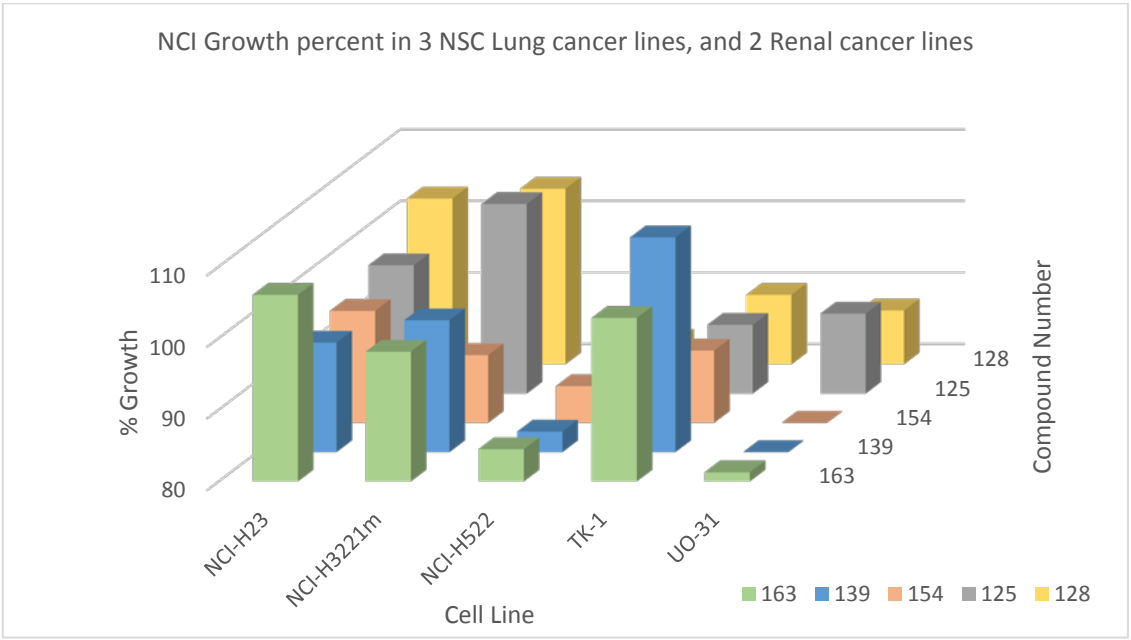
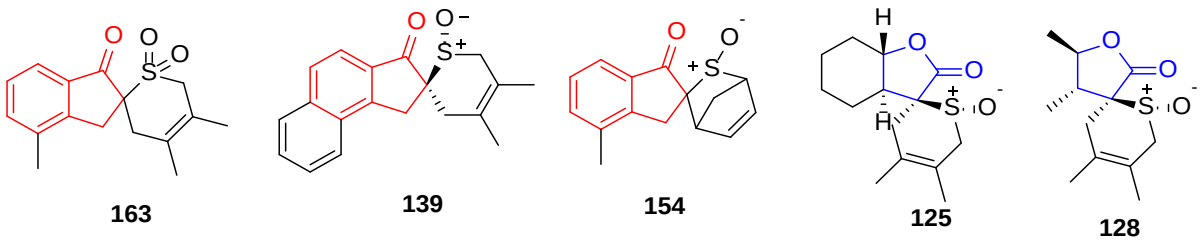


Figure 100: Range of sulfoxide cycloadducts generated by Diels-Alder cycloaddition reactions, that were screened for their anticancer activity.

The five cycloadducts were investigated for their anticancer activity using the one-dose (10 mM) cell line screening, with an aim of comparing the electronic and steric effects on biological activity. None of this set of cycloadducts exhibited exciting anticancer activity, with mean growth percentages consistently around 100, showing inactivity. Some of the cancer cell lines did show a cytotoxic effect however, most notably against three non small cell lung cancer lines (NCI-H23, NCI-H322M, NCI-H522) and 2 renal cancer cell lines (TK-1, UO-31) (Graph 2). The best result was achieved on the cancer cell line UO-31 which is derived from renal cell carcinoma.



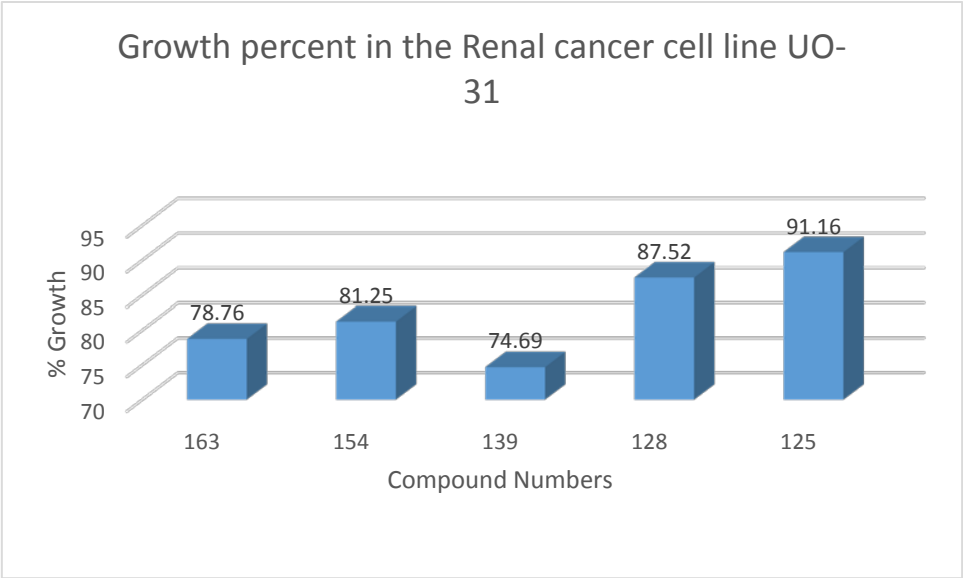
Graph 2



163 **139** **154** **125** **128**

Figure 101

Also, it seems that these five compounds exhibited a minor cytotoxic effect on the cell line NCI-H522 with all growth percentages less than 90%. With these results obtained for these cycloadducts, none of the compounds exhibited the biological activity required for five dose screening by the NCI. The one dose mean graphs obtained, from the NCI for each of the compounds are contained in appendix I.



Graph 3: Growth inhibition results obtained of the thiopyan-S-oxide derivatives on UO-31.

The greatest cytotoxic effect, for this specific cell line is observed with the naphthalene derived thiopyran-*S*-oxide **139** (Graph 3). This may be due to the planar bicyclic system with extended aromaticity. Additionally it is noted that the sulfone derivative **163** had a mean growth percent of 100.98%. This is in comparison to the sulfoxide derivative which was previously tested by Buckley and had a mean growth percent of 77%. [16]

2.11.2.3 Biological activity of oxathiazole-*S*-oxide cycloadducts

The synthesis of a range of novel oxathiazole-*S*-oxides from 1,3-dipolar cycloadditions of α-oxo sulfines in this work represents a route to a series of novel, highly functionalised, spirocyclic

heterocyclics. In addition to the heterocyclic motif, the indanone moiety is common to each of the 1,2,5-oxathiazole-*S*-oxides tested (see Section 2.7). No reports on the biological activity or more specifically, anticancer activity, of 1,4,2- or 1,2,5-oxathiazole-*S*-oxides exist in the literature, however there are reports on the biological activity of some related heterocycles; 1,4,2-oxathiazoles. The most closely related compound reported in the literature to have been tested for biological activity is the glucopyranosylidene-spiro-oxathiazole **340** (Figure 102).[162] This report describes how the rigid-spiro bicyclic structure with a hydrophobic aromatic moiety, (which is also common to our compounds) provides an optimal interaction against the RMGPb enzyme leading to enhanced biological activity. The glucose substituted oxathiazole derived compounds described in this report, are the most potent glucose based inhibitors of GP to date with an inhibition in the nanomolar range.[162] Similarly, the oxathiazole-2-one derivatives **341** (Figure 102) which is structurally similar to Bortezomib **335** (Figure 96) has been shown to be active against a human 20S proteasome[163] and other small molecule derivatives have shown excellent activity and selectivity for the mycobacterium proteasome. [164] 1,4,2-Oxathiazoles have been described as sulfur analogues of 1,2,4-oxadiazoles, such as **342** (Figure 102) which have been found to show anticancer activity by inducing apoptosis.[165]

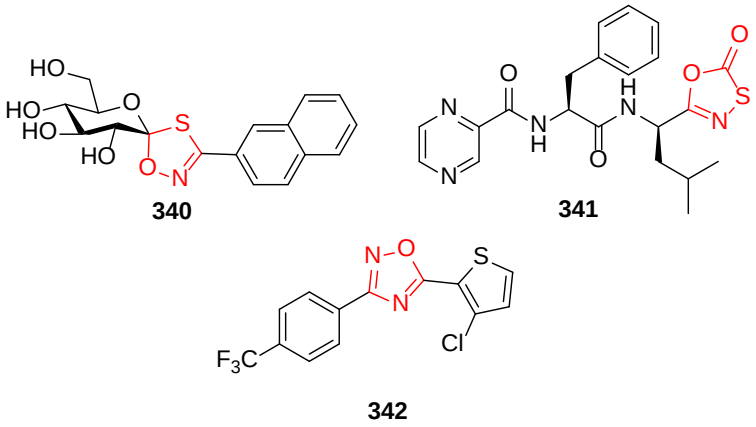


Figure 102: Heterocycles similar to the oxathiazole-S-oxides, which have shown substantial biological activity.

With this literature precedent in mind, and the known activity of the indanone moiety, seven oxathiazole-*S*-oxides were submitted for testing of their anticancer activity, including six novel 1,2,5-oxathiazole-*S*-oxides (**246**, **253**, **250**, **271**, **274**, **268**) and one novel 1,4,2-oxathiazole-*S*-oxide (**296**) (Figure 103).

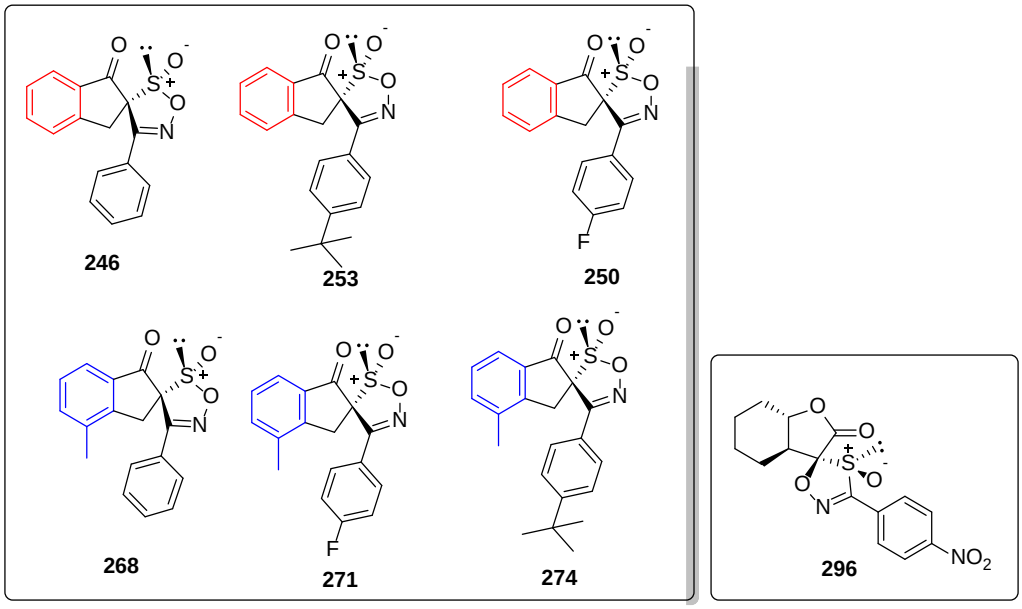
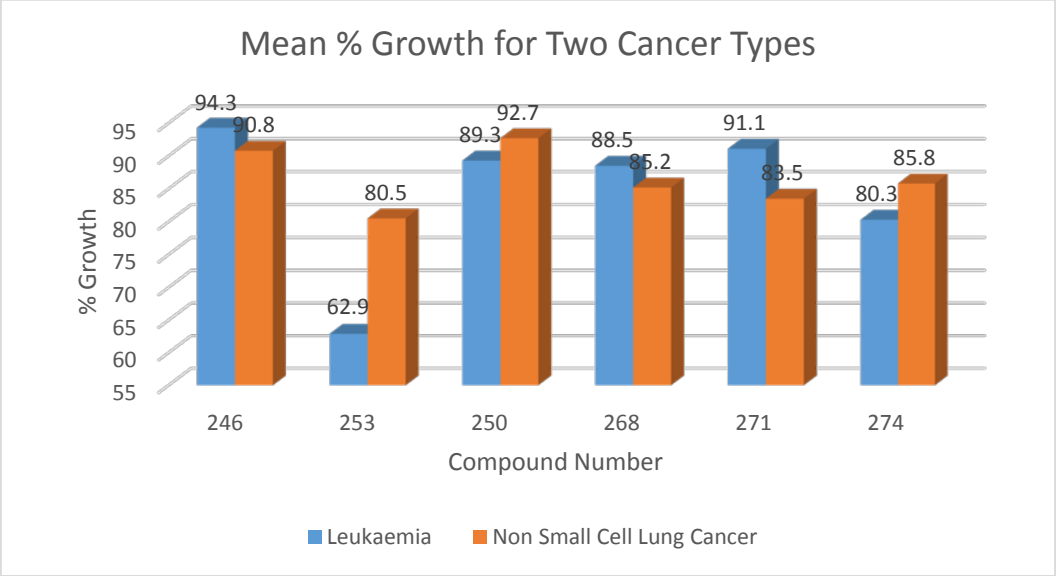


Figure 103: The range of 1,2,5-oxathiazole-S-oxide analysed for anticancer activity.

The six 1,2,5-oxathiazole-*S*-oxide derivatives submitted for testing included three with an unsubstituted indanone moiety and three with a methyl group in the 2-position. Interestingly, each of the 1,2,5-oxathiazole-*S*-oxides tested showed selectivity for both leukaemia and non-small cell lung cancer with mean growths between 62.9 – 94.3% and 80.3 – 92.7% respectively (Graph 4). The best results achieved on the leukaemia cancer cell lines was a mean growth percent of 62.9% for the compound **253** (Figure 104). Notably, in three of the cell lines growth was reduced to approx. 50% in the presence of **253**.

Panel/Cell Line	Growth Percent	Mean Growth Percent - Growth Percent
Leukemia		
CCRF-CEM	60.13	
HL-60(TB)	97.98	
K-562	54.76	
MOLT-4	54.69	
RPMI-8226	63.28	
SR	46.91	

Figure 104: Mean growth result for **253** *on leukemia cancer cell lines.*



Graph 4: Growth percentages of the 1,2,5-oxathiazole-S-oxides on leukemia and non small cell lung cancer.

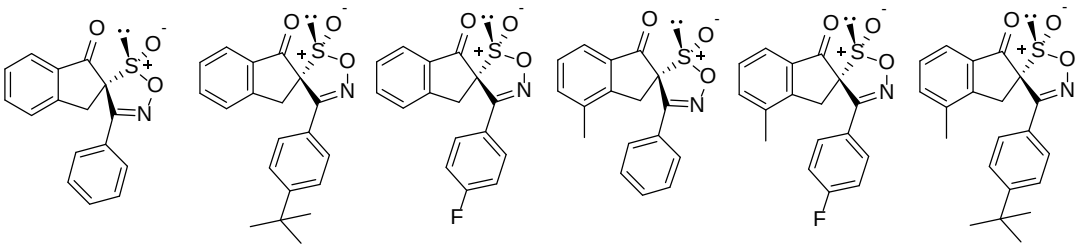
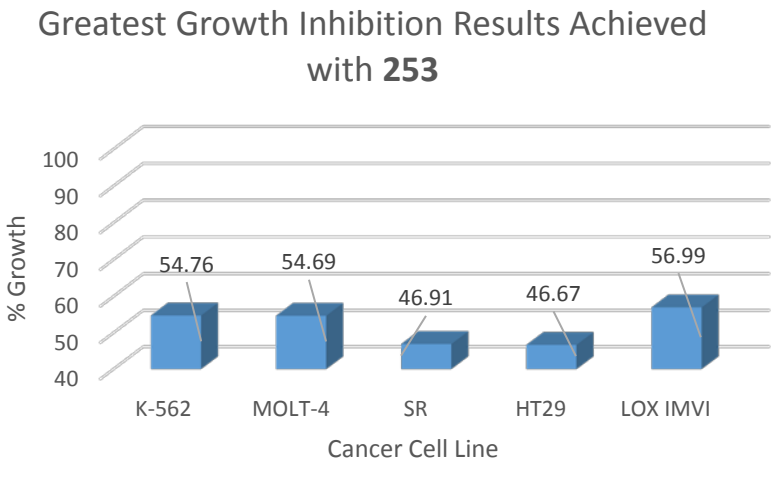
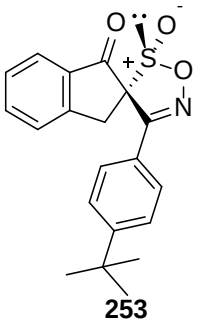


Figure 105: Range of 1,2,5-oxathiazole-S-oxides tested.

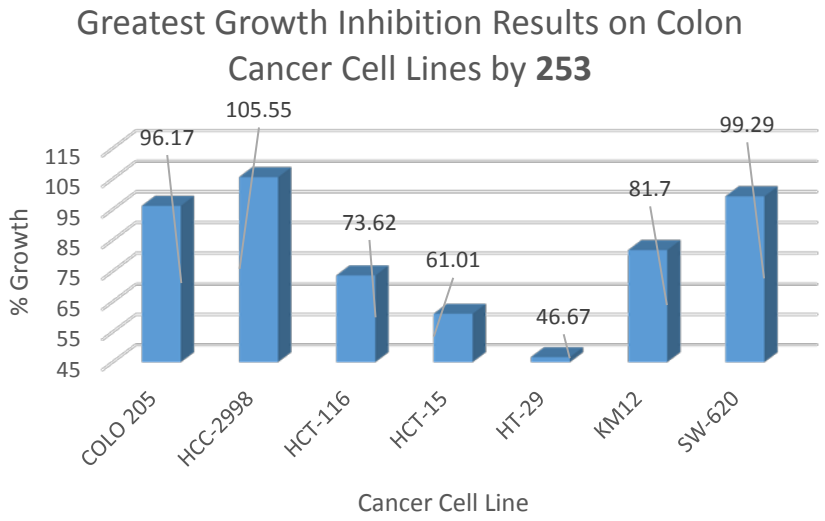
However, the overall best result achieved with compound **253** was a growth percent of 46.67% on the cancer cell line HT29. HT29 is part of the colon cancer cell lines and this result is quite interesting as with each of the other 1,2,5-oxathiazole-*S*-oxide derivatives, no growth inhibition is observed. This suggests that the unsubstituted indanone moiety combined with the sterically demanding *t*-butyl group on the aromatic ring leads to selectivity and cytotoxicity, suggesting for future projects that larger groups on the aromatic ring of a nitrile oxide, combined with smaller substituents on the α-oxo sulfine may lead to more active derivatives. Compound **253** had the lowest mean growth percent of all the compounds tested. Some of the cell lines which experience the greatest growth inhibition are outlined below (Graph 5).

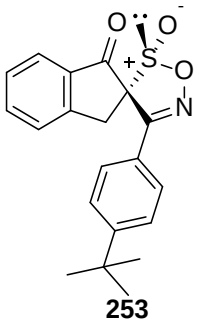




Graph 5: Best mean growth results achieved with ***253****.*

Also unique to the compound **253** is its growth inhibition on four out of the seven colon cancer cell lines screened. Each of other 1,2,5-oxathiazole-*S*-oxides did not exhibit a similar growth inhibition. The most significant result was on HT29 which is adenocarcinoma originating from colon tissue, with a mean growth percent of 46.67 %.

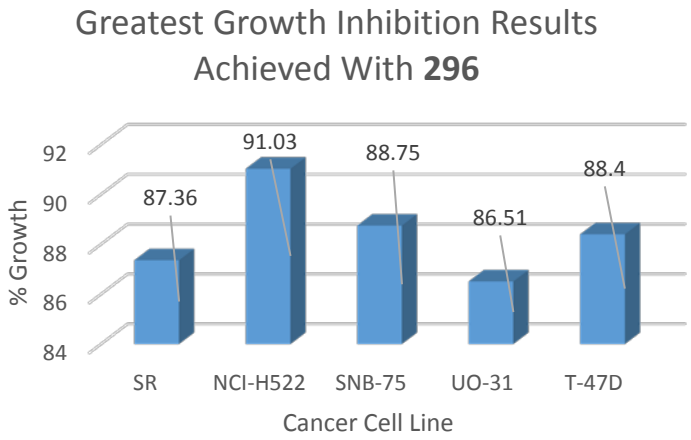


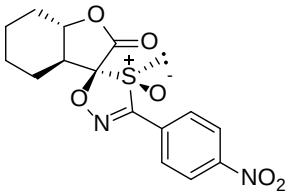


Graph 6: Mean growth results of **253** *on colon cancer cell lines specifically.*

1,2,5-Oxathiazole-*S*-oxide **253** with the t-butyl substituent displayed greater impact on growth inhibition than the other related compounds tested. For the unsubstituted indanone derivatives, the compound with the greatest growth inhibition is the *t*-butyl substituted **253**, followed by the unsubstituted phenyl ring **246**, followed by the *p*-fluoro derivative **250**. For the 2-methyl substituted indanone derivatives, the most cytotoxic is again the *t*-butyl derivative **274**, this time followed by the p-fluoro derivative **271**, and least cytotoxic was the unsubstituted derivative **268**.

Interestingly, the NCI agreed to test the *p*-nitrophenyl substituted 1,4,2-oxathiazole-*S*-oxide **296** also. Experience within the group has been that compounds containing nitro groups are often not accepted for one dose testing. The best results achieved with this compound were on a renal cancer cell line UO-31 (86.51%) and a leukaemia cell line SR (87.36%).



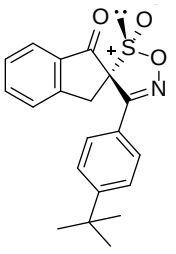


296

Graph 7: Best mean growth results achieved with ***296****.*

2.11.3 Conclusion of biological evaluation

From the 12 compounds submitted to the NCI for biological testing all of these were accepted for one dose testing and their anticancer activity was subsequently assessed and the resulting growth inhibition results collated by mean growth graphs. Four sulfoxide cycloadducts (**128**, **125**, **154**, **139**) along with a sulfone (**163**) were tested with limited promising outcomes. A new series of indanone derived 1,2,5-oxathiazole-*S*-oxides (**246**, **253**, **250**, **271**, **274**, **268**) and a furanone derived 1,4,2-oxathiazole-*S*-oxide (**296**) were generated and accepted for analysis of their cytotoxicity. However, the series of 1,2,5-oxathiazole-S-oxides tested possessed promising selectivity for leukaemia and non small cell lung cancer cell lines in comparison to the other cell lines. One derivative (**253**) showed good growth inhibition levels with growth inhibition of almost 55% on the SR cell line. A preliminary structure activity relationship shows an unsubstituted indanone moiety and bulky, sterically demanding substituents on the phenyl ring are beneficial to biological activity.



253

Figure 106: The 1,2,5-oxathiazole-S-oxide **253** *with the lowest mean growth result.*

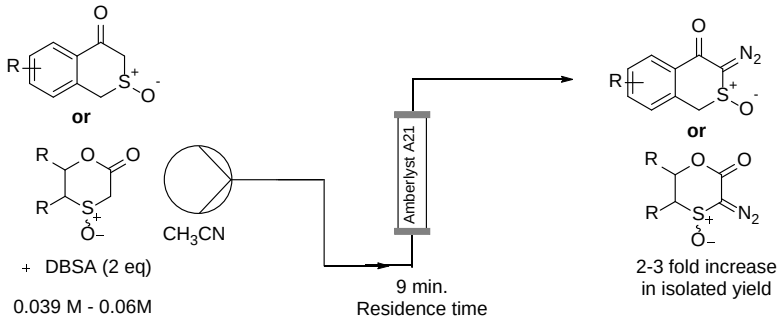
The scope for further functionalisation and derivatisation is evident as structural modifications on both the indanone and aromatic ring is easily undertaken in an attempt to further increase both the selectivity and activity.

2.12 Concluding remarks

In conclusion, the most notable achievements in this research were the successful development of a continuous flow methodology for the synthesis of lactone and ketone derived α-diazosulfoxides, as well as the development of 1,3-dipolar cycloadditions of α-oxo sulfines with both nitrone and nitrile oxide dipoles resulting in the successful isolation, characterisation and biological testing of a number of heterocycles.

While our group has worked with α-diazosulfoxides for many years, the greatest challenge in this work is the very low yield in the synthesis of the α-diazosulfoxides, typically less than 30%, which has inhibited the ability to explore their reactivity.

Through optimisation of the diazo transfer process in continuous flow and utilisation of solid supported bases, in particular Amberlyst A21, we have significantly enhanced the synthesis of α-diazosulfoxides resulting in a notable increase in isolated yield. The new conditions (2 eq. DBSA **87**, 5 eq. Amberlyst A21, 9 min residence time) are consistently performing well across a range of lactone and ketone derived α-diazosulfoxide substrates with 2 – 3 fold increase in yield over the standard batch reaction conditions. This method is a substantial improvement on previous work reported from within the group and highlights the suitability of flow for the synthesis of compounds that may be sensitive to the reaction conditions, in this case, base. Use of continuous flow allows the synthesis in a manner which is safer, more scalable and more time efficient. Interestingly, this new method, enables access to very labile ketone derived α-diazosulfoxides (**81**,**82**) which could not be successfully isolated from batch reaction conditions.



Scheme 111

Through the insight gained during the optimisation of the continuous flow process, a new batch protocol (Et_3N, CH_3CN, DBSA) was developed, utilizing dropwise addition of base to control base concentration and decreasing reaction time to limit exposure to basic medium, which proved to be successful in increasing the yields for the synthesis of the lactone and the ketone derived α-diazosulfoxides in batch reaction conditions. Additionally, the major impact of this work is, using

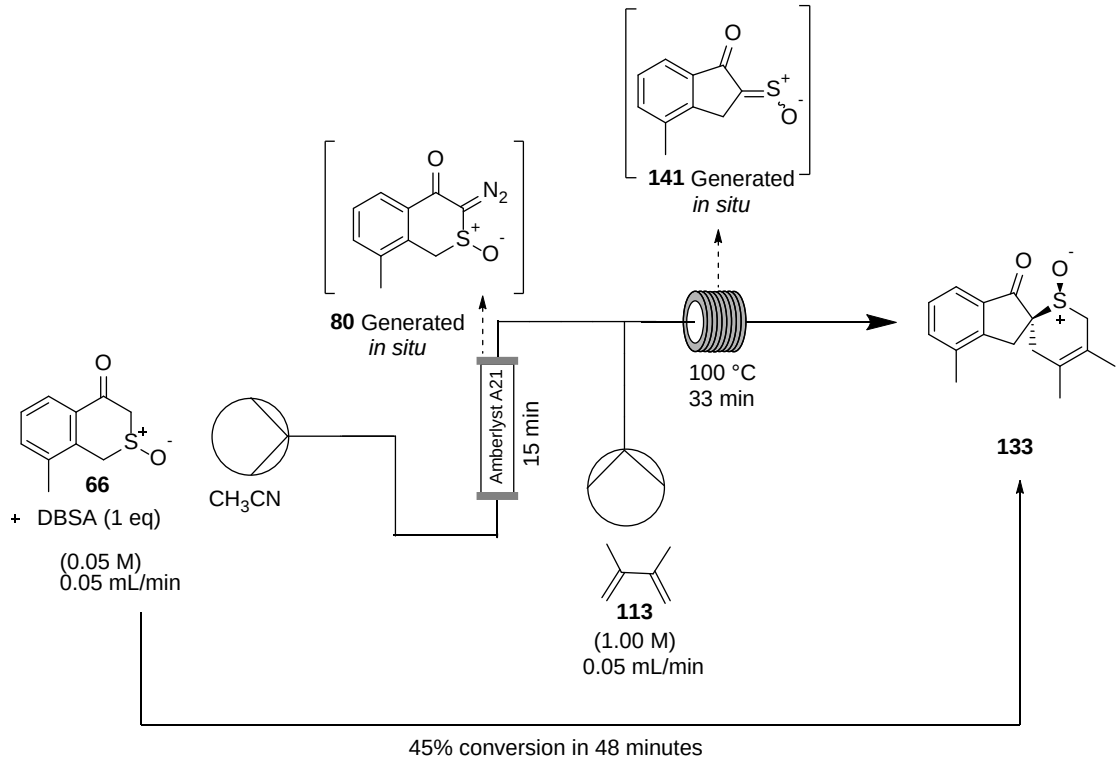
either the new batch conditions or the continuous flow diazo transfer conditions, that it is now possible to easily access α-diazosulfoxides in synthetically useful quantities. The yield of the lactone derivatives from continuous flow is consistently higher than the new or old batch reactions conditions, whereas the yield of the ketone derivatives are comparable from the continuous flow conditions and the new batch conditions. Therefore, use of continuous flow conditions for the isolation of high yields of lactone derived α-diazosulfoxides, and use of the new batch conditions for the isolation of high yields of ketone derived α-diazosulfoxides provide optimum outcomes, at least in the compounds studied to date.

Access to α-diazosulfoxides in synthetically useful amounts for the first time enabled the investigation of reactions of α-diazosulfoxides in continuous flow, under transition metal catalysis, thermolysis or photolysis, which was building on earlier work, conducted in batch reaction conditions, carried out within the group. It was established that α-diazosulfoxides can be converted to α-oxo sulfines very cleanly in continuous flow under mild, metal free reaction conditions, focusing on the lactone series for this part of the work. The α-oxo sulfine is generated with a view to intercepting and trapping this reactive intermediate. In the absence of this, the α-oxo sulfines can subsequently undergo a range of different transformations to form a number of byproducts. The outcome of the sulfine degradation in the absence of trapping, is remarkably consistent and predictable across a range of very different reationo conditions with the same major products, including sulfur extrusion, dominating. Clearly, alteration of the conditions leads to changes in the relative ratios, but globally the outcome is consistent.

Having demonstrated successful transformations to the α-oxo sulfine in continuous flow (transition metal catalysis, thermolysis, photolysis), successful Diels-Alder cycloadditions proved efficient in continuous flow, using thermolysis or rhodium acetate catalysis, resulting in good diastereoselectivity and excellent yields. The thermally induced cycloaddition reactions also have the added advantage of being metal free and catalyst free. As the ketone and lactone α-diazosulfoxides differ in their reactivity profiles the temperature required to initiate the hetero-Wolff rearrangement is different with the ketones rearranging efficiently at 100°C in acetonitrile/dichloromethane mixtures while higher temperature of 120°C was employed with the lactone derivatives achieved in a solvent mixture of toluene/dichloromethane. Critical to the success of the α-oxo sulfine cycloaddition was use of a sufficiently concentrated diene trap. The diastereoselectivity of the reactions is comparable (or better) across the series, compared to transition metal catalysed batch reactions, but consistently higher yields of both lactone and ketone derived cycloadducts are obtained. In some cases, this methodology has the added

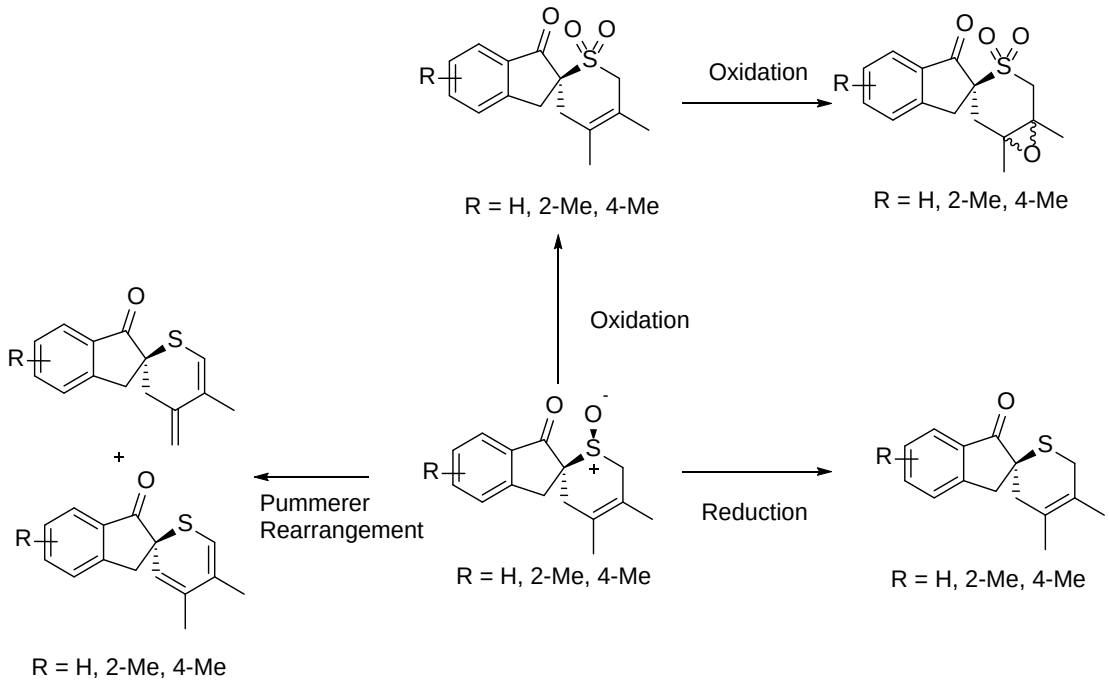
advantage of purification by recrystallisation or reslurry of the desired cycloadducts rather than column chromatography.

Combining the α-oxo sulfine generation and trapping studies, with the diazo transfer, led to proof of concept for telescoping the diazo transfer process with subsequent Diels-Alder cycloaddition reaction. We established the ability to go from stable sulfoxide precursors through to labile α-diazosulfoxides, thermally promote the rearrangement to the reactive α-oxo sulfine, and subsequently trap in a Diels-Alder cycloaddition reaction resulting in a stable thiopyran-*S*-oxide cycloadduct, with clear potential benefits from a safety and scale up perspective.



Scheme 112

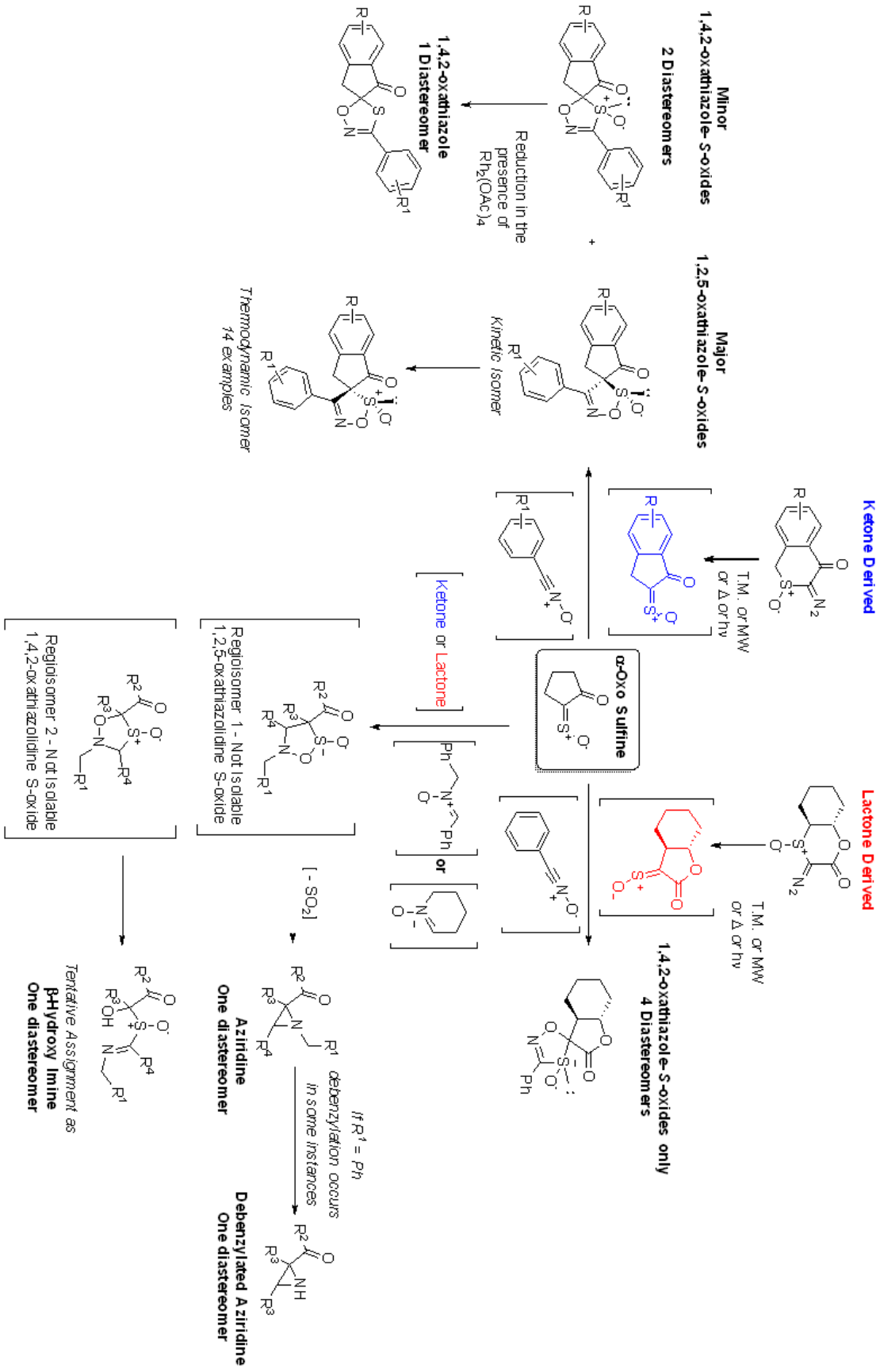
Indeed, this telescoped process step allows access to the thiopyran-*S*-oxides in synthetically useful yields for the first time, enabling further derivatisation of these compounds. Illustrative examples such as oxidation, reductions, and Pummerer rearrangements were carried out leading to a series of novel sulfides and sulfones, and in some cases β-epoxy-sulfones.



Scheme 113

The 1,3-dipolar cycloadditions of both lactone and ketone derived α-oxosulfines was a significant advance in this research programme (Scheme 114). For reaction of ketone derived α-oxo sulfines, two sets of reaction conditions were successfully established for the preferential formation of either the kinetic isomer or the thermodynamic isomer of a 1,2,5-oxathiazole-*S*-oxide cycloadducts by trapping of α-oxo sulfines with nitrile oxides. These cycloadducts are exceptionally rare in the literature with only two reported examples. A range of 1,4,2-oxathiazole-*S*-oxides was also isolated (both diastereomers) and well as three 1,4,2-oxathiazole reduction products (only formed under rhodium catalysed reaction conditions), one of which was confirmed by X-ray crystallography. It became apparent during the course of this study that the 1,2,5-oxathiazole-*S*-oxides have the unexpected property of interconversion from a kinetic isomer to a thermodynamic isomer (Scheme 114). The stereochemistry and regiochemistry of the cycloadducts were unambiguously defined using single crystal X-ray analysis of four cycloadducts. A brief study was carried out with lactone derived α-oxo sulfine with nitrile oxides which showed they had the opposite regiochemical outcome to the ketone derivatives.

When the 1,3-dipolar cycloaddition reactions of lactone and ketone derived α-oxo sulfines were carried out with nitrones, the intact cycloadducts, Regioisomer 1 and 2 (Scheme 114) were not isolated in any case. However, a consistent pattern was seen across all reactions with the transformation of Regioisomer 1 to aziridines *via* sulfur extrusion, and rearrangement of Regioisomer 2 to the tentatively assigned β-hydroxy imines.


Ketone Derived
Lactone Derived
T.M. or MW
or Δ or hv
α-Oxo Sulfine
Ketone or Lactone
Ph
N+
O-
or
1,4,2-oxathiazole-S-oxides only
4 Diastereomers
Minor
1,4,2-oxathiazole-S-oxides
2 Diastereomers
Major
1,2,5-oxathiazole-S-oxides
Reduction in the
presence of
Rh2(OAc)4
1,4,2-oxathiazole
1 Diastereomer
Kinetic Isomer
Thermodynamic Isomer
14 examples
Regioisomer 1 - Not Isolable
1,2,5-oxathiazolidine S-oxide
Regioisomer 2 - Not Isolable
1,4,2-oxathiazolidine S-oxide
[- SO2]
If R1 = Ph
debenzylation occurs
in some instances
Aziridine
One diastereomer
Debenzylated Aziridine
One diastereomer
Tentative Assignment as
β-Hydroxy Imine
One diastereomer

Scheme 114

Biological testing was carried out determining the anticancer activity of twelve compounds across the research programme. Four of these were sulfoxide cycloadducts from Diels-Alder cycloaddition reactions, one sulfone derivative, six 1,2,5-oxathiazole-*S*-oxides and one 1,4,2-oxathiazole-*S*-oxide. On analysis of the results from this study, some interesting selectivity patterns were identified and may be worthy of further study in the future.

Outputs from this research have included a review in the *European Journal of Organic Chemistry,* and papers in both the *Journal of Flow Chemistry* and the *Journal of Organic Chemistry,* with a fourth publication (on the 1,3-dipolar cycloadditions) currently in preparation.

"*All things are difficult before they are easy*"

Dr. Thomas Fuller

Chapter 3

Experimental Procedures

3.0 General Procedures

All solvents were distilled prior to use by the following methods: dichloromethane was distilled from phosphorus pentoxide; ethyl acetate was distilled from potassium carbonate; acetone was distilled from potassium permanganate followed by potassium carbonate; toluene was distilled from sodium benzophenone ketyl and stored over 4 Å molecular sieves; and methanol was distilled from magnesium methoxide and stored over 3 Å molecular sieves. Distilled diethyl ether was obtained commercially from Riedel de Haën and HPLC grade acetonitrile, available from Labscan Ltd., was used for diazo transfer reactions. All reagents were used without further purification except for *p*-toluenesulfonyl chloride, which was used after any tosic acid impurities had been precipitated using dichloromethane and hexane.[166] 3-Chloroperoxybenzoic acid (77% max.) supplied by Aldrich was used without further purification unless otherwise stated; the active oxygen content was determined by iodometric titration.[167]

^{1}H (300.13 MHz) and ^{13}C (75.5 MHz) NMR spectra were recorded on a Bruker Avance 300 NMR spectrometer. ^{1}H NMR (400.13 MHz) and ^{13}C (100 MHz) spectra were recorded on a Bruker Avance 400 NMR spectrometer. All spectra were recorded at 20 °C, in deuterated chloroform ($CDCl_3$), using tetramethylsilane (TMS) as an internal standard, and on the Bruker Avance 400 NMR spectrometer unless otherwise stated. Chemical shifts (δ_H and δ_C) are reported as parts per million (ppm) relative to TMS and coupling constants are expressed in Hertz (Hz). Splitting patterns in ^{1}H NMR spectra are designated as s (singlet), br s (broad singlet), br d (broad doublet), d (doublet), t (triplet), q (quartet), dd (doublet of doublets), dt (doublet of triplets), td (triplet of doublets), qd (quartet of doublets), m (multiplet) and ABq (AB quartet). While the term AB quartet is used throughout this report, this is perhaps more accurately described as an AB system consisting of two doublets. ^{13}C NMR spectra were calibrated using the solvent signals *i.e.* $CDCl_3$: δ_C 77.0 ppm. All spectroscopic details for compounds previously made were in agreement with those reported unless otherwise stated. Diastereomeric ratios (d.r.) and product ratios were determined by ^{1}H NMR spectroscopy. Infra red spectra were recorded Perkin Elmer FTIR UATR2 spectrometer. Microwave-assisted synthesis was carried out using the CEM Discover Synthesiser in conjunction with ChemDriver software (Version 3.5.0) and the CEM Discover S-class Synthesiser in conjunction with Synergy software (Version 1.19). Both microwaves apply a maximum power of 300 W and reaction temperatures were measured by an IR sensor with an accuracy of ±5 °C. Continuous flow reactions were carried out on Vaportec R-Series or E-Series flow reactors. Melting points were measured on a Uni-Melt Thomas Hoover capillary melting point apparatus and are uncorrected.

Wet flash column chromatography was carried out on silica gel using Kieselgel 60, 0.040-0.063 mm (Merck). Thin layer chromatography (TLC) was carried out on precoated silica gel plates (Merck 60 PF254). Visualisation was achieved by UV light detection (254 nm), vanillin staining, iodine staining and potassium permanganate staining as appropriate.

Low resolution mass spectra were recorded on a Waters Quattro Micro triple quadrupole instrument in electrospray ionization (ESI) mode using 50% acetonitrile-water containing 0.1% formic acid as eluent; samples were made up in acetonitrile. High resolution precise mass spectra (HRMS) were recorded on a Waters LCT Premier TOF LC-MS instrument in electrospray ionization (ESI) mode using 50% acetonitrile-water containing 0.1% formic acid as eluent; samples were made up in acetonitrile.

Single crystal X-ray analysis was conducted by Dr. S. E. Lawrence, Dr. Kevin Eccles and Uday Khandivalli, Department of Chemistry, University College Cork using a Nonium Mach 3 diffractometer with graphite monochromatised Mo-Kα radiation (λ = 0.71069 Å). Calculations were performed on a PC with the SHELXL-97 (G.M. Sheldrick, University of Gottingen, 1998) and Platon (A.L. Spek, University of Utrecht, 1998) suite of programs.

Thermogravimetric analysis (TGA) was carried out on a Thermal Analysis (TA) Q500 Thermogravimetric Analysis instrument.

Glassware, gloves and any materials which were in contact with thioglycolic acid or any malodorous sulfur compounds were soaked for at least 24 h in a bleach bath.

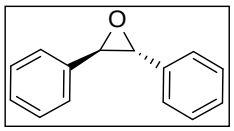
3.1 Synthesis of α-diazosulfoxides

3.1.1 Procedure for Generating Sodium Methoxide

Sodium metal was cut into small pieces and washed with hexane to remove any paraffin oil. The sodium was then added, slowly and in small portions, to methanol which was stirring at 0 °C under a nitrogen atmosphere. Any sodium residues which may have remained in the hexane washing were quenched with a small amount of methanol.

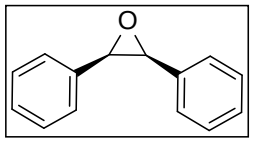
3.1.2 Synthesis of Epoxides

trans-2,3-Diphenyloxirane 12



trans-Stilbene **46** (2.75 g, 15.25 mmol, 1 eq) was dissolved in dichloromethane (25 mL) and stirred in a dry round bottomed flask under a nitrogen atmosphere. 3-Chloroperoxybenzoic acid (3.69 g, 21.38 mmol, 1.4 eq, 77%) was dissolved in dichloromethane (35 mL) and added dropwise to the stirring solution at 0°C over 15 min. The reaction mixture was stirred at 0°C for 3 h and then at room temperature for a further 13 h. The reaction mixture was filtered to remove the precipitated 3-chlorobenzoic acid. The filtrate was washed with aqueous $NaHCO_3$ (10%, 2 x 15 mL), water (1 x 15 mL), and brine (1 x 15 mL). The resulting solution was concentrated *in vacuo* to give *trans*-stilbene oxide **12** as a white crystalline solid (2.56 g, 86%). ν_{max}/ cm^{-1} (neat): 2923, 1452; δ_H (400 MHz) 3.87 (2H, s, CH), 7.30 – 7.42 (10H, m, Aromatic CH); δ_C (75.5 MHz) 62.87 (2 x CH), 125.5 (4 x CH), 128.3 (2 x aromatic CH), 128.5 (4 x aromatic CH), 137.1 (2 x aromatic Cq); HRMS (ESI +): Exact mass calculated for $C_{14}H_{12}O$ $[M+H]^+$, 197.0960. Found: 197.0960. Spectral characteristics in agreement with those reported in the literature. [16]

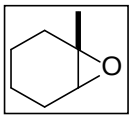
cis-2,3-Diphenyloxirane 45



cis-Stilbene **47** (1.95 g, 11.00 mmol, 1 eq) in dichloromethane (25 mL) was stirred in a dry round bottomed flask under a nitrogen atmosphere. 3-Chloroperoxybenzoic acid (2.84 g, 16.51 mmol, 1.4 eq, 77%) was dissolved in dichloromethane (35 mL) and added dropwise to the stirring solution at 0°C over 15 min. The reaction mixture was stirred at 0°C for 3 h and then at room temperature for a further 13 h. The reaction mixture was filtered to remove the precipitated *m*-chlorobenzoic acid, which had precipitated. The filtrate was washed with aqueous $NaHCO_3$ (10%, 2 x 15 mL), water (1 x 15 mL), and brine (1 x 15 mL). The resulting solution was concentrated *in vacuo* to give *cis*-stilbene oxide **45** as a yellow oil (1.99 g, 93%). ν_{max}/ cm^{-1} (neat): 3024, 1448; δ_H (400 MHz): 4.34 (2H, s, CH), 7.06 – 7.25 (10H, m, Aromatic CH); δ_C (75.5 MHz)

59.8 (2 x CH), 126.9 (4 x Aromatic CH), 127.5 (2 x Aromatic CH), 127.8 (4 x Aromatic CH), 134.4 (2 x Aromatic Cq). Spectral characteristics in agreement with those reported in the literature. [16]

1-Methyl-7-oxabicyclo [4.1.0] heptane 6

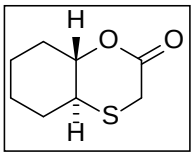


1-Methylcyclohexene (4.5 g, 48 mmol, 1 eq) was dissolved in dichloromethane (25 mL) and stirred in a dry round bottomed flask under a nitrogen atmosphere. 3-Chloroperoxybenzoic acid (11.5 g, 48 mmol, 1.4 eq, 77%) was dissolved in dichloromethane (35 mL) and added dropwise to the stirring solution at 0°C over 15 min. The reaction mixture was stirred at 0°C for 3 h and then at room temperature for a further 13 h. The reaction mixture was filtered to remove the precipitated 3-chlorobenzoic acid. The filtrate was washed with aqueous $NaHCO_3$ (10%, 2 x 30 mL), water (1 x 30 mL), and brine (1 x 30 mL). The resulting solution was concentrated *in vacuo* to give the epoxide **6** as a colourless oil (2.6 g, 58 %). δ_H (400 MHz) 1.19-1.50 (overlapping signals including 3H of cyclohexyl ring and a 3H, s at 1.29), 1.61 - 1.71 (1H, m, cyclohexyl ring), 1.80 - 1.94 (4H, m, cyclohexyl ring), 2.96 (1H, s, CHO); δ_C (75.5 MHz) 19.6 (CH_3), 20.0, 23.9, 24.7, 29.8 (4 x CH_2) 57.4 (Cq, CqO), 59.4 (CH, CHO). Spectral characteristics in agreement with those reported in the literature. [16]

3.1.3 Synthesis of sulfides

3.1.3.1 Synthesis of lactone derived Sulfides

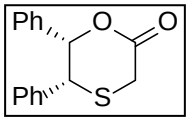
***trans*-Hexahydro-benzo [1, 4] oxathiin-2-one 4**



(a) A solution of thioglycolic acid **2** (3.18 mL, 45.7 mmol, 1 eq.) in methanol (25 mL) was added slowly over 10 min, to a freshly prepared solution of sodium methoxide (2.12 g sodium, 92.2 mmol, 2 eq in 100 mL methanol) while stirring at 0 °C under a nitrogen atmosphere. The colourless solution was stirred for 5 min and a solution of 1-cyclohexene oxide (4.5 g, 45.7 mmol, 1 eq.) in methanol (20 mL) was added dropwise to the solution while stirring at 0°C. The temperature was maintained at 0°C until the addition of the epoxide was complete. The reaction mixture was then heated under reflux conditions for 3 h under a nitrogen atmosphere. The reaction mixture was cooled and the solvent removed *in vacuo* to leave a white solid which was dissolved in water (60 mL) and acidified to pH 1 with concentrated hydrochloric acid. The aqueous solution was extracted with diethyl ether (3 × 35 mL). The combined ethereal layers were washed with water (20 mL), brine (20 mL), dried with anhydrous $MgSO_4$ and concentrated *in vacuo* to leave the hydroxy acid **3** (8.69 g) as a colourless oil.

(b) The crude hydroxy acid **3** was dissolved in toluene (100 mL) and a catalytic amount of tosic acid (40 mg, 0.2 mmol) was added. The reaction mixture was heated under reflux conditions for 6 h under Dean-Stark conditions. The solution was cooled and washed with sodium bicarbonate solution (10%, 3 × 30 mL), water (20 mL), brine (20 mL), and dried with anhydrous $MgSO_4$. The organic layer was concentrated under reduced pressure to give the sulfide **4** as a pale yellow solid (5.93 g, 75% over the two steps). Analysis by ^1H NMR spectroscopy indicated that the material was sufficiently pure to be carried on to the next step without further purification; ν_{max}/ cm^{-1} (neat): 2932, 1721, 1039; δ_H (400 MHz) 1.11-1.64 (4H, m, cyclohexyl ring), 1.69-1.81 (1H, m, cyclohexyl ring), 1.82-1.92 (1H, m, cyclohexyl ring), 1.96-2.12 (1H, m, cyclohexyl ring), 2.19-2.30 (1H, m, cyclohexyl ring), 3.00 (1H, overlapping ddd, *J* 11.6, 10.4, 4.0, CHS), 3.23 (1H, d, *J* 14.7, A of ABq, one of SCH_2), 3.69 (1H, d, *J* 14.7, B of ABq, one of SCH_2), 4.17 (1H, overlapping ddd appears as dt, *J* 10.6, 10.6, 4.3, CHO); δ_C (300 MHz): 23.7, 25.1, 26.8, 32.2, 32.6 (5 x CH_2), 43.0 (CH, CHS), 81.7 (CH, CHO), 168.0 (Cq, C=O); HRMS (ESI +): Exact mass calculated for $C_8H_{12}O_2S$ $[M+H]^+$, 173.0612 Found: 173.0622. Spectral characteristics are in agreement with those reported in the literature.[13]

***cis*-5, 6-Diphenyl-1,4-oxathian-2-one 9**

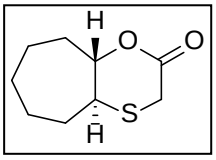


(a) A solution of thioglycolic acid **2** (4.58 mL, 49.73 mmol, 1 eq.) in methanol (10 mL) was added slowly to a freshly prepared solution of sodium methoxide (2.28 g sodium, 99.46 mmol, 2 eq in 150 mL methanol) over 10 min, while stirring at 0 °C under a nitrogen atmosphere. The colourless solution was stirred for 5 min and *trans*-stilbene oxide **12** (9.76 g, 49.73 mmol, 1 eq.) was added in one portion to the solution while stirring at 0 °C. The reaction mixture was then heated under reflux conditions for 3 h under a nitrogen atmosphere. The reaction mixture was cooled and the solvent removed *in vacuo* to leave a pale yellow solid which was dissolved in water (50 mL) and acidified to pH 1 with concentrated hydrochloric acid. The aqueous solution was extracted with diethyl ether (3 × 35 mL). The combined ethereal layers were washed with water (20 mL), brine (20 mL), dried with anhydrous $MgSO_4$ and concentrated *in vacuo* to leave the hydroxy acid (16.1 g) as a colourless oil.

(b) The crude hydroxy acid was dissolved in toluene (100 mL) and a catalytic amount of tosic acid (40 mg, 0.2 mmol) was added. The reaction mixture was heated under reflux conditions for 4 h under Dean-Stark conditions. The solution was cooled and washed with sodium bicarbonate solution (10%, 3 × 30 mL), water (20 mL), brine (20 mL), and dried with anhydrous $MgSO_4$. The organic layer was then concentrated *in vacuo* to give the sulfide **9** as a pale yellow solid which was recrystallized from hot ethyl acetate to give the sulfide as a white crystalline solid (7.36 g, 55%). δ_H (400 MHz) m.p. 145–146

°C (lit., 145–147 °C)[15]; ν_{max}/cm^{-1} (neat) 1748, 1253; δ_H (300 MHz) 3.53 (1H, d, A of ABq, *J* 14.4, 0.5, one of SCH_2), 3.99 (1H, d, B of ABq, *J* 14.4, SCH_2), 4.55 (1H, incompletely resolved d, *J* 3.3, CHS), 5.74 (1H, d, *J* 3.2, CHO), 6.87 – 7.04 (4H, m, 4 x Aromatic CH), 7.08–7.25 (6H, m, 6 x Aromatic CH); δ_C (100 MHz) 27.9 (CH_2), 49.4 (CH, CHS), 81.6 (CH, CHO), 126.3, 127.3, 127.9, 128.4, 128.6, 129.8 (10 x Aromatic CH) 135.1, 136.0 (2 x Aromatic Cq), 168.3 (Cq, C=O). Spectral details in agreement with those reported in the literature. [15]

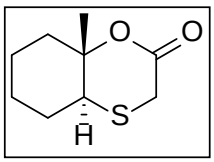
Hexahydro-5*H*-cyclohepta[*b*] [1, 4] oxathiin-2(3*H*)-one 7



(a) A solution of thioglycolic acid **2** (3.81 mL, 54.6 mmol, 1 eq.) in methanol (25 mL) was added slowly to a freshly prepared solution of sodium methoxide (2.51 g sodium, 109.3 mmol, 2 eq in 100 mL methanol) while stirring at 0 °C under a nitrogen atmosphere. The colourless solution was stirred for 5 min and a solution of cycloheptene oxide **10** (6.13 g, 54.6 mmol, 1 eq.) in methanol (20 mL) was added dropwise to the solution while stirring at 0°C. The temperature was maintained at 0°C until the addition of the epoxide **10** was complete. The reaction mixture was then heated under reflux conditions for 3 h under a nitrogen atmosphere. The reaction mixture was cooled and the solvent removed *in vacuo* to leave a white crystalline solid which was dissolved in water (40 mL) and acidified to pH 1 with concentrated hydrochloric acid. The aqueous solution was extracted with diethyl ether (3 × 35 mL). The combined ethereal layers were washed with water (20 mL), brine (20 mL), dried with anhydrous $MgSO_4$ and concentrated *in vacuo* to leave the hydroxy acid (8.46 g) as a colourless oil.

(b) The crude hydroxy acid was dissolved in toluene (80 mL) and a catalytic amount of tosic acid (40 mg, 0.2 mmol) was added. The reaction mixture was heated under reflux conditions for 6 h under Dean-Stark conditions. The solution was cooled and washed with sodium bicarbonate solution (10%, 3 × 30 mL), water (20 mL), brine (20 mL), and dried with anhydrous $MgSO_4$. The organic layer was then concentrated *in vacuo* to give the sulfide **7** as a white crystalline solid (5.59 g, 55% over the two steps); ν_{max}/ cm^{-1} (neat): 1732, 1264; δ_H (400 MHz) 1.38–1.94 (9H, m, cycloheptyl ring), 2.05–2.22 (1H, m, cycloheptyl ring), 3.14 (1H, overlapping ddd appears as dt, *J* 9.8, 9.8, 3.0, C*H*S), 3.22 (1H, d, A of ABq, *J* 14.7, one of SCH_2), 3.68 (1H, d, B of ABq, *J* 14.5, one of SCH_2), 4.17–4.37 (1H, m, CHO); δ_C (75.5 MHz) 22.0, 25.5, 27.27, 27.31, 30.8 (5 x CH_2 of cycloheptyl ring), 33.5 (CH_2, SCH_2), 46.3 (CH, CHS), 85.4 (CH, CHO), 168.9 (Cq, C=O); Spectral details in agreement with those reported in the literature. [15]

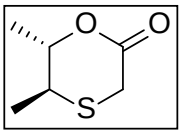
(8aS)-8a-Methylhexahydrobenzo[*b*][1,4]oxathiin-2(3*H*)-one 5



A solution of thioglycolic acid **2**(1.26 g, 0.95 mL, 13.7 mmol, 1 eq.) in methanol (25 mL) was added slowly to a freshly prepared solution of sodium methoxide (0.63 g sodium, 27.4 mmol, 2 eq in 100 mL methanol) over 10 min, while stirring at 0°C under a nitrogen atmosphere. The colourless solution was stirred for 5 min and a solution of 1-methylcyclohexene oxide **6** (1.54 g, 13.7 mmol, 1 eq.) in methanol (20 mL) was added dropwise to the solution while stirring at 0 °C. The temperature was maintained at 0 °C until the addition of the epoxide **6** was complete. The reaction mixture was then heated under reflux conditions for 5 h under a nitrogen atmosphere. The reaction mixture was cooled and the solvent removed *in vacuo* to leave a pale yellow solid which was dissolved in water (50 mL) and acidified to pH 1 with concentrated hydrochloric acid. The aqueous solution was extracted with diethyl ether (3 × 35 mL). The combined ethereal layers were washed with water (20 mL), brine (20 mL), dried with anhydrous $MgSO_4$ and concentrated *in vacuo* to leave the hydroxy acid (4.92 g) as a colourless oil.

(b) The crude hydroxy acid was dissolved in toluene (80 mL) and a catalytic amount of tosic acid (40 mg, 0.2 mmol) was added. The reaction mixture was heated under reflux conditions for 6 h under Dean-Stark conditions. The solution was cooled and washed with sodium bicarbonate solution (10%, 3 × 30 mL), water (20 mL), brine (20 mL), and dried with anhydrous $MgSO_4$. The organic layer was then concentrated *in vacuo* to give the sulfide **5** as a white crystalline solid (2.10 g, 82% over the two steps). δ_H (400 MHz) 1.20-1.94 (10H, m, contains 7H of cyclohexyl ring and CH_3 s at 1.57), 2.00-2.12 (1H, m, CH of cyclohexyl ring), 3.12 (1H, dd, *J* 12.0, 3.8, CHS), 3.46 (1H, d, A of ABq, *J* 17.0, one of SCH_2), 3.64 (1H, d, B of ABq, *J* 17.0, one of SCH_2); δ_C (100 MHz) 19.3 (CH_3), 22.5, 25.6, 25.6, 28.4, 39.1 (5 x CH_2), 46.0 (CH, CHS), 86.0 (Cq, CqO), 165.8 (Cq, C=O). Spectral characteristics are in agreement with those reported in the literature.[13] Signals corresponding to residual tosic acid (<5%) are observed in the ^{13}C NMR spectrum at 128.2 and 129.0 ppm.

***trans*-5,6-Dimethyl-1,4-oxathian-2-one 8**



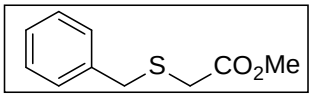
A solution of thioglycolic acid **2** (0.96 mL, 13.86 mmol, 1.15 eq.) in methanol (25 mL) was added slowly to a freshly prepared solution of sodium methoxide (0.64 g sodium, 27.72 mmol, 2.3 eq in 100 mL methanol) over 10 min, while stirring at 0 °C under a nitrogen atmosphere. The colourless solution was stirred for 5 min and a solution of *cis*-2,3 epoxybutane **11** (0.86 g, 12 mmol, 1 eq.) in methanol (20 mL) was added dropwise to the solution while stirring at 0 °C. The temperature was maintained at 0 °C until the addition of the epoxide **11** was

complete. The reaction mixture was then heated under reflux conditions for 1.5 h under a nitrogen atmosphere. The reaction mixture was cooled and the solvent removed *in vacuo* to leave a yellow solid which was dissolved in water (30 mL) and acidified to pH 1 with concentrated hydrochloric acid. The aqueous solution was extracted with diethyl ether (3 × 35 mL). The combined ethereal layers were washed with water (20 mL), brine (20 mL), dried with anhydrous $MgSO_4$ and concentrated *in vacuo* to leave the hydroxy acid (1.83 g) as a colourless oil.

(b) The crude hydroxy acid was dissolved in toluene (80 mL) and a catalytic amount of tosic acid (40 mg, 0.2 mmol) was added. The reaction mixture was heated under reflux conditions for 3.5 h under Dean-Stark conditions. The reaction mixture was cooled and washed with sodium bicarbonate solution (10%, 3 × 30 mL), water (20 mL), brine (20 mL), and dried with anhydrous $MgSO_4$. The organic layer was then concentrated *in vacuo* to give the sulfide **8** as a colorless oil (1.21 g, 70% over the two steps). ν_{max}/cm^{-1} (neat): 1721, 1264; δ_H (400 MHz) 1.24 (3H, d, *J* 7.5, CH_3CS), 1.36 (3H, d, *J* 6.6, CH_3CO), 2.97–3.05 (1H, symmetrical m, CHS), 3.10 (1H, d, A of ABq, *J* 14.7, one of $SOCH_2$), 3.60 (1H, d, B of ABq, *J* 14.6, one of $SOCH_2$), 4.18 – 4.25 (1H, m, CHO); δ_H (100 MHz) 18.7, 18.9 (2 x CH_3), 25.6 (CH_2), 39.8 (CH, CHS), 80.2 (CH, CHO), 168.4 (Cq, C=O); (ESI+) $(M+H)^+$ 147 (100%); HRMS (ESI +): Exact mass calculated for $C_6H_{11}O_2S$ $[M+H]^+$, 147.0480 Found : 147.0476.

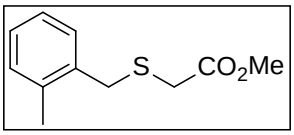
3.1.3.2 Synthesis of ketone derived sulfides

Methyl 2-(benzylthio)acetate 19



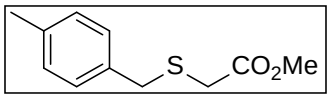
Potassium carbonate (18.60 g, 134 mmol, 2 eq) was slowly added to a solution of methyl thioglycolate **18** (6.02 mL, 67 mmol, 1 eq) in methanol (100 mL) over 5 min at 0 °C. The ice bath was removed and the reaction mixture was allowed to slowly return to room temperature. A solution of benzyl bromide (8.00 mL, 67.0 mmol, 1 eq) in methanol (10 mL) was added over 20 min. The reaction mixture was stirred for 3 h and filtered to remove the inorganic salts which had precipitated. The filtrate was concentrated *in vacuo* and the residue partitioned between water (150 mL) and diethyl ether (150 mL). The layers were separated and the combined ethereal layers were washed with sat. sodium bicarbonate solution (50 mL), water (50 mL), brine (50 mL) and dried with anhydrous $MgSO_4$. The solution was concentrated *in vacuo* to give methyl 2-(benzylthio)acetate **19** as a clear oil which was used without further purification (9.10 g, 69%); ν_{max}/cm^{-1} 1736; δ_H (400 MHz) 3.08 (2H, s, CH_2), 3.71 (3H, s, CH_3), 3.82 (2H, s, CH_2), 7.18-7.47 (5H, m, 5 x Aromatic CH); δ_C (100 MHz) 32.1 (CH_2), 36.4 (CH_2), 52.3 (CH_3), 127.3, 128.6, 129.2 (3 signals representing 5 × Aromatic CH), 137.2 (Aromatic Cq), 170.8 (Cq, C=O). Spectral details are in agreement with those reported in the literature.[16]

Methyl 2-(2-methylbenzylthio)acetate[168] **26**



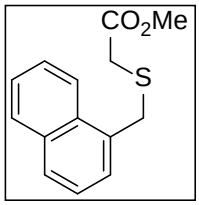
Potassium carbonate (11.59 g, 82.5 mmol, 1.5 eq) was added directly to a solution of 2-methylbenzyl chloride **25** (7.86 g, 55.0 mmol, 1 eq), methyl thioglycolate **18** (5 mL, 55.0 mmol, 1 eq) and sodium iodide (0.42 g, 5 mol%) in acetone (80 mL). This mixture was heated under reflux for 14 h, then concentrated under reduced pressure and the residue was dissolved in ethyl acetate (60 mL) and washed with water (2 x 50 mL). The layers were separated and the organic layer was dried with $MgSO_4$. The dried solution was concentrated *in* vacuo to give methyl 2-(2-methylbenzylthio)acetate **26** as a pale yellow oil which was used without further purification (8.32 g, 75 %). ν_{max}/cm^{-1} (neat) 1736; δ_H (400 MHz) 2.41 (3H, s, $ArCH_3$), 3.11 (2H, s, CH_2), 3.74 (3H, s, CH_3), 3.82 (2H, s, CH_2), 7.07-7.23 (4H, m, Aromatic CH); δ_C (100 MHz) 19.1 (CH_3), 32.4 (CH_2), 34.5 (CH_2), 52.4 (CH_3), 125.8, 127.6, 130.0, 130.8 (4 × Aromatic CH), 134.8 (Aromatic Cq), 137.0 (Aromatic Cq), 171.0 (Cq, C=O). Spectral characteristics are in agreement with those reported in the literature.[16]

Methyl 2-((4-methylbenzyl)thio)acetate 30[169]



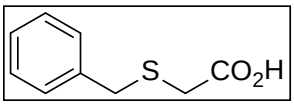
Potassium carbonate (7.84 g, 56.70 mmol, 1.5 eq) was added directly to a solution of 4-methylbenzyl bromide **28** (7.00 g , 37.8 mmol, 1 eq), methyl thioglycolate **18** (3.40 mL, 37.8 mmol, 1 eq) and sodium iodide (0.28 g, 1.89 mmol, 5 mol %) in acetone (80 mL). The reaction mixture was heated under reflux for 20 h, cooled to room temperature and concentrated under reduced pressure to a while solid. The residue was dissolved in ethyl acetate (60 mL) and washed with water (2 x 50 mL). The layers were separated and the organic layer dried with $MgSO_4$. The dried solution was concentrated *in* vacuo to give methyl 2-((4-methylbenzyl)thio)acetate **30** as a pale yellow oil which was used without further purification (7.77 g, 98%). ν_{max}(neat)/cm^{-1} 1737; δ_H (400 MHz) 2.32 (3H, s, $ArCH_3$), 3.07 (2H, s, CH_2), 3.70 (3H, s, CH_3), 3.78 (2H, s, CH_2), 7.09 - 7.16 (2H, m, Aromatic CH), 7.18 - 7.23 (2H, m, Aromatic CH); δ_C (100 MHz) 21.1 ($ArCH_3$), 32.1 (CH_2), 36.1 (CH_2), 52.3 (CH_3), 129.1, 129.2 (2 signals representing 4 × Aromatic CH), 134.1 (1 x Aromatic Cq), 136.9 (1 x Aromatic Cq), 170.9 (Cq, C=O); m/z (ESI+) 211 [(M+H)+, 17%)]. Spectral characteristics are in agreement with those reported in the literature.[16]

Methyl 2-((naphthalen-1-ylmethyl)thio)acetate 31[20]



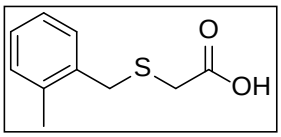
The title compound was prepared following the same procedure described for **19** using 1-chloromethylnaphthalene **29** (4.24 mL, 28.30 mmol, 1 eq), potassium carbonate (5.87 g, 42.45 mmol, 1.5 eq), methyl thioglycolate **18** (2.53 mL, 28.30 mmol, 1 eq) and sodium iodide (0.21 g, 1.42 mmol, 5 mol%) in acetone (60 mL). Following work-up the crude ester **31** was isolated as a viscous yellow oil (7.01 g, 95%). ν_{max}/cm^{-1} 1732; δ_H (400 MHz) 3.12 (2H, s, CH_2), 3.71 (3H, s, CH_3), 4.29 (2H, s, CH_2), 7.35-7.57 (4H, m, Aromatic CH), 7.72-7.87 (2H, m, Aromatic CH), 8.13 (1H, d, *J* 8.4, Aromatic CH); δ_C (100 MHz) 32.6 (CH_2), 34.1 (CH_2), 52.4 (CH_3), 124.0, 125.1, 125.9, 126.3, 127.8, 128.5, 128.8 (7 × Aromatic CH), 131.4, 132.4, 134.2 (3 × Aromatic Cq), 171.0 (Cq, C=O); Spectral characteristics are in agreement with those provided in the literature.[16,20]

2-(Benzylthio)acetic acid 20[18]



Methyl 2-(benzylthio)acetate **19** (8.3 g, 42.33 mmol) was added to a solution of acetic acid and water (50:50, 100 mL). The reaction mixture was heated under reflux conditions for 30 h and cooled to room temperature. The reaction mixture was extracted with diethyl ether (2 × 40 mL). The combined ethereal layers were washed with water (6 × 150 mL), brine (20 mL), dried with anhydrous $MgSO_4$ and concentrated *in vacuo* to give 2-(benzylthio)acetic acid **20** as a white crystalline solid which was used without further purification (7.24 g, 94 %); ν_{max}/cm^{-1} 3431, 1708; δ_H (400 MHz) 3.10 (2H, s, CH_2), 3.86 (2H, s, CH_2), 7.21-7.48 (5H, m, 5 x Aromatic CH), 10.25 (1H, br s, OH); δ_C (100 MHz) 31.9 (CH_2), 36.4 (CH_2), 127.4, 128.6, 129.2 (3 signals representing 5 × Aromatic CH), 136.9 (Aromatic Cq), 176.7 (Cq, C=O); HRMS (ESI+) m/z (ESI-) 181 [(M-H)-, 90%]. Spectral characteristics are in agreement with those provided in the literature.[16,18]

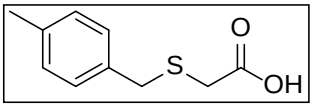
2-(2-Methylbenzylthio)acetic acid 27[16,168]



Methyl 2-(2-methylbenzylthio)acetate **26** (7.35 g, 35.06 mmol) was added to a solution of acetic acid and water (50:50, 100 mL). The reaction mixture was heated under reflux conditions for 20 h and cooled to room temperature. The mixture was extracted with diethyl ether (2 × 40 mL). The combined ethereal layers were washed with water (6 × 150 mL), brine (20 mL), dried with anhydrous $MgSO_4$ and concentrated *in vacuo* to give 2-(2-methylbenzylthio)acetic acid **27** (6.11 g, 94%), as a white crystalline solid which was used without further purification. ν_{max}/cm^{-1} (neat) 3019, 1706; δ_H (400 MHz) 2.41 (3H, s, CH_3), 3.14 (2H, s, CH_2), 3.88 (2H, s, CH_2), 7.12-7.26 (4H, m, 4 x Aromatic CH), 9.50 (1H, br s, OH); δ_C (75.5

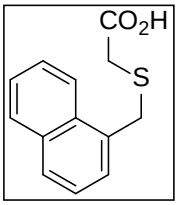
MHz) 19.1 (CH_3), 32.3 (CH_2), 34.5 (CH_2), 125.9, 127.8, 130.1, 130.9 (4 × Aromatic CH), 134.5 (1 x Aromatic Cq), 137.0 (1 x Aromatic Cq), 176.9 (Cq, C=O). Spectral details are in agreement with those reported in the literature. [16]

2-((4-Methylbenzyl)thio)acetic acid 32[170]



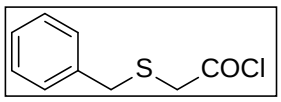
The title compound was prepared following the procedure described for the sulfide **20** using methyl 2-(4-methylbenzylthio)acetate **30** (6.85 g, 32.6 mmol), acetic acid and water (50 : 50, 80 mL), however it was heated under reflux for a total of 36 h. Following work-up, 2-(4-methylbenzylthio)acetic acid **32**, and some remaining acetic acid (3:1) was isolated as a clear oil and was used without further purification (6.39 g, 94 %). ν_{max}(neat)/cm^{-1} 3431, 1642; δ_H (400 MHz) 2.33 (3H, s, CH_3), 3.09 (2H, s, CH_2), 3.82 (2H, s, CH_2), 7.13 (2H, d, *J* 7.9, 2 x Aromatic CH), 7.22 (2H, d, *J* 8.0, 2 x Aromatic CH), 10.56 (1H, br s, OH); δ_C (100 MHz) 21.1 (CH_3), 32.0 (CH_2), 36.1 (CH_2), 129.1 (2 × Aromatic CH), 129.3 (2 × Aromatic CH), 133.8 (Aromatic Cq), 137.1 (Aromatic Cq), 177.1 (Cq, C=O). Signals detected for remaining acetic acid: δ_H (400 MHz) 2.11 (3H, s, CH_3); δ_C (75.5 MHz) 20.8 (CH_3), 178.0 (Cq, C=O). Spectral details are in agreement with those provided in the literature.[170]

2-((Naphthalen-1-ylmethyl)thio)acetic acid 33[20]



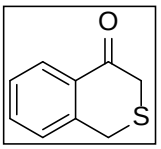
Methyl 2-((naphthalen-1-ylmethyl)thio)acetate **31** (6.50 g, 24.9 mmol) was added to a solution of acetic acid and water (50 : 50, 100 mL). The reaction mixture was heated under reflux conditions for 20 h and cooled to room temperature. The mixture was extracted with diethyl ether (2 × 40 mL). The combined ethereal layers were washed with water (6 × 150 mL), brine (20 mL), dried with anhydrous $MgSO_4$ and concentrated *in vacuo* to give the product as an off white crystalline solid (4.82 g, 89%). Analysis by ^{1}H NMR spectroscopy showed the product to be 95% pure with the impurity being the residual ester **31**. δ_H (400 MHz) 3.16 (2H, s, CH_2), 4.35 (2H, s, CH_2), 7.36-7.62 (4H, m, 4 x Aromatic CH), 7.75-7.85 (1H, d, *J* 7.9, Aromatic CH), 7.85-7.92 (1H, d, *J* 8.2, Aromatic CH), 8.12 (1H, d, *J* 8.4, Aromatic CH), 11.20 (1H, br s, OH); δ_C (75.5 MHz) 32.5 (CH_2), 34.1 (CH_2), 123.9, 125.1, 126.0, 126.3, 127.9, 128.6, 128.9 (7 × Aromatic CH), 131.3, 132.1, 134.2 (3 × Aromatic Cq), 176.3 (Cq, C=O). Spectral details are in agreement with those reported in the literature.[20]

2-(Benzylthio)acetyl chloride 21[18]



Thionyl chloride (3.86 g, 32.5 mmol, 2.35 mL, 2 eq) in dichloromethane (20 mL) was added dropwise to 2-(benzylthio)acetic acid **20** (2.96 g, 16.2 mmol, 1 eq) in dichloromethane (60 mL) over 10 min at 0 °C. The reaction mixture was allowed to slowly reach room temperature and stirred for a further 16 h. The solvent and excess thionyl chloride were removed in vacuo to leave 2-(benzylthio)acetyl chloride **21** as a yellow oil which was used without further purification (3.31 g, 98 %); ν_{max}(neat)/cm^{-1} 1791; δ_H (400 MHz) 3.51 (2H, s, CH_2), 3.82 (2H, s, CH_2), 7.21-7.49 (5H, m, 5 x Aromatic CH); δ_C (100 MHz) 36.2 (CH_2), 43.6 (CH_2), 127.7, 128.8, 129.2 (3 signals representing 5 × Aromatic CH), 136.1 (Aromatic Cq), 170.1 (Cq, C=O). Spectral details in agreement with those reported in the literature.[18]

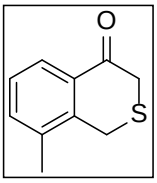
Isothiochroman-4-one 16[18]



Anhydrous aluminium chloride (2.88 g, 26.9 mmol, 1.4 eq) in dichloromethane (30 mL) was added slowly in portions to a solution of 2-(benzylthio)acetyl chloride **21** (3.60 g, 18 mmol, 1 eq) in dichloromethane (80 mL) at room temperature. The reaction mixture was stirred overnight at room temperature. A solution of conc. hydrochloric acid in water (50:50, 60 mL) was added and the layers were separated. The organic layer was washed with sat. sodium bicarbonate solution (2 × 20 mL), water (20 mL) and brine (20 mL) and was dried with anhydrous $MgSO_4$. The solution was concentrated *in vacuo* to give isothiochroman-4-one **16** as a brown solid which was used without further purification (1.89 g, 75 %). m.p. 61-62°C; ν_{max}(neat)/cm^{-1} 1673; δ_H (400 MHz) 3.56 (2H, s, CH_2), 3.93 (2H, s, CH_2), 7.20 (1H, d, *J* 7.9, 1 x Aromatic CH), 7.34-7.40 (1H, m, 1 x Aromatic CH), 7.43-7.49 (1H, m, 1 x Aromatic CH), 8.09 (1H, d, *J* 7.9, 1 x Aromatic CH); δ_C (100 MHz) 30.6 (CH_2, $ArCH_2$), 37.1 (CH_2), 127.7, 127.8, 129.0 (3 × Aromatic CH), 131.9 (1 x Aromatic Cq), 133.0 (1 x Aromatic CH), 141.8 (1 x Aromatic Cq), 191.0 (Cq, C=O). Spectral details in agreement with those reported in the literature.[16,19]

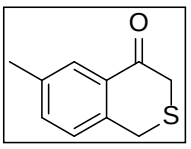
Note: *In the following reactions using P_2O_5, the paste/residues left in the round bottomed flask after the reaction mixture has been decanted, need to be carefully quenched. The order of addition of quenching solvents is isopropyl alcohol, absolute ethanol, 95% ethanol and finally water.*

8-Methylisothiochroman-4-one 22[16]



Phosphorous pentoxide (14.27 g, 100.60 mmol, 3 eq) was added portionwise over 10 min, to a stirring solution of 2-(2-methylbenzylthio)acetic acid **27** (6.11 g, 33.5 mmol, 1 eq) in hot toluene (60 °C, 100 mL). The mixture was stirred vigorously under reflux for 3 h. The oil bath was removed, the reaction mixture was allowed cool to room temperature and a further 2 eq. phosphorous pentoxide (9.51 g, 67.00 mmol) were then added portionwise. The mixture was stirred for an additional 2 h under reflux and cooled to room temperature. The organic solution was decanted from the brown insoluble mass, which was extracted with hot toluene (60 °C, 2 × 40 mL). The combined organic layers were concentrated *in vacuo* and gave the crude product as a light brown solid which was purified by flash chromatography (95:5 hexane:ethyl acetate) to give 8-methylisothiochroman-4-one **22** (1.40 g, 23 %) as a yellow solid. ν_{max}/cm^{-1} (neat) 1681; δ_H (400 MHz) 2.31 (3H, s, CH_3), 3.46 (2H, s, CH_2), 3.83 (2H, s, $ArCH_2$), 7.22-7.27 (1H, m, Aromatic CH), 7.33 (1H, d, *J* 6.9, Aromatic CH), 7.94 (1H, d, *J* 7.8, Aromatic CH); δ_C (100 MHz) 19.6 (CH_3), 27.5 (CH_2), 35.9 ($ArCH_2$), 127.6 (1 x Aromatic CH), 127.7 (1 x Aromatic CH), 132.6 (1 x Aromatic Cq), 134.3 (1 x Aromatic CH), 135.4 (1 x Aromatic Cq), 139.8 (1 x Aromatic Cq), 191.1 (Cq, C=O). Spectral details in agreement with those reported in the literature. [168]

6-Methylisothiochroman-4-one 23

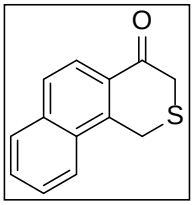


Phosphorous pentoxide (39.41 g, 139.2 mmol, 3 eq) was added portionwise over 10 min, to a stirring solution of 2-(2-methylbenzylthio)acetic acid **32** (9.10 g, 46.4 mmol, 1 eq) in hot toluene (60 °C, 250 mL). The mixture was stirred vigorously under reflux for 3 h. The oil bath was removed, the reaction mixture was allowed cool to room temperature, and a further 2 eq. phosphorous pentoxide (28.01 g, 92.5 mmol, 2 eq) were then added portionwise. The mixture was stirred for an additional 3 h under reflux and cooled to room temperature. The organic solution was decanted from the brown insoluble mass, which was extracted with hot toluene (60 °C, 2 × 80 mL). The combined organic layers were concentrated *in vacuo* and gave the crude product as a light brown solid which was purified by flash chromatography (95 : 5 hexane-ethyl acetate) to give 6-methylisothiochroman-4-one **23** (2.29 g, 28 %). m.p. 51-52 °C (lit.,[171] 52-53 °C); ν_{max} (neat)/cm^{-1} 1678 (Cq, C=O); δ_H (400 MHz) 2.22 (3H, s), 3.36 (2H, s, CH_2), 3.70 (2H, s, $ArCH_2$), 6.92 (1H, d, *J* 7.8, 1 x

Aromatic CH), 7.10 (1H, m, 1 x Aromatic CH), 7.73 (1H, s, 1 x Aromatic CH); δ_C (75.5 MHz) 21.0 (CH_3), 30.3, 37.1 (2 x CH_2), 127.7, 129.2 (2 x Aromatic CH), 131.6 (1 x Aromatic Cq), 133.9 (1 x Aromatic CH), 137.5 (1 x Aromatic Cq), 138.9 (1 x Aromatic Cq), 191.5 (Cq, C=O). Spectral details in agreement with those reported in the literature.[171]

1-Oxo-3-thia-1,2,3,4-tetrahydrophenanthrene 24[20]

Method 1: Phosphorus pentoxide and Celite®in toluene at reflux (3 h) – method by Aitken.[19]



A suspension of the acid **33** (1.5 g, 6.87 mmol, 1 eq) in toluene was heated to 80°C until the solid dissolved. A thick paste of Celite® (1.95 g) and phosphorus pentoxide (3.91 g, 13.75 mmol, 2 eq) in toluene (25 mL) was added slowly to the vigorously stirred mixture. The solution was heated under reflux for 3 h and on cooling to room temperature was worked up. The solution was filtered and the filtrate washed with an aqueous NaOH solution (1M, 15 mL). The organic layer was separated and washed with water (20 mL) and brine (20 mL). The solution was concentrated under reduced pressure to give the crude product as a thick yellow oil. Analysis by ^{1}H NMR spectroscopy showed the presence of the sulfide **24** along with the acid **33** and ester **31**. Purification by recrystallization from hot ethanol provided the target sulfide (0.115 g, 8%).

Method 2: Phosphorus pentoxide in toluene at reflux (5 h) - method by Buckley.[16]

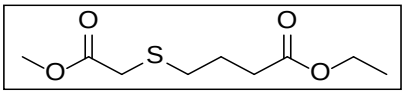
Phosphorous pentoxide (5.52 g, 19.4 mmol, 3 eq) was directly added to a stirring solution of the acid **33** (1.42 g, 6.4 mmol, 1 eq) in hot toluene (60 °C, 100 mL). The mixture was stirred vigorously under reflux for 3 h. The oil bath was removed, the reaction mixture was cooled to room temperature, and another portion of phosphorous pentoxide (3.7 g, 12.8 mmol, 2 eq.) was added. The mixture was stirred for an additional 2 h under reflux and cooled to room temperature. The organic solution was decanted from the brown insoluble mass, which was extracted with hot toluene (60 °C, 2 × 40 mL). The combined organic layers concentrated *in vacuo* and gave the crude product as a light brown solid which was purified by column chromatography on silica gel to give the sulfide **24** as a yellow solid (0.295 g, 30%). ν_{max} (neat)/cm^{-1} 1678; δ_H (400 MHz) 3.58 (2H, s), 4.37 (2H, s), 7.58-7.65 (2H, m, 2 x Aromatic CH), 7.81 (1H, d, *J* 8.0, 1 x Aromatic CH), 7.84-7.91 (1H, m, 1 x Aromatic CH), 8.00-8.11 (1H, m, 1 x Aromatic CH), 8.15 (1H, d, *J* 7.9, 1 x Aromatic CH); δ_C (100 MHz) 26.9, 35.6 (2 x CH_2), 124.0, 124.1, 127.3, 127.8, 128.5, 129.0 (6 x Aromatic CH), 129.8, 130.5, 135.3, 139.4 (4 x Aromatic Cq), 191.2 (Cq, C=O). Spectral details in agreement with those reported in the literature.[20,16]

Method 3: Phosphorus pentoxide and Celite®in toluene at reflux (5 h) - Combination of methods by both Aitken and Buckley.[16,19]

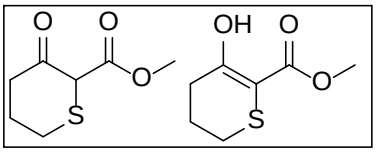
A suspension of the acid **33** in toluene was heated to 80°C until the solid dissolved. A thick paste of Celite®(1.95 g) and phosphorus pentoxide (3.91 g, 13.75 mmol, 2 eq) in toluene (25 mL) was added slowly to the vigorously stirred mixture. The solution was heated under reflux for 2 h and on cooling to room temperature another portion of phosphorus pentoxide was added (5.86 g, 20.62 mmol, 3 eq). The solution was heated under reflux for a further 3 h. After decanting the reaction mixture and rinsing the brown residue with hot toluene (60°C, 2 x 30 mL), the organic solution was concentrated *in vacuo* the crude product was isolated as a brown oil and on analysis by ^{1}H NMR spectroscopy showed the absence of the desired cyclised product.

3.1.3.3 Synthesis of monocyclic sulfides

Dihydro-2H-thiopyran-3(*4H*)-one 34[172]

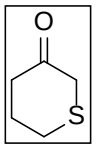


(a) A solution of methyl thioglycolate **18** (6.00 g, 5.08 mL, 56.5 mmol, 1 eq) in methanol (10 mL) was added to a solution of sodium methoxide (sodium 1.30 g, 56.57 mmol, 1 eq) in methanol (60 mL) at 0 °C under a nitrogen atmosphere. The reaction mixture was stirred for 10 min and ethyl 4-bromobutyrate **36** (11.02 g, 8.10 mL, 56.5 mmol, 1 eq) in methanol (10 mL) was added slowly. The reaction mixture was stirred for 15 h at room temperature. The mixture was filtered to remove any inorganic salts which had precipitated, and the filtrate was concentrated *in vacuo* to give a colourless oil. Water (100 mL) was added to the oil and the mixture was extracted with diethyl ether (3 × 50 mL). The combined ethereal layers were washed with water (20 mL), brine (20 mL), dried over anhydrous $MgSO_4$ and concentrated *in vacuo* to give ethyl 4-[(2-methoxy-2-oxomethyl)thio]butanoate **35**[173] as a colourless oil (11.63 g, 88 %) which was used without further purification; ν_{max}(film)/cm^{-1} 1736; δ_H (400 MHz) 1.10 (3H, t, *J* 7.1, CH_2CH_3,), 1.72 – 1.81 (2H, m), 2.27 (2H, t, *J* 6.7), 2.52 (2H, t, *J* 6.9), 3.06 (2H, d, *J* 9.6), 3.57 (3H, s, CH_3), 3.96 (2H, q, *J* 7.4, 6.9, CH_2CH_3).



(b) Potassium *t*-butoxide (5.32 g, 47.4 mmol, 2 eq) was added directly to a solution of methyl 4-[(2-methoxy-2-oxomethyl)thio]butanoate **35** (5.22 g, 23.7 mmol, 1 eq) in diethyl ether (100 mL) at 0 °C. The solution was allowed to slowly reach room temperature while stirring for 4 h. The mixture was hydrolysed with water/acetic acid solution (80 : 20, 60 mL). The aqueous phase was separated and extracted with diethyl ether (2 × 30 mL). The combined ethereal layers were

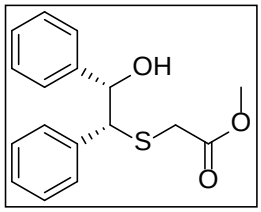
washed with water (5 × 60 mL), brine (20 mL), dried with anhydrous $MgSO_4$ and concentrated in vacuo to give the cyclised keto ester and enol mixture **37** as a yellow oil which was used directly in the next step.



(c) The crude keto ester and enol mixture **37** (1 : 3, 3.54 g) was stirred under reflux in aqueous sulfuric acid solution (15%, 20 mL) overnight and then cooled to room temperature. Aqueous sodium hydroxide solution (10%) was added dropwise to pH 7. The mixture was extracted with ethyl acetate (3 × 40 mL). The combined ethereal layers were washed with water (20 mL), brine (20 mL), dried with anhydrous $MgSO_4$ and concentrated in vacuo to give the crude product as a brown oil, which was purified by column chromatography on silica gel using hexane-ethyl acetate (60 : 40) as eluent to give the pure sulfide **34** as a yellow oil (1.21 g, 44% over 2 steps). ν_{max}(neat)/cm^{-1} 1708; δ_H (400 MHz) 2.39-2.48 (4H, m, 2 x CH_2), 2.77-2.80 (2H, m, CH_2), 3.21 (2H, s, CH_2); δ_C (75.5 MHz) 28.6, 33.4, 38.6, 41.9 (4 × CH_2), 203.9 (Cq, C=O); m/z (ESI+) 117 [(M+H)+, 20%]. Spectral details in agreement with those reported in the literature. [172]

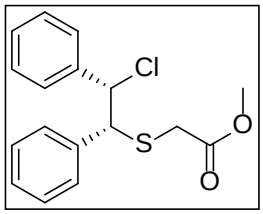
3.1.3.4 Lactam derived sulfides

erythro-(2-Hydroxy-1,2-diphenyl-ethylsulfanyl)-acetic acid methyl ester 48[22]



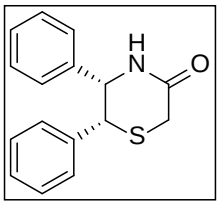
Methyl thioglycolate **18** (3.30 g, 2.78 mL, 31 mmol, 1.15 eq.) in methanol (20 mL) was added dropwise over 10 min, to a stirring solution of freshly prepared sodium methoxide (sodium 0.09 g, 4.20 mmol, 0.15 eq.) in methanol (40 mL) followed by *trans*-stilbene oxide **12** (5.51 g, 28.90 mmol, 1 eq.) in methanol (70 mL). The reaction mixture was heated under reflux for 2 h and stirring was continued at room temperature overnight. The reaction mixture was hydrolysed with water (40 mL), extracted with dichloromethane, the layers were separated and the organic layer dried with $MgSO_4$. The solvent was removed under reduced pressure to give the *erythro*-hydroxy ester **48** as a yellow clear oil which gradually crystallised on standing to a yellow solid (6.78 g, 80%) which was sufficiently pure by ^{1}H NMR spectroscopy to be brought forward to the next step. ν_{max}/cm^{-1} (neat) 3493, 1731; δ_H(400 MHz) 2.43 (1H, br s, OH), 2.88 (1H, d, *J* 15.2, A of ABq, one of SCH_2), 2.95 (1H, d, *J* 15.2, B of ABq, one of SCH_2), 3.61 (3H, s, CH_3O), 4.31 (1H, d, *J* 6.9, CHS), 5.02 (1H, d, *J* 6.9, CHO), 7.31-7.42 (10H, m, 10 x Aromatic CH); δ_C (100 MHz) 32.8 (SCH_2), 52.3 (OCH_3), 57.4 (CHS), 76.7 (CHO), 126.8 (2 x aromatic CH), 127.9, 128.1 (2 x Aromatic CH), 128.2, 128.5, 129.3, (3 signals representing 6 x Aromatic CH), 137.6, 140.7 (2 x Aromatic Cq), 170.7 (Cq, C=O). Spectroscopic details matched those reported in the literature.[22]

***erythro*-(2-Chloro-1,2-diphenyl-ethylsulfanyl)-acetic acid methyl ester 50**[22]



Thionyl chloride (3.04 mL, 41.8 mmol, 2.0 eq.) was added over 10 min to a stirring solution of the hydroxy ester **48** (6.33 g, 20.9 mmol) in dichloromethane (50 mL) at room temperature. The mixture was stirred at room temperature for 18 h and then the solvent and excess thionyl chloride were removed under reduced pressure to give the *erythro*-chloro ester product **50** as a white solid (6.55 g, 97 %); mp 71-73°C (lit.,[22] 74-76°C); ν_{max}/cm^{-1} (neat) 1732; δ_H (400 MHz) 2.74 (2H, s, SCH_2), 3.60 (3H, s, CH_3O), 4.64 (1H, d, *J* 9.8, CHS), 5.22 (1H, d, *J* 9.8, CHCl), 7.10-7.55 (10H, m, 10 x Aromatic CH); δ_C (75.5 MHz) 33.0 (SCH_2), 52.3 (OCH_3), 56.7 (CHS), 65.7 (CHCl), 127.9, 128.1, 128.5, 128.7, 128.3, 128.9 (6 signals representing 10 x Aromatic CH), 138.3, 139.1 (2 x Aromatic Cq), 170.3 (Cq, C=O); *m/z* (ESI+) 320 [$(M+H)^+$, 10%]. Spectroscopic details matched those reported in the literature.[22]

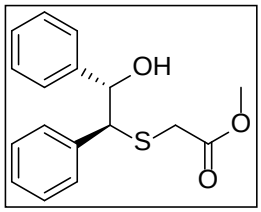
***cis*-5,6-Diphenylthiomorpholin-3-one 44**[22]



The chloro ester **50** (6.76 g, 21.07 mmol) was dissolved in acetonitrile (150 mL). and aqueous ammonium hydroxide (110 mL, 20%) was added. The solution was stirred at room temperature for 60 h and then extracted with dichloromethane (150 mL). After evaporation of the dried extracts the crude product (4.68 g) was isolated as white solid and purified by column chromatography on silica gel, using hexane – ethyl acetate as eluent (40 : 60) to give the *cis* sulfide **44** as a white crystalline solid (2.13 g, 38%); ν_{max}/cm^{-1} (neat) 1662; δ_H(400 MHz) 3.44 (1H, d, *J* 16.3, A of ABq, one of SCH_2), 3.86 (1H, d, *J* 16.3, B of ABq, one of SCH_2), 4.57 (1H, d, *J* 4.0, CHS), 4.97 (1H, t, *J* 3.9, CHN), 6.18 (1H, br s, NH), 6.80 – 6.89 (2H, m, 2 x Aromatic CH),7.09 – 7.40 (7H, m, 7 x Aromatic CH) 7.49-7.55 (1H, m, 1 x Aromatic CH); δ_C ($CDCl_3$) 31.1 (CH_2, SCH_2), 50.0 (CH, CHS), 62.7 (CH, CHN), 127.8, 128.0, 128.1, 128.2, 128.3, 128.8 (6 signals representing 10 x Aromatic CH), 136.4, 136.8 (2 x Aromatic Cq), 168.1 (Cq, C=O); HRMS (ESI+) Exact mass calculated for $C_{16}H_{15}NOS$ $[M+H]^+$, 270.0953, Found 270.0946. Spectroscopic details matched those reported in the literature.[22]

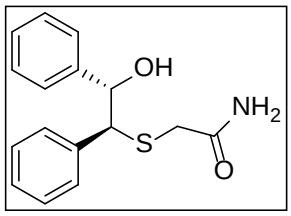
Note: This procedure was repeated using aqueous ammonium hydroxide (33%), and recrystallization from hot ethyl acetate (instead of purification by column chromatography on silica gel), followed by rinsing with water, and **44** was isolated in 64% yield.

threo-(2-Hydroxy-1,2-diphenyl-ethylsulfanyl)-acetic acid methyl ester 52[22]



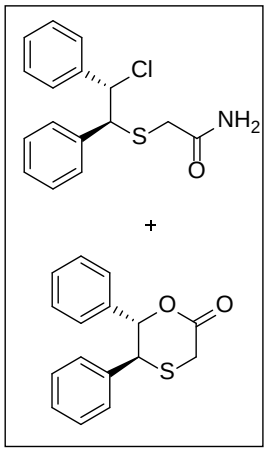
Methyl thioglycolate **18** (2.69 g, 2.26 mL, 25.36 mmol, 1.15 eq.) in methanol (20 mL) was added dropwise over 10 min to a stirring solution of freshly prepared sodium methoxide (sodium 0.76 g, 5.39 mmol, 0.15 eq.) in methanol (40 mL), followed by the addition of *cis*-stilbene oxide **45** (7.00 g, 33.9 mmol, 0.15 eq.) in methanol (70 mL) over 10 min. The reaction mixture was heated under reflux for 2 h and stirring was continued at room temperature overnight. The reaction mixture was hydrolysed with water (60 mL), extracted with dichloromethane (60 mL), the layers were separated and the organic layer dried with $MgSO_4$. The solvent was removed under reduced pressure to give the *threo*-hydroxy ester **52** as a pale yellow oil (6.64g, 99%)*. ν_{max}/cm^{-1} (neat) 3493, 1731; δ_H(400 MHz) 3.06 (1H, d, *J* 15.2, A of ABq, one of SCH_2), 3.19 (1H, d, *J* 15.2, B of ABq, one of SCH_2), 3.22 (1H, br s, OH), 3.63 (3H, s, OCH_3), 4.26 (1H, d, *J* 8.3, CHS), 4.93 (1H, d, *J* 8.3, CHO), 7.12-7.20 (10H, m, 10 x Aromatic CH); δ_c (100 MHz); 33.1 (SCH_2), 52.3 (CH_3O), 59.6 (CHS), 77.5 (CH, CHO) 126.7 (2 x aromatic CH), 127.5, 127.8 (2 x Aromatic CH), 128.0, 128.3, 128.8, (3 signals representing 6 x Aromatic CH), 138.5, 141.1 (2 x Aromatic Cq), 170.9 (Cq, C=O). *Residual peaks for methyl thioglycolate **18** were present ~2%.

threo-2-(2-Hydroxy-1,2-diphenyl-ethylsulfanyl)-acetamide 53[22]



Aqueous ammonium hydroxide (40 mL, 33%) was added over 10 min, to a solution of the hydroxy ester **52** (7.33 g, 24.23 mmol) in acetonitrile (160 mL) at room temperature. The solution was stirred at room temperature for 24 h and then extracted with dichloromethane (4 x 40 mL). The crude product was recrystallised from hot ethyl acetate to give the desired amide **53** as a white crystalline solid (5.71 g, 80%); mp 133-134°C (lit.,[22] 131-132°C); ν_{max}/cm^{-1} (neat) 3465, 1682; δ_H(400 MHz) 2.92 (1H, br s, OH), 3.06 (1H, d, *J* 16.6, A of ABq, one of SCH_2), 3.22 (1H, d, *J* 16.6, B of ABq, one of SCH_2), 4.04 (1H, d, *J* 7.7, CHS), 5.01 (1H, finely split singlet, CHO), 5.50 (1H, br s, one of $CONH_2$), 6.42 (1H, br s, one of $CONH_2$), 7.12-7.26 (10H, m, 10 x Aromatic CH); δ_c (75.5 MHz) 34.1 (CH_2, SCH_2), 60.9 (CH, CHS), 78.2 (CH, CHO), 126.5 (2 x aromatic CH), 127.7, 127.9 (2 x aromatic CH), 128.2, 128.5, 128.6, (6 x Aromatic CH), 136.6, 141.2 (2 x Aromatic Cq), 171.3 (Cq, C=O). Spectroscopic details matched those reported in the literature.[22]

***threo*-2-(2-Chloro-1,2-diphenyl-ethylsulfanyl)-acetamide 54**[14,22]

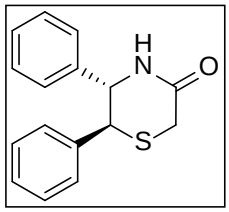


Thionyl chloride (1.56 mL, 21.49 mmol, 2.0 equiv) was added over 10 min, to a stirring solution of the hydroxy amide **53** (3.09 g, 10.74 mmol, 1 equiv) in dichloromethane (250 mL) at room temperature. The mixture was stirred at ambient temperature for 16 h and then the solvent and excess thionyl chloride were removed under reduced pressure to give a mixture of the *threo*-chloro amide **54** and lactone **51** in a ratio of 1:1 as yellow solid (3.07 g).

The reaction was repeated on a separate sample of **53**, at 0°C for 5 min to give the chloro amide **54 :** lactone **51** (97 : 3, 3.04 g, 94%). This material was used in the next step without further purification. mp 126-128°C; δ_H(400 MHz) 2.92 (1H, d, *J* 16.7, A of ABq, one of SCH_2), 3.15 (1H, d, *J* 16.7, B of ABq, one of SCH_2), 4.33 (1H, d, *J* 8.7, CHS), 5.20 (1H, d, *J* 8.7, CHCl), 5.40 (1H, br s, one of $CONH_2$), 6.56 (1H, br s, one of $CONH_2$), 7.12-7.22 (10H, m, 10 x Aromatic CH); δ_c (75.5 MHz) 34.9 (SCH_2), 59.6 (CHS), 66.4 (CHCl), 127.6 (2 x aromatic CH), 128.2 (1 x aromatic CH), 128.3 (2 x aromatic CH), 128.5 (1 x aromatic CH), 128.6, 128.7 (4 x Aromatic CH), 137.5, 138.7 (2 x Aromatic Cq), 172.1 (Cq, C=O). Spectral characteristics are in agreement with those reported in the literature. [13,14] The ^{1}H NMR signals of the corresponding lactone **51** are seen as follows: 3.43 (1H, d, *J* 14.5, one of SCH_2), 4.04 (1H, d, *J* 14.5, one of SCH_2), 4.39 – 4.47 (overlapping signals including 1H, d, CHS), 5.43 (1H, d, *J* 8.0, CHO).

Temperature	Time	Ratio of chloro amide 54 : lactone 51
Room Temperature	16 h	1 : 1
Room Temperature	5 min	85 : 15
0°C	5 min	97 : 3

***trans*-5,6-Diphenylthiomorpholin-3-one 43**[14,22]



Aqueous ammonium hydroxide (55 mL, 33%) was added over 10 min to a solution of the chloro amide **54** (chloro amide **54**: **51** lactone, 97:3, 2.74 g, 8.95 mmol) in acetonitrile (155 mL) at room temperature. The reaction mixture was stirred at room temperature for 60 h and then extracted with dichloromethane (4 x 40 mL). The crude product was purified by recrystallization from hot ethyl acetate to give the desired sulfide **43** as a white crystalline solid (1.69 g, 70 %); mp 143-144°C; ν_{max}/cm^{-1} (neat) 1660; δ_H (400 MHz) 3.46 (1H, d, *J* 17.1, A of ABq, one of SCH_2), 3.75 (1H, d, *J* 17.1, B of ABq, one of SCH_2), 4.06 (1H, d, *J* 9.6, CHS), 4.93 (1H, d, *J* 9.6, CHN), 6.02 (1H, br s, NH), 6.92 -7.41 (10H, m, 10 x Aromatic

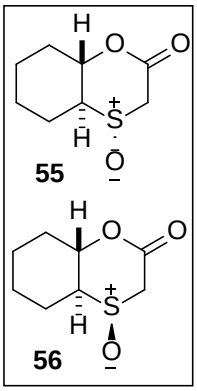
CH); δ_C (100 MHz) 31.2 (CH_2, SCH_2), 50.8 (CH, CHS), 66.4 (CH, CHN), 127.1, 128.1, 128.6 (3 signals corresponding to 10 x ArCH), 136.8, 133.8 (2 x Aromatic Cq), 167.3 (Cq, C=O). Spectral characteristics are in agreement with those reported in the literature. [13,14]

3.1.4 Synthesis of Sulfoxides

Note: While dr's were comparable to those reported by earlier researchers, in some instances partial dissolution of diastereomeric mixtures in deuterated chloroform, or withdrawing a solid sample from a mixture may have lead to altered dr's.

3.1.4.1 Lactone derived sulfoxides

(4aS*, 8aS*)-hexahydrobenzo[*b*][*1,4*]oxathiin-2(*3H*)-one 4-oxide 55 and **(4aS*, 8aS*)-hexahydrobenzo[*b*][*1, 4*]oxathiin-2(*3H*)-one 4-oxide 56** [13]

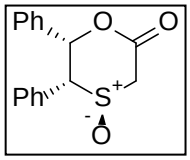


A solution of 3-chloroperoxybenzoic acid (70%, 1.52 g, 8.8 mmol, 1 eq) in dichloromethane (15 mL) was added dropwise over 20 min to a solution of the sulfide **4** (1.09 g, 6.3 mmol, 1 eq) in dichloromethane (20 mL) while stirring at 0 °C. The reaction mixture was stirred for 1.5 h while slowly returning to room temperature. The solution was filtered to remove precipitated 3-chlorobenzoic acid, washed with sodium bicarbonate solution (10%, 3 × 30 mL), water (30 mL) and brine (30 mL). The organic layer was dried with anhydrous $MgSO_4$ and concentrated *in vacuo* to produce the crude sulfoxides **56** and **55** as a mixture of diastereomers (1 : 1) and as a white solid (1.01 g, 85 %). The crude residue was dissolved in dichloromethane and loaded onto Celite®. Repeated purification by column chromatography on silica gel using hexane-ethyl acetate (50 : 50) led to separation of the two diastereomers both as white solids.

Equatorial sulfoxide **55**: δ_H (400 MHz) 1.20-2.65 (8H, m, 4 × CH_2), 2.66-2.80 (1H, ddd appears as m, CHS), 3.78 (1H, d, *J* 15.5, A of ABq, one of $SOCH_2$), 3.88 (1H, d, *J* 15.5, B of ABq, one of $SOCH_2$), 4.04 (1H, ddd appears as dt, *J* 11.0, 11.0, 4.8, CHO); δ_C (75.5 MHz, $CDCl_3$) 23.7, 25.2, 27.2, 32.4 (4 × CH_2), 51.1 (CH_2, $SOCH_2$), 67.7 (CH, CHS), 77.2 (CH, CHO), 163.7 (Cq, C=O).

Axial sulfoxide **56**: δ_H (400 MHz) 1.20-2.45 (8H, m, 4 × CH_2), 2.50-2.68 (1H, ddd appears as m, CHS), 3.62 (1H, d, *J* 16.1, A of ABq, one of $SOCH_2$), 4.02 (1H, d, *J* 16.1, A of ABq, one of $SOCH_2$), 4.88 (1H, ddd appears as dt, *J* 10.5, 10.5, 5.0, CHO); δ_C (75.5 MHz, $CDCl_3$) 23.4, 24.2, 24.8, 32.2 (4 × CH_2), 52.1 (CH_2, $SOCH_2$), 57.3 (CH, CHS), 73.8 (CH, CHO), 163.2 (Cq, C=O). Spectral characteristics are in agreement with those reported in the literature.[13]

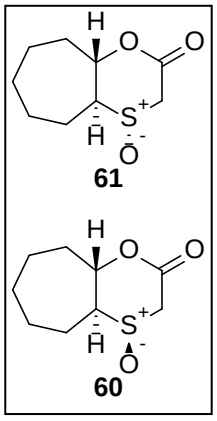
(4R*,5R*,6S*)-5,6-Diphenyl-1,4-oxathian-2-one 4-oxide 59[15]



A solution of 3-chloroperoxybenzoic acid (1.61 g, 9.32 mmol, 1 eq, 77%) in dichloromethane (50 mL) was added dropwise over 20 min to a solution of the sulfide **9** (1.96 g, 7.23 mmol, 1 eq) in dichloromethane (20 mL) while stirring at 0 °C. The

reaction mixture was stirred for 1.5 h while slowly returning to room temperature. The reaction mixture was filtered to remove precipitated 3-chlorobenzoic acid, washed with sodium bicarbonate solution (10%, 3 × 30 mL), water (30 mL) and brine (30 mL). The layers were separated, the organic layer was dried with anhydrous $MgSO_4$ and concentrated *in vacuo* to produce the crude sulfoxide **59** as one diastereomer and as a white crystalline solid (1.34 g, 64%). ν_{max}/cm^{-1} (neat) 1735, 1224, 1052; δ_H (400 MHz) 3.71 (1H, d, *J* 16.4, A of ABq, one of $SOCH_2$), 4.08 (1H, d, *J* 16.4, B of ABq, one of $SOCH_2$), 4.38 (1H, br s, CHS), 6.62 (1H, finely split singlet, CHO), 7.01–7.12 (2H, m, 2 x Aromatic CH), 7.18–7.41 (8H, m, 8 x Aromatic CH); δ_C (100 MHz, $CDCl_3$) 49.7 (CH_2), 66.8 (CHS), 75.5 (CHO), 126.0 (2 x Aromatic CH), 128.4 (1 x Aromatic Cq), 128.6 (1 x Aromatic CH), 128.7 (2 x Aromatic CH), 129.2 (1 x Aromatic CH), 129.3 (2 x Aromatic CH), 129.5 (2 x Aromatic CH), 134.8 (1 x Aromatic Cq), 163.4 (Cq, C=O). Spectral details are in good agreement with those reported by O'Sullivan.[15]

(4S*, 4aS*, 9aS*)-hexahydro-*5H*-cyclohepta[*b*][1, 4]oxathiin-2(*3H*)-one 4-oxide 61 and **(4R*, 4aS*, 9aS*)-hexahydro-*5H*-cyclohepta[*b*][1, 4]oxathiin-2(*3H*)-one 4-oxide 60** [15]



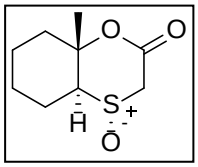
A solution of sodium metaperiodate (2.89 g, 13.52 mmol, 1.05 eq) in water (60 mL) was added slowly to a solution of the sulfide **7** (2.4 g, 12.88 mmol, 1 eq) in methanol (60 mL) over 20 min, while stirring at 0 °C. After 5 min, a white precipitate had formed. The reaction was monitored by TLC and stirred for 2.5 h while returning to room temperature. The precipitate was removed by filtration and the filtrate concentrated in vacuo to leave the sulfoxides **60, 61** and remaining salt mixture as a light brown solid. Dichloromethane (30 mL) was added and the mixture was stirred for 10 min. The remaining solid was removed by filtration and the solution concentrated under reduced pressure to give the crude product as a white crystalline solid (1 : 1, equatorial : axial, **61** : **60**, 1.46 g). The crude residue was dissolved in dichloromethane and loaded onto Celite®. Purification by column chromatography on silica gel using hexane-ethyl acetate (25 : 75) as eluent led to elution of the sulfoxides **60, 61** as a white solid (0.73 g, 28%, 1:1). ν_{max}/cm^{-1} (neat) 1742, 1018; m/z (ESI+) 203 [(M+H)+, 56%];

Equatorial diastereomer **61**: δ_H (400 MHz) 1.39–2.27 (9H, m, cycloheptyl ring), 2.35 – 2.47 (1H, m, 1 x cycloheptyl CH), 2.87 (1H, overlapping ddd appears as dt, *J* 10.0, 10.0, 3.3, CHS), 3.73 (1H, d, *J* 15.8, A of ABq, one of $SOCH_2$), 3.96 (1H, d, *J* 15.8, B of ABq, one of $SOCH_2$), 4.11 (1H, overlapping ddd appears as dt, *J* 10.4, 10.4, 5.5, CHO). Spectral characteristics are in good agreement with those reported by O'Sullivan.[15]

Axial diastereomer **60**: δ_H (400 MHz) 1.39–2.44 (10H, m, cycloheptyl ring), 2.62 (1H, ddd appears as dt, J 9.2, 9.2, 2.9, CHS), 3.51 (1H, d, *J* 16.0 Hz, A of ABq, one of $SOCH_2$), 4.24 (1H, d, *J* 16.0, B of ABq, one of $SOCH_2$), 5.08–5.18 (1H, symmetrical m, CHO); δ_C (75.5 MHz) 21.9, 24.8, 27.0, 28.1, 32.8 (5 x CH_2, cycloheptyl ring), 53.2 (CH_2, $SOCH_2$), 61.5 (CH, CHS), 75.8 (CH, CHO), 164.4 (C, C=O); Spectral characteristics are in agreement with those reported by O'Sullivan.[15]

Note: It was found later that recrystallization of a 1 : 1 mixture of axial and equatorial sulfoxides from hot ethyl acetate, led to preferential crystallisation of the axial diastereomer **60**. Purification of the mother liquor by column chromatography on silica gel using hexane – ethyl acetate as eluent (30 : 70 increasing to 10 : 90) led to elution of the pure equatorial sulfoxide **61**.

(4S*, 4aS*, 8aS*)-8a-methylhexahydrobenzo[*b*][1, 4]oxathiin-2(*3H*)-one 4-oxide 57 [3,14]

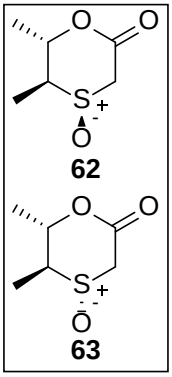


A solution of 3-chloroperoxybenzoic acid (77%, 2.20 g, 12.7 mmol, 1.29 eq) in dichloromethane (40 mL) was added dropwise over 20 min to a solution of the sulfide **5** (1.84 g, 9.8 mmol, 1 eq) in dichloromethane (40 mL) while stirring at 0 °C. The reaction mixture was stirred over 1.5 h while slowly returning to room temperature. The solution was filtered to remove precipitated 3-chlorobenzoic acid, washed with sodium bicarbonate solution (10%, 3 × 30 mL), water (30 mL) and brine (30 mL). The layers were separated and the organic layer was dried with anhydrous $MgSO_4$ and concentrated *in vacuo* to produce the crude sulfoxides **57** and **58** as a mixture of diastereomers (90 : 10, **57** : **58**) Purification by column chromatography on silica gel using hexane: ethyl acetate (50 : 50) lead to elution of a fraction with the major diastereomer **57** as the major component (9.5 : 1, **57 : 58**) and as a white crystalline solid (1.67 g, 70%).

Major equatorial sulfoxide **57**; δ_H(400 MHz) 1.32-2.20 (10H, m, contains 7H m of cyclohexyl ring and CH_3 s at 1.41), 2.50-2.61 (1H, m, appears as br d, CH of cyclohexyl ring), 2.88 (1H, dd, *J* 12.6, 4.2, CHS), 3.55 (1H, d, *J* 16.7, A of ABq, one of $SOCH_2$), 4.46 (1H, d, *J* 16.7, B of ABq, one of $SOCH_2$); δ_C (100 MHz) 21.3 (CH_3), 22.7, 24.4, 24.8, 39.7 (4 x CH_2), 54.3 (CH_2S), 65.8 (CHS), 82.0 (Cq, CqO, 162.9 (Cq, C=O). Spectral characteristics in agreement with those reported in the literature. [3,14]

Characteristic signals for the minor axial sulfoxide **58** observed in the ^{1}H NMR spectrum of the crude material include; δ_H(400 MHz) 3.73 (1H, d, *J* 16.8, A of AB_q of $SOCH_2$), 4.41 (1H, d, *J* 16.8, B of AB_q of $SOCH_2$); δ_C (100 MHz) 20.1 (CH_3), 22.3, 23.8, 25.8, 41.3, 52.4 (5 x CH_2), 58.8 (CHS), 84.8 (Cq, CqO), 162.7 (Cq, C=O).

(4R*, 5S*, 6S*)-5,6-dimethyl-1,4-oxathian-2-one 4-oxide 62 and **(4S*,5S*,6S*)-5,6-dimethyl-1,4-oxathian-2-one 4-oxide 63**



A solution of Oxone® (1.42 g, 2.31 mmol, 0.5 eq) in water (20 mL) was added dropwise to a solution of the sulfide **8** (0.680 g, 4.6 mmol, 1 eq) in acetone (30 mL) over 15 min while stirring at 0 °C. The reaction mixture was stirred for 3 h while returning slowly to room temperature. Water (10 mL) was then added to the flask to dissolve the inorganic salts. The resulting solution was extracted with dichloromethane (3 × 20 mL) and the combined organic layers washed with water (10 mL), brine (10 mL), dried with anhydrous $MgSO_4$ and concentrated *in vacuo* to give the crude product as a colourless oil (0.180 g, 24%) which was sufficiently pure to be carried on to the next step. The material was characterised as a mixture of diastereomers (axial **62** : equatorial **63,** 1 : 0.3); ν_{max}/cm^{-1} (neat) 1730, 1254, 1036; MS: (M+H) 163 (30%) HRMS (ESI+) Exact mass calculated for $C_6H_{11}O_3S$ $[M+H]^+$, 163.0429 Found: 163.0431.

***Note**:* In later experiments, the major axial diastereomer **62** (less polar) could be separated from the equatorial diastereomer **63** (more polar) by careful chromatography on silica gel.

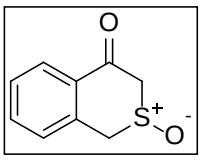
Axial sulfoxide **62** : δ_H (300 MHz) 1.39 (3H, d, *J* 7.3, CH_3CS), 1.54 (3H, d, *J* 6.6, CH_3CO), 2.74 – 2.82 (2 overlappping signals including 1H, symmetrical m, CHS), 3.65 (1H, A of ABq, *J* 16.2, one of $SOCH_2$), 4.10 (1H, B of ABq, *J* 16.2, one of $SOCH_2$), 4.97 - 5.04 (1H, m, CHO); δ_C (75.5 MHz) 10.8, 18.5 (2 x CH_3), 51.6 (CH_2), 54.0 (CHS), 73.2 (CHO), 163.4 (Cq, C=O).

Equatorial sulfoxide **63** : δ_H (300 MHz) 1.46 (3H, d, *J* 7.3, CH_3CS), 1.52 (3H, d, *J* 6.6, CH_3CO), 2.74 – 2.82 (2 overlappping signals including 1H, symmetrical m, CHS), 3.69 – 3.81 (2H, ABq, *J* 16.0, $SOCH_2$), 4.18 – 4.25 (1H, m, CHO); δ_C (75.5 MHz) 12.6, 19.2 (2 x CH_3), 49.3 (CH_2), 63.4 (CHS), 76.6 (CHO), 163.7 (Cq, C=O).

In some spectra of mixtures of **62** and **63** the AB_q at δ_H 3.69 – 3.81 ppm appears as a broad singlet at δ_H 3.9 ppm.

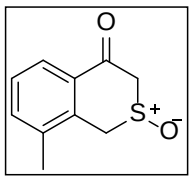
3.1.4.2 Benzofused Ketone derived sulfoxides

Isothiochroman-4-one *S*-oxide 64[16]



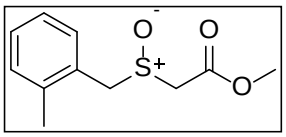
A solution of sodium metaperiodate (2.38 g, 11.12 mmol, 1 eq) in water (25 mL) was added slowly over 10 min to a solution of isothiochroman-4-one **16** (1.82 g, 11.12 mmol, 1 eq) in methanol (40 mL) while stirring at 0 °C. After 5 min, a white precipitate had formed. The reaction was monitored by TLC and stirred for 4 h while returning to room temperature. The precipitate was filtered and the filtrate concentrated in vacuo to leave the sulfoxide **64** and remaining salt mixture as a light brown solid. Dichloromethane (30 mL) was added and the mixture stirred for 10 min. The remaining solid was removed by filtration and the filtrate concentrated in vacuo to give isothiochroman-4-one *S*-oxide **64** as a brown solid which was recrystallised from hot ethyl acetate to afford light brown crystals (1.27 g, 64%). m.p. 169-171 °C (lit., [174] 170-171 °C); ν_{max}(neat)/cm^{-1} 1681, 1024; δ_H (400 MHz) 3.94 (1H, d, *J* 15.4, A of ABq, CH_2), 3.98 (1H, d, *J* 15.4, B of ABq, CH_2), 4.32 (1H, d, *J* 15.3, A of ABq, $ArCH_2$), 4.36 (1H, d, *J* 15.3, B of ABq, $ArCH_2$), 7.36 (1H, d, *J* 7.6, 1 x Aromatic CH), 7.46-7.53 (1H, m, 1 x Aromatic CH), 7.61-7.67 (1H, m, 1 x Aromatic CH), 8.13 (1H, d, *J* 7.9, 1 x Aromatic CH); δ_C (100 MHz) 52.4 (CH_2), 59.0 (CH_2), 128.3, 129.2, 131.1 (3 × Aromatic CH), 131.4, 131.6 (2 x Aromatic Cq), 135.4 (1 x Aromatic CH), 187.9 (Cq, C=O). Spectral characteristics are in agreement with those previously reported in the literature. [16, 174]

8-Methylisothiochroman-4-one *S*-oxide 66[16]



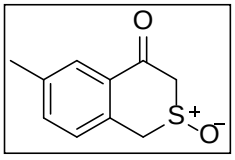
Oxone® (2.42 g, 3.93 mmol, 0.5 eq) in water (25 mL) was added dropwise to a stirring solution of 8-methylisothiochroman-4-one **22** (1.40 g, 7.87 mmol) in acetone (50 mL) at 0 °C. The mixture was allowed to slowly reach room temperature while stirring over 2 h 20 min when TLC analysis (100% ethyl acetate) showed all starting material was consumed. Water (10 mL) was then added to the flask to dissolve the inorganic salts. The resulting solution was extracted with dichloromethane (2 × 20 mL) and the combined organic layers washed with water (10 mL), brine (10 mL), dried with anhydrous $MgSO_4$ and concentrated *in vacuo* to give the crude product as a yellow crystalline product. Purification by flash chromatography on silica gel using ethyl acetate (100%) as eluent gave pure 8-methylisothiochroman-4-one *S*-oxide **66** as a white crystalline solid (0.945 g, 61%). Found C, 61.36; H 5.71, $C_{10}H_{10}O_2S$ requires C, 61.83; H 5.19; R_f 0.37 using 100% ethyl acetate as eluent; ν_{max}/cm^{-1} (neat) 1680, 1047; δ_H (400 MHz) 2.42 (3H, s, CH_3), 3.96 (1H, d, *J* 14.7, A of AB_q, CH_2), 4.02 (1H, d, *J* 14.7, B of AB_q, CH_2), 4.23 (1H, d, *J* 16.0, A of AB_q, $ArCH_2$), 4.30 (1H, d, *J* 16.0, B of AB_q, $ArCH_2$), 7.33-7.39 (1H, m, 1 x Aromatic CH), 7.52 (1H, d, *J* 18.2, 1

x Aromatic CH), 7.98 (1H, d, *J* 18.2, 1 x Aromatic CH); δ_C (75.5 MHz) 20.0 (CH_3), 48.5 (CH_2), 58.3 (CH_2), 126.2 (1 x Aromatic CH), 128.4 (1 x Aromatic CH), 129.9 (1 x Aromatic Cq), 131.8 (1 x Aromatic Cq), 137.1 (1 x Aromatic CH), 138.1 (1 x Aromatic Cq), 188.5 (Cq, C=O). Spectral characteristics are in agreement with those previously reported by Buckley. [16]



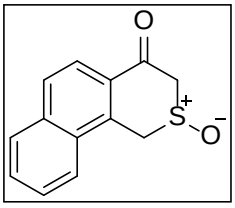
Additionally, when the reaction was carried out on an impure sample of the β-keto sulfide **22** and purified by column chromatography on silica gel using gradient hexane-ethyl acetate as eluent (50 : 50 increasing to 0 : 100) the sulfoxide **69** eluted as a colorless oil, before the cyclised β-keto sulfoxide **66**. ν_{max}/cm^{-1} (neat) 1737, 1047; δ_H (400 MHz) 2.41 (3H, s, $ArCH_3$), 3.60 (1H, d, *J* 13.8, A of ABq, one of CH_2), 3.71 (1H, d, *J* 13.8, B of ABq, one of CH_2), 3.78 (3H, s, CO_2CH_3), 4.21 (1H, d, *J* 12.9, A of ABq, one of CH_2), 4.32 (1H, d, *J* 12.9, B of ABq, one of CH_2), 7.14 – 7.33 (4H, m, 4 x Aromatic CH); δ_C (75.5 MHz) 19.8 ($ArCH_3$), 52.8 (CH_3, CO_2CH_3), 54.2 (CH_2), 57.1 (CH_2), 126.6 (CH, 1 x Aromatic CH), 128.1 (Cq, 1 x Aromatic Cq), 128.9, 130.9, 131.2 (CH, 3 x Aromatic CH), 137.6 (Cq, 1 x Aromatic Cq), 165.7 (Cq, C=O).

6-Methylisothiochroman-4-one 2-oxide 67[16]



Oxone® (1.48 g, 2.4 mmol, 0.5 eq) in water (25 mL) was added dropwise to a stirring solution of 6-methylisothiochroman-4-one **23** (0.860 g, 4.8 mmol, 1 eq) in acetone (50 mL) at 0 °C. The mixture was allowed to slowly reach room temperature while stirring over 2 h at which point TLC analysis (100% ethyl acetate) showed all starting material was consumed. Water (10 mL) was then added to the flask to dissolve the inorganic salts. The resulting solution was extracted with dichloromethane (2 × 20 mL) and the combined organic layers washed with water (10 mL), brine (10 mL), dried with anhydrous $MgSO_4$ and concentrated *in vacuo* to give the crude product as a white solid. Recrystallisation from hexane and dichloromethane led to recovery of the sulfoxide **67** as a white crystalline solid (0.750 g, 80%). δ_H (400 MHz) 2.41 (3H, s), 3.94 (1H, d, *J* 15.6, A of AB_q), 4.02 (1H, d, *J* 15.6, B of AB_q), 4.25 (1H, d, *J* 14.9, A of AB_q), 4.32 (1H, d, *J* 14.9, B of AB_q), 7.26 (1H, d, *J* 15.6, 1 x Aromatic CH), 7.46 (1H, d, *J* 15.6, 1 x Aromatic CH), 7.93 (1H, s, 1 x Aromatic CH); δ_C (75.5 MHz) 21.1 (CH_3), 52.4, 59.3 (2 x CH_2), 128.1 (CH, Aromatic CH), 131.4 (CH, Aromatic CH), 136.4 (CH, Aromatic CH). Signals corresponding to the aromatic Cq's and the carbonyl were not observed in the ^{13}C NMR spectrum however the remaining spectral characteristics are in agreement with those reported by Buckley.[16]

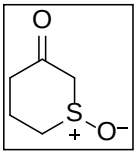
1H-Benzo[h]isothiochromen-4(*3H*)-one 2-oxide 68[16]



Oxone® (0.263 g, 0.43 mmol, 1 eq) in water (10 mL) was added dropwise to a stirring solution of sulfide **24** (0.184 g, 0.85 mmol) in acetone (10 mL) at 0 °C. The mixture was allowed to slowly reach room temperature while stirring over 2 h 20 min when TLC analysis (100% ethyl acetate) showed all starting material was consumed. Water (10 mL) was then added to the flask to dissolve the inorganic salts. The resulting solution was extracted with dichloromethane (2 × 20 mL) and the combined organic layers washed with water (10 mL), brine (10 mL), dried with anhydrous $MgSO_4$ and concentrated *in vacuo* to give the crude product as a yellow crystalline solid. Purification by flash chromatography on silica gel using ethyl acetate (100%) as eluent gave the sulfoxide **68** as a white crystalline solid (0.102 g, 52%). ν_{max} (neat)/cm^{-1} 1680, 1041; δ_H (400 MHz) 4.10 (1H, d, *J* 14.9, A of AB_q), 4.19 (1H, d, *J* 14.9, B of AB_q), 4.64 (1H, d, *J* 15.2, A of AB_q), 4.86 (1H, d, *J* 15.2, B of AB_q), 7.64-7.78 (2H, m, 2 x Aromatic CH), 7.83-8.00 (2H, m, 2 x Aromatic CH), 8.05-8.20 (2H, m, 2 x Aromatic CH); δ_C (100 MHz) 48.1, 58.7 (2 x CH_2) 122.8, 124.3, 128.0, 129.3, 129.3, 129.4 (6 x Aromatic CH), 129.7, 129.9, 131.3, 136.7 (4 x Aromatic Cq), 188.4 (Cq, C=O). Spectral characteristics are in good agreement with those reported by Buckley.[16]

3.1.4.3 Monocyclic ketone derived sulfoxides

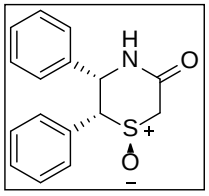
Dihydro-2H-thiopyran-3(*4H)*-one *S*-oxide 65[16,175,]



A solution of sodium metaperiodate (0.77 g, 3.62 mmol, 1 eq) in water (10 mL) was added slowly to a solution of dihydro-2H-thiopyran-3(4H)-one **34** (0.420 g, 3.62 mmol, 1 eq) in methanol (40 mL) over 10 min, while stirring at 0 °C. After 5 min, a white precipitate had formed. The reaction was monitored by TLC and stirred for 1.5 h while returning to room temperature. The precipitate was filtered, and the filtrate concentrated *in vacuo* to leave the sulfoxide **65** and remaining salt mixture as an off-white solid. Dichloromethane (40 mL) was added and the mixture stirred for 10 min. The remaining solid was removed by filtration and the filtrate concentrated in vacuo to give the crude sulfoxide as a pale yellow solid. Purification by column chromatography on silica gel using ethyl acetate (100%) as eluent led to elution of the pure sulfoxide **65** (0.31 g, 65%), which stained blue by vanillin on heating. m.p. 87-88 °C; ν_{max}(neat)/cm^{-1} 1715; δ_H (400 MHz) 2.26-2.36 (1H, m, one of CH_2), 2.51-2.64 (2H, m, 1 x CH_2), 2.78-2.94 (1H, m, one of CH_2), 2.95-3.05 (1H, m, one of CH_2), 3.08-3.16 (1H, m, one of CH_2), 3.63 (1H, A of ABq, *J* 13.3, one of CH_2), 3.69 (1H, B of ABq, *J* 13.3, one of CH_2); δ_C (100 MHz) 19.3, 41.4, 46.6, 59.8 (4 × CH_2), 199.7 (Cq, C=O). Spectral characteristics are in agreement with the literature. [16,175]

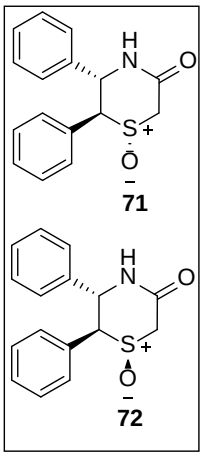
3.1.4.4 Lactam derived sulfoxides

cis-5,6-Diphenylthiomorpholin-3-one _S_-oxide 70[14]



A solution of 3-chloroperoxybenzoic acid (77%, 1.38 g, 8.00 mmol, 1 eq.) in dichloromethane (20 mL) was added slowly over 15 min at 0°C to a solution of *cis*-5,6-diphenylthiomorpholin-3-one **44** (1.66 g, 6.16 mmol, 1 eq.) in dichloromethane (20 mL). The ice bath was removed after 15 min and the reaction mixture stirred for another 2 h. The organic layer was washed with $NaHCO_3$ (10%, 2 x 15 mL), water (15 mL) and brine (15mL). The layers were separated and the organic layer was dried with $MgSO_4$ and concentrated under reduced pressure to give the crude sulfoxide **70** as a white solid (only one diastereomer present on analysis by ^{1}H NMR spectroscopy). The crude material was recrystallized from hot ethyl acetate to give the sulfoxide **70** as a white crystalline solid (1.46 g, 84%). mp; 212-214 °C (lit.,[14] 215°C); ν_{max}/cm^{-1} (neat) 1667, 1048; δ_H(400 MHz, $CDCl_3$) 3.51 (1H, A of ABq, *J* 17.3, one of $SOCH_2$), 3.69 (1H, B of ABq, *J* 17.3, one of $SOCH_2$), 4.38 (1H, d, *J* 3.2, CHS), 5.68 (1H, d, *J* 3.2, CHN), 6.94 (1H, br s, NH), 7.12-7.53 (10H, m, 10 x Aromatic CH); δ_C (75.5 MHz, $CDCl_3$) 47.6 (CH_2, $SOCH_2$), 52.8 (CH, CHN), 64.9 (CH, CHS), 126.9, 128.5, 129.0, 129.2, 129.3, 129.8 (7 signals representing 10 x aromatic CH and 1 x aromatic Cq), 136.3 (1 x aromatic Cq), 165.4 (Cq, C=O); ESI+ 285 (M^+, 15%). Spectral characteristics are in agreement with those reported in the literature. **[14]**

trans-5,6-Diphenylthiomorpholin-3-one S-oxides 72 and 71[14]



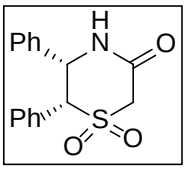
A solution of 3-chloroperoxybenzoic acid (0.787 g, 4.56 mmol, 1 equiv) in dichloromethane (40 mL) and *trans*-5,6-diphenylthiomorpholin-3-one **43** (0.96 g, 3.5 mmol, 1 equiv) in dichloromethane (40 mL) were used following the procedure described for the preparation of **70** above, to give the crude product as a white solid (1 : 1, axial : equatorial, **72 : 71**). Purification by column chromatography on silica gel using ethyl acetate (100 %) gave the pure sulfoxides **72** and **71** as a white solid and as a mixture of diastereomers (1 : 1, 0.70 g, 70 %); The material was characterised as a mixture of diastereomers. mp 174-176 °C (lit.,[14] 181-183°C); ν_{max}/cm^{-1} (neat) 1667, 1042.

Axial diastereomer **72** and Equatorial diastereomer **71**: δ_H(400 MHz) 3.74 – 3.96 (4H, m, containing A and B of ABq of $SOCH_2$, of **72,** CHS of **72,** and 1H, d, *J* 15.5, A of ABq of $SOCH_2$ of **71**), 4.06 (1H, d, *J* 10.9, CHS of **71**), 4.19 (1H, d, B of AB_q *J* 15.5, B of AB_q, one of $SOCH_2$ of **71**), 4.79 (1H, d, *J* 10.9, CHN of **71**) 5.54 (1H, d, *J* 10.8, CHN of **72**), 6.13 – 6.24 (2H, m, NH of both **72** and **71**), 6.99-7.37 (20H, m, 10 x Aromatic CH of **72** and 10 x Aromatic H of **71**); δ_C(100 MHz) 51.2 (CH_2, $SOCH_2$ of **71**), 54.3 ($SOCH_2$ of

72), 55.6 (CHN of **72**), 59.4 (CHN of **71**), 63.7 (CHS of **71**), 74.4 (CHS of **72**), 127.1, 127.7, 128.7, 128.9, 129.1, 129.3, (6 signals representing 10 x Aromatic CH), 131.4, 132.8, 136.9, 137.1, (4 x Aromatic Cq), 162.7 , 163.6 (2 x Cq, C=O of **72** and **71**).

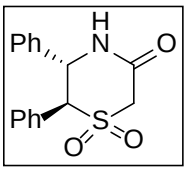
3.1.5 Synthesis of Sulfones

(5S*,6R*)-5,6-Diphenylthiomorpholin-3-one 1,1-dioxide 73



A solution of 3-chloroperoxybenzoic acid (1.63 g, 9.44 mmol, 3 eq), in dichloromethane (50 mL) was added dropwise over 15 min to a stirring solution of *cis*-5,6-diphenylthiomorpholin-3-one *S*-oxide **70** (0.89 g, 3.14 mmol, 1 eq) at 0°C. The reaction mixture was stirred for 8 h while slowly returning to room temperature. The reaction mixture was washed with $NaHCO_3$ (10%, 2 x 20 mL), water (20 mL), and brine (20 mL), dried and concentrated under reduced pressure to give the sulfone **73** as a white crystalline solid (0.26 g, 27%); mp 236-238 °C; ν_{max}/cm^{-1} (neat) 1668, 1125; δ_H (400 MHz) 4.06 (1H, d, *J* 17.3, 2.2, A of AB_q, CH_2), 4.21 (1H, d, *J* 17.3, B of AB_q, CH_2), 4.38 – 4.41 (1H, m, CHS), 5.65 (1H, d, *J* 4.0, CHN), 6.55 (1H, br s, NH), 7.14 – 7.19 (2H, m, 2 x Aromatic CH), 7.23 – 7.46 (8H, m, 8 x Aromatic CH); δ_C (75.5 MHz) 53.5 (CH_2, SO_2CH_2), 57.3 (CH, CHN), 69.6 (CH, CHS), 126.7 (2 x Aromatic CH), 128.0 (1 x Aromatic Cq), 128.2, 129.1, 129.7 (3 signals representing 8 x Aromatic CH), 133.6 (Aromatic Cq), 163.6 (Cq, C=O); HRMS (ESI+) Exact mass calculated for $C_{16}H_{15}NO_3S$ $[M+H]^+$, 302.0827 Found: 302.0839.

(5S*,6S*)-5,6-Diphenylthiomorpholin-3-one 1,1-dioxide 74



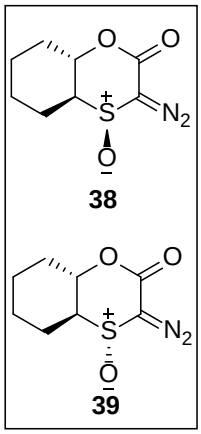
A solution of 3-chloroperoxybenzoic acid (1.09 g, 6.31 mmol, 3 eq), in dichloromethane (50 mL) was added dropwise over 15 min to a stirring solution of *trans*-5,6-diphenylthiomorpholin-3-one *S*-oxide **72** and **71** (0.60g, 2.10 mmol, 1 eq) at 0°C. The reaction mixture was stirred for 8 h while slowly returning to room temperature. The reaction mixture was washed with $NaHCO_3$ (10%, 2 x 20 mL), water (20 mL), and brine (20 mL), dried and concentrated under reduced pressure to give the desired sulfone **74** as a white crystalline solid (0.29 g, 45%). mp 229 – 231 °C; ν_{max}/cm^{-1} (neat) 1671, 1314, 1122; δ_H (400MHz) 4.18 (1H, d, *J* 17.3, A of AB_q, CH_2), 4.26 (1H, d, *J* 17.3, B of AB_q, CH_2), 4.30 (1H, d, *J* 10.2, CHS), 5.23 (1H, d, *J* 11.0, CHN), 6.16 (1H, br s, NH), 7.12 – 7.14 (2H, m, 2 x Aromatic CH), 7.21 – 7.34 (8H, m, 8 x Aromatic CH); δ_C (100 MHz) 56.3 (CH_2, SO_2CH_2), 59.7 (CH, CHN), 69.2 (CH, CHS), 125.4 (Aromatic Cq), 127.3, 129.0, 129.2, 129.4, 129.9, 130.3 (6 signals representing 10 x Aromatic CH), 136.1 (Aromatic Cq), 161.8 (Cq, C=O); HRMS (ESI+) Exact mass calculated for $C_{16}H_{15}NO_3S$ $[M+H]^+$ 302.0851 Found: 302.0854.

3.1.6 Synthesis of α-diazosulfoxides under standard batch conditions

Note: *Care should be taken while handling diazo compounds to limit personal exposure. While no explosion or detonation occurred during these studies it is prudent to handle diazo compounds behind a blast shield.*

Note: *DBSA was sourced from commercial suppliers (TCI Chemical or Sigma Aldrich, CAS Number 79791-38-1) as a mixture of isomers, and was used without purification.*

Axial and equatorial 3-diazo-*trans*-hexahydrobenzo[1,4]oxathiin-2-one *S*-oxides 38 and 39[14]



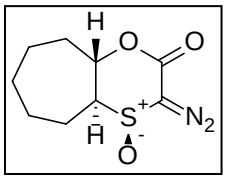
A solution of triethylamine (0.24 mL, 1.7 mmol, 1 eq) in acetonitrile (20 mL) was added dropwise to a mixture of the sulfoxides **56** and **55** (1:1, 0.33 g, 1.7 mmol, 1 eq) in acetonitrile (50 mL) while stirring at 0 °C under a nitrogen atmosphere. The reaction mixture was stirred for 5 min and then a solution of tosyl azide (0.33 g, 1.7 mmol, 1 eq) in acetonitrile (10 mL) was added dropwise, again while stirring at 0 °C under a nitrogen atmosphere. Once the additions were complete the ice bath was removed and the bright orange solution was stirred at ambient temperature under inert atmosphere overnight for 17 h. The solvent was removed under reduced pressure to give the crude product as a viscous dark orange oil (**38** : **39**, 1 : 0.8) which was adsorbed onto Celite® and purified by column chromatography on silica gel using hexane/ethyl acetate (50:50) to isolate the axial and equatorial diazosulfoxides, **38** and **39**. (1 : 0.7, 0.101 g, 27% total mass recovery). Repeated chromatography of the mixture enables separation of the mixture of diastereomers.

Axial **38**: ν_{max}/cm^{-1} (neat) 2129, 1690; δ_H(400 MHz) 1.20-1.80 (4H, m, 4H of CH_2 ring), 1.85-2.05 (2H, m, 2H of CH_2 ring), 2.05-2.27 (1H, m appears as br d, 1H of CH_2 ring), 2.30-2.51 (1H, m appears as br d, 1H of CH_2 ring), 2.82 (1H, ddd appears as dt, *J* 10.9, 10.9, 4.8, CHS), 4.89 (1H, ddd appears as dt, *J* 10.9, 10.9, 4.8, CHO); δ_C(100 MHz) 22.9, 24.3, 24.9, 31.9 (4 × CH_2 ring), 57.9 (CH, CHS), 71.8 (CH, CHO), 158.7(Cq, C=O).

Equatorial **39**: ν_{max}/cm^{-1} (neat) 2127, 1704; δ_H(400 MHz) 1.25-1.82 (4H, m, 4H of CH_2 ring), 1.85-2.02 (2H, m, 2H of CH_2 ring), 2.23-2.36 (1H, m appears as br d, 1H of CH_2 ring), 2.57-2.68 (1H, m appears as br d, 1H of CH_2 ring), 2.95 (1H, ddd appears as dt, *J* 11.0, 11.0, 4.9, CHS), 4.04 (1H, ddd appears as dt, *J* 11.0, 11.0, 4.9, CHO); δ_C(100 MHz) 23.6, 24.7, 27.3, 31.9 (4 × CH_2 ring), 67.8 (CH, CHS), 71.3 (C=N_2), 74.3 (CH, CHO), 160.8 (Cq, C=O); HRMS (ESI+) Exact mass calculated for $C_8H_{10}N_2O_3S$ $[M+H]^+$, 215.0490

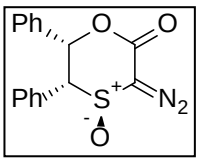
Found: 214.0491 (80%). Spectral characteristics are in agreement with those reported in the literature.[13,14,29] In a separate experiment, using a 1 : 1 mixture of the sulfoxides **56** and **55** an isolated yield of 35% of **38** and **39** was achieved.

(4S*, 4aS*, 9aS*)-3-diazohexahydro-5H-cyclohepta[*b*][1,4]oxathiin-2(*3H*)-one 4-oxide 75[15]



A solution of triethylamine (0.24 mL, 0.17 g, 1.7 mmol, 1 eq) in acetonitrile (5 mL) was added dropwise to a solution of the axial sulfoxide **60** only (0.33 g, 1.6 mmol, 1 eq) in acetonitrile (30 mL) while stirring at 0 °C under a nitrogen atmosphere. The reaction mixture was stirred for 5 min and a solution of DBSA **87** (0.598 g, 1.70 mmol, 1.05 eq) in acetonitrile (10 mL) was then added slowly while stirring at 0°C under a nitrogen atmosphere. The solution slowly reached room temperature while stirring over 9 h, under the inert atmosphere. The solvent was removed under reduced pressure to yield the crude product as a red solid (0.76 g). The oil was adsorbed on to Celite® and purified by column chromatography on silica gel using hexane – ethyl acetate as eluent (40 : 60 – 0 : 100% ethyl acetate) to give the axial α-diazosulfoxide **75** as a yellow crystalline solid (0.170 g, 46%). ν_{max}/cm^{-1} (neat) 2127, 1697, 1051; δ_H (300 MHz) 1.37–1.92 (6H, m, 3 x CH_2 of cycloheptyl ring), 1.98–2.34 (4H, m, 2 x CH_2 of cycloheptyl ring), 2.84 (1H, td, *J* 9.5, 2.6, CHS), 5.17 (1H, overlapping ddd, *J* 4.8, 4.8, 4.8, CHO); δ_C (75.5 MHz) 22.0. 26.8, 27.3, 29.1, 33.2 (5 x CH_2 of cycloheptyl ring), 61.6 (CH, CHS), 74.4 (CH, CHO), 160.3 (Cq, C=O); m/z (ESI+) 229 [$(M+H)^+$, 40%]. Spectral characteristics are in agreement with those reported by O'Sullivan.[15]

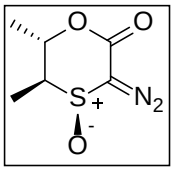
(4S*, 5R*, 6S*)-3-Diazo-5,6-diphenyl-1,4-oxathian-2-one 4-oxide 77[15]



A solution of triethylamine (0.121 g, 0.16 mL, 1.2 mmol, 1.05 eq) in acetonitrile (10 mL) was added dropwise over 10 min to a solution of the sulfoxide **70** (axial diastereomer only, 0.32 g, 1.13 mmol, 1 eq) in acetonitrile (40 mL) while stirring at 0 °C under a nitrogen atmosphere. The reaction mixture was stirred for 5 min and a solution of DBSA **87** (0.418 g, 1.2 mmol, 1.05 eq) in acetonitrile (10 mL) was then added slowly while stirring at 0°C under a nitrogen atmosphere. The solution was allowed to slowly reach room temperature while stirring under the inert atmosphere for 9 h. The solvent was removed under reduced pressure to yield the crude product as a red oil (0.409 g). The oil was adsorbed on to Celite® and purified by column chromatography on silica gel using hexane – ethyl acetate as eluent (50 : 50) to give the pure α-diazosulfoxide **77** as a yellow crystalline solid (0.098 g, 28%). ν_{max}/cm^{-1} (neat) 2154, 2135, 1679; δ_H (300 MHz) 4.30 (1H, d, *J* 2.0, CHS), 6.57 (1H, d, *J* 2.0, CHO), 7.14–7.41 (10H, m, aryl rings); δ_C (75.5 MHz) 68.1 (CH, CHS), 74.3 (CH, CHO), 126.2, 128.7, 128.8, 129.3, 129.7, 129.8 (6 signals

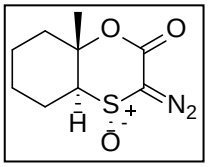
corresponding to 10 x Aromatic CH), 126.8, 135.0 (2 × Aromatic Cq). Spectral characteristics are in agreement with those reported by O'Sullivan.[15]

(4S*, 5R* ,6R*)-3-Diazo-5,6-dimethyl-1,4-oxathian-2-one 4-oxide 78



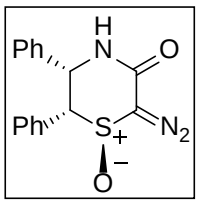
A solution of triethylamine (0.121 g, 0.16 mL, 1.2 mmol, 1.05 eq) in acetonitrile (10 mL) was added dropwise over 10 min to a solution of the axial sulfoxide only **62** (0.32 g, 1.13 mmol, 1 eq) in acetonitrile (40 mL) while stirring at 0 °C under a nitrogen atmosphere. The reaction mixture was stirred for 5 min and a solution of DBSA **87** (0.418 g, 1.2 mmol, 1.05 eq) in acetonitrile (10 mL) was then added over 5 min while stirring at 0°C under a nitrogen atmosphere. The solution was allowed to reach room temperature while stirring under the inert atmosphere for 9 h. The solvent was removed under reduced pressure to yield the crude product as a red oil (0.409 g). The oil was adsorbed on to Celite® and purified by column chromatography on silica gel using hexane-ethyl acetate as eluent (50 : 50 increasing to 0 : 100) to give the pure axial α-diazosulfoxide **78** as a yellow oil (0.098 g, 28%). ν_{max}/cm^{-1} (neat) 2122, 1688, 1091 cm^{-1}; δ_H (400 MHz) 1.42 (3H, d, *J* 7.2, CH_3), 1.52 (3H, d, *J* 6.6, CH_3), 2.91 (1H, dq appears as q, *J* 9.8, 7.2, CHS), 5.07 (1H, dq, *J* 9.8, 6.5, CHO); δ_C (100 MHz) 12.0, 18.4 (2 x CH_3), 55.5 (CH, CHS), 71.1 (CH, CHO), 71.7 (Cq, $C=N_2$), 159.4 (Cq, C=O).

(4S*, 4aS*, 8aS*)-3-Diazo-8a-methylhexahydrobenzo[*b*][1,4]oxathiin-2(*3H*)-one 4-oxide 76



A solution of triethylamine (0.203 g, 0.28 mL, 2.0, 1.05 eq) in acetonitrile (10 mL) was added dropwise over 5 min, to a solution of the sulfoxide **57** (0.388 g, 1.91 mmol, 1 eq) in acetonitrile (40 mL) while stirring at 0 °C under a nitrogen atmosphere. The reaction mixture was stirred for 5 min and a solution of DBSA **87** (0.687 g, 1.95 mmol, 1.02 eq) in acetonitrile (10 mL) was then added slowly while stirring at 0°C under a nitrogen atmosphere. The solution was allowed to slowly reach room temperature and continued stirring under the inert atmosphere for 16 h. The solvent was removed under reduced pressure to yield the crude material as a red oil (0.823 g). The oil was adsorbed on to Celite® and purified by column chromatography on silica gel using gradient hexane-ethyl acetate as eluent (50 : 50 – 0 : 100) to give the pure α-diazosulfoxide **76** as a yellow crystalline solid (0.144 g, 33%). δ_H ($CDCl_3$) 1.30-2.05 (10H, m containing s at 1.42, 7H of cyclohexyl ring and CH_3), 2.57 (1H, br d, *J* 14.1, 1H of CH_2), 3.02 (1H, dd, *J* 12.7, 4.1, CHS); δ_C ($CDCl_3$) 19.6 (CH_3), 22.8, 25.3, 25.5, 39.8 (4 × CH_2), 68.1 (CH, CHS), 81.5 (Cq, CqO), 159.7 (Cq, C=O). Spectroscopic data is in agreement with those previously published in the literature.[13]

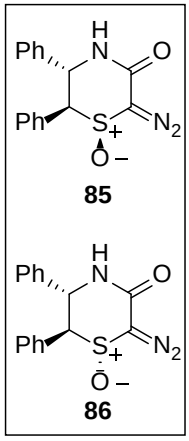
***cis*-2-Diazo-5,6-diphenylthiomorpholin-3-one *S*-oxide 84[14]**



Sodium hydride (60% dispersion in mineral oil, 0.134 g, 3.35 mmol, 1.2 eq.) was weighed into a dry 250 mL roundbottomed flask and placed under nitrogen. Dry THF (40 mL) was added *via* a syringe and the suspension was stirred at 0°C. *cis*-5,6-Diphenylthiomorpholin-3-one *S*-oxide **70** (0.80 g, 2.7 mmol, 1 eq.) in THF (5 mL) was added dropwise to the stirring suspension. Stirring was continued for 10 min at 0°C and then a solution of *p*-toluenesulfonyl azide (0.551 g, 2.7 mmol, 1 eq.) in dry THF (5mL) was added dropwise over 10 min to give a yellow coloured solution. The solution was allowed to slowly reach room temperature and continued stirring under the inert atmosphere for 16 h. The THF was removed under reduced pressure to give the crude product as an orange oil (0.791 g). Repeated column chromatography on silica gel using 100% chloroform as eluent led to elution of the pure α-diazosulfoxide **84** as an orange crystalline solid (0.10 g, 12%); m.p. 152-155 °C decomp; ν_{max}/cm^{-1} (neat) 2113, 1651, 1061 cm^{-1}; δ_H(400 MHz, $CDCl_3$) 4.10 (1H, d, *J* 2.9, CHS), 5.83 (1H, d, *J* 2.9, CHN), 5.91 (1H, br s, NH), 7.08-7.42 (10H, m, aromatic); δ_C (75.5 MHz, $CDCl_3$) 52.4 (CH, CHN), 68.6 (CH, CHS), 127.2, 128.2, 128.9, 129.0, 129.6, 130.0 [6 signals representing 10 x Aromatic CH and 1 x Aromatic Cq (128.2)], 136.2 (1 x Aromatic Cq), 161.3 (Cq, C=O); m/z 283 (M^+-N_2, 10%); HRMS (ESI+) Calculated $C_{16}H_{13}N_3O_2S$ $[M+H]^+$ 312.0813 Found 312.0811 (30%) 284.0764 (M-N_2. 70%).

***trans*-2-Diazo-5,6-diphenylthiomorpholin-3-one *S*-oxides 85 and 86[14]**

Note: *The polymer supported benzenesulfonyl azide is swollen by stirring in the reaction solvent for 20 min, prior to addition to the reaction mixture to increase the porosity of the solid supported reagent, therefore enabling greater access to the reactive sites.* [176]



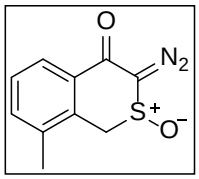
Sodium hydride (60% dispersion in mineral oil, 0.22 g, 0.92 mmol, 1.2 eq.) was weighed into a dry 100 mL roundbottomed flask and placed under nitrogen atmosphere. Dry THF (20 mL) was added *via* syringe and the suspension was stirred at 0°C. *trans*-5,6-Diphenylthiomorpholin-3-one *S*-oxides **71,72** (1 : 1, 0.22 g, 0.77 mmol, 1 eq) in THF (15 mL) was added dropwise to the stirring suspension. Stirring was continued for 15 min at 0°C and then polymer supported benzenesulfonyl azide (0.77 g, 1.15 mmol, 1.5 eq.) which had been swollen in dry THF for 15 mins was added to give a yellow coloured solution. The reaction mixture was stirred for 1 h at 0°C, then overnight at room temperature with a gradual colour change to orange. The polymer supported reagent was filtered off and rinsed with dichloromethane (2 x 5 mL). The solvent was removed under reduced pressure to give a yellow/brown residue. This residue was dissolved in dichloromethane (1 mL), loaded on to alumina and purified using 100% chloroform as

eluent to give the pure α-diazosulfoxides **85** and **86** as a yellow crystalline solid (0.06 g, 27%) and as a mixture of diastereomers (1 : 5.5, equatorial : axial, **86 : 85**). m.p 169-171 °C; ν_{max}/cm^{-1} (neat) 2111, 1644, 1065; HRMS (ESI+) Exact mass calculated for $C_{16}H_{13}N_3O_2S$ $[M+H]^+$ 312.0823 Found 312.0821 (30%) 284.0764 (M – N_2. 100%)

Major diastereomer **85** (axial): δ_H(400 MHz) 4.22 (1H, d, *J* 10.9, CHS), 5.64 (1H, d, *J* 10.9, CHN), 5.99 (1H, br s, NH), 7.18-7.30 (10H, m, 10 x aromatic CH); δ_c (75.5 MHz, $CDCl_3$); 54.0 (CH, CHN), 66.9 (CH, CHS), 125.6, 128.0, 128.8, 129.0, 129.1, 129.7, (6 signals representing 10 x Aromatic CH), 131.7, 136.9 (2 x ArCq) 158.7 (Cq, C=O).

Minor diastereomer **86** (equatorial): δ_H (400 MHz $_3$) 4.43 (1H, d, *J* 8.8, C*H*S), 4.94 (1H, d, *J* 8.8, CHN), 6.23 (1H, br s, N*H*), 7.18-7.30 (10H, m, 10 x aromatic CH); δ_c (75.5 MHz, $CDCl_3$); 55.3 (CH, CHS), 65.0 (CH, CHN), 125.5, 127.8, 128.6, 129.3, 129.5, (5 signals corresponding to 10 x Aromatic CH), 162.4 (Cq, C=O). Note: For this minor diastereomer **86** two Cq signals and a sixth aromatic CH signal were not observed in the ^{13}C NMR spectrum .

3-Diazo-8-methylisothiochroman-4-one *S*-oxide 80[16]



A solution of triethylamine (0.30 mL, 2.10 mmol, 1eq) in acetonitrile (5 mL) was added dropwise over 10 min to a solution of isothiochroman-4-one *S*-oxide **66** (0.42 g, 2.1 mmol, 1 eq) in acetonitrile (30 mL) while stirring at 0 °C under a nitrogen atmosphere. The reaction mixture was stirred for 5 min and a solution of tosyl azide (0.430 g, 2.10 mmol, 1 eq) in acetonitrile (10 mL) was then added slowly while stirring at 0°C under a nitrogen atmosphere. The solution was allowed to slowly reach room temperature while stirring under the inert atmosphere for 9 h. The solvent was removed under reduced pressure to yield the crude product as a red solid (0.68 g). The oil was adsorbed on to Celite® and purified by column chromatography on silica gel using hexane-ethyl acetate as eluent (50 : 50 – 0 : 100) to give the pure α-diazosulfoxide **80** as a yellow crystalline solid (149 mg, 31%). m.p. 72-74 °C (decomp.); ν_{max}/cm^{-1} (neat) 2114, 1624; δ_H (400 MHz) 2.44 (3H, s, CH_3), 4.07 (1H, d, *J* 15.5, A of ABq, one of CH_2), 4.58 (1H, d, *J* 15.5, B of ABq, one of CH_2), 7.42 (1H, t, *J* 7.7, Aromatic CH), 7.49 (1H, d, *J* 7.0, Aromatic CH), 8.01 (1H, d, *J* 6.9, Aromatic CH); δ_C (75.5 MHz) 19.9 (CH_3), 48.8 (CH_2), 78.7 ($C=N_2$), 125.6 (1 x Aromatic CH), 128.6 (1 x Aromatic CH), 131.6 (1 x Aromatic Cq), 135.9 (1 x Aromatic CH), 138.5 (1 x Aromatic Cq), 176.5 (Cq, C=O). Spectral characteristics are in agreement with those reported in the literature.[16]

3.1.7 Synthesis of α-diazosulfoxides in continuous flow

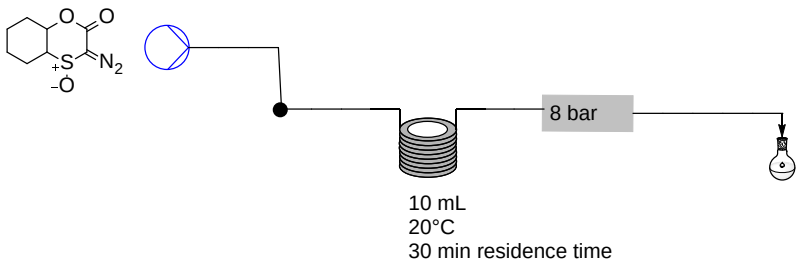
The *Vaportec R-Series* flow reactor consists of 4 reactor positions and 4 HPLC/piston pumps. It allows for manual or automated control. To prepare the reactor for operation, pumps were purged with the required solvent All reaction tubing, coils, inlets and connections were also purged thoroughly in a similar manner. An 8 bar back pressure regulator was fitted to the sytem for all reactions.

The *Vapourtec E-Series* flow reactor consists of 3 peristaltic pumps and up to two temperature controlled reactors. In the same manner used for preparation of the R-Series system, each pump needed for the reaction was purged with the required solvent. All reaction tubing, coils, inlets and connections were also purged thoroughly in a similar manner. An 8 bar back pressure regulator was fitted to the sytem for all reactions.

Table 46

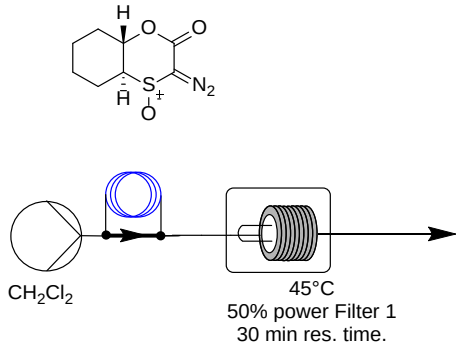
General Specification	
Material of tubing	PFA
Diameter of tubing	1 mm
Working flow rates	0.1 mL/min – 10 mL/min
Tubular reactor working volumne	10 mL
Temperature range	-70°C – 150°C
Column reactor internal diameter (ID)	10 mm
Column reactor length	100 mm
Column reactor operating temperatures	Ambient to 150°C

When the substrates are pumped directly from a feeder vessel the reaction scheme will show it being pumped directly, as in Scheme 115;



Scheme 115: Direct pumping of reagents.

When injection loops are used (blue) for the introduction of substrate/reagents, the following symbol is included on the scheme, as in Scheme 116;



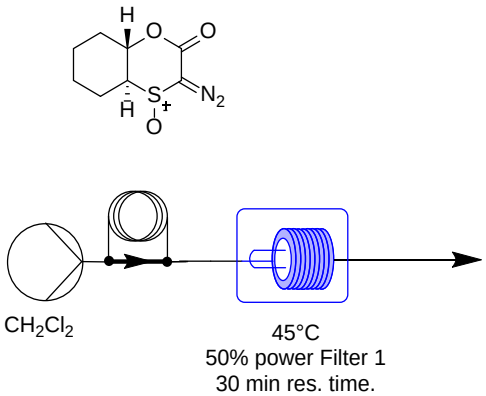
Scheme 116: Pumping of reagents via injection loop.

When reactions are carried out with the UV-150 Photochemical Reactor, it is strongly recommended by Vapourtec that a filter is always used in the UV-150 reactor as they will absorb a significant amount of the unwanted infra-red energy. The three filters supplied with the UV-150 photochemical reactor have different cut-off wavelengths (Table 47);

Table 47: Cut-off wavelengths of UV-150 photochemical reactor filters.

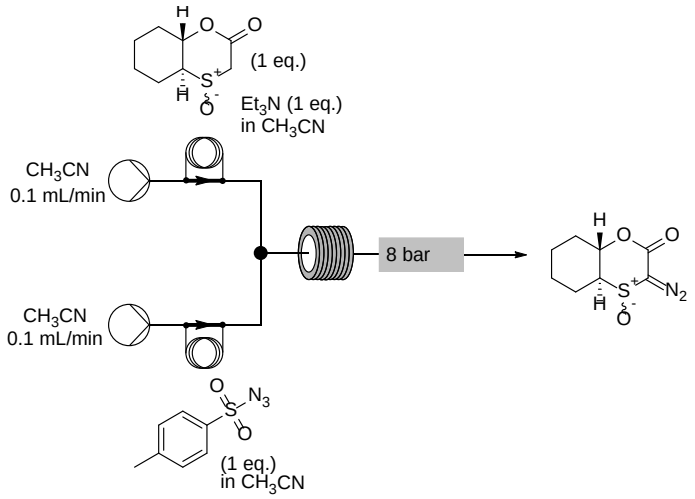
Filter	Wavelength
Type 1 (Silver)	190 – 2000 nm
Type 2 (Gold)	250 – 390 nm
Type 3 (Red)	300 – 2000 nm

Additionally, The fluoropolymer tubing has good UV transmission in the range 220 – 400 nm with an internal bore of 1.3 mm and a wall thickness of 0.15 mm. The maximum pressure limit at 80°C (for the 10 mL UV-150 reactor) is 12 bar.



Scheme 117: Photochemical UV-150 reactor.

3.1.7.1 General method for diazo transfer in continuous flow using homogeneous bases



Scheme 118

Acetonitrile was pumped through the system at a flow rate of 0.1 mL min^{-1} for 10 min to purge the system by means of a HPLC pump. A substrate (1 eq) and amine base (1 eq) were dissolved in acetonitrile (5 mL). Separately, a sulfonyl azide (1 eq) was dissolved in acetonitrile (5 mL). The substrate solution was pumped into a T-piece where it met the sulfonyl azide solution (0.1 mL min^{-1} each). The combined stream passed through a 10 mL reactor coil before passing the volume through a back pressure regulator (8 bar). The product was collected and concentrated under reduced pressure. Results of this optimisation procedure are outlined in Table 48.

Table 48: The use of triethylamine as base in continuous flow

Entry	Residence Time (min)[b]	Et_3N (eq.)	Tosyl Azide (eq.)	Temp	Conversion (%)[a]
1	25	1	1	22	22
2	50	3	1	25	26
3	50	1	1	25	17
4	50	1	1	40	22
5	50	1.9	2	40	38
6	25	1	1	40	26
7	50	1	1 (DBSA)	25	38
8	50	2	1 (DBSA)	40	40

[a] Conversions determined by ^1H NMR spectroscopy.
[b] Residence times of 50 minutes have a flow rate of 0.2 mL/min, residence times of 25 minutes have a flow rate of 0.4 mL/min.

Table 49: Variation of the homegeneous base for diazo transfer to sulfoxides in continuous flow.

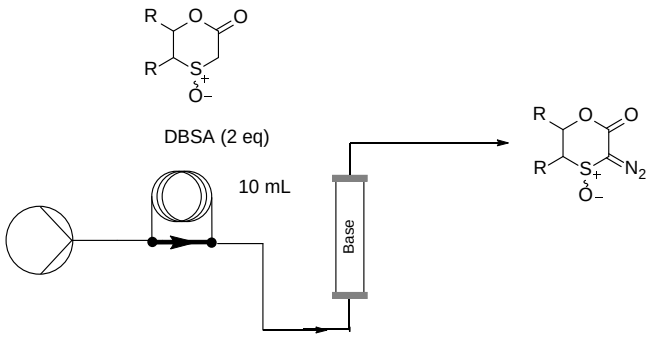
Entry	Base (eq.)	Diazo transfer reagent (eq.)	Residence time (min.)	Conversion (%)[a]
1	Et_2NH (1.05)	Tosyl Azide (1.05)	25	9
2	Et_3N (2)	DBSA (1)	50	40[b]
3	Et_3N (1.9)	Tosyl Azide (2)	50	38[b]
4	DIPEA (1.05)	Tosyl Azide (1.05)	25	4
5	DBU (1.05)	Tosyl Azide (1.05)	25	-[c]

[a] Conversions were determined by ^{1}H NMR Spectroscopy.
[b] These reactions were carried out at 40°C.
[c] The percentage conversion to α-diazosulfoxide could not be determined due to the decomposition of the product to multiple unidentifiable products.

3.1.7.2 Diazo transfer in a continuous flow system using solid supported bases.

Note:

- *Polymer bound DBU was obtained from Sigma Aldrich and has a particle size of 100 – 200 mesh, is 1% cross linked with divinylbenzene and has a loading of 1.5 – 2.5 mmol/g. Amberlyst A21 has a divinylbenzene backbone also, with a particle size of 22 – 30 mesh and a loading of 4.8 mmol/g. Dimethylamine is the active functionality of Amberlyst A21.*
- *For setting up each reaction, the solid supported reagent was loaded into the Omnifit™ glass column reactor with a substantial amount of headspace left for expansion of the reagent on swelling with solvent. The desired solvent is passed over the reagent at 0.2 mL/min for 10 - 15 min at which point the reactor column is disconnected. The adjustable endpiece (as opposed to the fixed endpiece) is tightened sufficiently to compress the solid supported reagent and remove excess solvent, allowing the volume of solvent to be accurately measured through weighing.*
- *In some cases, the Amberlyst A21 is dispersed amongst acid washed sand within the column reactor, resulting in a larger volume within the reactor. This larger volume is sometimes necessary to increase the residence time, when the flow rate of the pump is at its minimum.*



Scheme 119

3.1.7.3 General procedure for diazo transfer using polystyrene supported 1,8-diazabicyclo undec-7-ene (PS - DBU) as base

A 6.6 mm ID Omnifit™ glass column was packed with polymer bound DBU (5 eq). Acetonitrile was pumped through the column at a flow rate of 0.1 mL min^{-1} for 10 min to prepare the system by means of a HPLC pump. Solutions of a sulfoxide substrate (1 eq) in acetonitrile (5 mL), *p*-tosyl azide (2 eq) in acetonitrile (5 mL) were both fed into the same stream and then into the column reactor (18°C, 40 min residence time) at a flow rate of 0.5 mL min^{-1}. The product was collected after passing through an 8 bar back pressure regulator. The collected material was then concentrated under reduced pressure to give the crude product as a pale yellow oil. Conversion was calculated by analysis of the ^{1}H NMR spectrum of the crude material.

3.1.7.4 General procedure for diazo transfer using solid supported bases

A 6.6mm ID Omnifit™ glass column was packed with Amberlyst A21 (20 eq). Acetonitrile was pumped through the column at a flow rate of 0.1 mL min^{-1} for 10 min to prepare the system by means of a HPLC pump. Solutions of a sulfoxide substrates (1 eq) in acetonitrile (5 mL), *p*-tosyl azide (2 eq) in acetonitrile (5 mL) were both fed into the same stream and then into the column reactor (18°C, 60 min residence time) at a flow rate of 0.7 mL min^{-1}. The product was collected after passing through a 8 bar back pressure regulator. The collected material was then concentrated under reduced pressure to give the crude product as a pale yellow oil. Conversion was calculated to be 100 % by analysis of the ^{1}H NMR spectrum.

Note: The results from the investigation using solid or solid supported bases are outlined in Table 50.

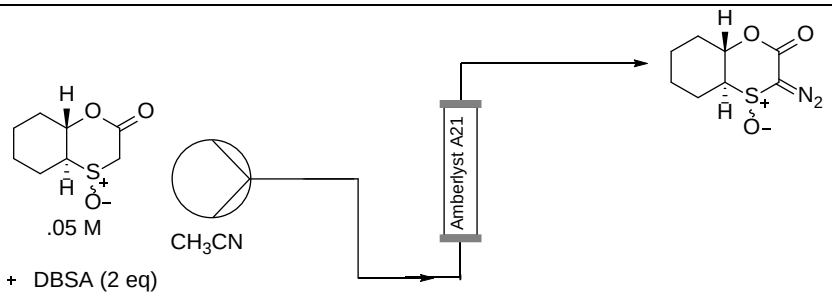
Table 50: Initial investigation with polystyrene supported/insoluble bases.

Entry	Base (eq.)	Diazo transfer reagent (eq.)	Residence time (min.)	Conversion (%)[a]
1	PS-DBU (5)	Tosyl Azide (2)	9	100
2	K_2CO_3 (5)	Tosyl Azide (2)	15	3
3	PS-NMe_2 (20)	Tosyl Azide (2)	9	100
4	PS-NMe_2 (20)	DBSA (2)	9	100

[a]Conversions determined by ^{1}H NMR spectroscopy.

The results from the optimisation investigation using Amberlyst A21 as the solid supported base are outlined in Table 51.

Table 51: Optimisation of diazo transfer process to α-diazosulfoxide in continuous flow using solid Amberlyst A21.

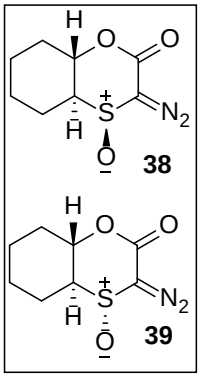


Entry	Amberlyst A21	Diazo Transfer Reagent (eq.)	Residence time (min.)	Conversion (%)	Yield (%)
1	(20 eq)	DBSA(2)	9.5	100	47
2	(20 eq)	DBSA (2)	9	100	49
3	(20 eq)	DBSA (2)	4.5	100	73
4	(20 eq)	DBSA(2)	2.25	98	73
5	(7 eq)	DBSA (2)	4.5	96	68
6	(7 eq)	TsN_3 (2)	6.5	100	-
7	(7 eq)	DBSA (1.2)	6.5	73	-
8	(7 eq)	DBSA (1.2)	9	82	-
9	(7 eq)	DBSA (1.5)	9	85	54
10	(5 eq)	DBSA (2)	4.5	77	68
11	(5 eq)	DBSA (2)	9.5	95	71
12	(5eq)	DBSA (2)	9	86	76

3.1.7.5 General Procedure for the Synthesis of α-Diazosulfoxides Using Amberlyst A21 (5 eq) as base.

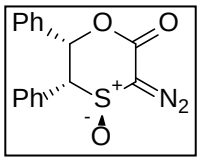
A packed bed reactor consisting of a fritted low pressure 10 mm ID× 10 mm long Omnifit™ glass column was packed with Amberlyst A21 (5 eq.) dispersed among acid washed sand (approx. 4.5 g) and mounted vertically. Acetonitrile was pumped through the column at a flow rate of 5 mL/min for 10 min to prepare the system by means of a peristaltic pump. The sulfoxide (1 eq.) was added to 5 mL of acetonitrile in a 10 mL volumetric flask. Dodecylbenzenesulfonyl azide (2 eq.) was added to the flask, and the solution was made up to the graduation mark with acetonitrile. The solution was pumped through the reactor with a residence time of 9 min at room temperature. The volume of the reactor was established by weighing the packed bed reactor while dry and again following saturation with acetonitrile. The system was fitted with an 8 bar back pressure regulator. The crude material was concentrated under reduced pressure without heating, and conversion was established by ^{1}H NMR spectroscopy. Purification by column chromatography on silica gel using gradient hexane-ethyl acetate as eluent (50 : 50 — 0 : 100) gave the pure α-diazosulfoxides in good to excellent yields.

3-Diazo-hexahydrobenzo[1,4]oxa-thiin-2(*3H*)-one *S*-oxides 38 and 39



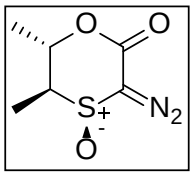
A (1 : 0.7, **55** : **56**, equatorial : axial) diastereomeric mixture of the sulfoxides (0.100 g, 0.53 mmol, 1 eq.) and DBSA **87** (0.373 g, 1.06 mmol, 2 eq.) in acetonitrile (10 mL) was pumped through a 10-mm ID packed bed reactor containing Amberlyst A21 (0.552 g, 2.65 mmol, 5 eq) and acid washed sand (approx. 4.6 g) with a residence time of 9 min. The crude product (0.432 g) was a thick yellow oil which showed a relatively clean product and conversion to be 86% on analysis by ^{1}H NMR spectroscopy. Purification by column chromatography on silica gel (ethyl acetate–hexane 50:50) gave the pure α-diazosulfoxides as a mixture of diastereomers (1 : 0.7, **39** : **38**, equatorial : axial) and as a yellow crystalline solid (0.085 g, 76%). Spectral characteristics are consistent with those outlined above, and in the literature.[14]

(4R*,5S*,6R*)-3-Diazo-5,6-diphenyl-[1, 4]-oxathian- 2-one *S*-oxide 77



A 10 mm ID Omnifit™ glass column was packed with Amberlyst A21 (0.395 g, 1.9 mmol, 5 eq.) and acid washed sand (approx. 4.6 g). The axial sulfoxide **59** (0.100 g, 0.35 mmol, 1 eq.) was added to 5 mL of acetonitrile in a 10 mL volumetric flask. Dodecylbenzenesulfonyl azide **87** (0.270 g, 0.70 mmol, 2 eq.) was added to the flask, and the solution was made up to the graduation mark with acetonitrile. The solution was pumped through the reactor at room temperature with a residence time of 9 min. The crude product (0.344 g) was a thick yellow oil which showed conversion to be 96% on analysis by ^{1}H NMR spectroscopy. Purification by column chromatography on silica gel using hexane-ethyl acetate as eluent (50 : 50) gave the pure α-diazosulfoxide **77** as a yellow crystalline solid (0.104 g, 88%). Spectral characteristics are consistent with those outlined above, and in the literature.[14]

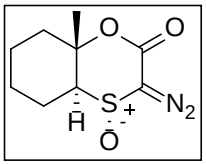
(4S*,5S*,6S*)-3-diazo-5,6-dimethyl-1,4-oxathian-2-one 4-oxide 78



A 6.6 mm ID Omnifit™ glass column was packed with Amberlyst A21 (0.625 g, 3.00 mmol, 5 eq) dispersed in acid washed sand (approx. 4.4 g). The axial sulfoxide **62** (0.102 g, 0.60 mmol, 1 eq) was added to 5 mL of acetonitrile in a 10 mL volumetric flask. Dodecylbenzenesulfonyl azide **87** (0.422 g, 1.201 mmol, 2 eq) was added to the flask and the solution made up to the graduation mark with acetonitrile. The solution was pumped through the reactor with a residence time of 9 min and a flow rate of 0.2 mL min $^{-1}$ at room temperature. The system was fitted with an 8 bar back pressure regulator and the resulting clear yellow solution was concentrated under reduced pressure. The crude product (0.488 g) was a thick yellow oil which showed complete consumption of the starting sulfoxide on analysis by ^{1}H NMR

spectroscopy. Purification by column chromatography on silica gel using ethyl acetate-hexane as eluent (50 : 50) gave the pure α-diazosulfoxide **78** as a yellow crystalline solid (0.101 g, 86%). mp 123-125°C; ν_{max} (neat)/cm^{-1} 2123, 1682, 1051 cm^{-1}; δ_H(400 MHz) 1.42 (3H, d, *J* 7.2, CH_3), 1.52 (3H, d, *J* 6.6, CH_3), 2.91 (1H, dq appears as q, *J* 9.8, 7.2, CHS), 5.07 (1H, dq, *J* 9.8, 6.5, CHO); δ_C (100 MHz) 12.5, 18.8 (2 x CH_3), 56.0 (CH, CHS), 71.5 (CH, CHO), 159.8 (Cq, C=O). Note: The $C=N_2$ signal was not observed in the ^{13}C NMR spectrum of the product.

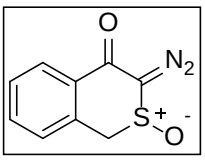
(4R*,4aS*,8aS*)-3-Diazo-8a-methyl-hexahydrobenzo [1,4]-oxathiin-2-one *S*-oxide 76



A 10 mm ID Omnifit™ glass column was packed with Amberlyst A21 (0.514 g, 5 eq.,mmol) dispersed in acid washed sand (approx. 4.5 g). The sulfoxides **57** and **58** (9.5 : 1, 0.100 g, 0.49 mmol, 1 eq.) were added to 5 mL of acetonitrile in a 10 mL volumetric flask. Dodecylbenzenesulfonyl azide **87** (0.347 g, 0.98 mmol, 2 eq.) was added to the flask, and the solution was made up to the graduation mark with acetonitrile. The solution was pumped through the reactor at room temperature with a residence time of 9 min. The crude product (0.451 g) was a thick yellow oil which showed conversion to be 98% by ^1H NMR spectroscopy. Purification by column chromatography (ethyl acetate–hexane 50 : 50) gave the pure α-diazosulfoxide **76** as a yellow crystalline solid (0.096 g, 86%). Spectral characteristics are consistent with those outlined above, and in the literature.[14]

Note: When the reaction was repeated at a concentration of 0.09 M the isolated yield of **76** was 60%.

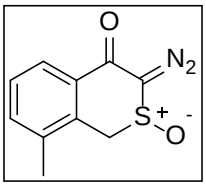
3-Diazoisothiochroman-4-one *S*-oxide 14



A 6.6 mm ID Omnifit™ glass column was packed with Amberlyst A21 (0.575 g, 2.76 mmol, 5 eq, total volume 1.9 mL made up by acid washed sand). A solution of the sulfoxide **64** (0.120 g, 0.5 mmol, 1 eq) and DBSA **87** (0.466 g, 1.0 mmol, 2 eq) in acetonitrile (10 mL) was fed into the column reactor (18°C, 9 min residence time) at a flow rate of 0.2 mL min^{-1}. The product was collected in a 50 mL round bottomed flask after passing through a 8 bar back pressure regulator. The collected material was then concentrated under reduced pressure to give the crude product as a pale yellow oil (0.652 g). Conversion was calculated to be 96 % by ^1H NMR spectroscopy. Purification of the crude reaction mixture by column chromatography on silica gel using gradient hexane-ethyl acetate as eluent (30 : 70 – 0 : 100) led to elution of the α-diazosulfoxide **14** as a pure yellow solid (0.105 g, 80%). m.p. 78-79 °C (decomp.); Found: C, 52.13; H, 2.67; N, 13.22. $C_9H_6N_2O_2S$ requires C, 52.42; H, 2.93; N, 13.58%; ν_{max}(neat)/cm^{-1} 2120, 1634, 1054 ; δ_H (400 MHz) 4.32 (2H, fine ABq appears as s, CH_2), 7.39 (1H, d, *J* 7.1, Aromatic CH), 7.52-7.65 (2H, m, Aromatic CH), 8.14 (1H, dd, *J* 7.6, 1.5, Aromatic CH); δ_C (100 MHz) 52.9 (CH_2, $ArCH_2$), 79.2 (Cq, $C=N_2$), 127.6 (CH, aromatic CH), 129.4 (CH, aromatic CH), 130.3 (Cq, aromatic Cq), 131.2 (Cq, aromatic Cq),

131.7 (CH, aromatic CH), 133.9 (CH, aromatic CH), 176.0 (Cq, C=O); HRMS (ESI+): Exact mass calculated for $C_9H_7N_2O_2S$ [M+H]+, 207.0228. Found 207.0228. Spectral characteristics are in agreement with those reported by Buckley. [16]

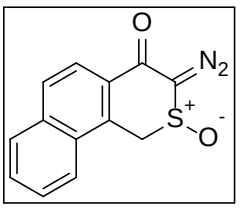
3-Diazo-8-methylisothiochroman-4-one 2-oxide 80



A 6.6 mm ID Omnifit™ glass column was packed with Amberlyst A21 (0.447 g, 2.15 mmol, 5 eq, total volume 2 mL made up by acid washed sand). A solution of the sulfoxide **66** (0.084 g, 0.43 mmol, 1 eq) and DBSA **87** (0.303 g, 0.86 mmol, 2 eq) in acetonitrile (10 mL) was fed into the column reactor (18°C, 9 min residence time) at a flow rate of 0.2 mL min^{-1}. The product was collected after passing through a 8 bar back pressure regulator and collected in a 50 mL round bottomed flask. The collected product was then concentrated under reduced pressure to give the crude product as a pale yellow oil (0.491 g). Conversion was calculated to be 96 % by ^{1}H NMR. Purification of the crude reaction mixture by column chromatography on silica gel using gradient hexane-ethyl acetate (30 : 70 – 0 : 100) as eluent, led to elution of the α-diazosulfoxide **80** as a bright yellow solid (0.082 g, 88%); m.p. 72-74 °C (decomp.); ν_{max}(neat)/cm^{-1} 2114 (C=N_2), 1624 (Cq, C=O); δ_H (400 MHz) 2.44 (3H, s, CH_3), 4.07 (1H, d, *J* 15.5, A of ABq, one of CH_2), 4.58 (1H, d, *J* 15.5, B of ABq, one of CH_2), 7.42 (1H, t, *J* 7.7, Aromatic CH), 7.49 (1H, d, *J* 7.0, Aromatic CH), 8.01 (1H, d, *J* 6.9, Aromatic CH); δ_C (100 MHz) 19.9 (CH_3), 48.8 (CH_2), 78.7 (C=N_2), 125.6 (1 x Aromatic CH), 128.6 (1 x Aromatic CH), 131.6 (1 x Aromatic Cq), 135.9 (1 x Aromatic CH), 138.5 (1 x Aromatic Cq), 176.5 (Cq, C=O)*. Spectral characteristics are in agreement with those reported by Buckley. [16]

*The ^{13}C NMR spectrum was obtained approx. 8 hours after the ^{1}H NMR spectrum and signals detected for the α-oxo sulfine were present in in the ^{13}C NMR spectrum, corresponding to approximately 5% of the material: δ_C (75.5 MHz) 17.7 (CH_3, $ArCH_3$), 32.1 (CH_2, $ArCH_2$), 122.5, 129.0 (CH, 2 x Aromatic CH), 135.8, 137.2 (Cq, 2 x Aromatic Cq), 137.2 (CH, 1 x Aromatic CH), 144.4 (Cq, 1 x Aromatic Cq), 184.8 (Cq, C=S=O), 188.9 (Cq, C=O).

3-Diazo-1H-benzo[h]isothiochromen-4(3H)-one 2-oxide 81

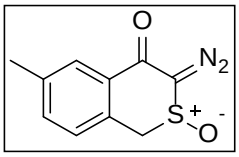


A 6.6mm ID Omnifit™ glass column was packed with Amberlyst A21 (0.453g, 2.2 mmol, 5 eq, total volume 1.9 mL made up by acid washed sand). The sulfoxide **68** (0.102 g, 0.44 mmol, 1 eq) and DBSA **87** (0.311 g, 0.88 mmol, 2 eq) were added to acetonitrile (8 mL) in a 10 mL volumetric flask and sonicated to ensure dissolution. The flask was made up to the graduation mark. This solution was pumped through the column reactor (18°C, 9 min residence time) at a flow rate of 0.2 mL min^{-1} to give a residence time of 9 min. The product was collected after passing through a 8 bar back pressure regulator and collected

in a 50 mL round bottomed flask as a clear yellow solution. The collected product was then concentrated under reduced pressure to give the crude product as a pale yellow solid (0.524 g). Conversion was calculated to be 65 % by ^{1}H NMR spectroscopy. Purification of the crude reaction mixture was carried out by column chromatography on silica gel using hexane-ethyl acetate as eluent (60 : 40 – 25 : 75) to elute the α-diazosulfoxide **81** as a crystalline bright yellow solid (0.044 g, 39%). Analysis by ^{1}H NMR spectroscopy showed some decomposition products present. An analytically pure sample was obtained by slow recrystallization from dichloromethane and diethyl ether. mp 118 – 120°C; ν_{max}(neat)/cm^{-1} 2126, 1681; δ_H (400 MHz) 4.35 (1H, d, *J* 15.8, one of CH_2), 5.20 (1H, d, *J* 15.9, one of CH_2), 7.64 – 7.66 (2H, m, 2 x Aromatic CH), 7.92 – 7.97 (2H, m, 2 x Aromatic CH), 8.08 – 8.10 (1H ,m, 1 x Aromatic CH), 8.18 – 8.20 (1H, d, *J* 7.8. 1 x Aromatic CH); δ_C (100 MHz) 31.8 (CH_2), 119.8, 124.5, 128.0, 129.4, 130.1, 130.4, (6 x Aromatic CH), 137.4. 146.7 (2 x Aromatic Cq), 183.9 (Cq, C=O); m/z (ESI+) 257 [(M+H)+, 10%]; Exact mass calculated for $C_{13}H_9N_2O_2S$ [M+H]+, 257.0385. Found 257.0378

Note: *Two Cq signals were not observed and no diazo carbon signal was observed in the ^{13}C NMR spectrum. Although DBSA has a high initiation temperature of 151°C, and was sonicated for less than 30 seconds, sonication of sulfonyl azides is not recommended as the sample may heat up.*

3-Diazo-6-methylisothiochroman-4-one 2-oxide 83

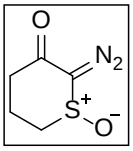


A 6.6mm ID Omnifit™ glass column was packed with Amberlyst A21 (0.589 g, 2.83 mmol, 5 eq, total volume 1.9 mL, made up by acid washed sand). The sulfoxide **67** (0.100 g, 0.56 mmol, 1 eq) and DBSA **87** (0.398 g, 1.13 mmol, 2 eq) were added to acetonitrile (15 mL) and sonicated to ensure dissolution. This solution was pumped through the column reactor (18°C, 9 min residence time) at a flow rate of 0.2 mL min^{-1} to give a residence time of 9 min. The product was collected after passing through a 8 bar back pressure regulator in a 50 mL round bottomed flask as a clear yellow solution. The collected product was then concentrated under reduced pressure to give the crude product as a crystalline pale yellow solid (0.468 g). Conversion was calculated to be 99 % by ^{1}H NMR spectroscopy. Purification of the crude reaction mixture was carried out on silica gel using hexane-ethyl acetate as eluent (60 : 40 – 25 : 75) to elute the α-diazosulfoxide **83** as a crystalline bright yellow solid (0.067g, 60%). A second fraction isolated was the sulfoxide **67** starting material (0.016 g). m.p. 64-65 °C (decomp.); ν_{max}(neat)/cm^{-1} 2112, 1680, 1084; δ_H (400 MHz) 2.43 (3H, s, CH_3), 4.27 (2H, fine ABq appears as s, CH_2), 7.27 (1H, d, *J* 6.4, one of Aromatic CH), 7.41 (1H, dd, *J* 7.7, 1.3, Aromatic CH), 7.94 (1H, unresolved d, *J* 1.1, Aromatic CH); δ_C (100 MHz) 21.2 (CH_3, $ArCH_3$), 52.8 (CH_2, $ArCH_2$), 79.2 (Cq, C=N_2), 127.2 (Cq, 1 x Aromatic Cq), 127.9 (CH, 1 x Aromatic CH), 130.9 (Cq, 1 x Aromatic Cq), 131.6 (CH, 1 x Aromatic CH), 134.6 (CH, 1 x Aromatic CH), 139.6 (Cq ,1 x Aromatic Cq), 176.2 (Cq, C=O); HRMS (ESI+): Exact mass calculated for $C_{10}H_9N_2O_2S$

[M+H]+, 221.1564. Found 221.1575. Spectral characteristics are in agreement with those reported by Buckley. [16]

Note: The isolated yield is 71% when corrected for recovered starting material.

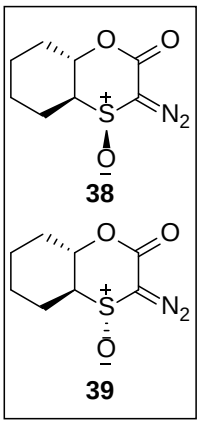
2-Diazo-dihydro-2H-thiopyran-3(*4H*)-one *S*-oxide 82



A 6.6mm ID Omnifit™ glass column was packed with Amberlyst A21 (0.922 g, 4.43 mmol, 5 eq, total volume 1.9 mL made up by acid washed sand). The sulfoxide **65** (0.118 g, 0.88 mmol, 1 eq) and DBSA **87** (0.622 g, 1.77 mmol, 2 eq) were added to acetonitrile (13 mL) and sonicated to ensure dissolution. This solution was pumped through the column reactor (18°C, 25 min residence time) at a flow rate of 0.2 mL min^{-1} to give a residence time of 9 min. The product was collected after passing through an 8 bar back pressure regulator in a 50 mL round bottomed flask as a clear yellow solution. The collected solution was then concentrated under reduced pressure to give the crude product as a crystalline pale yellow solid (0.702 g). Conversion was calculated to be 72 % by ^{1}H NMR spectroscopy. Purification of the crude reaction mixture by column chromatography on silica gel using ethyl acetate-methanol as eluent (90 : 10) led to elution of the the α-diazosulfoxide **82** as a crystalline bright yellow solid (0.027 g, 19%). υ_{max} (neat)/cm^{-1}, 2118 , 1641, 1161; δ_H (400 MHz) 2.19-2.28 (1H, m), 2.41-2.55 (1H, m), 2.70-2.80 (1H, sym m), 2.86-3.06 (2H, m), 3.05-3.21 (1H, m); δ_C (100 MHz) 14.5 (CH_2), 37.3 (CH_2), 48.1 (CH_2), 81.6 (Cq, $C=N_2$), 186.5 (Cq, C=O); HRMS (ESI+): Exact mass calculated for $C_5H_7N_2O_2S$ $[M+H]^+$, 159.0228. Found 159.0231; m/z (ESI+) 159 [$(M+H)^+$, 22 %]. Signals corresponding to the hetero-Wolff rearrangement product, the α-oxosulfine are present in the ^{13}C NMR spectrum at 19.5, 31.1, 39.3 and 185.6 ppm.

3.1.8 New batch conditions for the synthesis of α-diazosulfoxides in batch reaction conditions.

Axial and equatorial 3-diazo-*trans*-hexahydrobenzo[1,4]oxathiin-2-one *S*-oxides 38 and 39[14]



A mixture of the sulfoxides (**56 : 55,** 4 : 3, axial: equatorial) (0.500 g, 2.65 mmol, 1 eq) was dissolved in acetonitrile (30 mL). DBSA **87** (1.86 g, 5.31 mmol, 2 eq) was added to the stirring solution at room temperature. Neat triethylamine (0.268 g, 2.65 mmol, 1 eq) was added dropwise to the reaction mixture at room temperature over 20 min. The reaction mixture was stirred for 1 h at which point analysis of an aliquot by ^{1}H NMR spectroscopy showed complete consumption of the axial sulfoxide **56** starting material (**56 : 55 : 38 : 39**, 0 : 35 : 54 : 11) (Figure 107). The reaction mixture was stirred at room temperature for a further 4 h. The crude mixture was concentrated under reduced pressure to give the crude material as a thick red oil (2.17 g). Analysis by ^{1}H NMR spectroscopy showed 69% conversion (**56 : 55 : 38 : 39**, 0 : 31 : 54 : 15) (Figure 107). Purification by column chromatography on silica gel using gradient hexane-ethyl acetate as eluent (80 : 20 – 0 : 100) led to elution of two fractions. The first contained a 1:1 mixture of the axial α-diazosulfoxide **38** and the equatorial α-diazosulfoxide **39** (0.224 g, 40%), the second contained **38** only (0.035 g, 6%). Spectral characteristics as outlined above.

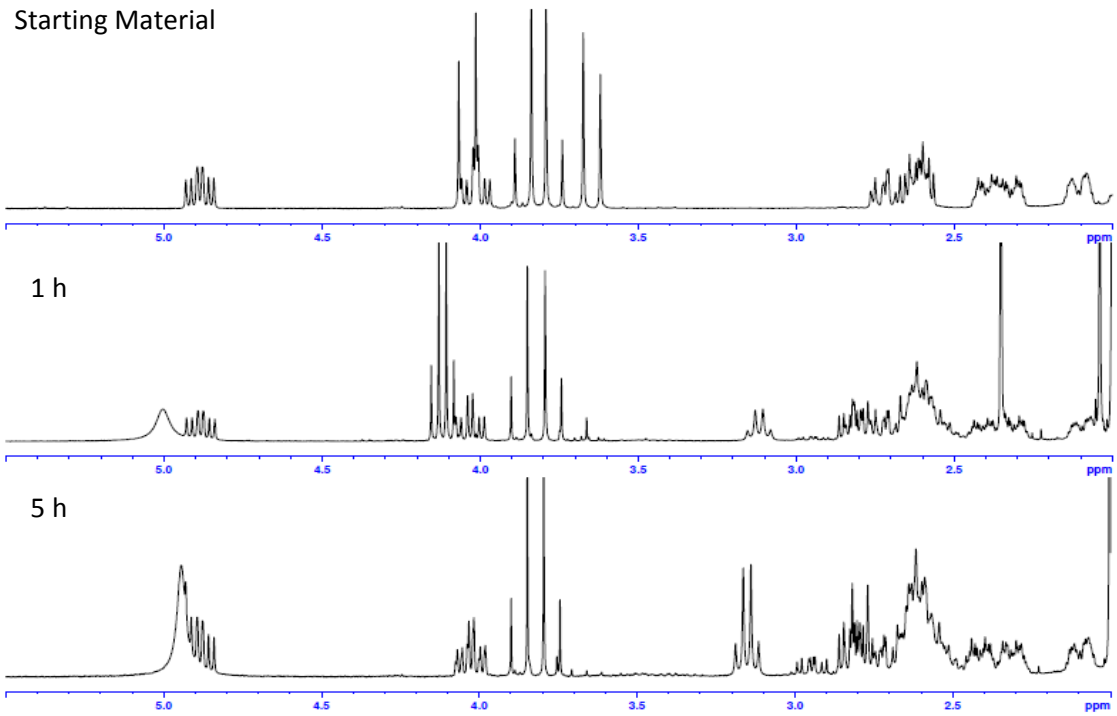
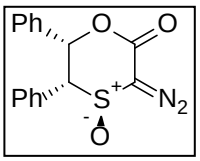


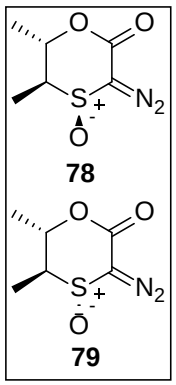
*Figure 107: ^{1}H NMR spectra of the sulfoxide starting material (top, **56 : 55,** 4 : 3), the reaction mixture after 1 h (centre) and 5 h (bottom). The disappearance of the AB_q of the axial sulfoxide shows it is consumed whereas the AB_q of the equatorial sulfoxide remains.*

(4S*,5R*,6S*)-3-Diazo-5,6-diphenyl-1,4-oxathian-2-one 4-oxide 77



The sulfoxide **59** (0.220 g, 0.79 mmol, 1 eq, presumed to be **59** only) and DBSA **87** (0.540 g, 1.53 mmol, 2 eq) were dissolved in acetonitrile (20 mL). Neat triethylamine (0.077 g, 0.79 mmol, 1 eq) was added portionwise (in drops) to the reaction mixture at room temperature over 20 min. The reaction mixture was stirred for 90 mins at which point analysis of an aliquot by ^{1}H NMR spectroscopy showed over 100% consumption of sulfoxide **59**, however peaks corresponding to a trace amount of the opposite diastereomer were present. The crude mixture was concentrated under reduced pressure to give the crude material as a thick orange oil. Purification by column chromatography on silica gel using hexane-ethyl acetate as eluent (50 : 50) led to elution of the desired α-diazosulfoxide **77** as a yellow solid (0.131 g. 55%). Spectral characteristics as outlined above. Notably, the quality of the material was unchanged after three months storage in the freezer.

3-Diazo-5,6-dimethyl-1,4-oxathian-2-one 4-oxide 78 and 79



78

79

A mixture of the sulfoxides **62** and **63** (1 : 0.2, 0.206 g, 1.26 mmol, 1 eq) and DBSA (0.892 g, 2.53 mmol, 2 eq) were dissolved in acetonitrile (20 mL). Neat triethylamine (0.128 g, 1.26 mmol, 1 eq) was added portionwise (in drops) to the reaction mixture at room temperature over 20 min. The reaction mixture was stirred for 4.5 h at which point analysis of an aliquot by ^{1}H NMR spectroscopy showed over 90% consumption of the starting material **62**. Diastereomer **62** reacts much faster than **63**, it is not clear if **63** reacts at all (Figure 108) The crude mixture was concentrated under reduced pressure to give the crude material as a thick orange oil. Purification by column chromatography on silica gel hexane-ethyl acetate as eluent (25:75) led to elution of the desired axial α-diazosulfoxide **78** as a yellow solid (0.112 g, 47%). Spectral characteristics are as outlined above.

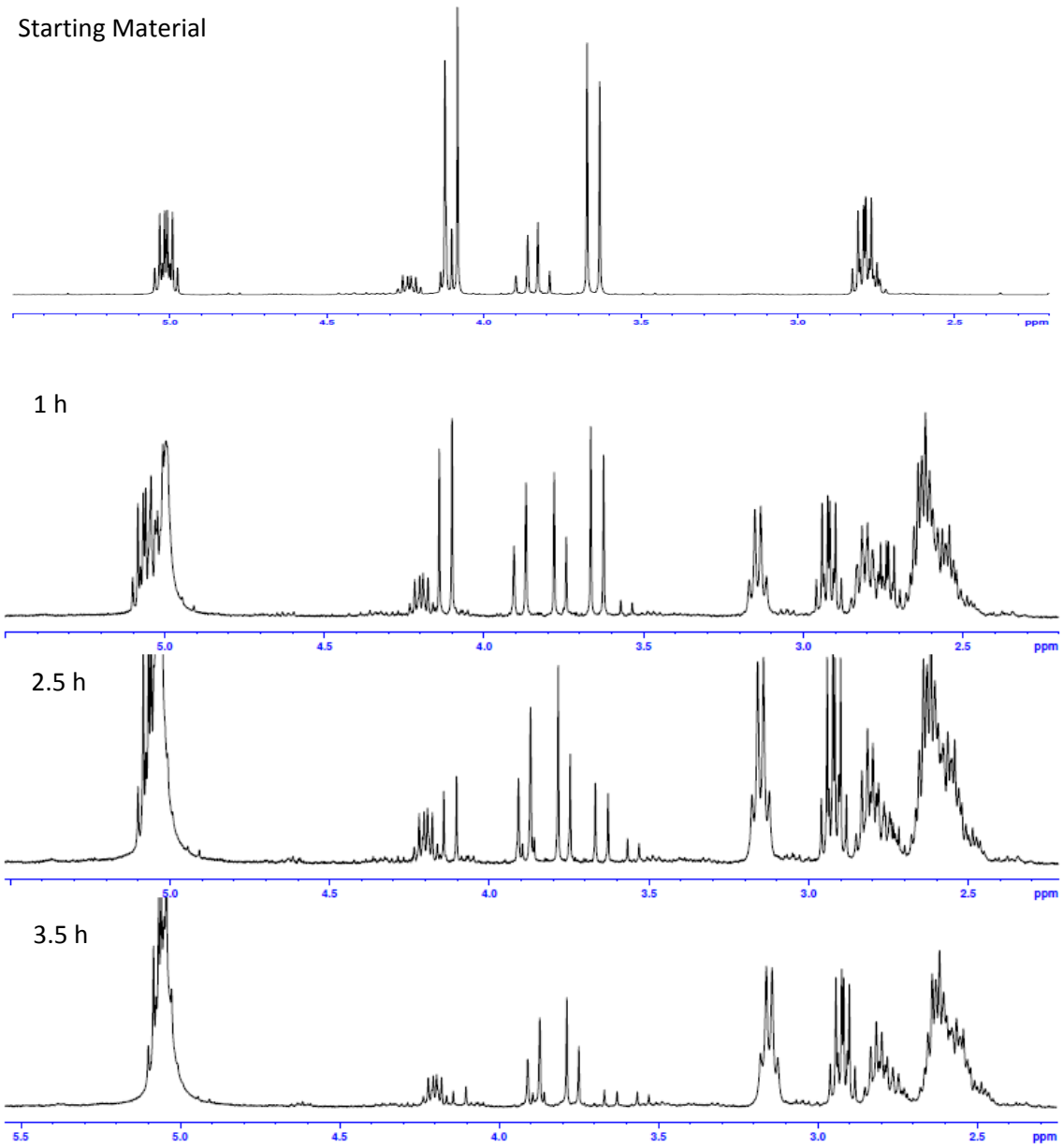
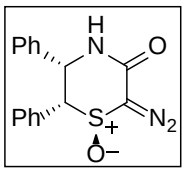


Figure 108: Stacked spectra from the monitoring of the diazo transfer to sulfoxides **62** *and* **63** *with DBSA. Notably, disappearance of the ABq system corresponding to the major axial sulfoxide* **62** *shows that axial* **62** *reacts more readily than the equatorial sulfoxide* **63**.

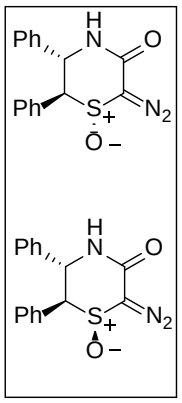
cis-2-Diazo-5,6-diphenylthiomorpholin-3-one *S*-oxide 84[14]



The sulfoxide **70** (0.232 g, 0.08 mmol, 1 eq) was dissolved in dry THF (20 mL). DBSA (0.572 g, 0.160 mmol, 2 eq) in dry THF (5 mL) was added to the stirring solution at room temperature. NaH (60% dispersion in mineral oil, 0.039 g, 0.089 mmol, 1.1 eq) was added portion wise to the reaction mixture at room temperature over 20 min. The reaction mixture was stirred for 3 h at which point analysis of an aliquot by ^{1}H NMR spectroscopy showed complete consumption of the starting material. The crude mixture was concentrated under reduced pressure to give the crude material as a thick red oil. Purification by column chromatography

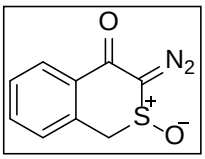
on silica gel using hexane-ethyl acetate as eluent (20 : 80 – 0 : 100) led to elution of the desired α-diazosulfoxide **84** as a yellow solid (0.150 g, 62%). Spectral characteristics as outlined above.

***trans*-2-Diazo-5,6-diphenylthiomorpholin-3-one *S*-oxides 85 and 86**[14]



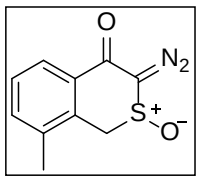
A mixture of the sulfoxides **71,72** (axial : equatorial, 1 : 1.2, 0.242 g, 0.08 mmol, 1 eq) was dissolved in dry THF (20 mL). DBSA **87** (0.580 g, 0.160 mmol, 2 eq) in dry THF (5 ml) was added to the stirring solution at room temperature. NaH (60% dispersion in mineral oil, 0.040 g, 0.089 mmol, 1.1 eq) was added portion wise to the reaction mixture at room temperature over 20 min. The reaction mixture was stirred for 75 min at which point analysis of an aliquot by ^{1}H NMR spectroscopy showed approx. 90% consumption of the starting material. The crude mixture was concentrated under reduced pressure to give the crude product as a thick red oil (0.774 g). Purification by column chromatography on silica gel using hexane-ethyl acetate as eluent (80 : 20 – 0 : 100) led to elution of the desired α-diazosulfoxides, axial **85** and equatorial **86** as a yellow solid (5 : 1, 0.063 g. 24%). Spectral characteristics as outlined above.

3-Diazoisothiochroman-4-one 2-oxide 14



The sulfoxide **64** (1.37 g, 7.69 mmol, 1 eq) was dissolved in acetonitrile (60 mL). DBSA **87** (5.41 g, 15.4 mmol, 2 eq) was added to the stirring solution at room temperature. Neat triethylamine (0.78 g, 1.06 mL, 1.26 mmol, 1 eq) was added dropwise to the reaction mixture at room temperature over 20 min. The reaction mixture was stirred for 2 h at which point analysis of an aliquot by ^{1}H NMR spectroscopy showed over 95% consumption of the starting material. The crude reaction mixture was concentrated under reduced pressure to give the crude material as a thick orange oil (7.06 g). Purification by column chromatography on silica gel using hexane-ethyl acetate as eluent (50 : 50 – 0 : 100) led to elution of the desired α-diazosulfoxide **14** as a yellow solid (1.14 g. 72%). m.p. 78-79 °C (decomp.); δ_H (400 MHz) 4.32 (2H, fine AB_q appears as s), 7.39 (1H, d, *J* 7.1), 7.52-7.65 (2H, m), 8.14 (1H, dd, *J* 7.6, 1.5, Aromatic CH); Spectral characteristics are in agreement with those reported by Buckley. [16]

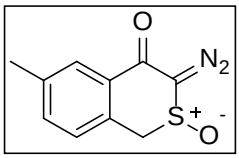
3-Diazo-8-methylisothiochroman-4-one *S*-oxide 80[16]



The sulfoxide **66** (0.950 g, 3.79 mmol, 1 eq) was dissolved in acetonitrile (20 mL). DBSA **87** (3.44 g, 7.39 mmol, 2 eq) was added to the stirring solution at room temperature. Neat triethylamine (0.383 g, 0.52 mL, 3.79 mmol, 1 eq) was added dropwise to the reaction mixture at room temperature over 20 min. The reaction mixture was stirred for 3.5 h at which point analysis of an aliquot by ^{1}H NMR spectroscopy showed

over 90% consumption of the starting material. The crude mixture was concentrated under reduced pressure to give the crude material as a thick orange oil (4.23 g). Purification by column chromatography on silica gel using hexane-ethyl acetate as eluent (50 : 50 – 0 : 100) gave pure 3-diazo-8-methylisothiochroman-4-one *S*-oxide **80** as a yellow crystalline solid (0.74 g. 68%). Spectral characteristics as outlined above.

3-Diazo-6-methylisothiochroman-4-one *S*-oxide 83



The sulfoxide **67** (0.712 g, 3.68 mmol, 1 eq) was dissolved in acetonitrile (50 mL). DBSA **87** (2.58 g, 7.37 mmol, 2 eq) was added to the stirring solution at room temperature. Neat triethylamine (0.371 g, 0.51 mL, 3.68 mmol, 1 eq) was added dropwise to the reaction mixture at room temperature over 20 min. The reaction mixture was stirred for 5 h at which point analysis of an aliquot by ^{1}H NMR spectroscopy showed over 95% consumption of the starting material (Figure 109). The crude mixture was concentrated under reduced pressure to give the crude material as a thick purple oil (3.21 g). Purification by column chromatography on silica gel using gradient hexane-ethyl acetate as eluent (50 : 50 – 0 : 100) led to elution of the desired α-diazosulfoxide **83** as a pale yellow crystalline solid (0.68 g, 84%). m.p. 64-65 °C; ν_{max} (neat)/cm^{-1} 2111, 1684, 1084; δ_H (400 MHz) 2.43 (3H, s), 4.27 (2H, fine AB_q appears as s), 7.27 (1H, d, *J* 6.4, Aromatic CH), 7.41 (1H, dd, *J* 7.7, 1.3, Aromatic CH), 7.94 (1H, unresolved d, *J* 1.1, Aromatic CH). Spectral characteristics are consistent with those reported by Buckley.[16]

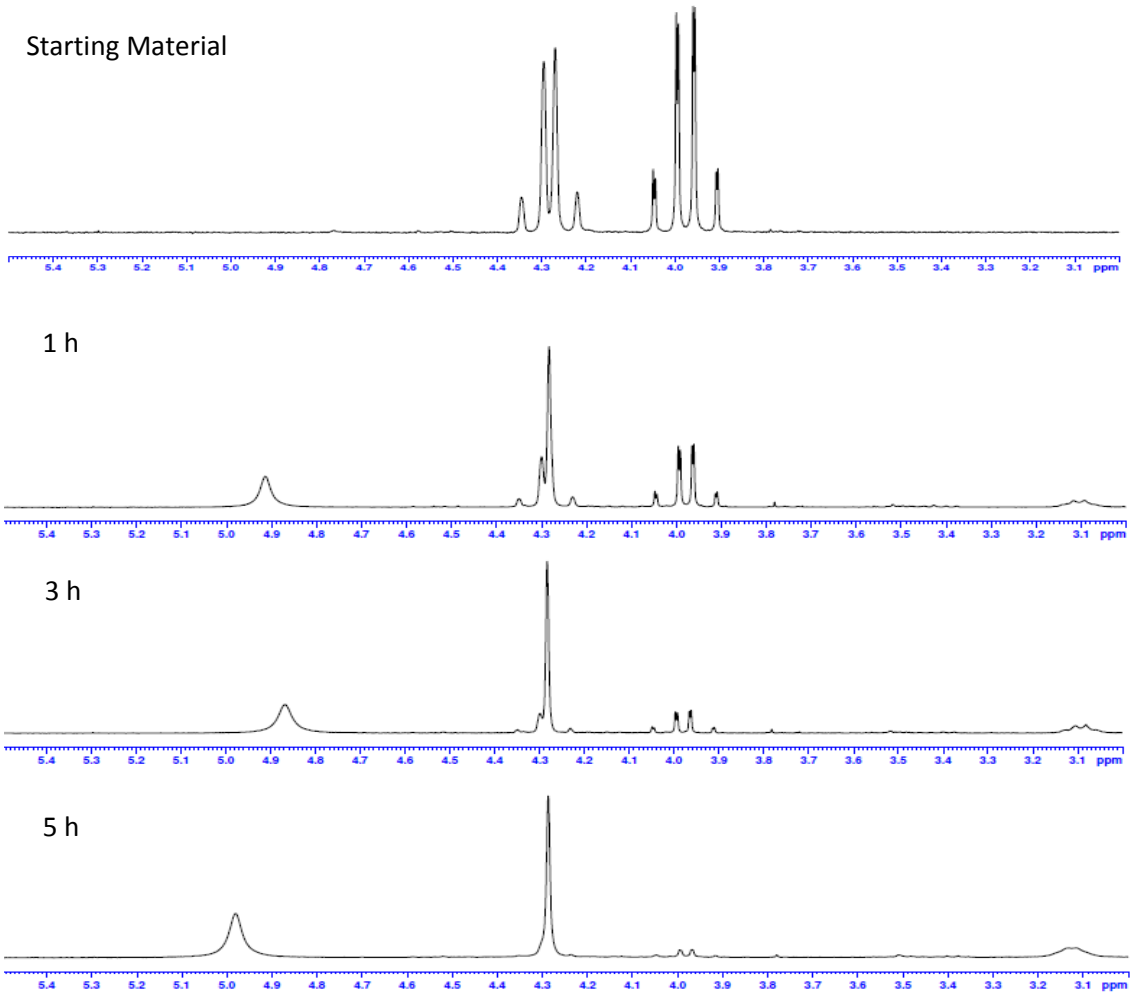
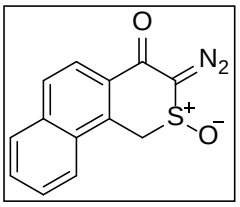


Figure 109: Monitoring the diazo transfer reaction to the sulfoxide **67** *shows the disappearance of the* $SOCH_2$ *signal over 5 h.*

3-Diazo-1H-benzo[*h*]isothiochromen-4(*3H*)-one 2-oxide 81



The sulfoxide **68** (0.080 g, 0.03 mmol, 1 eq) was dissolved in acetonitrile (20 mL). DBSA **87** (0.160 g, 0.045 mmol, 2 eq) was added to the stirring solution in acetonitrile (5 mL) at room temperature. Neat triethylamine (0.035 g, 0.03 mmol, 1 eq) was added portion wise in drops to the reaction mixture at room temperature over 20 min. The reaction mixture was stirred for 105 min at which point analysis of an aliquot by ^{1}H NMR spectroscopy showed over 90% consumption of the starting material. The reaction mixture was concentrated under reduced pressure to give the crude material as a thick red oil (0.215 g). Purification by column chromatography on silica gel using hexane - ethyl acetate as eluent (50 : 50 – 0 : 100) led to elution of the desired α-diazosulfoxide **81** as a yellow solid (0.041 g. 46%). mp 118 – 120°C; ν_{max}(neat)/cm^{-1} 2126, 1681; δ_H (400 MHz) 4.35 (1H, d, *J* 15.8, A of AB_q of $ArCH_2$), 5.20 (1H, d, *J* 15.9, B of AB_q of $ArCH_2$), 7.64 – 7.66 (2H, m, 2 x Aromatic CH), 7.92 – 7.97 (2H, m, 2 x Aromatic CH),

8.08 – 8.10 (1H, m, 1 x Aromatic CH) 8.18 – 8.20 (1H, d, *J* 7.0, 1 x Aromatic CH). Spectral characteristics are in agreement with those described above.

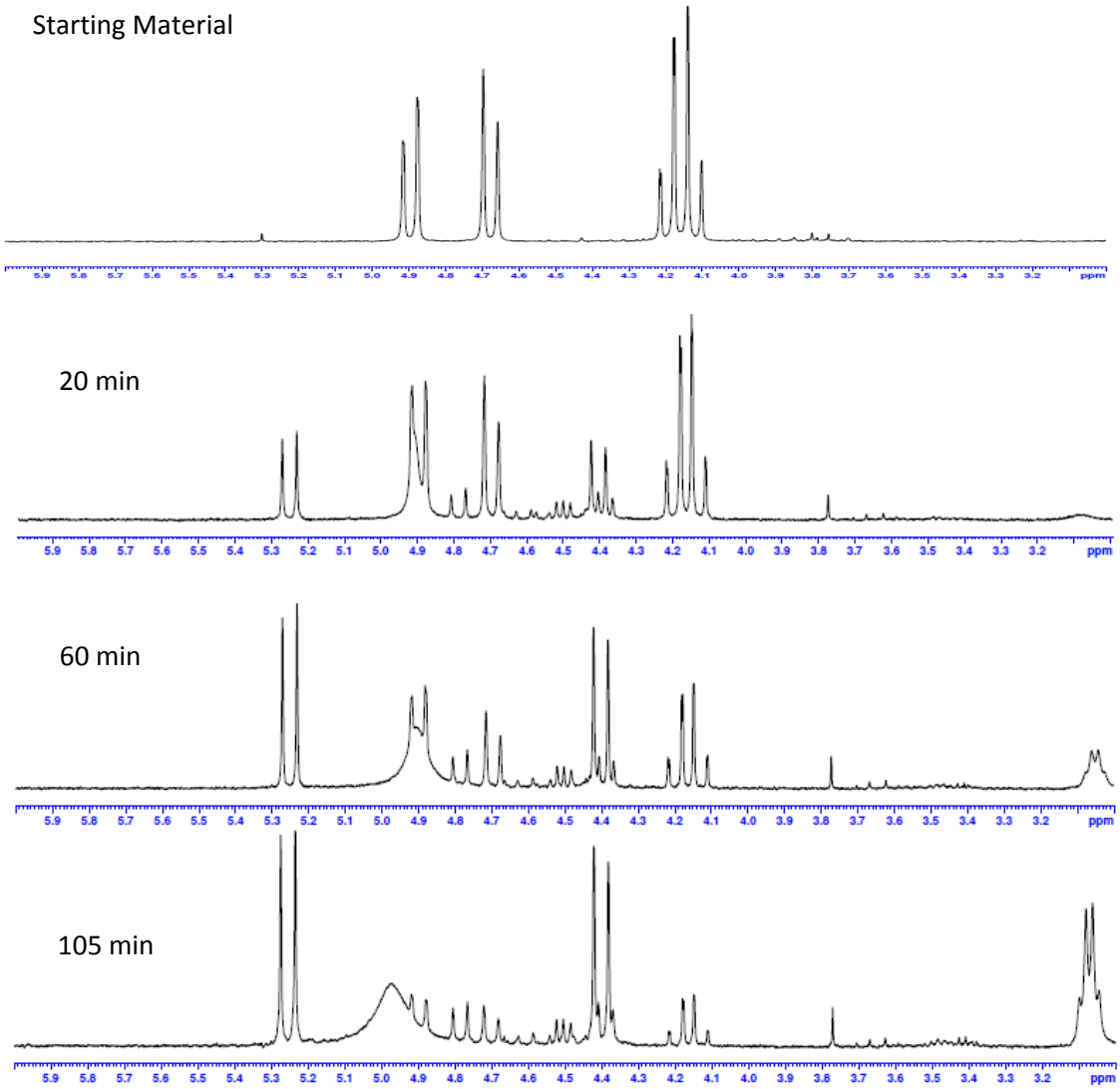
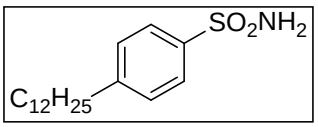


Figure 110: Stacked spectra of the ^{1}H NMR spectra obtained when monitoring the diazo transfer to the sulfoxide **68** *over time.*

3.2 Reactivity of α-diazosulfoxides in continuous flow.

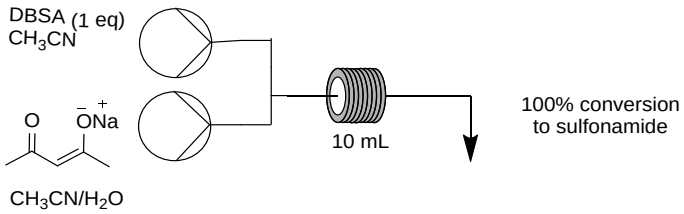
3.2.1 Sacrifical quench of Dodecylbenzenesulfonyl azide in batch [29]

4-Dodecylbenzenesulfonamide 88



NaOH pellets (0.016 g, 4.2 mmol, 1.5 eq) and acetyl acetone (0.042 g, 4.2 mmol, 1.5 eq) were dissolved in acetonitrile : water (1 : 1, 2.5 mL). Dodecylbenzenesulfonyl azide **87** (0.100 g, 0.28 mmol, 1 eq) was added directly to the sodium salt solution, and stirred at room temperature for 15 min. A colour change from colourless to yellow was observed. The reaction mixture was extracted with dichloromethane (2 x 3 mL). The combined organic extracts were washed with water (2 mL), brine (2 mL) and dried with anhydrous $MgSO_4$. The solution was concentrated under reduced pressure to give the crude product as a yellow oil. Analysis by ^{1}H NMR spectroscopy showed the presence of the sulfonamide **88** and sulfonyl azide **87** in a ratio of 2 : 1 (0.061 g, 66%). Characteristic peaks of the sulfonamide; 5.17 (2H, br s, SO_2NH_2), 7.27 (2H, d, *J* 8.6, 2 x Aromatic CH), 7.84 (2H, d, *J* 8.2, 2 x Aromatic CH). Characteristic peak of the sulfonyl azide; 7.37 (2H, d, *J* 8.6, 2 x Aromatic CH), 7.87 (2H, d, *J* 6.7, 2 x Aromatic CH).

3.2.2 Application of a sacrificial sulfonyl azide quench as reported in the literature by Maguire *et al*.[29]

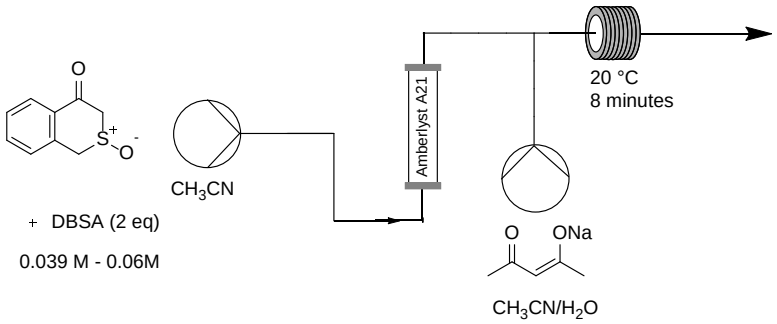


Scheme 120

NaOH pellets (0.032 g, 8.4 mmol, 1.5 eq) and acetyl acetone (0.084 g, 8.4 mmol, 1.5 eq) were dissolved in acetonitrile : water (1 : 1, 2 mL). Separately, dodecylbenzenesulfonyl azide **87** (0.200 g, 0.56 mmol, 1 eq) was dissolved in acetonitrile (2 mL). Both solutions were loaded in to separate injection loops (2 mL) on the Vapourtec R-series reactor. The reaction solutions were pumped at 0.33 mL/min where they mixed at a T-piece and continued through a 10 mL reactor coil at room temperature, with a residence time of 15 min. A colour change from colourless to yellow was observed in the reactor coil. The crude reaction mixture was extracted with dichloromethane (2 x 6 mL). The combined organic extracts were washed with water (4 mL), brine (4 mL) and dried with anhydrous $MgSO_4$. The solution was concentrated under reduced pressure to give the sulfonamide **88** only (0.102, 55%) as a yellow oil which was pure by ^{1}H NMR spectroscopy. δ_H (400 MHz, $CDCl_3$) 0.73 – 0.88 (6H, br m, 6H of $C_{12}H_{25}$),

0.99 – 1.35 (14H, br m, 14H of $C_{12}H_{25}$), 1.46 – 1.68 (4H, m, 4 H of $C_{12}H_{25}$), 2.49 – 2.66 (1H, br m, 1H of $C_{12}H_{25}$), 5.17 (2H, br s, SO_2NH_2), 7.27 (2H, d, *J* 8.6, 2 x Aromatic CH), 7.84 (2H, d, *J* 8.2, 2 x Aromatic CH). Spectroscopic data was consistent with those reported in the literature.

3.2.3 Telescoped sacrificial quench study in continuous flow – modified procedure from Maguire *et al.*[29]



Scheme 121

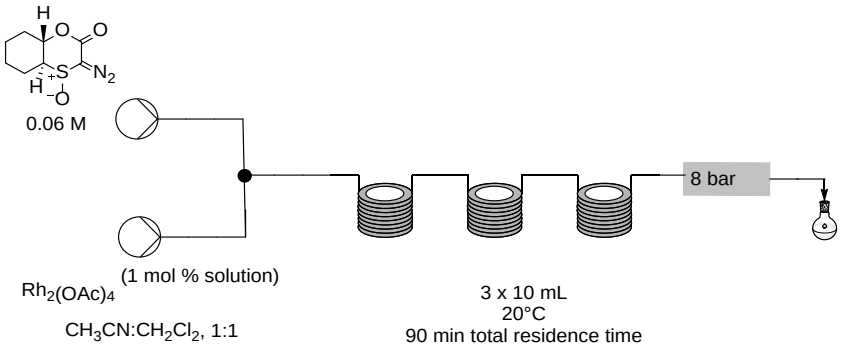
The sulfoxide **64** (0.087 g, 0.4 mmol, 1 eq) and DBSA **87** (0.285 g, 0.8 mmol, 2 eq) were dissolved in acetonitrile (8 mL) and pumped through a 6.6 mm internal diameter Omnifit™ column packed with Amberlyst A21 (0.416 g, 5 eq) with a residence time of 9 min. The outlet was pumped to a T-piece where it met the sacrificial quench solution **100** (20 mL acetonitrile, 20 mL DCM, 2.7 g acetyl acetone, 1.08 g NaOH). The solution of α-diazosulfoxide **64** and sacrificial quench solution **100** were pumped through a 10 mL reactor coil with a residence time of 8 min. Intense red coloration was observed within the coil. The reaction mixture was collected and concentrated under reduced pressure to give the crude product as a brown oil (0.416 g). Analysis of the material by ^{1}H NMR spectroscopy showed complete consumption of the DBSA **87** to form the sulfonamide **88** byproduct, however no sulfoxide **64** or α-diazosulfoxide **14** signals were identifiable in the mixture. The material was a complex mixture of unidentifiable products and so the crude material was not purified.

3.2.4 Reactivity and transformations of α-diazosulfoxides in continuous flow.

Note: The following set of reactions were carried out to investigate the effect of continuous flow reaction conditions on the outcome of the transformation from the α-diazosulfoxides **38,39** to the intermediate α-oxo sulfine **101** and subsequent rearrangements. Previously similar reactions were carried out in batch reaction conditions by Collins[14] with successful isolation and characterisation of a range products including the alkene dimer **41**, the disulfide dimer **40** and the enol **42**.

3.2.5 Reactivity of cyclohexyl derived α-diazosulfoxide.

Method 1: Generation of the α-oxo sulfine **101** using rhodium acetate dimer, in continuous flow, in the absence of a diene trap, with a 90 minute residence time.



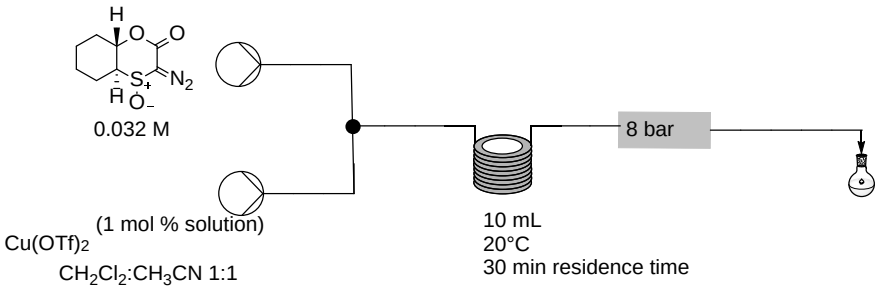
Scheme 122

A mixture of the α-diazosulfoxides **38,39** (1 : 0.7, 0.070 g, 0.3 mmol, 1 eq) was added to a 5 mL volumetric flask and the flask was filled to the graduation mark with acetonitrile to generate a 0.06 M solution of the α-diazosulfoxides. Rhodium acetate dimer (0.001 g, 1 mol %) was added to a mixture of acetonitrile and dichloromethane (1:1, 5 mL) generating a purple coloured solution. Both solutions were pumped at a rate of 0.17 mL/min with a combined flow rate of 0.34 mL/min through 3 x 10 mL reactor coils connected in series, giving a residence time of 90 min. The reactor temperature was set at 20°C. The collected solution was concentrated under reduced pressure to a brown oil as the crude product (0.058 g). Analysis of the crude product by ^{1}H NMR spectroscopy showed the sulfine **101** to be the major product with trace amounts of the alkene dimer **41**, disulfide **40**, and enol **42** rearrangement products.

Table 52

Product	Sulfine 101	Alkene dimer 41	Enol 42	Disulfide 40
Ratio	1.0	0.42	0.07	0.11

Method 2: Reactivity with copper triflate in the absence of a diene trap.



Scheme 123

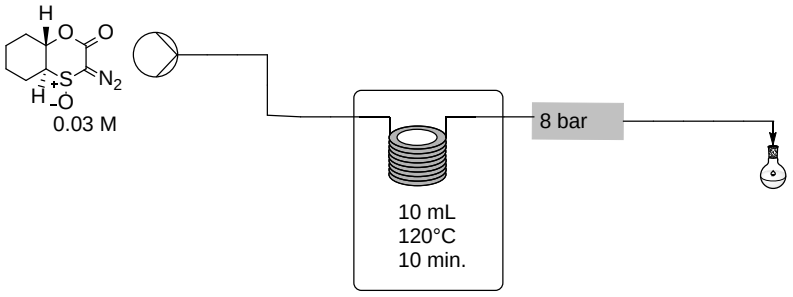
A mixture of the α-diazosulfoxides **38,39** (1 : 0.7, 0.033 g, 0.15 mmol, 1 eq) was added to a 5 mL volumetric flask and the flask was filled to the graduation mark with acetonitrile to generate a 0.032 M solution of the diazo. Separately, copper trifluoromethane sulfonate (0.002 g, 0.003 mmol, 1 mol %) was added to a solution of acetonitrile and dichloromethane (1 : 1, 5 mL). The reactor temperature was set at 20°C. The flow rates for both pumps were set at 0.15 mL/min giving an overall flow rate of 0.3 mL/min and a residence time of 33.33 min with a 10 mL coil reactor. The collected solution was concentrated under reduced pressure to give a brown solid as the crude product (0.032 g). Analysis of the crude product by ^{1}H NMR spectroscopy showed the sulfine **101** to be the major product with trace amounts of the enol **42** and the disulfide **40**. The crude reaction mixture was not purified further. The characteristic peaks of the sulfine **101** are present at δ_H 2.91 (1H, br d, *J* 12.5, one of CH_2), 3.88 (1H, ddd, *J* 11.6, 11.6, 3.6, CHO); The characteristic peaks of the enol **42** are present at δ_H 2.89 (dd, *J* 14.5, 4.5) and 4.54 (1H, dd, *J* 11.3, 6.2); The characteristic peaks of the disulfide **40** are present at δ_H 2.40-2.65 (2H, m, 2 of H of CH_2), 3.11 (2H, d, *J* 11.9, CH), 4.74 (2H, dd, *J* 11.2, 5.8, CHO). A signal indentified as belonging to an unknown component is observed at 4.84 ppm as a broad multiplet.

Note: Repeating the reaction, on the same scale, at 65°C, resulted in an increase of the amount of enol product **42**, relative to the disulfide **40**, caused by sulfur extrusion at the elevated temperature.

Table 53

Temperature	Sulfine 101	Alkene dimer 41	Enol 42	Disulfide 40
Ambient	1.82	0	0.43	1
65°C	3.5	0	0.97	1

Method 3: Generation of the α-oxo sulfine **101** using thermolysis in toluene, in the absence of a diene trap.



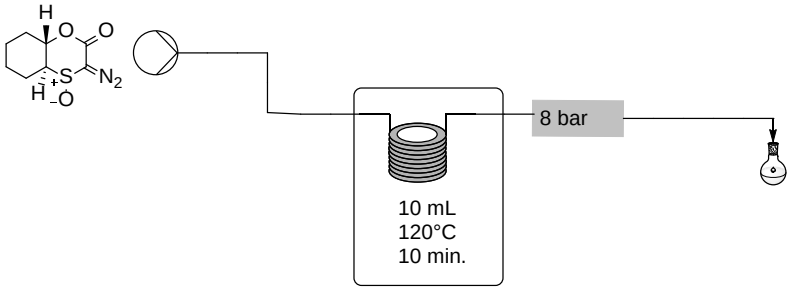
Scheme 124

A mixture of the α-diazosulfoxides **38,39** (1 : 0.7, 0.036 g, 0.16 mmol, 1 eq) was added to a 5 mL volumetric flask and the flask was filled to the graduation mark with toluene to generate a solution of the α-diazosulfoxides (0.03 M). The reactor temperature was set at 120°C. The flow rate for the pump was set at 1 mL/min giving a residence time of 10 min with the 10 mL reactor coil. The solution was pumped through the reactor. The collected solution was concentrated under reduced pressure to a brown oil as the crude product (0.027 g). Analysis of the crude material by ^{1}H NMR spectroscopy showed a very complex crude product mixture with identifying signals belonging to the enol **42** and the disulfide **40** present and large amounts of unknown impurities. The crude reaction mixture was not purified.

Table 54

Product	Sulfine 101	Alkene dimer 41	Enol 42	Disulfide 40
Ratio	0	0.31	0.13	1

Method 4: Generation of the α-oxo sulfine **101** using thermolysis in dichloromethane, in the absence of a diene trap.



Scheme 125

The α-diazosulfoxides **38,39** (0.064 g, 0.29 mmol, 1 eq) were added to a 5 mL volumetric flask and the flask was filled to the graduation mark with dichloromethane to generate a solution of the α-diazosulfoxides (0.06 M). The reactor temperature was set at 120°C. The flow rate for the pump was set at 1 mL/min giving a residence time of 10 min with the 10 mL coil reactor. The solution was pumped through the reactor.

Note: We wanted to confirm that concentration of the crude reaction mixture under reduced pressure was not affecting the ratio of rearrangement products, therefore, before the crude reaction mixture was concentrated, a sample was analysed by infrared spectroscopy with the major absorption peaks recorded at 1080, 1756 (C=O) and 2942 cm^{-1}. The collected solution was subsequently concentrated under reduced pressure to a yellow solid as the crude product (0.051 g), and again, analysed by IR spectroscopy.

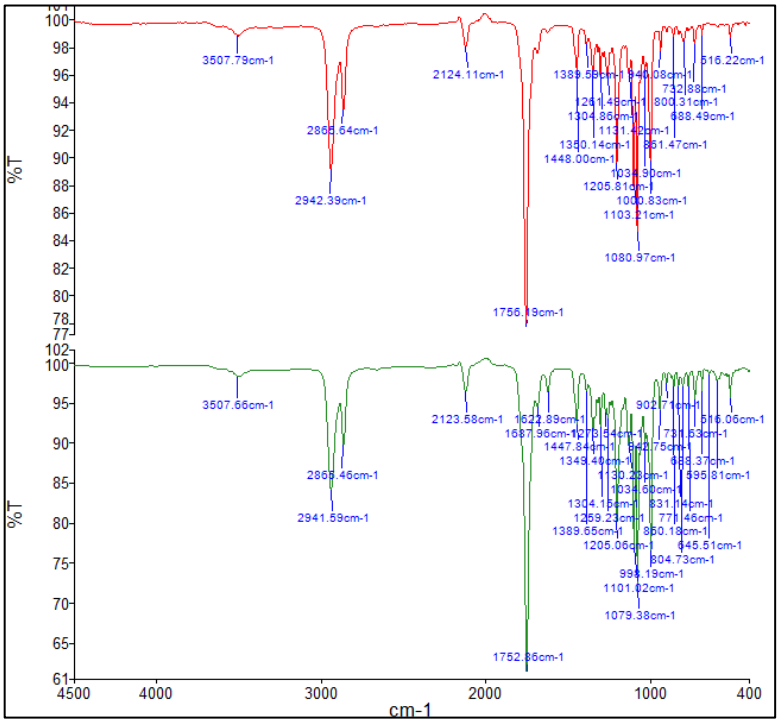


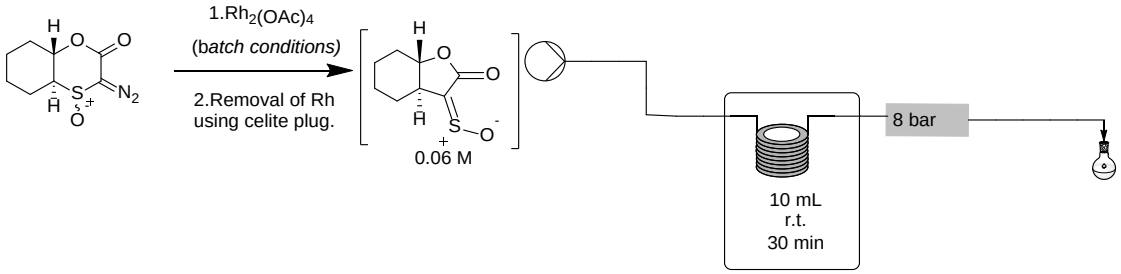
Figure 111: Red; Analysis of crude material before concentration under reduced pressure showing the carbonyl absoprtion of the α-oxo sulfine **101** *to be the major product and; green; after concentration under reduced pressure whereby no change in the infrared spectrum is observed.*

Analysis of the crude product by ^{1}H NMR spectroscopy showed the sulfine **101** to be the major product with additional formation of the enol **42** and disulfide dimer **40**. The crude reaction mixture was not purified further. On analysis of the reaction mixture after a further 18 h the ratio of products had changed further through rearrangement of the intermediate α-oxo sulfine **101**.

Table 55

Product	Sulfine 101	Alkene dimer 41	Enol 42	Disulfide 40
Ratio (after reaction)	1.0	0	0.04	0.21
After 18 h	1.0	0	0.19	0.98

Method 5: Pregeneration of α-oxosulfine **101** in batch, with subsequent pumping through continuous flow system (investigating the effect of back pressure on rearrangement products).



Scheme 126

α-Diazosulfoxides **38,39** (0.114 g, 0.53 mmol, 1 eq) were dissolved in dichloromethane (8 mL) to generate a 0.06 M solution of the diazo. Rhodium acetate dimer (0.001 g, 1 mol %) was added to this solution. Monitoring by IR spectroscopy (solution evaporating on top of ATR crystal) showed complete disappearance of the diazo stretch after 15 min.

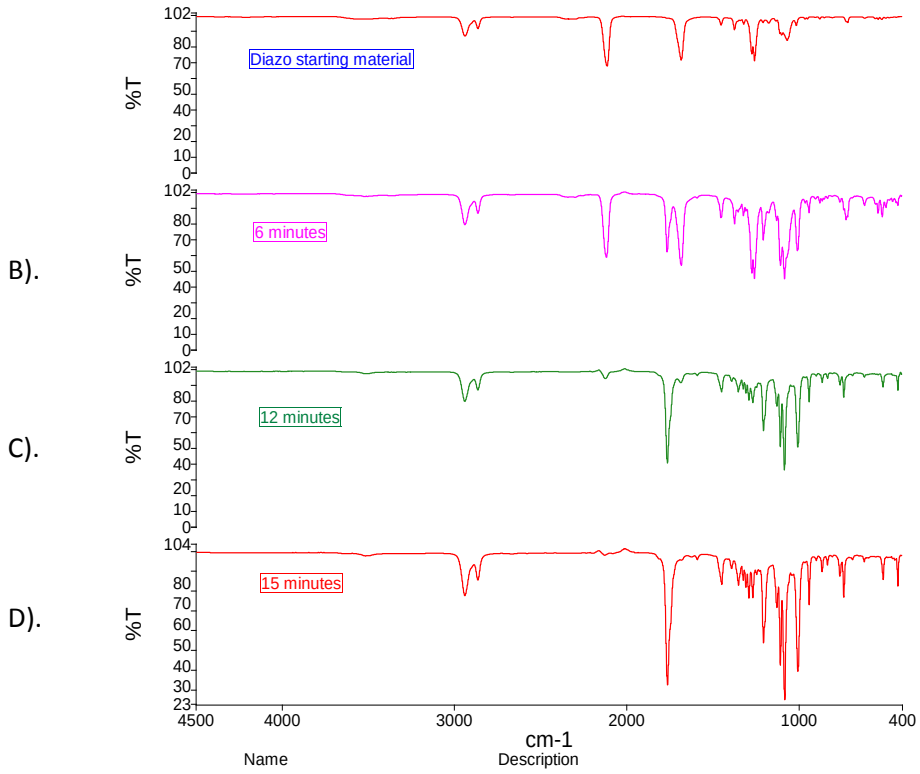


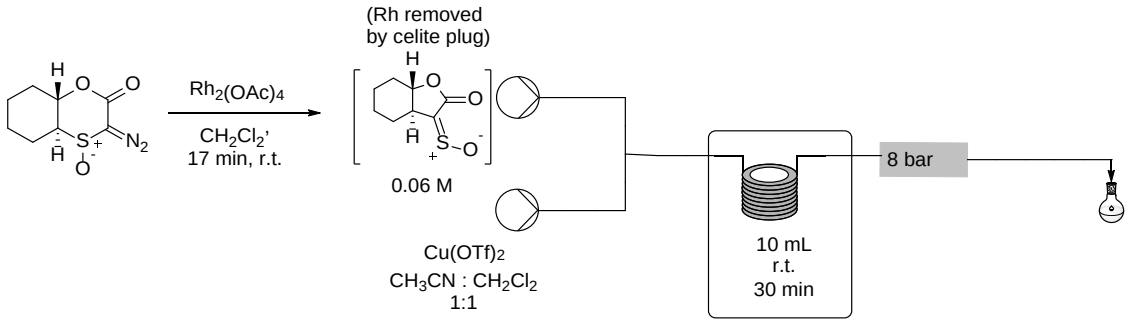
Figure 112: Loss of diazo moiety monitored by infrared specroscopy. A). Shows the IR spectrum of the α-diazosulfoxide starting material B). Shows appearance of the carbonyl for the α-oxo sulfine **101** *and a decrease in the intensity of the diazo absorption at 2129 cm^{-1}. C). Shows a significant decrease in the absorption of the diazo moiety. D). Shows complete disappearance of the diazosulfoxide carbonyl and diazo moiety absorptions.*

The solution of the α-oxo sulfine **101** was filtered through a Celite® plug. This slightly yellow solution (8 mL) was pumped through a 10 mL reactor coil at a rate of 0.33 mL/min giving a residence time of 30 min. The collected colorless solution was concentrated under reduced pressure to give a brown oil as the crude product (0.096 g). Analysis of the crude product by ^{1}H NMR spectroscopy showed the alkene dimer **41** to be the major product with trace amounts of the enol **42** and disulfide **40** products. Spectroscopic data are the same as outlined above.

Table 56

Product	Sulfine 101	Alkene dimer 41	Enol 42	Disulfide 40
Ratio	0	4.4	1.0	1.07

Method 6: Pregeneration of sulfine **101** in batch conditions, followed by pumping through flow system with copper triflate transition metal catalyst, in the absence of a diene trap.

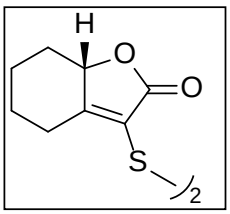


Scheme 127

α-Diazosulfoxides **38,39** (0.105 g, 0.49 mmol, 1 eq) were dissolved in dichloromethane (8 mL) to generate a 0.06 M solution of the diazo. Rhodium acetate dimer (0.001 g, 1 mol %) was added to this solution. Monitoring by IR showed complete disappearance of the diazo stretch after 17 min. The solution of α-oxo sulfine **101** was filtered through a Celite® plug. In a separate vial copper(II) triflate (0.002 g, 0.004 mmol, 1 mol %) was dissolved in a mixture of acetonitrile and dichloromethane (1 : 1, 8 mL). Both solutions were pumped to a T-piece at a rate of 0.17 mL/min giving a residence time of 30 min. The collected colorless solution was concentrated under reduced pressure to a brown oil as the crude product (0.078 g). Analysis of the crude product by ^{1}H NMR spectroscopy showed the disulfide dimer **40** to be the major product with trace amounts of enol **42** and alkene dimer **41**.

Table 57

Product	Sulfine 101	Alkene dimer 41	Enol 42	Disulfide 40
Ratio	0	1.5	1.0	4.95



Purification of the crude reaction mixture led to elution of the disulfide dimer **40** as a white crystalline solid (0.029 g, 35%). ν_{max}(neat)/cm^{-1} 1759, 1001; δ_H($CDCl_3$) 1.10-1.75 (6H, m, 6H of CH_2), 1.80-2.15 (4H, m, 4H of CH_2), 2.17-2.35 (2H, m, 2H of CH_2), 2.40-2.65 (2H, m, 2H of CH_2), 3.11 (2H, d, *J* 11.9, CH), 4.74 (2H, dd, *J* 11.2, 5.8, CHO); δ_C ($CDCl_3$) 22.7, 26.3, 27.8, 34.2 (4 x CH_2), 80.8 (CH, CHO), 120.0 (C), 169.7 (Cq, C=O), 174.0 (Cq). Spectral characteristics are in agreement with those reported in the literature.[14]

3.2.6 Photochemical Decomposition Reactions:

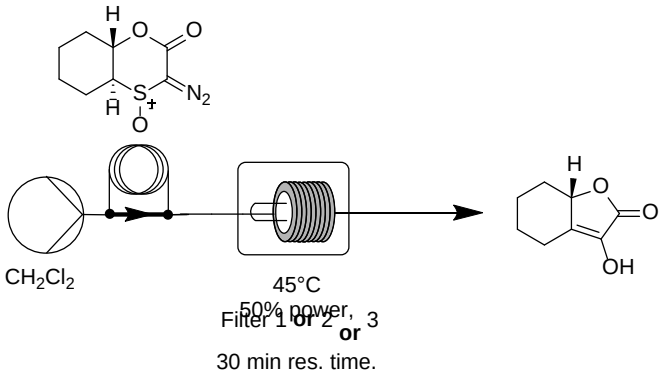
Note: *It is strongly recommended by Vapourtec that a filter is always used in the UV-150 reactor as they will absorb a significant amount of the unwanted infra-red energy. The three filters supplied with the UV-150 photochemical reactor have different cut-off wavelengths;*

Filter	***Wavelength***
Type 1 (Silver)	*190 – 2000 nm*
Type 2 (Gold)	*250 – 390 nm*
Type 3 (Red)	*300 – 2000 nm*

Additionally, The fluoropolymer tubing has good UV transmission in the range 220 – 400 nm with an internal bore of 1.3 mm and a wall thickness of 0.15 mm. The maximum pressure limit at 80°C (for the 10 mL UV-150 reactor) is 12 bar.

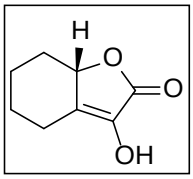
3.2.7 Photochemically induced transformations of α-diazosulfoxides.

For the following photochemical reaction a mixture of the α-diazosulfoxides **38,39** (1 : 0.7, 0.07 g, 0.3 mmol, 1 eq) was dissolved in dichloromethane (6 mL) to generate a 0.06 M solution of the α-diazosulfoxides. This solution was partitioned in to 3 x 2 mL portions. Each 2 mL portion underwent a photochemical transformation using a different filter. In all cases, the UV-150 reactor temperature was set at 45°C, with a power input of 50%, and the flow rate for the pump was set at 0.33 mL/min giving a residence time of 30 min with the 10 mL coil reactor.



Scheme 128

Method 1: Photochemical decomposition of α-diazosulfoxide 38,39 using Filter type 1 (190 – 2000 nm)



The filter number 1 was used. 2 mL of the solution was pumped through the UV-150 reactor using the injection loops. The collected solution was concentrated under reduced pressure to a brown oil as the crude product (0.022 g). Analysis of the crude product by ^{1}H NMR spectroscopy showed the enol **42** to be the major product with >90% purity with the characteristic signals being present at δ_H 2.89 (1H, dd, *J* 14.5, 4.5, cyclohexyl CH) and 4.54 (1H, dd, *J* 11.3, 6.2, CHO); ν_{max} (neat)/cm^{-1}; 1752, 1262,732 cm^{-1}.

Method 2: Photochemical decomposition of α-diazosulfoxide 38,39 using using Filter type 2 (250 – 390 nm)

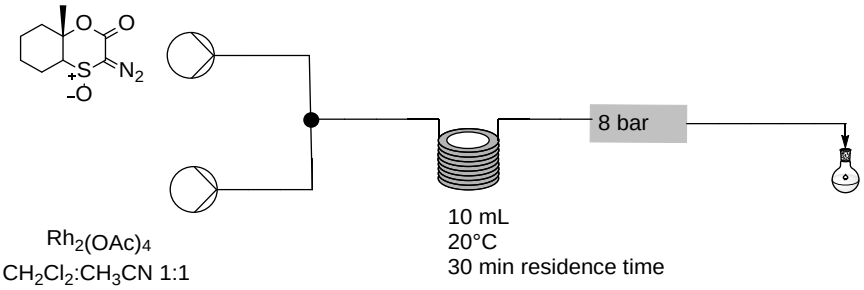
The filter number 2 was used. 2 mL of the solution were pumped through the reactor using the UV-150 reactor using the injection loops. The collected solution was concentrated under reduced pressure to a brown oil as the crude product (0.020 g). Analysis of the crude product by ^{1}H NMR spectroscopy showed the enol **42** to be the major product, with minor impurities (< 10 %) present with the corresponding signals as singlets at 5.77, 5.88 and 5.95 ppm.

Method 3: Photochemical decomposition of α-diazosulfoxides 38,39 using using Filter type 3 (300 – 2000 nm)

The filter number 3 was used. 2 mL of the solution were pumped through the reactor using the UV-150 reactor using the injection loops. The collected solution was concentrated under reduced pressure to a brown oil as the crude product (0.022 g). Analysis of the crude product by ^{1}H NMR spectroscopy showed the enol **42** to be the major component of the crude reaction mixture, along with some unidentified impurities. Signals assigned to the minor impurities include singlets at 5.5, 5.7, 5.9 and 6.0 ppm. The crude reaction mixture was not purified further.
Note: On comparison of the three ^{1}H NMR spectra from the three crude reaction mixtures, Filter 3 was the most complex, while Filters 1 and 2 were extremely similar.

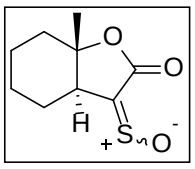
3.2.8 Reactivity of the methyl bridgehead α-diazosulfoxide 76 in a continuous flow system.

Method 1: Generation of the α-oxo sulfine in continuous flow processing using transition metal catalysis – and subsequent trapping to generate the cycloadduct; Semi continuous process for the [4+2] Diels-Alder cycloaddition.



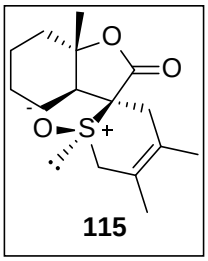
Scheme 129

The α-diazosulfoxide **76** (0.154 g, 0.67 mmol, 1 eq) was dissolved in dichloromethane (10 mL) giving a bright yellow solution. Separately, rhodium acetate dimer (0.002 g, 1 mol %) was added to a mixture of dichloromethane and acetonitrile (1 : 1, 10 mL) generating a purple coloured solution. Both solutions were pumped at a flow rate of 0.17 mL/min where they met at a T-piece and reacted in a 10 mL reactor coil giving a residence time of 30 min. An 8 bar back pressure regulator was inline before collection. The crude reaction mixture was filtered through a Celite® plug and concentrated under reduced pressure to give the crude product as a green/blue residual oil. Analysis by ^{1}H NMR spectroscopy showed the mixture to consist of the α-oxo sulfine **111** and trace amounts of the unknown product **112** which has a doublet of doublets at approx. 4.8 ppm.



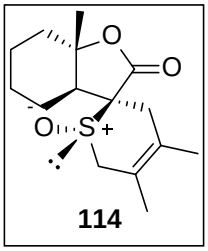
α-Oxo sulfine **111**; δ_H ($CDCl_3$, 400 MHz) 1.20-2.12 (10H, m containing s at 1.42, 7H of CH_2 and CH_3), 2.79 (1H, br d, *J* 14.0, 1H of CH_2), 3.00 (1H, dd, *J* 11.9, 2.7, CH); δ_C ($CDCl_3$) 20.7 (CH_3), 22.4, 22.9, 25.0, 35.4 (4 × CH_2), 59.8 (CH), 86.6 (Cq), 166.2 (Cq, C=O), 177.0 (C=S=O). Spectral characteristics are in agreement with those reported by Collins.[14]

The α-oxo sulfine **111** was redissolved in dichloromethane (10 mL) in a round bottomed flask, and 2,3-dimethyl-1,3-butadiene **113**, (0.554 g, 10 eq, 0.76 mL) was added neat, dropwise to the stirring solution at room temperature. The green solution was stirred at room temperature for 2 h at which point an aliquot was extracted and analysed by ^{1}H NMR spectroscopy, showing complete consumption of the intermediate α-oxo sulfine **111**. The crude reaction mixture (0.142 g) consisted of a major



115

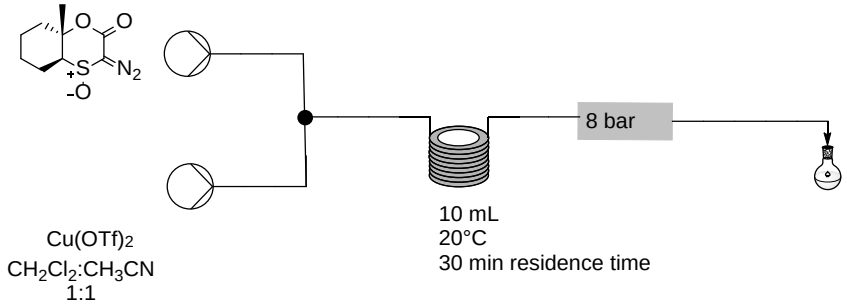
cycloaddition product **114**, a minor cycloaddition product **115**, and the unknown in a ratio of 1 : 0.2 : 0.04. Purification of the reaction mixture by column chromatography on silica gel using hexane-ethyl acetate as eluent (80 : 20), led to the elution of 3 major fractions. The first fraction contained the relatively non-polar disulfide **117** as described in Section 3.2.8, Method 3. The second fraction contained a mixture of the two diastereomeric cycloadducts **115** and **114**, and the third fraction contained the pure major cycloadduct **114** as an off white crystalline solid (**393** in O'Sullivans thesis[15])[xii]. Characteristic signals of the minor cycloadduct **115** (**394** in O'Sullivans thesis[15]) include doublets at 3.0, 3.17 and 3.74 ppm.



114

The third fraction contained **114** only (0.048 g, 26%) υ_{max}/cm^{-1} 1766; 1049; δ_H (400 MHz) 1.23–1.81 (19 H, broad multiplet with overlapping signals including; 3 x CH_3 singlets at 1.59, 1.78, 1.81 and 10 H from 4 x CH_2 and 2 x CH), 2.88 (1H, br d, *J* 18.1, 1 x CH), 3.27 (1H, A of ABq, *J* 17.2, $SOCH_2$), 3.55 (1H, B of ABq, *J* 17.1, $SOCH_2$); δ_C (75.5 MHz) 19.6, 19.9, 21.5 (3 x CH_3, methyl groups), 22.9, 23.0, 26.4, 34.2 (4 x CH_2, 4 x cyclohexyl CH_2), 38.9 (CH_2, allylic H_2), 49.5 (CH_2, $SOCH_2$), 56.4 (CH) 60.8 (Cq), 85.2 (Cq, CqO), 114.9, 124.6 (2 x Cq, C=C), 173.3 (Cq, C=O); Spectral characteristics are in agreement with those reported by O'Sullivan.[15]

Method 2: Generation of the α-oxo sulfine of the methyl bridgehead derived α-diazosulfoxide using copper triflate as the transition metal catalyst.



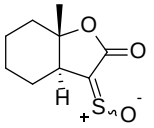
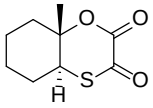
Scheme 130

The α-diazosulfoxide **76** (0.021 g, 0.09 mmol, 1 eq) was dissolved in dichloromethane (2 mL) generating a 0.045 M solution. In a separate vial, copper(II) triflate (0.001 g, 5 mol % relative to **76**) was dissolved in dichloromethane and acetonitrile (1:1, 2 mL) generating a colourless 0.001 M solution. Both solutions were pumped at a flow rate of 0.165 mL/min giving a combined flow rate of 0.33 mL/min and an overall residence time of 30 min in the 10 mL reactor coil, at room temperature. The crude

[xii] Compound numbers **393** and **394** refer to compounds **114** and **115** in the thesis of O'Sullivan.

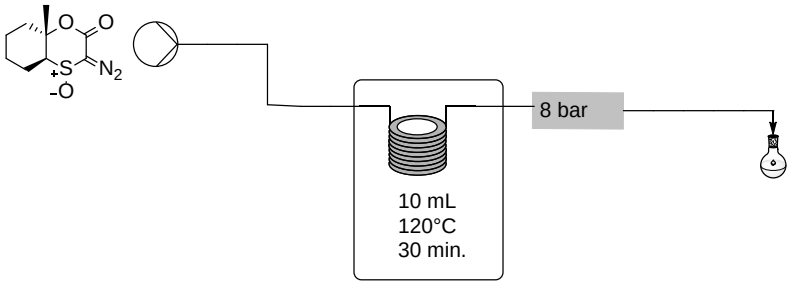
reaction mixture was collected as a yellow oil and concentration under reduced pressure gave the crude mixture of products as a yellow oil (0.02 g). Analysis of the crude reaction mixture showed the major product to be the α-oxo sulfine **111** with the formation of an unknown **112**, and thioester **116**, previously characterised by O'Sullivan also present.

Table 58

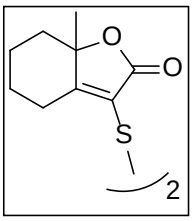
Compound	Sulfine 111	Unknown 112	Thioester 116
			
Ratio	3.5	1	1.2

Characteristic peaks of of the sulfine **111** include: 2.79 (1H, d, *J* 10.4), 3.00 (1H, dd, *J* 8.8, 2.3) Characteristic peaks of the unknown are; 4.79 (1H, d, *J* 10.4) and 4.86 (1H, d, *J* 10.3). The characteristic peak of the thioester **116** is as a doublet at 4.01 (1H, d, *J* 12.8) as described by O'Sullivan.[15]

Method 3: Thermolysis of α-diazosulfoxide **76** in toluene.

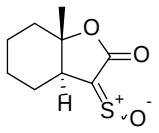
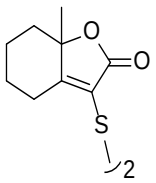


Scheme 131



The α-diazosulfoxide **76** (0.033 g, 0.14 mmol) was dissolved in toluene (4 mL) generating a 0.035 M solution. This yellow solution was pumped through a 10 mL reactor coil heated to 120°C at a flow rate of 0.33 mL/min giving a residence time of 30 min. The crude reaction mixture was collected and concentrated under reduced pressure providing the crude product as a brown oily residue (0.028 g). On analysis of the crude reaction mixture by ^{1}H NMR spectroscopy, complete consumption of the starting material was observed. The ratio of the products present were as follows.

Table 59: Ratio of products formed with the thermolysis of α-diazosulfoxide **76** *in toluene.*

Product	Sulfine 111	Disulfide 117	unknown 112
			
Ratio	1.27	2	1

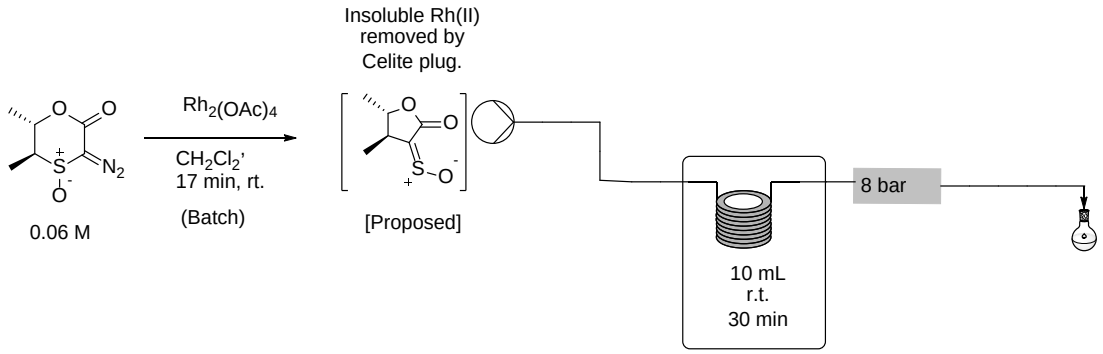
Purification of the crude reaction mixture by column chromatography on silica gel using hexane-ethyl acetate as eluent (90 : 10 – 75 : 25) led to the elution of a first fraction that contained the disulfide **117** and unknown **112** in a ratio of 1 : 0.2. δ_C (100 MHz, $CDCl_3$); 22.2 (CH_3), 22.8, 27.0, 27.4, 40.0 (4 × CH_2). The quaternary carbon signals were not observed however the recorded spectral characteristics are in agreement with those previously reported in the literature.[14] Characteristic signals from the impurity are 4 singlets between 4.68 and 4.90 ppm as reported by Collins.[14]

The second fraction contained pure disulfide **117** as a white solid (0.014 g, 25%). δ_H (400 MHz, $CDCl_3$); 1.40-2.15 (16H, m containing s at 1.50, 5 x CH_2 and 2 × CH_3), 2.20-2.35 (4H, m, 4H of CH_2), 3.00 (2H, dt, *J* 13.7, 2.1, 2 x 1 of CH_2).

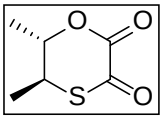
3.2.9 Reactivity of the *trans* - dimethyl α-oxo sulfine in continuous flow, with pre-generation of the α-oxo sulfine using transition metal catalysis.

Note: In an attempt to form a second example of a serically hindered alkene generated through dimerization of an α-oxo sulfine, the conditions which generated the alkene dimer **41** in highest yield from the corresponding α-diazosulfoxides **38,39**, were applied to the α-diazosulfoxide **78**.

(5R*,6R*)-5,6-dimethyl-1,4-oxathiane-2,3-dione 119



Scheme 132



α-Diazosulfoxide **78** (0.067 g, 0.35 mmol, 1 eq) was dissolved in dichloromethane (5.9 mL) to generate a 0.06 M solution of the diazo. Rhodium acetate dimer (0.001 g, 1 mol %) was added to this solution. Monitoring of aliquots of the reaction mixture by IR spectroscopy showed complete disappearance of the diazo stretch at 2126 cm^{-1} after 20 min and formation of a carbonyl stretch at 1752 cm^{-1} tentatively assigned as an α-oxo sulfine.

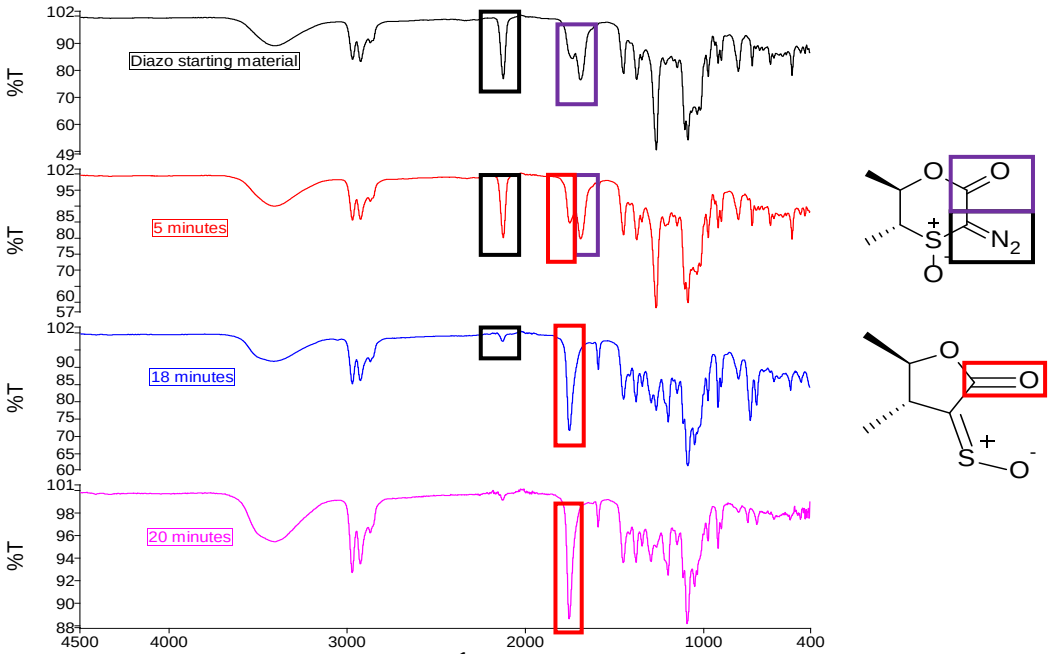


Figure 113: *Generation of the proposed α-oxo sulfine* **118** *from the α-diazosulfoxide* **78** *in batch using rhodium acetate dimer as the transition metal catalyst. The samples were analysed be evaporation of the solvent on the ATR. Disappearance of the diazo stretch at 2126 cm^{-1}.*

The solution of proposed α-oxo sulfine **118** (0.06 M) was filtered through a Celite® plug to remove any insoluble rhodium acetate catalyst. This colorless solution (6 mL) was pumped through a 10 mL coil reactor at a rate of 0.33 mL/min giving a residence time of 30 min. The collected solution was concentrated under reduced pressure to the crude product as a brown oil (0.067 g). Analysis of the crude material indicated the presence of one predominant compound, presumably a rearrangement product of the α-oxo sulfine **118**. The infrared spectrum of this crude material was identical to the infrared spectrum abtained after a 20 minute reaction time of the α-diazosulfoxide **78** with rhodium acetate dimer. Tentatively assigned as either diketone **119**, the *E* and *Z* sulfine **118**, the alkene dimer **120** or another unknown.

Signals corresponding to the tentatively assigned diketone **119** isolated as a brown oil. ν_{max}(neat/cm^{-1}) 1084, 1447, 1752; δ_H($CDCl_3$, 300 MHz) 1.19 (3H, d, *J* 6.7, 1 x CH_3), 1.29 (3H, dd, *J* 7.2, 2.7, 1 x CH_3)* 2.77 (1H, dq, *J* 7.0, 7.0, CH), 3.73 (1H, ddq, *J* 6.5, 6.5, 1.5, CHO); δ_C ($CDCl_3$, 75.5 MHz) 15.8 (CH_3, 1 x

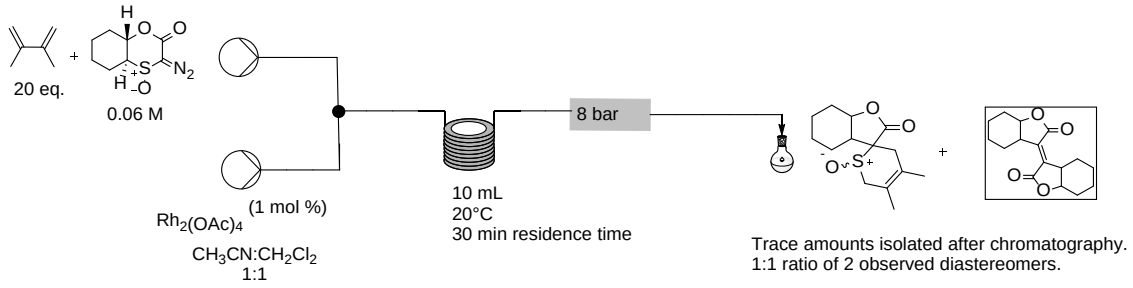
CH_3), 18.5, 18.7 (two signals of equal intensity are seen, corresponding to 2 x CH_3), 53.8, 54.2 (two signals of equal intensity are seen, corresponding to 2 x CHS), 69.2, 69.3 (two signals of equal intensity are seen, corresponding to 2 x CHO).

Minor signals belonging to an impurity are apparent in the ^{13}C NMR spectrum at 15.1, 19.7, 28.7, 45.3, 82.1, 179.4 and 191.4 ppm.

*This signal may be two overlapping doublets.

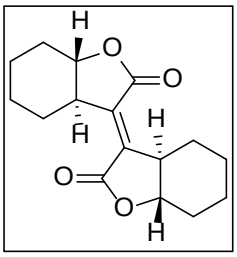
3.3 Diels-Alder cycloadditions

Method 1: Diene **113** and α-diazosulfoxides **38,39** in the same stream and rhodium acetate in the other stream.



Scheme 133

A mixture of the α-diazosulfoxides **38,39** (1 : 0.7, 0.138 g, 0.006 mol, 1 eq) and 2,3-dimethyl-1,3-butadiene **113** (0.529 g, 0.73 ml, 0.006 mol, 10 eq) were added to a 10 mL volumetric flask and the flask was filled to the graduation mark with acetonitrile to generate a 0.064 M solution of the diazo. In a separate 10 mL volumetric flask, rhodium acetate dimer (0.003 g, 1 mol %) was added and dissolved in a solution of acetonitrile and dichloromethane (1 : 1, 10 mL) to generate a purple coloured solution (0.0006 M). The reactor temperature was set at 20°C. The flow rates for both pumps were set at 0.15

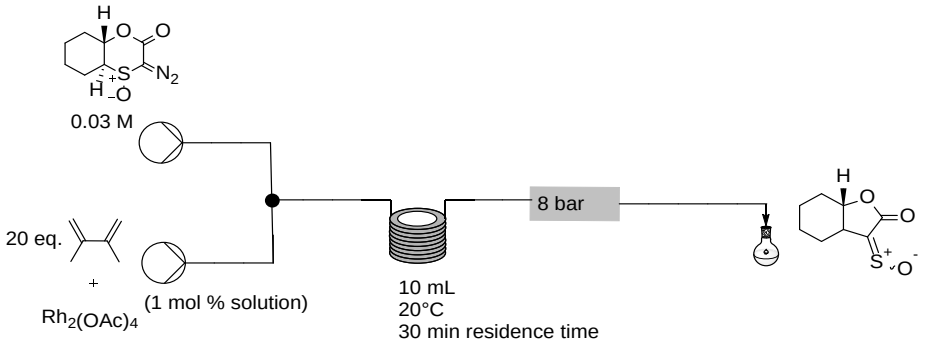


mL/min giving an overall flow rate of 0.3 mL/min and a residence time of 33.33 min with a 10 mL reactor coil. 9.5 mL of both solutions were pumped through the reactor. The collected solution was concentrated under reduced pressure to give the crude product as a brown oil (0.166 g). Analysis by ^{1}H NMR spectroscopy showed a complex mixture with the alkene dimer **41** comprising approx. 70% of the mixture. Purification by column chromatography on silica gel using gradient hexane-ethyl acetate as eluent (90 : 10 – 50 : 50) led to elution of the major product, the alkene dimer **41**, as a white crystalline solid (0.049 g, 56%). Mp 191-193 °C (lit[14] 190-192 °C); δ_H (400 MHz) 1.10 – 2.01 (6H, m, 6H of cyclohexyl CH_2), 2.20-2.38 (1H, sym m, one H of cyclohexyl CH_2), 2.71-2.80 (1 H, sym m, CHCq), 2.91 (1H, br d, *J* 12.5, one H of cyclohexyl CH_2), 3.88 (1H, ddd, *J* 11.6, 11.6, 3.6, CHO); δ_C (100 MHz); 23.9, 25.3, 26.7, 30.6 (4 x CH_2), 51.1 (CH, CHCq), 83.7 (CH, CHO), 138.3 (Cq, C=C), 169.1 (Cq, C=O).

One residual fraction isolated from the column, showed the presence of two diastereomeric cycloadducts in a ratio of 1:1 with characteristic signals appearing in the ^{1}H NMR spectrum as doublets at 3.19, 3.50, 3.75 and 4.40 ppm .

Method 2: α-Diazosulfoxides **38,39** in one stream, and rhodium acetate dimer and diene **113** together in a separate stream.

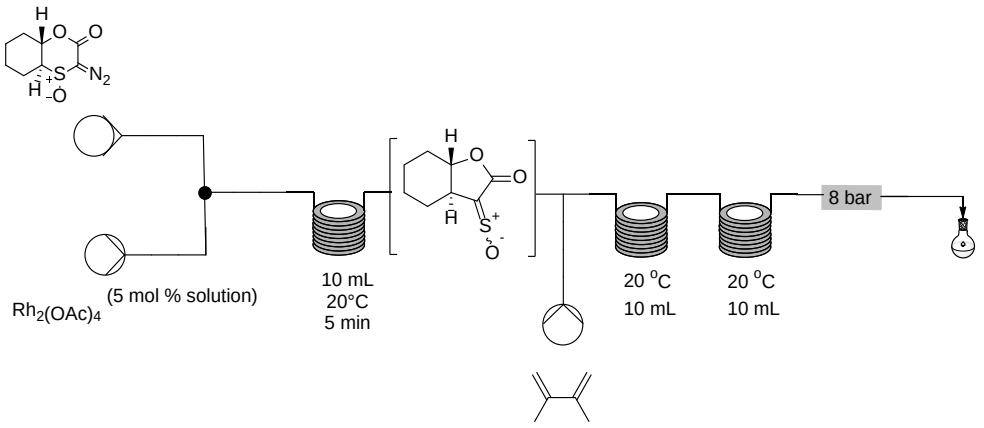
Note: In an attempt to reduce the frequency of dimerisation, the diazosulfoxides **38,39** are twice as dilute as the previous reaction.



Scheme 134

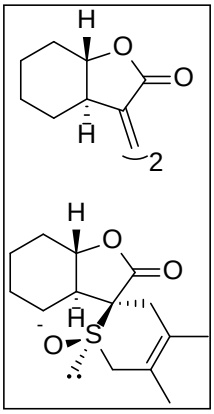
A mixture of the α-diazosulfoxides **38,39** (0.070 g, 0.003 mol, 1 eq) was added to a 10 mL volumetric flask and the flask was filled to the graduation mark with acetonitrile to generate a 0.032 M solution of the α-diazosulfoxides. Separately, 2,3-dimethyl-1,3-butadiene **113** (0.536 g, 0.74 ml, 0.0064 mol, 20 eq) was added to a solution of acetonitrile and dichloromethane (1:1, 10 mL), rhodium acetate dimer (0.0012 g, 1 mol %) was added to this solution, and the volumetric flask was filled up to 10 mL. The reactor temperature was set at 20°C. The flow rates for both pumps were set at 0.15 mL/min giving an overall flow rate of 0.3 mL/min and a residence time of 33.33 min with a 10mL coil reactor. 9.5 mL of both solution were pumped through the reactor. The crude material collected was concentrated under reduced pressure to a brown oil as the crude product (0.068 g). Analysis of the crude product by ^{1}H NMR spectroscopy showed the α-oxo sulfine **101** only as the crude product.

Method 3: Attempted trapping of the *E* (thermodynamic) isomer of the α-oxo sulfine **101**; by generation of the *Z* (kinetic) α-oxo sulfine in situ using rhodium acetate dimer and providing a 5 min residence time to allow isomerisation from the kinetic sulfine to the thermodynamic sulfine.



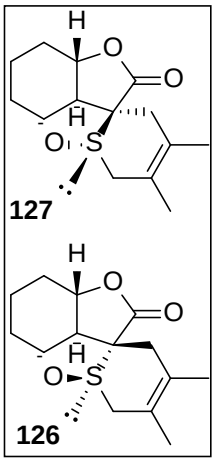
Scheme 135

A mixture of the α-diazosulfoxides **38,39** (0.144 g, 6.7 mmol, 1 eq) was dissolved in dichloromethane (1.4 mL, 0.48 M). Separately, rhodium acetate dimer (0.003 g, 5 mol %) was added to a mixture of acetonitrile and dichloromethane (1:1, 1.4 mL) generating a purple solution. The two solutions were pumped at a rate of 1 mL/min each for five min resulting in a residence time of 5 min in the first 10 mL reactor coil. At this point, 2,3-dimethyl-1,3-butadiene **113** (1.10 g, 1.5 mL, 20 eq) was introduced. All three pumps were manually set to flow at 0.222 mL/min giving a combined flow rate of 0.666 mL/min and a total residence time of 30 min over the 2 x 10 mL reactor coils. The crude reaction mixture was collected and concentrated under reduced pressure to provide the crude solution as a pale yellow oil (0.162 g). Following analysis by ^{1}H NMR spectroscopy the cycloadduct **125** formed by trapping of the *Z* (kinetic) sulfine, unreacted α-oxo sulfine **101**, and 2 cycloadducts **126,127** formed by trapping of the thermodynamic sulfine were present in a ratio of 3.3 : 3.8 : 1 : 0.6. Following purification of the reaction mixture by column chromatography the following products were isolated as white solids.



The first fraction contained the alkene dimer **41** (16 mg, 18%); δ_H (400 MHz) 1.10 – 2.01 (6H, m, 6H of cyclohexyl CH_2), 2.20-2.38 (1H, sym m, one H of cyclohexyl CH_2), 2.71-2.80 (1 H, sym m, CHCq), 2.91 (1H, br d, *J* 12.5, one H of cyclohexyl CH_2), 3.88 (1H, ddd, *J* 11.6, 11.6, 3.6, CHO); δ_C (100 MHz); 23.9, 25.3, 26.7, 30.6 (4 x CH_2), 51.1 (CH), 83.7 (CHO), 138.3 (C=C), 169.1 (Cq, C=O), the second fraction contained the diastereomer **125** (10 mg, 6%) formed from trapping of the kinetic sulfine, characteristic peaks include; 3.54 (1H, sharp d, *J* 15.1, one of $SOCH_2$), 3.95 (1H, br d, *J* 15.1, one of $SOCH_2$), 4.55 (1H, ddd appears as dt, *J* 10.1, 10.1, 3.8, CHO).

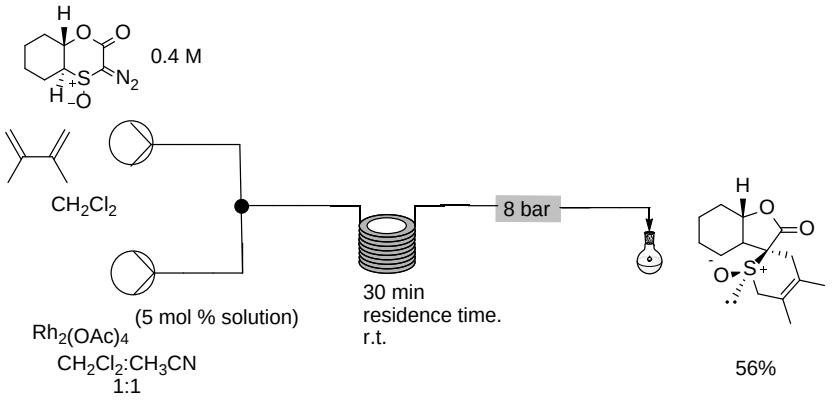
A flush of the column led to the elution of a third and final fraction which contained a mixture of the two most polar cycloadducts, **127** : **126**, (1 : 2) (43 mg, 26 %). Spectral details of both are as follow;.



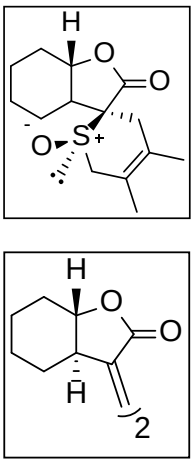
Distinguishable peaks for **127**[15]; 3.23 (1H, d, *J* 16.9), 3.76 (1H, d, *J* 16.9); δ_C (75.5 MHz) 19.5, 19.8 (2 x CH_3), 23.6, 25.2, 26.3, 30.3, 30.4 (5 x CH_2), 45.0 (CH, bridgehead CH), 51.4 (CH_2, $SOCH_2$), 64.1 (Cq, C_{spiro}), 81.3 (CH, CHO), 118.5, 124.9 (2 x C, C=C). No carbonyl peak was observed in the ^{13}C NMR spectrum.

Distinguishable peaks for **126**[15]; 3.56 (1H, d, *J* 15.7), 3.97 (1H, td, *J* 11.5, 4, CHO), 4.42 (1H, d, *J* 15.4); δ_C (75.5 MHz) 19.9, 20.1 (2 x CH_3), 23.4, 23.7, 24.8, 31.0, 31.1, (5 x CH_2), 45.6, (CH, bridgehead CH), 50.0 (CH_2, $SOCH_2$), 61.3 (Cq, C_{spiro}), 79.4 (CH, CHO), 120.2, 123.3 (2 x C, C=C), 171.0 (Cq, C=O).

Method 4: Trapping of the α-oxo sulfine **101** *in situ* using transition metal catalysis – differs to **method 1** by a significant increase in concentration.

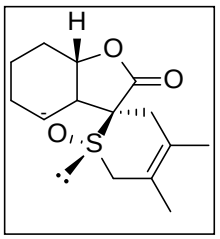


Scheme 136



A mixture of the α-diazosulfoxides **38,39** (0.090 g, 0.42 mmol, 1 eq) and 2,3-dimethyl-1,3-butadiene **113** (0.689 g, 8.4 mmol, 20 eq) were dissolved in dichloromethane (1 mL) generating a 0.4 M solution of **38,39**. In a separate vial, rhodium acetate dimer (0.001 g, 0.02 mmol, 5 mol %) was disolved in a solution of acetonitrile and dichloromethane (1:1, 10 mL) generating a purple coloured solution. The reactor temperature was set at 20°C. The flow rates for both pumps were set at 0.15 ml/min giving an overall flow rate of 0.3 mL/min and a residence time of 33.33 min with a 10 mL coil reactor. The collected solution was concentrated under reduced pressure to a brown oil as the crude product (0.098 g), analysis by ^1H NMR spectroscopy showed successful cycloaddition to form two cycloadducts, the major product **125** from trapping of the kinetically favoured Z-isomer and the minor product **127** from trapping of the thermodynamic *E*-isomer **127**, as well as the α-oxo sulfine **101** (45 : 10 : 45). Purification by column

chromatography on silica gel using hexane-ethyl acetate as eluent (90 : 10 – 50 : 50) led to elution of the major product **125** as a white crystalline solid (0.063 g, 56%) and the least polar fraction contained the alkene dimer **41** (0.022 g, 19%). Spectral characteristics of the major cycloadduct **125** are reported in section 3.3.2 and the alkene dimer **41** is reported in section 3.3 method 1.

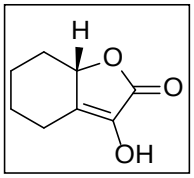


The characteristic signal of the minor diastereomer **127** recorded in the ^{1}H NMR of the crude material is a doublet at 4.43 ppm (1H, d, *J* 16.2) as reported by Collins.[14]

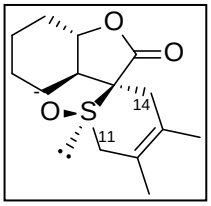
3.3.1 UV-150 reaction promoted Diels-Alder cycloaddition.

Diels-Alder cycloaddition of α-oxo sulfine 101 with 2,3-dimethyl-1,3-butadiene 113

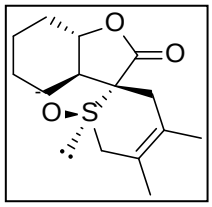
The α-diazosulfoxides **38,39** (1 : 1, 0.145 g, 0.067 mmol, 1 eq) were dissolved in acetonitrile/dichloromethane (4:1, 12 mL) to make a 0.06M solution. 2,3-dimethyl-1,3-butadiene **113** (1.10 g, 1.34 mmol, 20 eq, 1.52 mL) was added to this solution. The solution was pumped through a UV-150 reactor coil with filter number 2 installed, at a flow rate 0.33 mL/min providing a residence time of 30 min. The crude material was collected as a brown solution and concentrated under reduced pressure to give a brown oil (0.126 g). The ^{1}H NMR spectrum of the crude reaction mixture showed 2 diastereomers and the enol product **42** present (major : minor : enol , **126** : **125 : 42,** 2 : 1 : 1). Purification of the reaction mixture by column chromatography on silica gel led to elution of the three separate fractions.



The first contained the enol decomposition product **42** (0.016 g, 16%). ν_{max}(neat)/cm^{-1} 2939, 1752, 1145; δ_H($CDCl_3$) 1.05-2.00 (7H, m, 7 of H of 4 x CH_2), 2.50 (1H, m, 1 H of 4 x CH_2), 2.89 (1H, dd, *J* 14.5, 4.5, CH), 4.54 (1H, dd, *J* 11.3, 6.2, CHO), 5.76 (1H, br s, OH); δ_C ($CDCl_3$) 22.7, 23.8, 25.4, 34.0 (4 × CH_2), 78.3 (CH, CHO), 133.8 (Cq, C=C), 134.2 (Cq, C=C), 170.5 (Cq, C=O); Exact mass calculated for $C_8H_{11}O_3$ $[M+H]^+$ 155.0708. Found 155.0705. Spectral characteristics are consistent with those previously reported by Collins.[14]



The second fraction contained the minor diastereomer **125** (0.012 g, 6%) . Spectroscopic details are in agreement with those reported in section 3.3.2.



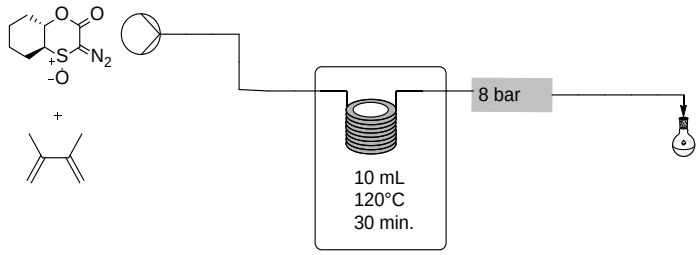
The third fraction contained the major diastereomer **126**, favoured under photochemical conditions (0.025 g, 14%). ν_{max}(neat)/cm^{-1} 1764, 1447, 1050; δ_H($CDCl_3$) 1.23-1.91 (overlapping signals including including 2 x 3H, s at 1.66 and 1.80 and 7H of cyclohexyl ring), 2.28 – 2.37 (1H, m, 1 of H of CH_2), 2.48 (1H, d, *J* 12.3, A of ABq, one of allylic CH_2), 2.62 – 2.72 (2H, m including one cyclohexyl CH and d, *J* 12.3, B of ABq at 2.59, allylic CH_2), 3.17 (1H, br d, *J* 16.4, one of $SOCH_2$), 3.68 (1H, br d, *J* 16.4, one of $SOCH_2$), 3.94 (1H, ddd appears as dt, *J* 11.1, 11.1, 3.8, CHO). δ_C ($CDCl_3$) 19.5, 19.9 (2 × CH_3), 23.6, 25.2, 26.4, 30.3 (4 × CH_2), 30.5 [CH_2, C(14)H_2], 45.1 [CH, CH(9)], 51.4 (CH_2, $SOCH_2$), 64.1 [Cq, C(3)], 81.3 (CH, CHO), 118.6 (Cq, C=C), 125.0 (Cq, C=C), 173.8 (Cq, C=O); m/z (ESI+) 269 [$(M+H)^+$, 100%].

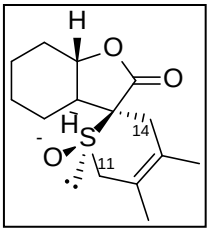
*This fraction contained about 5% of the minor diastereomer with corresponding signals observed a a doublet at 3.55 ppm and 4.41 ppm in the ^{1}H NMR spectrum and at 20.1, 23.4, 23.7, 24.8, 31.1, 45.6, 50.1, 61.3, 79.4, 120.2, 123.3, 171.1 in the ^{13}C NMR Spectrum.

3.3.2 Diels-Alder cycloadditions using thermolysis.

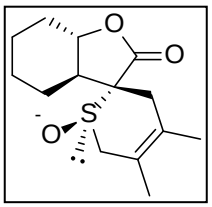
Generation of the intermediate α-oxo sulfine using thermolysis in continuous flow leading to trapping of the α-oxo sulfine *in situ*.

(1'S,3S,3aS,7aS)-4',5'-Dimethyl-3a,3',4,5,6,6',7,7a-octahydro-*2H*-spiro[benzofuran-3,2'-thiopyran]-2-one 1'-oxide 125



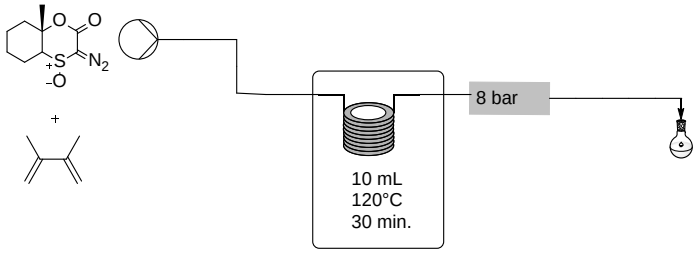


The α-diazosulfoxides **38,39** (0.068 g, 0.31 mmol, 1 eq) was dissolved in the minimum amount of toluene and dichloromethane (1.5 mL, 4 : 1), generating a 0.2 M solution, and 2,3-dimethyl-1,3-butadiene **113** (0.521 g, 0.63 mmol, 20 eq, 0.72 mL) was added to this solution. The solution was pumped through a 10 mL reactor coil heated to 120°C at a flow rate of 0.333 mL/min providing a residence time of 30 min. An 8 bar back pressure regulator was fitted to the system. The crude solution was collected as a pale yellow solution and concentrated under reduced pressure to give a yellow oil (0.085 g) which crystallised overnight. The ^{1}H NMR spectrum of the crude reaction mixture showed **125** and **126** present in a ratio of 84 : 16. Purification of the reaction mixture by column chromatography on silica gel using hexane – ethyl acetate as eluent (50 : 50) led to elution of the product **125** as a white crystalline solid (0.063 g, 74%). Found C, 61.70; H 7.36; $C_{14}H_{20}O_3S$ requires C, 62.66; H 7.51; Mp 187-190 °C; υ_{max}(neat/cm^{-1}) 1765, 1448, 1197, 1031; δ_H($CDCl_3$) 1.20-1.55 (3H, m, 3 x H from CH_2 on cyclohexyl ring), 1.66 (3H, s, CH_3), 1.76 (3H, s, CH_3), 1.82-2.30 (6H, m, CH_2 and CH of cyclohexyl ring), 2.40 [2H, br s, allylic C(14)H_2], 3.54 (1H, sharp d, *J* 15.1, one of $SOCH_2$), 3.95 (1H, br d, *J* 15.1, one of $SOCH_2$), 4.55 (1H, ddd appears as dt, *J* 10.1, 10.1, 3.8, CHO); δ_C($CDCl_3$) 18.9, 20.1 (2 x CH_3), 23.4, 23.7, 25.6, 31.2, 38.7, (5 x CH_2) 51.5 (CH_2S), 54.5 (CHCS), 63.7 (qC), 81.7 (CHO), 118.4 (CH), 126.2 (CH), 173.4 (Cq, C=O); m/z (ESI+) 269 [(M+H)$^+$, 100%]. Spectroscopic detail are in agreement with those previously reported in the literature.[14]

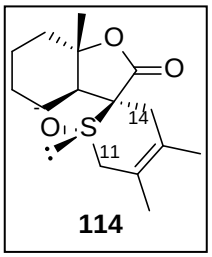


Distinguishable signals observed for the minor diastereomer **126** in another fraction of the column; $\delta_H(CDCl_3)$ 1.18-2.10 (overlapping signals including 2 x CH_3 singlets at 1.55 and 1.71 ppm, and 8H from cyclohexyl ring) 3.57 (1H, br d, *J* 16.4, A of AB_q of $SOCH_2$), 3.94 (1H, ddd appears as dt, *J* 11.1, 11.1, 3.8, C*H*O), 4.40 (1H, br d, *J* 16.4, B of AB_q of $SOCH_2$).Characteristic spectra are in agreement with those reported by O'Sullivan.[15]

(1'S,3S,3aS,7aS)-4',5',7a-Trimethyl-3a,3',4,5,6,6',7,7a-octahydro-*2H*-spiro[benzofuran-3,2'-thiopyran]-2-one 1'-oxide 114

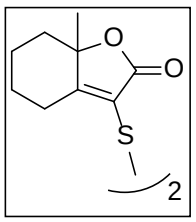


Scheme 137



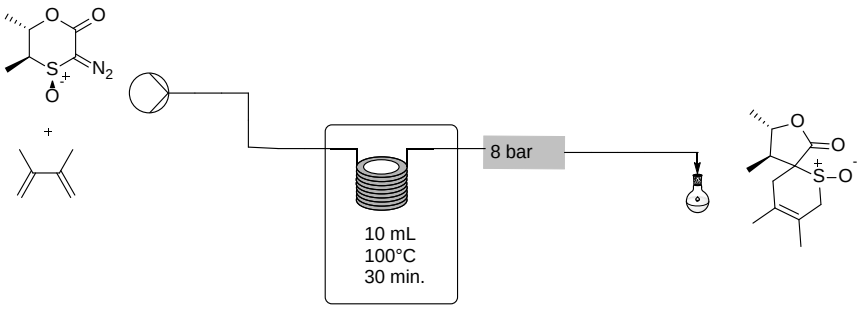
114

The α-diazosulfoxide **76** (0.073 g, 0.32 mmol, 1 eq) was dissolved in the minimum amount of toluene and dichloromethane (1.4 mL, 4 : 1) and 2,3-dimethyl-1,3-butadiene **113** (0.262 g, 3.19 mmol, 10 eq) was added to the solution (0.2 M). This reaction mixture was pumped through a 10 mL reactor coil heated to 120°C at a flow rate of 0.333 mL/min giving a residence time of 30 min. The crude reaction mixture was collected as a pale yellow solution and concentration under reduced pressure gave the crude product as an off white crystalline solid (0.085 g). Analysis of this mixture by ^{1}H NMR spectroscopy showed the presence of **114** and **115** in a ratio of 97 : 3. The crude product was dissolved in dichloromethane and purified by column chromatography on silica gel using gradient hexane-ethyl acetate as eluent, (20:80 – 0:100). The second and major fraction was the cycloadduct **114** (0.055g, 62%). Found C, 63.45; H 7.76; $C_{15}H_{22}O_3S$ requires C, 63.80; H 7.85; ν_{max}(neat/cm^{-1}) 1763, 1048; δ_H (400 MHz) 1.23–2.12 (19H, m containing 4 x CH_2, 1 x CH, bridgehead CH, 3 x CH_3 at 1.59 and br s at 1.78 and 1.81), 2.88 [1H, br d, *J* 18.1, 1 x CH, 1H of C(14)H_2], 3.27 (1H, d, A of ABq, *J* 17.2, $SOCH_2$), 3.55 (1H, br d, B of ABq, *J* 17.1, $SOCH_2$); δ_C (75.5 MHz) 19.6, 20.0, 21.5 (3 x CH_3, methyl groups), 22.9, 23.0, 26.4, 34.2 (4 x CH_2, 4 x cyclohexyl CH_2), 38.9 [CH_2, C(14)H_2], 49.5 [CH_2, SOC(11)H_2], 56.4 (CH), 60.8 (Cq), 85.2 (Cq, bridgehead), 114.9, 124.6 (2 x Cq, C=C), 173.3 (Cq, C=O); m/z (ESI+) 283 [(M+H)$^+$, 100%]. Spectral characteristics are in agreement with those reported by O'Sullivan.[15]

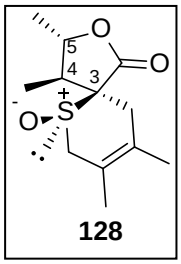


The first fraction consisted of the disulfide **117** (0.010, 16%), as described earlier, and trace amounts of other impurities.

3,4,8,9-Tetramethyl-2-oxa-6-thiaspiro[4.5]dec-8-en-1-one 6-oxide 128 and 129

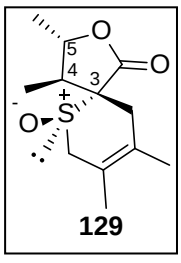


Scheme 138



128

The α-diazosulfoxide **78** (0.112 g, 0.59 mmol, 1 eq) was dissolved in the minimum amount of toluene and dichloromethane (2.5 mL, 4 : 1) and 2,3-dimethyl-1,3-butadiene **113** (0.977 g, 11.9 mmol, 20 eq) was added to the solution (0.2M). This reaction mixture was pumped through a 10 mL reactor coil heated to 120°C at a flow rate of 0.333 mL/min giving a residence time of 30 min. The crude reaction mixture was collected as a pale yellow solution and concentration under reduced pressure gave the crude product as a yellow crystalline solid (0.120 g). Analysis of this crude mixture by ^{1}H NMR spectroscopy showed the presence of a major and minor diastereomer (**128 : 129**, 72 : 28) . The crude product was dissolved in dichloromethane and purified by column chromatography on silica gel using gradient hexane-ethyl acetate as eluent (80 : 20 – 40 : 60). The first least polar fraction (5 mg) contained decomposition products and plasticiser. The second fraction contained the major diastereomer **128** (0.042 g, 30%) and the final fraction contained the major product as well as trace amounts of a second diastereomer (8 : 1, **128 : 129**, 0.042 g, 30%). The second fraction was recrystallised from ether/hexane. **128**; m.p. 189–190 °C, ν_{max}/cm^{-1} (neat) 1750, 1205, 1041; δ_H (400 MHz) 1.39 [3H, d, *J* 7.4, CH_3C(4)], 1.45 [3H, d, *J* 6.8, CH_3C(5)], 1.66 (3H, br s, CH_3), 1.75 (3H, br s, CH_3), 2.23 – 2.50 (3 overlapping signals containing 1H, m, C(4)H, 1H, d, A of ABq, *J* 18.3, allylic CH_2 and 1H, d, B of ABq, *J* 18.5, allylic CH_2), 3.54 (1H, d, *J* 15.4, A of ABq, one of $SOCH_2$), 3.93 (1H, br d, *J* 15.4, B of ABq, one of $SOCH_2$), 4.58 (1H, overlapping dq, *J* 8.8, 6.8, CHO); δ_C (100 MHz) 9.7 [CH_3, C(4)CH_3], 18.98, 19.00, 20.3 (3 × CH_3, methyl



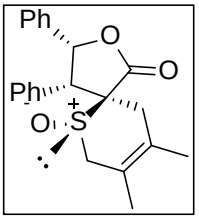
129

groups), 38.6 (CH_2, allylic CH_2), 49.1 (CH, CHC), 50.8 (CH_2, $SOCH_2$), 65.4 (Cq, C_{Spiro}), 80.7 (CH, CHO), 118.4, 126.1 (2 × Cq, C=C), 172.7 (C, C=O); m/z (ESI+) 243 [$(M+H)^+$, 45%], HRMS (ESI+): Exact mass calculated for $C_{12}H_{19}O_3S$ $[M+H]^+$, 243.1055. Found 243.1055. Spectral characteristics are in good agreement with those reported by

Collins.[14] Characteristic peaks of the minor diastereomer **129** are; δ_H (400 MHz) 3.29 (1H, d, *J* 17.3, A of AB_q, one of CH_2), 4.12 – 4.22 (1H, m, CHO), 4.31 (1H, d, *J* 15.7 B of AB_q, one of CH_2).

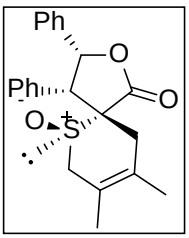
8,9-Dimethyl-3,4-diphenyl-2-oxa-6-thiaspiro[4.5]dec-8-en-1-one 6-oxide 130 and 131

The α-diazosulfoxide **77** (0.062 g, 0.2 mmol, 1 eq) was dissolved in the minimum amount of toluene and dichloromethane (2 mL, 4 : 1) and 2,3-dimethyl-1,3-butadiene (0.326 g, 0.40 mmol, 20 eq) was added to the solution. This reaction mixture was pumped through a 10 mL reactor coil heated to 120°C at a flow rate of 0.333 mL/min giving a residence time of 30 min. The crude reaction mixture was collected as a pale yellow solution and concentration under reduced pressure gave the crude product as a yellow crystalline solid. (0.071 g). Analysis of this crude mixture by ^{1}H NMR spectroscopy showed the presence of 2 diastereomers (~ 1 : 1). The crude product was dissolved in dichloromethane and purified by column chromatography on silica gel (20 % ethyl acetate in hexane, increasing to 100 % ethyl acetate). The first fraction isolated contained two diastereomers in a 1:1 ratio. The cycloadducts were characterised as a mixture (0.043 g, 60%). ν_{max}/cm^{-1} (neat) 1758, 1073; m/z (ESI+) 367 [$(M+H)^+$, 30%], HRMS (ESI+): Exact mass calculated for $C_{22}H_{23}O_3S$ $[M+H]^+$, 367.1362. Found 367.1368.



The distinguishable peaks corresponding to the first diastereomer **130** were δ_H (400 MHz) 1.76, 1.93 (2 x 3H, 2 x br s, 2 x CH_3), 2.57 (1H, d, *J* 17.8, A of ABq, one of allylic CH_2), 2.94 (2H, br s, $SOCH_2$), 3.26–3.46 (1H, m, contains B of ABq of allylic CH_2), 3.76 (1H, d, *J* 5.9, CHC), 5.99 (1H, d, *J* 5.9, CHO), 6.86 – 7.19 (10H, m, aryl rings); δ_C (100 MHz) 19.8, 20.4 (2 x CH_3, methyl groups), 30.2 (CH_2, allylic CH_2), 48.1 (CH_2, $SOCH_2$), 54.9 (CH, C(4)H), 62.6 (Cq, C(3)S), 81.8 (CH, CHO), 116.8, 124.7 (2 x Cq, C=C), 125.5, 127.9, 128.3, 129.8 (4 x CH appear for 6 of CH of aryl rings), 131.5, 134.1 (2 x C, C of aryl rings), 175.0 (C, C=O);

O'Sullivan reports the two CH_3 singlets as being present at 1.63 and 1.92 ppm, however in this work these singlets appear at 1.76 and 1.93 ppm in the ^{1}H NMR spectrum.



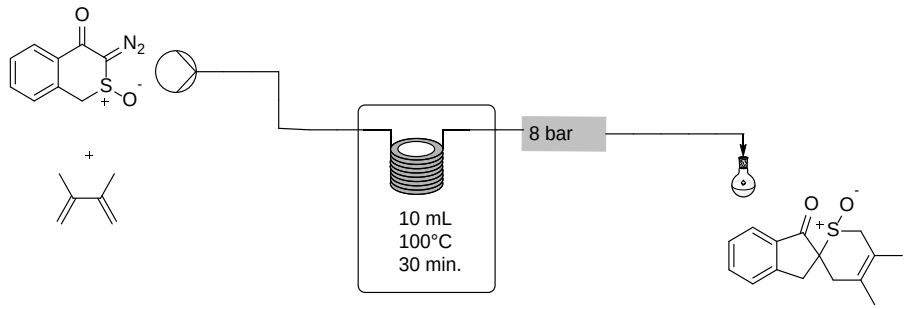
The peaks corresponding to the second diastereomer in the mixture, **131**, were; δ_H (400 MHz) 1.79, 1.82 (2 x 3H, 2 x br s, 2 x CH_3), 2.77 (1H, A of ABq, *J* 17.6, one of allylic CH_2), 3.10 (1H, A of ABq, *J* 18.0, one of $SOCH_2$), 3.26–3.46 (1H, m, contains B of AB_q of allylic CH_2), 3.92 (1H, d, *J* 5.4, CHC), 4.05 (1H, B of ABq, *J* 18.3, one of $SOCH_2$), 6.14 (1H, d, *J* 5.4, CHO), 6.86 – 7.19 (10H, m, aryl rings); δ_C (100 MHz) 19.5, 20.1 (2 x CH_3, 2 x methyl groups), 32.0 (CH_2, allylic CH_2), 49.9 (CH_2, $SOCH_2$), 58.0 (CH, CHC), 64.5 (C, CS), 81.3 (CH, CHO), 117.9, 121.9 (2 x Cq, C=C), 127.6, 128.0, 128.34, 128.4 (4 x CH appearing for 6 of CH of aryl rings), 132.6, 134.7 (2 x Cq, Cq of aryl rings), 171.5 (Cq, C=O).

3.3.3 Thermolysis conditions for Diels-Alder cycloadditions of ketone derived α-oxo sulfines.

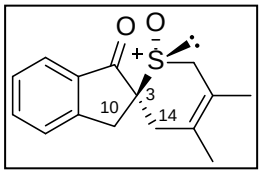
Note: Due to the ketone derived α-diazosulfoxides being insoluble in toluene, acetonitrile was used as the solvent for the thermolysis. Thermogravimetric analysis and melting point data had shown the temperature of rearrangement to be approx. 100°C which is achievable in continuous flow reactors using acetonitrile as the solvent, due to the back pressure imposed.

The signals corresponding to C(14)H_2 and the SOCH_2 protons are consistently broadened across the series due to long range unresolved coupling with the hydrogens of the vinylic methyl groups.

(1'S,2S)-4',5'-Dimethyl-3',6'-dihydrospiro[indene-2,2'-thiopyran]-1(*3H*)-one 1'-oxide 135



Scheme 139

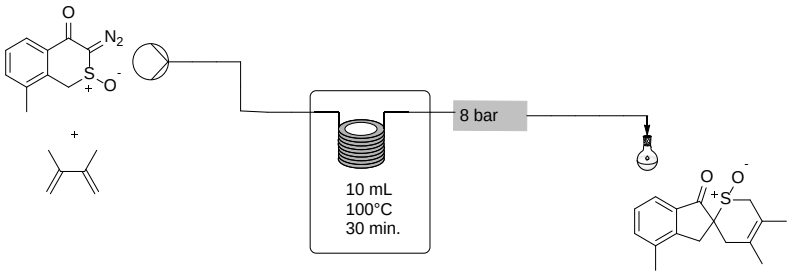


The α-diazosulfoxide **14** (0.166 g, 0.82 mmol, 1 eq) was dissolved in acetonitrile and dichloromethane (4:1, 2 mL). 2,3-dimethyl-1,3-butadiene **113** (1.34 g, 16.41 mmol, 1.86 mL, 20 eq) was added to this solution. The reactor was set to maintain a temperature of 100°C. The solution was pumped through the heated 10 mL reactor coil with a flow rate of 0.33 mL/min providing an overall residence time of 30 min. The crude reaction mixture was collected and concentrated under reduced pressure to give a brown oil containing a major diastereomer **135** and minor diastereomer **136** in a ratio of 95 : 5 (0.188 g). The crude material was purified by column chromatography on silica gel using hexane-ethyl acetate (50 : 50) as eluent giving the pure product **135** as a light brown crystalline solid (0.134 g, 63%). m.p. 131–133 °C, ν_{max} (neat)/cm^{-1} 1705, 1051; δ_H (400 MHz) 1.67 (3H, s, CH_3), 1.73 (3H, s, CH_3), 2.29 [1H, d, *J* 18.3, A of ABq, C(14)H_2], 3.00 [1H, d, *J* 18.3, B of ABq, C(14)H_2], 3.21 [1H, d, *J* 18.0, A of ABq, C(10)H_2], 3.38-3.51 [2H, m, consisting of 1H, d, B of ABq, C(10)H_2, and 1H, d, A of ABq, SOCH_2], 3.72 (1H, d, *J* 17.9, B of ABq, SOCH_2), 7.38-7.48 (2H, m, Aromatic CH), 7.60-7.67 (1H, m, Aromatic CH), 7.79 (1H, d, *J* 7.7, Aromatic CH); δ_C (100 MHz) 19.8 (CH_3), 19.9 (CH_3), 35.2 [CH_2, C(14)H_2], 37.2 [CH_2, C(10)H_2], 50.5 (CH_2, SOCH_2), 63.7

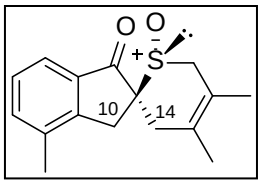
[Cq, C(3)], 117.4 (Cq, C=C), 124.5 (Aromatic CH), 125.9 (Cq, C=C), 126.1, 128.2, 135.6 (3 × Aromatic CH), 136.3 (Aromatic Cq), 150.6 (Aromatic Cq), 201.3 (Cq, C=O); MS (ESI+) 261 [$(M+H)^+$, HRMS (ESI+): Exact mass calculated for $C_{15}H_{17}O_2S$ $[M+H]^+$, 261.0949 Found 261.0943.

The signal observed in the ^1H NMR spectrum of the crude material corresponding to the minor diastereomer **136** is δ_H (400 MHz) 2.78 [1H, d, *J* 18.2, 1H of $C(14)H_2$].

4,4',5'-Trimethyl-3',6'-dihydrospiro[indene-2,2'-thiopyran]-1(*3H*)-one 1'-oxide 133



Scheme 140

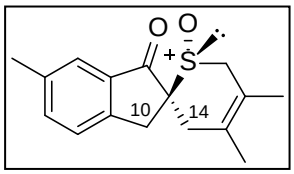


The α-diazosulfoxide **80** (0.234 g, 1.06 mmol, 1 eq) was dissolved in acetonitrile and dichloromethane (2.5 mL, 4 : 1). 2,3-Dimethyl-1,3-butadiene (1.75 g, 21.24 mmol, 20 eq) was added to this solution. The reactor was set to maintain a temperature of 100°C. The solution was pumped through a 10 mL reactor coil heated to 100°C with a flow rate of 0.33 mL/min providing an overall residence time of 30 min. The crude reaction mixture was collected and concentrated under reduced pressure to give a light yellow oil (0.300 g). Analysis of the material by ^1H NMR spectroscopy showed <5% of the diastereomer **134** present. The oil was dissolved in ether and concentrated under reduced pressure to give a pale yellow crystalline solid. This solid was stirred in a 1:1 mixture of diethyl ether and hexane to dissolve trace impurities but not the cycloadduct product. Filtration of the insoluble product led to isolation of the cycloadduct **133** as a white crystalline solid (0.189 g, 64%). Mp 187-189°C; ν_{max}/cm^{-1} (neat) 1708, 1273; δ_H (400 MHz, $CDCl_3$) 1.74 (3H, s, CH_3), 1.81 (3H, s, CH_3), 2.30 [1H, d, *J* 18.4, A of AB_q, $C(14)H_2$], 2.35 (3H, s, $ArCH_3$), 3.03 - 3.10 [overlapping doublets consisting of 1H, d, *J* 18.4, B of AB_q, $C(14)H_2$ and 1H, d, *J* 17.8, A of AB_q $C(10)H_2$], 3.30 [1H, d, *J* 17.8, B of AB_q, $C(10)H_2$], 3.51 (1H, d, *J* 17.0, A of AB_q, $SOCH_2$), 3.75 (1H, d, *J* 17.0, B of AB_q, $SOCH_2$), 7.30-7.34 (1H, m, Aromatic CH), 7.43 (1H, d, *J* 7.3, Aromatic CH), 7.61 (1H, d, *J* 7.6, Aromatic CH); δ_C (100 MHz, $CDCl_3$) 17.8 (CH_3, $ArCH_3$), 19.8, 19.9 (2 x CH_3), 35.3 [CH_2, $C(14)H_2$], 36.1 [CH_2, $C(10)H_2$], 50.5 (CH_2, $SOCH_2$), 63.5 [Cq, C(3)], 117.4 (Cq, C=C), 122.0 (Aromatic CH), 125.9 (Cq, C=C), 128.5 (Aromatic CH), 135.3 (Aromatic Cq), 136.0 (Aromatic Cq), 136.1 (Aromatic CH), 149.5 (Aromatic Cq), 201.5 (Cq, C=O); m/z (ESI+) 275 [$(M+H)^+$, 60%], HRMS (ESI+): Exact mass calculated for $C_{16}H_{19}O_2S$ $[M+H]^+$, 275.1106 Found 275.1100.

The signal observed in the ^{1}H NMR spectrum of the crude material corresponding to the minor diastereomer **134** is δ_H (400 MHz) 2.80 [1H, d, *J* 18.3, 1H of C(14)H_2].

The structure of **133** was determined by single crystal x-ray diffraction on a crystalline sample recrystallized from acetonitrile. Crystal data for: $C_{16}H_{18}O_2S$, *Mr* = 274.36, monoclinic, $P2_1/c$, a = 7.7313(8) Å, b = 10.8286(14) Å, c = 17.607(2) Å, β = 101.601(4)°, *V* = 1443.9(3) Å^3, *Z* = 4, D_c = 1.262 g cm^{-3}, F_{000} = 584, Cu Kα radiation, λ = 0.71073 Å, *T* = 300.(2) K, $2\theta_{max}$ = 25.03°, μ = 0.219 mm^{-1}, 9084 reflections collected, 2524 unique (R_{int} = 0.0354), final GooF = 1.002, R_1 = 0.0421, wR_2 = 0.0967 (1869 obs. data: $I > 2\sigma(I)$); R_1 = 0.0611, wR_2 = 0.1066 (all data).

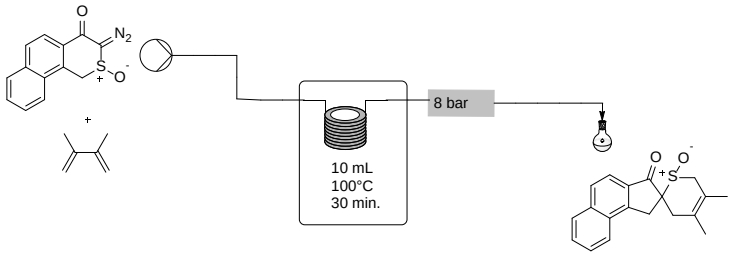
4',5',6-Trimethyl-3',6'-dihydrospiro[indene-2,2'-thiopyran]-1(*3H*)-one 1'-oxide 137



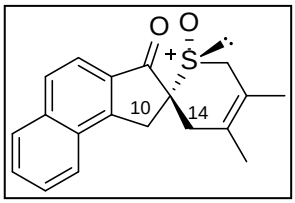
The α-diazosulfoxide **83** (0.200 g, 0.91 mmol, 1 eq) was dissolved in acetonitrile and dichloromethane (2.3 mL, 4 : 1). 2,3-dimethyl-1,3-butadiene **113** (0.75 g, 1.82 mmol, 20 eq) was added to this solution. The reactor was set to maintain a temperature of 100°C. The solution was pumped through a 10 mL reactor coil heated to 100°C with a flow rate of 0.33 mL/min providing an overall residence time of 30 min. The crude reaction mixture was collected and concentrated under reduced pressure to give a red oil (0.284 g). Analysis of the material by ^{1}H NMR spectroscopy showed <5% of the other diastereomer **138** present. The oil was dissolved in the minimum amount of dichloromethane and loaded on to silica to be purified by column chromatography (10% ethyl acetate in hexane increasing to 40% ethyl acetate). The cycloadduct **137** was isolated as a white solid (0.196 g, 78 %). m.p. 139-140 °C; ν_{max} (neat)/cm^{-1} 1704, 1048, 725; δ_H (400 MHz) 1.73 (3H, s, CH_3), 1.79 (3H, s, CH_3), 2.27 [1H, d, *J* 18.2, A of ABq, C(14)H_2], 2.40 (3H, s, ArCH_3), 3.01 [1H, d, *J* 18.0, B of ABq, C(14)H_2], 3.16 [1H, d, *J* 18.0, A of ABq, C(10)H_2], 3.36 [1H, d, *J* 17.7, B of ABq, C(10)H_2], 3.47 (1H, d, *J* 16.8, A of ABq, SOCH_2), 3.70 (1H, d, *J* 16.7, B of ABq, SOCH_2), 7.33 (1H, d, *J* 7.6, Aromatic CH), 7.43-7.46 (1H, m, Aromatic CH), 7.57 (1H, br s, Aromatic CH); δ_C (100 MHz) 19.5 (CH_3), 19.9 (CH_3), 21.1 (ArCH_3), 35.1 [CH_2, C(14)H_2], 36.8 [CH_2, C(10)H_2], 50.5 (CH_2, SOCH_2), 64.0 (Cq, C_{spiro}), 117.2 (Cq, C=C), 124.3 (CH, Aromatic CH), 125.7 (CH, Aromatic CH), 126.0 (Cq, C=C), 136.4 (Cq, Aromatic Cq), 136.9 (CH, Aromatic CH), 138.3 (Cq, Aromatic Cq), 147.9 (Cq, Aromatic Cq), 201.2 (Cq, C=O); HRMS (ESI+): Exact mass calculated for $C_{16}H_{19}O_2S$ [M+H]+, 275.1106. Found 275.1093; m/z (ESI+) 275 [(M+H)+, 40%].

The signal observed in the ^{1}H NMR spectrum of the crude material corresponding to the minor diastereomer **138** is δ_H (400 MHz) 2.78 [1H, d, *J* 18.2, 1H of C(14)H_2].

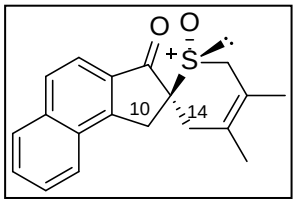
4',5'-Dimethyl-3',6'-dihydrospiro[cyclopenta[a]naphthalene-2,2'-thiopyran]-3(*1H*)-one 1'-oxide 139 and 140.



The α-diazosulfoxide **81** (0.042 g, 0.16 mmol, 1 eq) was dissolved in acetonitrile and dichloromethane (0.5 mL, 4 : 1). 2,3-dimethyl-1,3-butadiene **113** (0.269 g, 3.28 mmol, 0.37 mL, 20 eq) was added to this solution. The continuous flow reactor was set to maintain a temperature of 100°C. The solution was pumped through the heated 10 mL reactor coil with a flow rate of 0.33 mL/min providing an overall residence time of 30 min. The crude reaction mixture was collected and concentrated under reduced pressure to give a brown oil (0.050 g). Analysis by ^{1}H NMR spectroscopy showed there to be a major and minor diastereomer present in a ratio of 73 : 27, **139** and **140** respectively, as well as a significant amount of unidentified decomposition products (~30%). The crude material was purified by column chromatography on silica gel using hexane-ethylacetate as eluent (50 : 50) leading to the elution of two diastereomeric products. The first fraction to elute was the less polar, minor diastereomer **140** as



a brown oily residue (0.010 g, 20%) ν_{max}/cm^{-1} (neat) 1697 (Cq, C=O), 1046 (S-O); δ_H (400 MHz, $CDCl_3$) 1.71 (3H, s, CH_3), 1.82 (3H, s, CH_3), 2.42 [1H, d, *J* 18.4, A of AB_q, C(14)H_2], 2.88 [1H, d, *J* 18.5, B of AB_q, C(14)H_2], 3.33 [1H, d, *J* 17.6, A of AB_q, C(10)H_2], 3.43 (1H, d, *J* 16.4, B of AB_q, $SOCH_2$) 3.75 (1H, d, *J* 17.6 B of AB_q, $SOCH_2$), 4.22 [1H, d, *J* 16.4, B of AB_q, C(10)H_2], 7.64-7.77 (3H, m, 3 x Aromatic CH), 7.83 – 7.85 (1H, d, 1 x Aromatic CH), 7.94 – 7.96 (1H, d, 1 x Aromatic CH), 8.08 – 8.10 (1H, d, 1 x Aromatic CH); δ_C (100 MHz, $CDCl_3$) 19.5 (CH_3), 19.9 (CH_3), 30.1 [CH_2, C(10)H_2], 39.2 [CH_2, C(14)H_2], 52.4 (CH_2, $SOCH_2$), 68.4 (Cq, C_{spiro}), 118.6 (Cq, C=C), 119.7 (Aromatic CH), 124.7 (Aromatic CH), 127.0 (Cq, C=C), 127.4 (Aromatic CH), 129.1 (Aromatic CH), 129.2 (Aromatic Cq), 129.3 (1 x Aromatic CH), 129.9 (Aromatic Cq), 130.0 (Aromatic CH), 133.2 (Aromatic Cq), 137.1 (Aromatic Cq), 154.5 (Aromatic Cq), 202.1 (Cq, C=O). This fraction contained about 15% of the major diastereomer **139**.

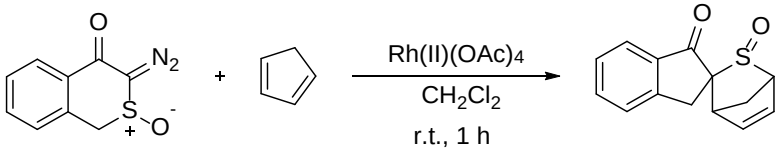


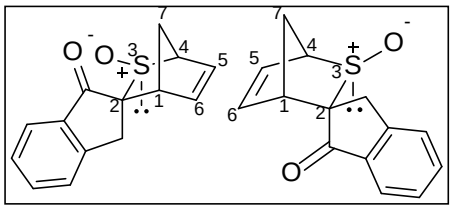
The second fraction was the major, more polar diastereomer **139**, as a yellow oily residue (0.017 g, 34%) ν_{max}/cm^{-1} (neat) 1697 (Cq, C=O), 1046 (S-O).; δ_H (400 MHz, $CDCl_3$) 1.77 (3H, s, CH_3), 1.84 (3H, s, CH_3), 2.39 [1H, d, *J* 18.4, A of AB_q, C(14)H_2], 3.10 [1H, d, *J* 18.4, B of AB_q, C(14)H_2], 3.49 – 3.60 (overlapping doublets, containing 1H, d, *J* 18.0, A of AB_q, C(10)H_2 and 1H, d, *J* 16.8, A of AB_q, $SOCH_2$), 3.70 -3.87 (overlapping doublets containing 1H, d, *J* 18.0, B of AB_q, C(10)H_2 and 1H, d, *J* 16.8, B of AB_q, $SOCH_2$), 7.63-7.76 (3H, m, 3 x Aromatic CH), 7.84 – 7.86 (1H, d, *J* 8.8 Aromatic CH), 7.94 – 8.01 (2H, m, 2 x Aromatic CH); δ_C (100 MHz, $CDCl_3$) 19.9 (CH_3), 20.0 (CH_3), 35.3 [CH_2, C(14)H_2], 35.7 [CH_2, ArC(10)H_2], 50.5 (CH_2, $SOCH_2$), 63.5 (Cq, C_{spiro}), 117.4 (Cq, C=C), 119.7 (Aromatic CH), 124.3 (Aromatic CH), 125.9 (Cq, C=C), 127.4 (Aromatic CH), 129.1 (Aromatic CH), 129.5 (Aromatic CH), 129.7 (Aromatic Cq), 129.8 (Aromatic CH), 133.9 (Aromatic Cq), 136.9 (Aromatic Cq), 152.0 (Aromatic Cq), 201.0 (Cq, C=O); m/z (ESI+) 311 [$(M+H)^+$, 40%], HRMS (ESI+): Exact mass calculated for $C_{19}H_{19}O_2S$ $[M+H]^+$, 311.1106 Found 311.1099. This fraction contained <12% of the minor diastereomer **140**.

3.3.4 Cycloaddition reaction with cyclopentadiene as the diene and α-oxo sulfines as the dieneophiles.

3-Thiaspiro[bicyclo[2.2.1]heptane-2,2'-inden]-5-en-1'(*3'H*)-one 3-oxide

Attempt 1: Generation of the α-oxo sulfine in batch using transition metal catalysis and *in situ* trapping.



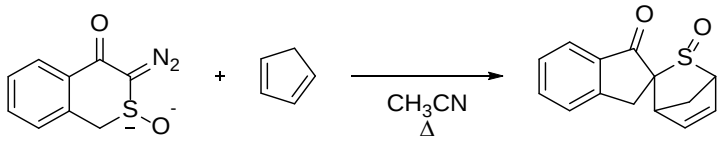


α-Diazosulfoxide **14** (0.072 g, 0.34 mmol, 1 eq) was dissolved in acetonitrile : dichloromethane (4 : 1, 3 mL, 0.1 M). Cyclopentadiene **149** (0.231 g, 3.4 mmol, 10 eq) was added to this solution. Lastly, rhodium acetate dimer (0.001 g, 1 %) was added to the reaction mixture. The reaction mixture was stirred at room temperature for 1 h and then the reaction mixture was concentrated under reduced pressure to give the crude product as a brown solid (0.187 g). Analysis of the crude material by ^{1}H NMR spectroscopy showed complete consumption of the starting material and the presence of two diastereomeric products (**151** : **152/153**, major : minor, 60 : 40) as well as a significant amount of unidentified impurities. The crude mixture was purified by column chromatography on silica gel using hexane-ethyl acetate as eluent (95 : 5) leading to isolation of Diastereomer B **152/153*** (0.018 g, 22%);

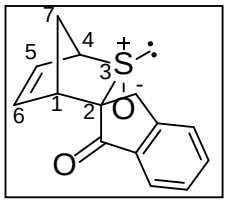
ν_{max}/cm^{-1} (neat) 1686, 1605, 1465; δ_H (400 MHz, $CDCl_3$) 2.41 [1H, dt, *J* 11.0, 2.7, one of C(7)H_2], 3.05 (1H, d, A of AB_q, *J* 17.2, one of $ArCH_2$), 3.28 [1H, s, C(1)H], 3.39 [1H, d, B of AB_q *J* 17.2, one of $ArCH_2$], 3.89 [1H, d, *J* 11.1, one of C(7)H_2], 4.15 [1H, s, C(4)H], 6.17 [1H, dd, *J* 5.7, 3.2, C(6)H], 6.56 [1H, dd, *J* 5.7, 2.9, C(5)H], 7.39 – 7.45 (2H, m, 2 x Aromatic CH), 7.61 (1H, t, *J* 7.5, 1 x Aromatic CH), 7.81 (1H, d, *J* 7.6, 1 x Aromatic CH); δ_C (100 MHz, $CDCl_3$) 38.0 (CH_2, $ArCH_2$), 45.7 [CH_2, C(7)H_2], 48.5 [CH, C(1)H], 70.6 [CH, C(4)H], 75.7 (Cq, C_{spiro}), 124.5, 125.5, 128.3 (3 x Aromatic CH), 130.2 [CH, C(6)H], 135.2 (1 x Aromatic CH), 137.6 (Aromatic Cq), 142.6 [CH, C(5)H], 150.0 (Aromatic Cq), 197.9 (Cq, C=O).

*This sample of the minor diastereomer **152/153** was isolated with some impurities present (< 10 %), full characterisation of a pure sample of the minor diastereomer **152/153** was successfully achieved from ***attempt 4*** for the cycloadditon of cyclopentadiene **149** and the α-diazosulfoxide **14** in continuous flow thermolysis conditions.

Attempt 2*:* Generation of the α-oxo sulfine in batch using thermolysis, and *in situ* trapping, 30 min reaction time.



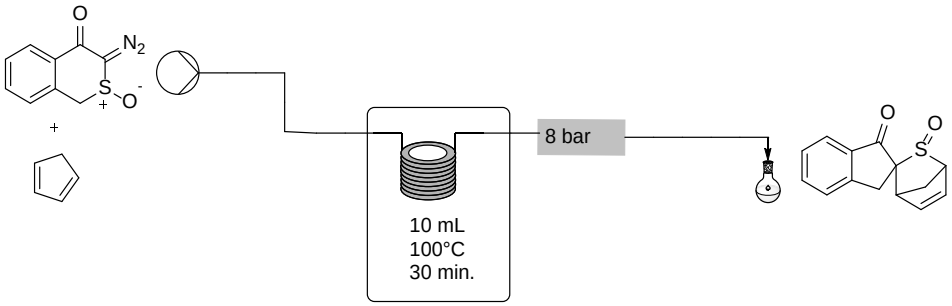
The α-diazosulfoxide **14** (0.075 g, 0.36 mmol, 1 eq) was dissolved in acetonitrile : dichloromethane (4 : 1, 3.5 mL, 0.1 M). Cyclopentadiene **149** (0.240 g, 3.64 mmol, 10 eq) was added to this solution. The reaction mixture was heated under reflux for 30 min. At this point the crude reaction mixture was concentrated under reduced pressure to give the crude product as a brown solid (0.193 g). Analysis of the crude material by ^{1}H NMR spectroscopy showed the clean formation of two diastereomeric products (**151** : **152/153**, A : B, 2 : 1). Purification of the crude reaction mixture by column chromatography on silica gel using hexane-ethyl acetate as eluent (95 : 5) led to the elution of one diastereomer, **151**. The diastereomer A **151** eluted first and was characterised as a white crystalline solid (0.054 g, 63 %).



Diastereomer A **151**; mp 128 – 130°C; ν_{max}/cm^{-1} (neat) 1682, 1604, 1011; δ_H (400 MHz, $CDCl_3$) 2.57 – 2.70 [2H, m, C(7)H_2], 2.99 (1H, d, *J* 17.8, A of AB_q, $ArCH_2$), 3.27 – 3.37 [1H, m, C(1)H], 3.63 (1H, d, *J* 17.8, B of AB_q, $ArCH_2$), 5.83 – 5.84 [2H, m, C(4)H, C(6)H], 6.20 – 6.22 [1H, m, C(5)H], 7.37 – 7.43 (2H, m, 2 x Aromatic CH), 7.55 – 7.59 (1H, m, Aromatic CH), 7.81 – 7.83 (1H, m, Aromatic CH); δ_C (100 MHz, $CDCl_3$) 32.4 (CH_2, $ArCH_2$) 36.0 [CH_2, C(7)H_2], 48.7 [CH, C(1)H], 70.4 (Cq, C_{spiro}), 98.3 [CH, C(4)H], 125.2, 125.7, 128.2 (3 x Aromatic Cq), 129.0 [CH, C(6)H], 134.59 (Aromatic CH), 134.63 (Aromatic Cq), 137.9

[CH, C(5)H], 149.4 (Aromatic Cq), 200.8 (Cq, C=O); m/z (ESI+) 245 [$(M+H)^+$, 20%], HRMS (ESI+): Exact mass calculated for $C_{14}H_{13}O_2S$ $[M+H]^+$, 245.0636, Found 245.0646.

Attempt 3: Generation of the α-oxo sulfine by thermolysis, in continuous flow and subsequent trapping – 30 min residence time.

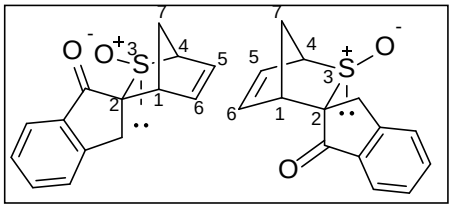


The α-diazosulfoxide **14** (0.114 g, 0.553 mmol, 1 eq) was dissolved in acetonitrile : dichloromethane (8 mL, 4 : 1). Cyclopentadiene **149** (0.365 g, 5.53 mmol, 10 eq) was added to this solution. The reactor was set to maintain a temperature of 100°C. The solution was pumped through a 10 mL reactor coil heated to 100°C with a flow rate of 0.33 mL/min providing an overall residence time of 30 min. The crude reaction mixture was collected and concentrated under reduced pressure to give a brown oil (0.196 g). The crude reaction mixture was purified by column chromatography on silica gel using hexane-ethyl acetate as eluent (95 : 5) leading to isolation of the Diastereomer B **152/153** only (0.024 g, 18%)

Attempt 4*:* Generation of the α-oxo sulfine in continuous flow using thermolysis, and *in situ* trapping. Residence time of 5 min.

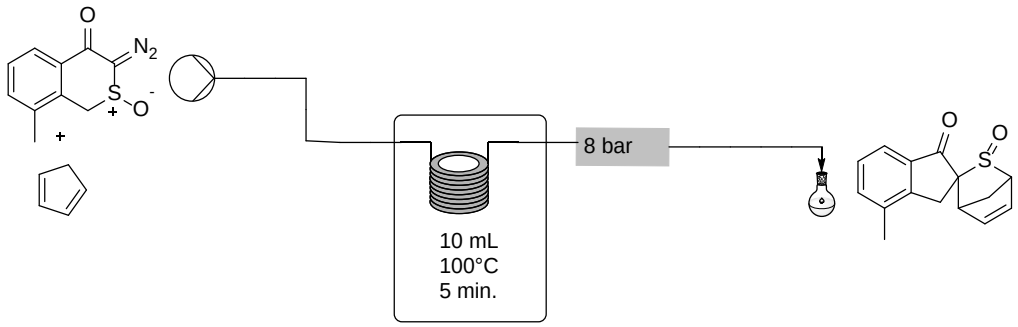
The α-diazosulfoxide **14** (0.105 g, 0.51 mmol, 1 eq) was dissolved in acetonitrile : dichloromethane (5 mL, 4:1). Cyclopentadiene **149** (0.336 g, 5.1 mmol, 10 eq) was added to this solution. The reactor was set to maintain a temperature of 100°C. The solution was pumped through a 10 mL reactor coil heated to 100°C with a flow rate of 2 mL/min providing an overall residence time of 5 min. The crude reaction mixture was collected and concentrated under reduced pressure to give a orange oil (0.120 g) and a mixture of diastereomers (approx. 1 : 1). The crude reaction mixture was purified by column chromatography on silica gel using hexane-ethylacetate (95 : 5) as eluent to elute the Diastereomer B **152/153** as a brown oily residue (0.048 g, 35%).

Diastereomer B **152/153**

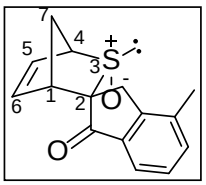


ν_{max}/cm^{-1} (neat) ν_{max}/cm^{-1} (neat) 1686, 1605, 1465; δ_H (400 MHz, $CDCl_3$) 2.41 [1H, dt, *J* 11.0, 2.7, one of C(7)H_2], 3.05 (1H, d, A of AB_q, *J* 17.2, one of ArCH_2), 3.28 [1H, s, C(1)H], 3.39 [1H, d, B of AB_q *J* 17.2, one of ArCH_2], 3.89 [1H, d, *J* 11.1, one of C(7)H_2], 4.15 [1H, s, C(4)H], 6.17 [1H, dd, *J* 5.7, 3.2, C(6)H], 6.56 [1H, dd, *J* 5.7, 2.9, C(5)H], 7.39 – 7.45 (2H, m, 2 x Aromatic CH), 7.61 (1H, t, *J* 7.5, 1 x Aromatic CH), 7.81 (1H, d, *J* 7.6, 1 x Aromatic CH); δ_C (100 MHz, $CDCl_3$) 38.0 (CH_2, ArCH_2), 45.7 [CH_2, C(7)H_2], 48.5 [CH, C(1)H], 70.6 [CH, C(4)H], 75.7 (Cq, C_{spiro}), 124.5, 125.5, 128.3 (3 x Aromatic CH), 130.2 [CH, C(6)H], 135.2 (1 x Aromatic CH), 137.6 (Aromatic Cq), 142.6 [CH, C(5)H], 150.0 (Aromatic Cq), 197.9 (Cq, C=O); m/z (ESI+) 245 [$(M+H)^+$, 40%], HRMS (ESI+): Exact mass calculated for $C_{14}H_{13}O_2S$ $[M+H]^+$, 245.0636 Found 245.0640. This fraction contained about 5% of a trace impurity with a doublet at 3.50 ppm, triplet at 4.0 ppm and a doublet at 4.73 ppm.

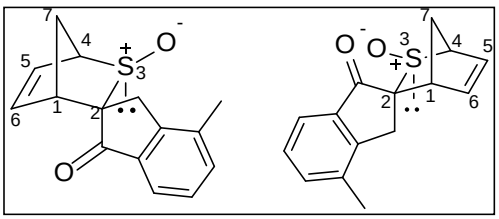
4'-Methyl-3-thiaspiro[bicyclo[2.2.1]heptane-2,2'-inden]-5-en-1'(*3'H*)-one 3-oxide; 154 and 155



The α-diazosulfoxide **80** (0.062 g, 0.28 mmol, 1 eq) was dissolved in acetonitrile : dichloromethane (4 mL, 4 : 1). Cyclopentadiene **149** (0.186 g, 2.8 mmol, 10 eq) was added to this solution. The reactor was set to maintain a temperature of 100°C. The solution was pumped through a 10 mL reactor coil heated to 100°C with a flow rate of 2 mL/min providing an overall residence time of 5 min. The crude reaction mixture was collected and concentrated under reduced pressure to give a yellow oil (0.070 g) and as a mixture of two diastereomers (A : B, 1.2 : 1, **154** : **155**/**156**). The crude reaction mixture was purified by column chromatography on silica gel using hexane-ethyl acetate as eluent (95 : 5) to elute the two diastereomers in two different fractions. The first fraction contained the major product from the crude material, diastereomer A **154** as a brown oily residue (0.010 g, 14%);



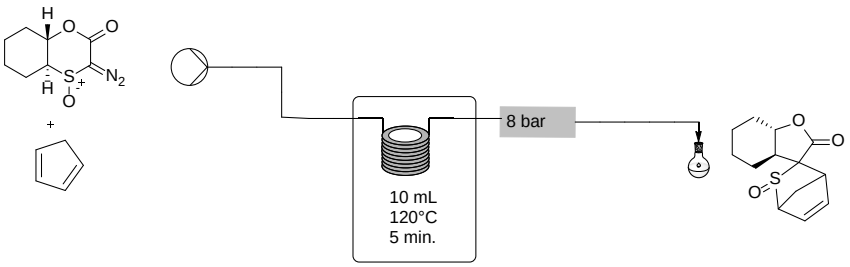
ν_{max}/cm^{-1} (neat) 1680, 1007; δ_H (400 MHz, $CDCl_3$) 2.31 (3H, s, $ArCH_3$), 2.65 – 2.67 [2H, m, C(7)H_2], 2.90 (1H, d, *J* 17.8, A of AB_q, $ArCH_2$), 3.29 – 3.37 [1H, m, C(1)H], 3.47 (1H, d, *J* 17.8, B of AB_q, $ArCH_2$), 5.82 – 5.88 (2H, m, C(4)H and C(6)H], 6.20 – 6.24 [1H, m, C(5)H], 7.33 (1H, t, *J* 7.5, 1 x Aromatic CH), 7.38 (1H, d, *J* 7.4 1 x Aromatic CH), 7.66 (1H, d, *J* 7.5, 1 x Aromatic CH); δ_C (100 MHz, $CDCl_3$) 17.8 (CH_3, $ArCH_3$), 31.3 (CH_2, $ArCH_2$), 36.0 [CH_2, C(7)H_2], 48.9 [CH, C(1)H], 70.2 (Cq, C_{spiro}), 98.3 [CH, C(4)H], 122.6, 128.4 (2 x Aromatic Cq), 129.1 [CH, C(6)H], 134.4, 134.9 (2 x Aromatic Cq), 135.2 (1 x Aromatic CH), 137.9 [CH, C(5)H] 148.3 (Aromatic Cq), 201.2 (Cq, C=O); m/z (ESI+) 259 [$(M+H)^+$, 20%]. HRMS (ESI+): Exact mass calculated for $C_{15}H_{15}O_2S$ $[M+H]^+$, 259.0793 Found 259.0788.



This was followed by elution of the diastereomer B **155/156** as a brown oily residue; (0.018 g, 25%). ν_{max} (cm^{-1}) 1699, 1051; δ_H (400 MHz, $CDCl_3$) 2.33 (3H, s, $ArCH_3$), 2.41 [1H, dt, *J* 11.0, 2.2, one of C(7)H_2] 2.88 (1H, d, *J* 17.6, A of AB_q, ArCH_2), 3.27 – 3.38 [2H, m, containing 1 H, *J* 17.6, B of AB*q* of $ArCH_2$ and 1H, br s, C(1)H], 3.71 [1H, d, *J* 11.0, one of C(7)H_2], 4.16 [1H, br s, C(4)H] 6.18 [1H, dd, *J* 5.6, 2.3, 1H of C(6)H], 6.58 [1H, dd, *J* 5.7, 2.9, 1H of C(5)H], 7.30 – 7.34 (1H, m, 1 x Aromatic CH), 7.42 (1H, d, *J* 7.4, 1 x Aromatic CH), 7.75 (1H, d, *J* 7.7, 1 x Aromatic CH); δ_C (100 MHz, $CDCl_3$) 17.8 (CH_3, $ArCH_3$), 36.9 (CH_2, $ArCH_2$), 45.8 [CH_2, C(7)H_2], 48.6 [CH, C(1)H], 70.6 [CH, C(4)H], 75.4 (Cq, C_{spiro}), 121.9, 128.5 (2 x Aromatic CH), 130.3 [CH, C(6)H], 135.2 (Aromatic Cq), 135.6 (Aromatic CH), 137.4 (Aromatic Cq), 142.6 [(CH, C(5)H] 149.0 (Aromatic Cq), 198.1 (Cq, C=O); m/z (ESI+) 259 [$(M+H)^+$, 100%]; HRMS (ESI+): Exact mass calculated for $C_{15}H_{15}O_2S$ $[M+H]^+$, 259.0793 Found 259.0782.

3.3.5 Cycloaddition of lactone derived α-diazosulfoxide 38,39 with cyclopentadiene 149 in continuous flow.

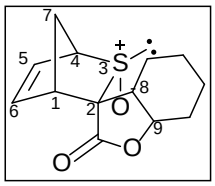
Lactone derived cycloadducts 158 and **161**



The α-diazosulfoxides **38,39** (1 : 0.7, 0.076 g, 0.35 mmol, 1 eq) were dissolved in toluene : dichloromethane (2 mL, 4 : 1, 0.15 M). Cyclopentadiene **149** (0.231 g, 2.8 mmol, 10 eq) was added to this solution. The reactor was set to maintain a temperature of 120°C. The solution was pumped

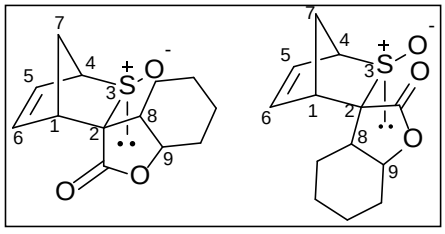
through a 10 mL reactor coil heated to 120°C with a flow rate of 2 mL/min providing an overall residence time of 5 min. The crude reaction mixture was collected and concentrated under reduced pressure to give a brown oil (0.147 g). Analysis of the crude reaction mixture showed the presence of unreacted axial α-diazosulfoxide starting material, and diastereomers A and B (38 : 30 : 32). The crude reaction mixture was purified by column chromatography on silica gel using hexane-ethyl acetate (95:5) as eluent to elute diastereomers A and B in two different fractions. The first fraction contained the Diastereomer A **158** and the second fraction contained Diastereomer B **161**/**162**.

Diastereomer A **158**:



Colorless oily residue; (0.017 g, 19%); ν_{max}/cm^{-1} (neat) 2931, 1739, 1025; δ_H (400 MHz, $CDCl_3$) 1.19 – 1.60 (3H, m, 1 x cyclohexyl CH_2, 1 x cyclohexyl CH), 1.80–2.10 (3H, m, 1 x cyclohexyl CH_2, 1 x cyclohexyl CH), 2.24 – 2.35 [3H, overlapping multiplet including td corresponding to C(8)H, and 1 x cyclohexyl CH_2], 2.48 – 2.55 [1H, dd, *J* 18.0, 2.1, A of AB_q, C(7)H_2], 2.61 – 2.66 [1H, d, *J* 18.0, B of AB_q, C(7)H_2], 3.38 – 3.43 [1H, unsymmetrical m, C(1)H], 3.81 [1H, t of d, *J* 3.7, 10.9, C(9)HO], 5.72 – 5.77 [2H, m, C(6)H and C(4)H], 6.11 – 6.13 [1H, m, C(5)H]; δ_C(100 MHz, $CDCl_3$) 23.6, 25.5, 27.5, 30.7 (4 x cyclohexyl CH_2), 33.5 [CH_2, C(7)H_2], 49.5 [CH, C(8)HC], 50.4 [CH, C(1)H], 69.1 (Cq, C_{spiro}), 83.5 [CH, C(9)HO], 97.8 [CH, C(4)H], 129.1 [CH, C(6)H], 137.5 [CH, C(5)H], 175.8 (Cq, C=O); m/z (ESI+) 253 [$(M+H)^+$, 20%], HRMS (ESI+): Exact mass calculated for $C_{13}H_{17}O_3S$ $[M+H]^+$, 253.0898 Found 253.0894. Trace amounts of impurities (approx. 5 %) recorded in the ^{1}H NMR spectra include a symmetrical quartet at 4.64 ppm and two broad singlets at 6.83 and 6.91 ppm respectively.

Diastereomer B **161**/**162** :

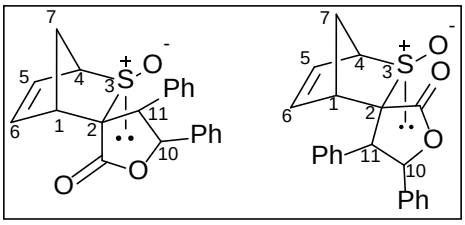


Brown oily residue (0.021 g, 24%); ν_{max}/cm^{-1} (neat) 1766, 1195, 1018; δ_H (400 MHz, $CDCl_3$) 1.01- 2.38 [overlapping signals containing 2 x cyclohexyl CH_2, 3 x cyclohexyl CH, 1 x C(8)H, appears as td, *J* 3.1, 12.7, 1H of C(7)H_2], 3.24 [1H, s, C(1)H], 3.51 [1H, d, *J* 11.11, one of C(7)H_2], 4.22 [1H, s, C(4)H], 4.26 [1H, t of d, *J* 10.8, 3.9, C(9)HO], 5.99 – 6.02 [1H, dd, *J* 5.7, 3.4, C(6)H], 6.46 – 6.48 [1H, dd, *J* 5.7, 3.0, C(5)H]; δ_C (100 MHz, $CDCl_3$) 23.6, 25.2, 28.5, 30.1 (CH_2, 4 x cyclohexyl CH_2), 45.5 [CH_2, C(7)H_2], 48.9 [CH, C(1)H], 51.6 [CH, C(8)H], 69.0 [CH, C(4)H], 81.7 [CH, C(9)HO], 129.0 [CH, C(6)H], 142.3 [CH, C(5)H], 171.0 (Cq, C=O); m/z (ESI+) 253 [$(M+H)^+$, 100%], Exact mass calculated for $C_{13}H_{17}O_3S$ $[M+H]^+$, 253.0898 Found 253.0890.

Note: In the ^{13}C NMR spectrum the spiro centre was not observed, but may be present under the $CDCl_3$ signal.

This fraction contains peaks corresponding to unknown impurities (<5%) which are observed in the ^{1}H NMR spectrum at δ_H 2.75 (td), 3.72 (td), 4.9 (br s), 5.3 (br s). In the ^{13}C NMR spectra, the corresponding signals are observed at δ_C 22.9, 24.0, 24.8, 31.9, 57.8, 59.1, 72.0, 73.5.

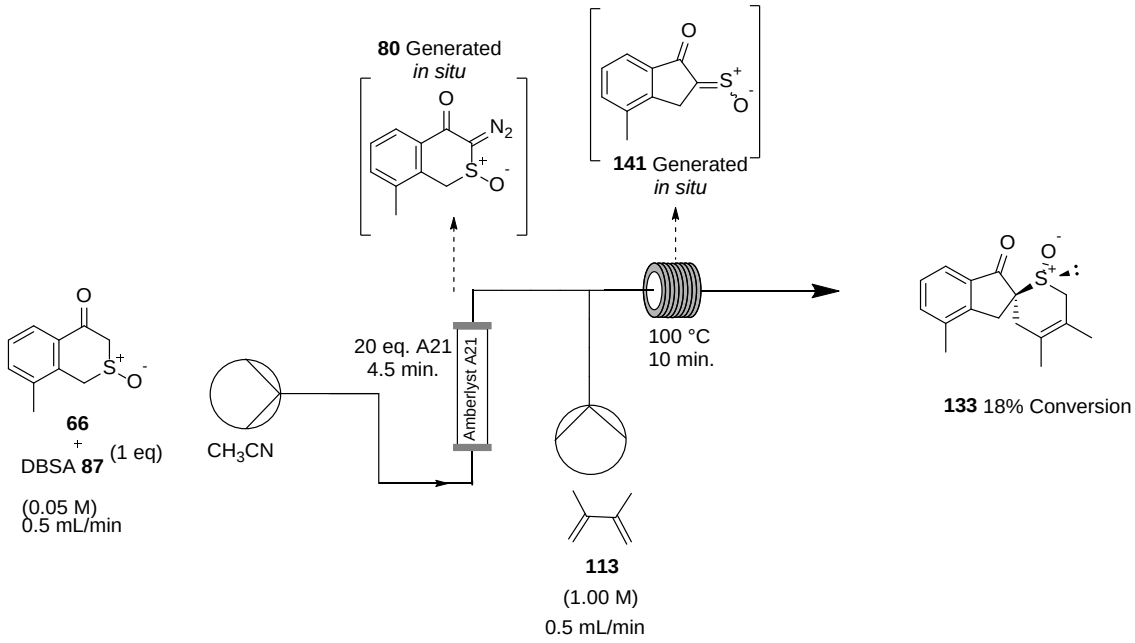
Lactone derived cycloadducts 159/160



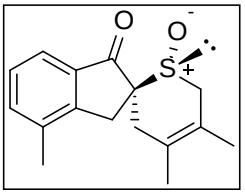
The α-diazosulfoxide **77** (0.072 g, 0.23 mmol, 1 eq) was dissolved in toluene : dichloromethane (2 mL, 4:1, 0.12 M). Cyclopentadiene (0.152 g, 2.3 mmol, 10 eq) was added to this solution. The reactor was set to maintain a temperature of 120°C. The solution was pumped through a 10 mL reactor coil heated to 120°C with a flow rate of 2 mL/min providing an overall residence time of 5 min. The crude reaction mixture was collected and concentrated under reduced pressure to give a yellow oil (0.094 g). Analysis of the crude reaction mixture showed the presence of unreacted starting material **77** and a mixture of a diastereomer A **157** and diastereomer B **159/160** (70 : 15 : 15). The crude reaction mixture was purified by column chromatography on silica gel using hexane-ethyl acetate as eluent (95 : 5) to elute two fractions. The first fraction isolated contained residual starting material only. The second fraction contained the diastereomer B **159/160** as a white crystalline solid (0.009 g, 11%). Mp 109-111°C; ν_{max}/cm^{-1} (neat) 1049, 1752; δ_H (400 MHz, $CDCl_3$) 2.34 [1H, dt, *J* 11.2, 2.7, 2.0, one of C(7)H_2], 3.53 [1H, s, C(1)H], 3.62 [1H, d, *J* 11.2, one of C(7)H_2], 3.84 [1H, d, *J* 7.0, C(11)H], 4.09 [1H, s, C(4)H], 5.78 [1H, dd, *J* 5.8, 3.2, C(6)H], 5.88 [1H, d, *J* 7.2, C(10)HO], 6.24 [1H, dd, *J* 5.7, 2.9, C(5)H], 7.02 – 7.40 (10H, m, 10 x Aromatic CH; δ_C (100 MHz, $CDCl_3$), 44.4 [CH_2, C(7)H_2], 50.4 [CH, C(1)H], 58.2 [CH, C(4)H], 68.9 [CH, C(11)H], 72.8 (Cq, C_{spiro}), 81.3 [CH, C(10)HO], 125.6, 126.2, 127.8, 128.0, 128.3, 128.5 (6 x Aromatic CH), 129.8 [CH, C(6)H], 135.0, 135.4 (2 x Aromatic Cq), 141.5 [CH, C(5)H] 171.0 (Cq, C=O); m/z (ESI+) 351 [$(M+H)^+$, 10%], HRMS (ESI+): Exact mass calculated for $C_{21}H_{17}O_3S$ $[M+H]^+$, 349.0898 Found 349.0899. Minor signals in the ^{1}H NMR spectrum belonging to an unknown impurity (<5%) are present at δ_H 4.97 (br s), 5.25 (br s), 6.75 (br s).

3.4 Telescoping the diazo transfer process, with the hetero-Wolff rearrangement and subsequent Diels-Alder cycloaddition reaction.

Method 1: Telecoping diazo transfer and cycloaddition using 1 equivalent of the diazo transfer reagent.

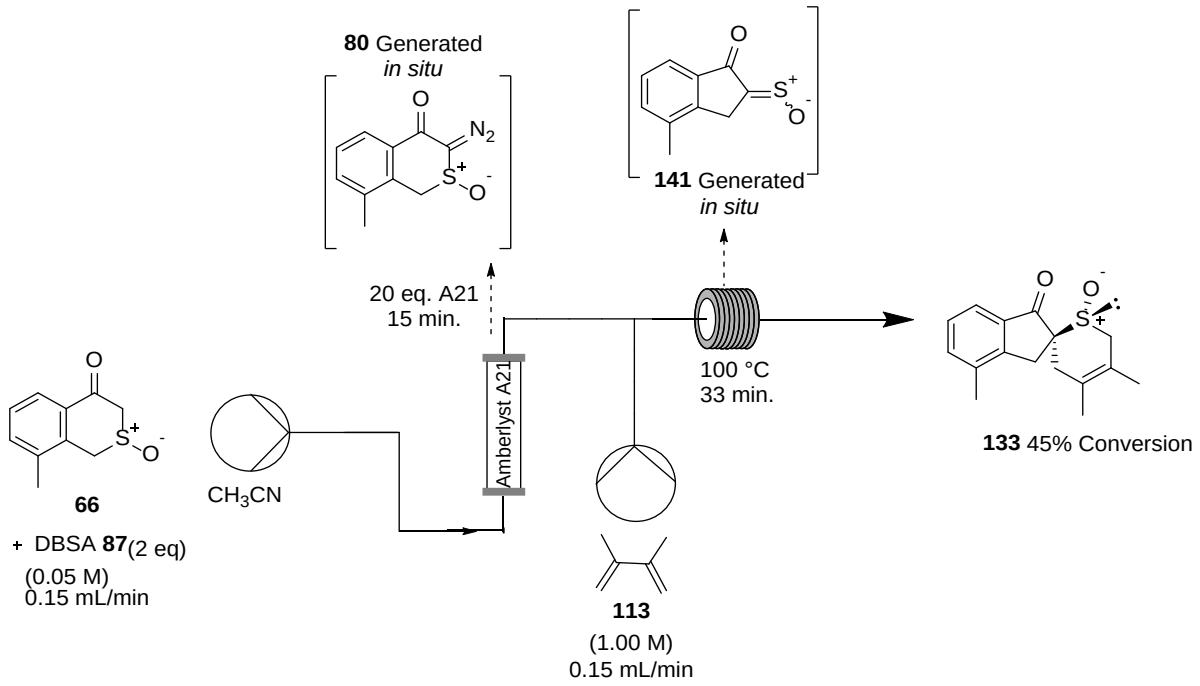


Scheme 141

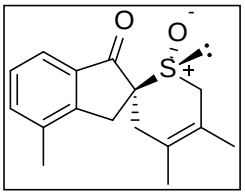


The sulfoxide **66** (0.150 g, 0.77 mmol, 1 eq) and DBSA **87** (0.271 g, 0.77 mmol, 1 eq) were dissolved in acetonitrile (15 mL) to generate a 0.05 M solution of both the sulfoxide **66** and DBSA **87**, and pumped through a 6.6 mm internal diameter Omnifit™ column packed with Amberlyst A21 (2.14 g, 20 eq, vol 2.3 mL) at a rate of 0.5 mL/min with a residence time of 4.5 min. The outlet was pumped to a T-piece where it met the 2,3-dimethyl-1,3-butadiene **113** solution (1.64 g in 20 mL dichloromethane, 1.0 M) pumped at 0.5 mL/min. The solution of α-diazosulfoxide **80** and 2,3-dimethyl-1,3-butadiene **113** was pumped through a 10 mL reactor coil with a residence time of 10 min. The reaction mixture was collected and concentrated under reduced pressure to give the crude product as a pale yellow soild (0.427 g). Analysis of the material by ^{1}H NMR spectroscopy showed the sulfoxide **66** starting material (82%), alongside the desired cycloadduct **133** (18%), residual DBSA **87**, and the sulfonamide byproduct **88**. The crude material was not purified by column chromatography due to the low conversion.

Method 2: Telecoping diazo transfer and cycloaddition using 2 equivalents of the diazo transfer reagent.

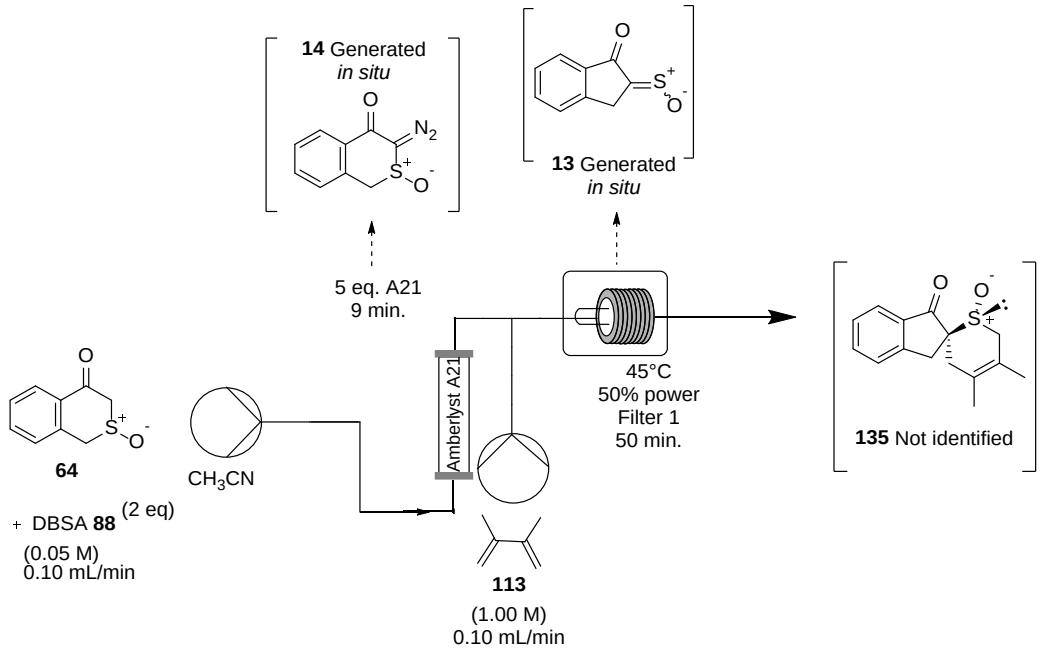


Scheme 142



The sulfoxide **66** (0.150 g, 0.77 mmol, 1 eq) and DBSA **87** (0.542 g, 1.54 mmol, 2 eq) were dissolved in acetonitrile (15 mL) generating a 0.05 M solution of the sulfoxide **66** and 0.1 M solution of DBSA **87**. 10 mL of this solution was pumped through a 6.6 mm internal diameter Omnifit™ column packed with Amberlyst A21 (2.14 g, 20 eq, vol 2.3 mL) at a rate of 0.15 mL/min with a residence time of 15 min. The outlet was pumped to a T-piece where it met the 2,3-dimethyl-1,3-butadiene solution **113** (1.64 g of 2,3-dimethyl-1,3-butadiene in dichloromethane 20 mL, 1.0 M) pumped at 0.15 mL/min. The solution of α-diazosulfoxide **80** and 2,3-dimethyl-1,3-butadiene **113** was pumped through a 10 mL coil with a residence time of 33 min. The reaction mixture was collected and concentrated under reduced pressure to give the crude product as a yellow oil (0.746 g). Analysis of the material by ^{1}H NMR spectroscopy showed the sulfoxide **66** starting material (55%) alongside the desired *in situ* trapped cycloadduct **133** (45%) and the DBSA **87** and sulfonamide byproduct **88**. The crude material was not purified by column chromatography. Spectral details for the cycloadduct are as described in section 3.3.3.

Method 3: Diazo transfer and hetero-Wolff rearrangement promoted by UV light.



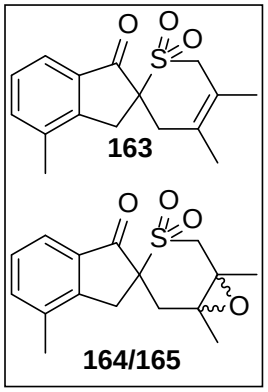
Scheme 143

The sulfoxide **64** (0.105 g, 0.51 mmol, 1 eq) and DBSA **87** (0.358 g, 1.02 mmol, 2 eq) were dissolved in acetonitrile (10 mL, 0.05 M). 8 mL of this solution was pumped through a 6.6 mm internal diameter Omnifit™ column packed with Amberlyst A21 (0.531 g, 5 eq) and acid washed sand at a rate of 0.10 mL/min with a residence time of 9 min on the Amberlyst A21. The outlet was pumped to a T-piece where it met the 2,3-dimethyl-1,3-butadiene solution **113** (1.09 g of 2,3-dimethyl-1,3-butadiene in dichloromethane 14 mL, 1.0 M) pumped at 0.10 mL/min. The solution of α-diazosulfoxide **80** and 2,3-dimethyl-1,3-butadiene **113** was pumped with a residence time of 50 min in the UV-150 reactor (Filter number 1). The reaction mixture was collected and concentrated under reduced pressure to give the crude product as a brown oil (0.316 g). Analysis of the material by ^{1}H NMR spectroscopy showed a complex mixture of unidentifiable products with no evidence of the α-diazosulfoxide **14** or subsequent photolysis induced rearrangement products as reported by Buckley.[16] The crude material was not purified by column chromatography.

3.5 Further fuctionalisation of Diels-Alder sulfoxide cycloadducts.

3.5.1 Oxidation to sulfone

4, 4', 5'-Trimethyl-3', 6'-dihydrospiro[indene-2, 2'-thiopyran]-1(*3H*)-one 1', 1'-dioxide 163

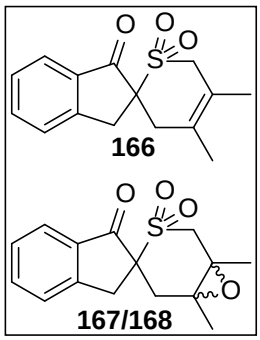


The sulfoxide **133** (0.050 g, 1 eq, 0.018 mmol, 1 eq) was dissolved in dichloromethane (3 mL) and cooled to 0°C with an ice bath. 3-Chloroperoxybenzoic acid (0.051 g, 1.5 eq, 0.29 mmol, 77%) was dissolved in dichloromethane (2 mL) and added dropwise to the stirring reaction mixture over 10 min. The ice bath was removed and the reaction mixture returned to room temperature, and stirred at that temperature for a further 3 h until TLC analysis showed consumption of the starting material. The reaction mixture was concentrated under reduced pressure to give a white crystalline solid (0.093 g). The ^{1}H NMR spectrum of the crude material showed the sulfone **163**, a major β-epoxy sulfone **164**, and a minor β-epoxy sulfone **165** in a ratio of 84 : 12 : 4 as well as the *m*-chlorobenzoic acid byproduct. Purification by column chromatography on silica gel using hexane-ethyl acetate (90 : 10) as eluent led to isolation of the β-keto sulfone **163**, as a white crystalline solid (0.042 g, 75%). ν_{max}/cm^{-1} (neat) 1707, 1273, 1117 cm^{-1}; Mp 187 – 188°C ; δ_H (400 MHz, $CDCl_3$) 1.71, 1.82 (2 x 3H, s, 2 x CH_3), 2.38 (CH_3, s, $ArCH_3$), 2.72 (1H, d, *J* 17.9, A of AB_q, $CqCH_2$), 2.90 – 2.92 (2 overlapping doublets including 1H, d, *J* 18.1, A of AB_q, $ArCH_2$ and 1H, d, *J* 17.9, B of AB_q, $CqCH_2$), 3.45 (1H, d, *J* 16.7, A of AB_q, SO_2CH_2), 3.95 (1H, d, *J* 18.1, B of AB_q, $ArCH_2$), 4.17 (1H, br d, *J* 16.7, B of AB_q, SO_2CH_2), 7.34 (1H, t, *J* 7.5, Aromatic CH), 7.46 (1H, d, *J* 7.3, Aromatic CH), 7.61 (1H, d, *J* 7.6, Aromatic CH); δ_C (100 MHz, $CDCl_3$) 17.8 (CH_3, $ArCH_3$), 19.3, 20.2 (2 x CH_3), 33.1 (CH_2, $ArCH_2$), 42.3 (CH_2, $CqCH_2$), 52.2 (CH_2, SO_2CH_2), 67.7 (Cq, C_{spiro}), 120.2 (Cq, C=C), 122.6 (CH, 1 x Aromatic CH), 124.2 (Cq, C=C), 128.7 (CH, 1 x Aromatic CH), 134.7, 135.7 (Cq, 2 x Aromatic Cq), 136.6 (CH, 1 x Aromatic CH), 149.8 (Cq, 1 x Aromatic Cq), 198.1 (Cq, C=O). m/z (ESI+) 291 [$(M+H)^+$, 100%], HRMS (ESI+): Exact mass calculated for $C_{16}H_{19}O_3S$ $[M+H]^+$, 291.1055. Found 291.1052.

Signals in the ^{1}H NMR of the crude material corresponding to the β-epoxy sulfone **164** include; 1.43, 1.56 (2 x 3H, 2 x s, 2 x CH_3), 3.04 (1H, d, *J* 18.3), 3.28 (1H, d, *J* 15.5), 3.54 (1H, d, *J* 14.8), 3.70 (1H, d, *J* 12.6), 3.74 (1H, d, *J* 15.4). Signals in the ^{1}H NMR of the crude material corresponding to the β-epoxy sulfone **165** include; 1.40, 1.55 (2 x 3H, 2 x s, 2 x CH_3)

In later work, section 3.5.2, an authentic sample of β-epoxy sulfones **167** and **168** were synthesised and isolated and have spectroscopic characteristics similar to **164**.

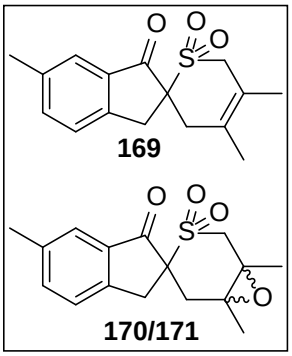
4', 5'-Dimethyl-3', 6'-dihydrospiro[indene-2, 2'-thiopyran]-1(*3H*)-one 1', 1'-dioxide 166



The sulfoxide **135** (0.083 g, 1 eq, 0.04 mmol, 1 eq) was dissolved in dichloromethane (3 mL) and cooled to 0°C with an ice bath. 3-Chloroperoxybenzoic acid (0.106 g, 1.5 eq, 0.61 mmol, 77%) was dissolved in dichloromethane (2 mL) and added dropwise to the stirring reaction mixture over 10 min. The ice bath was removed and the reaction mixture returned to room temperature, and stirred at that temperature for a further 3 h until TLC analysis showed consumption of the starting material. The reaction mixture was concentrated under reduced pressure to give a reddish/brown crystalline solid (0.093 g). The ^{1}H NMR spectrum of the crude material showed clean reaction to form the sulfone **166**, and the β-epoxy sulfones **167** and **168** in a ratio of 84 : 10 : 6, as well as the *m*-chlorobenzoic acid byproduct.* Purification by column chromatography on silica gel using hexane-ethyl acetate (90:10) as eluent led to isolation of the β-keto sulfone **166** (with trace amounts of an unknown impurity, ~5%) as a white crystalline solid (0.063 g, 72%). Mp 108 – 110°C; ν_{max}/cm^{-1} (neat) 1712, 1306, 1117 cm^{-1}; δ_H (400 MHz, $CDCl_3$) 1.64, 1.73 (2 x 3H, s, 2 x CH_3), 2.67 (1H, d, *J* 17.3, A of AB_q, $CqCH_2$), 2.82 (1H, d, *J* 17.3, B of AB_q, $CqCH_2$), 2.96 (1H, d, *J* 18.0, A of AB_q, $ArCH_2$), 3.38 (1H, d, *J* 16.8, A of AB_q, SO_2CH_2), 3.91 – 4.12 (2 overlapping signals including a 1H, d, *J* 17.9, B of AB_q, SO_2CH_2 and a 1H, d, *J* 17.1, B of AB_q, $ArCH_2$), 7.34 – 7.36 (1H, m, 1 x Aromatic CH), 7.43 (H, d, *J* 7.7, Aromatic CH), 7.59 (1H, t, 1 x Aromatic CH), 7.70 (1H, d, *J* 7.7, 1 x Aromatic CH);** δ_C (100 MHz, $CDCl_3$) 19.3, 20.1 (2 x CH_3), 34.1 (CH_2, $ArCH_2$), 42.1 (CH_2, Cq-CH_2), 52.2 (CH_2, SO_2CH_2), 67.8 (Cq, C_{spiro}), 120.1 (Cq, C=C), 124.2 (Cq, C=C), 125.2 (CH, 1 x Aromatic CH), 126.3 (CH, 1 x Aromatic CH), 128.4 (CH, 1 x Aromatic CH), 134.9 (Cq, 1 x Aromatic Cq), 136.1 (CH, 1 x Aromatic CH), 150.8 (Cq, 1 x Aromatic Cq), 197.8 (Cq, C=O); HRMS (ESI+): Exact mass calculated for $C_{15}H_{17}O_3S$ $[M+H]^+$, 277.0898. Found 277.0894.

*Characteristic signals of the β-epoxy sulfone **167** in the ^{1}H NMR spectrum of the crude material are 2 x CH_3 singlets at 1.44,and 1.54 ppm and signals corresponding to β-epoxy sulfone **168** in the ^{1}H NMR spectrum of the crude material include 2 x CH_3 singlets at 1.40 and 1.55 ppm. **Signals corresponding to an unidentified impurity were recorded in the ^{1}H NMR spectrum as a doublet at 3.76 ppm and a singlet at 4.45 ppm and in the ^{13}C NMR spectrum at 53.4, 54.4 and 59.5 ppm.

4', 5', 6-Trimethyl-3', 6'-dihydrospiro[indene-2,2'-thiopyran]-1(*3H*)-one 1', 1'-dioxide 169



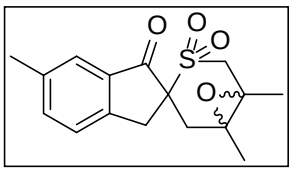
The sulfoxide **137** (0.275 g, 1 eq, 1.00 mmol, 1 eq) was dissolved in dichloromethane (10 mL) and cooled to 0°C with an ice bath. 3-Chloroperoxybenzoic acid (0.259 g, 1.50 mmol, 1.5 eq, 77%) was dissolved in dichloromethane (5 mL) and added dropwise to the reaction mixture over 15 min. The ice bath was removed and the reaction mixture returned to room temperature, and stirred overnight. The reaction mixture was concentrated under reduced pressure to give a pale yellow crystalline solid (0.485 g). The ^{1}H NMR of the crude material showed formation of the desired sulfone **169**, as well as the over oxidation product the β-epoxy sulfone (**169** : **170** : **171**, 52 : 37 :11, sulfone : major β-epoxy sulfone : minor β-epoxy sulfone) as well as the 3-chloroperoxybenzoic acid byproduct. Mass spec. analysis on the crude material identified the presence of:

(1) the sulfone **169**; m/z (ESI+) 291 [$(M+H)^+$, 70%], HRMS (ESI+): Exact mass calculated for $C_{16}H_{19}O_3S$ $[M+H]^+$, 291.1055. Found 291.1052 and

(2) the β-epoxy sulfones **170** and **171**; m/z (ESI+) 307 [$(M+H)^+$, 100%], HRMS (ESI+): Exact mass calculated for $C_{16}H_{19}O_4S$ $[M+H]^+$, 307.1004 Found 307.1001.

Purification of the crude material by column chromatography on silica gel using hexane-ethyl acetate (50 : 50) as eluent led to isolation of the β-keto sulfone **169** as a white crystalline solid in the first fraction (0.140 g, 48%). ν_{max}/cm^{-1} (neat) 1709, 1306, 1281, 1119, cm^{-1}; Mp 128 – 130 °C; δ_H (400 MHz, $CDCl_3$) 1.70, 1.80 (3H, s, 2 x CH_3), 2.40 (3H, s, $ArCH_3$), 2.72 (1H, d, *J* 17.9, A of AB_q, $CqCH_2$), 2.88 (1H, d, *J* 17.9, B of AB_q, $CqCH_2$), 2.97 (1H, d, *J* 18.0, A of AB_q, of $ArCH_2$), 3.44 (1H, d, *J* 17.0, A of AB_q, SO_2CH_2), 4.02 (1H, d, *J* 18.0, B of AB_q, $ArCH_2$), 4.12 (1H, br d, *J* 17.0, B of AB_q, SO_2CH_2), 7.35 (1H, d, *J* 7.9, 1 x Aromatic CH), 7.48 (1H, d, *J* 7.9, 1 x Aromatic CH), 7.56 (1H, s, 1 x Aromatic CH); δ_C (75.5 MHz, $CDCl_3$) 19.3, 20.2, 21.1 (3 x CH_3), 33.8 (CH_2, $ArCH_2$), 42.1 (CH_2, $CqCH_2$), 52.2 (CH_2, SO_2CH_2), 68.2 (Cq, C_{spiro}), 120.1 (Cq, C=C), 124.3 (Cq, C=C), 125.0 (CH, 1 x Aromatic CH), 125.9 (CH, 1 x Aromatic CH), 135.1 (Cq, 1 x Aromatic Cq), 137.4 (CH, 1 x Aromatic CH), 138.5 (Cq, 1 x Aromatic Cq). 148.3 (Cq, 1 x Aromatic Cq), 197.8 (Cq, C=O).

The β-epoxy sulfones **170** and **171** were isolated as a mixture of isomers in the second fraction.



A single fraction was isolated cleanly with a 1 : 0.7 mixture of the epoxides **170** and **171** (0.030 g, 10%) and was characterised as a mixture. ν_{max}/cm^{-1} (neat) 1713, 1312, 1124 cm^{-1}; δ_H (300 MHz, $CDCl_3$) 1.39 (3H, s, CH_3 of **171**),

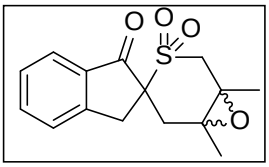
1.43, 1.53 (2 x 3H, s, 2 x CH_3 of **170**), 1.55 (3H, s, CH_3 of **171**), 2.39 (6H s, $ArCH_3$ from **170** and **171**),

$CqCH_2$ of epoxide **171** : 2.50, 2.86 *J* 15.8
$CqCH_2$ of epoxide **170**: 2.61, 2.86 *J* 15.8
$ArCH_2$ of **171**: 2.98, 4.05 *J* 17.2
$ArCH_2$ of **170**: 3.13, 3.79 *J* 18.4
SO_2CH_2 of **171**: 3.26, 4.15 *J* 15.2
SO_2CH_2 of **170**: 3.67, 4.50 *J* 15.5
} 6H of **170** and 6H of **171**

7.34 – 7.40 (2H, m, 1 x ArH from each diastereomer), 7.44 – 7.50 (2H, m, 1 x ArH from each diastereomer), 7.53 – 7.63 (2H, m, 1 x ArH from each diastereomer); δ_C (75 MHz, $CDCl_3$) of **170**; 20.6, 21.0, 21.1, (3 x CH_3, 1 x $ArCH_3$, 2 x $CqCH_3$), 35.3 (CH_2, $ArCH_2$), 40.0 (CH_2, $CqCH_2$), 54.0 (CH_2, SO_2CH_2), 60.0, 62.2 (Cq, 2 x CqO), 67.63 (Cq, C_{spiro}), 124.8, 125.8, (CH, 2 x Aromatic), 135.1 (Cq, 1 x Aromatic Cq), 137.7 (CH, 1 x Aromatic CH), 138.6 (Cq, 1 x Aromatic Cq), 149.0 (Cq, 1 x Aromatic Cq), 197.0 (Cq, 1 x C=O); δ_C (75 MHz, $CDCl_3$) of **171**; 20.8, 21.1 , 21.5 (3 x CH_3, 1 x $ArCH_3$, 2 x $CqCH_3$), 35.2, (CH_2, $ArCH_2$), 40.9 (CH_2, $CqCH_2$), 53.8, (CH_2, SO_2CH_2), 58.4, 60.5, (2 x Cq, 2 x CqO), 67.60 (Cq, C_{spiro}), 125.2, 126.0 (2 x CH, 2 x Aromatic CH), 135.0 (Cq, 1 x Aromatic Cq), 137.3 (CH, 1 x Aromatic CH), 138.7 (Cq, 1 x Aromatic Cq), 147.0 (Cq, 1 x Aromatic Cq), 196.0 (Cq, 2 x C=O).

3.5.2 Oxidation to β-epoxy sulfone.

1,6-Dimethyl-7-oxa-4-thiaspiro[bicyclo[4.1.0]heptane-3,2'-inden]-1'(*3'H*)-one



The α,β-unsaturated sulfone **166** (0.153 g, 0.55 mmol, 1 eq) was dissolved in dichloromethane (10 mL). 3-Chloroperoxybenzoic acid (77%, 0.143 g, 1.5 eq, 0.83 mmol) was dissolved in dichloromethane (8 mL) and added to the sulfone **166** dropwise, at 0°C over 10 min. The ice bath was allowed to melt and the reaction mixture returned to room temperature over 2 h and was stirred for a further 14 h. The colorless solution (without a precipitate) was concentrated under reduced pressure to give a white crystalline solid (0.255 g). Analysis by ^{1}H NMR spectroscopy showed complete consumption of the starting material and a mixture of the β-epoxy sulfones **167** and **168** (83 : 17). Purification by column chromatography on silica gel led to the elution of three fractions. The first, least polar fraction contained one diastereomer (0.052 g, 32%). The second contained a 1:1 mixture of diastereomers, **167** : **168** (0.052 g, 32%) and the final fraction contained the second diastereomer (0.008 g, 5%). m/z (ESI+) 293 [$(M+H)^+$, 100%], HRMS (ESI+): Exact mass calculated for $C_{15}H_{17}O_4S$ $[M+H]^+$, 293.0848 Found 293.0835.

Less polar major epoxide **167**:

(0.052 g, 32%) ν_{max}/cm^{-1} (neat) 1712, 1313, 1125, cm^{-1}; δ_H (300 MHz, $CDCl_3$) 1.43, 1.53 (2 x 3H, s, 2 x CH_3), 2.63 (1H, d *J* 15.9, A of ABq, Cq-CH_2), 2.86 (1H, d, *J* 15.9, B of AB_q, 1H of Cq-CH_2), 3.19 (1H, d, *J* 18.4, A of ABq, $ArCH_2$), 3.50 (1H, d *J* 15.2, A of AB_q, SO_2CH_2), 3.67 (1H, d, *J* 15.2, B of AB_q, SO_2CH_2), 3.85 (1H, d *J* 18.4, B of AB_q, $ArCH_2$) 7.40 – 7.51 (2H, m, 2 x Aromatic CH), 7.70 (1H, td, *J* 7.4, 1.2, 1 x Aromatic CH). 7.82 (1H, d, *J* 7.5, 1 x Aromatic CH); δ_C (100 MHz, $CDCl_3$) 20.7, 21.1 (2 x CH_3), 35.6 (CH_2, $ArCH_2$), 39.9 (CH_2, Cq-CH_2), 53.9 (CH_2, SO_2CH_2), 59.9, 62.2 (Cq, 2 x CqO), 67.3 (Cq, Cq, Cspiro), 125.0, 126.3, 128.4, 136.4 (CH, 4 x Aromatic CH), 135.0, 151.5 (Cq, 2 x Aromatic Cq), 197.1 (Cq, C=O).

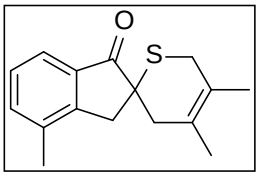
More polar minor epoxide **168**:

(0.08 g, 5%) ν_{max}/cm^{-1} (neat) 1717, 1312, 1125 cm^{-1}; δ_H (300 MHz, $CDCl_3$) 1.40, 1.55 (3H, s, 2 x CH_3), 2.52 (1H, d *J* 15.9, A of ABq of Cq-CH_2), 2.85 (1H, d, *J* 15.9, B of AB_q of Cq-CH_2), 3.04 (1H, d *J* 17.9, A of ABq, $ArCH_2$), 3.26 (1H, d *J* 15.5, A of AB_q, SO_2CH_2), 4.10 (1H, d *J* 17.2 B of AB_q, $ArCH_2$), 4.18 (1H, d B of AB_q *J* 15.4, SO_2CH_2) 7.39 – 7.51 (2H, m, 2 x Aromatic CH), 7.62– 7.67 (1H, m, 1 x, Aromatic CH), 7.77 (1H d, *J* 8.4, 1 x Aromatic CH); δ_C (100 MHz, $CDCl_3$) 19.5, 20.6 (2 x CH_3), 34.5 (CH_2, $ArCH_2$), 39.9 (CH_2, Cq-CH_2), 52.8 (CH_2, SO_2CH_2), 57.3, 59.5 (Cq, 2 x CqO), 66.2 (Cq, C_{spiro}), 124.5, 125.1, 127.5 (CH, 3 x Aromatic CH), 133.7 (Cq, 1 x Aromatic Cq), 134.9, (CH, 1 x Aromatic CH), 148.5 (Cq, 1 x Aromatic Cq), 195.1 (Cq, C=O).

3.5.3 Reduction to sulfides.

Procedure as per Drabowicz *et al.*[91]

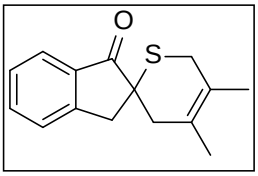
4,4',5'-Trimethyl-3',6'-dihydrospiro[indene-2,2'-thiopyran]-1(*3H*)-one 172



The sulfoxide cycloadduct **133** (0.054 g, 0.196 mmol, 1 eq) was dissolved in acetone (2 mL). Solid sodium iodide (0.070 g, 0.472 mmol, 2.4 equiv) was added in one portion. The reaction mixture was cooled to 0°C with an ice bath and trifluoroacetic anhydride (0.078 g, 0.37 mmol, 1.9 eq, 0.05 mL) was added dropwise as a solution in acetone (1 mL) over 2 min. The reaction mixture immediately turned from yellow to brown showing the liberation of I_2. TLC analysis showed the reaction to be complete after 20 min. The solution was concentrated under reduced pressure to give the crude product as a dark brown residue. This was dissolved in water (5 mL) and extracted with diethyl ether (2 x 10 mL). The ether washings were rinsed with saturated sodium thiosulfate pentahydrate (3 x 5 mL), followed by water (5 mL) and brine (5 mL). The yellow solution was dried with anhydrous $MgSO_4$ and concentrated under reduced pressure to give the product **172** as a yellow oil (0.042g, 84%) which was pure by ^1H NMR analysis. ν_{max}/cm^{-1} (neat) 1706, 1270 cm^{-1}; δ_H (400 MHz, $CDCl_3$) 1.73, 1.82 (2 x 3H, s, 2 x CH_3), 2.28 –

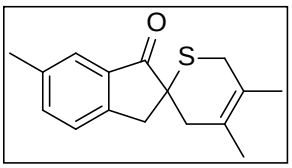
2.32 (2 overlapping signals including 1H, d *J* 15.4, A of ABq, Cq-CH_2, overlapping with 3H, s at 2.31, $ArCH_3$), 2.58 (1H, d, *J* 17.4, B of AB_q, 1H of Cq-CH_2), 3.04 – 3.19 (3H, m, overlapping multiplet containing 1H, A and B of ABq of $ArCH_2$, *J* 17.5, and A of ABq of SCH_2), 3.40 (1H, d, *J* 16.9, B of AB_q, SCH_2), 7.30 (1H, t, *J* 7.2, Aromatic CH), 7.40 (1H, d, *J* 7.8, Aromatic CH), 7.62 (1H, d, *J* 7.6, Aromatic CH); δ_C (100 MHz, $CDCl_3$) 17.8 (CH3, $ArCH_3$), 19.5, 20.5 (2 x CH_3), 30.7 (CH_2, $ArCH_2$), 39.3 (CH_2, Cq-CH_2), 41.6 (CH_2, SCH_2), 49.8 (Cq, C_{spiro}), 122.4 (CH, 1 x Aromatic CH), 123.1 (Cq, C=C), 125.5 (Cq, C=C), 128.1 (CH, 1 x Aromatic CH), 134.5 (Cq, 1 x Aromatic Cq), 135.4 (Cq, 1 x Aromatic Cq), 135.5 (CH, 1 x Aromatic CH), 149.9 (Cq, 1 x Aromatic Cq), 203.2 (Cq, C=O). m/z (ESI+) 259 [$(M+H)^+$, 100%], HRMS (ESI+): Exact mass calculated for $C_{16}H_{19}OS$ $[M+H]^+$, 259.1157. Found 259.1153

4',5'-Dimethyl-3',6'-dihydrospiro[indene-2,2'-thiopyran]-1(*3H*)-one 173



The sulfoxide cycloadduct **135** (0.040 g, 0.153 mmol, 1 eq) was dissolved in acetone (2 mL). Solid sodium iodide (0.055 g, 0.368 mmol, 2.4 equiv) was added in one portion. The reaction mixture was cooled to 0°C with an ice bath and trifluoroacetic anhydride (0.061 g, 0.29 mmol, 1.9 eq, 0.041 mL) was added dropwise as a solution in acetone (1 mL) over 2 min. The reaction mixture immediately turned from yellow to brown showing the liberation of I_2. TLC analysis showed the reaction to be complete after 20 min. The solution was concentrated under reduced pressure to give the crude product as a dark brown residue. This was dissolved in water (5 mL) and extracted with diethyl ether (2 x 10 mL). The ether washings were rinsed with saturated sodium thiosulfate pentahydrate (3 x 5 mL), followed by water (5 mL) and brine (5 mL). The yellow solution was concentrated under reduced pressure to give the product **173** as a yellow oil (0.030 g, 81%) which was pure on analysis by ^1H NMR. ν_{max}/cm^{-1} (neat) 1705, 1276 cm^{-1}; δ_H (400 MHz, $CDCl_3$) 1.73, 1.81 (2 x 3H, s, 2 x CH_3), 2.32 (1H, d *J* 17.7, A of ABq, one of Cq-CH_2,), 2.59 (1H, d, *J* 17.7, B of AB_q, one of Cq-CH_2), 3.05 (1H, d, *J* 17.2, A of ABq, one of $ArCH_2$), 3.19 – 3.31 (2H, compact AB_q, *J* 17.4, SCH_2), 3.40 (1H, d, *J* 17.7, B of AB_q, one of $ArCH_2$) 7.36 – 7.42 (2H, m, 2 x Aromatic CH), 7.55 – 7.63 (1H, m, 1 x, Aromatic CH), 7.78 (1H, d, *J* 7.6, Aromatic CH); δ_C (100 MHz, $CDCl_3$) 19.5, 20.4 (CH_3, 2 x CH_3), 30.7 (CH_2, $ArCH_2$), 38.9 (CH_2, Cq-CH_2), 42.7 (CH_2, SCH_2), 49.9 (Cq, C_{spiro}), 123.1 (Cq, C=C) 125.1 (CH, 1 x Aromatic CH), 125.4 (Cq, C=C), 126.2 (CH, 1 x Aromatic CH), 127.9 (CH, 1 x Aromatic CH), 134.6 (Cq, 1 x Aromatic Cq), 135.0 (CH, 1 x Aromatic CH), 150.4 (Cq, 1 x Aromatic Cq), 202.9 (Cq, C=O). HRMS (ESI+): Exact mass calculated for $C_{15}H_{17}OS$ $[M+H]^+$, 245.1000. Found 245.0999.

4',5',6-Trimethyl-3',6'-dihydrospiro[indene-2,2'-thiopyran]-1(*3H*)-one 174



The sulfoxide cycloadduct **137** (0.030 g, 0.109 mmol, 1 eq) was dissolved in acetone (2 mL). Solid sodium iodide (0.039 g, 0.26 mmol, 2.4 equiv) was added in one portion. The reaction mixture was cooled to 0°C with an ice bath and trifluoroacetic anhydride (0.043 g, 0.21 mmol, 1.9 eq, 0.03 mL) was added dropwise as a solution in acetone (1 mL) over 2 min. The reaction mixture immediately turned from yellow to brown showing the liberation of I_2. TLC analysis showed the reaction to be complete after 50 min. The solution was concentrated under reduced pressure to give the crude product as a dark brown residue. This was dissolved in water (5 mL) and extracted with diethyl ether (2 x 10 mL). The ether washings were rinsed with saturated sodium thiosulfate pentahydrate (3 x 5 mL), followed by water (5 mL) and brine (5 mL). The yellow solution was dried with anhydrous $MgSO_4$, and concentrated under reduced pressure to give the product **174** as a yellow oil (0.021 g, 75%) which was pure by ^{1}H NMR analysis. ν_{max}/cm^{-1} (neat) 1708, 1281 cm^{-1}; δ_H (300 MHz, $CDCl_3$) 1.73, 1.80 (3H, s, 2 x CH_3), 2.28 (1H, d, *J* 17.3, A of ABq, Cq-CH_2), 2.40 (CH_3, s, $ArCH_3$), 2.56 (1H, d, *J* 17.4, B of AB_q, 1H of Cq-CH_2), 3.05 (1H, d, *J* 17.1 AB_q, A of ABq, one of $ArCH_2$), 3.19 – 3.29 (2H, compact AB_q, *J* 17.4, SCH_2), 3.41 (1H, d, *J* 17.7, B of AB_q, one of $ArCH_2$), 7.27 (1H, d, *J* 7.1, 1 x Aromatic CH), 7.40 (1H, d, *J* 8.1, 1 x Aromatic CH), 7.57 (1H, br s, 1 x Aromatic CH); δ_C (75.5 MHz, $CDCl_3$) 19.5, 20.4, 21.1 (3 x CH_3), 30.7 (CH_2, $ArCH_2$), 39.1 (CH_2, Cq-CH_2), 42.4 (CH_2, SCH_2), 50.3 (Cq, C_{spiro}), 123.1 (Cq, C=C), 125.0 (CH, 1 x Aromatic CH), 125.5 (Cq, C=C), 125.9 (CH, 1 x Aromatic CH), 134.8 (Cq, 1 x Aromatic Cq), 136.1 (CH, 1 x Aromatic CH), 137.8 (Cq, 1 x Aromatic Cq), 147.6 (Cq, 1 x Aromatic Cq), 202.8 (Cq, C=O); m/z (ESI+) 259 [$(M+H)^+$, 100%], HRMS (ESI+): Exact mass calculated for $C_{16}H_{19}OS$ $[M+H]^+$, 259.1157. Found 259.1161.

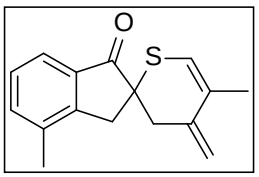
3.5.4 Pummerer rearrangements

Procedure as per Gulea *et al.* [71]

Pummerer rearrangement of cycloadduct 133

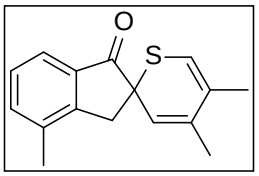
The sulfoxide **133** (0.060 g, 0.2 mmol, 1 eq) was dissolved in dry THF (1 mL) while stirring at 0°C under a nitrogen atmosphere. Trifluoroacetic anhydride (0.050 g, 0.22 mmol, 1.1 eq), was added dropwise over 10 min. The ice bath was removed and the mixture was stirred for 1 h at room temperature and then diluted with dichloromethane (5 mL). The reaction mixture was washed with aqueous $NaHCO_3$ (10%, 2 x 10 mL), water (1 x 10 mL) and brine (1 x 10 mL), dried with $MgSO_4$ and concentrated under reduced pressure to give the crude product as a yellow oil (0.042 g) and as a 1:1 mixture of isomers **182** and **183** and 5% residual starting material **133**; m/z (ESI+) 257 [$(M+H)^+$, 40%], HRMS (ESI+): Exact mass calculated for $C_{16}H_{17}OS$ $[M+H]^+$, 257.1000. Found 257.1000

Purification of the crude reaction mixture by careful column chromatography on silica gel using gradient hexane – ethyl acetate as eluent (100 : 0 – 90 : 10) led to the elution of two isomeric products.



The less polar fraction was the isomer **182** isolated as a brown oil (0.015 g, 27%). ν_{max}/cm^{-1} (neat) 1715, 1268 cm^{-1}; δ_H (400 MHz, $CDCl_3$) 2.02, 2.31 (3H, s, 2 x CH_3), 2.48 (1H, d, *J* 14.8, A of AB_q, $CqCH_2$), 3.03 (1H, d, *J* 14.8, B of AB_q, $CqCH_2$), 3.13 – 3.27 (2H, m, AB_q, *J* 17.5, $ArCH_2$), 4.89 (1H, s, one of $C=CH_2$), 5.23 (1H, s, one of $C=CH_2$), 6.11 (1H, s, SCH), 7.33 (1H, dd, *J* 8.8, 7.6, 1 x Aromatic CH), 7.44 (1 H, d, *J* 8.1, Aromatic CH), 7.65 (1H, d, *J* 7.6, Aromatic CH); δ_C (100 MHz, $CDCl_3$) 17.8, 20.8 (CH_3, 2 x CH_3), 40.6 (CH_2, $CqCH_2$), 42.5 (CH_2, $ArCH_2$), 54.1 (Cq, C_{spiro}), 114.1 (CH_2, $C=CH_2$), 117.7 (CH, SCH=), 122.4 (CH, 1 x Aromatic CH), 127.6 (Cq, $Cq=CH_2$), 128.2 (CH, 1 x Aromatic CH), 134.0 (Cq, 1 x Aromatic Cq), 135.7 (Cq, 1 x Aromatic Cq), 136.1 (CH, 1 x Aromatic CH), 139.3 (Cq, SCH=Cq), 150.4 (1 x Aromatic Cq), 203.4 (Cq, C=O).

*The other isomer **183** is present in approximately 10% with corresponding signals present in the ^1H NMR spectrum at 1.92, 1.97, 5.30 and 5.94 ppm.



The more polar fraction was the isomer **183** isolated as a yellow crystalline solid (0.011 g, 20 %); ν_{max}/cm^{-1} (neat) 1717, 1274 cm^{-1}. Mp 80 – 81°C; δ_H (400 MHz, $CDCl_3$) 1.92, 1.97 (3H, s, 2 x CH_3), 2.30 (3H, s, $ArCH_3$), 3.20 (1H, d, *J* 17.5, A of AB_q, $ArCH_2$), 3.33 (1H, d, *J* 17.5, B of AB_q, $ArCH_2$), 5.30, 5.94 (2 x 1H, 2 x s, 2 x vinyic CH), 7.32 (1H, t, *J* 7.7, Aromatic CH), 7.42 (1H, d, *J* 7.4, Aromatic CH), 7.65 (1H, d, *J* 7.7, Aromatic CH); δ_C (100 MHz, $CDCl_3$) 17.7, 20.4, 20.8 (3 x CH_3), 44.0 (CH_2, $ArCH_2$), 52.2 (Cq, C_{spiro}), 112.7 (CH, SCH), 117.4 (CH, CH=C), 122.7 (CH, 1 x Aromatic CH) 128.3 (CH, 1 x Aromatic CH), 131.2 (Cq, CH=Cq), 133.5 (Cq, 1 x Aromatic Cq), 135.4 (Cq, 1 x Aromatic Cq), 135.9 (CH, 1 x Aromatic CH), 136.5 (Cq, SCH=Cq), 149.4 (Cq, 1 x Aromatic Cq), 201.9 (Cq, C=O).

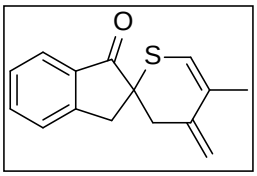
*This fraction contained 14% residual starting material **133**.

Pummerer rearrangement of sulfoxide cycloadduct 135

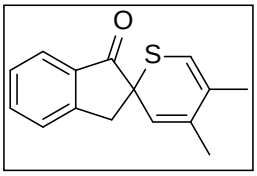
The sulfoxide **135** (0.114 g, 0.4 mmol, 1 eq) was dissolved in dry THF (2.5 mL) at 0°C under a nitrogen atmosphere while stirring. Trifluoroacetic anhydride (0.101 g, 0.44 mmol, 1.1 eq), was added dropwise over 10 min. The ice bath was removed and the mixture was stirred for 1 h at room temperature and then diluted with dichloromethane (5 mL). The reaction mixture was washed with aqueous $NaHCO_3$ (10%, 2 x 10 mL), water (1 x 10 mL) and brine (1 x 10 mL), dried with $MgSO_4$ and concentrated under reduced pressure to give the crude product as a brown oil (0.080 g) and a mixture of isomers (1 : 1,

180 : **181**). Mass spec. analysis on the crude material identified the molecular formula; m/z (ESI+) 243 [$(M+H)^+$, 35%], HRMS (ESI+): Exact mass calculated for $C_{15}H_{15}OS$ $[M+H]^+$, 243.0844. Found 243.0832.

Purification of the crude reaction mixture by careful column chromatography on silica gel using gradient hexane-ethyl acetate as eluent (100 : 0 – 90 : 10) led to the elution of two isomeric products.



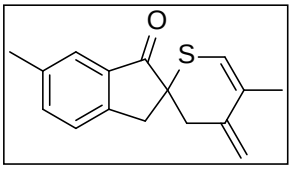
The less polar fraction was the isomer **180** isolated as a brown oil (0.024 g, 23%); ν_{max}/cm^{-1} (neat) 1708, 1606 cm^{-1} δ_H (400 MHz, $CDCl_3$) 2.01 (3H, s, CH_3), 2.50 (1H, d, *J* 14.5, A of AB_q, one of $CqCH_2$), 3.02 (1H, d, *J* 14.5, B of AB_q, one of $CqCH_2$), 3.26 – 3.38 (2H, m, AB_q, *J* 18.0, $ArCH_2$), 4.89 (1H, s, one of $C=CH_2$), 5.22 (1H, s, one of $C=CH_2$), 6.09 (1H, s, SCH=), 7.39-7.43 (2H, m, 2 x Aromatic CH), 7.63 (1H, t, *J* 7.7, 1 x Aromatic CH), 7.82 (1H, d, *J* 7.1 1 x Aromatic CH); δ_C (100 MHz, $CDCl_3$) 20.9 (CH_3, CH_3), 40.6 (CH_2, $CqCH_2$), 43.2 (CH_2, $ArCH_2$), 54.2 (Cq, C_{spiro}), 114.1 (CH_2, $Cq=CH_2$), 117.6 (CH, SCH=C), 125.0 (CH, 1 x Aromatic CH), 126.5 (CH, 1 x Aromatic CH), 127.6 (Cq, $CH_2=Cq$), 128.0 (CH, 1 x Aromatic CH), 134.6 (Cq, 1 x Aromatic Cq), 135.6 (CH, 1 x Aromatic CH), 139.2 (Cq, SCH=Cq), 151.3 (Cq, 1 x Aromatic Cq), 203.0 (Cq, C=O). This fraction contained 5% of the isomer **181**.



The more polar fraction was the isomer **181** isolated as a yellow crystalline solid (0.026 g, 25%); mp. 79-81°C; ν_{max}/cm^{-1} (neat) 1712, 1605, cm^{-1}; δ_H (400 MHz, $CDCl_3$) 1.91, 1.96 (3H, s, 2 x CH_3), 3.29 – 3.47 (2H, AB_q, *J* 17.7, A and B of AB_q of $ArCH_2$), 5.30 (1H, s, CqCH), 5.92 (1H, s, SCH), 7.36 – 7.42 (2H, m, 2 x Aromatic CH), 7.60 (1H, t, *J* 7.6, 1 x Aromatic CH), 7.81 (1H, d, *J* 7.6, 1 x Aromatic CH); δ_C (100 MHz, $CDCl_3$) 20.5, 20.8 (CH_3, 2 x CH_3), 44.8 (CH_2, $ArCH_2$), 52.2 (Cq, C_{spiro}), 112.6 (CH, SCH=), 117.2 (CH, CqCH=), 125.5 (CH, 1 x Aromatic CH), 126.2 (CH, 1 x Aromatic CH), 128.2 (CH, 1 x Aromatic CH), 131.2 (Cq, CH=Cq), 133.6 (Cq, 1 x Aromatic Cq), 135.3 (CH, 1 x Aromatic CH), 136.7 (Cq, SCH=Cq), 150.4 (Cq, 1 x Aromatic Cq), 201.2 (Cq, C=O).

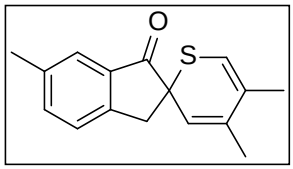
Pummerer rearrangement of cycloadduct 137

The sulfoxide **137** (0.150 g, 0.54 mmol, 1 eq) was dissolved in dry THF (4 mL) at 0°C under a nitrogen atmosphere while stirring. Trifluoroacetic anhydride (0.126 g, 0.60 mmol, 1.1 eq) was added dropwise over 10 min. The ice bath was removed and the mixture was stirred for 1 h and then diluted with dichloromethane (5 mL). The reaction mixture was washed with aqueous $NaHCO_3$ (10%, 2 x 10 mL), water (1 x 10 mL) and brine (1 x 10 mL), dried with $MgSO_4$ and concentrated under reduced pressure to give the crude product as a brown oil (0.159 g) and a mixture of isomers (1 : 1, **185** : **184**). Purification of the crude reaction mixture by careful column chromatography on silica gel using hexane-ethyl acetate as eluent (100 : 0 – 90 : 10) led to the elution of the two isomeric products.



The less polar fraction was the isomer **184** isolated as a bright yellow oil (0.047 g, 32%). ν_{max}/cm^{-1} (neat) 1710, 1493, 1280 cm^{-1} ; δ_H (400 MHz, $CDCl_3$) 2.01 (3H, d, *J* 1.2, CH_3), 2.42 (3H, s, $ArCH_3$), 2.49 (1H, d, *J* 14.8, A of AB_q, one of $CqCH_2$), 3.02 (1H, d, *J* 14.8, B of AB_q, one of $CqCH_2$), 3.20 – 3.33 (2H, m, AB_q, *J* 17.7, $ArCH_2$), 4.88 (1H, s, one of $C=CH_2$), 5.22 (1H, s, one of $C=CH_2$), 6.09 (1H, s, SCH=), 7.24 – 7.31 (1H, m, 1 x Aromatic CH), 7.41 – 7.47 (1H, m, 1 x Aromatic CH), 7.61 (1H, br s, 1 x Aromatic CH); δ_C (100 MHz, $CDCl_3$) 20.8, 21.1 (2 x CH_3), 40.6 (CH_2, $CqCH_2$), 42.9 (CH_2, $ArCH_2$), 54.6 (Cq, C_{spiro}), 113.9 (CH_2, $Cq=CH_2$), 117.7 (CH, SCH=), 124.8 (CH, 1 x Aromatic CH), 126.2 (CH, 1 x Aromatic CH), 127.5 (Cq, $CH_2=Cq$), 134.7 (Cq, 1 x Aromatic Cq), 136.9 (CH, 1 x Aromatic CH), 138.0 (1 x Cq, Aromatic Cq), 139.4 (Cq, SCH=Cq), 148.7 (Cq, 1 x Aromatic Cq), 203.0 (Cq, C=O); m/z (ESI+) 257 [$(M+H)^+$, 100%]; HRMS (ESI+): Exact mass calculated for $C_{16}H_{17}OS$ $[M+H]^+$, 257.1000. Found 257.1011.

This fraction contained approx. 10% of the other isomer **185**, corresponding signals identified in the ^1H NMR spectrum include 2 x CH_3 singlets at 1.91 and 1.96 ppm, and CH singlets at 5.2 and 5.8 ppm. Signals identified in the ^{13}C NMR for the other isomer were observed at 44.5, 52.5, 112.7, 117.4, 125.4, 125.9 and 147.7 ppm.

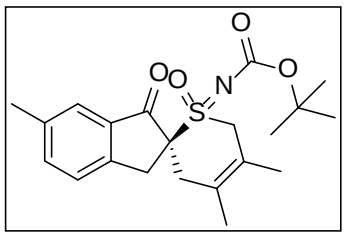


The more polar fraction was the isomer **185** isolated as a bright yellow oil (0.030 g, 21%); ν_{max}/cm^{-1} (neat) 1714, 1280 cm^{-1}; δ_H (400 MHz, $CDCl_3$) 1.91, 1.96 (2 x 3H, 2 x CH_3), 2.40 (3H, br s, $ArCH_3$), 3.20 – 3.40 (2H, AB_q, *J* 17.4, A and B of AB_q of $ArCH_2$), 5.28 (1H, s, CqCH=), 5.91 (1H, s, SCH=), 7.23 – 7.26 (1H, m, 1 x Aromatic CH), 7.42 (1H, dd, *J* 8.0, 1.4, 1 x Aromatic CH), 7.60 (1H, br s, 1 x Aromatic CH); δ_C (100 MHz, $CDCl_3$) 20.4, 20.8, 21.1 (3 x CH_3), 44.6 (CH_2, $ArCH_2$), 52.5 (Cq, C_{spiro}), 112.7 (CH, SCH=), 117.4 (CH, CqCH=), 125.4 (CH, 1 x Aromatic CH), 125.9 (CH, 1 x Aromatic CH), 131.0 (Cq, CH=Cq), 133.8 (Cq, 1 x Aromatic Cq), 136.54 (CH, 1 x Aromatic CH), 136.58 (Cq, SCH=Cq) 138.2 (Cq, 1 x Aromatic Cq), 147.7 (Cq, 1 x Aromatic Cq), 201.2 (Cq, C=O). m/z (ESI+) 257 [$(M+H)^+$, 100%].

3.5.5 Attempted synthesis of sulfoximine 190

Procedure as per Bull *et al.*[99]

Attempted synthesis of tert-Butyl (4',5',6-trimethyl-1'-oxido-1-oxo-1,3,3',6'-tetrahydro-1'l6-spiro[indene-2,2'-thiopyran]-1'-ylidene)carbamate 190



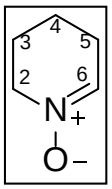
BOC carbamate **189** (0.028 g, 0.24 mmol, 1.5 eq), MgO (0.026 g, 0.64 mmol, 4 eq) and $Rh_2(OAc)_4$ (2.5 mol %) were added to a suspension of the sulfoxide **137** (0.045 g, 0.16 mmol, 1 eq) in dichloromethane (1.5 mL), followed by diacetoxyiodobenzene (0.079 g, 0.24 mmol, 1.5 eq) at room temperature. The reaction mixture was heated to 40°C and

stirred for 5 h. The reaction mixture was then filtered through a Celite® plug, and concentrated *in vacuo* to give the crude material as a white solid (0.113 g). Purification by column chromatography on silica gel led to recovery of the BOC carbamate **189** and the sulfoxide starting material **137** in two separate fractions, with no evidence for the formation of the desired sulfoximine product. Spectral characteristics for the sulfoxide **137** are consistent with those outlined above.

3.6 Synthesis of dipole precursors and dipoles.

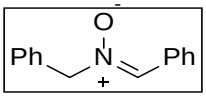
3.6.1 Generation of Nitrones.

2, 3 ,4 ,5 -Tetrahydropyridine 1-oxide 212



Yellow mercuric oxide (1.14 g, 5.2 mmol, 2 eq) was added slowly to a stirring solution of 1-hydroxypiperidine **214** (0.28 g, 2.6 mmol, 1 eq) in dichloromethane (4 mL) at 0°C. The ice-bath was removed, and as the reaction progressed, the slurry turned from orange in colour to dark green. Following stirring at room temperature for 20 min, TLC analysis indicated the reaction had gone to completion. The slurry was filtered through Celite® which was washed with dichloromethane (5 mL). After evaporation of the solvent under reduced pressure, the crude nitrone **212** was obtained as a pale yellow oil; δ_H (400 MHz, $CDCl_3$) 1.77-1.85, 1.97-2.09 [2 x 2H, m, C(3)H_2, C(4)H_2], 2.48-2.55 [2H, m, C(5)H_2], 3.84-3.91 [2H, m, C(2)H_2], 7.23 – 7.28 [1H, m, C(6)H]. Spectral characteristics are consistent with those reported in the literature. [119,122]

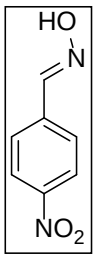
***N*-Benzyl-1-phenylmethanimine oxide 211**[177]



To a stirred solution of dibenzylamine **215** (3.5 g, 17.7 mmol, 1 eq) in a mixture of acetonitrile : THF : 0.01 M disodium EDTA (24.7 mL : 6.2 mL : 24.6 mL) at 5°C, was added $NaHCO_3$ (7.45 g, 88.7 mmol, 5 eq). While cooling to maintain the temperature at 5°C, Oxone® (11.45 g, 18.58 mmol, 1.05 molar eq) was added portionwise over 2 h with vigorous stirring. The mixture was stirred for a further 1 h at 5°C and then ethyl acetate was added (80 mL). The organic layer was separated and the aqueous layer was extracted with ethyl acetate (3 x 50 mL). The combined organic extracts were dried with anhydrous magnesium sulfate and concentrated under reduced pressure to provide nitrone **211** as an off-white crystalline solid (2.77 g, 74%) ; mp 69 – 70°C. ν_{max}/cm^{-1} (neat) 1458, 1153, 690; δ_H (400 MHz, $CDCl_3$) 4.96 (2H, s, ArCH_2), 7.24 – 7.46 (9H, m, 8 x Aromatic CH and CH=N), 8.18 – 8.22 [2H, m, 2 x Aromatic CH ortho to CH=N(O)Bn]; δ_C (75.5 MHz, $CDCl_3$) 71.7 (CH_2), 128.4, 128.5, 128.6, 128.9, 129.2, 130.4 (CH, 6 signals representing 10 x Aromatic CH), 130.5 (CH, CHN), 133.4, 134.4 (Cq, 2 x Aromatic Cq). All spectral characteristics are consistent with those reported in the literature.[177]

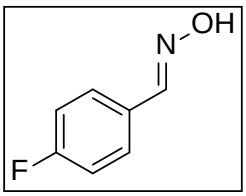
3.6.2 Syntheis of Oximes

(*E*)-4-Nitrobenzaldoxime 217[178]



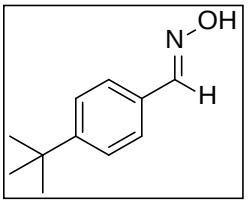
p-Nitrobenzaldehyde **223** (8.54 g, 56.5 mmol, 1 eq), hydroxylamine hydrochloride (3.93 g, 56.5 mmol, 1 eq) and anhydrous sodium acetate (11.59 g, 141.3 mmol, 2.5 eq) were heated under reflux in aqueous ethanol (90%, 100 mL) for 24 h. The solvent was then removed under reduced pressure. The resulting residue was dissolved in sodium hydroxide solution (2 M, 20 mL) and water (20 mL) and subsequently filtered, leaving a dark orange solution of the oxime anion in the filtrate. The filtrate was acidified with acetic acid resulting in the precipitation of the oxime **217** as a pale yellow solid. The crystals were isolated by vacuum filtration and washed with water. The solid was recrystallized from ethanol: water (3 : 1) to yield the oxime **217** as a yellow solid (6.95 g, 84 %). Found C, 58.77; H 5.49; N 22.50, $C_7H_6N_2O_3$ requires C, 59.01; H 4.95 ; N 22.94; mp 125 – 126°C (lit.[125] 119 – 120°C); ν_{max}/cm^{-1} (neat) 1605, 1532, 1347; δ_H (300 MHz, $CDCl_3$) 7.75 (2H, d, *J* 8.7, 2 x Aromatic CH), 7.98 (1 H, s, OH), 8.21 (1H, s, CH), 8.25 (2H, d, *J* 8.7, 2 x Aromatic CH); δ_C (100 MHz, $CDCl_3$) 124.1 (1 signal corresponding to 2 x Aromatic CH), 127.7 (1 signal corresponding to 2 x Aromatic CH), 138.2 (Cq, 1 x Aromatic Cq), 148.5 (CH, CH=N), 148.6 (Cq, 1 x Aromatic Cq). Spectroscopic characteristics are in good agreement with the literature.[178]

(*E*)-4-Fluorobenzaldehyde oxime 218[178]



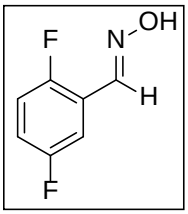
To a suspension of the 4-fluorobenzaldehyde **224** (1.5 g, 12.08 mmol, 1 eq) in water/ethanol/ice (1 : 1 : 2, 12 mL) was added hydroxylamine hydrochloride in one portion (0.84 g, 12.08 mmol, 1 eq). NaOH solution (1.20 g NaOH, 2.5 eq, 50% in water) was added dropwise over 10 min keeping the temperature under 30°C. The reaction mixture was stirred for 1 h at room temperature, after which TLC analysis (40% ethyl acetate, 60% hexane as eluent) showed complete consumption of starting material. The reaction mixture was extracted with ether (20 mL), the aqueous layer was separated and acidified to pH 6 with concentrated HCl. The aqueous layer was extracted with diethyl ether (3 x 20 mL). The combined organic layers were dried with $MgSO_4$ and concentrated under reduced pressure to give the oxime **218** as a white crystalline solid (1.65 g, 98%). ν_{max}/cm^{-1} (neat) 3256, 1606, 1509; δ_H (400 MHz, $CDCl_3$) 7.04 – 7.12 (2H, m, 2 x Aromatic CH), 7.54 – 7.57 (2H, m, 2 x Aromatic CH), 8.14 (1H, s, CH=N), 9.13 (1H, br s, OH); δ_C (100 MHz, $CDCl_3$) 116.0 (2 x CH, 2 x Aromatic CH, d, $^2J_{CF}$ 22.0), 128.1 (Cq, 1 x Aromatic Cq, $^4J_{CF}$ 3.3), 128.9 (2 x CH, 2 x Aromatic CH, d, $^3J_{CF}$ 8.4), 149.4 (CH, CH=N), 163.8 (ArCF, d, $^1J_{CF}$ 250.5); m/z (ESI+) 140 [$(M+H)^+$, 20%]; HRMS (ESI+): Exact mass calculated for C_7H_7NOF $[M+H]^+$, 140.0512. Found 140.0519. The spectral data are in agreement with those reported in the literature. [178]

(*E*)-4-(*tert*-Butyl)benzaldehyde oxime 220[126,127]



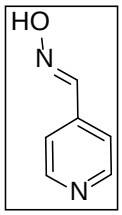
To a suspension of the 4-*t*-butylbenzaldehyde **226** (1.63 g, 10 mmol, 1 eq) in water/ethanol/ice (1 : 1 : 2, 12 mL) was added hydroxylamine hydrochloride in one portion (0.69 g, 10 mmol, 1 eq). NaOH solution (0.99 g NaOH, 2.5 eq, 50% in water) was added dropwise over 10 min keeping the temperature under 30°C. The reaction mixture was stirred for 1 h at room temperature at which point TLC analysis (40% ethyl acetate, 60% hexane as eluent) showed complete consumption of the starting material. The reaction mixture was extracted with ether (20 mL) and the layers separated. The aqueous layer was acidified to pH 6 with concentrated HCl. The aqueous layer was subsequently extracted with diethyl ether (3 x 20 mL). The combined organic layers were dried with $MgSO_4$ and concentrated under reduced pressure to give the oxime **220** as a white crystalline solid (1.56 g, 89 %). mp 88 – 90° C; ν_{max}/cm^{-1} (neat) 3252, 1607, 1510; δ_H (400 MHz, $CDCl_3$) 1.36 (9H, s, 3 x CH_3), 7.41 (2H, d, *J* 7.8, 2 x Aromatic CH), 7.50 – 7.59 (2H, m, 2 x Aromatic CH), 8.13 (1H, s, CH=N), 9.0 (1H, br s , OH); δ_C (100 MHz, $CDCl_3$) 31.2 (1 signal corresponding to 3 x CH_3), 34.9 [Cq, $Cq(CH_3)_3$], 125.8 (2 x CH, 2 x Aromatic CH), 126.9 (CH, 2 x Aromatic CH), 129.1 (Cq, 1 x Aromatic Cq), 150.2 (CH, CH=N), 153.5 (Cq, 1 x Aromatic Cq). HRMS (ESI+): Exact mass calculated for $C_{11}H_{16}NO$ $[M+H]^+$ 178.1232. Found 178.1225

(*E*)-2, 5-Difluorobenzaldehyde oxime 219[126,179]



To a suspension of the 2,5-di-fluorobenzaldehyde **225** (2.84 g, 20 mmol, 1 eq) in water/ethanol/ice (1 : 1 : 2, 20 mL) was added hydroxylamine hydrochloride in one portion (2.77 g, 20 mmol, 1 eq). NaOH solution (1.99 g NaOH, 2.5 eq, 50% in water) was added dropwise over 10 min keeping the temperature under 30°C. The reaction mixture was stirred overnight at room temperature at which point TLC analysis (40% ethyl acetate, 60% hexane as eluent) showed complete consumption of starting material. The reaction mixture was extracted with ether (20 mL), the aqueous layer was separated and acidified to pH 6 with concentrated HCl. The aqueous layer was extracted with diethyl ether (3 x 20 mL). The combined organic layers were dried with $MgSO_4$ and concentrated under reduced pressure to give the oxime **219** as a white crystalline solid (1.44 g, 47%). mp 104 - 106° C; ν_{max}/cm^{-1} (neat) 3232, 1488, 1191, 805; δ_H (400 MHz, $CDCl_3$) 7.00 – 7.20 (2H, asymmetric multiplet, 2 x Aromatic CH), 7.42 – 7.46 (1H, m, 1 x Aromatic CH), 8.33 (1H, br s, CH=N), 8.63 (1H, br s, OH); δ_C(100 MHz, $CDCl_3$) 112.9 (dd, $^2J_{CF}$ 25.5, $^3J_{CF}$ 3.3, Aromatic CH), 117.2 (dd, $^2J_{CF}$ 24.4, $^3J_{CF}$ 8.4, Aromatic CH) 118.2 (dd, $^2J_{CF}$ 24.8, $^3J_{CF}$ 9.0, Aromatic CH), 121.1 (dd, $^2J_{CF}$ 13.2, $^3J_{CF}$ 8.4, Aromatic Cq), 143.5 (apparent br t, J_{CF} 2.8, CH=N), 156.8 (dd, $^1J_{CF}$ 248.4, $^4J_{CF}$ 2.6, ArCF), 158.7 (dd, $^1J_{CF}$ 243.0, $^4J_{CF}$ 2.4, ArCF). m/z (ESI+) 158 [$(M+H)^+$, 80%]. HRMS (ESI+): Exact mass calculated for $C_7H_6NOF_2$ $[M+H]^+$ 158.0417 Found 158.0417.

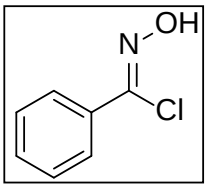
Isonicotinaldehyde oxime 221[130]



To a suspension of isonicotinaldehyde **227** (4.20 g, 40 mmol, 3.74 mL, 1 eq) in water/ethanol/ice (1 : 1 : 2, 40 mL) was added hydroxylamine hydrochloride in one portion (2.72 g, 40 mmol, 1 eq). NaOH solution (3.92 g NaOH, 2.5 eq, 50% in water) was added dropwise over 10 min keeping the temperature under 30°C. The reaction mixture was stirred for 1 h at room temperature, TLC analysis (40% ethyl acetate, 60% hexane as eluent) showed complete consumption of starting material. The reaction mixture was extracted with ether (20 mL), the aqueous layer was carefully acidified to pH 7 with concentrated HCl (avoiding formation of the HCl salt). The aqueous layer was extracted with diethyl ether (3 x 40 mL). The organic layers were combined and dried with $MgSO_4$ and concentrated under reduced pressure to give the oxime **191** as a pale yellow crystalline solid (3.33 g, 70 %). Found C, 58.97 H 4.98 N 22.31, $C_6H_6N_2O$ requires C, 59.01; H 4.95 ; N 22.94; Mp 124 - 125° C; ν_{max}/cm^{-1} (neat) 1601, 1310, 818; δ_H (400 MHz, $CDCl_3$) 7.55 (2H, finely split s, 2 x Aromatic CH), 8.14 (1H, s, CH=N), 8.61 (2H, finely split s, 2 x Aromatic CH), 11.90 (1H, br s, OH); δ_C (100 MHz, $CDCl_3$), 121.3 (2 x Aromatic CH), 141.2 (Aromatic Cq), 147.1 (CH=N), 149.5 (2 x Aromatic CH); m/z (ESI+) 123 [$(M+H)^+$, 100%].

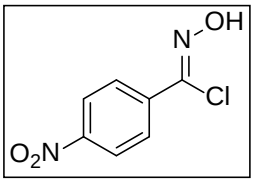
3.6.3 Synthesis of Imidoyl chlorides

Benzohydroximoyl chloride 193[119,122,128]



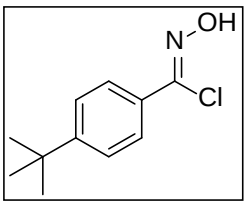
Chlorine gas (generated by the dropwise addition of concentrated hydrochloric acid to solid potassium permanganate) was bubbled through a cooled (-10°C) solution of benzaldoxime **216** (3.00 g, 0.24 mol) in chloroform (36 mL), with a calcium chloride guard tube fitted to the reaction flask. The temperature was maintained at -10°C by use of a cryocooler and the chlorine gas caused the solution to go from clear through yellow, yellow/orange, green, blue/green, green, yellow and finally dark orange, indicating saturation. Excess chlorine gas was purged with nitrogen and the colour changed to a pale yellow. The solvent was removed by concentration under reduced pressure and the resulting residue was dissolved in hexane and placed in a freezer overnight. The resultant solid was isolated by vacuum filtration to yield benzohydroximoyl chloride **193** as a white solid (1.94 g, 50%). δ_H (400 MHz, $CDCl_3$) 7.37-7.52 (3H, m, 3 x Aromatic CH), 7.82-7.85 (2H, m, Aromatic CH), 8.61 (1H, s, OH). Spectral characteristics are in agreement with those reported in the literature.[119]

_N_-Hydroxy-4-nitrobenzimidoyl chloride 228[124]



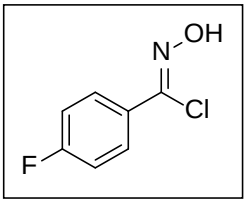
To a solution of the oxime **217** (4 g, 24.1 mmol, 1 eq) in DMF (35 mL) was added the first portion of NCS (0.578 g, 0.043 mmol, 0.2 eq) and the reaction mixture is heated to 40°C. A small amount of HCl gas, extracted from the headspace of a conc. HCl bottle, is bubbled through the solution to initiate the reaction.[125] The remaining portion of NCS (2.61 g, 0.196 mmol, 0.8 eq) was added in small portions over 20 min while keeping the reaction temperature below 45°C. The mixture was stirred at room temperature overnight, poured on to water (300 mL) and extracted with ether (3 x 90 mL). The organic layers were combined and washed with brine (20 mL), dried with $MgSO_4$ and concentrated under reduced pressure to give the imidoyl chloride **228** as a pale yellow crystalline solid (3.68 g, 76%). mp: 124-125 °C; ν_{max}/cm^{-1} (neat) 3112, 1601, 1523; δ_H (300 MHz, $CDCl_3$) 8.04 (2H, d, *J* 9.0, 2 x Aromatic CH), 8.26 (2H, d, *J* 9.0, 2 x Aromatic CH), 8.41 (1H, br s, OH),; δ_C (75.5 MHz) 123.6 (CH, 2 x Aromatic CH), 128.0 (CH, 2 x Aromatic CH), 138.21 (Cq, Aromatic Cq-NO_2), 138.25 (Cq, 1 x Aromatic Cq), 145.5 (Cq, C=N).

4-(*tert*-Butyl)-*N*-hydroxybenzimidoyl chloride 231[127]



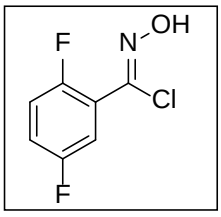
To a solution of the oxime **220** (0.500 g, 0.28 mmol, 1 eq) in DMF (3 mL) was added one fifth of the NCS (0.75 g, 0.056 mmol, 0.2 eq) and the reaction mixture is heated to 40°C. A small amount of HCl gas, extracted from the headspace of a conc. HCl bottle is bubbled through the solution to initiate the reaction.[125] The remaining portion of NCS (0.300 g, 0.224 mmol, 0.8 eq) was added in small portions over 20 min while keeping the reaction temperature below 45°C. The mixture was stirred at room temperature overnight, poured onto water (30 mL) and extracted with ether (3 x 10 mL). The organic layers were combined and washed with brine (10 mL), dried with $MgSO_4$ and concentrated under reduced pressure to give the imidoyl chloride **231** as a colourless oily residue (0.435 g, 73%). ν_{max}/cm^{-1} (neat) 2962, 1607, 1249, 936; δ_H (400 MHz, $CDCl_3$) 1.30 (9H, s, 3 x CH_3), 7.40 (2H, d, *J* 8.8, 2 x Aromatic CH), 7.75 (2H, d, *J* 8.8, 2 x Aromatic CH), 9.85 (1H, s, OH). δ_C (100 MHz, $CDCl_3$) 31.2 (3 x CH_3), 34.9 [Cq, Cq(CH_3)$_3$], 125.6 (CH, 2 x Aromatic CH), 127.1 (CH, 2 x Aromatic CH), 129.8 (Cq, 1 x Aromatic Cq), 140.1 (Cq, C=N), 154.1 (Cq, 1 x Aromatic Cq). HRMS (ESI+): Exact mass calculated for $C_{11}H_{15}NO^{35}Cl$ $[M+H]^+$, 212.0842. Found 212.0839.

4-Fluoro-*N*-hydroxybenzimidoyl chloride 229[129]



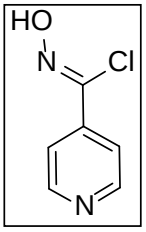
To a solution of the oxime **218** (1.65 g, 11.86 mmol, 1 eq) in DMF (12 mL) was added NCS (0.28 g, 2.37 mmol, 0.2 eq) in one portion. The reaction mixture was heated to 40°C, a small amount of HCl gas, extracted from the headspace of concentrated HCl bottle was bubbled through the solution to initiate the reaction.[125] The remaining NCS (1.25 g, 9.48 mmol, 0.80 eq) was added portionwise while keeping the reaction temperature below 45°C. The mixture was stirred at room temperature overnight, poured onto water (120 mL) and extracted with ether (3 x 30 mL). The organic layers were combined and washed with brine (30 mL), dried with $MgSO_4$, and concentrated under reduced pressure to give the imidoyl chloride **229** as a white crystalline solid (~92% pure, 8% residual starting material **218**) (0.79 g, 36%*). mp 59 - 61° C; ν_{max}/cm^{-1} (neat) 3368, 1598, 1505, 1234; δ_H (400 MHz, $CDCl_3$) 7.09 (2H, t, *J* 9.7, 8.3, 2 x Aromatic CH), 7.81 – 7.84 (2H, m, 2 x Aromatic CH), 8.64 (1H, br s, OH); δ_C (100 MHz, $CDCl_3$) 115.7 (2 x CH, d, $^2J_{CF}$ 22.4, 2 x Aromatic CH), 128.6 (d, $^4J_{CF}$ 3.3, 1 x Aromatic Cq), 129.3 (2 x CH, d, $^3J_{CF}$ 8.8, 2 x Aromatic CH), 139.1 (Cq, C=N), 164.2 (Cq, 1 x Aromatic CF, d, $^1J_{CF}$ 251.6); HRMS (ESI+): Exact mass calculated for $C_7H_5{}^{35}ClFNO$ $[M+H]^+$, 174.0122 Found 174.0115. *Corrected yield for the presence of the residual starting material.

2,5-difluoro-*N*-hydroxybenzimidoyl chloride 230[127]



To a solution of the oxime **219** (1.37 g, 8.7 mmol, 1 eq) in DMF (8 mL) was added NCS (0.26 g, 1.74 mmol, 0.2 eq) in one portion. The reaction mixture was heated to 40°C. a small amount of HCl gas, extracted from the headspace of a bottle was bubbled through the solution to initiate the reaction.[125] The remaining NCS (1.07 g, 6.96 mmol, 0.8 eq) was added in small portions while keeping the reaction temperature below 45°C. The mixture was stirred at room temperature overnight, poured onto water (80 mL) and extracted with ether (3 x 30 mL). The organic layers were combined and washed with brine (30 mL), dried with $MgSO_4$ and concentrated under reduced pressure to give the crude product as a white solid. This was recrystallized from DCM/hexane to give the desired product as a white crystalline solid **230** (1.53 g, 93 %). mp 118 - 120° C; ν_{max}/cm^{-1} (neat) 3283, 1490, 1167, 990; δ_H (400 MHz, $CDCl_3$) 7.11 – 7.15 (2H, m, 2 x Aromatic CH), 7.38 – 7.41 (1H, m, 1 x Aromatic CH) 8.81 (1H, br s, OH); δ_C (100 MHz, $CDCl_3$) 117.3 (CH, dd, $^2J_{CF}$ 18.4, $^3J_{CF}$ 10.0, ArCH-3), 117.9 (CH, dd, $^2J_{CF}$ 23.1, $^3J_{CF}$ 10.4, ArCH-6), 118.7 (CH, dd, $^2J_{CF}$ 19.1, $^3J_{CF}$ 13.7, ArCH-4), 122.1 (dd, $^2J_{CF}$ 12.7, $^3J_{CF}$ 9.0, ArC-1), 134.3 (d, $^3J_{CF}$ 4.7, C=N), 155.9 (dd, $^1J_{CF}$ 253.2, $^4J_{CF}$ 4.0, 1 x ArCF), 158.2 (dd, $^1J_{CF}$ 245.3, $^4J_{CF}$ 4.0, 1 x ArCF); HRMS (ESI+): Exact mass calculated for $C_7H_5NOF_2{}^{35}Cl$ $[M+H]^+$, 192.0028 Found 192.0029.

_N_-Hydroxyisonicotinimidoyl chloride 232[130]

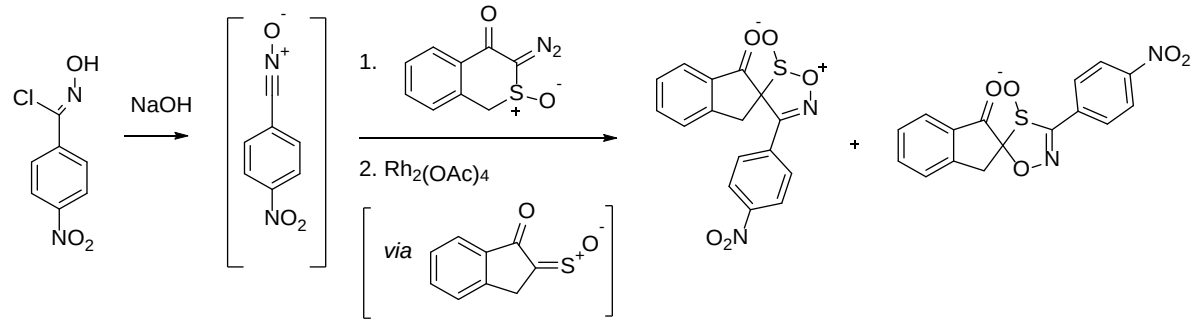


A solution of the oxime **221** (3.20 g, 26.2 mmol, 1 eq) in DMF (25 mL) was heated to 50°C. NCS (3.49 g, 26.2 mmol, 1 eq) was added portionwise over 15 min. A small amount of HCl gas, extracted from the headspace of a bottle was bubbled through the solution to initiate the reaction.[125] The mixture was stirred at this temperature for 5 h, poured onto water (250 mL) and extracted with ether (3 x 80 mL). The organic phase was washed with brine (60 mL), dried with $MgSO_4$ and concentrated under reduced pressure to give the imidoyl chloride **232** as a pale brown crystalline solid (1.64 g, 40 %). mp 142 - 143° C; ν_{max}/cm^{-1} (neat) 1601, 1009, 683; δ_H (400 MHz, DMSO-d_6) 7.76 (2H, d, *J* 4.7, 2 x Aromatic CH), 8.69 (2H, d, *J* 4.7, 2 x Aromatic CH), 13.00 (1H, br s, OH); δ_C (100 MHz, DMSO-d_6) 120.7 (CH, 2 x Aromatic CH), 133.7 (Cq, Aromatic Cq), 140.66 (Cq, C=N), 149.5 (CH, 2 x Aromatic CH). HRMS (ESI+): Exact mass calculated for $C_6H_6N_2O^{35}Cl$ $[M+H]^+$, 157.0169. Found 157.0179. Spectral characteristics are consistent with those reported in the literature.[130] Minor peaks belonging to an unidentified impurty observed in the ^{13}C NMR spectra include signals at 122.8, 150.3 and 166.0 ppm.

3.7 1,3-Dipolar cycloaddition reaction

3.7.1 Nitrile oxide and ketone derived α-oxo sulfine dipolar cycloaddition reactions

Note: The isolated yields described for this section are of the isolated pure material only. In most cases, more of the cycloadduct was present in other fractions with other components. The fractions isolated by column chromatography were evaporated to dryness, test tube by test tube to isolate pure compounds both for spectroscopic analysis and biological activity screening. This approach was necessary in separating diastereomers and regiosisomers all of similar polarity.



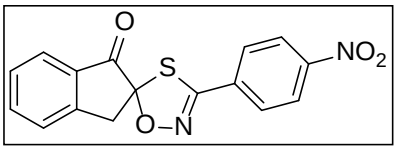
Scheme 144

3.7.1.1 Optimisation reactions for the dipolar cycloadditons of nitrile oxide and ketone derived α-oxo sulfine.

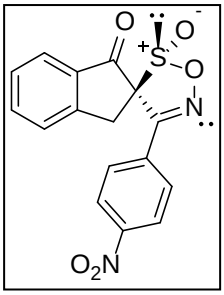
Method 1: Batch reaction conditions, rhodium acetate as catalyst, 1 h.

The imidoyl chloride **228** (0.278 g, 1.38 mmol, 2.3 eq) was added portionwise over 10 min, at room temperature to a vigorously stirred solution of aqueous NaOH (1M, 10 mL) and dichloromethane (10 mL). After complete addition, the mixture was stirred for a further 10 min. The layers were separated, and the organic layer was dried with anhydrous $MgSO_4$ and concentrated under reduced pressure. The white solid was dissolved in 1 : 1 dichloromethane/ethyl acetate (1 : 1, 5 mL) and the α-diazosulfoxide **14** (0.122 g, 0.59 mmol, 1 eq) was added in one portion as a solid, followed by rhodium acetate dimer (0.013 g, 5 mol %). The solution gradually changed colour from red/brown to orange. After stirring for 1 h the reaction mixture was monitored by ^{1}H NMR spectroscopy which showed complete consumption of both the α-diazosulfoxide **14** and intermediate sulfine **13**. The reaction mixture was concentrated *in vacuo* to give the crude product as a brown solid and a mixture of components by ^{1}H NMR analysis. The mixture consisted of the major kinetic 1,2,5-oxathiazole-*S*-oxide **236**, the minor thermodynamic 1,2,5-oxathiazole-*S*-oxide **237**, a 1,4,2-oxathiazole-*S*-oxide Regioisomer B **238** and a 1,4,2-oxathiazole **239** in the ratio of 40 : 29 : 22 : 9. The crude reaction mixture was dissolved in DCM

and purified by column chromatography on silica gel using gradient hexane-ethyl acetate as eluent (100 : 0 – 20 : 80), leading to the elution of two distinct fractions. The less polar fraction to elute was the 1,4,2-oxathiazole **239** (0.031 g, 15%); mp 175 – 177°C; ν_{max}/cm^{-1} (neat) 1715, 1597, 1518; δ_H (400 MHz, $CDCl_3$) 3.82 (1H, d, *J* 17.9, A of AB_q, one of $ArCH_2$), 3.95 (1H, d, *J* 17.9, B of AB_q, one of $ArCH_2$), 7.48 – 7.53 (2H, m, 2 x Aromatic CH), 7.72 – 7.76 (1H, m, 1 x Aromatic CH), 7.87 – 7.91 (3H, m, 3 x Aromatic CH), 8.30 (2H, d, *J* 7.8, 2 x Aromatic CH); δ_C ($CDCl_3$, 100 MHz) 42.3 (CH_2, $ArCH_2$), 102.2 (Cq, C_{spiro}), 124.1 (CH, 2 x Aromatic CH), 126.0, 126.4 (CH, 2 x Aromatic CH), 128.9 (CH, 2 x Aromatic CH), 129.1 (CH, 1 x Aromatic CH), 131.2 (Cq, Aromatic Cq), 132.2 (Cq, Aromatic Cq), 133.4 (Cq, Aromatic Cq), 137.0 (CH, 1 x Aromatic CH), 149.1 (Cq, Aromatic Cq), 153.3 (Cq, C=N), 195.6 (Cq, C=O). Signal belonging to an unknown impurity present in about 10% are at 3.25 (1H, d, *J* 18.5), 3.39 (1H, d, *J* 18.5), 6.63 (1H, d, *J* 8.9).



The more polar second fraction to elute was the kinetic isomer **236** (0.048 g, 24%); mp 168 - 170°C; ν_{max}/cm^{-1} (neat) 1711, 1517; δ_H (400 MHz, $CDCl_3$) 3.61 (1H, d, *J* 18.3, A of AB_q, one of $ArCH_2$), 3.88 (1H, d, *J* 18.3, B of AB_q, one of $ArCH_2$), 7.62 (2H, t, *J* 8.3, 2 x Aromatic CH), 7.67 (2H, d, *J* 8.8, 2 x Aromatic CH_2, 7.81 – 7.89 (1H, m, 1 x Aromatic CH), 7.97 (1H, d, *J* 7.6, 1 x Aromatic CH), 8.21 (2H, d, *J* 8.9, 2 x Aromatic CH); δ_C ($CDCl_3$, 100 MHz) 31.5 (CH_2, $ArCH_2$), 92.5 (Cq, C_{spiro}), 124.4 (CH, 2 x Aromatic CH), 125.9, 127.2 (CH, 2 x Aromatic CH), 129.2 (CH, 2 x Aromatic CH), 129.8 (CH, 1 x Aromatic CH), 131.6, 136.2 (Cq, 2 x Aromatic Cq), 137.3 (CH, 1 x Aromatic CH), 148.8 (Cq, 1 x Aromatic Cq), 149.4 (Cq, 1 x Aromatic Cq), 157.5 (Cq, C=N), 190.4 (Cq, C=O).



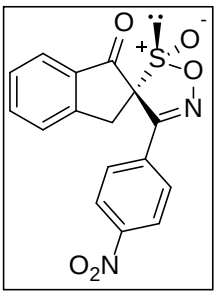
Characteristic signals of the 1,4,2-oxathiazole-*S*-oxide Regioisomer B **238** are 3.70 and 4.21 ppm in the ^{1}H NMR spectrum.

Note: As the ^{13}C NMR spectrum was carried out approx. 5 h after the first ^{1}H NMR spectrum of the isolated column fraction, some interconversion from the kinetic diastereomer **236** to the thermodynamic diastereomer **237** was observed (Table 60, entry 2). Characteristic signals of the thermodynamic isomer **237** (< 10%) can be observed at 3.42 and 4.12 ppm in the ^{1}H NMR spectrum and 28.4 and 96.6 ppm in the ^{13}C NMR spectrum. As the interconversion from the kinetic isomer to the thermodynamic isomer progressed, the change was monitored by ^{1}H NMR spectroscopy.

Table 60: After purification of the crude matierial by column chromatography the column fraction that contained the kinetic isomer was monitored by ^{1}H NMR to observe the interconversion from the kinetic isomer **236** *to the thermodynamic isomer* **237**.

Entry	Time	Ratio of products **236 : 237** **kinetic : thermodynamic**
1	5 h after reaction stopped. (This is the time difference between obtaining the ^{1}H NMR spectrum of the crude material and isolating the kinetic isomer only, from the reaction mixture, by column chromatography on silica gel)	1 : 0
2	10 h after reaction stopped [The ^{1}H NMR of the fraction from the column was obtained (entry 1) and left in deuterated chloroform for a further 5 h while waiting to obtain the ^{13}C NMR spectrum]	9 : 1
3	4 weeks (The sample was left in toluene/dichloromethane attempting to grow a single crystal)	55 : 45

A single crystal from this fraction, ca. 3 weeks after isolation from the reaction mixture (which was originally 100% kinetic isomer **236**) was selected and the corresponding structure solved. Subsequent analysis of the crystal by ^{1}H NMR spectroscopy on a 600 MHz NMR spectroscopy showed the material to be the opposite diastereomer (**237**) to which was originally present (**236**).



237; mp 159-161°C; ν_{max}/cm^{-1} (neat) 1699, 1522, 1345; δ_H (400 MHz, $CDCl_3$) 3.42 (1H, d, *J* 19.3, A of AB_q, CH_2), 4.12 (1H, d, *J* 19.3, B of AB_q, CH_2), 7.52 (2H, d, *J* 8.9, 2 x ArH on $ArNO_2$), 7.62 (2H, t, *J* 8.2, 7.2 2 x Aromatic CH), 7.84 (1H, t, *J* 7.4, 8.4, 1 x Aromatic CH), 7.99 (1H, d, *J* 7.7, 1 x Aromatic CH) 8.23 (2H, d, *J* 8.9, 2 x ArH on $ArNO_2$); HRMS (ESI+) Exact mass calculated for $C_{16}H_{11}N_2O_5S$ $[M+H]^+$, 343.0389. Found: 343.0388

Note: A ^{13}C NMR spectrum was not obtained of the crystal, however the thermodynamic isomer **237**, was later fully characterised from another reaction (see **Method 2**).

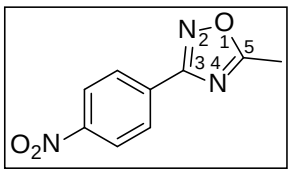
The relative stereochemistry of the thermodynamic isomer **237** was established by single crystal X-ray diffraction on a crystal grown by slow recrystallization from dichloromethane and toluene over 4 - 5 weeks.

Crystal data for **237**: $C_{16}H_{10}N_2OS$, *Mr* = 342.32 , triclinic *P*-1, a = 7.5520(11) Å, b = 8.2283(11) Å, c = 12.8010(18) Å, α = 74.726 (4), β =86.674 (5)°, γ = 72.819 (4) *V* = 732.95 (18) Å^3, *Z* = 2, D_c = 1.55 g cm^{-3}, F_{000} = 352, Mo Kα radiation, λ = 0.7107 Å, *T* = 300(2) K, $2\theta_{max}$ = 26.40°, μ = 0.252 mm^{-1}, 15211 reflections

collected, 2275 unique (R_{int} = 0.0445), final GooF = 1.054, R_1 = 0.0510, wR_2 = 0.1583 (2275 obs. data: $I > 2\sigma(I)$); R_1 = 0.0643, wR_2 = 0.1729 (all data).

Method 2: Thermolysis in batch reaction conditions, 4 equivalents of dipole.

The imidoyl chloride **228** (0.108 g, 2 mmol, 4 eq) was added portionwise as a solid, over 10 min, to a mixture of aqueous NaOH (1M, 20 mL) and DCM (10 mL). After complete addition the biphasic mixture was stirred for ten min. The layers were separated, and the organic layer was dried with $MgSO_4$ and concentrated under reduced pressure to approx. 5 mL DCM. The α-diazosulfoxide **14** (0.105 g, 0.5 mmol, 1 eq) was dissolved in acetonitrile (5 mL) and added to the pre-generated dipole. The mixture was heated under reflux while stirring under a nitrogen atmosphere. The reaction mixture was analysed by withdrawing an aliquot, concentration under reduced pressure, and analysis by ^{1}H NMR in time intervals as per Table 61 to determine the ratio of products **236** and **237** (Table 61). After stirring for 7 h the reaction mixture was concentrated under reduced pressure to give a mixture of the the kinetic isomer **236**, the thermodynamic isomer **237**, and an acetonitrile cycloadduct **242** in a ratio of 1 : 3.3 : 11.3. Purification was undertaken by column chromatography on silica gel using gradient hexane-ethyl acetate as eluent (100 : 0 – 20 : 80). The desired thermodynamic isomer **237** was isolated as a white crystalline solid (0.042 g, 25%) and the ^{1}H NMR characteristics are in agreement with those outlined above. δ_C ($CDCl_3$, 100 MHz) 28.4 (CH_2, $ArCH_2$), 96.6 (Cq, C_{spiro}), 124.5 (CH, 2 x Aromatic CH), 126.3, 127.1 (CH, 2 x Aromatic CH), 129.1 (CH, 2 x Aromatic CH), 129.6 (CH, Aromatic CH), 131.9, 134.0 (Cq, 2 x Aromatic Cq), 137.5 (CH, 1 x Aromatic CH), 149.5, 151.2 (Cq, 2 x Aromatic Cq), 156.5 (Cq, C=N), 192.0 (Cq, C=O). HRMS (ESI+) Exact mass calculated for $C_{16}H_{11}N_2O_5S$ $[M+H]^+$, 343.0389. Found: 343.0388



The oxadiazole 5-methyl-3-(4-nitrophenyl)-1,2,4-oxadiazole **242** (0.045, 42%). Mp 132 – 133 °C; ν_{max}/cm^{-1} (neat) 1347, 1511, 1582; δ_H (400 MHz, $CDCl_3$) 2.70 (3H, s, CH_3), 8.26 (2H, d, *J* 8.9, 2 x Aromatic CH_2), 8.34 (2H, d, *J* 8.9 2 x Aromatic CH); δ_C ($CDCl_3$, 100 MHz) 12.4 (CH_3, $CqCH_3$), 124.1 (CH, 2 x Aromatic CH), 128.3 (CH, 2 x Aromatic CH), 132.7 (Cq, Aromatic Cq), 149.4 (Cq, Aromatic Cq-NO_2), 166.9 [Cq, C(3)=N], 177.4 [Cq, C(5)=N]; HRMS (ESI+) Exact mass calculated for $C_9H_8N_3O_3$ $[M+H]^+$, 206.0566. Found: 206.0563.

Table 61: The interconversion between the thermodynamic isomer **237** *and the kinetic isomer* **236** *was monitored over time, at reflux conditions.*

Entry	Time (h)	Ratio of products[a] 236 : 237 : 242
1	0.5	1 : 1.2 : 5.3
2	3.5	1 : 2.6 : 10
3	7.0	1 : 3.3 : 11.3

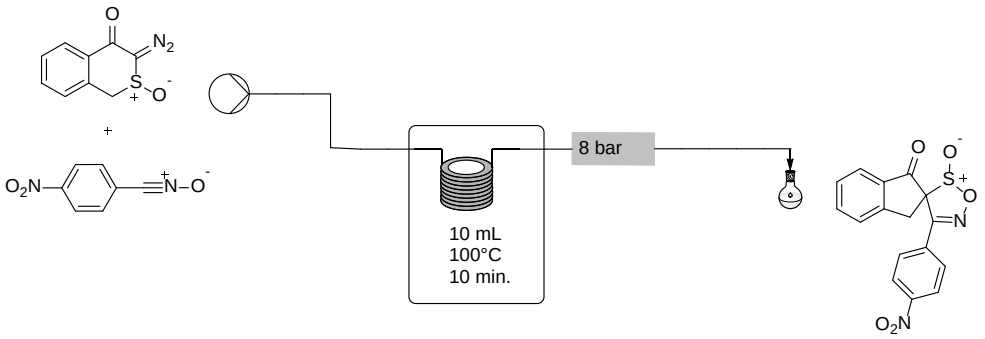
[a] The ratio of products **236** to **237** was determined by integration of the diasterotopic AB quartet system in the ^{1}H NMR spectra.

Method 3: Batch reaction conditions, rhodium acetate as catalyst, 4 equivalents of dipole and 1.5 h reaction time.

The imidoyl chloride **228** (0.249 g, 1.24 mmol, 4 eq) was added portionwise over 10 min, at room temperature to a vigorously stirred solution of aqueous NaOH (1M, 10 mL) and dichloromethane (10 mL). After complete addition, the mixture was stirred for a further 10 min. The layers were separated, and the organic layer dried with $MgSO_4$ and concentrated under reduced pressure to approximately half the initial volume. The α-diazosulfoxide **14** (0.064 g, 0.31 mmol, 1 eq) was added in one portion, followed by rhodium acetate dimer (0.013 g, 5 mol %). The solution gradually changed colour from red/brown to orange and nitrogen evolution was observed. After stirring for 1.5 h an aliquot was taken from the reaction mixture and was checked by ^{1}H NMR spectroscopy. The resulting spectrum showed no signals corresponding to either the α-diazosulfoxide **14** or the intermediate sulfine **13**. The reaction mixture was concentrated *in vacuo* to give the crude product as a brown solid (0.196 g) and a mixture of the kinetic product **236** and the thermodynamic product **237** in a ratio of 4 : 3. The crude reaction mixture was dissolved in DCM and purified by column chromatography on silica gel using gradient hexane-ethyl acetate as eluent (100 : 0 – 20 : 80), leading to elution of a mixture of the thermodynamic cycloadduct **237** and the kinetic cycloadduct **236** in a ratio of 76 : 24 and as an off white crystalline solid (0.018 g, 17%). Spectral characteristics are in agreement with those outlined above.

Minor signals for the 1,4,2-oxathiazole-*S*-oxide Regioisomer B **238** are seen at 3.70 and 4.21 ppm in the ^{1}H NMR spectrum of the crude material.

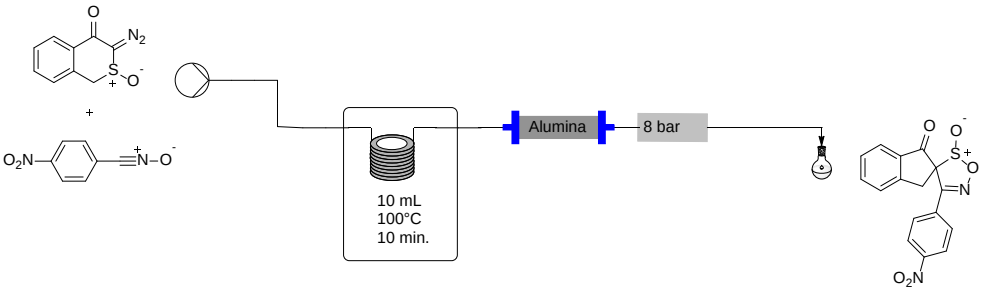
Method 4: Thermolysis in continuous flow with a 10 min residence time and dichloromethane as solvent.



Scheme 145

The dipole **235** was generated using the protocol described in method 1 above using the imidoyl chloride **228** (0.543 g, 2.71 mmol, 4 eq). After concentration *in vacuo* the dipole **235** was isolated as a white solid and dissolved in dichloromethane (15 mL). The α-diazosulfoxide **14** (0.140 g, 0.67 mmol, 1 eq) was added to the solution of the dipole **235** in dichloromethane as a solid in one portion and spontaneously dissolved to give a deep red solution. This solution was pumped through a 10 mL reactor coil heated to 100°C, at a rate of 1 mL/min giving a residence time of 10 min. After the reactor coil, precipitation was observed in the lines and before the back pressure regulator, caused by cooling of the solution. The crude reaction mixture was collected and concentrated *in vacuo*. Analysis by ^{1}H NMR indicated 100% consumption of the α-diazosulfoxide starting material **14** to form a mixture of products. The products formed were the kinetic 1,2,5-oxathiazole-*S*-oxide diastereomer **236**, the thermodynamic diastereomer **237** and an unknown in the ratio of 1 : 2 : 1. Due to the mass loss that occurred from the blockages and resolving this issue, the crude material was not purified to obtain a yield. The characteristic signals of the unidentified impurity are singlets at 3.76 and 4.4 ppm.

Method 5: Thermolysis in continuous flow with a 10 min residence time, alumina column inline and ethyl acetate/dichloromethane as solvent.



Scheme 146: Thermolysis in continuous flow followed by alumina column.

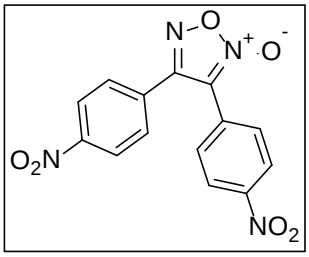
The dipole **235** was generated using the protocol described in method 1 above using the imidoyl chloride **228** (0.203 g, 1.01 mmol, 2 eq). After concentration *in vacuo* the dipole **235** was isolated as a

white solid and dissolved in ethyl acetate/dichloromethane (1 : 1, 5 mL). The α-diazosulfoxide **14** (0.105 g, 0.51 mmol, 1 eq) was disolved in ethyl acetate/dichloromethane (1 : 1, 5 mL) and subsequently added to the solution of the dipole **235**. This solution was pumped through a 10 mL reaction coil heated to 100°C at a rate of 1 mL/min giving a residence time of 10 min, followed by a 10 mm id Omnifit™ glass column packed with Alumina (volume ~ 1 mL).[136] The crude material was collected as an orange solution and concentrated under reduced pressure to give the crude product as an orange crystalline solid (0.195 g). Analysis by ^{1}H NMR spectroscopy showed the material to be a mixture of the thermodynamic (**237**) and kinetic (**236**) cycloadducts along with a Regioisomer B (**238**) and an unknown impurity* (56 : 10 : 14 : 30). The crude material was re-slurried in ether and stirred for 10 mins, following trituration with ether, isolation of a crop of the thermodynamic isomer **237** was achieved as an off white crystalline solid (0.089 g, 52%). **Note:** An unusual doubling of signals occurred in the ^{1}H NMR spectrum of the isolated material.

*The characteristic signal of the impurity in the ^{1}H NMR spectra of the crude material is a singlet at 3.76 ppm.

Method 6: Microwave irradiation, dichloromethane as solvent, 100°C.

The dipole **235** was generated using the protocol described in method 1 above using the imidoyl chloride **228** (0.235 g, 1.17 mmol, 2.5 eq). After concentration *in vacuo* the dipole **235** was isolated as a white solid and dissolved in dichloromethane (4 mL). The α-diazosulfoxide **14** (0.100 g, 0.46 mmol, 1 eq) was added as a solid in one portion. The reaction mixture was heated in the microwave at 100°C for 10 min with a ramp time of 3 min and a cool down time of 8 min. The crude reaction mixture was a brown solution and after concentration under reduced pressure the crude product was isolated as a brown solid (0.236 g). Analysis of the crude reaction mixture by ^{1}H NMR spectroscopy showed the presence of the kinetic isomer **236**, the thermodynamic isomer **237,** the Regioisomer B **238** and an unknown (characteristic signal as a singlet at 3.76 ppm in the ^{1}H NMR spectrum) in the ratio of 9 : 81 : 5 : 5. Purification of the crude reaction mixture was carried out by column chromatography on silica gel using hexane/ethyl acetate as eluent. The first fraction to elute contained the furoxan dimer **344** as a white crystalline solid.[180] δ_H (400 MHz, $CDCl_3$) 7.70 – 7.78 (4H, m, 4 x Aromatic CH), 8.31 – 8.41 (4H, m, 4 x Aromatic CH); δ_C ($CDCl_3$, 100 MHz) 112.5 (Aromatic Cq), 124.5, 124.6 (2 x 2 x Aromatic CH), 128.5 (Aromatic Cq), 129.5, 129.6 (2 x 2 x Aromatic CH), 132.0 (Aromatic Cq), 148.8 (Aromatic Cq), 149.6 (C=N), 154.0 (C=N); m/z 329 ($M+H^+$, 20%), HRMS (ESI+) Exact mass calculated for $C_{14}H_9N_4O_6$ $[M+H]^+$, 329.0522, Found: 329.0516. The characteristic details are in agreement with the literature. [180]



The second fration to elute was the thermodynamic isomer **237** as a white crystalline solid (0.029 g, 18%). Spectral characteristics are consistent with those reported above.

Method 7: Literature procedure for the synthesis of a 1,2,5-oxathiazole-*S*-oxide.[137]

The imidoyl chloride **228** (0.091 g, 0.45 mmol, 1 eq) was added portionwise over 10 min, at room temperature to a vigorously stirred solution of aqueous NaOH (1M, 10 mL) and dichloromethane (10 mL). After complete addition, the mixture was stirred for a further 10 min. The layers were separated and the organic layer was dried with $MgSO_4$ and concentrated under reduced pressure give the dipole **235** as a crystalline white solid. The solid was dissolved in ether (10 mL) and cooled to -20°C. The α-diazosulfoxide **14** (0.092 g, 0.45 mmol, 1 eq) was added in one portion, followed by rhodium acetate dimer (0.005 g, 1 %). The α-diazosulfoxide **14** had not dissolved in the ether after stirring for 1 h and so dichloromethane (5 mL) was added to the flask. The reaction mixture was stirred for a further 2 h. At this point, the reaction mixture was concentrated under reduced pressure to give a brown solid as the crude product (0.128 g). Analysis by ^{1}H NMR spectroscopy showed a complex mixture of products with trace amounts of the cycloadducts present and the α-oxo sulfine (characteristic peak is a singlet at 4.26 ppm in the ^{1}H NMR spectrum) as the major component. The crude mixture was not purified by column chromatography.

Method 8: Thermolysis in continuous flow with a 30 min residence time and 2 equivalents of dipole.

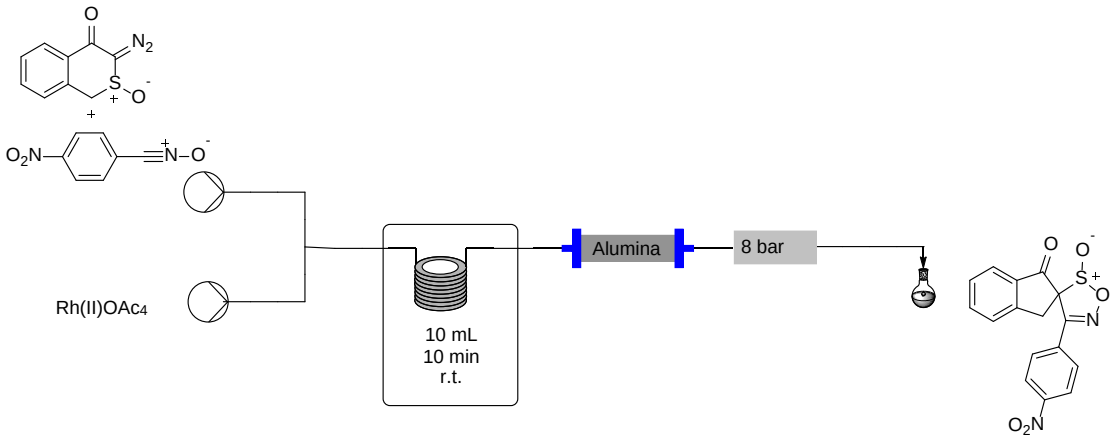
The dipole **235** was generated using the protocol described in method 1 above using the imidoyl chloride **228** (0.201 g, 1.01 mmol, 2 eq). After concentration *in vacuo* the dipole **235** was isolated as a white solid and dissolved in ethyl acetate/dichloromethane 1:1 (15 mL). The α-diazosulfoxide **14** (0.105 g, 0.51 mmol, 1 eq) was added to this solution in one portion. This solution was pumped through a 10 mL reaction coil heated to 100°C, with a residence time of 30 min, followed by a 10 mm id Omnifit™ glass column packed with Alumina (volume ~ 1 mL). The crude material was collected as an orange solution and concentrated under reduced pressure to give the crude product as an orange crystalline solid (0.195 g) consisting of the kinetic isomer **236**, the thermodynamic isomer **237,** the Regioisomer B **238** (10 : 83 : 7) and furoxan dimer **344** (indicated by excess aromatic signals). The ^{1}H NMR of the crude material was very clean (notably with no singlet at 3.7 ppm) however blockages in the line caused mass loss due to cooling and precipitation at the slow flow rate and so the crude product was not purified by column chromatography.

Method 9: Thermolysis in continuous flow with a 10 min residence time and 4 equivalents of dipole.

The dipole **235** was generated using the protocol described in method 1 above using the imidoyl chloride **228** (0.427 g, 2.13 mmol, 4 eq). After concentration *in vacuo* the dipole was isolated as a white

solid and dissolved in ethyl acetate/dichloromethane 1 : 1 (15 mL). The α-diazosulfoxide **14** (0.110 g, 0.53 mmol, 1 eq) was added to this solution in one portion. This solution was pumped through a 10 mL reaction coil heated to 100°C with a residence time of 10 min, followed by a 10 mm id Omnifit™ glass column packed with Alumina (volume ~ 1.5 mL). The orange solution was collected and concentrated under reduced pressure to give the crude product as a bright orange crystalline solid (0.453 g) consisting of the thermodynamic isomer **237**, the kinetic isomer **236,** the Regioisomer **238** (17 : 72 : 11) and furoxan dimer **344** (indicated by excess aromatic signals). Blockages in the line, formed by cooling induced precipitation of the excess dipole/furoxan dimer **344**, caused mass loss due to the slow flow rate and so the crude product was not purified by column chromatography.

Method 10 : Attempting to favour formation of the kinetic isomer in flow using Rhodium acetate dimer as the transition metal catalyst.



Scheme 147

The dipole **235** was generated using the protocol described in method 1 above using the imidoyl chloride **228** (0.096 g, 0.48 mmol, 2 eq). After concentration *in vacuo* the dipole **235** was isolated as a white solid and dissolved in ethyl acetate/dichloromethane 1 : 1 (10 mL). The α-diazosulfoxide **14** (0.05 g, 0.24 mmol, 1 eq) was added to this solution in one portion. Separately, rhodium acetate dimer (1 mg, 1 mol %) was dissolved in dichloromethane : acetonitrile (8 : 2, 10 mL).[30] Both solutions were pumped at a rate of 0.5 mL/min where they met at a T-piece. The combined stream passed through a 10 mL reactor coil at 20°C with a residence time of 10 min followed by a 10 mm id Omnifit™ glass column packed with Alumina (volume ~ 1.0 mL). The orange solution was collected and concentrated under reduced pressure to give the crude product as a bright orange crystalline solid (0.128 g). Analysis by ^{1}H NMR spectroscopy showed the material to be a mix of the kinetic isomer **236**, thermodynamic isomer **237** and the Regioisomer **238** in a ratio of 52 : 38 :10, along with the unknown with a singlet at 3.76 ppm. The reaction mixture was not further purified.

Method 11: Batch reaction conditions, rhodium acetate as catalyst, 30 min at r.t.

The dipole **235** was generated using the protocol described in method 1 above using the imidoyl chloride **193** (0.100 g, 0.98 mmol, 2 eq). After concentration *in vacuo* the dipole was isolated as a white solid and dissolved in ethyl acetate/dichloromethane (1 : 1, 5 mL). The α-diazosulfoxide **14** (0.05 g, 0.24 mmol, 1 eq) was added to this solution in one portion followed by rhodium acetate dimer (1 mg, 1 mol %). The solution underwent a gradual colour change from red to orange and was stirred at room temperature for 30 mins followed by concentration under reduced pressure. The crude product was isolated as an orange crystalline solid (0.131 g). Analysis of the crude material by ^{1}H NMR spectroscopy showed the presence of the kinetic isomer (**236**), thermodynamic isomer (**237**) and Regioisomer B (**238**) in a ratio of 47 : 35 : 18.

The characteristic signal of the 1,4,2-oxathiazole-*S*-oxide Regioisomer B **238** was visible at 4.21 ppm in the ^{1}H NMR spectrum as a 1H, d.

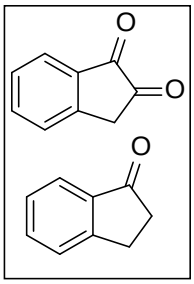
Method 12: Batch reaction conditions, rhodium acetate as catalyst, 30 min at 0°C.

The dipole **235** was generated using the protocol described in method 1 above using the imidoyl chloride **193** (0.100 g, 0.98 mmol, 2 eq). After concentration *in vacuo* the dipole was isolated as a white solid and dissolved in dichloromethane (5 mL). This solution was cooled to 0°C using an ice bath. The α-diazosulfoxide **14** (0.05 g, 0.24 mmol, 1 eq) was added to this solution in one portion followed by rhodium acetate dimer (1 mg, 1 mol %). The solution underwent a gradual colour change from red to orange and was stirred at room temperature for 30 mins followed by concentration under reduced pressure. The crude product was isolated as a red crystalline solid. Analysis of the crude material by ^{1}H NMR spectroscopy showed the kinetic isomer **236**, the thermodynamic isomer **237** and the Regioisomers **238** and **239** in a ratio of 58 : 29 : 3 : 10. Characteristic signals are outlined in **Method 1**.

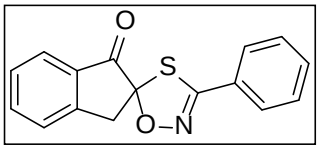
3.7.1.2 Cycloaddition reactions of α-diazosulfoxide 14 with nitrile oxide dipoles under both batch and continuous flow conditions.

Method 1: Batch reaction conditions, rhodium acetate as catalyst, 1 h.

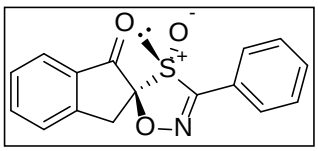
The nitrile oxide dipole **192** was generated using the method previously described in Section 3.7.1, from the imidoyl chloride **193** (0.155 g, 1.00 mmol, 2.3 eq). The solution of dipole **192** was concentrated under reduced pressure and added to the α-diazosulfoxide **14** (0.090 g, 0.43 mmol, 1 eq) in dichloromethane/ethyl acetate (1 : 1, 15 mL). This was followed by the addition of rhodium acetate dimer (0.009 g, 0.02 mmol, 5 mol %). The reaction mixture was stirred at room temperature under a nitrogen atmosphere for 1 h. The crude reation mixture was concentrated under reduced pressure to give the crude material as an orange oil. Analysis of the crude material by ^{1}H NMR spectroscopy showed no signals corresponding to either the α-diazosulfoxide **14**, or the intermediate α-oxo sulfine



13, as well as the presence of the thermodynamic isomer **246**, and trace amounts of diketone rearrangement product **146** and monoketone rearrangement product **142**. The characteristic signal of the diketone product **146** is the 2H singlet at 3.64 ppm and the characteristic signal of the monoketone product **142** is a 2H multiplet at 2.67 – 2.72 ppm and a 2H multiplet at 3.13 – 3.21 ppm as described by Buckley.[16] Purification of the reaction mixture by flash chromatography on silica gel led to the elution of multiple fractions. The first fraction was isolated as a white crystalline solid and was identified as as the furoxan dimer **233**.

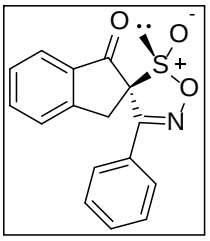


The second fraction to elute was the 1,4,2-oxathiazole **249** as a yellow crystalline solid (0.026 g, 9%); mp 89 – 90°C; ν_{max}/cm^{-1} (neat) 1719, 1273, 1083, 743; δ_H (400 MHz, $CDCl_3$); 3.79 (1H, d, *J* 18.0, A of AB_q, one of CH_2), 3.92 (1H, d, *J* 18.0, B of AB_q, one of CH_2), 7.40 – 7.52 (6H, m, 6 x Aromatic CH), 7.68 – 7.73 (2H, m, 2 x Aromatic CH), 7.89 (1H, d, *J* 7.6, 1 x Aromatic CH); δ_C ($CDCl_3$, 100 MHz); 42.7 (CH_2, $ArCH_2$), 101.1 (Cq, C_{spiro}), 125.8, 126.4 (CH, 2 x Aromatic CH), 127.5 (Cq, 1 x Aromatic Cq), 128.2 (CH, 2 x Aromatic CH), 128.7 (CH, 2 x Aromatic CH), 131.3 (CH, 1 x Aromatic CH), 132.6 (Cq, 1 x Aromatic Cq), 136.7 (CH, 1 x Aromatic CH), 149.2 (Cq, 1 x Aromatic Cq), 155.2 (Cq, C=N), 196.2 (Cq, C=O).



The third fraction was a mixture of thermodynamic isomer **246** and regiosiomer B **248**, regio : thermodynamic, 0.73 : 1, **248** : **246** (spectral characteristics for the thermodynamic isomer **246** described in (**Method 2** below) The material was characterised as a mixture and spectral characteristics for the 1,4,2-oxathiazole-*S*-oxide Regioisomer B **248** are; (0.023 g, 8%); ν_{max}/cm^{-1} (neat) 1714, 1367, 1154; δ_H (400

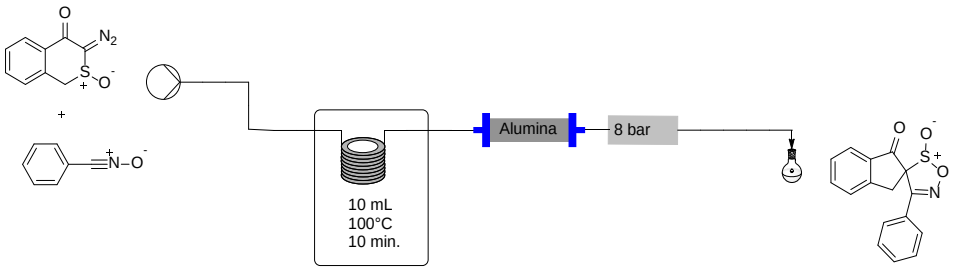
MHz, $CDCl_3$); 3.66 (1H, d, *J* 18.9, A of AB_q, one of CH_2), 4.28 (1H, d, *J* 18.4, B of AB_q, one of CH_2), 7.29 – 7.98 [multiple overlapping signals including (3H, m, 3 x ArH), (3H, m, 3 x Aromatic CH), (1H, m, 1 x Aromatic CH), (1H, m, 1 x Aromatic CH) and (1H, m, 1 x Aromatic CH)]; δ_C ($CDCl_3$, 100 MHz); 28.6 (CH_2, $ArCH_2$), 110.8 (Cq, C_{spiro}), 125.6 (Cq, Aromatic Cq), 125.7, 126.8 (CH, 2 x Aromatic CH), 127.6 (1 x Aromatic Cq), 128.7 (2 x Aromatic CH), 128.8 (1 x Aromatic CH), 129.5 (CH, 2 x Aromatic CH), 133.0 (Cq, Aromatic Cq), 137.1 (CH, Aromatic CH), 149.0 (Cq, Aromatic Cq), 158.7 (Cq, C=N), 193.2 (Cq, C=O); (M+H) 298 (30%); HRMS (ESI+) Exact mass calculated for $C_{16}H_{11}NO_3S$ $[M-H]^+$, 298.0538. Found: 298.0533



The fourth fraction contained the kinetic diastereomer **247** (0.014 g 6%). ν_{max}/cm^{-1} (neat) 1716, 1601, 1168, 760; δ_H (400 MHz, $CDCl_3$); 3.64 (1H, d, A of AB_q *J* 18.8, one of CH_2), 3.83 (1H, d, B of AB_q, *J* 18.2, one of CH_2), 7.34 – 8.10 [overlapping signals including (2H, t, *J* 7.6, 8.1, 2 x ArH), a (3H, m, 3 x Aromatic CH), a (2H, m, 2 x Aromatic CH), a (1H, t, *J* 7.3, 8.5, 1 x Aromatic CH) and (1H, d, *J* 7.8 1 x Aromatic CH).

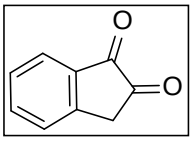
Note: *On obtaining a ^{13}C NMR spectrum of the sample on 600MHz after a period of approximately 8 months, the ^1H NMR showed 90% conversion to the thermodynamic diastereomer* **246***. Characteristic signals in the ^{13}C NMR include; 31.9 (CH_2) and 97.4 (C_{spiro}). And in the ^1H NMR spectrum signals corresponding to the thermodynamic isomer* **246** *were seen at 3.49 and 4.07 ppm.*

Method 2: Thermolysis in continuous flow with a 10 min residence time.

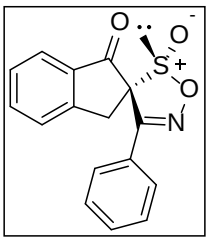


Scheme 148

The imidoyl chloride **193** (0.380 g, 1.90 mmol, 2 eq) was added portionwise over 10 min, at room temperature to a vigorously stirred solution of aqueous NaOH (1M, 10 mL) and dichloromethane (10 mL). After complete addition, the mixture was stirred for a further 10 min. The layers were separated and the organic layer was dried with $MgSO_4$ and concentrated under reduced pressure to half the initial volume. The α-diazosulfoxide **14** (0.196 g, 0.95 mmol, 1 eq) was added and the volume of dichloromethane/ethyl acetate 1:1 made up to 28 mL, (0.034 M). The



solution was pumped through a 10 mL reaction coil heated to 100°C, with a 10 min residence time, followed by a 10 mm id Omnifit™ glass column packed with Alumina (volume ~ 1 mL). The crude reaction mixture was collected as an orange solution and concentrated under reduced pressure to give the crude product as an orange crystalline solid (0.378 g) which on analysis by ^{1}H NMR consisted of the thermodynamic isomer **246**, kinetic isomer **247**, Regioisomer B **248**, Regioisomer A **264** and diketone **146** In a ratio of 63 : 12 : 15 : 7 : 18. The crude reaction mixture was dissolved in the minimum amount of dichloromethane and purified by column chromatography on silica gel to give the thermodynamic isomer **246** as a white crystalline solid (0.089 g, 32%). Found C, 64.41; H 3.91; N 4.77. $C_{16}H_{11}NO_3S$ requires C, 64.63; H 3.73 ; N 4.71; mp 101-102°C; ν_{max}/cm^{-1} (neat) 1713, 1157; δ_H (400 MHz, $CDCl_3$) 3.49 (1H, d, *J* 19.2, A of AB_q, CH_2), 4.07 (1H, d, *J* 19.2, B of AB_q, CH_2), 7.29 – 7.60 (7H, m, 7 x Aromatic CH), 7.79 (1H, t, *J* 8.5, 1 x Aromatic CH), 7.96 (1H, d, *J* 7.8, 1 x Aromatic CH); δ_C ($CDCl_3$, 100 MHz); 28.9 (CH_2, $ArCH_2$), 97.4 (Cq, C_{spiro}), 125.6 (Cq, Aromatic Cq), 126.1, 127.0 (2 x CH, 2 x Aromatic CH), 128.0 (CH, 2 x Aromatic CH), 129.2, (CH, 1 x Aromatic CH), 129.4 (CH, 2 x Aromatic CH), 131.7 (CH, 1 x Aromatic CH), 134.3 (Cq, 1 x Aromatic Cq), 137.1 (CH, 1 x Aromatic CH), 151.6 (Cq, Aromatic Cq), 158.0 (Cq, C=N), 192.6 (Cq, C=O); HRMS (ESI+) Exact mass calculated for $C_{16}H_{10}NO_3S$ $[M-H]^+$, 296.0381. Found: 296.0375.



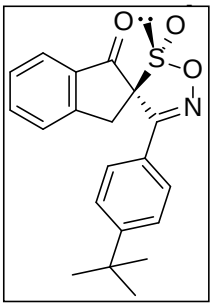
The relative stereochemistry of the cycloadduct **246** was determined by single crystal X-ray diffraction on a crystalline sample of **246**[181] recrystallized from dichloromethane/hexane. Crystals of **246** are triclinic, space group *P* -1. Crystal data for $C_{16}H_{11}NO_3S$, *Mr* = 297.32, a = 7.342 (2) Å, b = 8.954 (3) Å, c = 11.714 (3) Å, α = 70.226 (9)°, β = 83.607 (9)°, γ = 72.230 (9), *V* = 960.1 (3) Å^3, *Z* = 2, D_c = 1.431 g cm^{-3}, F_{000} = 308, Mo Kα radiation, λ = 0.710 Å, *T* = 300 K, $2\theta_{max}$ = 1.000°, μ = .243 mm^{-1}, 6640 reflections collected, 2407 unique (R_{int} = 0.0360), final GooF = 1.055, R_1 = 0.0405, wR_2 = 0.1080 (1976 obs. data: $I > 2\sigma(I)$); R_1 = 0.0503, wR_2 = 0.1166 (all data).

Characteristic signals of the 1,4,2-oxathiazole-*S*-oxide Regioisomer A **264** is a 1H doublet at 3.32 ppm in the ^{1}H NMR spectrum of the crude material. The characteristic signal of the diketone product **146** is the 2H singlet at 3.64 ppm as described by Buckley.[16]

4'-(4-(tert-Butyl)phenyl)spiro[indene-2,3'-[1,2,5]oxathiazol]-1*(3H)*-one *S*-oxide

Method 1: Batch reaction conditions, rhodium acetate as catalyst, 1 h.

The *para*-*t*-butyl nitrile oxide **244** was generated using the method previously described in Section 3.7.1 from the imidoyl chloride **231** (0.403 g, 1.90 mmol, 2.6 eq). The solution was concentrated under reduced pressure and added to the α-diazosulfoxide **14** (0.151 g, 0.73 mmol, 1 eq) in

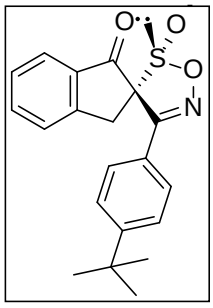


dichloromethane/ethyl acetate (1 : 1, 15 mL). This was followed by the addition of rhodium acetate dimer (0.009 g, 0.02 mmol, 5 mol %). The reaction mixture was stirred at room temperature under a nitrogen atmosphere for 1 h. The reaction mixture was concentrated under reduced pressure to give the crude material as a thick brown oil (0.452 g). Analysis of the crude material by ^{1}H NMR spectroscopy showed no evidence of the α-diazosulfoxide starting material **14** or intermediate sulfine **13**, with the formation of the desired kinetic isomer **254** and a Regiosiomer **255** in a ratio of 80 : 20. Purification of the reaction mixture by flash chromatography on silica gel led to the elution of the kinetic cycloadduct **254** (0.040 g, 16%) white crystalline solid. Mp 128 – 129 °C; ν_{max}/cm^{-1} (neat) 753, 1165, 1712; δ_H (400 MHz, $CDCl_3$); 1.24 (9H, s, 3 x CH_3), 3.62 (1H, d, *J* 18.4, A of AB_q, one of $ArCH_2$), 3.81 (1H, d, *J* 18.4, B of AB_q, one of $ArCH_2$), 7.35 – 7.44 (4H, symmetrical q, *J* 8.7, 4 x Aromatic CH), 7.56 – 7.64 (2H, m, 2 x Aromatic CH), 7.80 (1H, t, *J* 7.5, 2 x Aromatic CH), 7.96 (1H, d, *J* 7.8, 1 x Aromatic CH); δ_C ($CDCl_3$, 100 MHz); 31.0 [CH_3, $C(CH_3)_3$], 32.0 (CH_2, $ArCH_2$), 35.0 [Cq, *C*$(CH_3)_3$], 93.4 (Cq, C_{spiro}), 122.3 (Cq, $CqCH_2$), 125.6 (CH, 1 x Aromatic CH), 126.3 (CH, 2 x Aromatic CH), 127.1 (CH, 1 x Aromatic CH), 128.0 (CH, 2 x Aromatic CH), 129.3 (CH, 1 x Aromatic CH), 136.6 (Cq, Aromatic Cq), 136.8 (CH, Aromatic CH), 149.2 (Cq, Aromatic Cq), 155.6 (Cq, Aromatic Cq-$C(CH_3)_3$), 158.8 (Cq, C=N), 191.0 (Cq, C=O); (M+H) 354 (10%); HRMS (ESI+) Exact mass calculated for $C_{20}H_{20}NO_3S$ $[M-H]^+$, 354.1164. Found: 354.1157.

Characteristic peaks of regiosiomer B **255** are seen at 3.44, 4.19 [2 x (1H, d, *J* 18.8)].

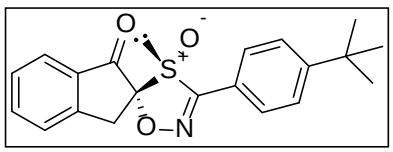
Method 2: Thermolysis in continuous flow with a 10 min residence time.

The imidoyl chloride **231** (0.355 g, 1.29 mmol, 2.6 eq) was converted to the nitrile oxide **244** as described in Section 3.7.1. The solution of the dipole **244** was concentrated under reduced pressure to give the dipole **244** as a yellow oily residue. This residue was dissolved in dichloromethane/ethyl acetate (1 : 1, 5 mL) and added to the α-diazosulfoxide **14** (0.133 g, 0.65 mmol, 1 eq) in dichloromethane/ethyl acetate (1 : 1, 10 mL) This deep orange solution was pumped through a 10 mL reactor coil heated to 100°C followed by a 10 mm id Omnifit™ glass column packed with Alumina (~3 g, volume ~ 1.8 mL, the bed of alumina has narrow beds of acid washed sand at either end), at a flow rate of 1 mL/ min giving a residence time of 10 min. The crude material was collected as an orange solution and concentrated under reduced pressure to give the crude product as a yellow oil (0.243 g) which on analysis by ^{1}H NMR spectroscopy showed the desired thermodynamic isomer **253**, the Regioisomer **265** and the kinetic isomer **254** in a ratio of 78 : 10 : 12. The crude reaction mixture was dissolved in the minimum amount of dichloromethane and purified by column chromatography on



silica gel to give two fractions. The first fraction contained the thermodynamic isomer **253** (0.066 g, 30%); as a yellow crystalline solid; mp 119 – 120°C; ν_{max}/cm^{-1} (neat) 2961, 1712, 1267, 1149; δ_H(400 MHz, $CDCl_3$) 1.29 (9H, s, 3 x CH_3), 3.54 (1H, d, *J* 19.4, A of AB_q, one of $ArCH_2$), 4.08 (1H, d, *J* 19.4, B of AB_q, one of $ArCH_2$), 7.22 – 7.26 (2H, m, 2 x Aromatic CH), 7.35 – 7.37 (2H, m, 2 x Aromatic CH), 7.56 – 7.59 (2H, m, 2 x Aromatic CH), 7.79 (1H, t, *J* 8.5, 1 x Aromatic CH), 7.96 (1H, d, *J* 7.8, 1 x Aromatic CH); δ_C ($CDCl_3$, 100 MHz); 29.0 (CH_2, $ArCH_2$), 31.0 (CH_3, 3 x CH_3), 35.0 [Cq, Cq(CH_3)$_3$], 97.5 (Cq, C_{spiro}), 122.6 (Cq, Aromatic Cq), 126.1 (CH, 1 x Aromatic CH), 126.4 (CH, 2 x Aromatic CH), 127.0 (CH, 1 x Aromatic CH), 127.8 (CH, 2 x Aromatic CH), 129.1 (CH, 1 x Aromatic CH), 134.3 (Cq, Aromatic Cq), 137.0 (CH, Aromatic CH), 151.7 (Cq, Aromatic Cq), 155.4 (Cq, Aromatic Cq), 157.8 (Cq, C=N), 192.7 (Cq, C=O); HRMS (ESI+) Exact mass calculated for $C_{20}H_{20}NO_3S$ $[M+H]^+$, 354.1164. Found: 354.1169.

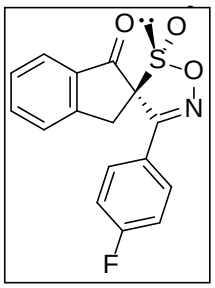
The relative stereochemistry of the cycloadduct **253** was determined by single crystal X-ray diffraction on a crystalline sample of **253**[181] recrystallized from dichloromethane/hexane. Crystals of **253** are monoclinic, space group *P* 21/*c*. Crystal data for $C_{20}H_{19}NO_3S$, *Mr* = 353.42, a = 11 .0131 (2) Å, b = 11.9246 (2) Å, c = 14.5681 (3) Å, $\alpha = \gamma = 90$ °C, $\beta = 107.106$ (10)°, *V* = 1828.55 (6) $Å^3$, *Z* = 4, D_c = 1.284 g cm^{-3}, F_{000} = 744, Cu Kα radiation, λ = 1.541 Å, *T* = 296 K, $2\theta_{max}$ = 0.750°, μ = 1.721 mm^{-1}, 22017 reflections collected, 3172 unique (R_{int} = 0.0256), final GooF = 1.060, R_1 = 0.0549, wR_2 = 0.1588, (3041 obs. data: $I > 2\sigma(I)$); R_1 = 0.0562, wR_2 = 0.1600 (all data).



The second fraction to elute contained the 1,4,2-oxathiazole-*S*-oxide Regioisomer A **265** (0.011 g, 5%) Yellow oil. ν_{max}/cm^{-1} (neat) 2962, 1726, 1272, 1083; δ_H (400 MHz, $CDCl_3$) 1.33 (9H, s, 3 x CH_3), 3.31 (1H, d, *J* 17.3, A of AB_q, one of $ArCH_2$), 3.47 (1H, d, *J* 17.3, B of AB_q, one of $ArCH_2$), 7.74 – 7.57 (4H, m, 4 x Aromatic CH), 7.76 (1H, t, *J* 7.8, 1 x Aromatic CH), 7.87 (2H, d, *J* 7.8, 2 x Aromatic CH), 7.97 (1H, d, *J* 7.8, 1 x Aromatic CH); δ_C ($CDCl_3$, 100 MHz); 31.0 (CH_3, 3 x CH_3), 33.6 (CH_2, $ArCH_2$), 35.2 [Cq, Cq(CH_3)$_3$], 107.9 (Cq, C_{spiro}), 122.1 (Cq, Aromatic Cq), 125.5 (CH, 1 x Aromatic CH), 126.7 (CH, 2 x Aromatic CH), 127.1, (CH, 1 x Aromatic CH), 128.8 (CH, 2 x Aromatic CH), 129.3 (CH, 1 x Aromatic CH), 135.3 (Cq, 1 x Aromatic Cq), 137.0 (CH, 1 x Aromatic CH), 147.5 (Cq, 1 x Aromatic Cq), 156.0 (Cq, 1 x Aromatic Cq), 159.4 (Cq, C=N), 189.2 (Cq, C=O); HRMS (ESI+) Exact mass calculated for $C_{20}H_{20}NO_3S$ $[M+H]^+$, 354.1164. Found: 354.1175.

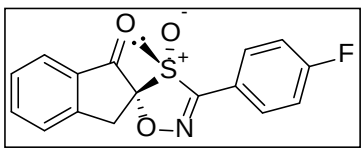
4'-(4-Fluorophenyl)spiro[indene-2,3'-[1,2,5]oxathiazol]-1(3H)-one 2'-oxide

Method 1: Batch reaction conditions, rhodium acetate as catalyst, 1 h.



The nitrile oxide **243** was generated using the method previously described in Section 3.7.1. from the imidoyl chloride **229** (0.229 g, 1.32 mmol, 2.6 eq). The solution was concentrated under reduced pressure and added to the α-diazosulfoxide **14** (0.105 g, 0.51 mmol, 1 eq) in dichloromethane/ethyl acetate 1:1 (10 mL). This was followed by the addition of rhodium acetate dimer (0.006 g, 0.015 mmol, 5 mol %). The reaction mixture was stirred at room temperature under a nitrogen atmosphere for 1 h. The crude reaction mixture was concentrated under reduced pressure to give the crude material as a thick brown oil (0.253 g). Analysis of the crude material by ^{1}H NMR spectroscopy showed no evidence of either the α-diazosulfoxide starting material **14** or intermediate sulfine **13**, along with the formation of the kinetic isomer **251**, the thermodynamic isomer **250**, the 1,4,2-oxathiazole-*S*-oxide Regioisomer A **252** and the diketone product **345** in a ratio of 68 : 14 : 7 : 11. Purification of the reaction mixture by flash chromatography on silica gel led to the elution of the kinetic diastereomer **251** and the Regioisomer A **252**. The first fraction contained the kinetic 1,2,5-oxathiazole-S-oxide **251** (0.045 g, 28%) Yellow oily residue; Found C, 60.54; H 3.40 N 4.30. $C_{16}H_{10}NFO_3S$ requires C, 60.95; H 3.20 ; N 4.44; ν_{max}/cm^{-1} (neat) 1716, 1602, 1508, 1160; δ_H (400 MHz, $CDCl_3$) 3.60 (1H, d, A of AB_q *J* 18.3, one of $ArCH_2$), 3.83 (1H, d, B of AB_q, *J* 18.3, one of $ArCH_2$), 7.04 (2H, t, *J* 8.6, 2 x Aromatic CH), 7.46 – 7.49 (2H, m, 2 x Aromatic CH), 7.58 – 7.65 (2H, m, 2 x Aromatic CH), 7.82 (1H, t, *J* 7.4, 1 x Aromatic CH), 7.96 (1H, d, *J* 7.7, 1 x Aromatic CH); δ_C ($CDCl_3$, 100 MHz); 31.8 (CH_2, $ArCH_2$), 93.2 (Cq, C_{spiro}), 116.7 (CH, 2 x Aromatic CH, d, $^{2}J_{CF}$ 22.3), 121.6 (Cq, d, $^{4}J_{CF}$ 3.5, 1 x Aromatic Cq), 125.7, 127.2, 129.5 (CH, 3 x Aromatic CH), 130.4 (CH, 2 x ArCH, d, $^{3}J_{CF}$ 9) ,136.4 (Cq, 1 x Aromatic Cq), 137.0 (CH, 1 x Aromatic CH), 149.0 (Cq, 1 x Aromatic Cq), 158.0 (Cq, C=N), 164.7 (CF, Aromatic CF, d, $^{1}J_{CF}$ 254.6), 190.8 (Cq, C=O). Spectral characteristics are consistent with those reported for **251** in Method 2 (below.)

Note: After 6 h in $CDCl_3$ the sample which was originally **251** only had become a 9 : 1 mixture of **251** and the thermodynamic isomer **250.**



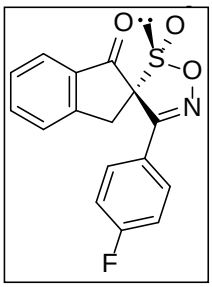
The second fraction to elute contained the 1,4,2-oxathiazole-*S*-oxide Regioisomer A **252** (0.018 g, 11%) Pale yellow crystalline solid; mp 159 - 161°C; ν_{max}/cm^{-1} (neat) 1721, 1073, 844; δ_H (400 MHz, $CDCl_3$) 3.33 (1H, d, *J* 17.2, A of AB_q, one of $ArCH_2$), 3.51 (1H, d, *J* 17.2, B of AB_q, one of $ArCH_2$), 7.18 – 7.24 (3H, m, 3 x Aromatic CH), 7.51 – 7.58 (2H, m, 2 x Aromatic CH), 7.77 (1H, t, *J* 8.7, 2 x Aromatic CH), 7.93 – 7.98 (2H, m, 2 x Aromatic CH); δ_C ($CDCl_3$, 100 MHz) 33.6 (CH_2, $ArCH_2$), 108.3 (Cq, C_{spiro}), 117.0 (CH, 2 x Aromatic CH, d, $^{2}J_{CF}$ 22), 125.6, 127.1, 129.4 (CH, 3 x Aromatic CH), 131.0 (CH, 2 x ArCH, d, $^{2}J_{CF}$ 9), 135.2

(Cq, 1 x Aromatic Cq), 137.1 (CH, 1 x Aromatic CH), 147.4 (Cq, 1 x Aromatic Cq), 158.4 (Cq, C=N), 188.9 (Cq, C=O).* Spectral characteristics are consistent with those reported for **252** in **Method 2** (below.)

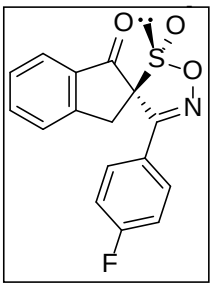
* The C_F bond was not observed in the ^{13}C NMR spectrum.

Method 2: Thermolysis in continuous flow with a 10 min residence time.

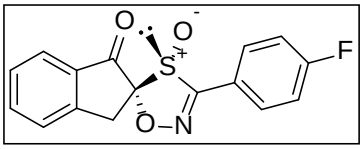
The imidoyl chloride **229** (0.283 g, 1.64 mmol, 2.6 eq) was converted to the nitrile oxide **243** as described in Section 3.7.1. The solution of the dipole **243** was concentrated under reduced pressure to give the dipole as a white crystalline solid. This residue was dissolved in dichloromethane/ethyl acetate (1 : 1, 5 mL) and added to the α-diazosulfoxide **14** (0.130 g, 0.64 mmol, 1 eq) in dichloromethane/ethyl acetate (1 : 1, 10 mL) This deep orange solution was pumped through a 10 mL reaction coil heated to 100°C followed by a 10 mm id Omnifit™ glass column packed with Alumina (~3 g, volume ~1.8 mL, the bed of alumina has narrow beds of acid washed sand at either end), at a flow rate of 1 mL/ min giving a residence time of 10 min. The output was collected as an orange solution and concentrated under reduced pressure to give the crude product as a yellow oil (0.227 g). Analysis of the crude reaction mixture by ^1H NMR spectroscopy showed the formation of the thermodynamic isomer **250**, the kinetic isomer **251**, a Regioisomer A **252** and the diketone rearrangement product **146** in a ratio of 63 : 18 : 12 : 7. The crude reaction mixture was dissolved in the minimum amount of dichloromethane and purified by column chromatography on silica gel to give three fractions:



The first fraction contained the thermodynamic isomer **250** (0.070, 35%) Yellow crystalline solid; Found C, 60.45; H 3.30 N 4.73. $C_{16}H_{10}NFO_3S$ requires C, 60.95; H 3.20 ; N 4.44; mp 107 - 109°C; ν_{max}/cm^{-1} (neat) 3073, 1715, 1154; δ_H (400 MHz, $CDCl_3$) 3.45 (1H, d, *J* 19.2, A of AB_q, one of $ArCH_2$), 4.08 (1H, d, *J* 19.2, B of AB_q, one of $ArCH_2$), 7.05 (2H, t, *J* 8.6, 2 x Aromatic CH), 7.29 – 7.33 (2H, m, 2 x Aromatic CH), 7.59 (2H, t, *J* 8.5, 2 x Aromatic CH), 7.80 (1H, t, *J* 8.9, 1 x Aromatic CH), 7.98 (1H, d, *J* 7.5, 1 x Aromatic CH); δ_C ($CDCl_3$, 100 MHz) 28.8 (CH_2, $ArCH_2$), 97.2 (Cq, C_{spiro}), 116.8 (CH, 2 x Aromatic CH, d, $^2J_{CF}$ 22), 121.8 (Cq, d, $^4J_{CF}$ 3.6, 1 x Aromatic Cq), 126.2, 127.1, 129.3 (CH, 3 x Aromatic CH), 130.2 (CH, 2 x ArCH, d, $^3J_{CF}$ 8), 134.1 (Cq, 1 x Aromatic Cq), 137.3 (CH, 1 x Aromatic CH), 151.5 (Cq, 1 x Aromatic Cq), 157.0 (Cq, C=N), 164.7 (Cq, 1 x Aromatic CF, d, $^1J_{CF}$ 257), 192.5 (Cq, C=O). $(M+H)^+$ 316 (10%); HRMS (ESI+) Exact mass calculated for $C_{16}H_{11}NO_3FS$ $[M+H]^+$, 316.0444. Found: 316.0447.



The second fraction contained the kinetic isomer **251** (0.023 g, 12%) Yellow oily residue; ν_{max}/cm^{-1} (neat) 1716, 1602, 1510, 1160; δ_H (400 MHz, $CDCl_3$) 3.60 (1H, d, *J* 18.5, A of AB_q, one of $ArCH_2$), 3.83 (1H, d, *J* 18.0, B of AB_q, one of $ArCH_2$), 7.04 (2H, t, *J* 8.6, 2 x Aromatic CH), 7.46 – 7.50 (2H, m, 2 x Aromatic CH), 7.58 – 7.65 (2H, m, 2 x Aromatic CH), 7.82 (1H, t, *J* 8.2, 1 x Aromatic CH), 7.96 (1H, d, *J* 7.7, 1 x Aromatic CH); δ_C ($CDCl_3$, 100 MHz) 31.8 (CH_2, $ArCH_2$), 93.2 (Cq, C_{spiro}), 116.7 (CH, 2 x Aromatic CH, d, $^2J_{CF}$ 21), 121.6 (Cq, d, $^4J_{CF}$ 3.6, 1 x Aromatic Cq), 125.7, 127.1, 129.5 (CH, 3 x Aromatic CH), 130.4 (CH, 2 x Aromatic CH, d, $^3J_{CF}$ 8.6), 136.4 (Cq, 1 x Aromatic Cq), 136.9 (CH, 1 x Aromatic CH), 149.0 (Cq, 1 x Aromatic Cq), 158.0 (Cq, C=N), 164.7 (Cq, 1 x Aromatic CF, d, $^1J_{CF}$ 255), 190.7 (Cq, C=O); MS: $(M+H)^+$ 316 (10%); HRMS (ESI+) Exact mass calculated for $C_{16}H_{11}NO_3FS$ $[M+H]^+$, 316.0444. Found: 316.0444.

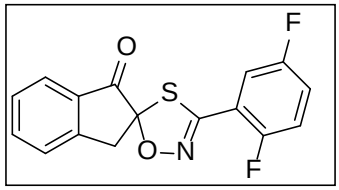


The third fraction to elute was the 1,4,2-oxathiazole-*S*-oxide Regiosiomer A **252** as a yellow crystalline solid (0.08 g, 4%); ν_{max}/cm^{-1} (neat) 1725, 1601, 1238. 1082; δ_H (400 MHz, $CDCl_3$) 3.33 (1H, d, *J* 17.0, A of AB_q, one of $ArCH_2$), 3.51 (1H, d, *J* 17.2, B of AB_q, one of $ArCH_2$), 7.19 – 7.24 (3H, m, 3 x Aromatic CH), 7.51 – 7.58 (2H, m, 2 x Aromatic CH), 7.78 (2H, t, *J* 8.5, 2 x Aromatic CH), 7.93 – 7.98 (2H, m, 2 x Aromatic CH); δ_C ($CDCl_3$, 100 MHz)*; 33.6 (CH_2, $ArCH_2$), 108.4 (Cq, C_{spiro}), 117.1 (CH, d, $^2J_{CF}$ 21, 2 x Aromatic CH), 125.6, 127.1 129.4 (CH, 3 x Aromatic CH), 131.0 (CH, d, $^3J_{CF}$ 9.2, 2 x Aromatic CH), 137.2 (CH, 1 x Aromatic CH), 147.4 (Cq, 1 x Aromatic Cq); MS: (M+H) 316 (15%); HRMS (ESI+) Exact mass calculated for $C_{16}H_{11}NO_3FS$ $[M+H]^+$, 316.0444. Found: 316.0454. **Note:***The C=O, C-F, one Aromatic Cq, and the C=N signal were not detected in the ^{13}C NMR spectrum.

4'-(2,5-Difluorophenyl)spiro[indene-2,3'-[1,2,5]oxathiazol]-1(*3H*)-one *S*-oxide

Method 1: Batch reaction conditions, rhodium acetate as catalyst, 1 h.

The nitrile oxide dipole **245** was generated using the method previously described in Section 3.7.1 from the imidoyl chloride **230** (0.372 g, 1.95 mmol, 2.6 eq). The solution was concentrated under reduced pressure and added to the α-diazosulfoxide **14** (0.150 g, 0.74 mmol, 1 eq) in dichloromethane/ethyl acetate 1 : 1 (15 mL). This was followed by the addition of rhodium acetate dimer (0.0016 g, 5 mol %). The reaction mixture was stirred at room temperature under a nitrogen atmosphere for 1 h. The crude reaction mixture was concentrated under reduced pressure to give the crude material as an orange oil. Analysis of the crude material by ^1H NMR spectroscopy showed no evidence for either the α-diazosulfoxide starting material **14** or intermediate sulfine **13** and the 1,4,2-oxathiazole **241** as the major



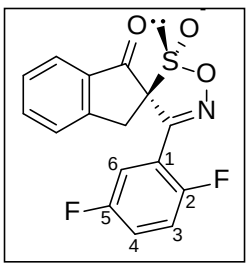
product, along with the kinetic isomer **257** and thermodynamic isomer **256** in a ratio of 54 : 23 : 23. Purification of the reaction mixture by flash chromatography on silica gel led to elution of the 1,4,2-oxathiazole **241** only as a pale yellow crystalline solid (0.018 g, 8%). mp 89 – 91°C; ν_{max}/cm^{-1} (neat) 1726, 1483, 1272; δ_H (400 MHz, $CDCl_3$) 3.78 (1H, d, *J* 18.0, A of AB_q, one of $ArCH_2$), 3.91 (1H, d, *J* 18.0, B of AB_q, one of $ArCH_2$), 7.10 – 7.19 (2H, m, 2 x Aromatic CH), 7.46 – 7.50 (2H, m, 2 x Aromatic CH), 7.57 – 7.61 (1H, m, 1 x Aromatic CH), 7.72 (1H, t, *J* 8.5, 1 x Aromatic CH), 7.88 (1H, d, *J* 7.6, 1 x Aromatic CH); δ_C ($CDCl_3$, 100 MHz) 42.5 (CH_2, $ArCH_2$), 101.1 (Cq, C_{spiro}), 115.8 (CH dd, $^2J_{CF}$ 26.0, $^3J_{CF}$ 3.0, 1 x Aromatic CH), 117.0 (Cq, dd, $^2J_{CF}$ 14.6, $^3J_{CF}$ 9.0, 1 x Aromatic Cq), 117.7 (CH, dd, $^2J_{CF}$ 25.5, $^3J_{CF}$ 8.7, 1 x Aromatic CH), 119.5 (CH, dd, $^2J_{CF}$ 25.5, $^3J_{CF}$ 8.8, 1 x Aromatic CH), 125.9. 126.4, 128.9 (CH, 3 x Aromatic CH), 132.4 (Cq, 1 x Aromatic Cq), 136.8 (CH, 1 x Aromatic CH), 148.8 (Cq, 1 x Aromatic Cq), 149.3 (Cq, C=N), 155.8 (Cq, 1 x Aromatic CF, d, $^1J_{CF}$ 251), 158.3 (Cq, 1 x Aromatic CF, d, $^1J_{CF}$ 245), 196.0 (Cq, C=O); m/z (ESI+) 334 $[M+H]^+$ (25%); HRMS (ESI+) Exact mass calculated for $C_{16}H_{10}NO_3F_2S$ $[M+H]^+$, 334.0349 Found: 334.0345.

Characteristic signals of the kinetic isomer **257** are seen at 3.68, 3.98 [2 x (1H, d, *J* 17.8)].

The relative stereochemistry of the cycloadduct **241** was determined by single crystal X-ray diffraction on a crystalline sample of **241**[181] recrystallized from dichloromethane/hexane. Crystals of **241** are monoclinic, space group *P* 21/*c*. Crystal data for $C_{16}H_9F_2NO_2S$, *Mr* = 317.30, a = 14.0083 (10) Å, b = 8.7108 (6) Å, c = 11.54178 (8) Å, $\alpha = \gamma = 90$ °C, $\beta = 105.733$ (2)°, *V* = 1355.62 (16) $Å^3$, *Z* = 4, D_c = 1.555 g cm^{-3}, F_{000} = 648, Cu Kα radiation, λ = 1.541 Å, *T* = 296 K, $2\theta_{max}$ = 0.753°, μ = 2.417 mm^{-1},15370 reflections collected, 2344 unique (R_{int} = 0.0332), final GooF = 1.100, R_1 = 0.0328, wR_2 = 0.0920 (2299 obs. data: $I > 2\sigma(I)$); R_1 = 0.0335, wR_2 = 0.0927 (all data).

<u>Note:</u> This fraction contained 7% of the ketone rearrangement product **142** with characteristic signals at 2.71 and 2.91 ppm.

Method 2: Thermolysis in continuous flow with a 10 min residence time.

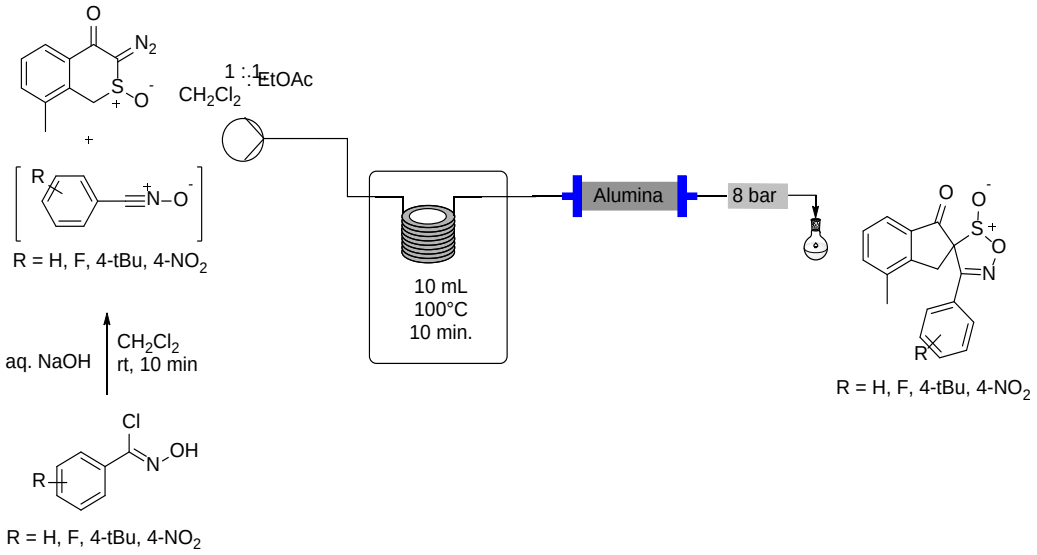


The imidoyl chloride **230** (0.350 g, 1.84 mmol, 2.6 eq) was converted to the nitrile oxide **245** as described in Section 3.7.1. The solution of the dipole **245** was concentrated under reduced pressure to give the dipole **245** as a viscous pale yellow oil. This residue was dissolved in dichloromethane/ethyl acetate (1 : 1, 5 mL) and added to the α-diazosulfoxide **14** (0.141 g, 0.70 mmol, 1 eq) in DCM/EtOAc (1:1, 10 mL) This deep orange solution was pumped through a 10 mL reaction coil heated to 100°C, followed by a 10 mm id Omnifit™ glass column packed with Alumina (~3 g, volume ~1.8 mL, the bed of alumina has narrow beds of acid washed sand at either end), at a flow rate of 1 mL/ min

giving a residence time of 10 min. The crude product was collected as an orange solution and concentrated under reduced pressure to give the crude product as a yellow oil (0.296 g). Analysis of the crude reaction mixture by ^{1}H NMR spectroscopy showed the formation of the thermodynamic isomer **256**, the monoketone **142**, diketone **146** and the Regioisomer B **266** in a ratio of 62 : 20 : 11 : 9. The crude reaction mixture was dissolved in the minimum amount of dichloromethane and purified by column chromatography on silica gel. Careful and repeated chromatography was required for isolation of the thermodynamic isomer **256** as a yellow oily residue (0.026 g, 11%). ν_{max}/cm^{-1} (neat) 1720, 1162, 1429; δ_H (400 MHz, $CDCl_3$) 3.37 (1H, d, *J* 18.8, A of AB_q, one of $ArCH_2$), 3.99 (1H, d, *J* 18.8, B of AB_q, one of $ArCH_2$), 6.99 – 7.04 (1H, complex m, 1 x Aromatic CH), 7.18 – 7.23 (1H, m, 1 x Aromatic CH), 7.76 (3H, t, *J* 8.9, 2 x Aromatic CH), 7.74 (1H, t, *J* 8.7, 1 x Aromatic CH), 7.92 (1H, d, *J* 7.6, 1 x Aromatic CH); δ_C ($CDCl_3$, 100 MHz) 28.3 (CH_2, $ArCH_2$), 97.1 (Cq, C_{spiro}), 115.3 (CH, dd, $^{2}J_{CF}$ 15.7, $^{3}J_{CF}$ 8.9, Aromatic C-3), 117.8 (CH, dd, $^{2}J_{CF}$ 24.7, $^{3}J_{CF}$ 8.5, Aromatic C-6), 118.1 (CH, dd, $^{2}J_{CF}$ 26.3, $^{3}J_{CF}$ 3.3, Aromatic C-4), 120.6 (CH, dd, $^{2}J_{CF}$ 24.1, $^{3}J_{CF}$ 9.1, Aromatic C-1), 125.9. 126.6, 128.9 (CH, 3 x Aromatic CH), 134.1 (Cq, 1 x Aromatic Cq), 136.5 (CH, 1 x Aromatic CH), 151.1 (Cq, 2 x Aromatic Cq), 154.4 (Cq, C=N), 156.3 (Cq, dd, $^{1}J_{CF}$ 251.3, $^{4}J_{CF}$ 5.9, 1 x C-F), 158.7 (Cq, d, $^{1}J_{CF}$ 244.8, 1 x C-F), 191.1 (Cq, d, $^{5}J_{CF}$ 4.2, C=O); MS (M^+) 333 (15%); HRMS (ESI+) Exact mass calculated for $C_{16}H_{10}NO_3F_2S$ $[M+H]^+$, 334.0360 Found: 334.0349.

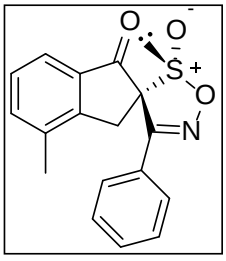
The crude product contained the ketone rearrangement product **142** with characteristic signals at 2.71 and 2.91 ppm in the ^{1}H NMR spectrum, the characteristic signal of the diketone product **146** is the 2H singlet at 3.64 ppm in the ^{1}H NMR spectrum and characteristic signals of the Regioisomer B **266** are present at 3.26 and 4.21 ppm [2 x (H, d, *J* 17.6)] in the ^{1}H NMR spectrum.

3.7.1.3 Dipolar cycloadditions of α-diazosulfoxide 80 with nitrile oxides.



Scheme 149

4-Methyl-4'-phenylspiro[indene-2,3'-[1,2,5]oxathiazol]-1(*3H*)-one *S*-oxide 268

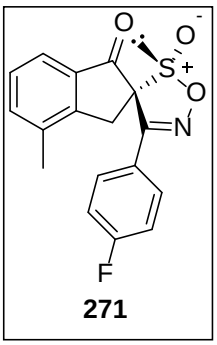


The imidoyl chloride **193** (0.230 g, 1.90 mmol, 2.6 eq) was added portionwise over 10 min, at room temperature, to a vigorously stirred solution of aqueous NaOH (1M, 10 mL) and dichloromethane (10 mL) to generate the dipole **192**. After complete addition, the mixture was stirred for a further 10 min. The layers were separated and the organic layer was dried with $MgSO_4$ and concentrated under reduced pressure to half the initial volume. The α-diazosulfoxide **80** (0.137 g, 0.64 mmol, 1 eq) was added and the volume made up to 14 mL of dichloromethane/ethyl acetate (1 : 1, 0.04 M). After this addition, the solution was immediately pumped through a 10 mL reactor coil heated to 100°C with a residence time of 10 min, followed by a 10 mm id Omnifit™ glass column packed with Alumina (2 g, volume, ~1.2 mL). The crude material was collected as an orange solution and concentrated under reduced pressure to give the crude product as an orange oil (0.256 g) and as a mixture of the thermodynamic isomer **268**, kinetic isomer **269**, and a 1,4,2-oxathiazole-*S*-oxide Regioisomer B **270** in a ratio of 74 : 18 : 8. The crude reaction mixture was dissolved in the minimum amount of dichloromethane, and purified by column chromatography on silica gel using gradient hexane-ethyl acetate as eluent (100 : 0 – 50 : 50) to give **268** only as a white crystalline solid (0.089 g, 30%). The first fraction contained the 1,2,5-oxathiazole-*S*-oxide thermodynamic isomer **268**; m.p. 150 – 151°C; ν_{max}/cm^{-1} (neat) 1709, 1156, 762; δ_H (400 MHz, $CDCl_3$) 2.38 (3H, s, CH_3), 3.32 (1H, d, *J* 19.0, A of AB_q, one of $ArCH_2$), 3.98 (1H, d, *J* 19.2, B of AB_q, one of $ArCH_2$), 7.29 – 7.31 (2H, m, 2 x Aromatic CH), 7.36 (2H, t, *J* 8.4, 2 x Aromatic CH), 7.46 – 7.51 (2H, m, 2 x Aromatic CH), 7.59 (1H, d, *J* 7.3, 1 x Aromatic CH), 7.80 (1H, d, *J* 7.6, 1 x Aromatic CH); δ_C ($CDCl_3$, 100 MHz) 17.8 (CH_3, $ArCH_3$), 27.9 (CH_2, $ArCH_2$), 97.4 (Cq, C_{spiro}), 123.5 (CH, 1 x Aromatic CH), 125.7 (Cq, 1 x Aromatic Cq), 127.9 (CH, 2 x Aromatic CH), 129.3 (CH, 1 x Aromatic CH), 129.4 (CH, 2 x Aromatic CH), 131.7 (CH, 1 x Aromatic CH), 134.1 (Cq, 1 x Aromatic Cq), 136.6 (Cq, 1 x Aromatic Cq), 137.7 (CH, 1 x Aromatic CH), 150.5 (Cq, 1 x Aromatic Cq), 158.0 (Cq, C=N), 192.8 (Cq, C=O); $(M)^+$ 311 (5%); HRMS (ESI+) Exact mass calculated for $C_{17}H_{14}NO_3S$ $[M+H]^+$, 312.0694. Found: 312.0687.

Characteristic peaks of the kinetic isomer **269** are 1H, d, at 3.42 and 3.75 ppm. Characteristic peaks of the 1,4,2-oxathiazole-*S*-oxide Regioisomer B **270** are 1H, d, at 3.72 and 4.28 ppm.

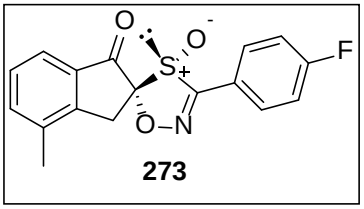
4'-(4-Fluorophenyl)-4-methylspiro[indene-2,3'-[1,2,5]oxathiazol]-1(*3H*)-one *S*-oxide

The imidoyl chloride **229** (0.301 g, 1.74 mmol, 2.6 eq) was added portionwise over 10 min, at room temperature, to a vigorously stirred solution of aqueous NaOH (1M, 10 mL) and dichloromethane (10 mL). After complete addition, the mixture was stirred for a further 10 min. The layers were separated and the organic layer was dried with $MgSO_4$ and concentrated under reduced pressure to half the


271

initial volume. The α-diazosulfoxide **80** (0.142 g, 0.66 mmol, 1 eq) was added to the solution of the dipole **243** and the volume made up to 14 mL of dichloromethane/ethyl acetate (1 : 1, 0.04 M). The solution was pumped through a 10 mL reaction coil heated to 100°C, with a residence time of 10 min, followed by a 10 mm id Omnifit™ glass column packed with Alumina (3 g, volume ~ 1.8 mL). The crude product was collected as an orange solution and concentrated under reduced pressure to give the crude product as an orange crystalline solid (0.386 g) which was a mixture of the thermodynamic isomer **271**, a kinetic isomer **272** and a 1,4,2-oxathiazole-*S*-oxide Regioisomer A **273** in a ratio of 77 : 11 : 12 The crude reaction mixture was dissolved in the minimum amount of dichloromethane and purified by column chromatography on silica gel to give the thermodynamic isomer **271** as a white crystalline solid (0.098 g, 45%); mp 147 - 149°C, ν_{max}/cm^{-1} (neat) 1714, 1232, 1154; δ_H (400 MHz, $CDCl_3$) 2.39 (3H, s, CH_3), 3.28 (1H, d, *J* 19.2, A of AB_q, one of CH_2), 3.98 (1H, d, *J* 19.2, B of AB_q, one of CH_2), 7.06 (2H, t, *J* 8.6, 2 x Aromatic CH), 7.29 – 7.33 (2H, m, 2 x Aromatic CH), 7.50 (1H, t, *J* 7.8, 1 x Aromatic CH), 7.60 (1H, d, *J* 7.3, 1 x Aromatic CH), 7.80 (1H, d, *J* 7.7, 1 x Aromatic CH); δ_C ($CDCl_3$, 100 MHz) 17.8 (CH_3, $ArCH_3$), 27.8 (CH_2, $ArCH_2$), 97.1 (Cq, C_{spiro}), 116.8 (CH, d, $^2J_{CF}$ 22, 2 x Aromatic CH), 121.9 (d, $^4J_{CF}$ 3.6, 1 x ArCq), 123.5 (CH, 1 x Aromatic CH), 129.4 (CH, 1 x Aromatic CH), 130.2 (1 signal representing 2 x ArCH, d, $^3J_{CF}$ 8), 134.0 (Cq, 1 x Aromatic Cq), 136.7 (Cq, 1 x Aromatic Cq), 137.8 (CH, 1 x Aromatic CH), 150.4 (Cq, 1 x Aromatic Cq), 157.0 (Cq, C=N), 164.6 (Cq, 1 x Aromatic CF, d, $^1J_{CF}$ 255), 192.8 (Cq, C=O); HRMS (ESI+) Exact mass calculated for $C_{17}H_{13}NO_3FS$ $[M+H]^+$, 330.0600. Found: 330.0588.

The relative stereochemistry of the cycloadduct **271** was determined by single crystal X-ray diffraction on a crystalline sample of **271** recrystallized from dichloromethane/hexane.[181] Crystals of **271** are orthorhombic, space group Pbca. α=β=γ= 90°C, Crystal data for $C_{17}H_{12}NFO_3S$ *Mr* = 329.34, a = 15.237 (3) Å, b = 11.212 (2) Å, c = 17.948 (3) Å, β = 90 (2)°, *V* = 3066.2 (10) $Å^3$, *Z* = 8, D_c = 1.427 g cm^{-3}, F_{000} = 1360, Mo Kα radiation, λ = 0.71073 Å, *T* = 296 K, $2\theta_{max}$ = 67.14°, μ = 2.111 mm^{-1}, 16848 reflections collected, 2637 unique (R_{int} = 0.0398), final GooF = 1.097, R_1 = 0.0448, wR_2 = 0.1302, (2617 obs. data: $I > 2\sigma(I)$); R_1 = 0.0448, wR_2 = 0.1303 (all data).

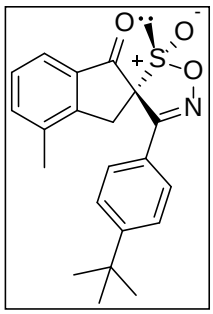

273

A second fraction isolated from the column contained the 1,4,2-oxathiazole-*S*-oxide Regioisomer A **273** (0.026 g, 12%) Yellow crystalline solid; ν_{max}/cm^{-1} (neat) 1724, 1600, 1238, 1080; δ_H (400 MHz, $CDCl_3$); 2.35 (3H, s, CH_3), 3.15 (1H, d, *J* 17.4, A of AB_q, one of CH_2), 3.41 (1H, d, *J* 17.4, B of AB_q, one of CH_2), 7.22 (2H, t, *J* 8.4, 2 x Aromatic CH), 7.47 (2H, t, *J* 8.8, 2 x Aromatic CH), 7.58 (1H, d, *J* 7.2, 2 x Aromatic CH), 7.82 (1H, d, *J* 7.4, 1 x Aromatic CH), 7.94 – 7.97

(2H, m, 2 x Aromatic CH); δ_C ($CDCl_3$, 100 MHz); 17.8 (CH_3, $ArCH_3$), 32.4 (CH_2, $ArCH_2$), 108.2 (Cq, C_{spiro}), 117.0 (CH, 2 x Aromatic CH, d, $^2J_{CF}$ 23.6), 121.5 (Cq, 1 x Aromatic Cq), 122.9, 129.5 (2 x CH, 2 x Aromatic CH), 131.0 (CH, 2 x Aromatic CH, d, $^3J_{CF}$ 8.8), 135.1, 136.4 (Cq, 2 x Aromatic Cq), 137.7 (CH, 1 x Aromatic CH), 146.5 (Cq, 1 x Aromatic Cq), 158.4 (Cq, C=N), 164.8 (Cq, 1 x Aromatic CF, d, $^1J_{CF}$ 256), 189.3 (Cq, C=O); ESI+ $(M+H)^+$ 330 (10%); HRMS (ESI+) Exact mass calculated for $C_{17}H_{13}NO_3FS$ $[M+H]^+$, 330.0600 Found: 330.0594.

Characteristic signals of the kinetic isomer **272** are observed as 1H, doublets, *J* 18.4, at 3.36 and 3.65 ppm.

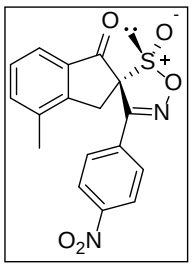
4'-(4-(tert-Butyl)phenyl)-4-methylspiro[indene-2,3'-[1,2,5]oxathiazol]-1(*3H*)-one *S*-oxide 274



The nitrile oxide **244** was generated from the imidoyl chloride **231** (0.275 g, 1.3 mmol, 2.6 eq) using the procedure outlined in Section 3.7.1. The α- diazosulfoxide **80** (0.092 g, 0.43 mmol, 1 eq) was added and the volume made up to 8 mL of dichloromethane/ethyl acetate (1 : 1, 0.04 M). The solution was pumped through a 10 mL reaction coil heated to 100°C, with a residence time of 10 min, and was followed by a 10 mm id Omnifit™ glass column packed with Alumina (~3 g, volume ~ 1.8 mL). The crude material was collected as an orange solution and concentrated under reduced pressure to give the crude product as an orange oil (0.218 g) and as a mixture of the thermodynamic isomer **274**, the kinetic isomer **275** and a 1,4,2-oxathiazole-*S*-oxide Regioisomer A **276** in a ratio of 78 : 15 : 7. The crude reaction mixture was dissolved in the minimum amount of dichloromethane and purified by column chromatography on silica gel to give the thermodynamic isomer **274** as a white crystalline solid (0.041 g, 26%). mp 105 - 106°C; ν_{max}/cm^{-1} (neat) 1721, 1269, 1173; δ_H (400 MHz, $CDCl_3$) 1.28 (9H, s, 3 x CH_3), 2.37 (3H, s, $ArCH_3$), 3.38 (1H, d, *J* 19.2, A of AB_q, one of CH_2), 3.98 (1H, d, *J* 19.2, B of AB_q, one of CH_2), 7.25 (2H, d, *J* 7.9, 2 x Aromatic CH), 7.37 (2H, d, *J* 8.5, 2 x Aromatic CH), 7.48 (1H, t, *J* 7.8, 1 x Aromatic CH), 7.59 (1H, d, *J* 7.3, 1 x Aromatic CH), 7.79 (1H, d, *J* 7.6, 1 x Aromatic CH); δ_C ($CDCl_3$, 100 MHz) 17.9 (CH_3, $ArCH_3$), 28.0 (CH_2, $ArCH_2$), 31.0 (CH_3, 1 signal representing 3 x CH_3), 35.0 [Cq, $Cq(CH_3)_3$], 97.4 (Cq, C_{spiro}), 122.7 (Cq, Aromatic Cq), 123.4 (CH, 1 x Aromatic CH), 126.4, 127.7 (CH, 2 signals representing 4 x Aromatic CH), 129.3 (CH, 1 x Aromatic CH), 134.1 (Cq, 1 x Aromatic Cq), 136.6 (Cq, 1 x Aromatic Cq), 137.6 (CH, 1 x Aromatic CH), 150.5, 155.4 (2 x Cq, 2 x Aromatic Cq), 157.8 (Cq, C=N), 193.0 (Cq, C=O); HRMS (ESI+) Exact mass calculated for $C_{21}H_{22}NO_3S$ $[M+H]^+$, 368.1320. Found: 368.1326.

Characteristic peaks of the kinetic 1,2,5-oxathiazole-*S*-oxide **275** in the ^{1}H NMR of the crude material were 3.40, 3.64 [2 x (1H, d, *J* 18.0)]. Characteristic peaks of a minor 1,4,2-oxathiazole-*S*-oxide Regioisomer A **276** in the ^{1}H NMR of the crude material were 3.04, 3.37 [2 x (1H, d, *J* 17.5)].

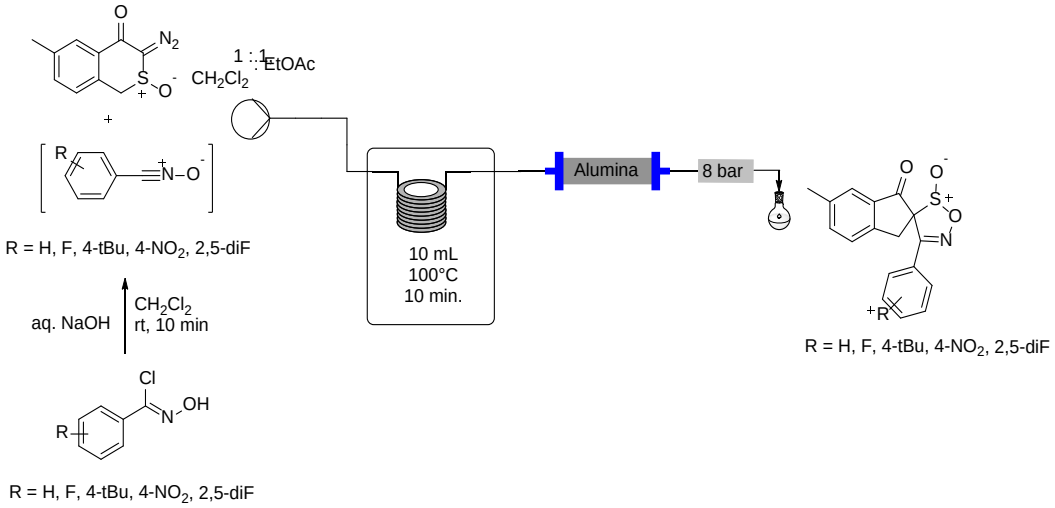
4-Methyl-4'-(4-nitrophenyl)spiro[indene-2,3'-[1,2,5]oxathiazol]-1(*3H*)-one *S*-oxide 277



The nitrile oxide dipole **235** was generated from the imidoyl chloride **228** (0.370 g, 1.85 mmol, 2.6 eq) using the procedure outlined in Section 3.7.1. The α-diazosulfoxide **80** (0.151 g, 0.7 mmol, 1 eq) was added and the volume made up to 15 mL of dichloromethane/ethyl acetate, (1 : 1, 0.04 M). The solution was pumped through a 10 mL reaction coil heated to 100°C at a flow rate of 1 mL/min giving a 10 minute residence time, and was followed by a 10 mm id Omnifit™ glass column packed with Alumina (~3 g, volume ~ 1.8 mL). The crude product was collected as an orange solution and concentrated under reduced pressure to give the crude product as an orange oil (0.344 g) and a mixture of the thermodynamic isomer **277**, the kinetic isomer **278** and a 1,4,2-oxathiazole-*S*-oxide Regioisomer B **279** in a ratio of 85 : 11 : 4 . The crude reaction mixture was dissolved in the minimum amount of dichloromethane and purified by column chromatography on silica gel using gradient hexane-ethyl acetate as eluent (100 : 0 – 60 : 40) to give the thermodynamic isomer **277** as a white crystalline solid. (0.049 g, 20%). mp 139 – 141°C; ν_{max}/cm^{-1} (neat) 1716, 1521, 1346, 1151; δ_H (400 MHz, $CDCl_3$); 2.32 (3H, s, $ArCH_3$), 3.25 (1H, d, *J* 19.2, A of AB_q, one of CH_2), 4.01 (1H, d, *J* 19.2, B of AB_q, one of CH_2), 7.50 – 7.54 [3H, m overlapping 2H doublet (2 x Aromatic CH) and 1H, m (1 x Aromatic CH)], 7.63 (1H, d, *J* 7.5, 1 x Aromatic CH), 7.82 (1H, d, *J* 7.5, 1 x Aromatic CH), 8.23 (2H, d, *J* 8.8, 2 x Aromatic CH); δ_C ($CDCl_3$, 100 MHz) 17.9 (CH_3, $ArCH_3$), 27.5 (CH_2, $ArCH_2$), 96.5 (Cq, C_{spiro}), 123.7 (CH, 1 x Aromatic CH), 124.5 (CH, 2 x Aromatic CH), 129.0 (CH, 2 x Aromatic CH), 129.7 (CH, 1 x Aromatic CH), 132.0, 133.8, 136.8 (3 x Cq, 3 x Aromatic Cq), 138.1 (CH, 1 x Aromatic CH), 149.5 (Cq, 1 x Aromatic Cq), 150.1 (Cq, 1 x Aromatic Cq), 156.6 (Cq, C=N), 192.3 (Cq, C=O); HRMS (ESI+) Exact mass calculated for $C_{17}H_{13}N_2O_5S$ $[M+H]^+$, 357.0545 Found: 357.0531.

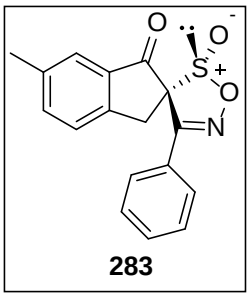
Characteristic peaks of the kinetic 1,2,5-oxathiazole-*S*-oxide **278** in the ^{1}H NMR of the crude material were 3.48, 3.87 [2 x (1H, d, *J* 18.2)]. Characteristic peaks of a minor 1,4,2-oxathiazole-*S*-oxide Regioisomer B **279** in the ^{1}H NMR of the crude material were 3.51, 4.31 [2 x (1H, d, *J* 17.3)].

3.7.1.4 Dipolar cycloaddition of α-diazosulfoxide **83** with nitrile oxides



Scheme 150

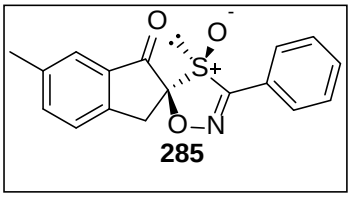
6-Methyl-4'-phenylspiro[indene-2,3'-[1,2,5]oxathiazol]-1(*3H*)-one *S*-oxide


283

The imidoyl chloride **193** (0.198 g, 1.30 mmol, 2.6 eq) was added portionwise over 10 min, at room temperature to a vigorously stirred solution of aqueous NaOH (1M, 10 mL) and dichloromethane (10 mL) to generate the dipole **192**. After complete addition, the mixture was stirred for a further 10 min. The layers were separated and the organic layer was dried with $MgSO_4$ and concentrated under reduced pressure to half the initial volume. The α-diazosulfoxide **83** (0.110 g, 0.50 mmol, 1 eq) was added and the volume made up to 11 mL of dichloromethane/ethyl acetate (1:1, 0.04M). The solution was pumped through a 10 mL reaction coil heated to 100°C with a residence time of 10 min and was followed by a 10 mm id Omnifit™ glass column packed with Alumina (~2 g, volume ~ 1.2 mL). The material was collected as a brown solution and concentrated under reduced pressure to give the crude product as an thick brown oil (0.238 g). The crude product was a mixture of the desired thermodynamic isomer **283**, a kinetic isomer **284**, a 1,4,2-oxathiazole-*S*-oxide Regiosiomer A **285** and an unknown (with a singlet at 3.77 ppm in the ^1H NMR spectrum), in a ratio of 64 : 16 : 11 : 9. The crude reaction mixture was dissolved in the minimum amount of dichloromethane and purified by column chromatography on silica gel using gradient hexane-ethyl acetate as eluent (100 : 0 – 60 : 40) to give the thermodynamic isomer **283** as a pale yellow solid (0.053g, 34%); Found C, 65.80; H 4.34; N 4.50. $C_{17}H_{13}NO_3S$ requires C, 65.58; H 4.21; N 4.50; m.p. 147-149 °C; ν_{max}/cm^{-1} (neat) 1712, 1276, 1153; δ_H (300 MHz, $CDCl_3$) 2.49 (3H, s, CH_3), 3.42 (1H, d, *J* 19.2, A of AB_q, one of $ArCH_2$), 4.02 (1H, d, *J* 19.2, B of AB_q, one of $ArCH_2$), 7.28 – 7.37 (4H, m, 4 x Aromatic CH), 7.45 – 7.47 (2H, m, 2 x Aromatic CH), 7.59 (2H, dd, *J* 7.7, 1.2, 1 x Aromatic CH), 7.75 (1H, br s, 1 x Aromatic CH); δ_C ($CDCl_3$, 75.5MHz) 21.1 (CH_3, $ArCH_3$), 28.5 (CH_2, $ArCH_2$), 97.7 (Cq, C_{spiro}),

125.7 (Cq, Aromatic Cq), 125.8 (CH, 1 x Aromatic CH), 126.6 (CH, 1 x Aromatic CH), 128.0, 129.3 (2 x CH, 4 x Aromatic CH), 131.6 (CH, 1 x Aromatic CH), 134.4 (Cq, 1 x Aromatic Cq), 138.4 (CH, 1 x Aromatic CH), 139.5 (Cq, 1 x Aromatic Cq), 149.0 (Cq, 1 x Aromatic Cq), 158.0 (Cq, C=N), 192.6 (Cq, C=O); m/z (ESI+) 312 (30%); HRMS (ESI+) Exact mass calculated for $C_{17}H_{14}NO_3S$ $[M+H]^+$, 312.0694 Found: 312.0683.

Characteristic signals for the 1,4,2-oxathiazole-*S*-oxide Regioisomer A **285** were apparent at 3.26 and 3.45 ppm, *J* 17.9, corresponding to <10% of the material.

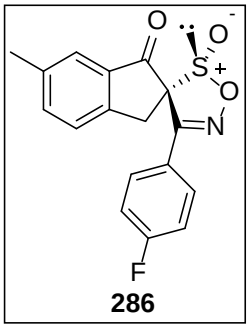


285

The second fraction to elute was the 1,4,2-oxathiazole-*S*-oxide Regioisomer A **285** (0.039 g, 25%) as a white crystalline solid; m.p. 152-154°C (decomp); ν_{max}/cm^{-1} (neat) 1726, 1492, 1282, 1084; δ_H (300 MHz, $CDCl_3$) 2.47 (3H, s, CH_3), 3.26 (1H, d, *J* 17.3, A of AB_q, one of $ArCH_2$), 3.45 (1H, d, *J* 17.3, B of AB_q, one of $ArCH_2$), 7.38 (1H, d, *J* 7.9, 1 x Aromatic CH), 7.48 – 7.59 (4H, m, 4 x Aromatic CH), 7.76 (1H, br s, 1 x Aromatic CH), 7.92 – 7.95 (2H, d, *J* 7.8, 2 x Aromatic CH); δ_C ($CDCl_3$, 75.5 MHz); 21.2 (CH_3, $ArCH_3$), 33.3 (CH_2, $ArCH_2$), 108.5 (Cq, C_{spiro}), 125.2 (Cq, 1 x Aromatic Cq), 125.4, 126.7, 128.8, 129.6, 132.1 (5 signals representing 7 x Aromatic CH), 135.4 (Cq, 1 x Aromatic Cq), 138.3 (CH, 1 x Aromatic CH), 139.7 (Cq, 1 x Aromatic Cq), 144.8 (Cq, 1 x Aromatic Cq), 159.4 (Cq, C=N), 189.0 (Cq, C=O); MS (ESI+) 312 (20%); HRMS (ESI+) Exact mass calculated for $C_{17}H_{14}NO_3S$ $[M+H]^+$, 312.0694. Found: 312.0704.

Characteristic peaks of the kinetic 1,2,5-oxathiazole-*S*-oxide isomer **284**, in the ^1H NMR spectrum of the crude material were 2 x 1H doublets at 3.44 and 3.52 ppm, *J* 17.5.

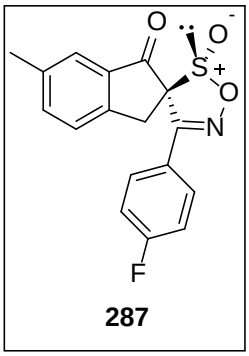
4'-(4-Fluorophenyl)-6-methylspiro[indene-2,3'-[1,2,5]oxathiazol]-1(*3H*)-one *S*-oxide



286

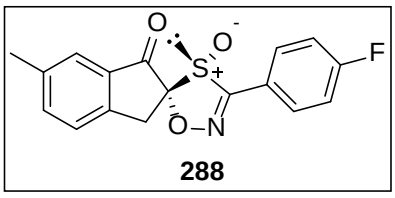
The nitrile oxide dipole **243** was generated from the imidoyl chloride **229** (0.090 g, 0.5 mmol, 1.95 eq) using the procedure outlined in Section 3.7.1. The α-diazosulfoxide **83** (0.06 g, 0.27 mmol, 1 eq) was added and the volume made up to 6 mL of dichloromethane/ethyl acetate (1:1, 0.04 M). The solution was pumped through a 10 mL reaction coil heated to 100°C, with a residence time of 10 min, followed by a 10 mm id Omnifit™ glass column packed with Alumina (~1 g, volume ~ 0.6 mL). The crude product was collected as a red solution and concentrated under reduced pressure to give the crude product as a red oil (0.128 g) which was a mixture of the desired thermodynamic isomer **286**, the kinetic isomer **287** and a 1,4,2-oxathiazole-*S*-oxide Regioisomer A **288** in a ratio of 73 : 14 : 13. The crude reaction mixture was dissolved in the minimum amount of dichloromethane and purified by column chromatography on silica gel using

gradient hexane-ethyl acetate as eluent (100 : 0 – 60 : 40) to give the thermodynamic isomer **286** (0.032 g, 36%) as white crystalline solid; Found C, 61.61; H 3.79; N 4.37. $C_{17}H_{12}NFO_3S$ requires C, 62.00; H 3.67; N 4.25; m.p. 156-158 °C ν_{max}/cm^{-1} (neat) 1711, 1162, 806; δ_H (300 MHz, $CDCl_3$); 2.49 (3H, s, CH_3), 3.40 (1H, d, *J* 19.7, A of AB_q, one of $ArCH_2$), 4.03 (1H, d, *J* 19.7, B of AB_q, one of $ArCH_2$), 7.05 (2H, t, *J* 8.9, 2 x Aromatic CH), 7.28 – 7.34 (2H, m, 2 x Aromatic CH), 7.46 (1H, d, *J* 8.0, 1 x Aromatic CH), 7.61 (1H, d, *J* 7.9, 1 x Aromatic CH), 7.74 (1H, br s, 1 x Aromatic CH); δ_C ($CDCl_3$, 100 MHz); 21.1 (CH_3, $ArCH_3$), 28.4 (CH_2, $ArCH_2$), 97.5 (Cq, C_{spiro}), 116.7 (CH, 1 signal representing 2 x Aromatic CH, d, $^2J_{CF}$ 22.2), 121.9 (Cq, 1 x Aromatic Cq, d, $^4J_{CF}$ 3.3), 125.9 (CH, 1 x Aromatic CH), 126.7 (CH, 1 x Aromatic CH), 130.2 (CH, 2 x ortho Aromatic CH, d, $^3J_{CF}$ 8.7), 134.4, (Cq, 1 x Aromatic Cq), 138.5 (CH, 1 x Aromatic CH), 139.6 (Cq, 1 x Aromatic Cq), 148.9 (Cq, Aromatic Cq), 157.0 (Cq, C=N), 164.6 (Cq, 1 x Aromatic CF, d, $^1J_{CF}$ 254.4), 192.5 (Cq, C=O); MS $(M)^+$ 330 (60%); HRMS (ESI+) Exact mass calculated for $C_{17}H_{13}FNO_3S$ $[M+H]^+$, 330.0600 Found: 330.0600

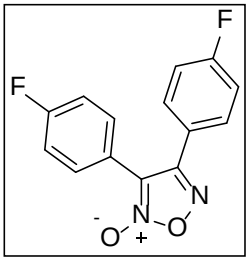

287

The second fraction to elute isolated contained the kinetic 1,2,5-oxathiazole-*S*-oxide **287** (0.004 g, 5%)δ_H (400 MHz, $CDCl_3$) 2.49 (3H, s, CH_3), 3.53 (1H, d, *J* 18.5, A of AB_q, one of $ArCH_2$), 3.77 (1H, d, *J* 18.5, B of AB_q, one of $ArCH_2$), 7.03 (2H, t, *J* 8.9, 2 x Aromatic CH), 7.45– 7.51 (3H, m, 3 x Aromatic CH), 7.58 – 7.63 (1H, m, 1 x Aromatic CH), 7.75 (1H, br s, 1 x Aromatic CH); $(M+H)^+$ 330 (25%), HRMS (ESI+) Exact mass calculated for $C_{17}H_{13}NO_3FS$ $[M+H]^+$, 330.0600. Found: 330.0605.

Note: On obtaining a ^{13}C NMR spectrum of the material after 6 months on a 600 MHz NMR spectrometer, the sample had completely converted to the thermodynamic isomer **286**, and spectroscopic characteristics are consistent with those reported above.

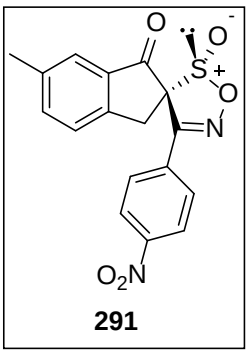

288

The third, most polar fraction to elute contained the 1,4,2-oxathiazole-*S*-oxide Regioisomer A **288** (0.008 g, 10%) as a colorless oil; ν_{max}/cm^{-1} (neat) 1722, 1282, 1157, 1083; δ_H (600 MHz, $CDCl_3$) 2.47 (3H, s, CH_3), 3.26 (1H, d, *J* 17.3, A of AB_q, one of $ArCH_2$), 3.45 (1H, d, *J* 17.3, B of AB_q, one of $ArCH_2$), 7.22 (2H, t, *J* 8.4, 2 x Aromatic CH), 7.39 (1H, d, *J* 7.7, 1 x Aromatic CH), 7.56 – 7.60 (1H, d, *J* 8.3, 1 x Aromatic CH), 7.76 (1H, s, 1 x Aromatic CH), 7.92 – 7.97 (2H, m, 2 x Aromatic CH); δ_C ($CDCl_3$, 125 MHz) 21.2 (CH_3, $ArCH_3$), 33.3 (CH_2, $ArCH_2$), 108.7 (Cq, C_{spiro}), 117.0 (CH, 2 x ArCH, d, $^2J_{CF}$ 22.6), 121.4 (Cq, d, $^4J_{CF}$ 3.3, 1 x Aromatic Cq), 125.4, 126.7 (CH, 2 x Aromatic CH), 131.0 (CH, 2 x Aromatic CH, d, $^3J_{CF}$ 9.4), 135.3 (Cq, 1 x Aromatic Cq), 138.4 (CH, 1 x Aromatic CH), 139.8, 144.7 (2 x Cq, 2 x Aromatic Cq), 158.4 (Cq, C=N), 164.9 (Cq, 1 x



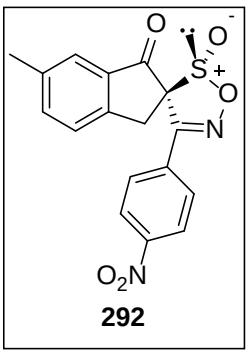
Aromatic CF, d, $^1J_{CF}$ 254), 188.9 (Cq, C=O); MS $(M)^+$ 329 (100%); HRMS (ESI+) Exact mass calculated for $C_{17}H_{12}FNO_3SNa$ $[M+Na]^+$, 352.0420 Found: 352.0425. **Note:** This fraction contained about 5% of the tentatively assigned furoxan dimer with characteristic multiplet peaks at 7.67 and 8.10 ppm in the ^1H NMR spectrum.

6-Methyl-4'-(4-nitrophenyl)spiro[indene-2,3'-[1,2,5]oxathiazol]-1(*3H*)-one *S*-oxide



291

The nitrile oxide **235** was generated from the imidoyl chloride **228** (0.325 g, 1.65 mmol, 2.6 eq) using the procedure outlined in Section 3.7.1. The α-diazosulfoxide **83** (0.140 g, 0.63 mmol, 1 eq) was added and the volume made up to 14 mL of dichloromethane/ethyl acetate (1:1, 0.04 M). The solution was pumped through a 10 mL reaction coil heated to 100°C at a flow rate of 10 mL/min giving a residence time of 10 min and was followed by a 10 mm id Omnifit™ glass column packed with Alumina (~ 2 g, volume ~ 1.2 mL). The material was collected as a yellow solution and concentrated under reduced pressure to give the crude product as a yellow crystalline solid (0.320 g) which on analysis by ^1H NMR spectroscopy was a mixture of the thermodynamic isomer **291**, the kinetic isomer **292**, and a 1,4,2-oxathiazole-*S*-oxide Regioisomer A **293** in a ratio of 77 : 17 : 6. The crude reaction mixture was dissolved in the minimum amount of dichloromethane and purified by column chromatography on silica gel using gradient hexane-ethyl acetate as eluent (100 : 0 – 60 : 40) to give the thermodynamic isomer **291** as a white crystalline solid (0.100 g, 45%). Found C, 56.95; H 3.49; N 7.75. $C_{17}H_{12}N_2O_5S$ requires C, 57.30; H 3.39 ; N 7.86; m.p. 128 – 130°C; ν_{max}/cm^{-1} (neat) 1707, 1523 1345, 1154; δ_H (300 MHz, $CDCl_3$) 2.50 (3H, s, CH_3), 3.35 (1H, d, *J* 19.4, A of AB_q, one of $ArCH_2$), 4.07 (1H, d, *J* 19.4, B of AB_q, one of $ArCH_2$), 7.47 – 7.53 [3H, 2 overlapping signals; (1H, d, *J* 8.5) and (2H, d, *J* 9.1, 2 x Aromatic CH)], 7.63 (1H, d, *J* 8.1, 1 x Aromatic CH), 7.77 (1H, br s, 1 x Aromatic CH), 8.22 (2H, d, *J* 9.0, 2 x Aromatic CH); δ_C ($CDCl_3$, 75 MHz) 21.2 (CH_3, $ArCH_3$), 28.1 (CH_2, $ArCH_2$), 96.8 (Cq, C_{spiro}), 124.5 (CH, 2 x Aromatic CH), 126.1 (CH, 1 x Aromatic CH), 126.8 (CH, 1 x Aromatic CH), 129.0 (CH, 2 x Aromatic CH), 132.0, 134.2 (Cq, 2 x Aromatic Cq), 138.8 (CH, 1 x Aromatic CH), 140.0, 148.6, 149.5 (Cq, 3 x Aromatic Cq), 156.0 (Cq, C=N) 192.0 (Cq, C=O); HRMS (ESI+) Exact mass calculated for $C_{17}H_{13}N_2O_5S$ $[M+H]^+$, 357.0545. Found: 357.0549.



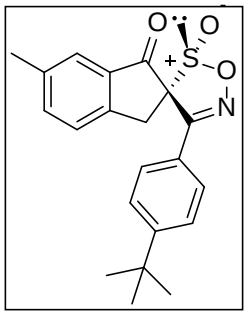
292

A second fraction contained the kinetic 1,2,5-oxathiazole-*S*-oxide diastereomer **292** (0.027 g, 11%); ν_{max}/cm^{-1} (neat) 1714, 1522, 1347; δ_H (300 MHz, $CDCl_3$) 2.51 (3H, s, CH_3), 3.54 (1H, d, *J* 18.0, A of AB_q, one of $ArCH_2$), 3.82 (1H, d, *J* 18.0, B of AB_q, one of $ArCH_2$), 7.49 – 7.54 (1H, m, 1 x Aromatic CH), 7.61 – 7.72 [3H, 2 overlapping signals (1H, m, 1 x Aromatic CH) and (2H, d, *J* 9.0, 2 x

Aromatic CH)], 7.75 (1H, br s, 1 x Aromatic CH), 8.20 (2H, d, *J* 9.0, 2 x Aromatic CH); δ_C ($CDCl_3$, 75 MHz) 21.2 (CH_3, $ArCH_3$), 31.3 (CH_2, $ArCH_2$), 92.8 (Cq, C_{spiro}), 124.21 (Cq, 1 x Aromatic Cq), 124.3 (CH, 2 x Aromatic CH), 125.6 (CH, 1 x Aromatic CH), 126.8 (CH, 1 x Aromatic CH), 129.1 (CH, 2 x Aromatic CH), 131.7 (Cq, 1 x Aromatic Cq), 136.5 (Cq, 1 x Aromatic Cq), 138.5 (CH, 1 x Aromatic CH), 140.3, 146.2 (Cq, 2 x Aromatic Cq), 157.6 (Cq, C=N), 190.3 (Cq, C=O); HRMS (ESI+) Exact mass calculated for $C_{17}H_{13}N_2O_3S$ $[M+H]^+$, 357.0545. Found: 357.0540. **Note:** This fraction contained about 10% of the thermodynamic diastereomer **291** with characteristic signals at 3.35 and 4.07 in the ^1H NMR spectrum.

Characteristic signals of another regioisomer, tentatively assigned as the minor 1,4,2-oxathiazole-*S*-oxide Regioisomer A **293**, in the ^1H NMR spectrum of the crude material are 3.42 and 3.56 [2 x (1H, d, *J* 17.2)].

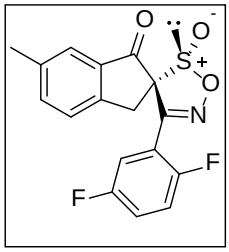
4'-(4-(tert-Butyl)phenyl)-6-methylspiro[indene-2,3'-[1,2,5]oxathiazol]-1(*3H*)-one *S*-oxide 289



The nitrile oxide **244** was generated from the imidoyl chloride **231** (0.299 g, 1.41 mmol, 2.6 eq) using the procedure outlined in Section 3.7.1. The α-diazosulfoxide **83** (0.120 g, 0.54 mmol, 1 eq) was added and the volume made up to 12 mL of dichloromethane/ethyl acetate (1:1, 0.04 M). The solution was pumped through a 10 mL reaction coil heated to 100°C, with a residence time of 10 min, followed by a 10 mm id Omnifit™ glass column packed with Alumina (~2 g, volume ~ 1.2 mL). The crude product was collected as a red solution and concentrated under reduced pressure to give the crude product as a thick orange oil (0.321 g) which consisted of the thermodynamic isomer **289**, the kinetic isomer **290** in a ratio of 80 : 20 and residual furoxan dimer **346**. The crude reaction mixture was dissolved in the minimum amount of dichloromethane and purified by column chromatography on silica gel using gradient hexane-ethyl acetate as eluent (100 : 0 – 60 : 40) to give the thermodynamic isomer **289** as a yellow oil (0.030 g, 15%). ν_{max}/cm^{-1} (neat) 2963, 1714, 1156, 814; δ_H (300 MHz, $CDCl_3$); 1.27 (9H, s, 3 x CH_3), 2.49 (3H, s, $ArCH_3$), 3.47 (1H, d, *J* 19.0, A of AB_q, one of $ArCH_2$), 4.03 (1H, d, *J* 19.0, B of AB_q, one of $ArCH_2$), 7.24 (2H, d, *J* 8.5, 2 x Aromatic CH), 7.36 (2H, d, *J* 8.6, 2 x Aromatic CH), 7.45 (1H, d, *J* 7.9, 1 x Aromatic CH), 7.59 (1H, d, *J* 7.8, 1 x Aromatic CH), 7.74 (1H, br s, 1 x Aromatic CH); δ_C ($CDCl_3$, 75.5 MHz) 21.1 (CH_3, $ArCH_3$) 28.7 (CH_2, $ArCH_2$), 31.0 (CH_3, 1 signal representing 3 x CH_3), 35.0 [Cq, $C(CH_3)_3$], 97.8 (Cq, C_{spiro}), 122.7 (Cq, Aromatic Cq), 125.8 (CH, 1 x Aromatic CH), 126.4 (CH, 2 x Aromatic CH), 126.6 (CH, 1 x Aromatic CH), 127.8 (CH, 2 x Aromatic CH), 134.6 (Cq, 1 x Aromatic Cq), 138.3 (CH, 1 x Aromatic CH), 139.4, 149.1, 155.3 (3 x Cq, 3 x Aromatic Cq), 157.8 (Cq, C=N), 192.7 (Cq, C=O); (M+H) 368 (60%); HRMS (ESI+) Exact mass calculated for $C_{21}H_{22}NO_3S$ $[M+H]^+$, 368.1320. Found: 368.1306.

Characteristic signals of another regioisomer, tentatively assigned as the kinetic 1,2,5-oxathiazole-*S*-oxide isomer **290** are 3.45 and 3.64 [2 x (1H, d, *J* 18.4)].

4'-(2,5-Difluorophenyl)-6-methylspiro[indene-2,3'-[1,2,5]oxathiazol]-1(*3H*)-one *S*-oxide 294



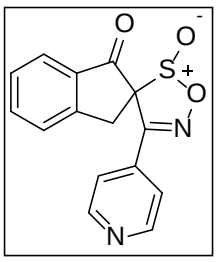
The nitrile oxide **245** was generated from the imidoyl chloride **230** (0.245 g, 1.27 mmol, 2.6 eq) using the procedure outlined in Section 3.7.1. The α-diazosulfoxide **83** (0.108 g, 0.49 mmol, 1 eq) was added and the volume made up to 11 mL of dichloromethane/ethyl acetate (1 : 1, 0.04 M). The solution was pumped through a 10 mL reaction coil heated to 100°C, with a residence time of 10 min, followed by a 10 mm id Omnifit™ glass column packed with Alumina (~2 g, volume ~ 1.2 mL). The crude material was collected as a red solution and concentrated under reduced pressure to give the crude product as a red oil (0.244 g) which on analysis of the ^{1}H NMR spectrum consisted of the thermodynamic isomer **294**, the kinetic isomer **295** and residual α-oxo sulfine (singlet at 4.21 ppm in the ^{1}H NMR spectrum) in a ratio of 53 : 11 : 36. The crude reaction mixture was dissolved in the minimum amount of dichloromethane and purified by column chromatography on silica gel to give the thermodynamic isomer **294** as the major component of one fraction as a brown oil (~90% pure, 0.026 g, 16%). ν_{max}/cm^{-1} (neat) 1720, 1490, 1429, 1163; δ_H (300 MHz, $CDCl_3$) 2.46 (3H, s, $ArCH_3$), 3.31 (1H, d, *J* 18.8, A of AB_q, one of $ArCH_2$), 3.94 (1H, d, *J* 18.6, B of AB_q, one of $ArCH_2$), 7.01 (1H, t of d, *J* 9.4, 4.3, 1 x Aromatic CH), 7.13 – 7.22 (1H, m, 1 x Aromatic CH), 7.39 (1H, d, *J* 7.9, 1 x Aromatic CH), 7.46 – 7.51 (1H, m, 1 x Aromatic CH), 7.55 (1H, d, *J* 7.5, 1 x Aromatic CH), 7.71 (1H, br s, 1 x Aromatic CH). Characteristic signals of **294** identified in the ^{13}C NMR spectrum include; δ_C ($CDCl_3$, 75.5 MHz); 21.1 (CH_3, $ArCH_3$) 27.9 (CH_2, $ArCH_2$), 97.5 (Cq, C_{spiro}), 117.5 – 118.3 (2 overlapping dd corresponding to 2 x Aromatic CH, including 1d $^{3}J_{CF}$ 8.8, 1d $^{4}J_{CF}$ 3.3), 120.5 (CH, 1 x Aromatic CH, dd, $^{2}J_{CF}$ 25, $^{3}J_{CF}$ 9.3), 125.8 (CH, 1 x Aromatic CH), 126.3 (CH, 1 x Aromatic CH), 137.8 (CH, 1 x Aromatic CH), 148.5 (Cq, C=N), 156.2 (Cq, 1 x Aromatic CF, d, $^{1}J_{CF}$ 260), 158.6 (Cq, 1 x Aromatic CF, d, $^{1}J_{CF}$ 246), 191.1 (Cq, C=O); MS $(M)^{+}$ 347 (15%), HRMS (ESI+) Exact mass calculated for $C_{17}H_{12}NO_3F_2S$ $[M+H]^{+}$, 348.0506. Found: 348.0515

Note: Signals for the 4 Aromatic Cq's of **294** were not seen in the ^{13}C NMR spectrum of the material. Signals seen which belong to an unidentified impurity include a symmetrical quartet at 3.5 – 3.6 ppm, a doublet at 3.8 ppm and 2 singlets at 4.2 and 4.7 ppm respectively.

Characteristic signals of another regioisomer, tentatively assigned as the kinetic 1,2,5-oxathiazole-*S*-oxide Isomer **295** are 3.50, 3.69 [2 x (1H, d, *J* 18.2)].

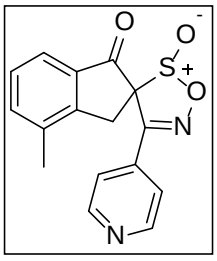
3.7.1.5 Attempted cycloaddition reactions with *N*-hydroxyisonicotinimidoyl chloride

4'-(Pyridin-4-yl)spiro[indene-2,3'-[1,2,5]oxathiazol]-1(*3H*)-one *S*-oxide 281



The nitrile oxide dipole **280** was generated from the imidoyl chloride **232** (0.234 g, 1.49 mmol, 2.6 eq) using the procedure outlined in Section 3.7.1. The α-diazosulfoxide **14** (0.115 g, 0.57 mmol, 1 eq) was added and the volume made up to 11 mL of dichloromethane/ethyl acetate (1 : 1, 0.04 M). The solution was pumped through a 10 mL reaction coil heated to 100°C, with a residence time of 10 min, followed by a 10 mm id Omnifit™ glass column packed with Alumina (~ 3 g, volume ~ 1.8 mL). The crude product was collected as an orange solution and concentrated under reduced pressure to give the crude product as a brown oil. Analysis of the mixture by ^{1}H NMR spectroscopy showed a complex mixture with no evidence of any cycloaddition product.

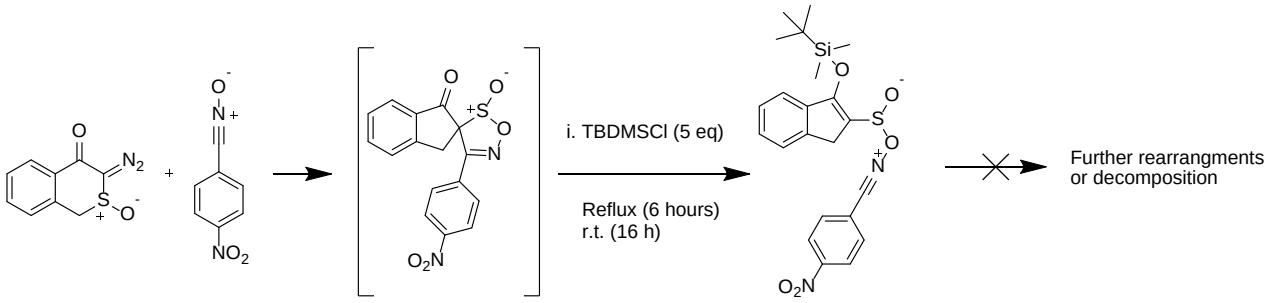
4-Methyl-4'-(pyridin-4-yl)spiro[indene-2,3'-[1,2,5]oxathiazol]-1(*3H*)-one *S*-oxide 282



The nitrile oxide dipole **280** was generated from the imidoyl chloride (0.288 g, 1.83 mmol, 2.6 eq) using the procedure outlined in Section 3.7.1. The α-diazosulfoxide **80** (0.150 g, 0.7 mmol, 1 eq) was added and the volume made up to 15 mL of dichloromethane/ethyl acetate (1 : 1, 0.04 M). The solution was pumped through a 10 mL reaction coil heated to 100°C, with a residence time of 10 min, followed by a 10 mm id Omnifit™ glass column packed with Alumina (~ 3 g, volume ~ 1.8 mL). The crude product was collected as an orange solution and concentrated under reduced pressure to give the crude product as an orange oily residue (0.344 g). Analysis of the mixture by ^{1}H NMR spectroscopy showed a complex mixture with no evidence of any cycloaddition product.

3.7.3.7 Attempted trapping of enolate intermediate

Method 1 for attempted trapping of enolate intermediate.



Scheme 151

The nitrile oxide dipole **235** was generated as per Section 3.7.1. from the para-nitroimidoyl chloride **228** (0.252 g, 1.26 mmol, 2.6 eq). This was concentrated under reduced pressure and added to the α-diazosulfoxide **14** (0.100 g, 0.48 mmol, 1 eq) in dichloromethane/ethyl acetate (15 mL, 1 : 1). Rhodium acetate dimer was added lastly to generate the sulfine **13** (0.010 g, 5 mol %). The reaction mixture was stirred at 1 room temperature for 1 h. TBDMSCl (0.365 g, 2.4 mmol, 5 eq) was added neat to the reaction mixture and the mixture was heated under reflux for 6 h, followed by stirring at room temperature for a further 16 h. The crude reaction mixture was concentrated under reduced pressure to give a brown/black sticky solid. This residue was dissolved in the minimum amount of DCM and purified by column chromatography on silica gel (100 % hexane – 100% ethyl acetate). No identifiable or clean products were isolated from the column.

Method 2 for attempted trapping of enolate intermediate.

The nitrile oxide dipole **235** was generated as per Section 3.7.1. using the para-nitroimidoyl chloride **228** (0.118 g, 0.59 mmol, 2.6 eq). The solution of dipole **235** was concentrated under reduced pressure and added to the α-diazosulfoxide **14** (0.074 g, 0.28 mmol, 1 eq). Total volume was 10 mL (dichloromethane/ethyl acetate, 1 : 1). Rhodium acetate dimer (0.010 g, 5 mol %) was added lastly, to generate the α-oxo sulfine. The reaction mixture was stirred at room temperature for 1 h. At this point, iodomethane (1.01 g, 5.6 mmol, 20 eq) was added neat to the reaction mixture and the mixture was heated under reflux for 6 h, followed by stirring at room temperature for further 16 h. The crude reaction mixture was concentrated under reduced pressure to give a brown/black sticky solid which consisted of a series of unidentiable decomposition products.

3.7.2 Nitrile oxide and lactone derived α-oxo sulfine dipolar cycloaddition reactions

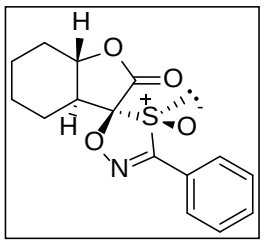
3'-Phenyl-3a,4,5,6,7,7a-hexahydro-2H-spiro[benzofuran-3,5'-[1,4,2]oxathiazol]-2-one *S*-oxide 267

Generation of the sulfine **101** *in situ* and trapping with benzonitrile oxide **192**.

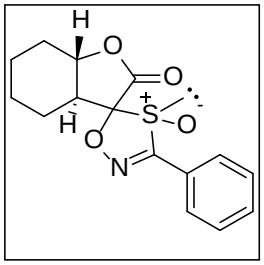
Benzohydroximoyl chloride **193** (0.371 g, 2.38 mmol, 4 eq) was over 10 min to a stirring solution of sodium hydroxide (1M, 3.6 mL) and ether (7 mL) cooled to 0°C with an ice bath. The ether layer containing the nitrile oxide **192** was separated, quickly dried over $MgSO_4$ and added to a solution of the α-diazosulfoxides **38,39** (1 : 1, 0.127 g, 0.59 mmol, 1 eq) in ether and dichloromethane. Rhodium acetate dimer (0.013 g, 0.029 mmol, 5 mol %) was added and the reaction mixture was put under a nitrogen atmosphere. After stirring at room temperature for 3 h a precipitate formed. The reaction mixture was monitored by TLC, which indicated that after 24 h all starting material had been consumed. The precipitate was collected by filtration through a sintered glass funnel (grade 4) to give the 1,4,2-oxathiazole-*S*-oxide as a white crystalline solid (0.077 g, 47 %) and a mixture of diastereomers (**267 : A**, 10:1). mp: 155-157°C; ν_{max}/cm^{-1} (neat) 2943, 1764, 1076; MS: (M+H) 306 (10%); HRMS (ESI+) Exact mass calculated for $C_{15}H_{15}NO_4S$ $[M+H]^+$, 306.0799. Found: 306.0800.

The material was characterised as a mixture of the major and minor components;

Note: The four possible diastereomers of the 1,4,2-oxathiazole-*S*-oxide are **267, 301**, **302** and **303** (see Results and Discussion, section 2.8). At this time, aside from **267**, it is not known which signal in the ^1H NMR spectrum corresponds to which cycloadduct, and therefore the cycloadduct present with unknown stereochemistry will be referred to as cycloadduct **A**.



Major Diastereomer **267**: δ_H (300 MHz, $CDCl_3$); 1.19-1.99 (7H, m, cyclohexyl ring), 2.25 (1H, ddd appears as dt, unresolved splitting, CHCSO), 2.40 (1H, cyclohexyl ring), 4.35 (1H, td, *J* 11.8, 3.4, CHO), 7.48 – 7.58 (3H, m, 3 x Aromatic CH), 7.82 – 7.97 (2H, m, 2 x Aromatic CH); δ_C (400 MHz, $CDCl_3$) 23.14, 23.17, 24.3, 30.1 (CH_2, 4 x cyclohexyl CH_2), 51.5 (CH, CHCSO), 82.3 (CH, CHO), 101.6 (qC, C_{spiro}), 124.5 (Cq, 1 x Aromatic Cq), 128.8 (CH, 2 x Aromatic CH), 129.7 (CH, 2 x Aromatic CH), 132.4 (CH, 1 x Aromatic CH), 160.2 (qC, C=N), 163.70 (Cq, C=O).



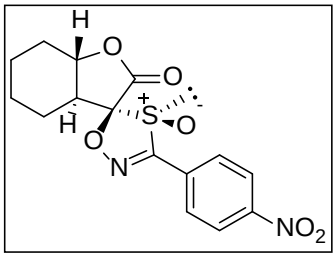
Characteristic signals belonging to the minor diastereomer, Cycloadduct **A** which was present as 10% of the mixture: δ_H (300 MHz, $CDCl_3$); 1.09-1.99 (7H, m, cyclohexyl ring), 2.40 (1H, 1 x CH of cyclohexyl ring), 2.57 (1H, ddd appears as a dt, *J* 10.8, 10.8, 4.2 CHCSO), 4.46 (1H, ddd appears as a td, *J* 10.9, 10.9, 3.9, CHO), 7.01- 7.82 (5H, m, 5 x Aromatic CH). Signals corresponding to the minor component were not observed in the ^{13}C NMR spectrum.

Following evaporation of the filtrate a ^1H NMR spectrum was recorded in which Cycloadduct **A** was a significant component of the mixture enabling identification of the signals as described above.

The relative stereochemistry of the major diastereomer **267** was determined by single crystal X-ray diffraction on a crystalline sample of **267** recrystallized from dichloromethane/hexane. Crystal data for $C_{15}H_{15}NO_4S$, *Mr* = 305.34, monoclinic, *C12/c*, a = 15.4674(14) Å, b = 8.4017(8) Å, c = 23.121(2) Å, β = 107.526 (2)°, *V* = 2865.2 (5) $Å^3$, *Z* = 8, D_c = 1.416 g cm^{-3}, F_{000} = 1280, Mo Kα radiation, λ = 0.71073 Å, *T* = 296 K, $2\theta_{max}$ = 26.75°, μ = 0.241 mm^{-1}, 10188 reflections collected, 3040 unique (R_{int} = 0.0323), final GooF = 1.030, R_1 = 0.0400, wR_2 = 0.0958 (3040 obs. data: $I > 2\sigma(I)$); R_1 = 0.0607, wR_2 = 0.1060 (all data).

3'-(4-Nitrophenyl)-3a,4,5,6,7,7a-hexahydro-2H-spiro[benzofuran-3,5'-[1,4,2]oxathiazol]-2-one *S*-oxide 296

Method 1: Generation of the sulfine *in situ* and trapping with *p*-nitrobenzonitrile oxide.

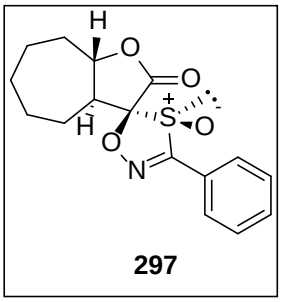


The α-diazosulfoxides **38,39** (0.125 g, 0.58 mmol, 1 eq) was dissolved in ether and dichloromethane (15 mL, 4:1). In a separate flask, *p*-nitrobenzohydroximoyl chloride **228** (0.468 g, 2.33 mmol, 4 eq) was added portion-wise at 0°C to a solution of ether (7 mL) and NaOH (1M, 3.6 mL). The biphasic mixture was stirred for 10 min and transferred to a separation funnel. The organic layer was separated, quickly dried using $MgSO_4$, and filtered in to the round bottomed flask containing the α-diazosulfoxides. Rhodium acetate dimer (0.012 g, 0.029 mmol, 5 mol %) was added to the reaction flask. The reaction mixture was stirred for 16 h and the precipitate was collected by filtration as the diastereomer **296** (0.049 g 25%). Mp 133-135°C; ν_{max}/cm^1 (neat) 1782, 1520, 1348, 1004; δ_H (400 MHz, $CDCl_3$) 1.30 – 2.10 (7H, m, CH_{2ring}), 2.32 (1H, t, *J* 9.5, 1H of CH_{ring}), 2.41 – 2.45 (1H, m, CHCS), 4.28 (1H, ddd appears as dt, *J* 12.4, 10.4, 4.1, CHO), 8.12 (2H, d, *J* 8.6, 2 x Aromatic CH), 8.38 (2H, d, *J* 8.3, 2 x Aromatic CH); δ_C ($CDCl_3$, 75.5 MHz); 23.0, 23.1, 24.3, 30.1 (CH_2¸4 x CH_2), 51.7 (CH, CHCS), 82.3 (CH, CHO), 102.7 (qC, C_{spiro}), 124.8 (CH, 2 x Aromatic CH),

129.5 (CH, 2 x Aromatic CH), 130.6 (Cq, Aromatic *Cq*-CN), 131.7 (Cq, Aromatic *Cq*, Cq-NO_2), 149.8 (Cq, C=N), 172.6 (Cq, C=O); MS: (M+H) 351 (10%).

3'-Phenyl-3a,5,6,7,8,8a-hexahydro-2H,4H-spiro[cyclohepta[b]furan-3,5'-[1,4,2]oxathiazol]-2-one *S*-oxide 297

Generation of the sulfine *in situ* and trapping with benzonitrile oxide **192**.



297

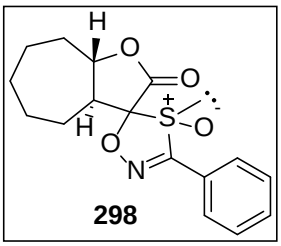
The α-diazosulfoxide **75** (0.141 g, 0.62 mmol, 1 eq) was dissolved in ether and dichloromethane (15 mL, 4:1). In a separate flask, benzohydroximoyl chloride **193** (0.382 g, 2.47 mmol, 4 eq) was added portion-wise at 0°C to a solution of ether (7 mL) and aqueous NaOH (1M, 3.6 mL). The mixture was stirred for 10 min and transferred to a separation funnel. The organic layer was separated, quickly dried using $MgSO_4$ and filtered in to the round bottomed flask containing the α-diazosulfoxide. Rhodium acetate dimer (0.013 g, 0.03 mmol, 5 mol %) was added to the reaction mixture flask. The reaction mixture was stirred for 2.5 h at which point an aliquot was removed, concentrated under reduced pressure and analysed by ^{1}H NMR spectroscopy. The ^{1}H NMR spectrum of an aliquot of the crude reaction mixture showed the presence of 4 compounds, 2 of which (**297** and **298**) were confirmed as being diastereomers of the desired product. A precipitate from the reaction was one diastereomer only (**297**) and the mother liquor, was again, a mixture of the 4 components (Table 62)

Table 62: Characteristic ^{1}H NMR signals and ratios of the four components in the crude material from the cycloaddition reaction.

Component	**1**	**2**	**3**	**4**
	299	**298**	**297**	**300**
Characteristic signal (CHO):	4.70 ppm	4.60 ppm	4.50 ppm	4.28 ppm
Crude Ratio:	1.00	0.12	0.63	0.37
Precipitate:	0	0	1	0
Mother Liquor:	1.00	0.12	0.26	0.32

The crude product was filtered off to give the precipitated diastereomer **297** only (0.041 g 21%). The mother liquor was concentrated and adsorbed on to Celite. Purification by column chromatography on silica gel using hexane-ethyl acetate as eluent (95:5) as eluent led to isolation of a second, minor diastereomer **298** (0.014 g, 7%).

Spectroscopic characteristics of the diastereomer **297**; mp: 145-147°C, ν_{max}/cm^{-1} (neat): 2932, 1763, 1243, 1087; δ_H (400 MHz, $CDCl_3$) 1.30 – 1.95 (9H, m, 4 x CH_2 and one of CH_2), 2.49 – 2.55 (1H, m, 1H of 1 cycloheptane CH_2), 2.64 – 2.70 (1H, m, CHCS), 4.50 (1H, ddd appears as dt *J* 11.9, 10.2, 3.7, CHO), 7.49 – 7.58 (3H, m, 3 x Aromatic CH), 7.92 (2H, d, *J* 7.3, 2 x Aromatic CH); δ_C ($CDCl_3$, 75.5 MHz); 22.8, 24.95, 25.01, 26.1, 33.6 (CH_2, 5 x CH_{2ring}), 49.0 (CH, CHCS), 83.0 (CH, CHO), 103.5 (qC, C_{spiro}), 124.6 (Cq, Aromatic Cq),128.8, 129.6, 132.3 (CH, 3 x Aromatic CH), 159.6 (Cq, C=N), 163.5 (Cq, C=O); MS: (M+H) 320 (20%); HRMS (ESI+) Exact mass calculated for $C_{16}H_{18}NO_4S$ $[M+H]^+$, 320.0957. Found: 320.0953.



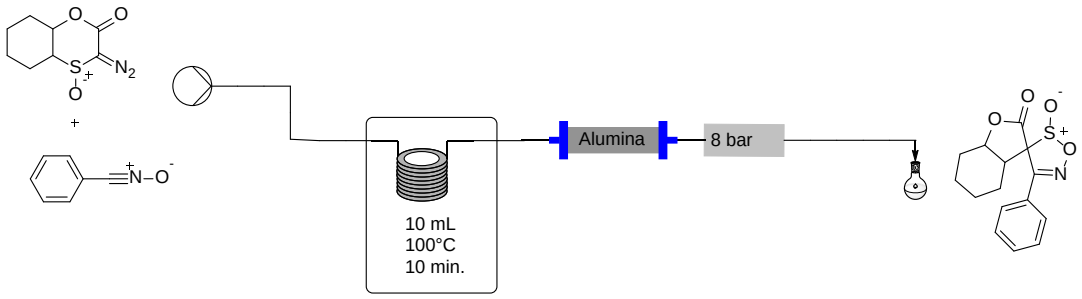
298

Spectroscopic characteristics of the minor product tentatively assigned as the cycloadduct **298** with unknown stereochemistry; δ_H (400 MHz, $CDCl_3$); 1.26 – 1.87 (9H, m, 9 x cycloheptyl CH), 2.46 – 2.54 (1H, m, 1H of 1 cycloheptyl CH_2), 2.58 – 2.65 (1H, m, CHCS), 4.61 (1H, ddd appears as dt, *J* 11.0, 10.1, 4.6, CHO*)*, 7.56 – 7.59 (2H, t, *J* 7.8, Aromatic CH), 7.63 – 7.67 (1H, m, 1 x Aromatic CH), 7.88 (2H, d, *J* 7.4, 2 x Aromatic CH)*;*

^{13}C NMR signals were obtained from an impure fraction of the product **298** which contained 5% of an impurity; ($CDCl_3$, 75.5 MHz) 24.1, 25.0, 25.1, 26.9, 33.1 (5 x CH_{2ring}), 41.6 (CH, CHCS), 84.9 (CH, CHO), 122.1 (Cq, C_{spiro}), 129.4 (Cq, 2 x Aromatic Cq), 130.3 (Cq, 2 x Aromatic Cq), 131.7 (Cq, Aromatic Cq), 134.2 (Cq, Aromatic Cq), 160.2 (Cq, C=N), 176.5 (Cq, C=O).

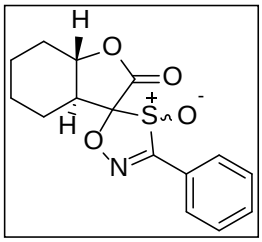
3.7.3 Cycloaddition reaction of lactone derived α-oxo sulfine with nitrile oxide dipole in continuous flow.

Note: A mixture of α-diazosulfoxides **38,39** believed to be equimolar was employed in the reactions described below. Each individual sample was not checked by ^{1}H NMR.



Scheme 152

Attempt 1: 10 min residence time at 100°C in DCM/EtOAc.



The nitrile oxide dipole **192** was generated from the imidoyl chloride **193** (0.338 g, 2.2 mmol, 2.6 eq) using the procedure outlined in Section 3.7.1. The α-diazosulfoxides **38,39** (1 : 1, 0.184 g, 0.85 mmol, 1 eq) were added and the volume made up to 18 mL of dichloromethane/ethyl acetate (1 : 1, 0.04M). The solution was pumped through a 10 mL reaction coil heated to 100°C followed by a 10 mm id Omnifit™ glass column packed with Alumina (~ 2.5 g, volume ~ 1.4 mL). The crude product was collected as a brown solution and concentrated under reduced pressure to give the crude product as a viscous brown oil (0.459 g). Analysis of the mixture by ^{1}H NMR spectroscopy showed a complex mixture consisting of starting material (approx. 80%) and unidentified decomposition products.

Attempt 2: 30 min, 120°C, Using conditions which were optimal for the ketone cycloadditions, but with a higher temperature because using a lactone derived α-oxo sulfine.

The nitrile oxide dipole **192** was generated from the imidoyl chloride **193** (0.194 g, 1.3 mmol, 2.6 eq) using the procedure outlined in Section 3.7.1. The α-diazosulfoxides **38,39** (1 : 1, 0.106 g, 0.49 mmol, 1 eq) were added and the volume made up to 14 mL of dichloromethane/ethyl acetate (1 : 1, 0.04 M). The solution was pumped through a 10 mL reaction coil heated to 120°C followed by a 10 mm id Omnifit™ glass column packed with Alumina (~2.5 g, volume ~ 1.4 mL). The crude product was collected as a brown solution and concentrated under reduced pressure to give the crude product as

a viscous brown oil (0.262 g). Analysis of the mixture by ^{1}H NMR spectroscopy showed a complex mixture of products and no evidence for the presence of the starting material. Purification of the material by column chromatography on silica gel led to the elution of multiple fractions each containing a mixture of diastereomeric cycloadducts.

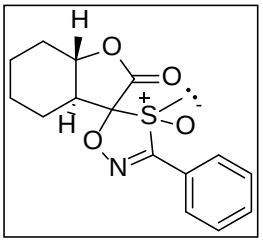
The first fraction (0.037 g, 25%) isolated from the column contained 4 cyclodducts **A**, **267**, **B** and **C** in a ratio of 0.88 : 1.18 : 0.31 : 1.0. The characteristic signals of the 4 cycloadducts are as follows

Table 63

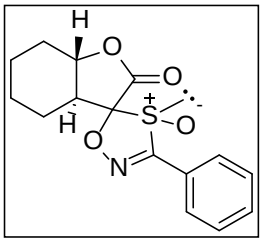
Diastereomer	Ratio	Corresponding peak
A	0.88	4.46 ppm (1H, td, *J* 10.8, 3.9, CHO), 2.89 (1H, td, CHCS)
267	1.18	4.35 ppm (1H, td, *J* 11.3, 10.8, CHO) (characterised by crystal structure)
B	0.31	4.11 ppm (1H, td, *J* 11.6, 10.9, CHO)
C	1.0	3.77 ppm (1H, td, *J* 11.8, 11.2, CHO)

The stereochemistry of the possible cycloadducts **267**, **301**, **302**, and **303** are shown in the Results and Discussion, Section 2.8. However, aside from **267**, it is not known which signal in the ^{1}H NMR spectrum corresponds to which cycloadduct, and therefore the cycloadducts with unknown stereochemistry will be referred to as cycloadducts **A, B** and **C**. At this point identification of which cycloadduct is **301**, **302**, or **303** is not possible.

A second fraction (0.017 g, 12%) contained the diastereomers **267, A**, **B,** and **C** in a ratio of 1 : 0.1 : 0.6 : 0.08 respectively. The compounds **A** and **B** were characterised as a mixture with the following characteristic signals;



Cycloadduct **A;** 2.89 (1H, td, *J* 11.4, 11.7, 3.3, CHCS), 4.46 (1H, td, *J* 10.8, 3.9, CHO), 7.92 (2H, dd, *J* 7.8, 1.8, 2 x Aromatic CH) δ_C ($CDCl_3$, 75 MHz); 23.2, 23.4, 24.7, 30.6 (4 x cyclohexyl CH_2), 47.1 (CH, CHCS), 83.4 (CH,CHO), 104.0 (Cq, C_{spiro}), 128.7 (2 x Aromatic CH), 129.5 (2 x Aromatic CH), 132.2 (1 x Aromatic Cq), 160.3 (Cq, C=N), 167.6 (Cq, C=O).



Cycloadduct **B;** 4.11 (1H, td, *J* 11.6, 10.9, 3.8, CHO), 7.84 (2H, dd, *J* 7.4, 1.6, 2 x Aromatic CH) δ_C ($CDCl_3$, 75 MHz); 24.0, 24.2, 24.8, 25.9 (4 x cyclohexyl CH_2), 46.1 (CH, CHCS), 83.5 (CH, CHO), 124.7 (Cq, C_{spiro}), 129.5 (2 x Aromatic CH), 130.5 (2 x Aromatic CH), 134.2 (1 x Aromatic Cq), 159.7 (Cq, C=N).

Attempt 3: Toluene/DCM, 30 min res time, 120°C, Alumina Column.

The nitrile oxide dipole **192** was generated from the imidoyl chloride **193** (0.132 g, 0.87 mmol, 2.6 eq) using the procedure outlined in Section 3.7.1. The α-diazosulfoxides **38**,**39** (0.072 g, 0.33 mmol, 1 eq) were added and the volume made up to 7 mL of dichloromethane/ethyl acetate (1 : 1, 0.04 M). The solution was pumped through a 10 mL reaction coil heated to 120°C followed by a 10 mm id Omnifit™ glass column packed with Alumina (~ 2.5 g, volume ~ 1.4 mL). The crude product was collected as a brown solution and concentrated under reduced pressure to give the crude product as a viscous brown oil (0.201 g). Analysis of the mixture by ^{1}H NMR spectroscopy showed a complex mixture of products and complete consumption of the starting material. Purification of the material by column chromatography on silica gel led to the elution of multiple fractions each containing a mixture of diastereomeric cycloadducts.

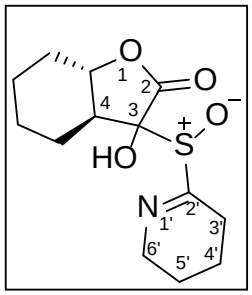
The first fraction (0.027 g, 25%) contained a mixture of the 1,4,2-oxathiazole-*S*-oxides **A** and **B** and an previously uncharacterised cycloadduct **304** in a ratio of 0.9 : 0.3 : 1.0. Characteristic spectroscopic signals are as described in Section 3.7.3. A second fraction (0.01 g, 8%) isolated from the column contained a mixture of **A** and **304** in a ratio of 0.9 : 1.0 respectively. Characteristic signals of **304** are 4.34 ppm in the ^{1}H NMR spectrum and 45.0 and 84.8 ppm in the ^{13}C NMR spectrum.

Comparison of flow reaction in superheated DCM/ethyl acetate to thermal reaction in batch.

The nitrile oxide dipole **192** was generated from the imidoyl chloride **193** (0.275 g, 1.81 mmol, 2.6 eq) using the procedure outlined in Section 3.7.1. The α-diazosulfoxides **38,39** (0.180 g, 0.7 mmol, 1 eq) were added and the volume made up to 15 mL of dichloromethane/ethyl acetate 1:1, (0.04M). Separately an oil bath was heated to 130°C (to allow for heat loss between the oil and the reaction vessel which the desired temperature was 120°C). The solution of diazo starting material **38,39** and nitrile oxide **192** was hot plunged in to the pre heated oil bath and heated under reflux for 30 mins. Concentration under reduced pressure gave back a bright yellow oily residue (0.384 g). Analysis of the crude reaction mixture by ^{1}H NMR spectroscopy showed the presence of the axial α-diazosulfoxide starting material **38** : **39** (8 : 1) with no indication of formation of the desired cycloadducts.

3.7.4 Nitrone and lactone derived α-oxo sulfine dipolar cycloaddition reactions

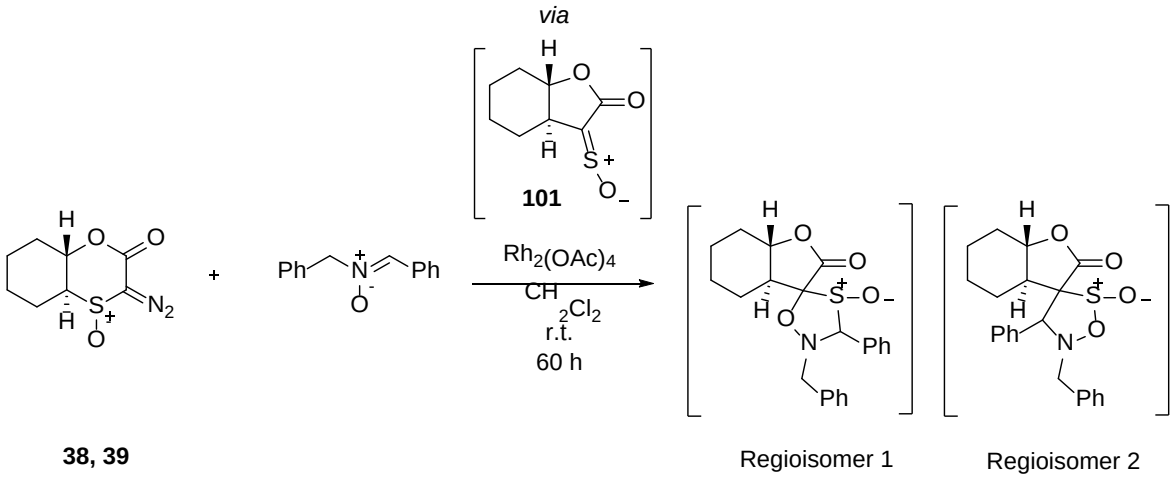
Dipolar cycloaddition of 2,3,4,5-tetrahydropyridine 1-oxide 212 with the α-oxo sulfine derived from α-diazosulfoxides 38,39



The α-diazosulfoxides **38,39** (1 : 0.7, 0.226 g, 1.03 mmol, 1 eq) were added to 2,3,4,5-tetrahydropyridine 1-oxide **212** [(freshly prepared for each reaction, see section 3.6), (0.154 g, 1.55 mmol, 1.5 eq)] in dichloromethane (20 mL). Rhodium acetate dimer (0.022 g, 0.051 mmol, 5 mol %) was added and the reaction mixture was stirred at room temperature for four days until TLC analysis showed no change. The reaction mixture was flitered through a Celite® plug and the solvent was removed under reduced pressure to give the crude product as an orange residue (0.312 g) which on analysis by ^{1}H NMR spectroscopy showed a complex mixture of unidentifiable products. Following purification by column chromatography on silica gel using hexane-ethyl acetate (70 : 30) as eluent, the product **307** was isolated as a yellow crystalline solid (0.047 g, 16%). mp 53-55°C; ν_{max}/cm^{-1} (neat) 2944, 1674, 1096; δ_H (400 MHz, $CDCl_3$) 1.26 – 2.04 (10H, m, 5 x CH_2), 2.12 – 2.29 (2H, m, CH_2), 2.32 – 2.61 [overlapping signals containing a 2H, t, of C(3')H_2, and a 1H, td of C(4)H], 3.30 [2H, br s, C(6')H_2], 3.59 (1H, td, *J* 11.4, 3.2, CHO), 8.62 (1H, br s, OH, exchanges in a D_2O shake); δ_C (75.5 MHz, $CDCl_3$) 19.6, 22.3. 24.3, 25.6, 26.4, 30.0, 30.4 (7 x CH_2), 41.4 (CH_2, NCH_2), 46.9 [CH, C(4)H], 84.1 (CH, CHO), 88.9 (Cq, C_{spiro}), 158.3 (Cq, C=N), 174.7 (Cq, C=O); HRMS (ES+) Exact mass calculated for $C_{13}H_{19}NO_4S$ $[M+H]^+$, 286.1113. Found 286.1122.

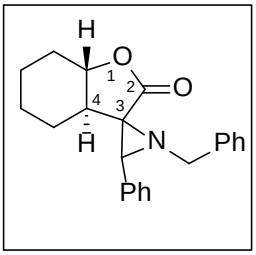
Note: In some instances, the ring opened rearrangement product **307** was prone to co-eluting with residual nitrone **212** with corresponding peaks at 24.5, 28.9, and 52.7 ppm in the ^{13}C NMR spectrum.

Dipolar cycloaddition of N-benzyl-1-phenylmethanimine oxide 211 with the α-oxo sulfine derived from α-diazosulfoxides 38,39

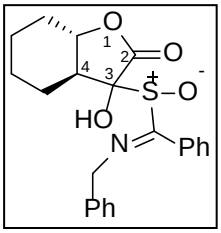


Scheme 153

The α-diazosulfoxides **38,39** (1 : 0.7, 0.176 g, 0.82 mmol, 1 eq) were dissolved in the minimum amount of dichloromethane (5 mL). The nitrone **211** [(can be synthesised and stored in the freezer, see section 3.6.1), (0.164 g, 0.780 mmol, 0.95 equiv)] was added dropwise as a solution in dichloromethane (5 mL). Lastly, rhodium acetate dimer was added (0.002 g, 0.041 mmol, 5 mol %). The reaction mixture was dark green on addition of the rhodium acetate dimer but gradually turned brown over 15 min. The reaction mixture was stirred at room temperature for 60 h and then concentrated under reduced pressure to leave a dark brown oily residue (0.271 g). This was dissolved in the minimum amount of dichloromethane and purified by column chromatography on silica gel. Purification by hexane-ethyl acetate (95 : 5, increasing to 70 : 30) led to the elution of three separate tentatively assigned products.

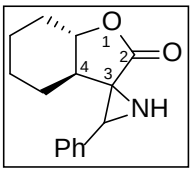


The first fraction to elute contained the aziridine **311** and some benzylamine (80 : 20) as a colourless oily residue (0.015 g, 5%); ν_{max}/cm^{-1} (neat); 1765, 1258, 1010; δ_H (400 MHz, $CDCl_3$); 0.71 – 1.52 (6H, m, 4 x cyclohexyl CH_2), 1.65 – 1.76 [2H, m, including C(4)H and 1H of cyclohexyl CH_2], 2.01 – 2.09 (1H, m, 1H of cyclohexyl CH_2), 3.14 (1H, td, *J* 12.0, 11.1, 3.6, CHO), 3.65 (1H, s, PhCH), 3.72 (1H, d, *J* 12.7, A of AB_q, $PhCH_2$), 4.20 (1H, d, *J* 12.7, B of AB_q, $PhCH_2$), 7.26 – 7.45 (10H, m, 10 x Aromatic CH); δ_C (75.5 MHz) 23.7, 24.7, 25.4, 30.4 (CH_2, 4 x cyclohexyl CH_2), 45.7 (CH, CHPh), 49.7 [CH, C(4)H], 50.1 (Cq, C_{spiro}), 56.3 (CH_2, CH_2Ph), 83.8 (CH, CHO), 127.50, 127.53 (CH, 2 x Aromatic CH), 127.6, 128.4, 128.5, 129.1, (CH, 4 signals representing 8 x Aromatic CH), 135.3, 138.6 (Cq, 2 x Aromatic Cq), 174.2 (Cq, C=O); MS: $(M+H)^+$ 397 (10%) HRMS (ESI+) Exact mass calculated for $C_{22}H_{24}NO_2$ $[M+H]^+$, 334.1807 Found: 334.1804. Characteristic peaks of the benzylamine are a CH_2 signal at 3.87 ppm in the ^1H NMR spectrum and at 50.1 ppm in the ^{13}C NMR spectrum.



The second fraction to elute was the ring opened rearrangement product **312** as a yellow oil (0.022 g, 7 %); ν_{max}/cm^{-1} (neat); 1688, 1596, 1221; δ_H (400 MHz, $CDCl_3$) 0.54 – 0.58 ppm, (1H, m, 1H of cyclohexyl CH_2), 0.73 (1H, qd, *J* 12.8, 4.2, 1H of cyclohexyl CH_2), 0.88 – 1.14 (1H, m, 1H of cyclohexyl CH_2), 1.19 – 1.36 (1H, m, 1H of cyclohexyl CH_2), 1.39 – 1.47 (1H, m, 1H of cyclohexyl CH_2), 1.54 (1H, qd, *J* 11.8, 3.8, 1H of cyclohexyl CH_2), 1.71 – 1.82 (1H, m, 1H of cyclohexyl CH_2), 2.09 – 2.17 (1H, m, 1H of cyclohexyl CH_2), 2.43 [1H, td, *J* 11.2, 3.1, C(4)H], 3.61 (1H, td, *J* 11.4, 3.4, CHO), 4.09 (2H, d, *J* 6.6, $PhCH_2$), 7.10 – 7.39 (10H, m, 10 x Aromatic CH), 8.54 (1H, br t, OH, exchanges rapidly in D_2O shake); δ_C (75.5 MHz) 24.2, 25.3, 28.6, 30.1 (4 x CH_2), 47.2 [CH, C(4)H], 47.4 (CH_2, CH_2Ph), 84.7 (CH, CHO), 94.2 (Cq, C_{spiro}), 126.9, 127.2, 128.6, 129.1 (4 signals representing 10 x Aromatic CH), 133.5, 139.3 (Cq, 2 x Aromatic Cq), 158.55 (Cq, C=N), 174.7 (Cq, C=O); MS: $(M)^+$ 397 (53 %) HRMS (ESI+) Exact mass calculated for $C_{22}H_{24}NO_4S$ $[M+H]^+$, 398.1426 Found: 398.1423.

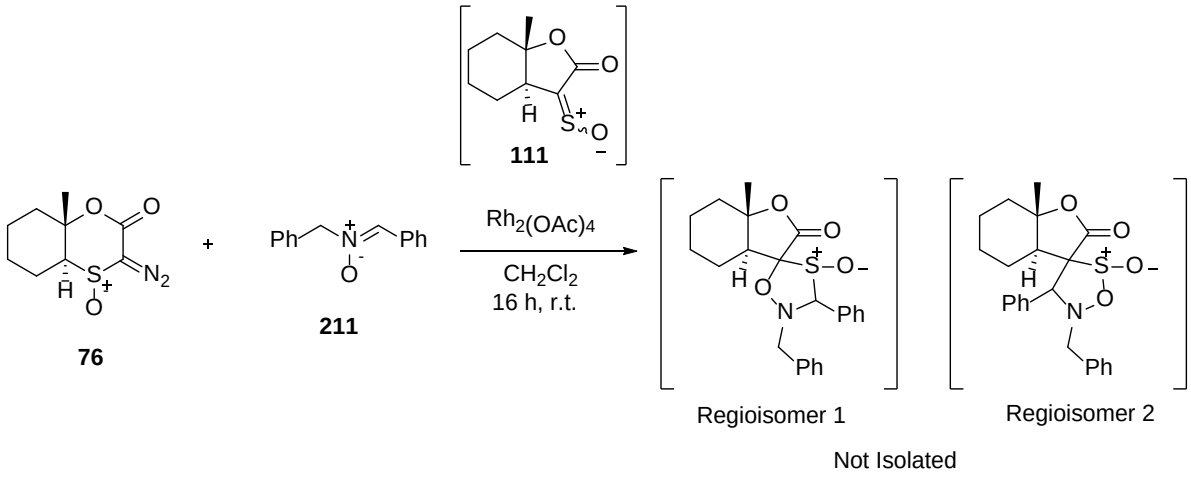
Signals corresponding to a minor impurity are present in the ^1H NMR spectrum as doublets at 4.19 and 4.55 ppm with *J* values of 14.4 Hz and a singlet at 4.81 ppm respectively. These signals correspond to 9% of the material.



The third fraction to elute was the debenzylated aziridine **313** as a white crystalline solid (0.024 g, 10%); m.p. 86 – 87°C, ν_{max}/cm^{-1} (neat); 1764, 1156; δ_H (400 MHz, $CDCl_3$) 1.28 – 1.50 (4H, m, 4H of cyclohexyl CH_2), 1.56 – 1.84 (4H, m, 3H of cyclohexyl CH_2, 1 x NH), 1.89 – 2.03 (2H, m, 2H of cyclohexyl CH_2), 2.30 (1H, d, *J* 11.6, 1 H of cyclohexyl CH_2), 2.58 [1H, qd, *J* 12.2, 3.3, C(4)H], 3.97 (CH, td, *J* 11.3, 3.7, CHO), 4.27 (1H, d, *J* 12.7, CHPh), 7.50 (2H, t, *J* 8.1, 2 x Aromatic CH), 7.62 (1H, t, *J* 8.1, 1 x Aromatic CH), 8.01 (2H, d, *J* 7.5, 2 x Aromatic CH); δ_C (75.5 MHz) 24.0, 25.1, 27.6, 30.1 (4 x CH_2, 4 x cyclohexyl CH_2), 47.2 [CH, C(4)H], 54.4 (CH, CHPh), 83.1 (CH, CHO), 128.76 (2 x CH, 2 x Aromatic CH), 129.2 (2 x CH, 2 x Aromatic CH), 133.9 (1 x CH, 1 x Aromatic CH), 136.4 (1 x Cq, 1 x Aromatic Cq), 172.2 (Cq, C=O); MS $(M+H)^+$ 244 (20%); HRMS (ES+) Exact mass calculated for $C_{15}H_{18}NO_2$ $[M+H]^+$, 244.1338. Found 244.1325.

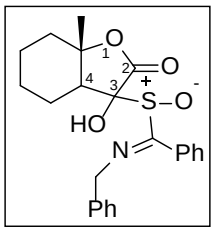
Note: No spiro signal was observed for this aziridine **313**. An extraneous signal was seen in the ^{13}C NMR spectrum at 193.4 pp, and may correspond to benzaldehyde formed in the reaction conditions.

Dipolar cycloaddition of N-benzyl-1-phenylmethanimine oxide 211 with with the α-oxo sulfine derived from α-diazosulfoxide 76



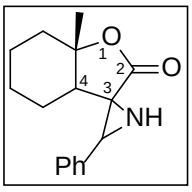
Scheme 154

The α-diazosulfoxide **76** (0.220 g, 0.96 mmol, 1 eq) was dissolved in the minimum amount of dichloromethane (5 mL). The nitrone **211** (0.204 g, 0.96 mmol, 1 eq) was added dropwise as a solution in dichloromethane (5 mL). Lastly, rhodium acetate dimer was added (0.004 g, 0.04 mmol, 5 mol %). The reaction mixture was dark green on addition of the rhodium catalyst but turned brown gradually over 15 min. The reaction mixture was stirred at room temperature for 60 h and then concentrated under reduced pressure to leave a dark brown oily residue (0.298 g). This residue was dissolved in dichloromethane and purified by column chromatography on silica gel. Purification by gradient hexane-ethyl acetate as eluent (100% hexane – 90 : 10) led to the elution of two separate products.



The first fraction was the ring opened rearrangement product **316** as a bright yellow oil (0.016 g, 4%); Bright yellow oil; ν_{max}/cm^{-1} (neat) 1688, 1055; δ_H(300 MHz, $CDCl_3$) 0.43 (1H, d, *J* 12.9, 1 x cyclohexyl CH), 0.72 – 1.15 (3H, m, 3 x cyclohexyl CH), 1.20 – 1.96 (7H, m, overlapping signals include a 3H s at 1.23 ppm and 4 x cyclohexyl CH), 2.65 [1H, dd, *J* 12.6, 3.4, C(4)H], 4.04 (2H, d, *J* 6.6, CH_2Ph), 7.08 – 7.36 (10 H, m, 10 x Aromatic CH), 8.36 – 8.40 (1H, br t, OH); δ_C (100 MHz, $CDCl_3$) 18.8 (CH_3, $CqCH_3$), 22.8, 24.7, 25.3, 36.7 (CH_2, 4 x cyclohexyl CH_2), 47.4 (CH_2, CH_2PH), 50.6 [CH, C(4)H], 84.7 (Cq, $CqCH_3$), 94.9 (Cq, C_{spiro}), 126.8, 127.0, 128.0, 128.5, 128.7, 128.9, (6 signals representing 10 x Aromatic CH), 133.5, 139.5 (Cq, 2 x Aromatic Cq), 157.8 (Cq, C=N), 174.5 (Cq, C=O); HRMS (ESI+) Exact mass calculated for $C_{23}H_{26}NO_4S$ $[M+H]^+$, 412.1579 Found: 412.1583.

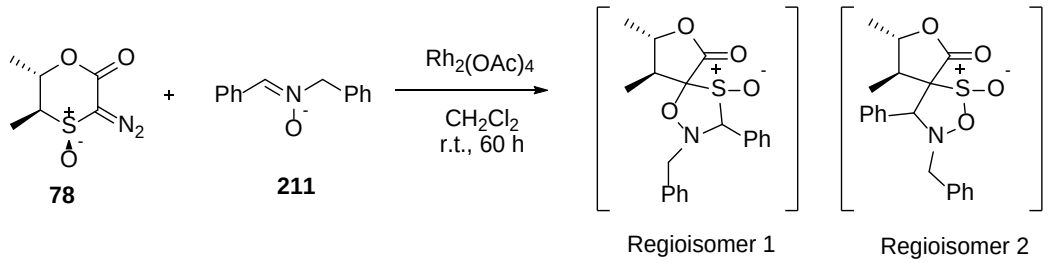
Signals for an unknown impurity are present in the ^1H NMR spectrum as doublets at 4.23, 4.38 and 4.57 ppm. These signals correspond to 15% of the material.



The second fraction to elute contained the debenzylated aziridine **317** as an off white crystalline solid (0.042 g, 13%); Found C, 74.26; H 7.73 $C_{16}H_{19}NO_2$ requires C, 74.68; H 7.44; m.p. 96 – 97°C, ν_{max}/cm^{-1} (neat); 2930, 1760, 1183; δ_H (400 MHz, $CDCl_3$) 1.21 – 1.69 (8H, m, containing 3H s at 1.42 ppm and 5 x cyclohexyl CH), 1.71 – 1.97 (4H, m, containing 3 x cyclohexyl CH and 1 x NH), 1.74 – 1.91 (4H, m, 4 x cyclohexyl CH), 2.03 – 2.11 (1H, m, 1 x cyclohexyl CH), 2.79 [1H, td, *J* 12.6, 2.9, C(4)H], 4.39 (1H, d, *J* 13.3, CHPh), 7.50 (2H, t, *J* 8.0, 2 x Aromatic CH), 7.58 – 7.63 (1H, m, 1 x Aromatic CH), 8.01 (2H, d, *J* 7.7, 2 x Aromatic CH); δ_C (75.5 MHz, $CDCl_3$) 19.1 (CH_3), 23.0, 24.3, 25.4, 36.9 (4 x CH_2, 4 x cyclohexyl CH_2), 49.6 [CH, C(4)H], 51.9 (CH, CHPh), 84.9 (Cq, CqO), 128.7 (2 x CH, 2 x Aromatic CH), 129.2 (2 x CH, 2 x Aromatic CH), 133.8 (1 x CH, 1 x Aromatic CH), 172.0 (Cq, C=O); MS (ESI+) tentative 257 M^+ (10%).

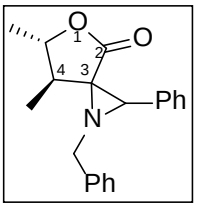
Note: The C_{spiro} is not seen in the ^{13}C NMR spectrum.

Dipolar cycloaddition of N-benzyl-1-phenylmethanimine oxide 211 with with the α-oxo sulfine derived from α-diazosulfoxide 78



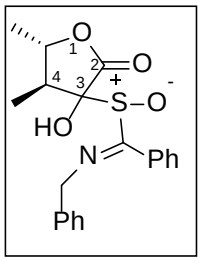
Scheme 155

The α-diazosulfoxide **78** (0.093 g, 0.49 mmol, 1 eq) was dissolved in the minimum amount of dichloromethane (5 mL). The nitrone **211** (0.104 g, 0.49 mmol, 1 equiv) was added dropwise as a solution in dichloromethane (5 mL). Lastly, rhodium acetate dimer was added (0.001 g, 0.02 mmol, 1 mol %). The reaction mixture was dark green on addition of the rhodium but gradually turned brown over 15 min. The reaction mixture was stirred at room temperature for 60 h and then concentrated under reduced pressure to leave a dark brown oil/residue. This was dissolved in the minimum amount of dichloromethane and purified by column chromatography on silica gel using gradient hexane-ethyl acetate as eluent (100% - 90 : 10) leading to the elution of three separate tentatively assigned products.



The first fraction contained the aziridine **319** as a colorless oil (0.016 g, 9%); ν_{max}/cm^{-1} (neat) 2926, 2125, 1757, 698; δ_H ($CDCl_3$, 400MHz) 0.71 (3H, d, *J* 7.2, CH_3), 1.17 (3H, d, *J* 6.2, CH_3), 1.48 – 1.62 [1H, m, C(4)H], 3.64 (1H, s, CHPh), 3.92 – 3.99 (1H, m, CHO) 4.21 (1H, d, *J* 13.6, A of AB_q, one of CH_2Ph), 4.32 (1H, d, *J* 13.6, B of AB_q, one of CH_2Ph), 7.26 – 7.45 (10H, m, 10 x Aromatic CH); δ_C ($CDCl_3$, 100MHz) 15.5, 20.6

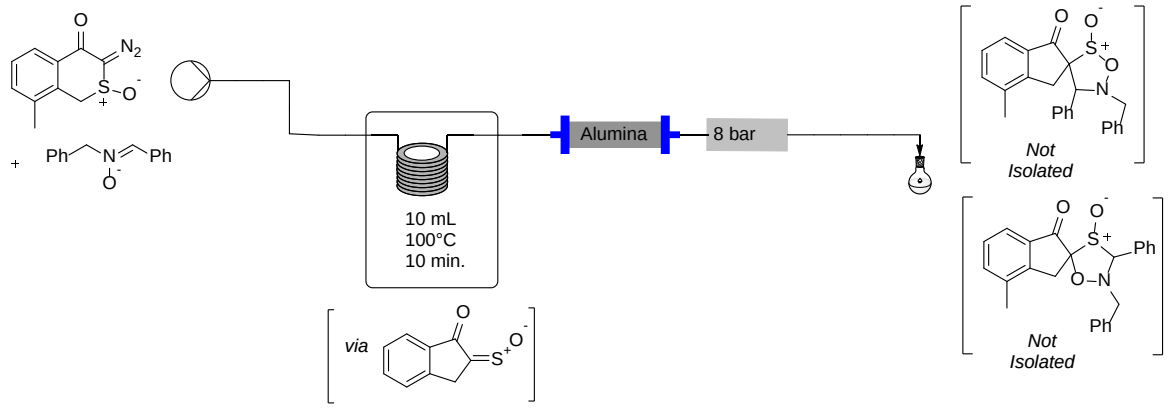
(CH_3, 2 x CH_3), 37.3 [CH, C(4)H], 50.1 (Cq, C_{spiro}), 53.1 (CH, CHPh), 54.8 (CH_2, CH_2Ph), 81.7 (CH, CHO), 127.2 (CH, 1 x Aromatic CH), 127.5 (CH, 2 x Aromatic CH), 127.7 (CH, 1 x Aromatic CH), 128.3, 128.4, 129.1 (CH, 3 signals representing 6 x Aromatic CH), 135.4, 138.8 (Cq, 2 x Aromatic Cq). No signal was seen for the C=O; MS (ESI M+H)$^+$ 308 (100%); HRMS (ES+) Exact mass calculated for $C_{20}H_{22}NO_2$ [M+H]$^+$, 308.1651. Found 308.1654.



The second fraction to elute was the ring opened rearrangement product **320** as a pale yellow oil (0.029 g, 16%); ν_{max}/cm^{-1} (neat) 1681, 1593, 1229; δ_H ($CDCl_3$, 400MHz) 0.64 (3H, d, *J* 6.5, CH_3), 1.31 (3H, d, *J* 6.6, CH_3), 2.43 – 2.50 [1H, m, C(4)H], 4.01 – 4.09 (1H, m, CHO), 4.12 (2H, dd, *J* 6.6, 2.1, CH_2Ph), 7.10 – 7.12 (2H, m, 2 x Aromatic CH), 7.20 – 7.29 (5H, m, 5 x Aromatic CH), 7.39 – 7.41 (3H, m, 3 x Aromatic CH), 8.79 (1H, br t, OH); δ_C ($CDCl_3$, 100 MHz) 20.4, 21.2 (CH_3, 2 x CH_3), 40.4 [CH, C(4)H], 47.7 (CH_2, CH_2Ph), 81.2 (CH, CHO), 94.8 (Cq, C_{spiro}), 126.9, 127.2, 128.6, 129.2 (CH, 4 signals representing 10 x Aromatic CH), 133.5, 139.2 (Cq, 2 x Aromatic Cq), 160.3 (Cq, C=N), 173.7 (Cq, C=O); MS (ESI+) tentative 371 M$^+$ (10%).

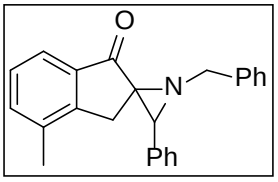
3.7.5 Nitrone and ketone derived α-oxo sulfine dipolar cycloaddition reactions

Cycloaddition reaction of the α-oxo sulfine derived from α-diazosulfoxide 80 with the dibenzylnitrone 211



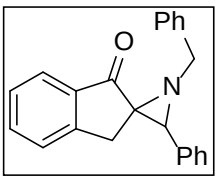
Scheme 156

The nitrone **211** (0.249 g, 1.18 mmol, 2.6 eq) was added to the α-diazosulfoxide **80** (0.100 g, 0.45 mmol, 1 eq) in dichloromethane/ethyl acetate (1 : 1, 10 mL, 0.04 M). The solution was pumped through a 10 mL reaction coil heated to 100°C, with a 10 minute residence time, followed by a 10 mm id Omnifit™ glass column packed with Alumina (~2 g, volume, ~ 1.2 mL). The crude material was collected as a brown solution and concentrated under reduced pressure to give the crude product as a viscous brown oil (0.359 g). Analysis of the mixture by ^{1}H NMR spectroscopy showed a complex mixture with no evidence of the α-diazosulfoxide **80** starting material, or intermediate α-oxo sulfine. Purification of the material using gradient elution with hexane - ethyl acetate (100 : 0 - 50 : 50) led to elution of the aziridine rearrangement product **329** as a yellow crystalline solid; which is formed as one diastereomer through the loss of SO_2 (0.056 g, 32%).; mp 127 - 128°C; ν_{max}/cm^{-1} (neat) 1698, 1277, 1048; δ_H (300

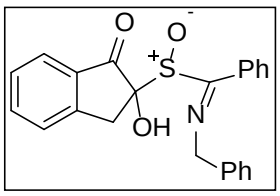


MHz, $CDCl_3$) 2.20 (3H, s, 1 x $ArCH_3$), 2.64 (1H, d, A of AB_q, *J* 18.1, one of $ArCH_2$), 2.94 (1H, d, B of AB_q, *J* 18.1, one of $ArCH_2$), 3.74 (1H, s, CHPh), 4.33 – 4.47 (2H, *J* 14.1, AB_q, benzylic CH_2), 7.13 – 7.40 (12H, m, 12 x Aromatic CH), 7.58 (1H, d, *J* 7.3, 1 x Aromatic CH); δ_C ($CDCl_3$, 75.5 MHz) 17.8 (CH_3, $ArCH_3$), 31.1 (CH_2, $ArCH_2$), 54.0 (CH_2, NCH_2), 54.6 (Cq, C_{spiro}), 55.1 (CH, CHPh), 120.6, 126.7, 127.5, 127.6, 128.1, 128.3, 128.3, 135.1 (8 signals representing 13 x Aromatic CH), 135.4, 137.2, 137.3, 139.6, 151.4 (5 signal representing 5 x Aromatic Cq), 201.6 (Cq, C=O). $(M+H)^+$ 340 (100%), HRMS (ESI+) Exact mass calculated for $C_{24}H_{22}NO$ $[M-H]^+$, 340.1701 Found: 340.1687.

Cycloaddition reaction of the α-oxo sulfine derived from α-diazosulfoxide 14 with the dibenzylnitrone 211

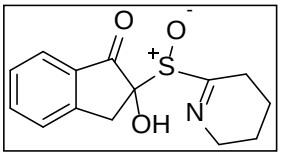


The nitrone **211** (0.399 g, 1.89 mmol, 2.6 eq) was added to the α-diazosulfoxide **14** (0.150 g, 0.73 mmol, 1 eq) in dichloromethane/ethyl acetate (1 : 1, 15 mL, 0.04 M). The solution was pumped through a 10 mL reaction coil heated to 100°C, with a 10 min residence time, followed by a 10 mm id Omnifit™ glass column packed with Alumina (~3 g, volume ~ 1.8 mL). The crude material was collected as a brown solution and concentrated under reduced pressure to give the crude product as a viscous brown oil (0.426 g). Analysis of the mixture by ^{1}H NMR spectroscopy showed the presence of **327** as a major component, with no evidence of the α-diazosulfoxide **14** starting material or intermediate α-oxo sulfine. Signals corresponding to residual nitrone **211** were apparent at 4.96 (2H, s), and 8.18 – 8.22 (2H, m). A singlet at 10.0 ppm is tentatively assigned to benzaldehyde. Purification of the crude product using gradient hexane - ethyl acetate as eluent (100 : 0 – 50 : 50) led to the elution of two products. The first fraction contained the aziridine rearrangement product **327** as a brown oil; (0.044 g, 18%); ν_{max}/cm^{-1} (neat) 1697, 1603, 1258, 726; δ_H (300 MHz, $CDCl_3$) 2.77 (1H, d, A of AB_q, *J* 18.2, one of $ArCH_2$), 3.07 (1H, d, B of AB_q, *J* 18.2, one of $ArCH_2$), 3.73 (1H, s, CHPh), 4.36 – 4.48 (2H, ABq, *J* 14.1, benzylic CH_2), 7.13 - 7.39 (12H, m, 12 x Aromatic CH), 7.49 – 7.54 (1H, t, *J* 7.3, 1 x Aromatic CH), 7.74 (1H, d, *J* 7.6, 1 x Aromatic CH); δ_C ($CDCl_3$, 75 MHz); 32.1 (CH_2, $ArCH_2$), 54.0 (CH_2, NCH_2), 54.5 (Cq, C_{spiro}), 55.2 (CH, CHPh), 123.3, 126.2, 126.7, 127.3 (CH, 4 x Aromatic CH), 127.5 (CH, 2 x Aromatic CH), 127.6 (CH, 1 x Aromatic CH), 128.0, 128.2, 128.3 (3 signals representing 6 x Aromatic CH), 134.5 (CH, 1 x Aromatic CH), 137.2, 137.5, 139.6, 152.3 (4 x Aromatic Cq), 201.3 (Cq, C=O); $(M+H)^+$ 326 (100%); HRMS (ESI+) Exact mass calculated for $C_{23}H_{20}NO$ $[M+H]^+$, 326.1545 Found: 326.1543.

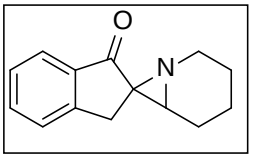


A second impure fraction was isolated as a dark brown residual oil (0.022 g, 8%). The ring opened rearrangement product **328** was the major component. Characteristic signals of the major component **328** are as follows; ν_{max}/cm^{-1} (neat) 1716 (weak), 1603, 1569, 1322; δ_H (300 MHz, $CDCl_3$); 3.27 (2H, s, $ArCH_2$), 4.30 (2H, d, *J* 6.7, $PhCH_2$), 7.16 – 7.52 (13H, m, 13 x Aromatic CH), 7.82 (1H, d, *J* 7.2, 1 x Aromatic CH), 10.97 (1H, br s, OH); δ_C ($CDCl_3$, 75 MHz) 32.1 (CH_2, $ArCH_2$), 48.1 (CH_2, $PhCH_2$), 105.3 (Cq, C_{spiro}), 122.6, 125.2, 126.8 (3 x Aromatic CH), 126.9 (CH, 2 x Aromatic CH), 127.3 (CH, 1 x Aromatic CH), 127.8 (CH, 2 x Aromatic CH), 128.6 (CH, 2 x Aromatic CH), 128.8 (CH, 2 x Aromatic CH), 129.2 (CH, 1 x Aromatic CH), 131.1 (CH, 1 x Aromatic CH), 133.8 (Cq, 1 x Aromatic Cq), 138.8 (Cq, 1 x Aromatic Cq), 141.5 (Cq, 1 x Aromatic Cq), 147.6 (Cq, 1 x Aromatic Cq), 161.2 (Cq, C=N), 191.4 (Cq, C=O). **Note:** repeated attempts to find the corresponding molecular ion by mass spectrometry were unsuccessful.

Cycloaddition reaction of the α-oxo sulfine derived from α-diazosulfoxide 14 with the piperidine derived nitrone 212



The nitrone 2,3,4,5-tetrahydropyridine 1-oxide **212** was freshly generated from 1-hydroxypiperidine (0.191 g, 1.89 mmol, 2.6 eq) (procedure described in section 3.6) and added to the α-diazosulfoxide **14** (0.150 g, 0.73 mmol, 1 eq) in dichloromethane/ethyl acetate (1:1, 15 mL, 0.04 M). The solution was pumped through a 10 mL reaction coil heated to 100°C followed by a 10 mm id Omnifit™ glass column packed with Alumina (~3 g, volume ~ 1.8 mL). The crude product was collected as an brown solution and concentrated under reduced pressure to give the crude product as a viscous brown oil (0.304 g). Analysis of the mixture by ^{1}H NMR spectroscopy showed a complex mixture including **333** and **332** with complete consumption of the α-diazosulfoxide **14**. Purification of the crude material using gradual hexane - ethyl acetate as eluent (100 : 0 – 50 : 50) led to elution of multiple products. The first fraction contained the rearrangement product **333** as a yellow crystalline solid (0.024 g, 12%). Mp 163 – 165°C; ν_{max}/cm^{-1} (neat) 1721, 1159; (300 MHz, $CDCl_3$) 1.78 – 1.89 (4H, m, 2 x CH_2), 2.57 (2H, t, *J* 7.1, 1 x CH_2), 3.40 – 3.48 (4H, m, $ArCH_2$ and NCH_2), 7.31 – 7.38 (1H, m, 1 x Aromatic CH), 7.40 – 7.42 (2H, m 2 x Aromatic CH), 7.76 (1H, d, *J* 7.3, 1 x Aromatic CH), 10.8 (1H, br s, OH); δ_C ($CDCl_3$, 75 MHz) 19.3, 22.3, 26.7 (CH_2, 3 x CH_2), 30.6 (CH_2, $ArCH_2$), 41.4 (CH_2, NCH_2), 102.6 (Cq, C_{spiro}), 122.1, 125.1, 126.6, 130.3 (CH, 4 x Aromatic CH), 142.0, 146.1 (Cq, 2 x Aromatic Cq), 160.1 (Cq, C=N), 188.7 (Cq, C=O); MS $(M)^+$ 277 (5%); HRMS (ESI+) Exact mass calculated for $C_{14}H_{16}NO_3S$ $[M+H]^+$, 278.0862 Found: 278.0851.



A second impure fraction isolated contained the aziridine rearrangement product **332** as the major component and as a brown oil (0.057g, 36%). ν_{max}/cm^{-1} (neat) 2934, 1710, 1603, 1044; (300 MHz, $CDCl_3$) 1.24 – 1.71 (5H, complex m containing 2 x CH_2, 1H of one CH_2), 2.09 – 2.21 (1H, symmetrical multiplet, one of CH_2), 2.65 (1H, dd, *J* 3.2, 7.5, CHN), 2.73 – 2.81 (1H, m, 1H, H_A of CH_2), 3.01 (1H, d, A of AB_q, *J* 17.5, one of $ArCH_2$), 3.19 (1H, d, B of AB_q, *J* 17.5, one of $ArCH_2$), 3.41 – 3.50 (1H, m, 1H, H_B of CH_2), 7.40 (1H, t, *J* 7.3, 1 x Aromatic CH), 7.52 – 7.63 (2H, m, 2 x Aromatic CH), 7.77 (1H, d, *J* 7.3, 1 x Aromatic CH); δ_C ($CDCl_3$, 75 MHz) 18.5, 19.9, 21.8, 26.9 (CH_2, 4 x CH_2), 41.5 (CH, CHN), 44.1 (CH_2, $ArCH_2$), 50.2 (Cq, C_{spiro}), 123.5, 126.3, 127.7, 134.4 (CH, 4 x Aromatic CH), 136.2, 151.2 (Cq, 2 x Aromatic Cq), 203.7 (Cq, C=O); MS $(M+H)^+$ 214 (100%); HRMS (ESI+) Exact mass calculated for $C_{14}H_{16}NO$ $[M+H]^+$, 214.1232 Found: 214.1224.

3.8 Bibliography

(1) Maguire, A. R.; Kelleher, P. G.; Ferguson, G.; Gallagher, J. F. *Tetrahedron Lett.* **1998**, *39*, 2819.
(2) Maguire, A. R.; Kelleher, P. G.; Lawrence, S. E. *Tetrahedron Lett.* **1998**, *39*, 3849.
(3) Maguire, A. R.; Collins, S. G.; Ford, A. *Arkivoc* **2003**, *7*, 96.
(4) O'Sullivan, O. C. M.; Collins, S. G.; Maguire, A. R.; Böhm, M.; Sander, W. *Eur. J. Org. Chem.* **2006**, 2918.
(5) O'Sullivan, O.; Collins, S.; Maguire, A. *Synlett* **2008**, 659.
(6) McCaw, P. G.; Buckley, N. M.; Collins, S. G.; Maguire, A. R. *Eur. J. Org. Chem.* **2016**, 1630.
(7) Zwanenburg, B. *J. Sulfur Chem.* **2013**, *34*, 142.
(8) Ebbinghaus, C. F.; Morrissey, P.; Rosati, R. L. *J. Org. Chem.* **1979**, *44*, 4697.
(9) Bremner, D. H.; Campbell, M. M. *J. Chem. Soc., Perk. Trans. 1* **1977**, 2298.
(10) Bremner, D. H.; Campbell, M. M. *J. Chem. Soc., Chem. Comm.* **1976**, 538.
(11) Hodson, D.; Holt, G. *J. Chem. Soc. C: Org.* **1968**, 1602.
(12) Kelleher, P. G., University College Cork, 2000.
(13) Collins, S. G.; O'Sullivan, O. C. M.; Kelleher, P. G.; Maguire, A. R. *Org. Biomol. Chem.* **2013**, *11*, 1706.
(14) Collins, S. G., National University of Ireland, Cork, 2006.
(15) O'Sullivan, O., University College Cork, 2009.
(16) Buckley, N. M., University College Cork, 2013.
(17) J.K., K. *Acta. Chem. Scand. Ser. B* **1984**, *38*, 101.
(18) Akkurt, M.; Yıldırım, S. Ö.; Kerbal, A.; Bennani, B.; Hadda, T. B.; Chohan, Z. H.; McKee, V. *J. Chem. Crystallogr.* **2010**, *40*, 165.
(19) Aitken, R. A.; Hauduc, C.; Hossain, M. S.; McHale, E.; Schwan, A. L.; Slawin, A. M. Z.; Stewart, C. A. *Aust. J. Chem.* **2014**, *67*, 1288.
(20) Ramadas, S. R.; Chenchaiah, P. C. *Steroids* **1981**, *37*, 353.
(21) Hamon, J.; Espaze, F.; Vignon, J.; Kamenka, J.-M. *Eur. J. Med. Chem.* **1999**, *34*, 125.
(22) Garcia Ruano, J. L.; Martinez, M. C.; Rodriguez, J. H.; Olefirowicz, E. M.; Eliel, E. L. *J. Org. Chem.* **1992**, *57*, 4215.
(23) Frieze, D. M.; Hughes, P. F.; Merrill, R. L.; Evans, S. A. *J. Org. Chem.* **1977**, *42*, 2206.
(24) McCaw, P. G.; Deadman, B. J.; Maguire, A. R.; Collins, S. G. *J. Flow Chem.* **2016**, *6*, 226.
(25) McCaw, P. G.; Buckley, N. M.; Eccles, K. S.; Lawrence, S. E.; Maguire, A. R.; Collins, S. G. *J. Org. Chem.* **2017**, *82*, 3666.
(26) Regitz, M. *Angew. Chem. Int. Ed.* **1967**, *6*, 733.
(27) Doyle, M. P.; McKervey, A.; Ye, T. *Modern Catalytic Methods for Organic Synthesis with Diazo Compounds: From Cyclopropanes to Ylides*; Wiley, 1998.
(28) Tarrant, E., College Cork, 2012.
(29) Deadman, B. J.; O'Mahony, R. M.; Lynch, D.; Crowley, D. C.; Collins, S. G.; Maguire, A. R. *Org. Biomol. Chem.* **2016**, *14*, 3423.
(30) Müller, S. T. R.; Murat, A.; Hellier, P.; Wirth, T. *Org. Pro. Res. Dev.* **2016**, *20*, 495.
(31) Müller, S. T. R.; Murat, A.; Maillos, D.; Lesimple, P.; Hellier, P.; Wirth, T. *Chem. Eur. J.* **2015**, *21*, 7016.
(32) Maas, G. *Angew. Chem. Int. Ed.* **2009**, *48*, 8186.
(33) Bollinger, F. W.; Tuma, L. D. *Synlett* **1996**, *1996*, 407.
(34) Hazen, G. G.; Weinstock, L. M.; Connell, R.; Bollinger, F. W. *Synth. Commun.* **1981**, *11*, 947.
(35) Tuma, L. D. *Thermochim. Acta* **1994**, *243*, 161.
(36) Kitamura, M.; Kato, S.; Yano, M.; Tashiro, N.; Shiratake, Y.; Sando, M.; Okauchi, T. *Org. Biomol. Chem.* **2014**, *12*, 4397.
(37) Potter, G. T.; Jayson, G. C.; Miller, G. J.; Gardiner, J. M. *J. Org. Chem.* **2016**, *81*, 3443.
(38) Rossini, E.; Netz, R. R.; Knapp, E.-W. *J. Chem. Theory Comput.* **2016**, *12*, 3360.

(39) Kaljurand, I.; Rodima, T.; Leito, I.; Koppel, I. A.; Schwesinger, R. *J. Org. Chem.* **2000**, *65*, 6202.
(40) Kupracz, L.; Hartwig, J.; Wegner, J.; Ceylan, S.; Kirschning, A. *Beilstein J. Org. Chem.* **2011**, *7*, 1441.
(41) Bihani, M.; Bora, P. P.; Bez, G.; Askari, H. *Comp. Rend. Chim.* **2013**, *16*, 419.
(42) Bonfils, F.; Cazaux, I.; Hodge, P.; Caze, C. *Org. & Biomol. Chem.* **2006**, *4*, 493.
(43) Tamborini, L.; Romano, D.; Pinto, A.; Bertolani, A.; Molinari, F.; Conti, P. *J. Mol. Catal. B: Enzym.* **2012**, *84*, 78.
(44) Bihani, M.; Bora, P. P.; Bez, G.; Askari, H. *ACS Sus. Chem. Eng.* **2013**, *1*, 440.
(45) Barrett, M. J.; Khan, G. F.; Davies, P. W.; Grainger, R. S. *Chem Comm.* **2017**, *53*, 5733.
(46) See reference 13 page 134.
(47) Ishikawa, T. *Superbases for organic synthesis: guanidines, amidines, phosphazenes and related organocatalysts*; John Wiley & Sons, 2009.
(48) Kirmse, W. *Eur. J. Org. Chem.* **2002**, *2002*, 2193.
(49) O'Sullivan, O. C. M.; Collins, S. G.; Maguire, A. R.; Bucher, G. *Eur. J. Org. Chem.* **2014**, 2297.
(50) Sander, W.; Strehl, A.; Maguire, A. R.; Collins, S.; Kelleher, P. G. *Eur. J. Org. Chem.* **2000**, 3329.
(51) Suzuki, E.; Watari, F. *Spec. Acta Part A: Mol. Biomol. Spec.* **1995**, *51*, 779.
(52) Leriverend, C.; Metzner, P.; Capperucci, A.; Degl'Innocenti, A. *Tetrahedron* **1997**, *53*, 1323.
(53) Cerreta, F.; Leriverend, C.; Metzner, P. *Tetrahedron Lett.* **1993**, *34*, 6741.
(54) El-Sayed, I. *Mona. Chem.* **2004**, *136*, 543.
(55) O'Sullivan, O. C. M., University College Cork, 2008.
(56) Saalfrank, R. W.; Rost, W. *Angew. Chem. Int. Ed.* **1985**, *24*, 855.
(57) Chevrie, D.; Metzner, P. *Tetrahedron Lett.* **1998**, *39*, 8983.
(58) Mol, N. J. d.; Henegouwen, G. M. J. B. v.; Gerritsma, K. W. *Photochem. Photobiol.* **1979**, *29*, 479.
(59) Vapourtec Ltd. Photochemical reactor datasheet, 2016.
(60) Cox, R. J.; Wang, P. S. *J. Chem. Soc., Perkin Trans. 1* **2001**, 2022.
(61) Alan Aitken, R.; M. Armstrong, J.; J. Drysdale, M.; C. Ross, F.; M. Ryan, B. *J. Chem. Soc. Perkin Trans. 1* **1999**, 593.
(62) O'Sullivan, O. C. M.; Collins, S. G.; Maguire, A. R.; Buche, G. *Eur. J. Org. Chem.* **2014**, 2297.
(63) McCaw, P. G.; Buckley, N. M.; Collins, S. G.; Maguire, A. R. *Eur. J. Org. Chem.* **2016**, *2016*, 1630.
(64) Lenz, B. G.; Haltlwanger, R. C.; Zwanenburg, B. *J. Chem. Soc., Chem. Comm.* **1984**, 502.
(65) Baltas, M.; Raouf-Benchekroun, K.; De Blic, A.; Cazaux, L.; Tisnès, P.; Gorrichon, L.; Hussein, K.; Barthelat, J. C. *Tetrahedron* **1996**, *52*, 14865.
(66) Zwanenburg, B.; Thijs, L.; Broens, J. B.; Strating, J. *Recl. Trav. Chim. Pays-Bas* **1972**, *91*, 443.
(67) Ogurok, V. M.; Siry, S. A.; Rusanov, E. B.; Shermolovych, Y. G. *J. Fluorine Chem.* **2016**, *189*, 119.
(68) Watanabe, Y.; Sakakibara, T. *Tetrahedron* **2009**, *65*, 599.
(69) Heras, M.; Gulea, M.; Masson, S. *Chem. Commun.* **2001**, 611.
(70) Bastin, R.; Albadri, H.; Gaumont, A.-C.; Gulea, M. *Org. Lett.* **2006**, *8*, 1033.
(71) Denancé, M.; Legay, R.; Gaumont, A.-C.; Gulea, M. *Tetrahedron Lett.* **2008**, *49*, 4329.
(72) Yoshimura, Y.; Yamazaki, Y.; Kawahata, M.; Yamaguchi, K.; Takahata, H. *Tetrahedron Lett.* **2007**, *48*, 4519.
(73) Smith, L. H.; Coote, S. C.; Sneddon, H. F.; Procter, D. J. *Angew. Chem. Int. Ed.* **2010**, *49*, 5832.
(74) Porta, R.; Benaglia, M.; Puglisi, A. *Org. Pro. Res. Dev.* **2016**, *20*, 2.
(75) Newman, S. G.; Jensen, K. F. *Green Chem.* **2013**, *15*, 1456.
(76) Fanelli, F.; Parisi, G.; Degennaro, L.; Luisi, R. *Beilstein J. Org. Chem.* **2017**, *13*, 520.
(77) Henry, C.; Bolien, D.; Ibanescu, B.; Bloodworth, S.; Harrowven, D. C.; Zhang, X.; Craven, A.; Sneddon, H. F.; Whitby, R. J. *Eur. J. Org. Chem.* **2015**, *2015*, 1491.
(78) Lamborelle, N.; Simon, J. F.; Luxen, A.; Monbaliu, J.-C. M. *Org. & Bio. Chem.* **2015**, *13*, 11602.
(79) Nakashima, E.; Yamamoto, H. *Chem. Commun.* **2015**, *51*, 12309.

(80) Chiroli, V.; Benaglia, M.; Cozzi, F.; Puglisi, A.; Annunziata, R.; Celentano, G. *Org. Lett.* **2013**, *15*, 3590.
(81) Abele, S.; Höck, S.; Schmidt, G.; Funel, J.-A.; Marti, R. *Org. Pro. Res. Dev.* **2011**, *16*, 1114.
(82) Chang, M.-Y.; Lee, T.-W.; Hsu, R.-T.; Yen, T.-L. *Synthesis* **2011**, *2011*, 3143.
(83) Platz, M. S. *J. Org. Chem.* **2014**, *79*, 2341.
(84) Burdzinski, G. T.; Wang, J.; Gustafson, T. L.; Platz, M. S. *J. Am. Chem. Soc.* **2008**, *130*, 3746.
(85) Dickson, R. S.; Dobney, B. J.; Eastwood, F. W. *J. Chem. Educ.* **1987**, *64*, 898.
(86) Shiri, L.; Kazemi, M. *Res. Chem. Intermed.* **2017**, 1.
(87) Bahrami, K.; Khodaei, M. M.; Karimi, A. *Synthesis* **2008**, *2008*, 2543.
(88) Bahrami, K.; Khodaei, M. M.; Sheikh Arabi, M. *J. Org. Chem.* **2010**, *75*, 6208.
(89) Brown, H. C.; Ravindran, N. *Synthesis* **1973**, *1973*, 42.
(90) Jang, Y.; Kim, K. T.; Jeon, H. B. *J. Org. Chem.* **2013**, *78*, 6328.
(91) Drabowicz, J.; Oae, S. *Synthesis* **1977**, *1977*, 404.
(92) Legnani, L.; Lunghi, C.; Albini, F. M.; Nativi, C.; Richichi, B.; Toma, L. *Eur. J. Org. Chem.* **2007**, *2007*, 3547.
(93) Bourdon, F.; Ripoll, J.-L.; Vallée, Y. *Tetrahedron Lett.* **1990**, *31*, 6183.
(94) Fujita, J.; Matsuda, H.; Yamamoto, K.; Morii, Y.; Hashimoto, M.; Okuno, T.; Hashimoto, K. *Tetrahedron* **2004**, *60*, 6829.
(95) Santoyo Gonzalez, F.; Garcia Mendoza, P.; Lopez Aparicio, F. J. *Carbohydr. Res.* **1988**, *183*, 227.
(96) Praefcke, K.; Weichsel, C. *Liebigs Ann. Chem.* **1979**, *1979*, 784.
(97) Chen, X. Y.; Park, S. J.; Buschmann, H.; De Rosa, M.; Bolm, C. *Biorg. Med. Chem. Lett.* **2012**, *22*, 4307.
(98) Nugent, B. M.; Buysse, A. M.; Loso, M. R.; Babcock, J. M.; Johnson, T. C.; Oliver, M. P.; Martin, T. P.; Ober, M. S.; Breaux, N.; Robinson, A.; Adelfinskaya, Y. *Pest Manag. Sci.* **2015**, *71*, 928.
(99) Zenzola, M.; Doran, R.; Luisi, R.; Bull, J. A. *J. Org. Chem.* **2015**, *80*, 6391.
(100) Huisgen, R. *Angew. Chem. Int. Ed.* **1963**, *2*, 565.
(101) Huisgen, R. *Angew. Chem. Int. Ed.* **1963**, *2*, 633.
(102) Carruthers, W. *Cycloaddition Reactions in Organic Synthesis*; Elsevier, 1990.
(103) Huisgen, R.; Mloston, G.; Polborn, K. *J. Org. Chem.* **1996**, *61*, 6570.
(104) Bonini, B. F.; Maccagnani, G.; Mazzanti, G.; Thijs, L.; Ambrosius, H. P. M. M.; Zwanenburg, B. *J. Chem. Soc., Perkin Trans. 1* **1977**, 1468.
(105) Zwanenburg, B. *Rec. Trav. Chim. Pays-Bas* **1982**, *101*.
(106) Bonini, B. F.; Maccagnani, G.; Mazzanti, G.; Pedrini, P.; Lammerink, B. H. M.; Zwanenburg, B. *J. Chem. Soc., Perkin Trans. 1* **1983**, 2097.
(107) Zwanenburg, B. *Recl. Trav. Chim. Pays-Bas* **1982**, *101*, 1.
(108) Bonini, B. F.; Maccagnani, G.; Wagenaar, A.; Thijs, L.; Zwanenburg, B. *J. Chem. Soc., Perkin Trans. 1* **1972**, 2490.
(109) Elsäßer, A.; Sundermeyer, W. G. *Chem. Ber.* **1985**, *118*, 4553.
(110) Mlostoń, G.; Linden, A.; Heimgartner, H. *Helv. Chim. Acta* **1996**, *79*, 31.
(111) Lim, Y. W.; Hewitt, R. J.; Burkett, B. A. *Eur. J. Org. Chem.* **2015**, 4840.
(112) Burkett, B. A.; Fu, P.; Hewitt, R. J.; Ng, S. L.; Toh, J. D. W. *Eur. J. Org. Chem.* **2014**, *2014*, 1053.
(113) Lemercier, B. C.; Pierce, J. G. *Org. Lett.* **2015**, *17*, 4542.
(114) Mloston, G.; Kowalski, M. K.; Obijalska, E.; Heimgartner, H. *J. Fluorine Chem.* **2017**, *199*, 92.
(115) Bonini, B.; Maccagnani, G.; Mazzanti, G.; Pedrini, P.; Zwanenburg, B. *Chem. Info.* **1978**, *9*.
(116) Handels, J. W. H., University of Nijmegen, 1979.
(117) Gella, C.; Ferrer, È.; Alibés, R.; Busqué, F.; de March, P.; Figueredo, M.; Font, J. *J. Org. Chem.* **2009**, *74*, 6365.
(118) Roca-Lopez, D.; Tejero, T.; Caramella, P.; Merino, P. *Org. Biomol. Chem.* **2014**, *12*, 517.
(119) Kissane, M., University College Cork, 2009.
(120) Louis, C.; Hootelé, C. *Tetrahedron: Asym.* **1997**, *8*, 109.

(121) Alsbaiee, A.; Ali, S. A. *Tetrahedron* **2008**, *64*, 6635.
(122) Kissane, M.; Lawrence, S. E.; Maguire, A. R. *Tetrahedron* **2010**, *66*, 4564.
(123) Kissane, M., University College Cork, 2009.
(124) Hogan, D., University College Cork.
(125) Liu, K.-C.; Shelton, B. R.; Howe, R. K. *J. Org. Chem.* **1980**, *45*, 3916.
(126) Schwarz, L.; Girreser, U.; Clement, B. *Eur. J. Org. Chem.* **2014**, *2014*, 1961.
(127) Zhang, D.-W.; Lin, F.; Li, B.-C.; Liu, H.-W.; Zhao, T.-Q.; Zhang, Y.-M.; Gu, Q. In *Chem. Pap.* 2 015; Vol. 69, p 1500.
(128) Heinrich, W. *Ber. Chem.* **1907**, *40*, 1667.
(129) Ratcliffe, P.; Abernethy, L.; Ansari, N.; Cameron, K.; Clarkson, T.; Dempster, M.; Dunn, D.; Easson, A.-M.; Edwards, D.; Everett, K.; Feilden, H.; Ho, K.-K.; Kultgen, S.; Littlewood, P.; Maclean, J.; McArthur, D.; McGregor, D.; McLuskey, H.; Neagu, I.; Nimz, O.; Nisbet, L.-A.; Ohlmeyer, M.; Palin, R.; Pham, Q.; Rong, Y.; Roughton, A.; Sammons, M.; Swanson, R.; Tracey, H.; Walker, G. *Biorg. Med. Chem. Lett.* **2011**, *21*, 4652.
(130) Zhu, J.; Ye, Y.; Ning, M.; Mándi, A.; Feng, Y.; Zou, Q.; Kurtán, T.; Leng, Y.; Shen, J. *ChemMedChem* **2013**, *8*, 1210.
(131) Harding, S. L.; Marcuccio, S. M.; Savage, G. P. *Beilstein J. Org. Chem.* **2012**, *8*, 606.
(132) Yu, Z.-X.; Caramella, P.; Houk, K. N. *J Amer. Chem. Soc.* **2003**, *125*, 15420.
(133) Bonini, B. F.; Maccagnani, G.; Mazzanti, G.; Thijs, L.; Veenstra, G. E.; Zwanenburg, B. *J. Chem. Soc., Perkin Trans. 1* **1978**, 1218.
(134) Hejmanowska, J.; Jasiński, M.; Mlostoń, G.; Albrecht, Ł. *Eur. J. Org. Chem.* **2017**, 950.
(135) O'Brien, A. G.; Levesque, F.; Seeberger, P. H. *Chem. Commun.* **2011**, *47*, 2688.
(136) Brasholz, M.; Saubern, S.; Savage, G. P. *Aust. J. Chem.* **2011**, *64*, 1397.
(137) Schwab, M.; Sundermeyer, W. *Chem. Ber.* **1988**, *121*, 75.
(138) Dyer, J. C.; Evans, S. A. *J. Org. Chem.* **1980**, *45*, 5350.
(139) Mlostoń, G.; Kowalski, M. K.; Obijalska, E.; Heimgartner, H. *J. Fluorine Chem.*
(140) Rewinkel, J. B. M.; Zwanenburg, B. *Recl. Trav. Chim. Pays-Bas* **1990**, *109*, 190.
(141) Kumar, S.; Kumar, V.; Singh, S. P. *Pericyclic Reactions: A Mechanistic and Problem-Solving Approach*; Elsevier Science, 2015.
(142) Gothelf, K. V.; Jørgensen, K. A. *Chem. Rev.* **1998**, *98*, 863.
(143) Zhao, Q.; Han, F.; Romero, D. L. *J. Org. Chem.* **2002**, *67*, 3317.
(144) Matysiak, J. *Biorg. Med. Chem.* **2006**, *14*, 2613.
(145) Grzesiek, S.; Cordier, F.; Jaravine, V.; Barfield, M. *Prog. Nucl. Magn. Reson. Spectrosc.* **2004**, *45*, 275.
(146) Hierso, J.-C. *Chem. Rev.* **2014**, *114*, 4838.
(147) Meissner, A.; Sørensen, O. W. *J. Mag. Res.* **2000**, *143*, 431.
(148) de Ceglie, M. C.; Musio, B.; Affortunato, F.; Moliterni, A.; Altomare, A.; Florio, S.; Luisi, R. *Chem. Eur. J.* **2011**, *17*, 286.
(149) Meyer, C.; Pete, J.-P.; Piva, O. *Recl. Trav. Chim. Pays-Bas* **1995**, *114*, 492.
(150) Cramer, S. A.; Jenkins, D. M. *J. Amer. Chem. Soc.* **2011**, *133*, 19342.
(151) Trost, B. M.; Saget, T.; Hung, C.-I. *Angew. Chem. Int. Ed.* **2017**, *56*, 2440.
(152) Bates, S. E.; Fojo, A. T.; Weinstein, J. N.; Myers, T. G.; Alvarez, M.; Pauli, K. D.; Chabner, B. A. *J. Cancer Res. Clin. Oncol.* **1995**, *121*, 495.
(153) Monks, A.; Scudiero, D.; Johnson, G.; Paull, K.; Sausville, E. *Anti-Cancer Drug Des.* **1997**, *12*, 533.
(154) Holbeck, S. L.; Camalier, R.; Crowell, J. A.; Govindharajulu, J. P.; Hollingshead, M. G.; Anderson, L. W.; Polley, E. C.; Rubinstein, L.; Srivastava, A. K.; Wilsker, D. F. *Cancer Research* **2017**, canres. 0489.2017.
(155) Shoemaker, R. H.; Monks, A.; Alley, M. C.; Scudiero, D. A.; Fine, D. L.; McLemore, T. L.; Abbott, B. J.; Paull, K. D.; Mayo, J. G.; Boyd, M. R. *Prog. Clin. Biol. Res.* **1987**, *276*, 265.

(156) Rubinstein, L.; Shoemaker, R.; Paull, K.; Simon, R.; Tosini, S.; Skehan, P.; Scudiero, D.; Monks, A.; Boyd, M. *J. Natl. Cancer Inst.* **1990**, *82*, 1113.
(157) Bailly, F.; Queffélec, C.; Mbemba, G.; Mouscadet, J.-F.; Pommery, N.; Pommery, J.; Hénichart, J.-P.; Cotelle, P. *E. J. Med. Chem.* **2008**, *43*, 1222.
(158) Ghosh, S.; Sinha, S.; Drew, M. G. B. *Org. Lett.* **2006**, *8*, 3781.
(159) Leoni, L. M.; Hamel, E.; Genini, D.; Shih, H.; Carrera, C. J.; Cottam, H. B.; Carson, D. A. *J. Natl. Cancer Inst.* **2000**, *92*, 217.
(160) Sugimoto, H. *Pure Appl. Chem.* **1999**, *71*, 2031.
(161) Saxena, H. O.; Faridi, U.; Srivastava, S.; Kumar, J. K.; Darokar, M. P.; Luqman, S.; Chanotiya, C. S.; Krishna, V.; Negi, A. S.; Khanuja, S. P. S. *Biorg. Med. Chem. Lett.* **2008**, *18*, 3914.
(162) Somsák, L.; Nagy, V.; Vidal, S.; Czifrák, K.; Berzsényi, E.; Praly, J.-P. *Biorg. Med. Chem. Lett.* **2008**, *18*, 5680.
(163) Gryder, B. E.; Guerrant, W.; Chen, C. H.; Oyelere, A. K. *MedChemComm* **2011**, *2*, 1083.
(164) Lin, G.; Li, D.; de Carvalho, L. P. S.; Deng, H.; Tao, H.; Vogt, G.; Wu, K.; Schneider, J.; Chidawanyika, T.; Warren, J. D.; Li, H.; Nathan, C. *Nature* **2009**, *461*, 621.
(165) Zhang, H.-Z.; Kasibhatla, S.; Kuemmerle, J.; Kemnitzer, W.; Ollis-Mason, K.; Qiu, L.; Crogan-Grundy, C.; Tseng, B.; Drewe, J.; Cai, S. X. *J. Med. Chem.* **2005**, *48*, 5215.
(166) Milner, S. E.; Maguire, A. R. **2012**.
(167) Vogel, A. *Longman: UK 1979* **1978**.
(168) Cagniant, P.; Jecko, G.; Cagniant, P. *Bull. Soc. Chim. Fr.* **1961**, 2225.
(169) Tamura, Y.; Annoura, H.; Fuji, M.; Okura, M.; Ishibasi, H. *Chem. Pharm. Bull.* **1986**, *34*, 540.
(170) Canalini, G.; Degari, I.; Fochi, R. *Ann. Chim. (Rome)* **1967**, *57*, 1045.
(171) Yang, G.; Peop. Rep. China . 2010, p 47pp.
(172) De Savi, C.; Morley, A. D.; Nash, I.; Karoutchi, G.; Page, K.; Ting, A.; Gerhardt, S. *Bioorg. Med. Chem. Lett.* **2012**, *22*, 271.
(173) Young, T. E.; Heitz, L. J. *J. Org. Chem.* **1973**, *38*, 1562.
(174) Matsumoto, K.; Yamaguchi, T.; Katsuki, T. *Heterocycles* **2008**, *76*, 191.
(175) Bergesen, K.; Carden, B. M.; Cook, M. J. *J. Chem. Soc., Perkin Trans. 2* **1978**, 1001.
(176) Laszlo, P. *Preparative Chemistry Using Supported Reagents*; Elsevier Science, 2012.
(177) Murahashi, S.; Mitsui, H.; Shiota, T.; Tsuda, T.; Watanabe, S. *J. Org. Chem.* **1990**, *55*, 1736.
(178) Ramón, R. S.; Bosson, J.; Díez-González, S.; Marion, N.; Nolan, S. P. *J. Org. Chem.* **2010**, *75*, 1197.
(179) Xie, F.; Ni, T.; Zhao, J.; Pang, L.; Li, R.; Cai, Z.; Ding, Z.; Wang, T.; Yu, S.; Jin, Y.; Zhang, D.; Jiang, Y. *Bioorg. Med. Chem. Lett.* **2017**, *27*, 2171.
(180) Quadrelli, P.; Invernizzi, A. G.; Falzoni, M.; Caramella, P. *Tetrahedron* **1997**, *53*, 1787.
(181) Single crystal X-ray analysis was carried out by Dr. Simon Lawrence and Dr. Udaya Khandavalli.